

Central Intelligence Agency



Washington, D.C. 20505

25 September 2017

Mr. Michael Morisy
MuckRock News
DEPT MR 17807
411A Highland Avenue
Somerville, MA 02144-2516

Reference: F-2015-01649

Dear Mr. Morisy:

This is a final response to your 8 May 2015 Freedom of Information Act (FOIA) request for **any and all internal reports on the risks of geomagnetic storms to the nation**. We processed your request in accordance with the FOIA, 5 U.S.C. § 552, as amended, and the CIA Information Act, 50 U.S.C. § 3141, as amended. Our processing included a search for records as described in our 7 July 2015 acceptance letter.

We completed a thorough search for records responsive to your request and located three documents, consisting of 338 pages, which we determined can be released in their entirety. Copies of the documents are enclosed at Tab A.

We also determined that four documents, consisting of 483 pages, can be released in segregable form with deletions made on the basis of FOIA exemptions (b)(1) and/or (b)(3). Exemption (b)(3) pertains to information exempt from disclosure by statute. The relevant statutes are Section 6 of the Central Intelligence Agency Act of 1949, as amended, and Section 102A(i)(1) of the National Security Act of 1947, as amended. Copies of the documents and an explanation of exemptions are enclosed at Tab B.

As the CIA Information and Privacy Coordinator, I am the CIA official responsible for this determination. You have the right to appeal this response to the Agency Release Panel, in my care, within 90 days from the date of this letter. Please include the basis of your appeal.

If you have any questions regarding our response, you may contact us at:

Central Intelligence Agency
Washington, DC 20505
Information and Privacy Coordinator
703-613-3007 (Fax)

Please be advised that you may seek dispute resolution services from the CIA's FOIA Public Liaison or from the Office of Government Information Services (OGIS) of the National Archives and Records Administration. OGIS offers mediation services to help resolve disputes between FOIA requesters and Federal agencies. You may reach CIA's FOIA Public Liaison at:

703-613-1287 (FOIA Hotline)

The contact information for OGIS is:

Office of Government Information Services
National Archives and Records Administration
8601 Adelphi Road – OGIS
College Park, MD 20740-6001
202-741-5770
877-864-6448
202-741-5769 (fax)
ogis@nara.gov

Contacting the CIA's FOIA Public Liaison or OGIS does not affect your right to pursue an administrative appeal.

Sincerely,

A handwritten signature in black ink, appearing to read 'Allison Fong', with a long horizontal flourish extending to the right.

Allison Fong
Information and Privacy Coordinator

Enclosures

TAB A

GEOMAGNETIC FACTORS IN SPONTANEOUS SUBJECTIVE TELEPATHIC,
PRECOGNITIVE AND POSTMORTEM EXPERIENCES

George B. Schaut and Michael A. Persinger

Department of Psychology
Laurentian University

ABSTRACT

This study was designed to test the reliability of the observation that (spontaneous) subjective telepathic experiences concerning death and crises have occurred on days when the geomagnetic activity was quieter than the days before or afterwards. Geomagnetic activity (aa index) at the time of three major classes of subjective psi reports: telepathic-clairvoyant (n=133), precognitive (n=105), and postmortem (n=140) experiences was compared. Highly statistically significant ($p < .001$) differences were found between the classes of experiences and for time by class interactions. Telepathic experiences occurred on days when the geomagnetic activity was much less than the days on which the precognitive or postmortem experiences occurred. In addition, the geomagnetic activity on the days of the telepathic experiences was significantly lower than for the days before or afterward the experiences and for the average of the month or year in which the cases occurred. This pattern was not found for the other two classes of experiences. The telepathy-geomagnetic pattern was internally consistent and very similar to the results of three other studies. The results strongly suggest that some factor associated with or enhanced by transient, sudden decreases in geomagnetic activity may facilitate the occurrence or the memory of the occurrence of telepathic experiences concerning death and crisis.

INTRODUCTION

Several studies (Persinger, 1985a; 1986; Schaut & Persinger, 1985a,b) have shown that subjective telepathic experiences tend to occur on days when the geomagnetic activity is quieter than the days before or after the experiences. The effect is quite strong statistically and is very similar in all three studies. Most of the experiences from the Schaut and Persinger (1985) study occurred between the years 1920 and 1967 while those from the Gurney, Meyers and Podmore analyses (Persinger, 1986a) occurred between the years 1868 and 1884. More than 98% of the cases involved episodes of sudden death, crisis, or illness to friends or family members.

The aa (average antipodal) index of global geomagnetic activity has been employed in all of the above studies. Daily or half-daily values refer to the average amplitude (in gammas) of geomagnetic activity (Mayaud, 1973). This measure is derived directly and quantitatively from magnetograms of observatories in England and Australia (hence the term "antipodal"). This particular measure of geomagnetic activity was selected because it provided a homogeneous quantitative series of highly reliable values that begins in the year 1868. In addition, 100 years of the data are easily accessible in the monograph (Mayaud, 1973) or on magnetic tape; consequent years are also available. The aa index is also strongly correlated with a variety of more recent geomagnetic activity indices that include dozens of measurements from tens of different stations throughout the world.

We decided to determine the reliability of the previous studies by analyzing the remaining cases of subjective telepathic-clairvoyant (T-C) experiences that were available to us. These cases had been reported in FATE magazine; its format was considered instrumental for the demonstration of the specificity of the geomagnetic effect on T-C experiences because both precognitive (PC) and postmortem (PM) experiences were also included. Except for the temporal displacement before or after the event, descriptions and details of precognitive and postmortem experiences are similar to TC phenomena. We considered the PC and PM experiences as both source (from FATE) and case controls. If the geomagnetic effect was specific to T-C, then it should not be evident in the PC or PM cases. If it were evident in all three classes, then some non-specific factor (such as just the display of unusual experiences) might be likely.

In the present study, we compared the three major classes of subjective psi phenomena: telepathic-clairvoyance (T-C), precognitive (PC), and postmortem (PM) experiences, with respect to the geomagnetic activity

during the weeks, months and years in which they occurred. The study was designed to allow comparison with previous analyses and to allow internal comparisons within subcategories of the major classes. Consequently, we also compared the geomagnetic conditions during different modes (impression, image, dream, apparition) of experiences, conditions of the putative agent (death or crisis) when appropriate and time of day. We were particularly interested in the internal (replication) consistency of the two collections of FATE cases.

METHOD

Data Base

All first person reports concerning telepathic-clairvoyant (T-C), precognitive (PC), and postmortem (PM) experiences that contained the day, month and year of occurrence were recorded from our library of FATE magazines. Most of the 234 issues were published between the years 1965 and 1985. The collection of reports were completed in two series (replications). The first replication, which was published elsewhere (Schaut & Persinger, 1985b), involved 57 T-C, 56 PC, and 75 PM experiences. The second (replication) study involved 75 T-C, 49 PC, and 65 PM cases.

Procedure

Each report was coded according to the following parameters: hour (if given), day, month, year, sex of the percipient (reporter), classification (T-C, PC, or PM experience), mode of experience (feeling/impression, image, dream, or apparition), and general geographical location of the percipient (continent). The classification code also indicated if the experience involved sickness, crisis or death.

Case Characteristics

For the T-C experiences, the putative agent's situations at the time of the experiences were sudden sickness (n=12), life-threatening crises (27), and death (n=94). For the PC experiences, crisis was involved with 42 cases and death occurred in 63 cases. Chi-square analyses indicated that there was no statistically significant ($p > .05$) differences between study 1 and study 2 with respect to frequencies of class type, sex of

percipient (reporter), crisis/death condition or mode; 81% of the percipients were female. There was a significant ($p < .001$) difference between mode (4 levels) and the class of experience ($\chi^2 = 119.50$, $df = 6$); this was due to the disproportionate number of apparitional forms (83%) in the PM experiences compared to the T-C (28%) and PC (25%) experiences. However, there was no significant difference between the proportion of different modes between telepathic and precognitive experiences only. Modes for T-C and PC experiences were not influenced by sex, crisis/death condition, or month of occurrence but they were associated with time of day ($\chi^2 = 10.16$, $df = 3$, $p = .02$). Dreams (62%) and apparitional (75%) experiences were more likely to occur between midnight and 0600 hrs (local time) than impressions (36%) or images (31%). Impressions and images were more frequent during the other hours (0700 to 2300). Comparisons of all three classes with respect to the temporal specificity of reports: 1) specific hour, 2) day vs night, or 3) the date, demonstrated no significant ($\chi^2 = 4.30$, $df = 4$) differences in distribution. Thus, reports of the specific time of the experience did not differ between the three classes of phenomena.

Geomagnetic Activity

AA values for the appropriate hemisphere in which the case occurred (north or south) were coded for the 3 days before, 3 days after and the day of the experiences. The mean aa value for the month and for the year in which the experience occurred were also coded. For those cases in which there was an hourly specification, simply the value for the day of the experience was used. For those cases in which the specific hour was specified, adjustments were made between local and universal time by using combinations of half-day values. This procedure has been discussed previously (Schaut & Persinger, 1985b).

The primary design employed multivariate analyses of variance (MANOVA) which allows repeated (dependent) measures to be combined with factors (non-repeated measures). In this instance, the repeated measures were the 7 successive days of aa values or the aa values for the day, month and year in which the experience occurred. The main factors were classes of experiences and replication. Other main factors that were considered before analyses began were class of experience and crisis vs death situations and class of experience (for T-C and PC) and the mode of the experience.

MANOVA were selected because it allows a dynamic (temporal) comparison of changes over time between geomagnetic conditions for separate classes or conditions of

experiences. Our previous analyses indicated that interactions (Persinger, 1985a; Schaut & Persinger, 1985a,b) between the day of the experience and the type of experience were the key phenomena. The rationale for selecting the key day (day of the experience) and the three days before and the three days after the experience was based upon both theoretical and empirical reasons. First, geomagnetic activity within 1+1 days is usually highly correlated (>0.60) or dependent; beyond three days, there is little correlation (days are independent). Secondly, several previous studies (Persinger, 1985a; Schaut & Persinger, 1985a,b) have shown that more than +3 days from the key day, geomagnetic values are usually not significantly different from the mean values of the month.

Because assumptions of homogeneity of variance are occasionally violated with geomagnetic indices (from outlier values; i.e., geomagnetic storms), log transformations of the daily, monthly, and yearly aa values were completed; MANOVA designs were applied to these values. Repeated measures for specific classes of experiences were completed separately to verify the results of the MANOVA and to more clearly delineate the temporal pattern of aa values; a posteriori correlated t-tests for within class comparisons and independent t-tests for between group comparisons were used. As an additional verification and data check, non parametric: repeated measure (Friedman's) and non-repeated measure (Kruskal-Wallis) were completed for the different classes. This is a routine procedure in our laboratory in order to control for possible nonlinearities within data. All analyses were completed with SPSSX software on a DEC 2020 computer.

The means and standard errors of the mean of the daily aa indices for the three days before, the three days after and the days of the experiences as well as the averages for the month and years in which the experiences occurred are shown in Figure 1. Multivariate analyses of variance (MANOVA) of the seven repeated measures (7 successive daily aa values) and two factors: the three classes of experiences (telepathic, precognitive, and postmortem) and the two replications (one vs two) demonstrated no significant difference ($F(1,372)=0.56, p>.01$) between replications but a highly significant ($F(2,372)=11.20, p<.001$) difference between classes of experiences. The results of the MANOVA were similar for the log (base 10) transformations of the aa values ($F(2,372)=10.67, p<.001$).

A a posteriori analyses (Scheffe's set at $p<.05$) on both the raw scores and log transformations indicated that the T-C experiences occurred when the aa activity of the week ($\bar{X} \pm S.E.M. = 19.3 \pm 0.9$) was lower than the values for either the PC (24.2 ± 1.1) or PM (22.8 ± 1.0) experiences which did not differ from each other. The results were identical for both absolute values and log transformations. Nonpara-

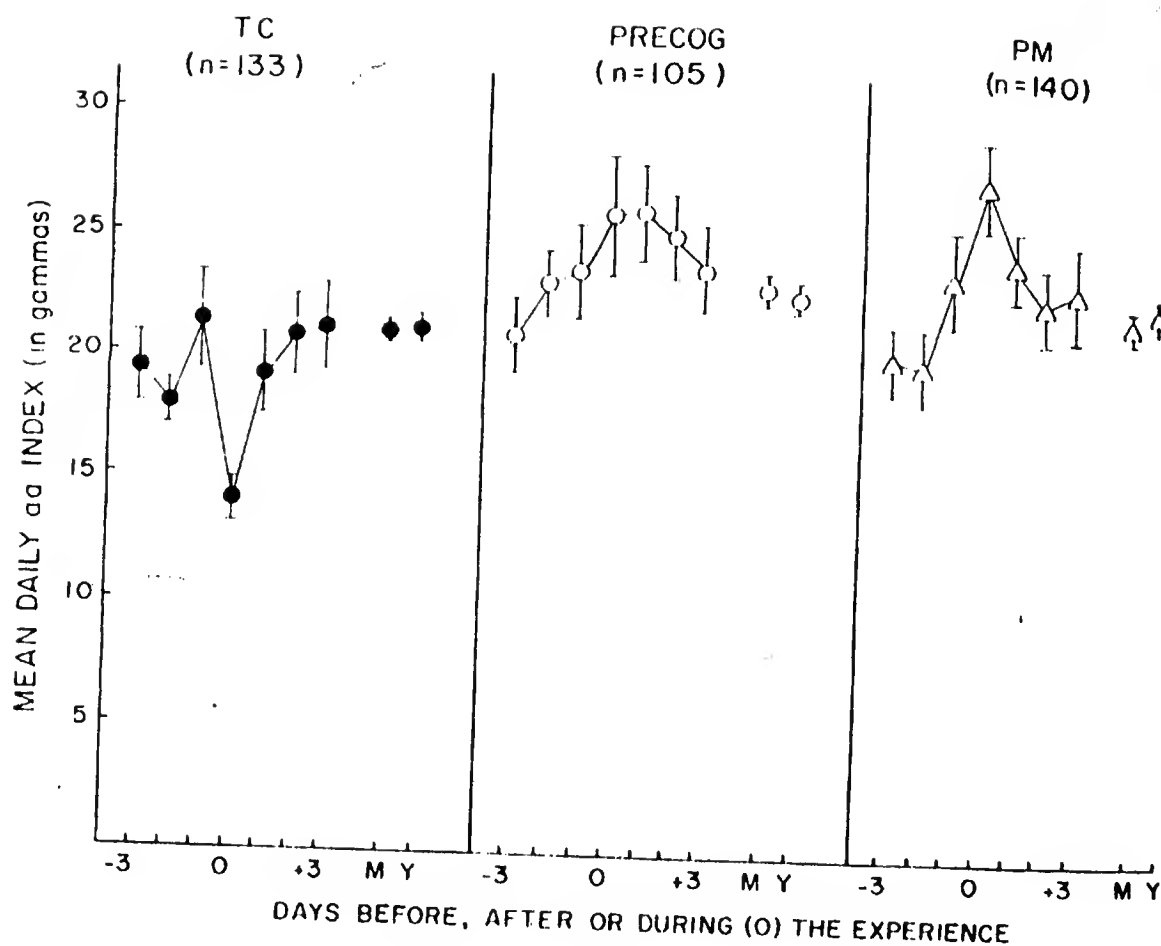


Figure 1: Mean daily values (in gamma) of the aa (antipodal) index of global geomagnetic activity for the three days before, three days after and the days of telepathic (T-C), precognitive (PC), and postmortem (PM) subjective experiences. n refers to the number of cases in each class of experience. M and Y refer to the means of the aa values for the months and years in which the experiences occurred. Vertical bars indicate ± 1 standard error of the mean.

metric analyses (Kruskal-Wallis) indicated that the geomagnetic activity was also quieter during the week of the T-C cases (mean ranks=161) than for the other two classes (ranks 213, 200) of experience ($\chi^2=15.41$, $p<.001$).

By far the most striking effect was the statistically significant class by days interaction. This was evident for both normal ($F(12,2332)=4.30$, $p<.001$) and log transformed data ($F(12,2232)=4.42$, $p<.001$). A posteriori contrasts indicated that this interaction was due to the quieter geomagnetic conditions on the day ($X=S.E.M.=13.9+1.0$) of the T-C experiences compared to the days on which the PC ($26.+2.2$) and PM ($27.5+1.9$) experiences occurred. None of the other interactions (replication by day; class by replication by day) were significant statistically. There was also no significant difference between days ($F(6,2232)=2.50$, $p>.01$). Differences were normal aa values on just the days of the experiences were highly significant ($F(2,375)=28.33$, $p<.001$). The variance of aa values for T-C cases only was significantly less on the key day compared to the other two classes (Bartlett Box $F=34.36$, $p<.001$). However, a Kruskal-Wallis test indicated a highly significant difference between classes for the mean ranks of the values ($\chi^2=59.54$, $p<.001$).

Additional MANOVA were completed to determine if the days of the experiences for the three classes were different from the monthly and yearly values. A posteriori correlated t-tests indicated that the T-C experiences occurred on days ($X+S.E.M.=13.9+1.0$) that were significantly quieter than the months ($20.9+0.5$) or the years ($21.3+0.4$) in which they occurred; however, there was no significant ($p>.05$) difference ($t=0.80$) between the aa values for the month and the years in which the T-C cases occurred. Similarly, there were no significant differences between the aa values for the days on which the precognition or apparitional cases occurred and their monthly aa ($22.9+0.8$, $21.9+0.6$, respectively) or yearly aa values ($22.6+0.5$, $22.4+0.4$, respectively). The aa values for the months and years in which the T-C experiences occurred were not significantly different ($p>.05$) from the aa values for the months and years in which the PC and PM experiences occurred.

We reasoned that if the relative decreases in geomagnetic activity on the days of T-C experiences were strong, the effect should be evident if we simply compared the differences in aa values between the days of the experiences and the months in which they occurred. Consequently the absolute aa value of the day of each experience was subtracted from the mean monthly value. The means and standard errors for these differences for each class of experiences were: T-C ($-6.8+0.9$), PC ($+3.4+2.0$), and PM ($5.6+1.8$). One-way analyses of variance indicated a highly significant ($F(2,377)=17.82$, $p<.001$) difference

between the groups. A posteriori Scheffe's set at $p < .05$ indicated that the effect was due solely to the relative decrease in geomagnetic activity during T-C experiences compared to both the PC and PM experiences that did not differ from each other. Calculations of relative changes for each case (key day aa value minus the monthly mean) divided by the monthly mean and multiplied by 100)) demonstrated values of $-32 \pm 4.1\%$, $14.4 \pm 9.4\%$, and $28.2 \pm 5\%$ for the three classes, respectively ($F = 21.36$, $p < .001$).

To determine the strength of the repeated measure (daily aa values) differences between days for the classes of experiences separately, both parametric and non-parametric repeated analyses were completed. The T-C cases demonstrated highly significant ($p < .001$) repeated measure differences ($F = 4.36$, $df = 6.792$; $\chi^2 = 34.33$, $df = 6$); A posteriori tests indicated that only the day of the experiences was significantly different than the other days. For the PM cases, a significant repeated measure effect also occurred ($F(6,834) = 5.70$, $p < .001$; $\chi^2 = 30.32$, $df = 6$, $p < .001$). A posteriori (contrast) correlated t-tests demonstrated that for apparitional experiences, the day of the experience was significantly more active relative to two to three days before the experience ($2.70 < t_s < 3.75$, $df = 139$). There were no significant ($p > .05$) repeated measure differences for the precognition experiences ($\chi^2 = 6.13$, $df = 6$; $F = 1.76$, $df = 6,734$).

Further tests were completed to determine the internal consistency and cross-reliability of the results. These analyses were completed as log 10 transformations of the aa values in order to reduce the possible distortions from extreme outlier values. The first step was to determine the internal reliability of the most significant effect: the marked, decreased geomagnetic activity on the days of T-C experiences compared to the days before and afterwards. As shown in Figure 2A, the two replications are almost identical. The experiences occurred when the geomagnetic activity became suddenly quieter compared to the days before and afterwards.

Cross-reliability with other analyses are shown in Figure 2B. Here the geomagnetic activity on the days of, the three days before and the 3 days after the T-C experiences are shown for the 17 new cases that contained specific dates from the Stevenson (1970) collection and for the 78 major cases that contained specific dates (between the years 1868 to 1885) from the Gurney, Myers and Podmore (1886) series. Monthly and yearly aa values for each of these collections are also displayed. As can be seen, in all three studies, the T-C experiences occurred on days when the geomagnetic activity became suddenly quieter compared to the days before and afterwards. In addition, the days of the T-C experiences were also quieter than the average monthly or yearly aa values. These differences

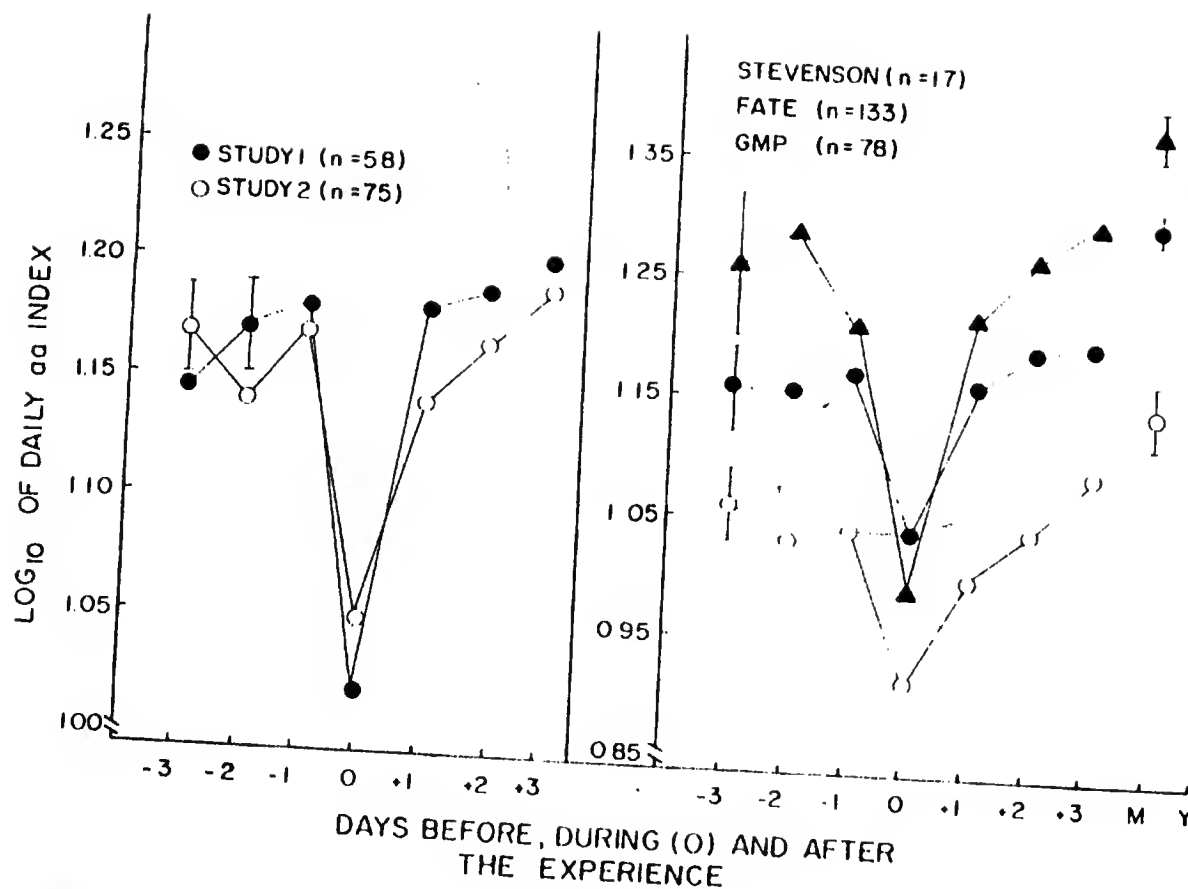


Figure 2: A) Log (base 10) transformations of the mean aa values for the three days before, three days after and the days of subjective telepathic experiences for replication 1 (n=57) and replication 2 (n=75). B) Log transformations of the mean aa values for the days during, before and after telepathic experiences from the Stevenson, present and Gurney, Myers and Podmore (GPM) series; the GPM series occurred between the years 1868 and 1885. Means for the log transformation of the aa values for the months (M) and years (Y) in which the experiences occurred are shown for each data base. Vertical lines indicate ± 1 standard error of the mean.

were highly statistically significant (Persinger, 1985a; Persinger, 1986a).

Because the chi-square analyses of T-C and precognitive cases indicated that more T-C cases involved putative agents who were dying compared to crises/sickness, MANOVA were completed for the seven days as function of the two classes of experiences (PC vs T-C) and whether the agent was dying or ill/in crisis). There was no significant difference between the condition of the agent ($F(1,222)=1.80$; $p>.05$) or class by agent interaction ($F<1$). Again, there was a highly significant main difference ($F(1,222)=11.74$; $p=.001$) between the two classes of experiences as well as the class by day interaction ($F(6,1332)=2.88$, $p=.009$).

Four modes of experiences had been designated in this study: impression/feeling, image, dream, and apparitions. To determine if the modes of the T-C experiences were differentially associated with the aa index of geomagnetic activity, MANOVA was completed for the seven days (key day +3 days) and the mode factor (four levels). There was a significant ($p=.002$) mode difference ($F=5.06$, $df=3,129$) and not surprisingly highly significant ($F=4.60$; $df=6,774$; $p<.001$) differences between daily aa values; there was no significant mode by day interaction. The day differences were due solely to the relative decrease in geomagnetic activity on the day of the T-C experiences (regardless of mode) compared to the days before or afterwards. The significant effect ($K-W \chi^2=12.40$, $p=.006$) between modes was due primarily to the higher overall geomagnetic activity during the week in which T-C experiences involving dreams occurred relative to those involving apparitional displays. We wondered whether or not T-C cases that contained the specific hour of the experience might demonstrate a more enhanced geomagnetic effect than those that referred to only the date or to a day vs night dichotomy. These results were interesting in light of the hypothesis that the decreased geomagnetic activity might facilitate the memory of the T-C experiences rather than their occurrence (D. Scott Rogo, personal communication). MANOVA demonstrated no significant difference between cases with different temporal specificity ($F<1$).

DISCUSSION

The results of this study replicate and extend the conclusions of other analyses. Quite clearly, subjective T-C experiences concerning death, crisis or unexpected illness have tended to occur when the geomagnetic activity was less than the days before or after the experiences. The V-shaped relationship of the geomagnetic activity during the period of the T-C experiences from FATE is similar in both direction and magnitude to two previous studies (Persinger, 1985a; 1986). Like these studies, the weeks and the days of the experiences from the FATE collection were quieter than the months or the years in which the experiences occurred (although the latter two were not different from each other). This suggests that the geomagnetic factor involved with T-C experiences exists in the order of days rather than months or years.

The major additional feature of the present study is the direct comparisons of three major classes of subjective psi experiences: T-C, precognition (PC), and postmortem (PM) phenomena. The latter two types of experiences were used as source (FATE) and case controls. PC and PM reports were source controls because they originated within the same potential editorial and selection biases as the T-C class. Reports of PC and PM experiences were case controls because they involved similar themes (death or crisis), hours and months of occurrence and gender proportions. Neither the PC nor the PM experiences demonstrated the geomagnetic pattern that was displayed by the T-C experiences.

Although the geomagnetic patterns around the days of the T-C, PC, and PM experiences differed markedly, there may be some global geomagnetic factor in the latter two classes. The most obvious possibility occurs with the PM experiences. Both parametric and nonparametric analyses indicated that PM experiences (which were primarily postmortem apparitions) occurred during periods when the geomagnetic activity was increasing; the days of the experiences were in fact significantly more active than the two to three days before the experiences. However, this elevated activity was not exceptional because there were no differences between these days and the monthly or yearly averages. This means that the PM experiences were more likely to have occurred when geomagnetic activity increased following a lull (quiet period) in geomagnetic activity.

The significance of this pattern is not clear. It may reflect as suggested by D. Scott Rogo (private communication) and E. Staton Maxey (private communication) that more people die during periods of increased geomagnetic activity. Because more than half of the

numbers of PM experiences occur within 3 days (Persinger, 1974a) of the empirical event (the death), these phenomena would simply be more frequent because deaths are more frequent. Indeed there is some evidence that increased incidence of myocardial infarction (Malin & Srivastava, 1979) and crisis/accident-related deaths (Persinger, 1983; Persinger & Nolan, 1984) may occur during increases in geomagnetic activity. This explanation assumes that the PM experiences are independent of geomagnetic activity and that the importance of this global factor is to simply increase the incidence of mortality or crises.

An alternative explanation is that enhanced geomagnetic activity actually contributes to the PM experiences. Several studies suggest that the electrical lability of the human brain may be influenced by some factor associated with geomagnetic activity. Rajaram and Mitra (1981) have shown that epileptic seizures occur more frequently during periods of increased geomagnetic activity; the pattern is obvious for both monthly analyses and during special (eclipse) conditions. The most frequent type of epilepsy in the adult population is temporal lobe or complex partial forms. Even in normal subjects, small microseizures are particularly likely during sleep, especially during rapid eye movements (REM) because of the intimate role of the hippocampus in the dream process.

Several empirical studies (Hess, Urech, & Wieser, 1982) involving depth electrical recordings indicate that the temporal lobe is particularly labile during dream periods and hence may become susceptible to environmental factors (Persinger, 1985b); day-night differences in the susceptibility of rodents to magnetic fields are well documented (see Kavaliers & Ossenkopp, 1985, for latest references). It is interesting that the hourly incidence of temporal lobe epileptic seizures is very similar to the occurrence of subjective spontaneous psi experiences. This pattern is evident even for the hourly occurrence of epileptic seizures (Spratling, 1904) that occurred during the last century, before the introduction of modern anti-convulsant drugs. One factor that is known to exacerbate temporal lobe instability are the corticosteroids and ACTH levels of the blood (Stevens, 1982). They are elevated during periods of stress, such as following the death of a family member or friend.

The variance of the daily aa values for the PC experiences was conspicuously and statistically higher than for the T-C and PM experiences. One initial explanation is that the label of precognitive experiences contains phenomena of heterogeneous sources. We also suspect (D. Lewicki & M. Persinger, unpublished data) that some accommodation must be made for the geomagnetic activity on the day of the experience compared to the day of the event. This is an important consideration and will be used to test

the hypothesis that PC experiences tend to occur when the geomagnetic activity is similar to what the activity will be on the day of the event. This effect would support a more traditional (temporal dimensional) interpretation of PC experiences.

The general trend of the slope in geomagnetic activity over days for PC experiences is still positive. This may support a second hypothesis that PC experiences tend to occur during slow, gradual increases in geomagnetic activity. These changes in activity could have become a learned cue (Persinger, 1979) through processes that facilitate unusual associations between subtle and overt environmental events. The processes would be due to the deepened and widened affect of the experiences because of their enhanced temporal lobe lability (Persinger, 1985b; Persinger & Roll, 1985).

Regardless of the interpretation of these patterns, the results indicate that the T-C geomagnetic relationship is not likely to be an artifact of either general psi "experiences" or reporting. Most of the experiences occurred long before the geomagnetic hypothesis was developed. In addition, the FATE cases are remarkably similar in general characteristics to the cases of more accepted data basis. The classic argument that FATE readers (or publishers) simply reiterated traditional T-C experiences is not supported. The critical data in the present study were the dates of the experiences. Geomagnetic activity on the days of T-C experiences was similar to that of the days of T-C experiences from other sources. These dates were not an experiential artifact since both PM and PC experiences did not demonstrate the pattern.

The next step is to determine the mechanism/s. Living systems can respond to geomagnetic variations of the magnitude that were involved in the present study. As reviewed by Ossenkopp and Barbeito (1978), homing capacity of pigeons is adversely affected by increased geomagnetic activity; quiet geomagnetic periods facilitate homing and probably migration behaviors. One hypothesis is that sudden, enhanced geomagnetic activity interferes with subtle natural electromagnetic phenomena that act as both directional and informational sources. That sudden enhancement of natural electromagnetic noise can interfere with communication between members of a species is well documented. Fish that communicate by interorganismic emission of ELF and VLF electric fields demonstrate marked deterioration in social communication and behaviors during local thunderstorms; presumably the sferics generated by the local storms masks the subtle organismic signals.

There is strong but not conclusive evidence that human beings may respond to geomagnetic variations or to the

stimuli generated by them (Persinger, 1974). A recent study by Subrahmanyam et al. (1985) has suggested that human beings can respond to slow electromagnetic variations that are similar in magnitude (5 or 50 gamma) to the continuous pulsations (Pc) of the geomagnetic field. They found discriminable changes in both electroencephalographic and subjective experiences when field frequencies between 0.01 Hz and 20 Hz were presented; maximum effects were noted with 0.01 Hz and 0.1 Hz fields. Of particular interest was the enhanced effect of these exposures when the volunteers were facing or lying north compared to the other three major directions. Similar patterns were found with non-human animals.

If this effect is replicated then two important and perhaps crucial conclusions are relevant for psi research. First, human beings can respond, both at subjective and objective neurobehavioral levels, to natural-intensity electromagnetic fields. Secondly, human beings respond to frequencies (or more appropriately, periods) that are commonly associated with geomagnetic fluctuations. They may occur for hours to days (and sometimes weeks) with periods ranging from a few seconds to several tens of minutes.

There is a potentially rich source of signals that are correlated with geomagnetic activity or that occur within these low frequency ranges (Campbell, 1967). In addition to the traditional ELF fields that are generated within the ionosphere-earth cavity, there are ULF (ultra low frequency) stimuli. Many of them occur as continuous pulsations (Pc). For example, Pc 1 variations have defined periods of 45-100 sec (0.01 Hz) and 150 to 600 sec, respectively. Whereas the typical amplitude values of Pc 1 are in the order of 1 gamma, the values for Pc 4 and Pc 5 are 10 and 100 gamma, respectively.

We expect that psi experiences, like other behaviors, should be influenced by the subtle, complex stimuli within the environment. The sensitivity of the living system and the complexity of these stimuli are just now becoming apparent. Even if one assumes that psi potential or experiences are homogeneous in time and space, the role of the human being as the neurobehavioral detection system cannot be ignored. Whereas the occurrence of psi may be geomagnetic field independent, the results of the present study suggest that at least the detection of psi stimuli is affected by the geomagnetic condition.

REFERENCES

- CAMPBELL, W.H. "Geomagnetic Pulsations." In S. Matsushita and W.H. Campbell (Eds.), Physics of Geomagnetic Phenomena Vol. II. New York: Academic Press, 1967, Pp. 821-909.
- HESS, R., URECH, E., and WIESER, H.G. "Arousal Patterns in Depth Recording from Epileptics." In M.B. Sterman, M.N. Shouse, and P. Passouant (Eds.), Sleep and Epilepsy. New York: Academic Press, 1982, Pp. 209-218.
- KAVALIERS, M. and OSSENKOPP, K.-P. "Tolerance to Morphine-Induced Analgesia in Mice: Magnetic Fields Function as Environmental Specific Cues and Reduce Tolerance Development." Life Sciences, 1985 (in press).
- MALIN, S.R.C. and SRIVASTAVA, B.J. "Correlation between Heart Attacks and Magnetic Activity." Nature, Vol. 277, 1979, 646-648.
- MAYAUD, P.N. "A Hundred Year Series of Geomagnetic Data 1868-1967." IAGA Bulletin, No. 33, 1973.
- OSSENKOPP, K.-P. and BARBEITO, R. "Bird Orientation and the Geomagnetic Field: A Review." Neuroscience and Biobehavioral Reviews, Vol. 2, 1978, 255-270.
- PERSINGER, M.A. The Paranormal: Part I: The Patterns. New York: M.S.S. Information, 1974. (a).
- PERSINGER, M.A. (Ed.). ELF and VLF Electromagnetic Field Effects. New York: Plenum Press, 1974. (b)
- PERSINGER, M.A. "ELF Field Mediation in Spontaneous PSI Events: Direct Information Transfer or Conditioned Elicitation?" Psychoenergetic Systems, Vol. 3, 1979, 155-169.
- PERSINGER, M.A. "The Effects of Transient and Intense Geomagnetic or Related Global Perturbations upon Human Group Behavior." In J.B. Calhoun (Ed.), Environment and Population: Problems of Adaptation. New York: Praeger, 1983, Pp. 28-30.
- PERSINGER, M.A. "Geophysical Variables and Behavior: XXX. Intense Paranormal Experiences Occur During Days of Quiet, Global, Geomagnetic Activity." Perceptual and Motor Skills, Vol. 61, 1985, 320-322. (a)

- PERSINGER, M.A. "Subjective Telepathic Experiences: Geomagnetic Activity and the ELF Hypothesis: Part II. Stimulus Features and Neural Detection." PSI Research, Vol. 4(2), 1985, 4-23. (b)
- PERSINGER, M.A. "Spontaneous Telepathic Experiences from the Gurney, Myers and Podmore Collection Occurred on Days that Displayed Low Geomagnetic Activity." Journal of the American Society for Psychical Research, 1986 (in press). (a)
- PERSINGER, M.A. and NOLAN, M. "Geophysical Variables and Behavior: XX. Weekly Numbers of Mining Accidents and the Weather Matrix: The Importance of Geomagnetic Variation and Barometric Pressure." Perceptual and Motor Skills, Vol. 59, 1984, 719-722.
- PERSINGER, M.A. and ROLL, W.G. "The Temporal Lobe Factor in PSI Phenomena." In Proceedings of the Parapsychological Association 28th Annual Convention, 12-16 August, 1985, Tufts University, Medford, Mass., Vol. 1, 1985, 439-449.
- RAJARAM, M. and MITRA, S. "Correlations between Convulsive Seizures and Geomagnetic Activity." Neuroscience Letters, Vol. 24, 1981, 187-191.
- SCHAUT, G.B. and PERSINGER, M.A. "Geophysical Variables and Behavior: XXXI. Global Geomagnetic Activity During Spontaneous Paranormal Experiences: A Replication." Perceptual and Motor Skills, Vol. 61, 1985, 412-414. (a)
- SCHAUT, G.B. and PERSINGER, M.A. "Subjective Telepathic Experiences, Geomagnetic Activity and the ELF Hypothesis: Part I. Data Analysis." PSI Research, Vol. 4(1), 1985, 4-11. (b)
- SPRATLING, W.P. Epilepsy and its Treatment. Philadelphia: W.B. Saunders, 1904.
- STEVENS, J.R. "Sleep is for Seizures: A New Interpretation of the Role of Phasic Ocular Events in Sleep and Wakefulness." In M.B. Sterman and M.N. Shouse (Eds.), Sleep and Epilepsy. New York: Academic Press, 1982, Pp. 149-264.
- STEVENSON, I. "Telepathic Impressions: A Review and Report of Thirty-Five New Cases." Proceedings of the American Society for Psychical Research, Vol. 29, 1970, 1-193.
- SUBRAHMANYAM, S., SANKER NARAYAN, P. V., and SRINIVASAN, T.M. "Effect of Magnetic Micropulsations on the Biological Systems: A Bioenvironmental Study." International Journal of Biometeorology, Vol. 29(3), 1985, 293-305.

SRI International



*Final Report
Covering the Period 15 November 1983 to 15 December 1984*

December 1984

GEOPHYSICAL EFFECTS STUDY (U)

SRI Project 6600

Copy No. **11**.....

This document consists of 58 pages.

UNCLASSIFIED

CONTENTS

LIST OF ILLUSTRATIONS.	v
LIST OF TABLES	v
I OBJECTIVE	1
II EXECUTIVE SUMMARY	3
III INTRODUCTION.	5
A. General.	5
B. Report Organization.	6
IV METHOD OF APPROACH.	7
A. Literature Search.	7
B. Data Acquisition	7
1. ELF Measurements.	7
a. Introduction	7
b. Los Altos Site (TRI)	8
c. SRI Site	10
2. Satellite Downlink Geophysical Data-Acquisition System.	11
3. Data-Acquisition System	13
4. Magnetic Data Tapes from NOAA	14
C. Data Analysis.	15
1. Integrated Data-Analysis System	15
2. Summary of Data Analyzed.	16
3. Summary of Data Unanalyzed.	17
D. Analysis Techniques and Data Preparation	18
1. Techniques Used	18
2. Description of Techniques	19
a. Epoch Analysis	19
b. Time-Lag Regression.	20
3. Description of Analysis Methods	20
a. RV Data.	20
b. Geophysical Data	21

UNCLASSIFIED

UNCLASSIFIED

V	RESULTS.	23
A.	Results of Geophysical Analysis	23
1.	Introduction	23
2.	Solar Flux	23
3.	Sunspot Number	24
4.	Solar Flares	25
5.	Magnetic Indices	28
6.	SIDs	30
B.	Results Pertaining to ELF	31
1.	Introduction	31
2.	Intercomparison of ELF System.	32
3.	ELF/RV Comparison.	32
VI	EVALUATION AND RECOMMENDATIONS	35
VII	SUMMARY.	37
	REFERENCES.	41
	BIBLIOGRAPHY.	43

UNCLASSIFIED

UNCLASSIFIED

ILLUSTRATIONS

1	ELF Data-Acquisition System.	9
2	Real-Time Geophysical Data Acquisition via Westar IV Downlink	12
3	Real-Time Geophysical Data-Acquisition System.	14
4	Geophysical/Performance Data-Analysis System	15

TABLES

1	Geophysical Data Bases	6
2	Description of RV Data	21

UNCLASSIFIED

I OBJECTIVE (U)

(U) The objective of this effort is to investigate the possible effects of ambient geophysical/extremely low-frequency electromagnetic factors on remote viewing (RV)* performance

* (U) RV (remote viewing) is the acquisition and description, by mental means, of information blocked from ordinary perception by distance or shielding.

II EXECUTIVE SUMMARY (U)

SRI International was tasked to investigate a potential correlation between remote viewing (RV) performance and ambient geophysical/extremely-low-frequency electromagnetic (ELF) activity. The possibility of such correlation is indicated, for example, by studies showing psychophysiological effects^{1, 2*} and behavioral changes^{3, 4} associated with ELF electromagnetic fields. The geophysical variables of interest include such factors as ELF intensity/fluctuations, ionospheric conditions, geomagnetic indices, sunspot number, and solar-flare characteristics. The questions addressed in this program are

- Do geophysical/performance correlations exist such that measurement of the ambient geophysical variables could be used as an indicator of expected performance?
- If so, can optimum performance windows be identified?

(U) The structure of the program to investigate the above issues consists of

- A literature search
- Real-time ELF measurements
 - SRI International (Menlo Park, California location)
 - Time Research Institute (Los Altos, California field station).
- Real-time geophysical data acquisition via the National Oceanic and Atmospheric Administration (NOAA) Westar IV satellite downlink.
- Computer correlation studies of RV performance versus variables of interest.

(U) In this report, we present findings from our over-six-year analysis of scored RV sessions--as they relate to geophysical environmental

* (U) References are listed at the end of this report.

UNCLASSIFIED

Table 1

(U) GEOPHYSICAL DATA BASES

- Solar terrestrial
 - Geomagnetic--ground-measured indices A_p , sum of K_p , C_p , C_9
 - Solar flux (MHz): 15,400, 8,800, 4,995, 2,800, 2,695, 1,415, 606, 410, 245
 - Sunspot number
 - Solar flares
- Ionospheric measurements
 - Sudden ionospheric disturbances (SID)
 - Sudden enhancements of signal strength (SES)
- ULF/ELF
 - 19 frequencies (from 1 to 30 Hz)

UNCLASSIFIED

B. (U) Report Organization

(U) The remainder of this report is organized to include: Method of Approach (Section IV), Results (V), Evaluation and Recommendations (VI), and Summary (VII). The Method of Approach section contains descriptions of the project tasks, which include Time Research Institute's data acquisition systems, other sources of geophysical data acquisition, lists of geophysical data that have been analyzed, and the analysis technique employed. The Results section contains the findings from the comparisons of both the ELF data sets among themselves, and the comparisons of RV performance data with the ELF and other geophysical data. The Evaluation and Recommendations section summarizes the findings and possible applications of our research, and identifies areas where further investigation is needed. The Summary section summarizes the overall effort and its implications with regard to RV performance enhancement and countermeasures development.

UNCLASSIFIED

UNCLASSIFIED

III INTRODUCTION (U)

A. (U) General

(U) In order to accomplish the goals listed in the Executive Summary, this program was designed to be a joint effort between SRI International and Time Research Institute (TRI) of Los Altos, California, with SRI as the prime contractor. Time Research Institute is a research organization that specializes in temporal analysis of geophysical variables and their potential correlation with phenomena of interest, such as weather patterns, earthquakes, and the like.

(U) Time Research Institute was responsible for establishing the appropriate hardware and software systems for collecting and analyzing data on environmental conditions and their correlation with RV performance. The purpose of the correlation study was to determine whether RV performance is enhanced or degraded by measurable changes occurring in the geophysical (including solar-terrestrial) environments. The specific geophysical data bases examined in this effort are given in Table 1.

(U) Should correlations between geophysical variables and RV performance be rigorously established over time, the application potential of the effort is twofold:

- Time periods in which enhanced RV performance might be expected could be identified, resulting in increased quality and accuracy of information obtained through such channels; similarly, time periods in which degraded RV performance might be expected could be avoided. Thus, optimum performance windows would be identified.
- An increased understanding of the types of environmental changes that correlate with RV performance could provide clues as to the mechanisms involved in RV functioning. Such knowledge would lead to a more focussed research on factors that could enhance RV performance, and would also provide information critical to the development of defensive countermeasures against RV.

UNCLASSIFIED

UNCLASSIFIED

IV METHOD OF APPROACH (U)

A. (U) Literature Search

(U) A literature search into the areas of known effects of static and low-frequency magnetic and electric fields on biological processes was carried out. Much of the literature available in the ELF range dealt with the effects (or lack thereof) of 60-Hz fields. Papers were sought that described both the gross effects of these fields and the mechanisms by which they could affect biological organisms. Some reports describing higher electromagnetic frequencies (e.g., microwave) were also included for their inferential value. (A bibliography appears as an appendix to this report.)

B. (U) Data Acquisition1. (U) ELF Measurementsa. (U) Introduction

(U) Although the ELF range (3 to 300 Hz) has been studied in some detail, many unknowns remain. Although it is known that extremely-low frequencies generated by geophysical means (e.g., electrical-storm activity) tend to distribute themselves globally, little information is available on the variation of the ELF environment from location to location. Therefore, local variations may exist that are caused by both man-made sources, and by the geological structure of the area. In the San Francisco Bay Area, man-made sources that generate ELF on a local scale include motors, telephone lines, power lines, and electrical subways [Bay Area Rapid Transit (BART)]; it needed to be determined whether the emission from such sources constitutes a significant contribution to the omnipresent global ELF field.

(U) In order to address the above issue, two ELF monitoring stations were set up--one at SRI Menlo Park (the RV laboratory), the other

UNCLASSIFIED

UNCLASSIFIED

(U)

at the TRI field station, 17 km distant. It was anticipated that the SRI environment might be an electrically "noisy" one due to the large amount of electrical and electronics activity in the area--a hypothesis that was verified. With the requirement that two ELF monitoring sites be implemented for the program, it was decided that the two systems would be made identical. In this way, differences between the systems would be minimized, thus reducing the opportunity for artifactual differences between the outputs.

b. (U) Los Altos Site (TRI)

(U) Since May 1982, TRI has been operating a prototype ELF monitoring site in Los Altos, where data have been collected twice daily for the purpose of correlating ELF disturbances against various phenomena of interest. In this period, analysis techniques were developed that were directly applicable to the present task.

(U) One of the first tasks was the upgrading of the Los Altos ELF monitoring site to provide coverage during power interrupts. Details of this effort can be found in an interim report prepared by SRI International.⁵

(U) The second task was the development of an upgraded high-data-rate ELF system (in duplicate) to be installed at the TRI and the SRI sites. Figure 1 is a block diagram of the basic upgraded ELF data-rate ELF system (in duplicate) to be installed at the TRI and the SRI sites. Figure 1 is a block diagram of the basic upgraded ELF data-acquisition system. The ELF signal is collected by an antenna, amplified, and then digitized by an analog-to-digital (A/D) converter so that the signal can be input into a computer for the purpose of analysis.

(U) The antenna is a "bioantenna" (a Live Oak tree). This procedure was based on one recommended by the Radioscience Laboratory at Stanford University. The detected signal is the voltage measured across a pair of electrodes implanted vertically approximately six feet apart along the lower tree trunk. A full description of the method is given in Reference 6, a reprint of which is included in the interim report mentioned above.

UNCLASSIFIED

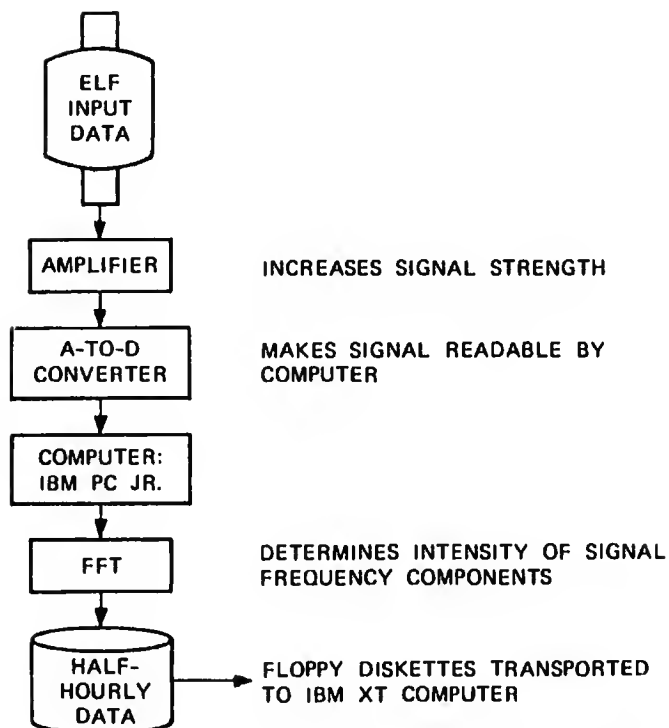
UNCLASSIFIED

FIGURE 1 (U) ELF DATA-ACQUISITION SYSTEM

(U) The system is configured around an IBM PC jr. micro-processor, which is not only cost-effective, but is compatible with an IBM XT computer where much of the ELF analysis is done. Data transfer and reduction is simple; floppy diskettes are transferable from one computer to the other.

(U) Software has been developed for the IBM PC jr. that reads input data from the A/D converter, performs a fast-Fourier transform (FFT), then outputs seven data files of 19 frequencies each to a floppy diskette. The system operates on universal time (UT), writing records of the means and standard deviations of 19 frequencies in the 1-to-30-Hz range--each half hour, half-UT day, UT day, and half Pacific-time day. This system is far superior in speed and accuracy to the prototype system. In the upgraded system, approximately 318 ELF samples are recorded each half hour. By comparison, the prototype ELF system sampled and processed

UNCLASSIFIED

UNCLASSIFIED

(U)

the ELF environment only 20 times in an equivalent period, for a total of about 420 samples in an entire day.

(U) The overall system calibration is as follows. A combined amplification of the signal is 1000X; the signal is amplified 10X in a preamplifier located at the antenna, and 100X in a main amplifier. This presents a maximum 5-V peak-to-peak signal at the A/D converter. The A/D converter operates on an input voltage in the range of 0 to 5.12 V. The output digital value is in the range of 0 to 256. Thus, each count on the digital output represents 20 mV at the input. The FFT algorithm converts the digital sample inputs into coefficients that are proportional to this input. A value of 100 counts at the frequency 1.6 Hz, for example, would be interpreted as indicating that the 1.6-Hz component of the measured signal has a voltage amplitude of 2 V at input to the A/D converter. The input signal having been amplified 1000X, this represents a 2-mV component at the antenna input.

(U) Further details concerning measurement and calibration, including special requirements in amplifier design, isolation circuit diagrams, and so forth, are available in the TRI subcontractor final report to SRI International.⁷

(U) The first new ELF data acquisition began five months after the start of the TRI subcontract with SRI International. TRI was able to initiate the first generation of the upgraded system in only five months in spite of delays in ordering specialized components for the new systems, and delays in the fabrication of the circuitry of the systems themselves. Further delays were experienced in ordering additional specialized components and in fabrication of a needed second-generation preamplifier. Final data acquisition was begun seven months after initiation of the subcontract.

c. (U) SRI Site

(U) The SRI ELF system was implemented after extensive testing of the upgraded system at Los Altos. A second-generation

UNCLASSIFIED

UNCLASSIFIED

(U)

preamplifier/amplifier was installed in August 1984. Some differences were immediately seen between the SRI and the TRI Los Altos stations. The dc output of the oak tree that was selected to be the ELF antenna at SRI was twice the level of the oak at Los Altos. It is a larger tree, and its dc potential with equivalent electrode spacing (300 mV) was twice that of the Los Altos site. This caused the amplified dc measurement component to exceed the limits of the A/D converter. Hence, no dc measurements are presently being made at the SRI site.

(U) As expected, the SRI location was found to be in an electrically-noisier area than the Los Altos station. The 60-Hz signal from power lines (and the like) at SRI was strong enough to approach the limits of the A/D converter when the amplification was adequate for ELF signal detection. The system software has been designed to omit data that exceed the A/D converter limits, then record the fact. To date, the system has operated successfully without losing data because limits were exceeded. There was a concern, however, that some large-amplitude ELF anomalies could cause the limits of the amplifier and the A/D converter to be exceeded, in which case data would be lost. A third-generation preamplifier has been designed, which contains the attributes of previous preamplifiers, but, a 60-Hz filter has been specially designed and added to the circuitry. This enables greater amplification of the ELF components of the signal without risk of exceeding the input limits to the A/D converter. The third-generation preamplifier is presently being fabricated and will be used in follow-on work.

2. (U) Satellite Downlink Geophysical Data-Acquisition System

(U) A near-real time satellite downlink system for solar-terrestrial data has recently become available from the National Oceanic and Atmospheric Administration (NOAA). With this unit, it is possible to provide immediate feedback and/or analysis in conjunction with RV sessions. (Normally, there are long delays in procuring solar-terrestrial data; without the downlink, delays of 10 days to 6 months are standard.)

UNCLASSIFIED

UNCLASSIFIED

(U)

By means of software developed at TRI,* the downlink system provides for accumulation of a detailed data base directly on computer diskettes.

(U) A satellite controller and a disk antenna for the downlink system were ordered and installed at the Los Altos site early in the project. The downlink system is configured around an IBM PC jr. micro-processor, as shown in Figure 2. Data transfer is accomplished by means

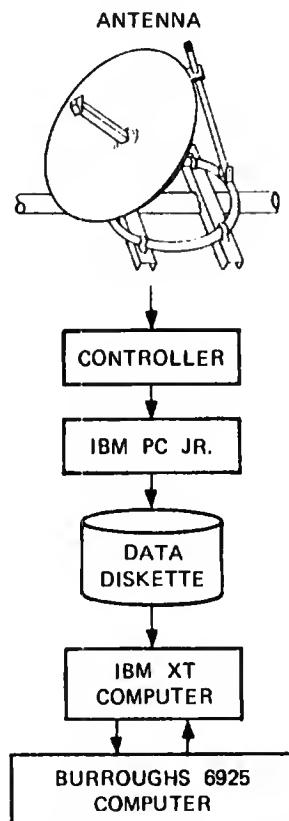


FIGURE 2 (U) REAL-TIME GEOPHYSICAL DATA ACQUISITION VIA WESTAR IV DOWNLINK

* (U) The format of the NOAA downlink is oriented toward text transmission, and is not well suited to data-base acquisition. Software for recording the data is not provided by NOAA.

UNCLASSIFIED

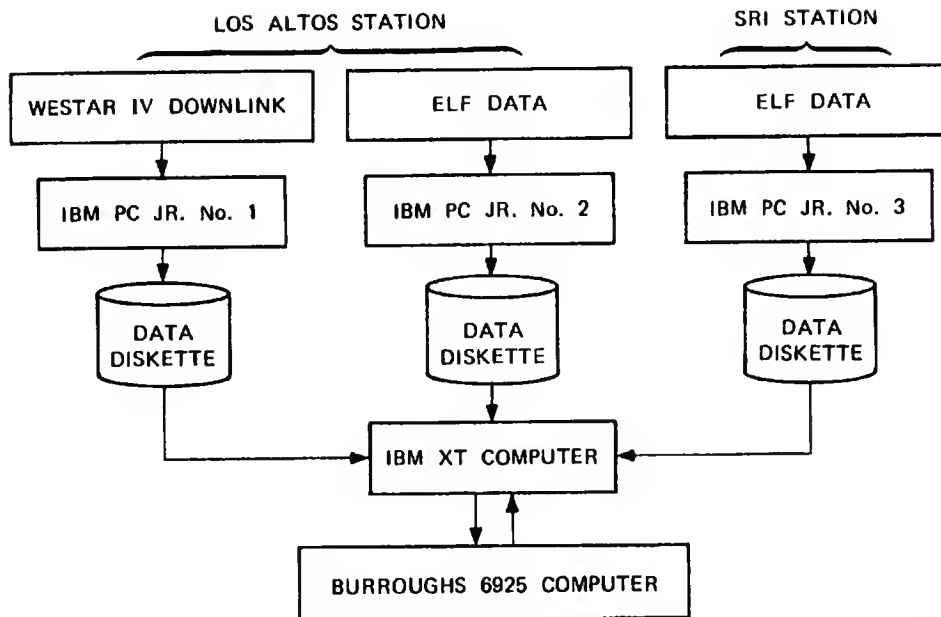
UNCLASSIFIED

FIGURE 3 (U) REAL-TIME GEOPHYSICAL DATA-ACQUISITION SYSTEM

(U)

Burroughs 6925 computer for use in that analysis requiring high-speed or large memory capacity.

4. (U) Magnetic Data Tapes from NOAA

(U) In addition to the above data collection from ELF and down-link systems, archived solar-geophysical data of interest were selected. Two criteria in this selection were used: first, the theoretical likelihood the data might correlate with RV performance, and second, its availability--based on appearance in the regularly published NOAA bulletin "Solar-Geophysical Data Prompt Reports." The data were ordered from the National Environmental Satellite Data and Information Service at the National Geophysical Data Center in Boulder, Colorado. Of 12 data sets requested, only 7 could be supplied; several of the data sets, although published in the "Solar-Geophysical Data Prompt Reports," were not available on magnetic tape.

UNCLASSIFIED

UNCLASSIFIED

(U)

similar to that of the ELF system; that is, by transport of floppy diskettes from the downlink computer to the larger IBM XT analysis computer.

(U) The geophysical data downlink began data acquisition in the third month of the TRI subcontract. The initial data were in the form of a direct recording, which was received from the satellite, on to computer diskettes. The intent was to acquire as long a data base as possible by acquiring raw data at the same time we were developing the software to reduce it. The kernel around which the software was written was a BASIC program from NOAA. The original NOAA software supplied the text data (received from the downlink) in the form of tabular summaries on a monitor. This software did not have the capability to store or record data to any medium. TRI made extensive modifications so that the numerical data could be stored onto computer diskettes for inclusion into a data base. The software is capable of averaging and storing about 20 geophysical variables at multiples of five-min intervals (e.g., 10- or 25-min averages), which were defined at the time the program was run. It writes six separate data files to the diskette.

(U) Initially, the program was set to average and write the data at five-min intervals. After a few months of operation, it was found that the disk drive of the PC jr. tended to fail with such frequent operation. The time-averaging span was changed to half-hourly intervals to save wear on the disk drive. This is the same time increment used for the ELF data. The two systems now operate in synchronization.

3. (U) Data-Acquisition System

(U) The three systems described above (the Los Altos and the SRI ELF stations, and the Geophysical Data downlink), operate in concert, forming the Geophysical Data-Acquisition System. Figure 3 shows the system components and their relationship to one another. Three IBM PC jrs. operate 24 hours a day collecting ELF and downlink solar-terrestrial data. Data from these microcomputers are processed in the IBM XT to form continuous data bases. Copies of these data bases are sent to the

UNCLASSIFIED

UNCLASSIFIEDC. (U) Data Analysis1. (U) Integrated Data-Analysis System

(U) Statistical analyses are performed on the data bases described above, preferably on the IBM XT for cost effectiveness. Figure 4 shows the Geophysical Data/Performance Analysis System. Data from all direct geophysical sources are input into the IBM XT, where they are preprocessed into continuous data bases stored on floppy diskettes. Some data extractions are also performed at this time. The data bases and the extracted data are read into the Burroughs 6925 computer. The data tapes from NOAA are also read directly into the Burroughs computer. The NOAA data files are long (16,000 records per year is common), and require the high speed of the mainframe computer (and our existing software residing there) to correct, process, and extract the geophysical data in usable form. NOAA data were further processed to extract subsets of data of

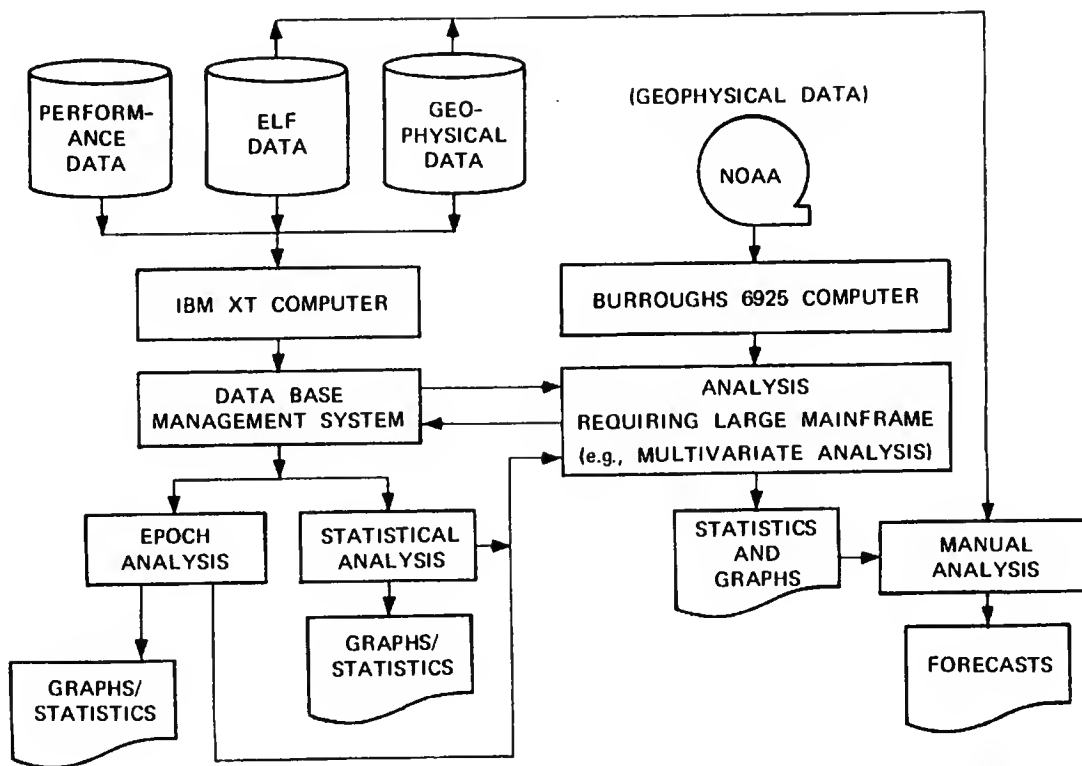


FIGURE 4 (U) GEOPHYSICAL/PERFORMANCE DATA-ANALYSIS SYSTEM

UNCLASSIFIED

UNCLASSIFIED

(U)

interest, and to summarize the daily number of occurrences of event-type data, e.g., solar flares (see analysis section below for details). These extracted and summarized data were down-loaded from the Burroughs by modem connection to the IBM XT, where statistical processing was performed.

2. (U) Summary of Data Analyzed

(U) Data were of two types: RV performance scores and geophysical. A detailed description of the analysis techniques appears in Section IV-D. In brief, the RV data were analyzed in five separate groups according to their generation in separate experimental series. These five groups were divided into highest- and lowest-score categories, and epoch analysis was performed on the eight subdivisions against each of the following geophysical variables:

- Geomagnetic indices:

A_p
Sum of K_p
C_p
C9

- Solar flux at the following frequencies:

15,400 MHz
8,800
4,995
2,800
2,695
1,415
606
410
245

- International Relative Sunspot numbers (Ri) or Zurich Sunspot numbers prior to 1981 (Rz).
- Sudden Ionospheric Disturbances partitioned by:
 - Sudden enhancement or decrease of LF atmospherics at approximately 27 kHz; further partitioned by the intensity of the disturbance.

UNCLASSIFIED

UNCLASSIFIED

(U)

- Solar Flares partitioned as follows:
 - All reported flares
 - Area of flares
 - Brilliance of flares
 - 10-deg segments of longitude
 - Flares larger than Sub-Brilliant (SB)
 - Area of flares
 - Brilliance of flares
 - 10-deg segments of longitude
- ELF Data:
 - 19 frequencies from 1 to 30 Hz.

3. (U) Summary of Data Unanalyzed

(U) Certain geophysical data were not analyzed for the following reasons:

- Magnetic Intensities at Satellite Altitudes, Solar Protons--
Although the Downlink system is operational, and the software functions well, there is a difficulty that is inherent to the Downlink system. The transmission error rate is exceedingly high; erroneous characters are transmitted frequently in the data, and would require hand editing--a time-consuming and labor-intensive task. Obtaining these data elsewhere was discussed with individuals at the SELDADS system, who were the data source. It was found that summaries of these data do not exist, and that the data are archived in a 3-s interval on magnetic tape. One month's data require an entire tape, at a cost of \$120 per tape. We would require about 20 of these tapes for a complete analysis of the RV data. Obtaining data by this means was impractical from the data-processing and tape-expense standpoints.
- Solar Wind--Only fragmentary time spans of these data were available from NOAA. It was explained that the antennas used to receive data from Pioneer XII and its predecessor satellites were redirected to receive signals from the Martian satellites.
- Radio Propagation Quality Indices--These data were not available on magnetic tape from NOAA.
- Stanford Mean Magnetic Field--These data were not available on magnetic tape from NOAA, however, partial analysis was

UNCLASSIFIED

UNCLASSIFIED

(U)

performed on data entered by hand at TRI. About half of the data were analyzed before software difficulties prevented completion.

- Auroral Electrojet, Equatorial Dst Values--Auroral electrojet data were not available for the entire time period. Existing data for Dst values were sent with an explanation that the Japanese were now in charge of acquisition of this data set, but had not submitted data since 1981. Dst values ended in December of 1983. Three of the RV data sets could have been analyzed, but format problems prevented it. Most of the NOAA data received on the tapes were in formats suitable for direct publication, with titles, headings, monthly averages, and comments occurring after each month's daily data. In some cases, the day or month was given only in the test heading. This format was unsuitable for computer data analysis, and extensive software had to be written to reorganize the data into a usable format. Although such software was written to extract data from many of the NOAA data sets, this one was bypassed because the data were incomplete.
- Cosmic Ray Indices--These data were sent by NOAA in a format that would have required extensive software development to extract daily values. Although daily values are published in the "Solar-Geophysical Data Prompt Reports," they are evidently not available on magnetic tape.

D. (U) Analysis Techniques and Data Preparation

1. (U) Techniques Used

(U) The analysis was performed on two computers: an IBM XT and a Burroughs 6925. All analyses that did not require the large memory and high speed of a mainframe were performed on the IBM XT, at a substantial cost savings. In particular, an epoch analysis program was translated from ALGOL to C for use on the XT. The C version for the XT has enhanced capabilities not available on the ALGOL version.

(U) Two statistical techniques were used in screening the data (1) epoch analysis, and (2) time-lag linear regression and correlation coefficients. The epoch analysis was performed primarily on the IBM XT machine; the time-lag regressions were done on the Burroughs. While the time-lag regressions allowed definitive statistical statements to be made,

UNCLASSIFIED

UNCLASSIFIED

(U)

execution of this program was generally very costly (up to \$150 per run), so such regressions were done sparingly.

2. (U) Description of Techniques

a. (U) Epoch Analysis

(U) The primary statistical program used to scan the data for possible relationships is called "epoch analysis." The purpose of epoch analysis is to detect time-lag relationships in noncontinuous, or nonscalar data sets of interest, such as "high-scoring viewing days." It will also show areas of nonexact time-lag relationships, where correlations will not (without further data manipulation such as running averages, and so forth). An overview of time periods that may relate to the data of interest is given in a quick and cost-effective way. Epoch analysis has been used here to indicate which time intervals will be appropriate to run time-lag regressions--a technique that is costly and frequently inaccurate if the timed relationships are approximate rather than exact.

(U) The epoch analysis technique compares events with other timed data sets (such as sunspot number) at intervals preceding and following the event. The program reads two files simultaneously. The first file is an event file, the second a data file. The program first reads an event, then scans the data temporally backward and forward in time around the event. This information is stored, a second event is read, and so forth. When all the events and surrounding data have been read, a printout is created that lists appropriate cross-correlation statistics between the event and data elements.

(U) As an example, the program calculates the average values of a variable, such as sunspot number, for discrete time intervals before or after a set of RV events of interest--say, high-scoring days. For all days, the technique determines the sunspot number one day prior to high-performance RV sessions (the events), the day of, the day after, and so forth. It will then calculate the average value for each day (e.g., -1, 0, +1), then tabulate and graph the results.

UNCLASSIFIED

UNCLASSIFIEDb. (U) Time-Lag Regression

(U) This is a standard regression analysis, which offsets the time base of the data in specified intervals. This program may be instructed to perform sets of regressions of many time lags at a time, even with data that are not continuous. Time lags are frequently encountered when analyzing solar-terrestrial data with respect to terrestrial events. For instance, approximately two to four days may elapse before magnetic storms resulting from solar flares are detected on earth. Assuming such mechanisms may also operate with respect to RV data, all geophysical correlations were carried out for a time-lag range of at least plus or minus five days.

3. (U) Description of Analysis Methodsa. (U) RV Data

(U) In order to determine whether RV performance correlates with geophysical activity, it is necessary to have access to RV data bases that have been quantified. Data bases that meet this criterion, both archival and those generated during the subcontract period, were made available to TRI for analysis.

(U) Four sets of RV data were analyzed initially; they constitute the primary data base.* Each data set is referred to by the year in which most of the data were gathered. Table 2 shows the name, number of samples, and begin- and end-date for each data set. The RV data were processed for the epoch analysis by selecting the dates of the highest and lowest scores or ratings for each data set.†

* (U) A fifth RV data base was examined near the end of the program, generally confirming the conclusions reached on the basis of the primary RV data base.

† (U) Selection was done by finding high and low scores in which the value range contained approximately one-third or less of the total data set. In most data sets, more than one session occurred on a given day-- frequently with different individuals. In some cases, two individuals had extremely high or low scores on a given day (there are comments later about individual variability). These data were left intact, e.g., if two individuals both scored high or low on the same day, those data were

UNCLASSIFIED

UNCLASSIFIED

Table 2

(U) DESCRIPTION OF RV DATA

Name	Sample Number	Begin Date	End Date	Comments
79	36	05/14/79	08/03/79	6 x 6 orientation
80	97	01/18/80	12/14/81	RVer I.S., Class B
81	48	07/30/81	10/21/81	Targeting
84 (II)	231	01/12/84	08/17/84	RV Training (II)
84 (I)	103	03/19/84	07/10/84	RV Training (I)

UNCLASSIFIED

b. (U) Geophysical Data

- (U) ELF Data--ELF data sets were prepared by concatenating the data from several diskettes into a single, long-term file for both the upgraded Los Altos and the SRI data. This was done for daily, half-daily, and half-hourly data.
- (U) NOAA Data--These data required extensive preprocessing and specialized software to be written. For example, two of the data sets, Sudden Ionospheric Disturbances (SID) and Solar Flares, contained multiple reports of the same event observed from different stations. Indices of location and magnitude of the event frequently do not agree from station to station. Software was written to eliminate duplicate reports by extracting the single largest report for each event. Extractions of single events were done when appropriate. Data files were constructed that contained the number or value of the events of interest for each calendar day, from 1 January 1978 until the end of the available data--usually 31 August 1984. The dates were checked for order and continuity. In event-oriented data files such as SID and Flares, events did not occur every day.

entered twice in the high or low data sets. If one individual scored extremely high, and another extremely low (on the same day), that day was entered in both the high and low data sets. The exception to this was the data set of RVer I.S., Class B sessions. Several sessions were carried out on a single day. To create the corresponding high and low data files, the mean score for each day was determined, and the high and low days were selected using the mean scores.

UNCLASSIFIED

UNCLASSIFIED

(U)

Records containing the appropriate null dates were inserted in these data files. Files were also prepared that were subsets of the event-type data files. Solar-flare data were cross-tabulated in 10-deg longitude segments by daily dates. Flares larger than Sub-Brilliant were cross-tabulated on a daily basis by area, brilliance, and longitude measurements. SIDs were extracted by LF Atmospheric and cross-tabulated on a daily basis by the intensity of the disturbance. The same was done for VLF Sudden Enhancements (SES).

UNCLASSIFIED

UNCLASSIFIED

V RESULTS (U)

A. (U) Results of Geophysical Analysis1. (U) Introduction

(U) For many years man has speculated that relationships exist between various biological functions and solar activity or its resulting geophysical activity. Some empirical observations on the quality of RV sessions during periods of known solar activity led to the idea that a screening of solar-geophysical variables for correlations might be fruitful. If, indeed, measurable geophysical disturbances affect RV performance, and these relationships could be defined, the reliability of RV-derived information could be determined by considering the geophysical environment at the times of RV sessions, and possibly enhanced by scheduling.

(U) This screening of geophysical variables in this report appears in the order of gross measurements to refined measurements, which may be closer to the actual mechanisms involved in influencing RV performance. Because of the fact that changes in most measurable geophysical data are initiated by solar activity, geophysical data sets co-vary. Hence, relationships were found in several data sets simultaneously. These correlations are most likely not due to cause and effect relationship between the covarying variables, but rather are the result of one or more of the geophysical processes that are driven by solar activity. Although correlations to noncausative variables may be useful for forecasting purposes, forecasts will be greatly enhanced when the correlations used are closest to the actual geophysical-biological mechanisms involved.

2. (U) Solar Flux

(U) The solar flux is a measurement of the electromagnetic output of the sun at several different frequencies in the megahertz range.

UNCLASSIFIED

UNCLASSIFIED

(U)

The measurement values are in units of $10^{-22} \text{ W m}^{-2} \text{ Hz}^{-3}$. These measurements are a gross indicator of the activity on the solar disk. Epoch analysis was performed for the high and the low scoring days of each of three RV data sets. (No solar-flux values were recorded for most of 1979 in the NOAA data, and the 84(I) data were not yet available when this analysis was performed.) The relationships found by epoch analysis in these data were generally unimpressive.

(U) Time lag correlations were run on two individuals from the 1981 experiment. Again, although certain correlations were found among the mass of data (some of them statistically significant), there was great variability between the individuals, and no definable pattern emerged.

3. (U) Sunspot Number

(U) Epoch analysis of RV versus sunspot number was performed. A low peak was found between 29 and 35 days prior to each of the four sets of high scoring sessions,* and a high peak preceded each of these sessions by 25 to 28 days. A low trough occurred 19 to 23 days before low-scoring sessions in each of the four data sets. On the day of the session, the sunspot number was at or above the epoch mean in each of the four low-data sets. Out of this analysis emerged three time intervals that may enable forecasting: 27 to 30 days, 16 to 19 days prior to the sessions, and (for theoretical reasons addressed later) two to four days after the sessions.

(U) To examine the time lags where possible correlations might exist, time lag correlations were performed for each individual in the groups from 1979, 1980, and 1984. Both positive and negative correlations to sunspot number were found. These results also indicated that clustering of correlations occurs near the time intervals both preceding and following session dates found in the epoch analysis. Overall, 779 correlations were performed. Up to 38 correlations at the $p = 0.05$ level would be expected

* (U) 84(I) data were not processed.

UNCLASSIFIED

UNCLASSIFIED

(U)

to occur by chance. Fifty-six correlations were observed, or about 50 percent over what would be expected by chance.

(U) Three time clusters were observed in the significant correlations. In a four-day interval, where 76 correlations are represented, the chance number of significant correlations at the $p = 0.05$ level is estimated to be 3.8. The interval from 27 to 30 days prior to the session (perhaps reflecting the solar-rotation rate) had eight individuals having significant correlations at $p < 0.05$; two other individuals were very close to significance. Another interval from 16 to 19 days prior to the sessions yielded eight significant correlations ranging from $p < 0.047$ to $p < 0.0003$. A third period appeared two to four days after the sessions. This three-day interval yielded five individuals having significant correlations, and four others having near-significant correlations.

(U) It can be surmised that because these correlations exist in patterns, there may be some phenomenon associated with sunspots that could be more closely linked to the actual mechanisms that influences RV performance. A likely candidate is the phenomenon of solar flaring, and its resulting effect on the terrestrial geomagnetic field. In particular, the finding that the strongest correlations to sunspot number consistently occurred two to three days after the sessions, points to flaring. At first one might dismiss observation of RV performance apparently forecasting sunspot number. However, if one considers that large flares from active regions on the sun (sunspots) can frequently be seen before the region rotates onto the solar disk, a hypothesis could be formed that incorporates flaring as a possible mechanism, because indeed, one can predict increases in sunspot numbers by observing flares on the east solar limb.

4. (U) Solar Flares

(U) Solar flares usually occur near sunspot groups called active regions. The sizes of these flares are classified in several ways by the intensity of various characteristics associated with them, i.e., according to their X-ray intensity, optical brilliance, area, and radio-wave

UNCLASSIFIED

UNCLASSIFIED

(U)

signatures. There does not seem to be a readily-available comprehensive index that takes all of the their characteristics into account. For this reason, flares were subdivided into several data sets prior to analysis:

- The first set was the total daily number of all recorded flares; these flares were further subdivided into location of origin in 10-deg longitudinal segments from the central meridian of the solar disk.
- The second data set was an extraction of the larger flares from the data. These flares were selected for their classification of both size and brilliance. Those classified as sub-brilliant or larger were used. (The flares were divided by longitude because flaring at certain longitudes on the solar disk is known to produce greater terrestrial effects than at other longitudes. For instance, relativistic energy showers most frequently originate from the northwest quadrant of the sun.)

(U) In exploring the theory that limb flaring (flares on the edge of the solar disk) may play a role in RV performance, special attention was given to this area of the sun. Indeed, as anticipated, significantly higher rates of limb flaring were found on the day of (or just before) four of five of the high-scoring data sets,* and on the day of (or just after) low-scoring data sets in four of five cases.* What this implies is that some confidence can be placed on the validity of relationship between solar flaring and RV performance.

(U) Of key interest is the finding that the flares occurring on the solar limbs (80 to 89 deg) tend to group with respect to high- and low-performance data sets. Large flares occurred on the limbs the day of sessions in three of four of the low-scoring data sets. In the fourth set, a flaring peak occurred three days later. The number of flares was significantly greater on low-scoring session days (more than two standard deviations above the epoch period mean) in each case. The days following low-scoring sessions continued to have high flare rates across the solar disk. (On the other hand, in three of four cases, high-scoring

* (U) 84(I) data were included.

UNCLASSIFIED

UNCLASSIFIED

(U)

data sets were preceded by an increase in limb flaring by one day. These values were near-significant. We shall return to this point below.) In addition to the tendency of flares to cluster on poor performance days, the numbers of flares was more than double the daily expected value for three of the low-scoring RV data sets.

(U) A speculation from the data is that low-viewing scores might be associated with flares (occurring on the east limb) rotating onto the solar disk (because of the numerous flare peaks observed at all locations on the disk following poor RV sessions). By contrast, high scoring might be associated with regions rotating off the west limb of the solar disk because of the fewer flare peaks following good sessions. Indeed, when diagrams of solar-active regions were examined for the first set of 1984 data, nine of ten of the low-scoring days showed active regions near the east limb. On the other hand, eight of ten of the high-scoring days showed active regions near the west limb.

(U) Based on the observation that, statistically, limb flares coincide with and follow degraded RV sessions, but precede enhanced RV performance by one day, a speculation could be made that there may be a close time relationship for enhanced and degraded RV sessions. In hypothesizing which solar-terrestrial changes could cause changes in RV performance, the observed rapidity of change and the reversal of the character of the effect must be taken into consideration. The following scenario is suggested. As a new active flaring region rotates over the solar limb, associated with it is some kind of a fast-acting phenomenon that requires a day or less to produce terrestrial effects. The terrestrial effect must be relatively brief, and of a character that is capable of both degrading and enhancing RV performance. An example of one such phenomenon is the Sudden Ionospheric Disturbances (SID) caused by X-ray and other electromagnetic-radiation bursts associated with the flaring process. SIDs can both enhance and decrease the quality of global electromagnetic signal propagation--possibly at biologically-active frequencies. A specific type of SID, a direct solar-flare effect (SFE), causes geomagnetic effects observed simultaneously with solar flares.

UNCLASSIFIED

UNCLASSIFIED

(U)

Another mechanism could be proton storms resulting from high-energy flares. Very-high-energy flares can accelerate particles at near-relativistic speeds; these particles are capable of reaching earth in a matter of a few hours. Magnetic storms may accompany the arrival of this high-speed solar wind. Either of these two mechanisms could explain the immediacy of the observed effect.

(U) With regard to the tendency for RV performance to first be degraded then enhanced, one might speculate on possible mechanisms for bipolar behavior based on, for instance, known patterns of magnetic storms. If RV performance were correlated with the intensity of the earth's magnetic field, then the following known variations that occur as part of the magnetic storm process might be capable of introducing the observed patterns into RV performance. Typically, the storms that begin suddenly start with.

- (1) A sudden increase in the horizontal (H) component of the earth's magnetic field; they then
- (2) Have an initial phase lasting a few minutes to a few hours, during which H decays to prestorm values;
- (3) This is followed by a main phase lasting about one to three days in which H is below the prestorm value, first decreasing, then increasing more slowly toward the prestorm value--many large random variations occur during this phase;
- (4) There is a postperturbation period after the end of the main phase, in which the value of H continues to rise toward, or perhaps above the prestorm value;
- (5) The last phase is an increase in the daily variation of H, which increases with increasing latitude. If RV performance correlated with magnetic intensity, patterns would certainly be found during the magnetic storm.

5. (U) Magnetic Indices

(U) Four magnetic indices, the sum of K_p , A_p , C_p , and $C9$ were screened with respect to RV performance. K_p is a quasi-logarithmic index of geomagnetic stations between latitudes 47 and 63 deg. K_p is specifically designed to measure solar particle radiation by its magnetic

UNCLASSIFIED

UNCLASSIFIED

(U)

effects. A_p is a daily index of magnetic activity on a linear scale rather than on the quasi-logarithmic scale of the K indices. It is the average of the eight values of an intermediate three-hourly index A_p , defined as approximately one-half the average gamma range of the most disturbed of the three force components D, H, and Z, in the three-hour interval at standard stations. The C_p index is derived from the K_p indices by converting the daily sum of A_p into the range of 0 to 2.5. The C9 index is a geomagnetic character figure obtained from the C_p index by reducing the C_p values to integers between 0 and 9 according to certain keys. All these values are closely related, and, not surprisingly, gave similar results in the epoch analysis comparing them to RV performance.

(U) The four sets of RV scores yielded remarkably similar patterns with respect to K_p , and corroborated the solar flare findings extremely well. In each case, values were above the epoch mean the day preceding low RV scores, decreasing in all cases on the day of the sessions. In three sets, the decrease fell below the mean; in the fourth case, the value dropped considerably and was only slightly above the mean. The next day's values of this data set continued to decrease and were below the mean. Conversely, in the sets of high-scoring days, all four sets showed K_p indices that were below the epoch mean the day before the sessions and increased to values above the mean in three of the four data sets. The fact that these patterns were replicated in the majority of the test data sets, and that high- and low-scoring data sets yielded inverse patterns with respect to K_p is a strong indication of a valid phenomenon existing. Therefore, what we found were strong similar patterns in the geomagnetic data with respect to RV performance. The geomagnetic field was quiet just before all high-scoring sessions, then became more active the day of the session. Magnetic activity was higher than normal one to five days prior to low-scoring sessions. This would suggest that RV sessions be performed when the activity of the geomagnetic field is on the increase after a quiet period.

(U) Comparing these consistent results with the results of the solar flare analysis shows that there is evidence for the standard

UNCLASSIFIED

UNCLASSIFIED

(U)

one-to-four day time lag between flare and subsequent magnetic activity. The magnetic indices are increasing on Day 0 (the day of the sessions), they continue to increase the day after the statistical flaring, then decrease in two to five days. Results using A_p , C_p , and C9 indices were similar; the best definition appeared to be seen with the K_p index followed by A_p , C_p , and C9. For forecasting purposes this is fortunate. The K_p (and A_p) are readily available by means of the satellite downlink, C_p and C9 are not.

6. (U) SIDs

(U) Sudden ionospheric disturbances result mostly from flaring of the sun, although not all flares cause SIDs, and SIDs can also result from unknown causes. SIDs are basically a disturbance of the upper ionized layer of the atmosphere called the ionosphere, specifically in the D region. During SIDs, radio waves at medium frequencies are strongly absorbed and long-distance communications fade out. Cosmic radio noise at 15 to 25 MHz is absorbed and also fades. At very low frequencies (15 to 40 kHz), however, the D region becomes a reflector, and atmospheric radio noise is enhanced. A SID is marked also by a sharp brief geomagnetic disturbance that behaves differently from a magnetic storm. SIDs are classified according to their intensity and types of terrestrial effects.

(U) Although many classifications exist, the two most common (known to enhance low-frequency transmission) were extracted from the data base; i.e., those classified as enhancing atmospherics, as measured at 27 kHz (SEA), and those which enhance signal strength in VLF transmissions (SES). (The effects of SIDs on ELF is not monitored and is unknown.)

(U) The results of the epoch analysis on SIDs correspond well to the results of the solar-flare and the magnetic analyses. While the SEAs showed some corroborative patterns, the results of the analysis on the SESs were remarkable. The results of the SIDs analysis are similar to the analysis of the occurrence of peaks of solar flares. That is, there

UNCLASSIFIED

UNCLASSIFIED

(U)

are fewer peaks occurring around the times of high-scoring sessions than low-scoring sessions. There are more strong SIDs peaks on the day of, and after low-scoring sessions. A SIDs peak of importance (magnitude "1" or greater occurs on the day of the low-scoring sessions in four of the data sets. Peaks of SIDs also occurred on the day of the session in four of five years of the high-scoring data sets, and on the day prior to the sessions in the other data set (1979). Therefore, nine of ten of the data sets had an SES-type SID occurring on the day of the session. The remaining data set had a peak in SIDs occurring in close proximity to the session--on the day before.

(U) It appears that SES-type SIDs are a good candidate for the previously hypothesized fast-acting result of solar activity that could influence RV performance. A peak of SES-type SIDs have occurred on or near every case of RV extreme-score sets. We speculate that there is some quality of the SID that is associated with the observed bipolar effect, resulting in both high- and low-quality RV performance. A quality of SIDs that might produce bipolar effects could be selective electromagnetic propagation. If SIDs selectively propagate certain VLF or ELF frequencies, it would not be surprising to find differing biological responses to frequency and intensity changes--assuming biological responses to ELF exist. Laboratory studies of ELF magnetic and electric fields (see references to work of Adey and others in Bibliography) suggest such ELF-biological relationships. An additional possibility to account for bipolar behavior might be the frequency characteristics of the atypical magnetic activity that accompanies SIDs. This can be accomplished by direct measurement of geomagnetic ELF, described in the section below.

B. (U) Results Pertaining to ELF

1. (U) Introduction

(U) The ELF environment, both naturally-occurring and man-made, is one good candidate for the mechanism by which many types of biological responses are produced. Laboratory studies have shown both sensitivity

UNCLASSIFIED

UNCLASSIFIED

(U)

and selectivity in biological responses to specific frequency and intensity windows. The intensities found to be biologically active are very weak, and fall in the same ranges as naturally-occurring magnetic and electrical fields. For our initial effort, we selected the frequency window of 0 to 30 Hz for two reasons, one pedagogical and one practical:

- It is the frequency range of the known electrical activity of a human being--particularly brainwave frequencies.
- It is necessary to filter out 60-Hz power-line noise, and simple electronic 60-Hz filters begin cutoff at about 30 Hz.

With regard to the latter point, although sharper filters are available, they are elaborate and expensive. For this exploratory investigation, the most cost- and time-effective route was chosen.

2. (U) Intercomparison of ELF Systems

(U) A number of comparisons between the various components of the ELF monitoring system have been made. The systems compared include the prototype system at TRI involving the use of the oak-tree bioantenna, the upgraded system at TRI involving use of both the oak tree and a coil antenna on loan from the Radioscience Laboratory at Stanford University, and a duplicate upgraded system at SRI involving use of an oak tree.

(U) Correlations were performed between ELF data sets generated on each of the systems. Although variations existed, by and large the correlations indicated statistically-significant tracking between the various systems, including the comparison of key concern--tracking between the duplicate upgraded systems at TRI and SRI, 17 km distant. In fact, tracking between the separated TRI and SRI systems, both utilizing oak-tree antenna, was somewhat better than tracking between the oak-tree and coil antennas, both at the TRI site.

3. (U) ELF/RV Comparison

(U) Epoch analyses were carried out to determine correlations between ELF and RV data sets for those periods of overlap in operation.

UNCLASSIFIED

UNCLASSIFIED

(U)

With regard to the prototype ELF system, whose data base began in May of 1982, the 1984 data base (before the fifth data base was added) was the only one available for comparison. Examination of the correlation graphs in the epoch analysis revealed some tendency (over time spans on the order of days) to inverse relationship between ELF and RV; that is, a tendency for ELF to be low in the vicinity of high-scoring days, and vice versa. There were not sufficient data of sufficient definition, however, to permit statistically-significant conclusions to be drawn.

(U) Beginning in June 1984, the upgraded ELF system became operational. RV data collected from then through August provided an opportunity to perform preliminary epoch analyses for a small sample of RV data (four cases each for high and low scores) on a half-hourly basis. (This is to be compared with the half-daily basis of the prototype ELF system.) An apparently consistent pattern that emerged in these analyses was a change from low-scoring sessions to high-scoring sessions during a rapid rise in ELF values; the separation between the two was on the order of an hour and a half (range one-half to two hours and a half). This appears as another example of bipolar effect mentioned earlier with respect to geomagnetic activity, where rapid crossing from below- to above-average activity on the days of extreme-scoring sessions was also observed. The time/funding scope of this level-of-effort project did not permit further exploration of this emerging relationship between ELF (and other geophysical activity) and potential rate-of-change effects on RV performance. This area appears to show exceptional promise, however, and will be pursued in a follow-on program.

(U) The emergence of a possible relationship between a period of time when the data are changing at a rapid rate (rather than peaking) is not surprising in light of known mechanism of biological processes. Several biological processes function by means of rates-of-change of stimuli in preference to any particular absolute values of those stimuli-- if the intensity of the stimuli fall within certain ranges.

UNCLASSIFIED

C02574264

UNCLASSIFIED
Approved for Release: 2017/09/11 C02574264

UNCLASSIFIED
Approved for Release: 2017/09/11 C02574264

UNCLASSIFIED

VI EVALUATION AND RECOMMENDATIONS (U)

(U) This study has a threefold purpose:

- To determine whether geophysical factors correlate with RV performance.
- If correlations are found, to identify which geophysical factors correlate with RV performance with enough lead time that RV performance could be forecast in advance.
- To optimize the potential for forecasting by seeking those geophysical factors that constitute the best candidates for the mechanism by which observed effects on RV performance are produced.

(U) Some degree of success has been achieved in all three categories. Significant correlations of some significance have been found to exist between RV performance and solar flux values, sunspot number, and magnetic indices M_p , A_p , C_p , and $C9$. Epoch analysis has shown that flares and resulting SIDs have a strong tendency to cluster in certain time intervals with respect to extreme-scoring RV sessions. Flares, especially those on the solar limbs, tend to occur on the day of low-performance RV sessions, and on the day preceding high-scoring sessions.

(U) SIDs resulting from flares may produce a bipolar effect, such that an intimate time relationship exists between high-scoring and low-scoring sessions. Epoch analysis on SIDs show enhanced sudden enhancement of signal strength in VLF (SES) on the day of, or before, both high- and low-scoring sessions.

(U) Evaluation of the ELF environment with data from the prototype ELF monitoring system revealed patterns in ELF measurements a number of days preceding the sessions which were oppositely configured over time with respect to high- and low-scoring sessions.

(U) A very encouraging aspect of this study is the corroboration of the findings by all of the various data sets examined. The relationship of geophysical phenomena to RV performance may be traced from solar

UNCLASSIFIED

UNCLASSIFIED

(U)

activity, to terrestrial activity--including SIDs and geomagnetic activity. All of these data sets appear at specific time intervals, which are known to occur with respect to each other, and at definable intervals with respect to the RV performance data.

(U) The following conclusions have been reached as a result of this data analysis:

- Correlations between several geophysical phenomena and RV performance are significant, and have a high probability of constituting a valid cause-effect phenomenon.
- Time periods of low-scoring sessions cluster (within 24 hours or less) with high-scoring sessions. This suggests that the mechanism that influences RV performance has a bipolar effect.
- ELF appears to be a reasonable candidate for a linking mechanism; it is capable of changing rapidly, is most likely affected by SIDs and other solar effects, and specific changes have been noted at the times of the sessions.
- Should further in-depth statistical studies confirm the results to date, a successful long-range forecasting system could possibly be developed using a combination of solar-terrestrial and monitored ELF data. Solar-terrestrial correlations were significant, but the time intervals are not yet defined accurately enough for reliable forecasting. Successful forecasting might be accomplished by using solar-terrestrial data to identify approximate time periods when enhanced and degraded performance is expected. Then, by monitoring the ELF environment during these periods, the exact effects can be known or anticipated.

(U) The objectives of a follow-on effort should be to (1) confirm the findings (especially with respect to the ELF data), (2) seek finer time resolution, and (3) clarify the mechanisms involved in the RV solar-terrestrial relationship. The final product of such an effort would be trial forecasts in a blind study in order to determine whether forecasting (and its companion, scheduling) can lead to increased reliability of the RV process.

UNCLASSIFIED

UNCLASSIFIED

VII SUMMARY (U)

(U) Past experiments in RV have shown considerable variability in RVer performance over time; that is, RVer are seen to perform better at some times than at others. This variability has not yet been fully explained nor examined in detail. The possibility exists a priori that performance might be affected by certain external factors. If this is the case, identifying these factors and understanding the way they influence a trainee's performance could lead to significant improvement in the RV product.

(U) As a starting point, human beings have been shown to be sensitive to certain forms of electromagnetic radiation that are known to exist in the geophysical environment; there is also some evidence that certain aspects of human behavior and performance are related to changes in yet other aspects of the geophysical environment. An important question relative to RV performance is the extent to which a trainee's performance is subject to such electromagnetic or geophysical factors. Investigation of this question is necessary in the course of developing a reliable RV capability. The results of such an investigation would show whether RV performance is influenced by these factors, and, if so, the degree to which such influences can be controlled, and whether they point to directions for further research into the fundamental nature of psi function in its broadest sense.

(U) The project described in this report is a first step in the process of determining the relationship between RV performance and various environmental factors. This project had a two-part aim. First, it was necessary to set up an environmental monitoring facility for real-time measurement of certain variables, and to identify available, reliable sources of other environmental data. Second, the degree of correlation between the available environmental data and the RV results needed to be developed. In this report, we describe the monitoring facility and the

UNCLASSIFIED

UNCLASSIFIED

(U)

specific environmental variables, and a preliminary analysis of the correlations between RV performance and these factors is given. Some interpretation is also provided as an aid to planning future work along these lines.

(U) Basically, in the monitoring facility we detect and record the local geomagnetic field, using a Fourier analysis technique to separate the various frequency components in the electromagnetic spectrum (in the range 0 to 30 Hz). A prototype facility had been in operation for more than two years, and some relatively coarse data were already available when the project began. These data, and the experience gained while gathering them, were used to design and calibrate more precise instrumentation for this program. Data from these systems were then used in the investigation to correlate against RV performance data for the corresponding time period of operation of this facility. An equally important part of the project consisted of correlating RV performance data against other geophysical observations available from the National Oceanographic and Atmospheric Administration--some of it by real-time acquisition from a Westar IV satellite downlink installed specifically for this purpose.

(U) As shown in this report, several significant correlations have been found between various geophysical factors and RV performance. These correlations have a strong tendency to cluster in certain time intervals with respect to high- and low-performance RV sessions. In some cases, the clustering precedes the correlated RV activity, thereby yielding the possibility of performance prediction, should such correlations continue to be viable in further work.

(U) Among the most interesting correlations to RV performance found are flares occurring on the sun, especially those on the edge (limbs) of the solar disk. These flares play an important role in producing upper atmospheric disturbances known as SIDs (sudden ionospheric disturbances), which influence terrestrial radio-signal propagation. SIDs are known to block higher-frequency communications, but at the same time, to enhance lower-frequency propagation at LF and VLF frequencies. Although the effect of SIDs on the yet lower-frequency ELF portion of the electromagnetic

UNCLASSIFIED

(U)

spectrum is unknown, it could provide a promising link between the solar-terrestrial environment and known electromagnetic effects on biological processes. With regard to ELF itself, preliminary evaluation of the ELF environment in half-hourly time intervals has shown a possible relationship to frequencies between 10 and 30 Hz, particularly as ELF intensities change from below average to above average values.

Considering the modest level-of-effort for the survey of geophysical/ELF factors, and their possible relationship to RV performance, a considerable amount of progress has been made in delineating potential correlations of value. What can be said at this point is that this pilot study provides evidence that the quality of RV functioning may be intimately related to the geophysical environment. What remains to be done is (1) an in-depth statistical evaluation of those findings of this study that were strongly intercorroborated by the various data sets used, and (2) a structured attempt at blind RV performance forecasting. As a result, continued collection and analysis of such data will be pursued to determine whether the correlations found are stable over time, and will thus provide a solid continuing basis for RV performance prediction. From both scientific and practical viewpoints, knowledge of this kind makes it possible' _____ to consider methods for enhancing the overall RV product.

C02574264

UNCLASSIFIED
Approved for Release: 2017/09/11 C02574264

UNCLASSIFIED
Approved for Release: 2017/09/11 C02574264

UNCLASSIFIED

REFERENCES (U)

1. Persinger, M. A., H. W. Ludwig, and H. P. Ossenkopp, "Psychophysiological Effects of ELF Electromagnetic Fields: A Review," Perceptual and Motor Skills, Vol. 36, pp. 1131-1159 (1973).
2. Weber, R., "Human Circadian Rhythms under the Influence of Weak Electric Fields and the Different Aspects of These Studies," Int. J. Biometeorology, Vol. 17, No. 3, pp. 227-232 (1974).
3. Friedman, H., R. Becker, and C. Bachman, "Effect of Magnetic Fields on Reaction-Time Performance," Nature, pp. 949-950 (4 March 1967).
4. Konig, H. L., "Behavioral Changes in Human Subjects Associated with ELF Electrical Fields," ELF and VLF Electromagnetic Field Effects, M. A. Persinger (ed.), Plenum Press, New York, pp. 81-99 (1974).
5. Puthoff, H. E. and M. Adams, "Geophysical Effects Study (U)," Interim Report, SRI 941/CL-0022, SRI International, Menlo Park, CA (July 1984), SECRET/NOFORN.
6. Fraser-Smith, A. C., "ULF Tree Potentials and Geomagnetic Pulsations," Nature, Vol. 271, No. 5646, pp. 641-642 (16 February 1978).
7. Adams, M. H., "The Effect of the Geophysical and ELF Environments on RV Performance (U)," Final Report, Time Research Institute, Los Altos, CA (28 November 1984), UNCLASSIFIED.

UNCLASSIFIED

C02574264

UNCLASSIFIED
Approved for Release: 2017/09/11 C02574264

UNCLASSIFIED
Approved for Release: 2017/09/11 C02574264

UNCLASSIFIED

BIBLIOGRAPHY (U)

- Adair, E. R. and B. W. Adams, "Microwaves Induce Peripheral Vasodilation in Squirrel Monkey," Science, Vol. 207, pp. 1381-1383, (1980).
- Adey, W. R., Chapter 15 in Functional Linkage in Biomolecular Systems, (Raven Press, New York), pp. 325-342, (1975).
- _____, "Frequency and Power Windowing in Tissue Interactions with Weak Electromagnetic Fields," Proc. IEEE, Vol. 68, No. 1, pp. 119-125, (1980).
- _____, "Tissue Interactions with Nonionizing Electromagnetic Fields," Physiological Rev., Vol. 61, No. 2, pp. 435-514, (1981).
- Adey, W. R. et al., "Effects of Weak Amplitude-Modulated Microwave Fields on Calcium Efflux from Awake Cat Cerebral Cortex," Bioelectromagnetics, Vol. 3, pp. 295-307, (1982).
- Archart-Treichel, J., "Electromagnetic Pollution: Is It Hurting Our Health?," Science News, Vol. 105, pp. 418-419, (1974).
- Bassett, G.A.L. et al., "Augmentation of Bone Repair by Inductively-Coupled Electromagnetic Fields," Science, Vol. 184, pp. 575-577, (1974).
- Bawin, S. M. and W. R. Adey, "Electric Fields and Nerve Activity," Proc. Natl Acad. Sci., (1976).
- Beal, J. B., "Spontaneous Electromagnetic Radiation from Natural Dielectrics," Planetary Assoc. for Clean Energy Newsletter, Vol. 3, No. 1, p. 30, (1981).
- Becker, R. O. et al., "The Direct Current Control System," N. Y. State J. Med., pp. 1169-1176, (1962).
- Becker, R. O., "Electromagnetic Forces and Life Processes," Technology Rev., pp. 32-38, (1972).
- _____, "The Significance of Bioelectric Potentials," J. Bioelectrochem. & Bioenergetics, (1974).
- "Biomedicine--How Electrical Healing Works," Science News, Vol. 122, p. 57, (1982).

UNCLASSIFIED

UNCLASSIFIED

- Bodznick, D. and R. G. Northcutt, "Electroreception in Lampreys: Evidence that the Earliest Vertebrates Were Electroreceptive," Science, Vol. 212, pp. 465-467, (1981).
- Borgens, R. B. and E. Roederer, "Enhanced Spinal Cord Regeneration in Lamprey by Applied Electric Fields," Science, Vol. 213, pp. 611-617, (1981).
- Bracken, T. Dan (Editor), "Proceedings of the Workshop on Electrical and Biological Effects Related to HVDC Transmission," Pacific Northwest Laboratory Report PNL-3121, Department of Energy, (1979).
- Buettner, K. J., "Present Knowledge on Correlations Between Weather Changes, Sferics, Air Electric Space Charges, and Human Health and Behavior," Bioclimatology-Federation Proceedings, pp. 631-637, (1957).
- Burr, H. S. and S. C. Northrup, "The Electro-Dynamic Theory of Life," Quart. Rev. of Biology, Vol. 10, (1935).
- Calhoun, J. B. (Editor), "Environment and Population: Problems of Adaptation," (Praeger Scientific), pp. 28-30, (1984).
- Chou, C. K. and A. W. Guy, "Holographic Assessment of Microwave Hearing," Science, Vol. 209, pp. 1143-1144, (1980).
- Deno, D. W. et al., "Measurements of Electric and Magnetic Fields in and Around Homes Near a 500-kV Transmission Line," presented at IEEE/PES Meeting, (1982).
- Dodge, C. H., "Clinical and Hygienic Aspects of Exposure to Electromagnetic Fields, from Biological Effects and Health Implications of Microwave Radiation," Symposium Proceedings, Richmond, VA, 17-19 September 1969, pp. 140-148, (1969).
- Eichmeier, J. and P. Buger, "Über den Einfluss Elektromagnetischer Strahlung auf die Wismutchlorid-Fällungsreaktion nach Paccardi," Int. J. Biometeor., Vol. 13, Nos. 3 and 4, pp. 239-256, (1969).
- Fischer, W. H. et al., "Laboratory Studies on Fluctuating Phenomena," Nat. J. Biometeor., Vol. 12, No. 1, pp. 15-19, (1968).
- Fraser-Smith, A. C., "ULF Tree Potentials and Geomagnetic Pulsations," Nature, Vol. 271, No. 5646, pp. 641-642, (1978).
- _____, "Some Statistics on Pc 1 Geomagnetic Micropulsation Occurrence at Middle Latitudes: Inverse Relation with Sunspot Cycle and Semi-Annual Period," J. Geophys. Res., Space Phys., Vol. 75, No. 25, pp. 4735-4745, (1 September 1970).

UNCLASSIFIED

UNCLASSIFIED

- Fraser-Smith, A. C., "Long-Term Predictions of Pc 1 Geomagnetic Pulsations: Comparison with Observations," Planet. Space Sci., Vol. 29, No. 7, pp. 1902-1907, (1964).
- Frey, A. H., "Biological Function as Influenced by Low-Power Modulated RF Energy," IEEE Trans. Microwave Theory and Tech., Vol. 19, No. 2, pp. 153-163, (1971).
- _____, "Neural and Behavioral Response to Changes in Weak Electromagnetic Fields," Workshop on Behavioral Sensitivities on Animals Possibly Relevant to Earthquake Prediction, Galveston, TX, 1979, pp. 1-10, (1979).
- Friedman, H. et al., "Geomagnetic Parameters and Psychiatric Hospital Admissions," Nature, Vol. 200, pp. 626-628, (1963)
- _____, "Psychiatric Ward Behaviour and Geophysical Parameters," Nature, Vol. 205, pp. 1050-1052, (1965).
- Friend, A. W., Jr. et al., "Low-Frequency Electric-Field-Induced Changes in the Shape and Motility of Amoebas," Science, Vol. 187, pp. 357-359, (1975).
- Garmon, L., "Something in the Air," Science News, Vol. 120, pp. 364-365, (1981).
- Gauquelin, M. and F. Gauquelin, "Review of Studies in the USSR on the Possible Biological Effects of Solar Activity," J. Interdiscipl. Cycle Res., Vol. 6, No. 3, pp. 249-252, (1975).
- Gavalas, R. J. et al., "Effect of Low-Level, Low-Frequency Electric Fields on EEG and Behavior in Macaca Nemistrina," Brain Res., Vol. 18, pp. 491-501, (1970).
- Gnevyshev, M. N. and K. F. Novikova, "Solar Activity and Manifestations in the Biosphere," National Research Council Report TT-1679, (1973).
- Goodman, R. et al., "Pulsing Electromagnetic Fields Induce Cellular Transcription," Science, Vol. 220, pp. 1283-1285, (1983).
- Guha, S. K. et al., "Electrical Field Distribution in the Human Body," Phys. Med. Biol., Vol. 18, No. 5, pp. 712-720, (1973).
- Hamer, J. R., "Effects of Low-Level, Low-Frequency Electric Fields on Human Time Judgment," Int. J. Biometeor., (1969).
- _____, "Biological Entrainment of the Human Brain by Low-Frequency Radiation," Technical Memorandum, Northrop Space Laboratories, (1965).

UNCLASSIFIED

UNCLASSIFIED

- Heiligenberg, W. and R. A. Altes, "Phase Sensitivity in Electoreception," Science, Vol. 199, pp. 1001-1004, (1978).
- Herin, R. A., "Electroanesthesia: A Review of the Literature (1819-1965)," Activitas Nervosa Superior, Vol. 10, No. 4, pp. 439-454, (1968).
- Heynick, L. N. and P. Polson, "Bioeffects of Radiofrequency Radiation: A Review Pertinent to Air Force Operations," USAF Report No. USAFSAM-TR-83-1, SRI International, Menlo Park, CA, (1983).
- Hicks, W. W., "A Series of Experiments on Trees and Plants in Electrostatic Fields," J. Franklin Inst., Vol. 64, No. 1, pp. 1-5, (1957).
- Hill, H. L. et al., Transmission Line Reference Book HVDC to 600 kV, (EPRI, Palo Alto, CA).
- _____, "Radio Interference," Transmission Line Reference Book HVDC to 600 kV, (EPRI, Palo Alto, CA), pp. 46-58.
- _____, "Direct Current Field Effects," Transmission Line Reference Book HVDC to 600 kV, (EPRI, Palo Alto, CA), pp. 73-96.
- Hillman, J. S. and J.D.C. Turner, "Association Between Acute Glaucoma and the Weather and Sunspot Activity," Brit. J. Ophthalmology, Vol. 61, pp. 512-516, (1977).
- Hirsch, F. G. et al., "The Psychologic Consequences of Exposure to High-Density Pulsed Electromagnetic Energy," Int. J. Biometeor., Vol. 12, No. 3, pp. 263-270, (1968).
- Houghton, A. et al., "Increased Incidence of Malignant Melanoma After Peaks of Sunspot Activity," The Lancet, pp. 759-760, (1978).
- Jitariu, P. et al., "L'Influence des Champs Electro-Magnetiques Pulsant sans Interruption sur les Fractions Proteiques Plasmatiques et sur Le Processus de la Coagulation chez les Lapins," Rev. Roum. Biol.--Zoologie, Vol. 12, No. 2, pp. 91-95, (1967).
- Kholodov, Y. A., "Effect of Electromagnetic and Magnetic Fields on the CNS," Foreign Sci. Bull., pp. 17-23, (1967).
- Kloss, D. A. and E. L. Carstensen, "Effects of ELF Electric Fields on the Isolated Frog Heart," IEEE Trans. Biomed. Eng., Vol. 30, No. 6, pp. 347-348, (1983).
- Konig, H., "Biological Effects of Extremely-Low-Frequency Electrical Phenomena in the Atmosphere," J. Interdiscipl. Cycle Res., Vol. 2, No. 3, pp. 317-323, (1971).
- Larkin, R. P. and P. J. Sutherland, "Migrating Birds Respond to Project Seafarer's Electromagnetic Field," Science, Vol. 195, pp. 777-778, (1977).

UNCLASSIFIED

UNCLASSIFIED

- Lawrence, A. F. and W. R. Adey, "Nonlinear Wave Mechanisms in Interactions Between Excitable Tissue and Electromagnetic Fields," Neurological Res., Vol. 4, Nos. 1 and 2, (Butterworth Publishers), pp. 115-152, (1982).
- Leach, J. F. et al., "Effect of Ozone Variation on Disease in Great Britain: I. Skin Cancer," Aviation, Space, and Environ. Med., Vol. 49, No. 3, pp. 512-516, (1978).
- Lerner, E. J. (Editor), "Biological Effects of Electromagnetic Fields," IEEE Spectrum, pp. 57-69, (1984).
- Lin-Liu, S. and W. R. Adey, "Low-Frequency Amplitude-Modulated Microwave Fields Change Calcium Efflux Rates from Synaptosomes," Bioelectromagnetics, Vol. 3, pp. 309-322, (1982).
- Lokken, J. E. et al., "A Note on the Classification of Geomagnetic Signals Below 30 Cycles per Second," Canadian J. of Phys., Vol. 40, pp. 1000-1009, (1962).
- Lokken, J. E. and J. A. Shand, "Man-Made Electromagnetic Interference at Extremely Low Frequencies," Canadian J. of Phys., Vol. 42, pp. 1902-1907, (1964).
- Lotmar, R. et al., "Dampfung der Gewebeatmung (Q02) von Mauseleber durch Kunstliche Impulsstrahlung," Int. J. Biometeor., Vol. 13, Nos. 3 and 4, pp. 231-238, (1969).
- Luben, R. W. et al., "Effects of Electromagnetic Stimuli in Bone and Bone Cells in vitro: Inhibition of Responses to Parathyroid Hormone by LF Fields," Proc. Natl. Acad. Sci., Vol. 79, p. 4188, (1982).
- Ludwig, H. W., "A Hypothesis Concerning the Absorption Mechanism of Atmospherics in the Nervous System," Int. J. Biometeor., Vol. 12, No. 2, pp. 93-97, (1968).
- Magnus, K., "Incidence of Malignant Melanoma of the Skin in the Five Nordic Countries: Significance of Solar Radiation," Int. J. Cancer, Vol. 20, pp. 477-485, (1977).
- Malin, S.R.C. and B. J. Srivastava, "Correlations Between Heart Attacks and Magnetic Activity," Nature, Vol. 277, pp. 646-648, (1979).
- Marha, K. et al., "Electromagnetic Field and the Living Environment," State Health Publishing House, (1968).
- Markson, R. J., "Geophysical Influences in Biological Systems," (thesis), Pennsylvania State University, (1967).
- Markson, R., "Tree Potentials and External Factors," (Masters thesis), Pennsylvania State University, (1967).

UNCLASSIFIED

UNCLASSIFIED

- Marshall, E., "ELF Resurrected After Drowning by Navy," Science, Vol. 212, pp. 644-645, (1981).
- Mayyasi, A. M. and R. A. Terry, "Effects of Direct Electric Fields, Noise, Sex and Age on Maze Learning in Rats," Int. J. Biometeor., Vol. 13, No. 2, pp. 101-111, (1969).
- Michaelson, S. M., "Human Exposure to Nonionizing Radiant Energy-Potential Hazards and Safety Standards," Proc. IEEE, Vol. 60, No. 4, pp. 389-421, (1972).
- _____, "Physiologic Regulation in Electromagnetic Fields," Bioelectromagnetics, Vol. 3, pp. 91-103, (1982).
- Michrowski, A., "USSR ELF Emissions Were Predicted for Remote Viewing and Mind-Control Capabilities," Planetary Assoc. for Clean Energy Newsletter, Vol. 3, No. 1, pp. 26-27, (1981).
- Moos, W. S. and R. Reiter, "Biological Effects of Electric, Magnetic and Electromagnetic Fields," (study group). Int. J. Bioelectricity, pp. 204-205, (1969).
- NRC Report, "Biologic Effects of Electric and Magnetic Fields Associated with Proposed Project Seafarer," National Research Council, pp. 27-54, (1977).
- Nordstrom, S. et al., "Reproductive Hazards Among Workers at High-Voltage Substations," Bioelectromagnetics, Vol. 4, No. 1, pp. 91-101 (1983).
- Park, C. G. and R. A. Helliwell, "Magnetospheric Effects of Power Line Radiation," Science, Vol. 200, pp. 727-730, (1978).
- Paschal, E. W., "Design of Broad-Band VLF Receivers with Air-Core Loop Antennas," Stanford Electronic Laboratories (SEL) Report, (1980).
- Persinger, M. A. et al., "Psychophysiological Effects of Extremely-Low-Frequency Electromagnetic Fields: A Review," Perceptual and Motor Skills, Vol. 36, pp. 1131-1159, (1973).
- Persinger, M. A., "Geophysical Models for Parapsychological Experiences," Psychoenergetic Systems, Vol. 1, pp. 63-74, (1975).
- _____, "Geophysical Variables and Human Behavior: VIII," Perceptual and Motor Skills, Vol. 56, pp. 243-249, (1983).
- Phillips, R. D. et al., "Effects of Electric Fields on Large Animals," Third Interim Report, EPRI Report No. EA-331, Research Proj. No. 799-1, Battelle, (1977).
- _____, "Effects of Electric Fields on Large Animals," Second Interim Report, EPRI Report No. EA-458, Research Proj. No. 799-1, Battelle, (1977).

UNCLASSIFIED

UNCLASSIFIED

- Phillips, R. D. and W. T. Kaune, "Biological Effects of Static and Low-Frequency Electromagnetic Fields: An Everview of United States Literature," EPRI Report No. EA-490-SR, Battelle, (1977).
- Phillips, R. D. et al., "Effects of Electric Fields on Large Animals (Section 4, Biological Studies)," EPRI Report No. EA-331, EPRI Research Proj. No. 799, Battelle, (1979).
- Pinneo, L. R., "Electrical Control of Behaviour by Programmed Stimulation of the Brain," Nature, Vol. 211, No. 5050, pp. 705-708, (1966).
- _____, "On Noise In The Nervous System," Psychological Rev., Vol. 73, No. 3, pp. 242-247, (1966).
- Pinneo, L. R. et al., Neuroelectric Research, Chapter 43, pp. 405-428, (1971).
- Poumailloux, M., "Repercussions Humaines De L'Activite Solaire Interne," Europe Medica, Vol. 10, No. 15, pp. 1201-1214, (1969).
- "The Radiofrequency Environment," Science News, Vol. 124, p. 92, (1983).
- Ravitz, L. J., "History, Measurement, and Applicability of Periodic Changes in the Electromagnetic Field in Health and Disease," Annals New York Acad. Sci., pp. 1144-1201.
- _____, "Electrodynamic Field Theory in Psychiatry," Southern Med. J., Vol. 46, No. 7, pp. 650-660, (1953).
- _____, "Electromagnetic Field Monitoring of Changing-State Function, Including Hypnotic States," J. Amer. Soc. Dent. & Med., Vol. 17, No. 4, pp. 119-129, (1978).
- Ray, J., "Citizens Protest High Power Lines," Bull. At. Scientists, Vol. 36, No. 4, pp. 28-30, (1980).
- Roller, W. L. and R. F. Goldman, "Estimation of Solar Radiation Environment," Int. J. Biometeor., Vol. 11, No. 3, pp. 329-336, (1967).
- Sazonova, T. E., "A Physiological Assessment of the Work Conditions in 400-500-kV Open Switching Yards," Abstract, (translation from Russian), IEEE Power Eng. Soc., (1965).
- Schiefelbein, S., "The Invisible Threat," Saturday Review, pp. 16-20, (1979).
- Scott-Walton, B. et al., "Potential Environmental Effects of 76 5-kV Transmission Lines: Views Before the N.Y. State Public Service Commission," (Section II), Department of Energy Report No. DDE/EV-0056, SRI International, Menlo Park, CA, pp. II-1-28, (1979).

UNCLASSIFIED

UNCLASSIFIED

- Senseman, D. M. and B. M. Salzberg, "Electrical Activity in an Exocrine Gland: Optical Recording with a Potentiometric Dye," Science, Vol. 208, pp. 1269-1271, (1980).
- Shoenholz, S., "Commentary--High Power Lines," Bull. At. Scientists, pp. 59-60, (1981).
- Shul'ts, N. A., "Effect of Solar Activity on the Frequency of Functional Leu-kopenias and Relative Lymphocytoses," NASA Report TT F-592, (1967).
- Sidaway, G. H. and G. F. Asprey, "Influence of Electrostatic Fields on Plant Respiration," Int. J. Biometeor., Vol. 12, No. 4, pp. 321-329, (1968).
- Solon, L. R., "A Public Health Approach to Microwave and Radiofrequency Radiation," Bull. At. Scientists, Vol. 39, No. 8, pp. 51-55, (1979).
- Southern, W. E., "Orientation of Gull Chicks Exposed to Project Sanguine's Electromagnetic Field," Science, Vol. 189, pp. 143-144, (1975).
- Steneck, N. H. et al., "The Origins of U.S. Safety Standards for Microwave Radiation," Science, Vol. 208, pp. 1230-1236, (1980).
- Stoupel, E., "Solar Terrestrial Prediction--Aspects for Preventive Medicine," International Solar Terrestrial Physics (ISTP) Workshop Paper, (1979).
- Takashima, S. and T. Asakura, "Desickling of Sickled Erythrocytes by Pulsed Radio-Frequency Field," Science, Vol. 220, pp. 411-413, (1983).
- Tell, R. A., "Broadcast Radiation: How Safe Is Safe?," IEEE Spectrum, pp. 43-51, (1972).
- Teorell, T., "Application of 'Square Wave Analysis' to Bioelectric Studies," Research Paper, University Uppsala, Sweden, pp. 235-254, (1946).
- Thomas, J. R. et al., "Microwave Radiation and Chlordiazepoxide: Synergistic Effects on Fixed-Interval Behavior," Science, Vol. 203, pp. 1357-1358, (1979).
- Venkataraman, K., "Epilepsy and Solar Activity--An Hypothesis," Neurology India, Vol. 24, No. 3, pp. 148-150, (1976).
- Verfaillie, G.R.M., "Correlation Between the Rate of Growth of Rice Seedlings and the P-Indices of the Chemical Test of Piccardi," Int. J. Biometeor., Vol. 13, No. 2, pp. 113-121, (1969).
- Vogelsang, R., "A Search for Electromagnetic Cortical Stimulation," Int. J. Bioelect., p. 131, (1969).

UNCLASSIFIED

UNCLASSIFIED

Weisburd, S., "DNA Helix Found to Oscillate in Resonance with Microwaves," Science News, Vol. 125, p. 248, (1984).

Wentworth, R. C., "Enhancement of Hydromagnetic Emissions after Geomagnetic Storms," J. Geophys. Res., Vol. 69, No. 11, pp. 2291-2298, (1 June 1964).

_____, "Evidence for Maximum Production of Hydromagnetic Emissions above the Afternoon Hemisphere of the Earth, 2. Analysis of Statistical Studies," J. Geophys. Res., Vol. 69, No. 13, pp. 2699-2705, (1 July 1964).

Wertheimer, N. and E. Leeper, "Electrical Wiring Configurations and Childhood Cancer," Amer. J. of Epidemiology, Vol. 109, No. 3, pp. 272-284, (1979).

Wever, R., "Human Circadian Rhythms under the Influence of Weak Electric Fields and the Different Aspects of These Studies," Int. J. Biometeor., Vol. 17, No. 3, pp. 227-232, (1973).

Wigle, D. T., "Malignant Melanoma of Skin and Sunspot Activity," The Lancet, p. 38, (1978).

Zaffanella, L. E. and D. W. Deno, "Electrostatic and Electromagnetic Effects of Ultrahigh-Voltage Transmission Lines," (Section 3), EPRI Report No. EL-802, General Electric Company, pp. 3-1 to 3-29, (1978).

_____, "Electrostatic and Electromagnetic Effects of Ultrahigh-Voltage Transmission Lines," (Section 5), EPRI Report No. EL-802, General Electric Company, pp. 5-1 to 5-46, (1978).

_____, "Electrostatic and Electromagnetic Effects of Ultrahigh-Voltage Transmission Lines," (Section 6), EPRI Report No. EL-802, General Electric Company, pp. 6-1 to 6-3, (1978).

_____, "Electrostatic and Electromagnetic Effects of Ultrahigh-Voltage Transmission Lines," (Section 7), EPRI Report No. EL-802, General Electric Company, pp. 7-1 to 7-105, (1978).

_____, "Electrostatic and Electromagnetic Effects of Ultrahigh-Voltage Transmission Lines," (Section 8), EPRI Report No. EL-802, General Electric Company, pp. 8-1 to 804, (1978).

UNCLASSIFIED

60000-C

fact

AIR TECHNICAL INTELLIGENCE TRANSLATION

1A-Proc
B-IR
C-BR

MAGNETIC STORMS AND SYSTEMS OF ELECTRIC CURRENTS
(MAGNITNYE BURI I SISTEMY ELEKTRICHESKIKH TOKOV)

BY

N. P. BEN'KOVA

FROM

TRUDY NAUCHNO-ISSLEDOVATEL'SKOGO INSTITUTA ZEMNOGO MAGNETIZMA

NO. 10(20), 1953

LENINGRAD

159 pp.



AIR TECHNICAL INTELLIGENCE CENTER
WRIGHT-PATTERSON AIR FORCE BASE
OHIO

ATIC-262920
F-TS-8974/V

Ministry of Agriculture and State Deliveries USSR

Central Administration of the Hydrometeorological Service

TRANSACTIONS OF THE RESEARCH INSTITUTE FOR TERRESTRIAL MAGNETISM

Number 10(20)

N.P.Ben'kova

MAGNETIC STORMS AND SYSTEMS OF ELECTRIC CURRENTS

Edited by

T.S.Kerblay

Candidate in Physical and Mathematical Sciences

Giziz

State Publishing House for Hydrology and Meteorology

Leningrad 1953

P-TS-8974/V

Ministry of Agriculture and State Deliveries USSR

Central Administration of the Hydrometeorological Service

TRANSACTIONS OF THE RESEARCH INSTITUTE OF TERRESTRIAL MAGNETISM

Number 10(20)

Giziz

GIDROMETEORIZDAT

(State Publishing House for Hydrology and Meteorology)

Leningrad 1953

F-TS-8974/V

NOTE

This work by N.P.Ben'kov is devoted to a study of magnetic storms and the electromagnetic processes responsible for them. It contains a survey of the literature on this topic, a classification of storms, a description of the morphology of the phenomenon, and a calculation of the extra-ionosphere, responsible for the regular parts of the magnetic disturbances. It also contains a description of individual storms and of related electric currents. One of the Chapters is devoted to the electric currents induced by the field of magnetic storms in the conducting layers of the earth. This work is of interest for specialists in geophysics, scientific workers, postgraduate students, students taking advanced courses, and specialists in the field of ionospheric physics.

F-TS-8974/V

1

INTRODUCTION

Magnetic storms, i.e., rapid random oscillations of the intensity vector of the geomagnetic field which from time to time disturb the normal march of the magnetic elements, constitute one of the most interesting geophysical phenomena. They were first discovered at the very dawn of the development of geomagnetic research, when the only magnetic instrument available was the magnetic needle, and have long attracted the attention of both navigators and scientists. The Arkhangel'sk seafarers, sailing on voyages in the basins of the White Sea and the North Arctic Ocean, noted unexpected and random fluctuations of the needle, frequently coinciding with auroral displays in the sky. "Our little mother deceives us when the North glows" * is a well-known maritime proverb which runs back to the middle of the Eighteenth Century. At present, when not only magnetic, gyro and astro-compasses but also complex radio-navigation and radio control systems are used for marine and aerial navigation, when shortwave radio is the principal means of communication in times of peace and war, the study of magnetic storms has become of still greater practical interest, being a necessary element of the theory and application of ionospheric propagation of radio waves.

The theoretical significance of the study of magnetic storms is likewise very great and not primarily, for geomagnetism itself, in which the problem of the irregularity of the magnetic field is one of the most important. The discovery of magnetic storms is usually attributed to Hiorter who, in 1741, discovered the irregular fluctuations of the magnetic needle. There is, however, reason (Bibl.30) to assume that they were known to Russian sailors in Northern waters.

lar variations occupies a particularly important place, but also for other divisions of geophysics, such as the physics of the upper layers of the atmosphere, the study of the aurora polaris, the cosmic rays and the earth currents. Since the electromagnetic processes of the earth's atmosphere are primarily due to solar radiations of all forms, there is an intimate relation between the departments of geophysics and of heliophysics. Magnetic storms, in particular, were the first geophysical phenomena for which a correlation with solar activity was discovered and which yielded abundant material from the solution of a number of problems related to solar radiation and behavior of the active regions of the solar envelopes.

The study of magnetic storms, the regularities in their course, and the electromagnetic processes causing them, constitute the subject matter of the present work.

Section 1. General Discussion of the Theories of Magnetic Storms

Despite the great efforts made by geophysicists of several generations in studying the morphology and nature of magnetic storms, many essential questions still remain controversial. This is explained, both by the complexity of the phenomenon which requires the attentive study of a large amount of empirical material for the clarification of any regularities at all, and its intimate connection with ionospheric physics and heliophysics. A quantitative theory of magnetic storms is given its necessary empirical base only when we know reliably the composition of the upper layers of the atmosphere, the velocity and laws of motion of air masses, the laws of radiation by the undisturbed solar surface, and by the active formations of the sun. The exceptionally rapid development of ionospheric and solar physics, which owes much to the work of Soviet scientists, allows us to expect that the combined efforts of geophysicists and astronomers will lead in the near future to a solution of these problems.

But even today, the basic stages of the theory of magnetic storms have already been marked out. As far back as 200 years ago, the hypothesis was postulated that magnetic storms are caused by minute particles of matter flying from the sun. The

data subsequently accumulated on the geographical distribution of magnetic activity, on its fluctuations with time, and on its correlation with solar activity, confirm this view, and the works of a number of geophysicists (Arrhenius, Angenheister, and mainly Stoermer, Birkeland, Chapman, and Alfven) laid the scientific foundation for the corpuscular theories of magnetic storms. The existence of a corpuscular radiation from the sun, proposed to explain magnetic storms and the aurora polaris and successfully used to solve a number of other problems, still remained a hypothesis until recent years. It was only in 1950-51 that measurements of the Doppler shift of the hydrogen lines in the spectra of the aurora confirmed the penetration of a stream of particles into the upper layers of the earth's atmosphere.

The modern corpuscular theories of storms are based on a chain of independent problems, beginning with the emission of the sun's geoeffective corpuscular radiation, the dynamics and electrodynamics of the corpuscular stream en route between the sun and the earth, and ending with the electromagnetic processes taking place on the earth's surface as a result of the interaction of the corpuscular stream with the permanent magnetic field of the earth and the earth's atmosphere. The construction of the system of electric currents, which constitutes the immediate cause of the fluctuation of the magnetic field during the time of a storm, occupies a position of considerable importance among the links of this chain. The mechanism of excitation of these currents is in many respects still obscure, and the very existence of the currents has not yet been confirmed by direct observations, as has been done for the currents responsible for the regular diurnal variations of the magnetic field *. In its present phase, however, geophysics offers no other hypothesis of equal value to

* Measurements of the magnetic field at great altitudes, by means of remote-reading magnetometers installed in rockets, have shown the existence of a discontinuity in the variation of the field at the height of the E layer of the ionosphere. This discontinuity confirmed the existence of electric currents at the level of 90-105 km, which might, judging by their intensity and diurnal variation, explain the quiet diurnal variations (S_q -variations) of the magnetic field. The hypothesis of currents flowing in the upper layers of the atmosphere was postulated by B. Stewart long before the experimental detection of the conducting properties of the ionosphere by radio methods.

F-TS-8974/V

explain the field of geomagnetic variations, without assuming electric currents external to the earth's surface. According to the Chapman-Ferraro and Alfvén corpuscular theories of magnetic storms, which are widely recognized today, the excitation of these currents in the upper layers of the earth's atmosphere, and beyond it, as a result of the action of a stream of solar corpuscles is a physical reality. Other authors consider the field of magnetic disturbance to be the direct field of flying, charged corpuscles of solar origin. This view evokes two remarks. First, motion of electric charges at high velocity is identical with an electric conduction current, and thus, this view cannot be opposed to the current theory of magnetic storms; second, considerably more theoretical and empirical arguments can be opposed to it than can be cited in its favor. The ultraviolet theory of magnetic storms*, according to which the prime causes of magnetic disturbances are outbursts of wave radiation, likewise reduces the effect of the disturbance of the upper layers of the atmosphere to the formation of certain additional current systems.

For an explanation of the S_q -variations, a diamagnetic theory had been advanced previously. According to this theory, the upper conducting layers of the atmosphere, due to the rotation of charged particles about the lines of force of the permanent magnetic field are, as it were, magnetized. The magnetic field of these layers, superimposed on the permanent field, forms the diurnal fluctuations of the magnetic elements. As a result of the work by Tamm (Bibl.31) and others, this hypothesis has been recognized as unfounded. However, even if the possible existence of a diamagnetic effect were not open to fundamental objections, it would be quite impossible to use the hypothesis for explaining such complex fluctuations as are observed during magnetic storms. For any view of the mechanism of action of a geoeffective solar stream on the magnetic field of the earth, it seems that the immediate causes of the fluctuations of the magnetic field during a disturbance are electric

* This theory developed by Meyers and Hulbert, is at present time the object of violent criticism.

currents* excited in some manner outside the earth's surface itself, and by induction in its depths. Thus an explanation of the morphology and nature of these currents is of fundamental significance for the development of the theories of magnetic storms. The calculation and discussion of the electric currents responsible for magnetic storms is the primary purpose of the present work.

Section 2. The Electric Current Systems of Magnetic Storms

The problem of finding the density and configuration of the currents from the magnetic field observed on the earth's surface is, in the general case, a many-valued one. However, by calling on supplementary information from other fields of geophysics, the number of possible solutions is narrowed, leaving only one or two parameters indeterminate. For example, the very plausible hypothesis was formulated

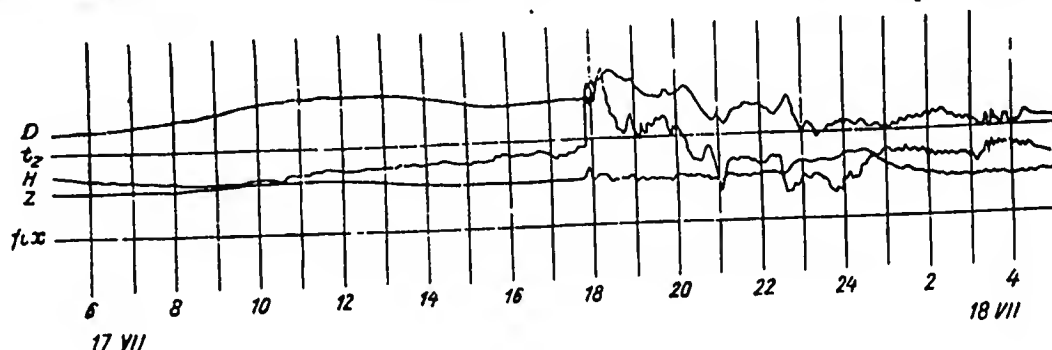


Fig.1 - Storm of 17 July 1947

Magnetograms of Krasnaya Pakhra Observatory

that the currents, responsible for the quiet diurnal variations, flow in a spherical layer concentric with the earth's surface. This allowed calculation of the system of currents of the S_q variations by means of spherical analysis and served as a basis for the formulation of the physical theories of the S_q . Only one parameter, the height of the current layer, still remained indeterminate in the calculations of the S_q -layer. Its value was found by consideration of experimental data on the ioniz-

* Not necessarily conduction currents. It is possible that the disturbances in the polar region are connected with a peculiar type of discharge currents.

0. ation of the D and E layers of the ionosphere.

2 The situation with respect to questions of the construction of the current.
4 systems responsible for the field of perturbation is considerably less favorable.
6 In spite of the large number of papers devoted to this subject, it has not yet been
8 definitively solved. The main reason for this is the above-mentioned complexity of
10 the fluctuations of the magnetic elements during a storm. If the calm (quiet) diurnal
12 variations are so regular (cf. left part of Fig.1) that a simple averaging of the
14 data for a few days in a month is sufficient to determine the law of variation of the
16 magnetic elements, magnetic storms (as will be seen from the right side of the same
18 figure) belong to those very capricious and at first glance completely random phen-
20 omena which are so abundant in geophysics. Magnetic storms are characterized not
22 only by complexity in the fluctuations of the vector of the magnetic field with time
24 (rapid fluctuations of various amplitudes and frequently of utterly irregular form,
26 follow each other without apparent regularity). The distribution of the vectors of
28 the disturbing force in space is also extremely complex. The form and amplitude of
30 the oscillations at different stations, particularly those located in different lat-
32 itudes, often bear little similarity to each other (Fig.2). The rough qualitative
34 characteristics of the field of magnetic storms (the disturbance is greater in high
36 than in low latitudes, greater in the evening than in the morning, etc.) have long
38 been known. However, in order to study with more rigor the morphology of the field,
40 by its spatial and time variations, the accumulation of a large amount of empirical
42 material was necessary, with long series of observatory data at a large number of
44 geographical points. While Schuster disposed of the annual data of seven observa-
46 tories in his calculation of the potential of the quiet diurnal variations, which
allowed him to get an idea of the system of currents that well represents the mean
features of the field, the workup of materials from 22 observatories to a few years
permitted Chapman to find only the general outlines of the morphology of the storm
field.

The second difficulty produced by the complex structure of the storm field in studying the causative electric currents, is the need for a special mathematical apparatus suitable for an analytical representation of the field and for the calculation of the current function. Spherical analysis, which is successfully used to represent the permanent field and the quiet diurnal variations, has permitted solutions of a number of fundamental problems of the structure of these fields, but it is practically useless for the investigation of fields with a complex geographical distribution.

All attempts made until now to construct a system of electric currents with fields equivalent to the fields of magnetic storms, were based on modest empirical material and were calculated by an approximate method (Chapman), or else were based on data relating to only a limited part of the earth's surface (for instance, a few polar stations) and were calculated under very narrow a priori assumptions (for instance, the postulate advanced by Birkeland, Gnevyshev, and others as to linearity of the current). As a result, these systems of electric currents do not represent (with the accuracy that is desirable for theoretical and practical problems) the geographic distribution and time regularities of the field of magnetic storms. Moreover, they have been constructed without proper division of the field observed on the earth's surface into the parts of external and internal origin, without investigating the question of potential, and without considering a number of other questions whose solution could be obtained only by means of the analytic representation of the field.

Most of the known current systems, and in particular the system of Chapman, which is cited in all manuals and textbooks on terrestrial magnetism, are average systems, equivalent to an average magnetic storm. The literature contains only few works devoted to the study of electric currents of individual magnetic storms and to the relations between the average and individual pictures. It follows from this that there is very great need for a new construction of the current systems of magnetic storms, based on the most complete possible empirical material and performed

by analytic methods.

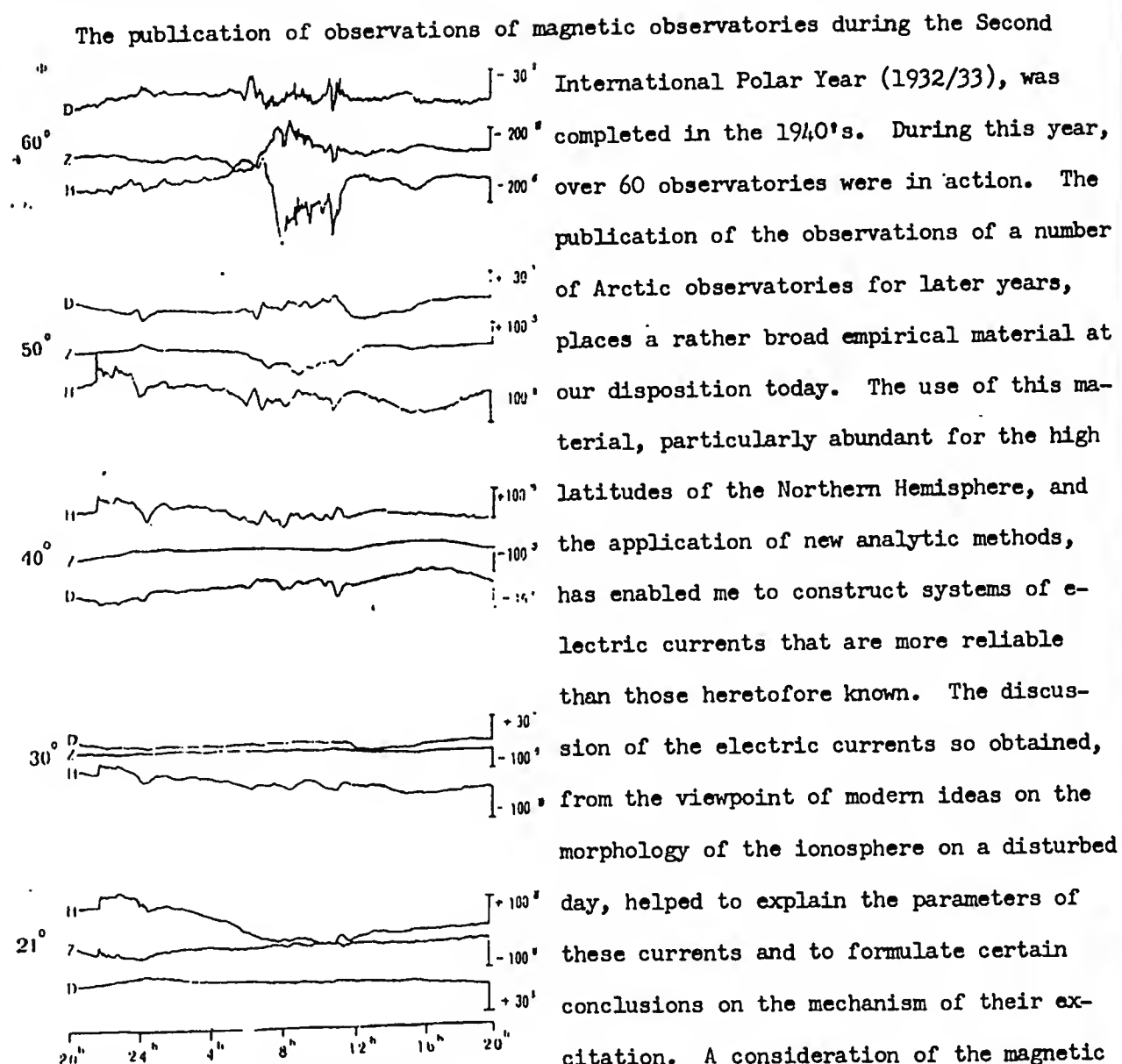


Fig.2 - Storm of 8 April 1947

Magnetograms of Observatories:

Sitka (60°), Tucson (50°),
Cheltenham (40°), San Juan (30°),
and Honolulu (21°)

result of fluctuations of an average system. The use of analytic methods made it pos-

International Polar Year (1932/33), was completed in the 1940's. During this year, over 60 observatories were in action. The publication of the observations of a number of Arctic observatories for later years, places a rather broad empirical material at our disposition today. The use of this material, particularly abundant for the high latitudes of the Northern Hemisphere, and the application of new analytic methods, has enabled me to construct systems of electric currents that are more reliable than those heretofore known. The discussion of the electric currents so obtained, from the viewpoint of modern ideas on the morphology of the ionosphere on a disturbed day, helped to explain the parameters of these currents and to formulate certain conclusions on the mechanism of their excitation. A consideration of the magnetic field on individual days made it possible to follow the development of the electric current systems of individual storms, and it was found that the current systems of individual storms may be regarded the re-

sible to divide the field of disturbance into parts of external and internal origin, and, on the basis of these parts, to judge the electromagnetic parameters of the interior of the earth.

Section 3. Content of this Report

It follows from the objects of this report, given in Section 2, that it includes two parts, a geophysical part comprising a study of the morphology of magnetic storms and of the disturbed ionosphere, and a mathematical part giving the development of practical methods of calculating the electric currents from the observed distribution of the magnetic field, to satisfy the specific requirements of our problem. The geophysical part covers the following points:

1. Classification of magnetic disturbances and separation of the perturbation field into individual parts. I consider that two groups of storms must be distinguished: world (M) and polar (P). The field of a worldwide storm, as stated by Chapman, is made up of three parts: an aperiodic part or, as it has been customarily called in all the earlier literature on geomagnetism, "the stormtime variations" (D_{st}), the disturbed diurnal variations (S_D), and the irregular part (D_i). However, the worldwide storms are always accompanied by a series of superimposed polar disturbances. The subdivision of the field of a worldwide storm must therefore be made by means of a four-term equation

$$D_{st} + S_D + D_i + P.$$

The methods of calculating the various parts of the field are described while Chapter II is devoted to the exposition of these questions.

2. Chapter III is devoted to a description of the geographical distribution of the field of D_{st} . The same Chapter gives the calculation results for the potential and currents of the field of D_{st} . The comparative simplicity of the field allowed us to use the method of spherical analysis. Two alternate systems of currents were calculated: the ionospheric layer of current, and an equatorial extra-ionospheric current ring. The ratio between the external and internal parts of the field was

obtained in good agreement with analogous data of other investigators.

3. The regularities of the S_D -variations has been considered: the dependence on geomagnetic coordinates, the role of Universal Time, the features of the distribution of S_D on the polar cap, and the longitudinal members. The external system of currents of the S_D variation was calculated by the method of surface integrals and compared with the Chapman system. The ratio of the external (V_e) to the internal (V_i) parts of the potential is discussed. We find that the ratio $\frac{V_e}{V_i}$ depends on the latitude and that its mean value is 0.89.

The above-enumerated questions are discussed in Chapter V.

4. A current system of an idealized polar storm (Chapter VI) is discussed, constructed from data of Silsbee and Vestine by expansion of the storm field into a series of Bessel functions. A resemblance of this system to the system of currents of the S_D variations was found.

5. The seasonal and 11-year fluctuations of the currents of the D_{st} - and S_D -variations are described (Chapter VII).

The current systems for individual seasons and years were calculated by approximate methods. It was found that the intensity of the D_{st} -current has cyclic fluctuations resembling the fluctuations of solar activity. The seasonal march of the D_{st} current has two waves (one annual and the other semiannual) and is completely explained from the viewpoint of the corpuscular theory of storms. The seasonal and 11-year fluctuations of the current systems of S are much more complex. The material presented by a number of observatories has shown that, during the course of the 11-year cycle and during the course of the year, both the intensities of the current eddies and the position of the auroral zone vary. The intensities of the currents in the middle and high latitudes obeys different regularities.

6. The D_{st} - and S_D -variation of the density of ionization of the F_2 layer of the ionosphere are discussed. It was found that the D_{st} -variations in the ionization of the F_2 layer cannot, either from their geographical distribution or from their

absolute value, be responsible for the ionospheric system of electric currents required for explaining the D_{st} -variations of the magnetic field. On this basis, the conclusion is drawn that the most probable cause of D_{st} -variations is an equatorial ring with a radius of 3-4 earth radii. A comparison of the S_D -currents may be explained, both in intensity and in form, under the assumption of a drift of the charged particles of the F_2 layer under the action of the earth's permanent magnetic field and of its gravitational field. Chapter VIII is devoted to an exposition of these questions.

7. The electric systems of currents of individual magnetic currents are calculated in Chapter IX. It is found that in all cases the currents, at a given instant of time, may be represented as the result of the superimposition of typical systems of D_{st} -, S_D -, and P-currents. However, the intensities and configurations of the D_{st} -, S_D -, and P-currents vary within wide limits from case to case.

8. The external (principal) part of the field of magnetic disturbances induces, secondary currents in the inner conducting parts of the earth, which in turn influence the magnetic field observed on the earth's surface. The separation of the potential of the field of D_{st} and the potential of the P-storms into an external and an internal part made it possible to calculate the conductivity of the deep parts of the earth and the thickness of the upper nonconducting layer. The calculations were made under three assumptions: 1) the conductivity of the deep parts of the earth is constant; 2) the conductivity increases with depth; and 3) the currents induced in the oceans and wet soil are allowed for. For the estimate of conductivity we use not only the data on the P-storms and the first harmonic of the D_{st} -field, but also the data on the S_q -variations. The results so obtained on the variation of conductivity with depth differ somewhat from those of previous authors and are in good agreement with modern ideas on the internal structure of the earth, based on seismic data. The division of the field for the harmonic P_3 of the D_{st} -variations cannot be

explained within the scope of the Chapman-Price induction theory. Chapter X is devoted to these questions.

The mathematical part of the work includes the following factors:

1. The method of surface integrals proposed by Vestine in 1941 was used for calculating the external and internal potentials of the S_D -field. This method, which is used for the first time in geomagnetism, required the development of practical methods of processing the material and of a technique of computation.

2. The author of the present work has proposed a method of calculating the current function on a sphere with a radius of a , if the potential observed on the surface of a sphere $R(R < a)$ is assigned in numerical or graphical form. The method is based on finding the current function for regions internal with respect to the sphere R , and on its extrapolation to outer space. The finding of the current function from the known potential on the sphere leads to the solution of the inner Dirichlet problem by the aid of a Fredholm equation of the second order. Practical calculation methods were worked out. The method is applied to a calculation of the currents of S_D . The questions connected with the integral method of analysis are discussed in Chapter IV.

The principal conclusions from the work are collected in the Conclusion.

Chapter I is devoted to a survey of the literature. Since this work is primarily devoted to questions of the morphology of the perturbation field and of the construction of the electric currents equivalent to it, out of the wide and varied literature on magnetic disturbances only studies devoted to the solution of these very questions are mentioned in the survey. Works devoted to other divisions of the theory of magnetic storms, to descriptions of individual phenomena, or to statistics of magnetic activity are not considered in the survey.

The equations are separately numbered in each Chapter. In referring to an equation given in the same Chapter, only its number is stated. In referring to an equation from a different Chapter, its number and the Chapter number are given.

CHAPTER I

SURVEY OF THE LITERATURE

Section 1. Basic Properties of Magnetic Storms. The Works of Birkeland

The magnetic field of the earth is rarely completely quiet. Very often, the smooth march of the magnetic elements, due to the quiet periodic variations (solar-diurnal, S_q ; lunar-diurnal, L ; annual, A) is disturbed by irregular fluctuations of varied form and amplitude. Any deviations of the magnetic field from the normal march are called disturbances. Some of them are so small (tenths and hundredths of a gamma) as to be detected only by special high-precision instruments (Bibl.16). The strongest disturbances, expressed in large and sharp fluctuations of the magnetic elements and lasting from several hours to several days, are called magnetic storms. Storms are observed simultaneously either over the entire earth or, at least, in the high latitudes. The amplitudes of fluctuation of the elements during extremely strong storms exceeds 1,000 γ in the middle latitudes and 2,000-3,000 γ in the high latitudes. During the time of a medium (moderate) storm, the fluctuations are of the order of 200-400-to 500-1,000 γ depending on the latitude. The rate of variation of the elements likewise fluctuates over a wide range, sometimes exceeding a few tens of gammas a second. Occasionally, very slow and smooth variations of the elements are observed (especially in the low latitudes, in the Z-component). The fluctuations of the magnetic elements during a storm are so diverse that, during the entire period over which the observatories have been recording the magnetic elements, i.e., for over 100 years, no two identical storms can be found.

Despite such randomness of fluctuations, statistical regularities obeyed by magnetic storms have long been known. These regularities are as follows: The intensity of storms (characterized by the frequency and amplitude of the fluctuations, the mobility of the curves, and the magnitude of the deviation from the normal values) depends on the latitude. It reaches its maximum values in the high latitudes, in the zone of maximum visibility of the aurora; as the pole is approached, the degree of disturbance again decreases. The number and intensity of the storms has a seasonal march with maxima at the epoch of the equinoxes, and also has an 11-year cycle. The maxima of the magnetic cycle lag 1-2 years behind the maxima of the solar cycles. There is a correlation between individual magnetic storms and the manifestations of solar activity: sunspots, flares, eruptions. This correlation is of a statistical nature for the weak and moderate storms. The strong storms, as a rule, are uniquely related to solar phenomena. Tendencies to a repetition of storms after a synodical revolution of the sun and to a lag of storms behind the passage of an active region across the central meridian, have been noted. Finally, the distribution of the intensity of a storm during the course of the day, the "diurnal march of magnetic activity", has been found.

An extensive section of the literature has been devoted to these regularities, and served, as already stated, as the basis for the development of the corpuscular theories of magnetic storms. Considerably fewer papers have been devoted to the study of the structure of the field of the storm field itself. A.Schmidt and van Bemmelen (Bibl.40) were among the first investigators who attempted to find the regularities obeyed by the storm field. According to them, the vector of the disturbance systematically varies its direction during the course of the storm, and the "eddies" into which the storm is divided are displaced along the earth's surface. Without taking up this idea of the storm in detail, based as it was on the erroneous assumption that storms are local and of terrestrial origin, let us turn to an exposition of the memoirs of Birkeland (Bibl.38), which have not lost their significance even

today. Having set himself the problem of studying the distribution of the vector of disturbance over the earth's surface and of explaining the origin of the storms, Birkeland commenced his investigations by accumulating observational data. He understood the particular importance of high-latitude observations and organized two special expeditions, in 1899/1900 and in 1902/03, during which a special system of temporary stations, provided with apparatus of the same type and operating under a common program, was used. In working up this material subsequently, Birkeland compiled, for several storms, maps of the geographical distribution of the vector of disturbance for successive most characteristic instants of time. Birkeland defines the vector of disturbance as follows: $F_d = F - F_n$, where F denotes the observed value of the magnetic field and F_n the normal undisturbed value. The construction of these "synoptic" maps showed Birkeland that, despite the apparent randomness of the fluctuations of the magnetic elements, a certain systematic character is manifest in the distribution of F_d . The vectors at closely adjacent stations are almost parallel; a definite relation exists between the vectors and the longitude of the station and, in particular, the latitude. Birkeland divided the listed magnetic storms, about 30 cases in all, into five types. Type 1, the most frequent, is characterized by the almost everywhere negative horizontal component of the vector F_d . The maximum magnitude of the vector is reached in the polar zone, declines sharply in the middle latitudes, and again increases somewhat in the equatorial belt. Storms of this type were called negative equatorial storms by Birkeland. Type 2, positive equatorial storms, are storms with a positive horizontal component of F_d ; the least disturbance embraces all latitudes, but its value is usually much weaker than the disturbance of negative storms. This type was rarely observed. Type 3 and 4 are positive and negative polar storms and are characterized by the fact that the vector of disturbance reaches high values only in the high latitudes, while the magnetic field of middle and low latitudes remains in fact almost undisturbed. Type 5, the cyclo-median storms, of small value, reach their greatest development on the daylight side of the

earth in low latitudes. As Chapman later pointed out, the cases of disturbances classified by Birkeland as Type 5 would be more correctly included among the bay disturbances accompanying sudden ionospheric disturbances and due to outbursts of ultraviolet radiation. These bay disturbances are anomalous intensifications of these S_q -variations, but not ordinary disturbances of corpuscular origin.

With respect to the equatorial storms Birkeland confined himself to the hypothesis that they were presumably due to certain systems of electric currents flowing not far from the equatorial region, and devoted all of his attention to a study of the polar storms. The most characteristic feature of the polar storms is a sharp increase of the H-component of the vector of disturbance and the passage of the Z-component through zero in the auroral zone. From this, Birkeland concluded that the polar storms were caused by a powerful linear current flowing at a certain height along the zone. Elementary counts, based on the use of the Biot-Savara law, allowed Birkeland to make an approximate estimate of the height (100-300 km) and the intensity (1×10^5 to 9×10^5 amp) of the current. The short duration of these storms (lasting from one to several hours) forced the assumption that the extension of the current along the zone is short: 10° , or a few tens of degrees. Birkeland postulated that his horizontal current was a part of a U-shaped current system, whose vertical branches extend beyond the limits of the atmosphere. The diagram of a typical field of a polar storm (Fig.3) shows the distribution of horizontal projections of the lines of force of the magnetic field (the solid curves), a graph of the variations of the vertical component (the lower part of the figure), and the system of isopotential lines (the broken lines). The hypothetical linear current flows in the direction of the principal axis of the disturbance, marked by the arrow. The maximum value of the vector H_d , as will be seen from the diagram, should be observed at the point C, the center of the disturbance.

The question of the closure of the Birkeland current system remained open, assuming the possibility of the existence, at a great distance from the earth, of a

very diffuse branch closing the current system, and also assuming the possibility of an unclosed system.

This current system is in agreement with the views of Birkeland and Stoermer on the origin of magnetic storms. According to the well-known Stoermer-Birkeland theory,

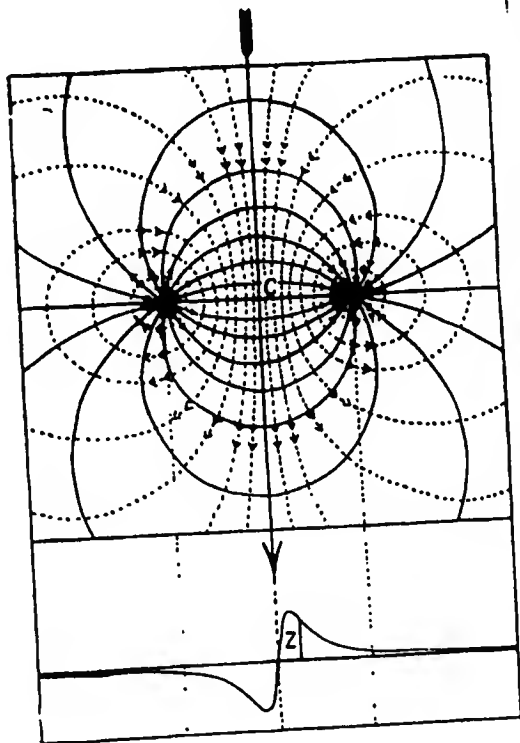


Fig.3 - Diagram of Magnetic Field of an Elementary Polar Storm (according to Birkeland).

The arrow shows the direction of the principal axis of the disturbance (C = Center of Disturbance; — Lines of Force; - - - Equipotential lines; Z = Vertical component of the storm field)

which is frequently set forth in the literature, the storm field is the field of a solar stream of charged particles of a single sign, deflected by the earth's magnetic field toward the polar zones. Solving the equation of motion of a charged particle, Stoermer calculated the possible forms of the paths and, in particular, obtained paths explaining the above described U-shaped current: the particles, moving along these paths, approach the earth from space, penetrate the atmosphere in the high-latitude region down to a height of 100-300 km, take a horizontal segment of their path in the atmosphere, as a rule along the auroral zone, and then once more leave the neighborhood of the earth. Experimental studies by Brueche (irradiation of a magnetized sphere by a narrow beam of cathode rays), which allowed him to follow the paths of individual particles, confirmed the possibility of such paths and thereby gave still greater significance to the Stoermer-

Birkeland theory. This theory is thus an attempt to systematize the data on magnetic disturbances, to establish an idea of the typical picture of a disturbance, to calculate the electric current equivalent to it, and to explain its origin. The

criticism of the physical bases of this theory is commonly known. Serious objections to the theory (a stream of particles with only a single sign could not reach the earth, due to the electrostatic repulsion of the particles; the invasion of the earth's atmosphere by particles of a single sign must lead to great fluctuations of electric potential during a storm, etc.) forced the various investigators subsequently to abandon the hypothesis of a singly-charged stream. Let us discuss the remarks provoked by the morphological part of the study. Since Birkeland's system of station was located in a narrow longitudinal sector of the Arctic (Iceland, Spitzbergen, Norway, Novaya Zemlya), he did not discover the fact that positive and negative polar disturbances are always observed simultaneously, but in different hemispheres. In reality, however, a polar disturbance usually covers all the longitudes of the polar region, the direction and magnitude of the vector of disturbance being different at different longitudes. It would thus seem more expedient to construct the system of electric currents determining the distribution of the magnetic field at all longitudes. Further, Birkeland had too small an observational material on the course of disturbances in moderate latitudes. The morphology of the equatorial storms therefore remained actually unstudied by him, and he did not get a clear idea on the currents responsible for them. The classification of storms introduced by Birkeland, as shown below, likewise does not seem usable.

Section 2. Chapman's Investigations and their Revisions

A completely different approach to the study of the morphology of magnetic storms is contained in the works of Chapman (Bibl.40). As far back as the beginning of the Twentieth Century, the works of Moos, Director of the Bombay Magnetic Observatory, contained indications that, during the storms, the horizontal component first increases (first phase of the storm), then decreases below the normal (second or chief phase, during which the fluctuations of the magnetic elements are greatest) and then slowly return to the normal state. The return to the normal state [in the literature, various terms are used - restoration phase, aftereffect, Nachstoerung,

postperturbation, and noncyclic variation noncyclic change] takes several days, even when the field is no longer disturbed by irregular fluctuations. The work of Moos gave Chapman ground for postulating that the storm field contains regular parts, for which certain stable systems of electric currents influencing the distribution of the vector of disturbance of the entire earth are responsible. The varied fluctuations of these currents result in the individual features of each storm, the random fluctuations superimposed on the average picture of the magnetic variations. Chapman worked up the variations of the magnetic elements H, D, and Z for 22 observatories located between 22° and 60° North Latitude. His calculations consisted in averaging of the values of the magnetic elements by hours, counting from the beginning of the storm. As a result of averaging a rather large number of cases (Chapman used the data of 40 moderate storms), the influence of the irregular fluctuations and of the regular part of the disturbance connected with the local time was to a large extent eliminated. He succeeded in finding the regular part of the storm field taking place at the same World Time at all longitudes of the same latitude. He termed this part of the field of a magnetic storm, the stormtime variations, i.e., the variations taking place according to a time reckoned from the beginning of the storm. During the 1930's and 1940's, the English term "stormtime variations" was still used in the Russian literature on terrestrial magnetism to designate this part of the storm field. It seems to us preferable to use the term "aperiodic disturbed variations" as we will do in future, while retaining nevertheless the symbol D_{st} -variations or D_{st} -field which is generally used today in the world literature. The D_{st} -variations of the H- (or X) component at all latitudes (or at least at the middle latitudes) were described similarly by Moos for Bombay. The D_{st} -variations of the Z-component, on the other hand, reduced to the decrease of the element in the first phase of the storm and to its increase in the second stage. The amplitude of the D_{st} -variations of the Z-component is smaller than the amplitude of the H-component. No regular aperiodic part could be found in the element D. During the entire storm, the fluctuations of

D, no matter how large they were, usually take place about the normal value of the element. This is evidence that the horizontal component of the vector of disturbance on the average is most often directed along the magnetic meridian. The D_{st} -variations during the course of moderate and great magnetic storms are the same in form and differ only in intensity. This made it possible for Chapman to conclude that the average picture of the D_{st} -variations was constant (or, more accurately, stable).

In analyzing the classification of storms proposed by Birkeland, Chapman concluded that the positive equatorial storms of Birkeland correspond to the first phase of the ordinary storm, and the negative ones to the second phase. The insufficiency of the material, in Chapman's opinion, prevented Birkeland from noting that the two types of storms are in reality only two successive phases of a single phenomenon. The averaging of the value of the magnetic elements (after eliminating the D_{st} -part for each storm) in accordance with the hours of the local days allowed discovery of the relation of the field of the magnetic storm on the time of day. This second regular part of the field of a magnetic storm is customarily termed the disturbed diurnal variation (abbreviated S_D). The existence of regular diurnal variations on days of magnetic storms, differing from the diurnal variations on quiet days, was noted, independently of Chapman, by a number of investigators. Chapman's calculation showed the existence of the S_D -variations in all the elements, and their regular change with latitudes. A characteristic feature of the S_D -variations in the H and Z components in the temperate latitudes is the minimum value of the elements in the morning hours and the maximum values in the evening.

The third part of the storm field, in Chapman's opinion, is the irregular fluctuations (D_1) superimposed on the regular parts and giving a random appearance to the variation of the magnetic field on disturbed days. Considering the regular parts of D_{st} - and S_D - to be the principal and most interesting parts, Chapman directed his efforts toward their further investigation, leaving the irregular part aside. Considering that the D_{st} - and S_D -variations we have described to be due to

electric currents flowing near the earth's surface (in the atmosphere itself or beyond it), Chapman formed an idea, from the observed magnetic variations, of the configurations and intensities of these currents. His systems of electric currents of magnetic storms entered the geophysical literature as the most probable representation of the electric currents, and served as a starting point for the development of the modern theoretical views on the nature of the phenomenon. His systems were constructed by an approximate method, without calculating the potential of the observed fields of variations. He started out from the following postulates:

1. By analogy with the S_Q -variations it may be assumed that the field of D_{st} or S_D observed on the earth's surface is the result of the composition of an external main field and an internal field due to induction in the conducting part of the earth. The ratio of the external field E to the internal field I , i.e., $E/I = 3/2$.
 2. The external system of electric currents is a spherical nonuniform current layer concentric with the earth's surface. The height of the current above the earth's surface $h = 200$ km.
 3. The direction and density of the current may be calculated from the observed magnetic field by the Biot-Savara law, by replacing at each point the action of the nonuniform spherical layer by the action of a uniform, plane current sheet of infinite extension. The current systems of the D_{st} - and S_D - variation so obtained are presented in Figs. 4a and 4b. It will be seen that the D_{st} currents flow everywhere westward in the direction of the parallels of latitude. The intensity of the current increases somewhat in the equatorial region, and increases strongly in the polar cap. The current along the auroral zone is represented in the form of a linear current of high density. The total intensity of the current flowing in each hemisphere is 200,000 amp; the current lines on the figures are drawn in such a way that a current of 10,000 amp flows between adjacent lines. During the first phase of magnetic storms (increasing H) the current should flow in the eastern direction.
- The current system of the S_D -variations is much more complex. An analysis of

the material as shown that on the whole the field of S_D -depends on the latitude and local times. For this reason, without taking into account the possible slight longitudinal asymmetry in the distribution of the field, Chapman constructed the current system in the same way as the system of the S_q -currents, i.e., fixed, if viewed from the sun. In order to explain the variation of the magnetic elements during the course of the day, the earth must be imagined to rotate inside this fixed system. The system S_D consists of four current loops in the moderate latitudes and a layer of almost parallel currents flowing about the polar cap. As in the case of D_{st} , an increased intensity of the current is observed in the auroral region. The currents presented in Figs. 4a and 4b correspond to a moderate magnetic storm with decrease of H in the principal phase equal to about 40 γ . During very strong storms, the currents can be expected to increase by a factor of 10-15.

The systems of currents of D_{st} and S_D , according to Chapman, call forth the following remarks:

1. The empirical material that served for their construction is, absolutely without question, insufficient. If the workup of the data of 22 observatories gave a sufficient idea of the distribution of the D_{st} - and S_D -variations in the moderate latitudes, then the regular part of the storms in the high latitudes would still remain in fact, unknown. Chapman judged the intensification of the D_{st} -variations in the auroral zone by the geographic distribution of the value of D_m . The symbol D_m denotes the difference between the mean diurnal values of the horizontal component on disturbed and quiet days, that is, $D = \bar{H}_q - \bar{H}_d$. Since the principal effect of the aperiodic storm variations reduces down to the decrease in the horizontal component, it follows that the difference of the mean diurnal values of H on quiet and disturbed days may serve as a certain characteristic of the value of the D_{st} -variations. Chapman judged the S_D -variations inside the zone by the diurnal march for all days, at the Antarctic Station of Cape Evans. The data from observatories lying in the auroral zone itself were not fully available to Chapman. As shown by the

materials collected by us for a number of high-latitude stations (cf. Chapter V), the distribution of variations is in reality somewhat different.

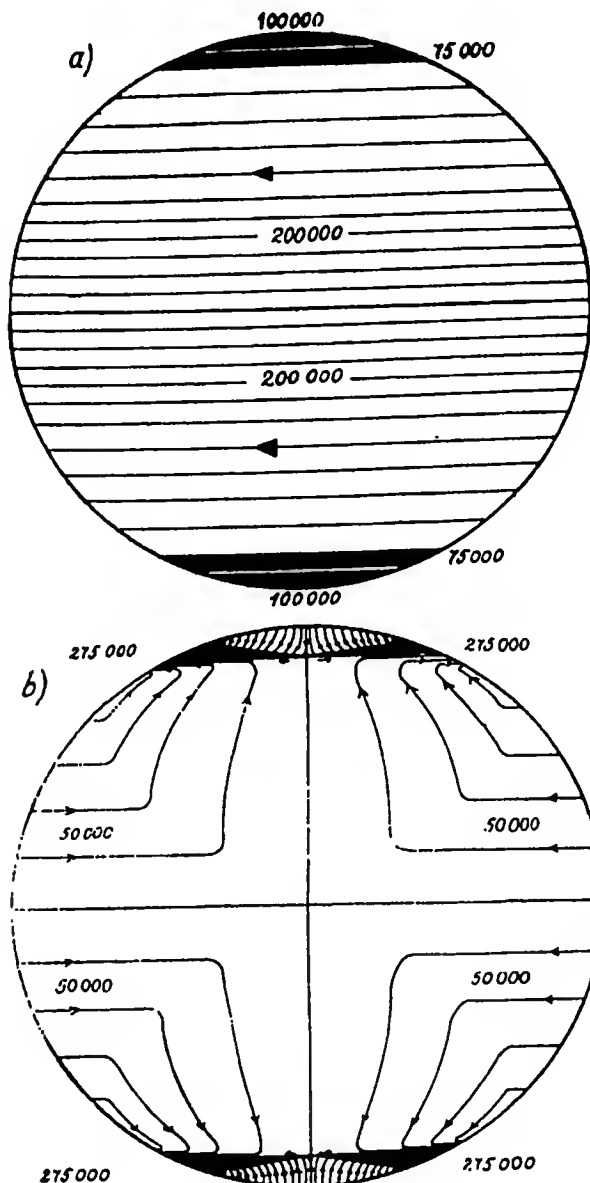


Fig.4 - Currents of the Regular Parts of the Storm Field (after Chapman).
Current strength in amperes (a - D_{st} -Variations; b - S_p -Variations)

2. The systems constructed by Chapman actually corresponds to worldwide storms (those observed over the entire earth). The absence of a distinct boundary line between world wide and polar storms (Chapman did not pay proper attention to the question of the classification of storms) lead to a certain distortion in the current systems in high latitudes (cf. Chapter II and III).

3. My own calculations of the potential of the external and internal parts of the S_D -variations have shown that the ratio I/E is not the same at all latitudes, and that in any case, the value $I/E = 0.6$ adopted by Chapman is exaggerated.

4. The height of the currents $h = 200$ km seems too low, which in turn would affect the numerical values of the current intensities found.

On comparing the Chapman and Birkeland systems, Vestine, in his paper written in collaboration with Chapman (Bibl.60) states that the Chapman system better reflects the actual course of a storm, and that the

Birkeland system does not withstand the test of comparison with empirical data. It seems to me that in comparing the Chapman and Birkeland systems it must above all be

borne in mind that these systems are responsible for different types of disturbances and have been constructed from material that is not entirely of full value: Chapman had almost no data on the high latitudes available to him, while Birkeland made little use of information on the course of disturbance in the middle and low latitudes.

The question of the necessity of verifying and elaborating the Chapman system from more complete magnetic data and applying more accurate methods to the calculation of the currents has repeatedly been raised in the literature. The most exhaustive revision made in the above mentioned work by Chapman and Vestine. Up to 1937, (the work was published in 1938) certain worked-up materials of magnetic observations made during the Second International Polar Year (II MPG 1932/1933) were available to the authors. In particular, there were observations within the auroral zone (the Thule and Godhavn Observatories) and immediately in the region of that zone (Bear Island, Matochkin Shar, etc). The values of the D_m - and S_D -variations had been calculated for all observatories, the S_D -variations being taken as the difference between the diurnal marches for international disturbed and quiet days*. This method of calculating S_D involves very little work and was subsequently used by a number of investigators.

The mathematical difficulties connected with the calculation of the electric currents corresponding to magnetic fields as complex in geographical distribution as S_D and D_{st} , forced the authors to abandon the solution of the direct problem (calculation of the currents from the observed field) and to take up instead the inverse problem (calculation of the magnetic field of the Chapman system of currents and its comparison with the observed field). For this purpose, the current systems of Figs. 4a and 4b were broken down into several principal forms: S_1 , surface current in the

* The International Association for Terrestrial Magnetism and Electricity, since 1905, has been selecting, from the magnetic characteristics of a worldwide system of observatories, the five quietest and the five most disturbed days in each month.

0 polar cap in the D_{st} -system; L_1 , linear current in the auroral zone in the D_{st} -system;
2 S_2 , current layer between two zones; etc. The magnetic field of each component part
4 of S , L , etc. was separately calculated by applying the Biot-Savara law to the el-
6 ements of the current and performing the corresponding integration over the surface
8 or outline. This method led to rather complicated computational work and made major
10 simplifications necessary. As an example we may say that the evaluation of the mag-
12 netic field of the L_1 -current, assuming it to be of circular form, led to the calu-
lation of integrals of the type $\int_0^{2\pi} \frac{p - a \cos \varphi}{r^3} d\varphi$, which are reduced to tabulated el-
liptic integrals; the surface currents over the polar cap in the middle latitudes
were assumed to be plane, and the evaluation of the surface currents S_4 (the middle-
latitude eddies in the S_d system) was not performed at all. As a result of graphic
integration, curves of the latitude dependence of the components of the S_d and D_{st}
fields were obtained. Their comparison with the observational data showed that the
Chapman systems do not contradict them, but still did not remove the question of the
desirability of a new construction of the systems, using all available material.

An attempt to elaborate the Chapman system was made in the paper by Vestine
(Bibl.58), based on the same starting material as the above-discussed work. It was
found that the Chapman systems had been constructed without allowing for the lati-
tudinal asymmetry in the distribution of the field. In the low and medium latitudes,
this asymmetry is actually small, but it is impossible to ignore it in the high lati-
tudes. Vestine expressed the very interesting thought that the asymmetry in the high
latitudes is due primarily to the noncoincidence between the magnetic and geographic
axes of the earth due to which fact the auroral zone is of an elliptical shape in-
stead of circular and is elongated in the direction of a line joining the magnetic
and geographic poles. For this reason, if we allow for the distance of a given point
of observation from the auroral zone, instead of simply taking into account the geo-
magnetic latitude of the point, then the longitudinal asymmetry is considerably dim-
inished. Vestine, on the basis of the magnetic data, determined the location of the

zone of linear polar current, which he found to be rather close to the position of the maximum isochasm obtained as early as 1867 by Fritz (for more details see Chapter V, Section 7). Thus Vestine's work not only solved certain questions as to the morphology of the S_D - and D_{st} -variations, but also disclosed the possibility of using magnetic data for pinpointing the position of the auroral zone. The magnetic data, being the result of continuous recording independent of the meteorological conditions can provide more reliable conclusions than those based on auroral statistics.

Among the worth that followed the investigations by Chapman, the paper by Chynk (Bibl.41) is worth mentioning. It points out the existence of a seasonal asymmetry in the distribution of the field of D_{st} -variations. According to Chynk, the seasonal march of D_m has a maxima in spring and autumn, like various measures of magnetic activity. However, in addition, it also has another maximum in the winter.

Section 3. Analytical Representation of the D_{st} -Variations

Attempts at an analytical representation of the potential field of disturbance are also contained in the geomagnetic literature. These attempts related only to the simplest part of the storm field, the aperiodic disturbed and noncyclic variations or, more exactly, only to the middle-latitude parts of these fields. All known papers on this subject (cf. Bibl.40 and 15) followed a definite object, namely separation of the observed field into an external and internal part, explanation of the internal part on the basis of the induction hypothesis, and definition of the conductivity in the depths of the earth required for such an explanation. Chapman and Whitehead calculated the external and internal potentials of the D_{st} -variations by expanding the spherical functions of the H and Z components of the field into series from the same data that had been used by Chapman for his approximate calculation of the D_{st} -currents. Since it was assumed that the field of D_{st} depends only on universal time and geomagnetic latitude, it followed that the values of the potential for a definite instant of time were represented by series of Legendre polynomials, and, since the potential was supposed to be symmetric with respect to the equator,

only the odd harmonics were retained in the series of polynomials. Thanks to the fact that the distribution of the D_{st} -field in the high latitudes was not taken into account, it was possible to represent the middle-latitude part of the field rather well by the three first harmonics P_1 , P_3 , and P_5 . The division of the field into an external and internal part (see Chapter III for more details) gave the following ratio: $I/E = 0.39$. It turned out that this ratio requires, for the explanation of the I-part within the framework of Lamb's induction theory, somewhat different electromagnetic parameters of the earth than those that follow from an analysis of the S_q -variations. A more detailed analysis of the results obtained by Chapman and Whitehead and other authors, and a comparison of those results with our own calculations, will be given in Chapter X.

McNish and Slautsitays, who performed the spherical analysis of the values of D_m , calculated the intensity of the external currents corresponding to those values and obtained interesting conclusions as to the ratio between the internal and external part.

No attempt has been made to date at an analytical representation of the distribution of the potential of the S_D -variations or of the irregular part of the disturbance.

Section 4. Position of the Points of Magnetic Storms. The Equatorial Ring

The papers enumerated in the preceding Sections exhaust all the studies of the morphology of the regular parts of the perturbation field and the calculation of the surface currents responsible for them. It goes without saying, however, that the construction of these systems is not a proof for their existence. If we make no supplementary postulates, then the problem of finding the currents from the magnetic field is an indeterminate, many-valued problem, and an infinite number of such systems can be calculated, each of a different configuration or at a different distance from the earth, whose field will likewise well represent the observed field of magnetic storms. The postulate made by Chapman, however, that the layer carrying

the currents is spherical appears entirely reasonable in the light of our knowledge of the structure of the ionosphere. In fact, if we assume for example that the height of the layer varies with the latitude or with the local time, by 100 km, then this would mean a variation of only 1.5% in the radius of the spherical surface. Under the assumption that the current layer is spherical, its radius (or the height of the current above the earth's surface) can be theoretically determined from the magnetic data just like the configuration of the lines of current or the intensity of current. If we assume that the field potential is represented by a series of spherical harmonics, then the cofactors of the expression $(\frac{a}{R})^n$ enter into each term, where a is the radius of the spherical current layer and R the radius of the earth. Then, by comparing the weight of the n_1^{th} , n_2^{th} , etc. terms in the expansion, the value of $\frac{a}{R}$ can be estimated. In practice, however, in view of the low accuracy in determining the coefficients with spherical functions, it is impossible to determine $\frac{a}{R}$ with an error of less than a few percent. Thus, to define the layer of the ionosphere in which the D_{st} -currents flow, using a spherical analysis of the type proposed by McNish and Slautsitays as basis, would hardly be possible. For any conclusion as to the height of the current layer, data on the structure of the ionosphere would have to be used, together with an attentive study of the structure, ionization density, number of collisions, and other parameters of the ionosphere, which would help to answer the question as to how far a certain layer meets the requirements that a current-carrying layer must meet. While it seems almost unquestionable today that the currents of the S_q -variations must be related to the lower part of the E layer and the D layer, there are still doubts as to the perturbation currents. The hypothesis that the disturbance currents are concentrated in the F_2 layer seems the most probable, since this layer shows the closest correlation with the magnetic disturbances. Nevertheless, in discussing the possible position of the S_D -currents, Chapman pointed out that their most characteristic feature was the evening maximum of intensity, while a maximum of ionization density in the evening is not observed

in a single one of the known layers*. In view of this, the question of the height of the S_D -currents remain unexplained in the papers of Chapman and his colleagues. As for the currents causing the D_{st} -variations, the thought is developed in the papers of Chapman and a number of other authors that these currents flow far beyond the limits of the earth's atmosphere, encircling the earth with a ring located in the equatorial plane. The idea of an equatorial ring current was first expressed by Störmer to explain the great polar distance of the auroral zone ($\theta_0 = 22 - 23^\circ$). The calculation of the paths of the particles under reasonable assumptions as to their velocities, and allowing only for the permanent magnetic field of the earth, leads to much lower values of θ_0 , equal, for example, to -2 to -4° for cathode rays, and to -16° to 19° for alpha particles. The magnetic field of the ring current in a westerly direction, reducing the horizontal component of the geomagnetic fields, leads to an increase of θ_0 to the necessary values. There are also other geophysical arguments in favor of the existence, in storm time, of an extra-ionospheric current ring. But it is precisely the great regularity in the course of the magnetic storms in the low latitudes (where the irregular fluctuations distort the quiet march of the elements only slightly and where the return of H to the normal state, is slow) that make both these phenomena difficult to explain under the assumption of an ionospheric location of the sources of the field. Forbush (Bibl.43), in studying the correlation between the magnetic storms and the cosmic rays, discovered such variations in the intensity of the cosmic rays as confirm the generation, at a certain distance from the earth, of a magnetic field diminishing the H component of the earth's magnetic field. A detailed theoretical consideration of the possible influence of the equatorial ring is also presented in the papers by Vallarta and Hess (Bibl.35). In recent years, a number of papers devoted to the effect of magnetic storms on the

* We will show later that the disturbed diurnal variations of ionization density of the F_2 layer satisfy this requirement, and thus eliminate the objection against placing the S_D currents in the F_2 layer.

cosmic rays have been published, most of them likewise confirming the Forbush hypothesis.

According to Stoermer's calculations, the ring should be of a very great radius, of the order of the distance from the earth to the moon, and should be formed as a result of the curvature of the paths of charged solar particles by the earth's magnetic field; the ring is not necessarily a closed one. The energy of such a ring must be great (current strength $\sim 10^7$ amp). As an argument in favor of Stoermer's calculated parameters, the "universe echo", i.e., the great delay of a radio signal returning to the earth, has sometimes been advanced. It has been supposed that, in passing through the ionosphere, a radio signal is reflected from the Stoermer electronic current*.

All later papers, however, express a different idea on the equatorial ring. Thus, according to the Chapman-Ferraro theory of magnetic storms, the solar stream, encountering the earth's magnetic field, forms a ring of much smaller radius, of the order of two to four earth radii. Since the corpuscular stream is assumed by these authors to be neutral, it follows that the formation of a ring current is explained by the difference in the velocity of motion of the positive and negative particles. The papers by Chapman and Ferraro contain no rigorous mathematical treatment of the question as to the formation of a ring out of the bodies of the corpuscular stream. They give only a system for the physical explanation of the process based on the retardation of the stream by the magnetic field of the earth**. The question as to the stability of a ring, if such a ring is actually formed, is treated with considerable rigor, explaining the conditions of dynamic equilibrium of the ring (i.e., determining the allowable fluctuations of radius and current density) and demonstrating the

* Special observations made in 1947-1949 with high-power transmitters (Bibl.65), failed to detect greatly lagging echoes.

** The USSR literature contains expositions of the Chapman-Ferraro theory [cf. for example, Eygenson (Bibl.34)].

impossibility of a prolonged existence of a ring with Störmer's parameters. In 1951, Martin (Bibl.48) considered the process of formation of the ring on the basis of the analogy between the electrodynamic processes connected with the motion of plasma in the magnetic field and hydrodynamic phenomena. The ionized stream flowing around a magnetic dipole is compared to a stream of incompressible fluid flowing around a body submerged in the fluid; in this case, the pressure due to the interaction between the electric currents induced in the body of the stream, with the magnetic field is identified with the hydrodynamic pressure. The parameters of the rings so obtained ($a = 5.5 R$ and $I = 10^6$ amp) proved to be of the same order as those calculated by Chapman and Ferraro. The literature also contains an attempt at determining the radius of the ring directly from empirical data, independent of any theoretical views on its formation. As is generally known, one of the most widely used characteristics of magnetic activity is the u-measure, equal to the difference between the diurnal values of the horizontal component on successive days. Considering that the descent of H during a storm, and, consequently, the value of the u-measure, is due to the magnetic field of the equatorial ring, the day-to-day variability of H may be equated to the increase in the horizontal component of the field of the current ΔH , thus permitting an evaluation of the ring parameters a and I , Yu.D.Kalinin (Bibl.19), who made these calculations under the assumption that the increment ΔH was due either to the variation in a from day to day (with the constant I), or to the variation in I (with the constant a), found that the radius of the ring must be of the order of two to four earth radii. As shown below in Chapter III, the spherical analysis of the field of D_{st} permits determining the quantities a and I independently, without assuming invariability of one or the other.

The above-mentioned investigations by Forbush also confirm the small radius of the ring (amounting a few earth radii). Indications pointing to other results have appeared in the literature. The studies of Hayakawa, Nagata, et al (Bibl.46) have shown that the observable effect of magnetic storms in the distribution of the

currents of cosmic rays cannot be explained under the assumption of a ring radius of $1.1 R_a < 100 R$ within the scope of the Stoermer-Forbush theory. These authors assume that the recalculation of the data based on the modifications introduced into the theories by Lemaitre and Vallart might help to explain the phenomenon. One of the authors of this report, Nagata (Bibl.51), estimated the parameters of the ring on the basis of the southward displacement of the auroral zone during the storm of 30 April 1933 and on the assumption of an intensification of the current in the equatorial ring during the course of the storm. It was found that, for agreement with empirical data, it is necessary to adopt a radius of the order of 20 earth radii for the ring.

Thus most investigators today tend toward the idea that an extra-ionospheric current ring exists, whose field explains the variations of the magnetic field and other geophysical phenomena (position of the auroral zone, influence of magnetic storm, and cosmic rays). But no definitive clarification has been obtained with respect to the parameters of the ring. The possibility of the existence of an ionospheric system of currents of the variations is likewise not completely excluded. At one time, Chapman (Bibl.40) advanced the following argument in favor of an ionospheric system. In view of the fact that the separation of the storm field into two parts is somewhat formal, it is necessary to approach with caution any attempts to explain these two parts by completely different causes; on the other hand, it would be extremely desirable to explain both regular parts of the field of disturbance by one and the same physical process. It is difficult to give an explanation of the disturbed diurnal radiations within the scope of a theory of an extra-ionospheric ring (for this it would be necessary to assume one of two improbable propositions: an elliptic ring or eccentricity of the earth's position). It would seem more natural to explain the S_D -variations under the assumption of currents flowing in the ionosphere, whose parameters depend explicitly on the diurnal rotation of the earth. This, in Chapman's opinion, does not allow complete rejection of the hypothesis of

an ionospheric system of D_{st} -currents. Sugiura (Bibl.56), without denying the existence of an extra-ionospheric ring current, considers a partial location of the D_{st} -currents in the ionosphere possible, in connection with the inductive action of the external ring on the conducting layers; as one of his arguments, he postulated a seasonal march of D_m , which is easily explained from the standpoint of ionospheric current systems.

These views on the electric currents of the perturbation field are based fundamentally on a study of the middle-latitude picture of magnetic storms and have the object of explaining this picture. In the following Section, we will discuss papers devoted to the electric currents flowing in the polar zones.

Section 5. Electric Currents of the Auroral Zone

The intensification of the regular and irregular parts of the perturbation fields in the high latitudes has compelled many investigators to assume that a powerful electric current flows along the auroral zone. We have already learned of Birkeland's ideas as to this current. Other authors have made similar calculations for individual instants of time of individual storms. These include McNish (Bibl.49).

McNish's work is interesting since the potential of the field on a bounded area of the surface, taken as a plane, is represented by the series

$$V = A_0 x + \sum_n e^{n^2 z} (A_n \cos nx + B_n \sin nx) + \sum_n e^{-n^2 z} (A_n \cos nx + B_n \sin nx),$$

where x is the abscissa of the point (distance from the zone of polar current) and z is the ordinate (height about earth's surface). The expansion of the H and Z components of the field into analogous series, from the data of certain observatories located near the polar zone, has allowed separation of the potential into parts of external and internal origin ($I/E \approx 1/4$) and has made it possible to calculate the height of the current. The best agreement with the observational data was given by a height of $h \approx 100$ km and the assumption that the current flows in a wide belt, a few tens of kilometers wide, over this zone. It must be noted that the simple in-

0 inspection of the magnetograms of polar observatories, without any computational op-
2 erations, forces us to assume the existence of electric currents at rather low levels
4 in the polar regions. The high degree of local variation in the distribution of the
6 vector of disturbance would be difficult to explain under the assumption that the
8 sources of the field were located far from the earth's surface.

10 The calculations of the linear electric currents responsible for the high-
12 latitude part of the S_D -variations were made by Harang (Bibl.44) and Sucksdorff
14 (Bibl.55). The materials used in both cases were the S_D variations for the Second
16 International Polar Year for several stations located close to the auroral zone. By
18 combining the observations of pairs of stations (cf. Chapter V for the formulas), the
20 authors calculated the position of the zone, the strength of the current flowing in
22 the zone, and the height of the current for various hours of the day. According to
24 Harang, the most probable value of the height is 100-200 km. According to Sucksdorff,
26 the height varies over a very wide range, from 100 to 1,000 km, and shows an obvious
28 dependence on the time of day. The great discrepancies between the values of the
30 parameters found by Harang and Sucksdorff indicate that a more careful selection of
32 the empirical material is necessary. Harang found the linear horizontal current to
34 be doubled in the polar zone, which is also confirmed by Yu.D. Kalinin (Bibl.20) on
36 the basis of the geographical distribution of the u-measure. Sucksdorff found that
38 for a better representation of the observed material, it is necessary to assume a
40 system of vertical currents descending from outer space to the earth's atmosphere in
42 regions close to the magnetic field. Sucksdorff's vertical current does not repre-
44 sent a closed contour, and it must be assumed that it is scattered due to a recombi-
46 nation of particles in the lower layers of the ionosphere. In performing his calcu-
48 lations, Sucksdorff started from Chapman's hypothesis that the internal part of the
50 perturbation field is equal to 2/3 of the external part. Harang in comparing the
52 calculated variations of the horizontal and vertical components, found that such an
54 idea leads to a poor correspondence of the H and Z variations, and that a lower

0 value of the ratio I/E , namely one of the order of 0.1, is more probable. As we will
2 see later in Chapter V, the calculation of the external and internal potentials of
4 S_D , for high latitudes, leads precisely to such small values of I/E .

6 The explanation of the field of a magnetic storm by a vertical current descending
8 in the auroral zone is likewise contained in the very interesting but somewhat con-
10 torversial papers by M.N.Gnevyshev (Bibl.12, 13). Let us first discuss the classi-
12 fication of storms proposed by him. In comparing the magnetic and ionospheric data
14 and considering the geographic distribution of the perturbation field, he came to the
16 conclusion that there are two types of storms: polar and worldwide, but his classi-
18 fication is not identical with that by Birkeland. He includes most of the moderate,
20 great, and violent storms usually observed over the entire earth, into the category
22 of worldwide storms. He considers that the maximum of the vector of disturbances
24 during these storms is observed in the auroral zone. He places a relatively small
26 number of storms in the second, or polar category; these are storms for which the
28 auroral zone plays no particular role and whose disturbance reaches a maximum at the
30 magnetic pole or near it. He supports this classification of storms with graphs of
32 the disturbance vector plotted against the geomagnetic latitude, and with comparisons
34 of the magnetic and ionospheric disturbance. The worldwide storms, according to
36 Gnevyshev, are caused by a vertical electric current descending from outer space and
38 reaching heights of 80-100 km (the lower boundary of the region at which the aurora
40 can be seen). He takes this stand on the basis of the Stoermer-Birkeland theory, as-
42 suming the direct superimposition on the geomagnetic field of particles of a singly-
44 charged stream. He circumvents the objections raised against that theory by assuming
46 very low flux densities (of the order of 5 cm^3), fairly high particle velocities, as
48 well as a pulsating radiation (noncontinuous) of the particles by the active foci of
50 the sun. Postulating a linear vertical current, he successfully calculates, from the
52 observed geomagnetic variations, the current strength, the polar distance of the zone,
54 the penetration of particles into the atmosphere, the cross section of the flux, the

velocity of the particles, and the nature of the particles (a mixture of doubly- and singly-ionized helium atoms). The decreased amount of disturbance in the middle and low latitudes is explained by him by their remoteness from the sources of the field, not admitting the existence of any special currents responsible for the disturbance in the middle and low latitudes. Gnevyshev's papers are of great value, since they show how the magnetic data can be used for judging the nature of the particles and the geometry of the corpuscular stream, but they do provoke certain objections. First, the classification adopted by the author is doubtful. A consideration of a series of magnetograms (cf. Chapter II for more details) shows that there are no grounds for putting storms with intensities increasing toward the pole in a separate category. Second, it is very difficult to explain the regular part of the perturbation field without assuming currents flowing above the middle latitudes (cf. Chapter V, Fig. 27). The flux densities obtained by Gnevyshev seem slightly too low*; in this connection, the question remains open as to how essential the theoretical objections, raised at one time against the Störmer-Birkeland theory, are for Gnevyshev's works.

Section 6. Penetration of Corpuscles into the Earth's Atmosphere. The Alfvén Theory

The penetration of solar charged particles of both signs into the earth's atmosphere in the high latitudes is considered by the majority of modern authors to be beyond doubt. This conviction is based on the factual data on the magnetic variations and the aurora. For example, a comparison of the intensity of the auroral displays with that of the magnetic disturbances enabled Harang (Bibl. 44) to calculate the velocity/spectrum of the particles penetrating the earth's atmosphere to various depths. In a number of other papers, radiosonde data are used to demonstrate the deep penetration of particles into the atmosphere. For example, the observations by Wells (Bibl. 64) showed that the intense polar storms, as a rule, are accompanied by the formation of

* We recall that the current density according to Chapman's data is equal to 10^2 cm⁻¹.

0 a strongly absorbing region at the level of the D layer. Less intense storms are
2 connected with the formation of a layer of abnormally high ionization at the level of
4 the E layer. In this case, the energy is obviously less, and, consequently, pene-
6 tration of the particles into the earth's atmosphere is not as deep. A correlation
8 in the high latitudes between the night layer E_g and the magnetic activity is noted
10 in a number of papers (cf. for example, Bibl. 1 and 2).

12 The definitive experimental proof for the penetration of solar particles into
14 the earth's atmosphere was obtained by spectrophotometry of the aurora. It is well
16 known that the absence of hydrogen lines in the auroral spectra was long a puzzle to
18 those interested. From the 1930's on, it has been possible, owing to the improved
20 technique of spectroscopic work, to find (but rather rarely) the H_α line in the a-
22 uroral spectra. In connection with this fact, Vegard postulated that hydrogen is not
24 a permanent component of the earth's atmosphere in the high latitudes, but is only a
26 stray brought in by the solar corpuscular stream. During a few auroral displays of
28 1950, he was able to discover (Bibl. 29) a Doppler broadening in the H_α , H_β and H_γ
30 lines, indicating the vertical displacement of hydrogen atoms at velocities of 800-
32 3,000 km/sec. Thus the question of the introduction of solar particles into the
34 earth's atmosphere must be considered definitively solved.

36 Much still remains unclarified with respect to the excitation of the currents
38 directly responsible for the fluctuations of the magnetic field. Since, with a
40 neutral stream (and there are not many grounds for doubting such a stream) the direct
42 influence of the field of particles of Birkeland-Gnevyshev is inapplicable. Therefore,
some mechanism responsible for the separation of the charges or the excitation of
some kind of currents must be introduced into the argument. The Chapman-Ferraro
theory, which is merely a theory on the formation of the equatorial ring (i.e., a
theory of the middle-latitude part of the D_{st} -variations), gives no answer to this
question. It is true that the above-mentioned note by Martyn does contain indi-
cations of the direction in which the theory would have to be further developed to

0 obtain an explanation of the polar part of the disturbance*. But these indications,
2 unsupported by any calculations, cannot be considered a reliable explanation of the
4 phenomenon.

6 An explanation of the disturbances in the high latitudes is worked out in more
8 detail in Alfven's theory, which is an attempt to reconcile the view of Stoermer and
10 Birkeland with those of Chapman and Ferraro. The Alfven theory (Bibl.4) is based on
12 the assumption of a stream consisting of charged particles of both signs, whose
14 motion from the sun to the earth takes place under the action of the inhomogeneous
magnetic fields of the sun and the earth and of the electric field created by the
stream itself. As in the Chapman-Ferraro theory, as a result of the encounter of
the corpuscular stream with the geomagnetic field, a "hollow" is formed, which is a
region surrounding the earth and which does not allow penetration of the charged
particles. Under the action of the inhomogeneous magnetic field of the earth, the
paths of the positive and negative particles separate, but since their total number
in unit volume is the same, the volume charge remains equal to zero. The electrons
which, in the equatorial plane, bend around the forbidden region in an easterly di-
rection, and the positive particles moving toward the west, form an electric current
of westerly direction, which is eccentric with respect to the earth (Fig.5). The
current comes closest to the earth on the evening side on which, in addition, the
greatest density is observed. This part of the current system is responsible for
the D_{st} - and S_D -variations of the middle latitudes. The dimensions of the forbidden

* It is postulated that the charged particles in the equatorial current torus, close
to its surface, might become detached from the body of the flux and be displaced to-
ward the earth along the lines of force of the magnetic field, which are lines of
very high conductivity. The entrance of these particles into the earth's atmosphere
at the latitude of the auroral zone causes luminescence of the atmosphere, and an
elevated ionization at the 90-100 km level, and would also produce a strong electric
field of meridional direction (the positive and negative particles would bombard dif-
ferent edges of the zone). This field, interacting with the permanent mag-
netic field of the earth, would produce a drift of the ionospheric ions of both signs
in a westerly direction. If the velocity of the positive and negative ions is as-
sumed to be different ($v_+ > v_-$), then a Hall current would flow along the zone, east-
ward on the evening side of the earth and westward on the morning side, which would
explain the polar part of the current system of S_D -variations.

0 zones depend on the parameters of the particles and therefore differ for the positive
2 and negative particles; the positive particles come closer to the earth than the neg-
4 ative ones. The penetration of positive particles into the region forbidden to the
6 electrons produces a great potential difference at the boundary of the region (accu-
mulation of positive particles on the day side and negative particles on the night
side). The conductivity of very rarefied gases in the presence of a magnetic field
is considerably greater along the direction of the field than in a direction perpen-
dicular to this. In view of this fact, positive and negative charges, tending to
neutralize each other, will move along the lines of force of the magnetic field from
the boundary of the forbidden zone to the upper layers of the earth's atmosphere in
the high latitudes. The invasion of the ionosphere by the corpuscles takes place in
the auroral zone. The conductivity of the polar ionosphere is relatively high so that
the positive particles will be displaced from the day side along the auroral zone to
the night side, and the negative particles in the opposite direction. Thus a peculiar
kind of discharge current, counterclockwise in the first half of the day (0-12^h) and
clockwise in the second half (12-14^h) will be established. Figure 6 gives a diagram
of the formation of the current. This current, in Alfven's opinion, is able to ex-
plain the polar disturbances and the aurora. This system of motion of charges was ob-
tained by Alfven as a result of the solution of the equations of motions of particles
in inhomogeneous magnetic and electric fields, allowing (it is true, only approxi-
mately) for the interaction of the particles. The Alfven theory successfully explains
certain regularities of the morphology of the aurora (position and diurnal displace-
ment of the auroral zone, certain forms of the auroral displays, etc.), as well as
the penetration of corpuscles into the polar ionosphere and the formation there of
currents causing the polar disturbances. Thus, the investigations by Alfven con-
tributed greatly to the development of the theory of magnetic storms. The concept of
the aurora as the result of discharge currents appears very probable in the light of
recent work by several Soviet scientists.

In spite of this, the work by Alfven evokes certain comments. First, according to Alfven, the polarization of particles in the stream and their motion from the sun

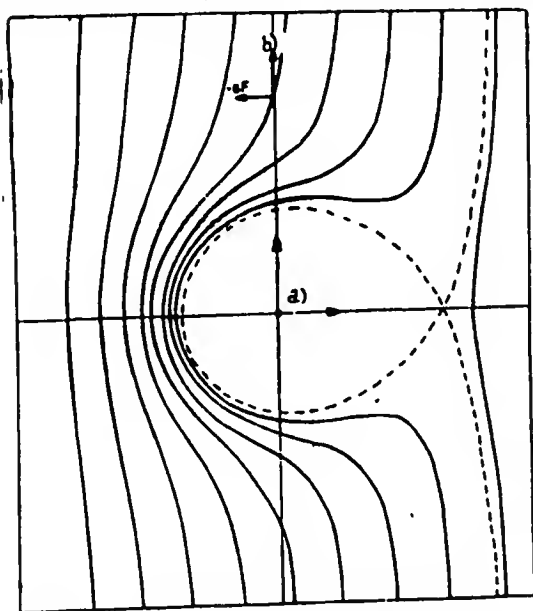


Fig.5 - Curvature of Stream in the Earth's Magnetic Field, According to Alfven (--- Boundaries of Forbidden Zone) a) Dipole; b) To the Sun

to the earth is due to the sun's magnetic field; Alfven takes 10^{34} cgs as the value of the magnetic moment of the sun, according to Khell's (Hull's) determinations. Repeated measurements by German and American authors resulted in much lower values, so that the question as to magnitude and constancy of the sun's magnetic field cannot be considered settled at present. The only fact which appears to be beyond doubt is that the magnetic field of the sunspots is many times greater than the general magnetic field of the sun. It would, therefore, appear that the magnetic field of the sunspots should have an influence on the process of formation and flight of the corpuscular polar stream, the more so

since the ejection of particles is undoubtedly from regions located near the spots. It is possible that the replacement in the Alfven equations of the value of the general magnetic field of the sun by the field of the sunspots, somewhat modifies the parameters of the stream, particularly on the first half of the path from sun to earth. Second, the explanation of the S_D -variations in the geomagnetic field by assuming an asymmetric location of the equatorial ring current seems improbable from the point of view of the morphology of the field of magnetic storms; according to the Alfven theory we would expect the field of S_D to increase toward the equator, just as is done by the D_{st} field. In reality, the S_D -variations are, on the contrary, almost entirely absent at the equator (cf. Chapter V). Third, according to Alfven, the polar

system of currents causing disturbances in the high latitudes is formed as a result of the accumulation of space charges in the equatorial ring. In this way, the increase in the amount of disturbance in the high latitude during worldwide storms could be explained, but this leaves the polar storms completely without explanation, i.e.,

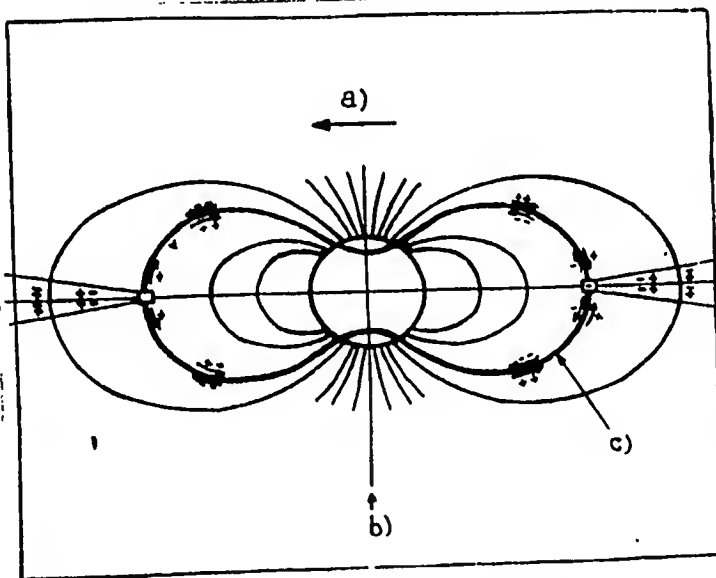


Fig.6 - Formation of Current Systems According to Alfven (— Lines of Force of Magnetic Field; - - - Boundary of Forbidden Zone)
a) To the sun; b) Magnetic axis; c) Boundary of Forbidden zone

it does not explain the disturbances affecting only the polar regions, which are obviously not connected with the formation of the equatorial ring. Besides these, and a number of analogous concrete objections, two other shortcomings of the Alfven theory, of a more general nature, must also be pointed out. First, the Alfven theory considers the formation of magnetic storms and of the aurora without any connection with the physics of the disturbed-day ionosphere. At the present stage, it would seem impossible to separate the explanations of the magnetic and

ionospheric disturbances, just as it is impossible to explain them independently of the aurora. Second, many stages of the theory have not been vigorously developed. There are numerous assumptions requiring physical or mathematical justifications (for example, the assumption that the electronic and ionic temperatures in the stream are unequal, and the like).

Thus, in spite of the fact that the Alfven theory has contributed much of value to the development of the ideas on magnetic storms and the aurora, it cannot be considered to resolve completely all questions of their origin.

Section 7. Dynamo Theory of Magnetic Storms

In this Section we will briefly discuss the dynamo theories of magnetic disturbances. It is well known that, during the first stage of development of the doctrine of magnetic storms, the dynamo theories occupied a prominent position (the Angenheister theory, the first version of the Chapman theory, the Lindemann theory, etc.). These authors explain the formation of the electric currents of magnetic storms by the vertical motion of the upper conducting layers (due either to thermal expansion, or to mechanical displacement under the action of the stream of particles penetrating into the atmosphere) in the permanent magnetic field of the earth. All these investigations, in time, were found to be unsound (Bibl.40), and today they are only of historical value. In 1946, Yu.D.Kalinin (Bibl.18) proposed a modification of the dynamo theory, explaining the middle-latitude part of the electric currents of the S_D -variations by the tidal motions of the upper layers of the atmosphere, under the action of the gravitational attraction of the mass of the flux. He described the conductivity of the ionosphere by the two-term expression $\rho = \rho_v + \rho_c$ where ρ_v denotes the portion of the conductivity due to the ionization under the action of the wave radiation of the sun, and ρ_c is the conductivity due to ionization by the corpuscular stream. Naturally, ρ_v depends on the zenith angle of the sun and ρ_c on the geomagnetic latitude of the point of observation. It was assumed that the integral conductivity of the entire layer of the ionosphere $\rho_v = 2 \times 10^7$, and $\rho_c = 5,100$ cgs. The calculations made by Kalinin showed that, under these assumptions, the current system would consist in each hemisphere of two eddy currents with centers located at latitudes $\pm 60^\circ$. On the evening side of the earth the eddy with the positive current direction is in the northern hemisphere, and on the morning side, the eddy with the negative direction. I myself consider that the mechanism of action of the stream on the earth's magnetic field, proposed by Kalinin is possible in principle, but I will demonstrate that the values of ρ_v and ρ_c , adopted by him are in need of review. The value of the ρ_v of the F_2 layer, in a direction perpendicular to the magnetic field (with which the S_D -

variations can be correlated), is possibly somewhat lower (for details, see Chapter VIII), while the value of ρ_c , taken by Kalinin as equal to 5,100, requires the corresponding justification.

Great attention has been paid in recent years by Japanese geophysicists to theoretical and morphological investigations of magnetic disturbances. A proposition common to them is the assertion that a dynamo effect is the fundamental cause of geomagnetic disturbances. The revival of the dynamo theories in the works of the Japanese authors is connected with the discovery, by radio methods, of horizontal motions in the ionosphere and of an anomalous rise in the ionization (and, consequently, in the conductivity) of the lower layers of the ionosphere in high latitudes. Here some authors connect the field of disturbance with motions of the E_s clouds. The correlation between the appearance of E_s in the high latitudes and magnetic activity, as we have already remarked, is no longer doubted and indicates the corpuscular nature of the E_s ionization. But the explanation of the S_D -currents flowing around the entire earth, as being due to the motion of the E_s clouds (and referring the current of the L-variations, on the other hand, to the level of the F_2 layer) would seem unreasonable. As shown below, the very frequent appearances of E_s in the equatorial regions well explain the behavior of S_q and L at Huancayo and by no means fit in with the regularities of the storm field. The papers by Nagata (Bibl.52) are of considerably greater interest. He considers only the polar part of the disturbance (position and displacement of the auroral zone, intensity of the current in it, and width of the zone) and shows that the polar current could be formed at the 60-100 km level as a result of an increase in ionization at this height by 20-40 times above its level on quiet days. In their papers, Nagata and Fukushima conduct a polemic with Alfven, pointing out that the configuration of the currents does not correspond to the form of the discharge currents postulated by Alfven. Nagata, using the McNish formulas for the representation of the field near the polar zone, also investigated the ratio of the external to the internal parts of the field, and obtained $E/I = 2.6$, which

0 does not contradict the data of other authors. Hasegawa (Bibl.45), in considering
2 the diurnal variations on quiet days and disturbed days in 19 polar observatories,
4 made use of harmonic analyses and calculated the electric conductivity of the upper
6 layers as well as the gradient of electric potential required to explain the S_D -
8 variations by dynamo currents. He also studied the form and displacement of the au-
10 roral zones during the course of the day and with the seasons of the year.

12 It seems that the excitation of dynamo currents in the lower layers of the iono-
14 sphere at high latitudes is very probable, taking account of the increase in ioniza-
16 tion during storms and of the existence of vertical and horizontal winds. It may be
18 that these play an important role in the formation of local polar disturbances. But
20 for all that, it does appear unclear, without more detailed investigations whether
22 these currents are responsible for the polar part of the S_D -variations, what role is
24 played by the current excited in the polar regions of the F_2 layer, and, a fortiori,
by what mechanism the low-latitude part of the S_D -currents is formed.

Section 8. Bay-Like Disturbances

In all the above papers, except for the investigations by Birkeland, the subject
of study was the fields of worldwide storms, i.e., of storms during which substantial
variations of the magnetic field were observed in all latitudes. After the investi-
gations by Birkeland, which unfortunately have not been sufficiently developed in
subsequent papers, it became clear that the polar magnetic storms accompanied in the
middle latitudes by small bay disturbances, constitute a special phenomenon charac-
terized by a different field structure and a different origin. A few papers devoted
to the statistics of bays in the middle latitudes are known (Bibl.8, 25). Thanks to
them, the questions of the diurnal, seasonal, or 11-year march of the frequency of
bays have been partially settled. Papers devoted to the considered of individual
bays are also known.

The most complete investigation of bay-like disturbances was made by Silsbee
and Vestine (Bibl.54) who subjected the bay-like disturbances observed by 13 obser-

0 vatories during the Second International Polar Year to statistical processing. They
2 investigated the problems of distribution of positive and negative bays during 24
4 hour periods and during the course of the year. This led to a concept as to the
6 mean (or more accurately the typical) bay, and a system of currents corresponding
8 to this typical bay was constructed. We will discuss the work of Silsbee and Ves-
10 tine in more detail in Chapter VI, which is specially devoted to bay-like distur-
12 bances. Silsbee and Vestine also calculated the linear polar currents for 20 indi-
14 vidual cases of bays. The direction of the current, in almost all cases, was paral-
16 lel to the auroral zone. The height of the current, even according to data from
18 closely adjacent observatories, varied over a wide range (for instance, 1^h 25^m on
20 3 July 1938, according to the data of one pair of stations, h was 100 km, while ac-
22 cording to the data of another pair, h was 560 km. At 0^h 50^m on 26 June 1933, h was
24 190 and 550 km, respectively). Such fluctuations of height must be considered an in-
26 dication that a linear current does not always well approximate the observed distri-
28 bution of the field of a polar storm.

30 Section 9. Current Systems of Individual Storms

32 As will be clear from the foregoing, the fundamental trend in geomagnetism dur-
34 ing the past two decades has been toward detection and explanation of the mean regu-
36 lar features of the perturbation field. A relatively small number of papers have
38 been devoted to a study of individual magnetic storms. In addition to the above-
40 mentioned calculations of the polar current of individual disturbances, there are
42 also a few cases where the surface-current systems of individual storms have been
44 considered. Thus, Yu.D. Kalinin (Bibl.21) in 1938 constructed isopotential lines by
46 the method of graphical integration for three successive instants of time for the
48 disturbance of 17 March 1933 for the northern part of Eurasia. Since the distribu-
50 tion of isopotential lines allows the configuration of the lines of the surface sys-
52 tem of currents to be judged to some extent, the conclusion may be drawn from these
54 maps of Kalinin that the current systems responsible for the disturbance of 17 March
56 1933 bear some resemblance to the mean systems of D_{st} and S_D represented in the works

of Chapman (Figs. 4a and 4b). From each map, the part of the middle latitude eddies and of the polar current of S_D may be found. Specifically for a solution of the question as to how much the electric currents, calculated for individual instants of time resemble the currents of the regular parts of the storm fields, Vestine (Bibl. 62) constructed current systems for five magnetic storms, of 14 October 1932, 30 April 1933, 5 August 1933, and 15 October 1932. As starting material, the mean-hourly values of the magnetic elements from observations of about 40 stations in the northern hemisphere were used. The methods of constructing the current lines was approximate, i.e., the same as that used by Chapman for the construction of the D_{st} and S_D -variations. The part due to the internal induced currents was eliminated from the observed values of the elements by multiplying the observed values of Z and dividing the observed values of H , by 0.8. This factor was compiled by Vestine instead of the factor 0.6 used earlier by Chapman, in connection with the papers cited in References 41 and 46, whose results were mentioned in the preceding Section. The maps of the current lines presented in the cited work show very plainly that, in all cases, it is possible to detect two intense eddies characteristic for the S_D -variation, a densification of current lines in the polar zone, and parallel current lines in the low latitudes, characteristic for the D_{st} -variations. The direction of the current corresponded in all cases to what would have been expected from a consideration of the average systems. Thus it may be considered that Vestine's experimental calculations yielded an interesting result substantiating the investigations by Chapman, devoted to the regular part of the fields of magnetic storms. It goes without saying that for a more trustworthy solution of the question posed by Vestine as to the ratio of the average to the individual current systems, it would be necessary to accumulate a large amount of material and to replace the mean values of the magnetic elements by their instantaneous values.

Section 10. Irregular Part of the Storm Field

The question of the irregular part D_i of the perturbation field is one of the

most obscure questions in geomagnetism. The statistical investigation of the magnetic disturbance, or activity, is usually conducted by using magnetic characteristics, i.e., by estimates of the degree of magnetic disturbance. Usually these characteristics take account of both the regular part of the field, the irregular fluctuations during storms, and the small disturbances. Thus the statistical regularities of the irregular part are studied in rather great detail. Unfortunately, only a few attempts have been made to correlate the study of the regular and irregular variations and to explain them within the framework of a single hypothesis. The well-known monograph by Chapman and Bartels, which considers in rather great detail the questions of magnetic disturbances, devotes a page and a half to the irregular part, in which it is stated that the high intensity of the field of D_1 in the polar cap may possibly be connected with local and rapid fluctuations in the ionization, which follow from the variability of the form and brightness of the auroral displays. The explanation of the irregular fluctuations in the temperate latitude differs according to what systems of currents (ionospheric or extra-ionospheric) were adopted to explain the regular part of the variations. Here Chapman states that, so long as no authentic theory of the regular parts of the disturbance has been constructed, scientists will be unable to give explanations for the irregular fluctuations.

A.P. Nikol'skiy (Bibl.26) has again raised the question as to the ratio of the irregular fluctuations to the regular parts of the disturbance, in a series of papers devoted to the statistics of magnetic activity in polar observatories. Like M.N. Gnevyshev, whose papers were mentioned above, Nikol'skiy is a proponent of the theory of the direct influence of the field of charged particles on the earth's magnetic field. Each pip or pulse on the magnetogram is in his opinion, a direct result of the invasion of the earth's atmosphere by a group of particles. The regular parts of the field of D_{st} -disturbances, at least in the high latitudes, are the results of formal averaging of individual and independent pulses and do not correspond to any real physical phenomenon. Since the distribution of the frequency of positive and

negative pulses during the course of a day obey definite regularities, the averaging of the values of the magnetic elements for a series of disturbances creates the impression that a regular diurnal march of the perturbation vector of S_D does actually exist. Since, in most cases, the pulses in the horizontal component are negative in sign, this leads to the false conclusion that H decreases uniformly during the time of a storm. The mean diurnal value of H_q^d for disturbed days, taken at selected quiet intervals in these days, coincides within an accuracy of 2-3 % with the mean diurnal value H_q for quiet days. This result, obtained by Nikol'skiy for a number of high-latitude observatories, indicated the absence of a general regular depression on stormy days. Without dwelling here on a criticism of this fundamental proposition by Nikol'skiy (we will return to it in the next Chapter) we may state that his work is of great value even if only because it has attracted attention to the study of D_i , and has forced a reconsideration "de novo" of the question as to the ratio of the regular to the irregular parts of the disturbance. Without a correct solution of this problem, to which an undeservedly small amount of attention has been given, a proper approach to the solution of a number of problems in the theory of magnetic disturbances is impossible.

Section 11. Conclusions

On the basis of the brief survey of recent papers on magnetic disturbances, given in the preceding sections, the following conclusions may be drawn:

1. The morphology of the field of disturbance has not yet been adequately been studied. More specifically, there is no complete clarity with respect to the classification of magnetic storms; the regular variations in the high latitudes have been little investigated (not only is their form unknown, but even, as indicated by the works of A.P. Nikol'skiy, there is not even confidence in their existence), etc.
2. In spite of the large number of papers devoted to the construction of electric currents, this question is still far from a definitive solution. Chapman's current systems, which are the most trustworthy, are based on insufficient material

and have been constructed by an extremely approximate method. It would be desirable to use all the observational material available today and to use objective analytical methods for continuing the investigations in this direction.

3. Too little material has been accumulated to judge the ratio of the regular parts of the field of disturbances to the irregular fluctuations, and to estimate the correspondence between the average current systems and the currents of individual storms.

4. There are also inadequate data with respect to the separation of the observed field of disturbance into parts of external and internal origin. The separation of the D_{st} field has shown that the ratio I/E for the disturbed variations and the quiet variations (S_q and L) is not the same. A knowledge of the ratio I/E is also important for a correct evaluation of the intensity and configuration of the external currents and for evaluating the conductivity of the deep layers of the earth.

5. There is almost a complete lack of comparisons of the current systems constructed on the basis of magnetic data with our modern ideas on the ionosphere of the disturbed day. The use of ionospheric data is necessary for any judgment as to the reality of the currents calculated and for refining their parameters.

6. The construction of a system of currents corresponding sufficiently well to the observed geomagnetic variations, is a necessary basis for working out physical explanations of the nature of magnetic storms.

The extensive materials on the geomagnetic variations, accumulated up to now in connection with the published summaries of the observations of a worldwide system for the Second International Polar Year and with the data of Soviet observatories, worked-up for a number of years, have induced me to review certain obscure questions in the morphology of magnetic storms and to carry out a new construction of the current systems. The following Chapters of the present work are devoted to a discussion of the results obtained.

CHAPTER II

DIVISION OF THE FIELD OF MAGNETIC STORMS

Section 1. Classification of Storms. Polar Storms

Before proceeding to a discussion of the regularities obeyed by the field of magnetic disturbances, the most acceptable classification of magnetic storms must be selected. After the work done by Birkeland, Gnevyshev, Vestine, and other authors, it is indisputable that magnetic storms, in all of their diversity, may be still subdivided into two main groups: polar storms and worldwide storms. The most correct definition of a polar storm, in my opinion, is the definition given by Silsbee and Vestine, according to which an elementary polar storm is a disturbance lasting from one to several hours, which in its form recalls a bay, of great amplitude in the polar latitudes and very small amplitude in the temperate latitudes. Polar storms (see Fig.7 for examples) may be observed on both quiet and disturbed days. It will be seen from the diagram that, at high latitudes, the amplitudes of a polar storm may be very great, over 1000 γ but that, with increasing distance from the auroral zone, the value of the amplitudes drops sharply. Figure 8 gives the latitude-dependence of the H and Z components of a polar storm (according to McNish). Figure 8 shows that the correspondence between the field of a polar storm and the field of the linear electric current flowing in the auroral zone is excellent. The decrease of the field in the temperate latitudes may be considered the result of the increasing distance from the sources of the field. Thus the polar storms, as we understand them, have the same geographical distribution as the worldwide storms in Gnevyshev's class-

ification. As for Birkeland's definition of polar storms, as already remarked in Chapter I, there is no necessity of dividing polar storms into positive and negative according to the sign of the horizontal component of the perturbation field. Figure 31 (cf. Chapter VI), which gives the distribution of the vectors of the field of a

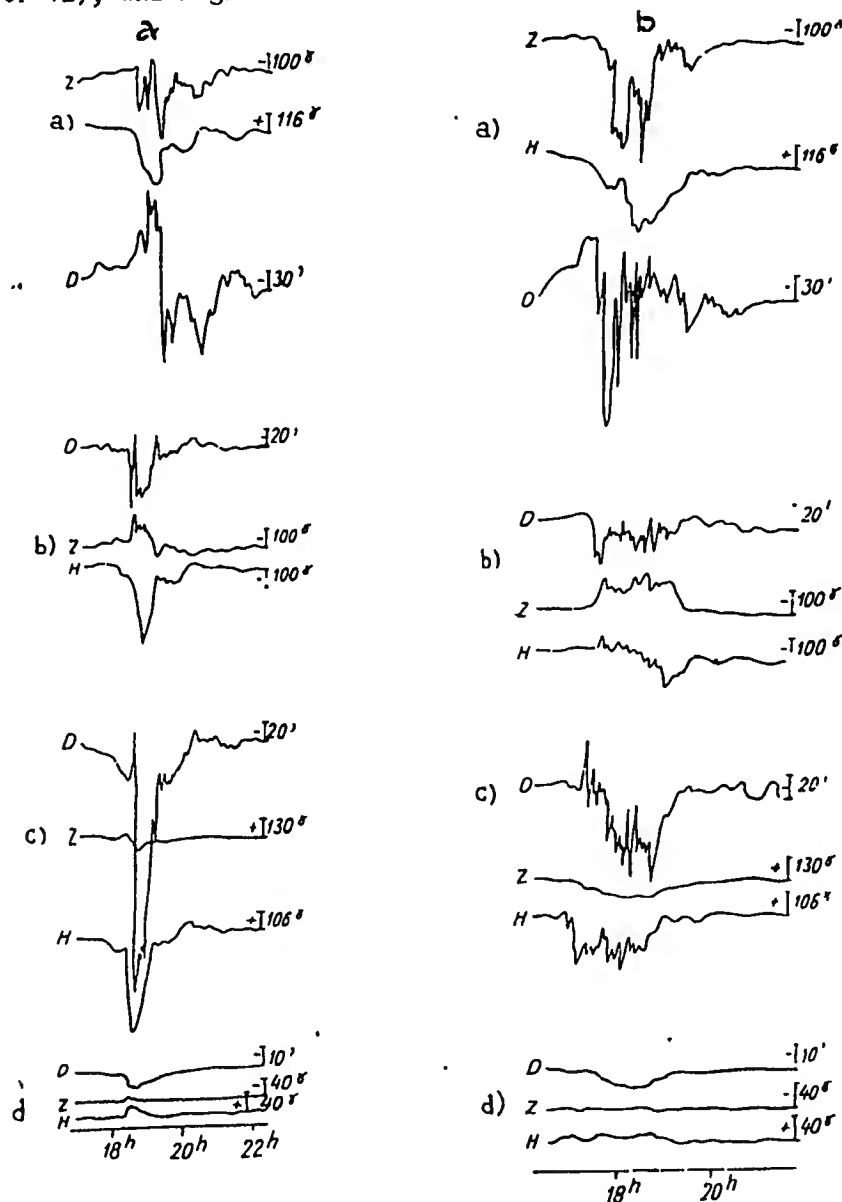


Fig.7 - Polar Storms. Universal Time (a - 11, March 1946; b - 13 March 1946).

a) Tikhaya Bay; b) Malochkin Shar; c) Dickson Island; d) Moscow

typical bay, shows very clearly that positive and negative polar storms are observed

simultaneously in the same latitude but in different longitudes. Polar storms are short-lived phenomena; the values of the magnetic elements return relatively rapidly

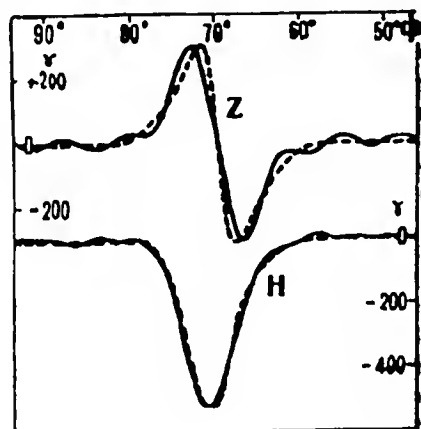


Fig.8 - H and Z Components of the Field of a Polar Storm, According to McFish (— Observed Values; ---- Linear Current Calculated for the Field)

to normal, and no prolonged aftereffect can be detected on the magnetograms. Nor is it possible to detect such a persistence by statistical methods. At the Tikhaya Bay Observatory, the mean values of H and Z were calculated for 38 quiet intervals following immediately after Polar bay disturbances, and for entirely quiet days during the same period of time. The small difference obtained (2γ in H and -3γ in Z) indicates the absence of any aftereffect. A consideration of individual cases of polar storms (Figs.7 and 9) and of the typical picture (Fig.31) forces us to consider that the field of a polar storm also lacks the aperiodic dis-

turbed variation (D_{st}) in the sense given to it in the papers by Chapman. Indeed, the field of the D_{st} -variations, by definition, depends only on the stormtime* and does not depend either on the longitude nor on the local time, while the disturbance vector of a polar storm differs at different longitudes of the same parallel of latitude. On the other hand, the disturbance vector of a polar storm depends explicitly on the local time, and thus, retaining the Chapman notation, we might consider that the two parts S_D and D_i were present in the field of a polar storm. However, in view of the fact that the duration of a polar storm is much shorter than a day, it would be meaningless to speak of its diurnal periodicity; it is more correct,

* The time reckoned from the beginning of a storm will everywhere henceforth be denoted by τ ; for this reason, we will denote the frequently aperiodic disturbed variations by the symbol $D_{st}(\tau)$.

without delimiting the regular and irregular parts of the storm field, to consider that the field of a polar storm (which we will denote by the symbol P) depends on the local time, i.e., $P(t)$. The frequency of distribution of the positive and negative P-storms is unequal during the course of a day (cf. Table 13), and the mean intensity of the disturbance is likewise unequal. It follows from this that, in calculating the mean diurnal values of the elements for days with P-storms, we will have a systematic decrease in H with respect to the quiet days and a systematic elevation in Z. This must be borne in mind in considering the distribution of $D_m = H_d - H_q$. Thus, it seems to us that the accuracy of Nikol'skiy's conclusions that there are

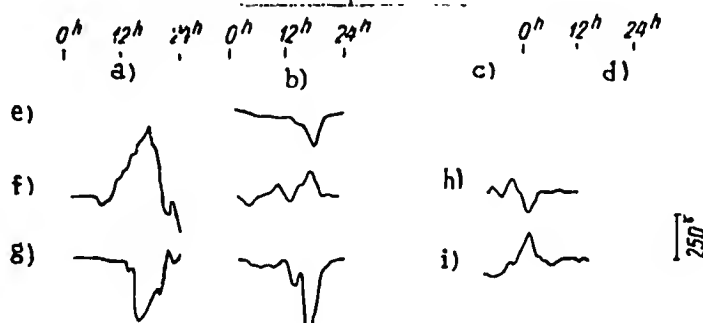


Fig.9 - Polar Storms of 1, 2 and 4 May 1933; Y-Component
Sveag. (Sveagruvan), $\Phi = 74^\circ$, $\Lambda = 131^\circ$; Chester. (Chesterfield),

$\Phi = 73^\circ$; $\Lambda = 324^\circ$; M. o-va (Bear Islands), $\Phi = 71^\circ$; $\Lambda = 124^\circ$;

R.S. (Rude Skou), $\Phi = 56^\circ$, $\Lambda = 98^\circ$; Azhin. (Agincourt), $\Phi = 55^\circ$, $\Lambda = 374^\circ$

a) 1 May; b) 4 May; c) 1 May; d) 2 May; e) Sveag.; f) Chester.;

g) Bear Island; h) Rude Skou; i) Agincourt

neither regular D_{st} -variations nor stable aftereffects is greatest for the P-storms.

Section 2. Worldwide Storms. D_{st} -Variations

For worldwide storms (cf. Figs. 1 and 2), the most characteristic feature is the distribution of the disturbance over all latitudes, although the high latitudes are still the most disturbed. A second feature of worldwide storms is the existence of

0 regular components of the field, the D_{st} - and S_D -variations. There can hardly be a
2 doubt as to the existence of D_{st} -variations in the temperate latitudes. Indeed, if
4 we consider magnetograms of low-latitude observatories, where the irregular fluctu-
6 ations distort only slightly the smooth parts of the elements, even during disturb-
8 ances, then, without any statistical treatment whatever, we will in each storm dis-
10 tinguish the positive and negative phases in the variations of the horizontal com-
12 ponent. The statistical computations described in Chapter I and the existence of a
very stable aftereffect, are other convincing arguments for the existence of these
variations. The slowness of the return of the magnetic elements to normal may be
judged from the noncyclic variations. The noncyclic variations, measured by the dif-
ference between the value of the element at 24^h and at 0^h on one and the same day,
are always positive for H and negative for Z, on international quiet days. This is
evidence that even on the quietest days, which are free from irregular fluctuations,
a slow return is observed (increase of H and decrease of Z) to the normal values of
the elements, i.e., the action of the D_{st} -current system is not interrupted.

However, the work by A.P.Nikol'skiy has made it necessary to answer the follow-
ing question: Do the D_{st} -variations exist in high latitudes? If they do, what are
the values of D_{st} in the auroral zone and on the polar cap? To answer this question
it is necessary to take account of the fact that, in the high latitudes, the irregu-
lar fluctuations are so great as to exceed, by many times, the possible value of the
regular part of the field. For this reason A.P.Nikol'skiy is justified in stating
that, if the irregular fluctuation obey any law (for instance, the predominant de-
crease of the H component), they will prevent elucidation of the true regularities
of the regular part of the field. In view of this fact, I decided, as A.P.Nikol'skiy
did, to evaluate the D_{st} field by calculating the mean diurnal value of the elements
at intervals for the stormy days free from irregular fluctuations. This method of
estimating D_{st} is somewhat arbitrary, since there are very few quiet intervals dur-
ing great magnetic storms, and their selection is not without subjectivity. In most

cases, the quiet intervals can be detected after the extinction of the great irregular fluctuations of the main phase, during the period of the aftereffect. By this method, I calculated the values of $H_q = H_q^d$ and of $Z_q - Z_q^d$ for the observatories of Honolulu, San Juan, Moscow, Cheltenham, Tucson, Sitka, Bear Islands, and Tikhaya Bay, whose magnetograms were available. As an example, Fig.10 gives graphs of $H_q - H_q^d$ and $Z_q - Z_q^d$ for 1932/33 and 1947*. Both parts of Fig.10a show, in agreement, that the difference $H_q - H_q^d$, which reaches an order of 100 γ in the equatorial region, declines monotonously with increasing latitudes, reaching practically zero at latitude 70° . No increase of $H_q - H_q^d$ in the auroral zone is detected, while the difference $D_m = H_q - H_q^d$, after a certain decrease at latitude 50° , increases sharply at latitude $65-70^\circ$ **. The values of $Z_q - Z_q^d$ are negative, and in absolute value increase from small values in the low latitudes to large values for the observatories at Sitka and Bear Islands. In the low latitudes, we have $H_q > D_m$, which may be explained most easily by the fact that $H_q - H_q^d$ was calculated for a few of the strongest storms, while D_m is the result of averaging the international disturbed days, most of which coincided with moderate and even small storms. The excess of $H_q - H_q^d$ over D_m in the high latitudes is to be explained, in all probability, by the fact that in these latitudes, there is another factor besides D_{st} , which likewise systematically lowers H during the time of a disturbance. This factor, in my opinion consists of the irregular fluctuations superimposed on the regular part of the field of worldwide disturbance.

* The values of $H_q - H_q^d$ for Tikhaya Bay are taken from the paper by A.P. Nikol'skiy, and since the data for the Second International Polar Year and 1947 were unavailable, the data for 1934 and 1946 were used instead. During the entire 12-year period of 1934-1946 for which Nikol'skiy gives data, however, the value of $H_q - H_q^d$ is at all times of the order of 2 γ .

** The graph of the latitude dependence of D_m for 1933, 1936, and 1938, constructed from data collected by me, is presented in Fig.32 (Chapter VII).

A consideration of magnetograms with polar storms on quiet days, magnetograms of moderately disturbed days, and of great magnetic storms will convince the investi-

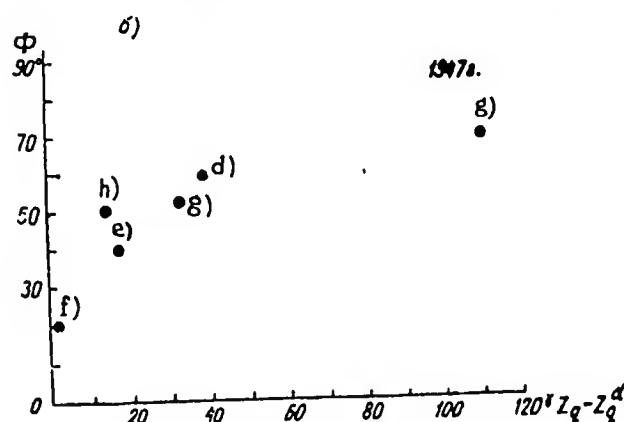
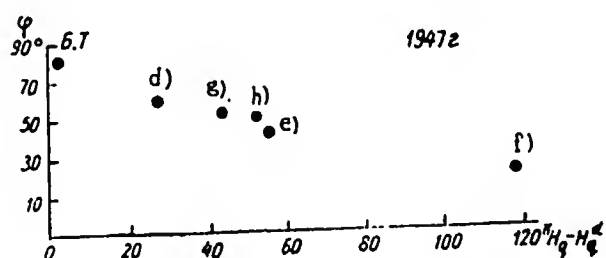
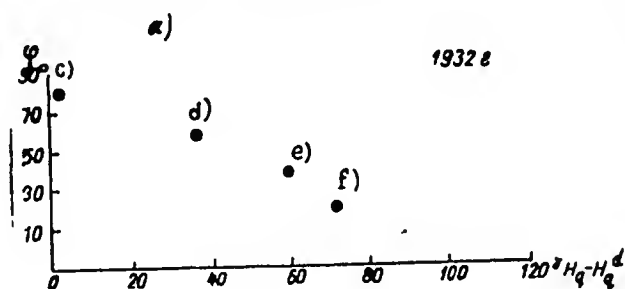


Fig.10 - Latitude Dependence: a) of $H_q - H_q^d$; and b) of $Z_q - Z_q^d$; c) Tikhaya Bay; d) Sitka; e) Thule; f) Honolulu; g) Bear Islands; h) Cheltenham

gator that the polar storms of a quiet day and the great irregular fluctuations during a worldwide storm are one and the same phenomenon; during a worldwide storm, a large number of polar storms of various amplitude and forms follow each other or are superimposed on each other, and, being accompanied by other forms of disturbances, give the impression of complex random fluctuations. This proposition has served as the basis for the conclusion drawn by Nikol'skiy that a magnetic storm is the sum of individual pulsations piled one on the other, a conclusion which in my opinion is erroneous. It is correct to assert that, during worldwide storms, a multitude of polar storms is always superimposed on the regular parts of the disturbance. A worldwide storm without polar storms is impossible; they are an inseparable part of it. But the worldwide storm is not a result of the simple summation of the fields of the individual

pulsations of polar storms. It has a fundamentally new property, the regular parts of the D_{st} and S_D field, which do not belong to the individual polar storms. This idea of the classification of storms into polar and worldwide, and of their inter-

relation, may well solve the contradictions between individual investigators on the questions of the morphology and classification of magnetic storms. For instance, Nikol'skiy's conclusion that the regular lowering of H is absent during storms, due to the presence of D_{st} -currents, can apparently be explained as follows: In calculating the mean values of H_q^d , Nikol'skiy used the tabular material on the hourly amplitudes of r_H and the mean hourly values of the H component. He selected the values of H in those quiet hours (at small values of r_H), which immediately followed strongly disturbed hours (at large values of r_H). In most cases, such sequences of a disturbed hour followed by a quiet hour take place on days of polar storms since in the days of worldwide storms, the number of quiet intervals in general is very small. It is therefore natural enough that the statistical treatment should have disclosed a regularity inherent in the P-storms but not in the M-storms*, i.e., an absence of any decrease in H . In the selection of quiet intervals for the calculation of H_q^d for Sitka, Bear Islands, and elsewhere, we used magnetograms of worldwide storms and, as shown by Fig.10, we obtained values of $H_q - H_q^d$ different from zero.

Chapman, as already stated, used the values of D_m to construct the polar part of the D_{st} -currents. In the high latitude, however, the value of the horizontal component of the field of P-storms, superimposed on the regular parts of the field of a worldwide storm, is considerably greater than this same component of the D_{st} part. It is, therefore, only natural that the calculation of D_m by simply taking the average should reveal the properties of P-storms, i.e., the sharp increase of $H_q - H_q^d$ in the polar zone.

We may also attempt to explain, from this point of view, M.N.Gnevyshev's views on the latitudinal distribution of the vector of disturbance. From Fig.1 and Table 1 of the Gnevyshev paper (Bibl.13) it would appear that, by the vector of disturbance ΔF , he means the deviation from the normal values at the instant of some distinct maximum (for example, 2000 Y at the Matochkin Shar Observatory), due to a great

* We will designate worldwide storms in this way to save space.

P-storm, considerably exceeding the D_{st} -part of the worldwide storm in value. It is understandable from this that the relation between ΔF and the distance from the auroral zone, which is depicted in Fig.4 of the paper cited, characterizes the geographic distribution of the field of a P-storm rather than that of an M-storm. This and analogous graphs served as grounds for Gnevyshev to dispute the current systems of the regular parts of the storm (the equatorial ring or the ionospheric systems of surface currents).

As for the storms in which the vector of disturbance increases toward the pole ("polar" storms, according to Gnevyshev's terminology), I am unfortunately unable to confirm or refute the existence of such storms, in view of the lack of empirical material that would be necessary for this. It goes without saying that the discovery of such storms, if indeed they exist, would be of great interest for the morphology and theory of magnetic disturbances.

The examples given above show very plainly the extent to which the ideas of an investigator about the morphology of a disturbance determine his theoretical views on the physical explanation of the phenomenon.

Section 3. S_D -Variations

Let us now discuss another regular part of the disturbed field, the S_D -variations, whose existence was doubted by Nikol'skiy. To study S_D I used the same method applied to D_{st} , namely, calculation of the variations for quiet intervals of disturbed days. Here I obtained about the same results for middle-latitude and high-latitude observatories as in calculating S_D by conventional methods, i.e., $S_D = S_d - S_q$. The diurnal marches for the Sitka observatory presented in Fig.11 show that there is a great resemblance between $S_d - S_q$ and $S_q^d - S_q$, except that the amplitudes of $S_d - S_q$ are greater than the amplitudes of $S_q^d - S_q$. The calculation of $S_d - S_q$ for the low-latitude station of Honolulu did not yield the expected results. In the low latitudes, the D_{st} -variations are so great that statistical treatment of a very large amount of material would be necessary in order to eliminate them, in spite of the

fact that the number of quiet intervals on stormy days there is very great. The quantity $S_q^d - S_d$ was not calculated for the polar observatories, due to the lack of the necessary number of magnetograms; however, a simple examination of the individual disturbed days is enough to show, as could hardly have been expected, that the amplitude of the $S_q^d - S_q$ -variations will decrease north of 60° . On the other hand, it would appear that these variations will behave in the high latitudes in the same way as S_D , i.e., their intensity will sharply increase in the auroral zone. Figure 11 allowed me to conclude that the second regular part of the field of worldwide storms, the disturbed diurnal variations, likewise has an existence quite as real as that of

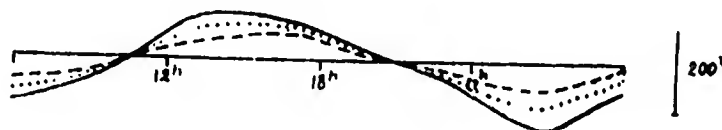


Fig.11 - S_D Variations of the Z-Component for Sitka Observatory
(Local Time)

— $S_q^d - S_q$, - - - $S_d - S_q$, $P(t)$

the D_{st} -variations, being found in all cases where the field is free from polar disturbances.

A second argument in favor of the existence of regular S_D -variations, evidently connected with the formation of a stable current system during worldwide storms, is the repetition of the active periods of a storm on successive days, which is well known to magnetologists. This repetition is manifested not only in the fact that the disturbance increases at one and the same hour of the day, but also in the fact that the main features and form of the fluctuations are sometimes repeated for several days in succession. This phenomenon is easily explained under the assumption of a current system encompassing the entire earth and fixed, if viewed from the sun. The

system exists for several days, at first developing and then weakening, repeating the fluctuations at the very same hours of each day. The S_D -current are apparently weaker in the low latitudes and considerably more intense in the high ones.

Returning to Fig.11, we may say that the S_D -variations of worldwide storms are very similar to the time-dependence of the field of polar storms. For comparison, we present in Fig.11 the diurnal variations of the Z component of the field of a typical polar storm (taken from the vector chart of Fig.31) for the latitude $\phi = 60^\circ$. It will be found that both curves, while differing somewhat in amplitude, have the same shape and the same times of the extremes. Thus the currents of the S_D -variations of worldwide storms and the currents of the P-storms, when superimposed, intensify each other without distorting each other.

Section 4. Division of the Field of Magnetic Storms

It follows from the above that the field of a worldwide magnetic storm may, in my opinion, be separated into four component parts:

$$M = D_{st}(\tau) + S_{DM}(t) + P(t) + D_i.$$

The value of the different parts in high and low latitudes is not the same. The part $P(t)$ has a great weight (greater than the first terms) in the high latitudes, while in the moderate and low latitude it is so small that here, without great error, we may adopt the Chapman three-term equation.

$$D_{st} + S_D + D_i$$

and calculate the regular parts of D_{st} and S_D with conventional methods, by appropriately averaging the available data for the mean hourly values of the magnetic elements. The value of D_m can serve as a good estimate of the order of D_{st} in these latitudes; the S_D -variations can be calculated as the difference $S_d - S_q$. Approaching the auroral zone, all the weight of the terms $P(t)$, $S_D(t)$, and D_i increases so much that it becomes difficult to separate the part of D_t by simple averaging, the more so since the value of D_{st} in the H component decreases; although it does increase in the Z component it still remains, in all probability, of the same order as in the temper-

ate latitudes*. As will be seen later (cf. Chapter III), an attempt to calculate the D_{st} of a polar observatory by the ordinary method is unsuccessful. The value of $D_m = H_q - H_d$ in the polar latitude ceases to characterize the value of D_{st} ; the predominance of negative polar storms has a strong influence on it. The S_d -variations in the polar latitudes, as in the low latitudes, may be taken as to $S_d - S_q$, bearing in mind the fact that in this way we are estimating both the regular part of the worldwide storm and the part due to the superimposition of the polar disturbances.

The properties and features of the polar storms are more easily studied by considering the isolated polar storms encountered on days free of worldwide storms, as has been done repeatedly by a number of authors.

The proposed division of the field of magnetic storms can be justified not only from the morphological point of view, but from the genetic as well. The D_{st} -variations can be considered as the field of the equatorial current ring, the S_p -variations as the field of the ionospheric currents encompassing the entire earth, and the P-storms as the result of the invasion of the ionosphere in high latitudes by corpuscles. For a worldwide storm, the presence of all three phenomena is characteristic: the formation of a ring current, the formation of ionospheric currents, and the deflection of the corpuscles toward the high latitudes. Penetration of the corpuscles in the high latitudes always accompanies the formation of great ionospheric and extra-ionospheric current systems, but such penetration can also take place without the formation of such systems. In such cases, only polar storms will be observed.

* If we assume that the D_{st} -variations are really caused by the equatorial current ring, whose field close to the earth's surface is almost uniform, then the value of Z at the pole should be about equal to H at the equator. While the graph of $Z_q - Z_q^d$ (cf. Fig. 10b) does not confirm this hypothesis, it still does not, in any case, contradict it.

The above point of view on the classification and division of the field of magnetic storms was used by us as a foundation for the workup and analysis of the material on magnetic disturbances. The D_{st} - and S_D -variations were isolated by statistical methods from the data on worldwide storms, and the three independent systems of electric currents, those of the D_{st} - and S_D -variations, and those of the P-storms, were calculated. The electric currents of several individual polar and worldwide storms were also studied, and their connection with the mean systems was shown.

CHAPTER III

THE D_{st} -VARIATIONSSection 1. The Starting Materials

To assure uniformity of the starting material, the observations at all observatories were taken for one and the same interval of time, namely for 1931-1933. There were two reasons for selecting these years: first, the largest number of data have been published for 1931-1933; second, these years are years of minimum solar activity. In years of high activity, the superimposition of one storm on another makes it difficult to separate the storms and complicates any statistical investigations.

For 1931-1933, I succeeded in collecting data of the hourly values of the magnetic elements for 66 observatories, whose names and coordinates are given in Table 1. The Table shows that there are a sufficient number of stations located at various latitudes in the eastern hemisphere. The number of stations in the western hemisphere is definitely inadequate.

For 1931-1933 I selected 65 moderate and violent storms with amplitudes at Slutsk ranging from 180 to 450 γ . It would have been desirable to determine the time of the beginning of the storm separately for each observatory. However, the lack of magnetograms from all observatories, that would be necessary for this, forced me to assume that the storms begin simultaneously over the entire earth, and to take the incipient moment according to the data of the Slutsk Observatory. A comparison of the beginnings of the storms for several observatories showed that the

Table 1

No.	Observatory	ϕ	λ	ψ	φ	λ	η	ϕ'
1	Thule (Tu.)	88° 0	0° 0	0° 0	76° 5	291° 1	- 19° 9	86° 9
2	Godhavn (God.)	79.8	32.5	- 17.5	69.2	306.5	- 11.2	78.2
3	Seoresby Sound (S.Z.)	75.0	81.8	- 36.2	70.5	338.0	- 6.8	73.8
4	Angmassalik (Ang.)	74.2	52.7	- 22.5	65.6	322.4	- 6.8	73.8
5	Sveagruvan (Sv.)	73.9	130.7	- 46.2	77.9	16.8	- 8.4	75.4
6	Chesterfield (Ch.)	73.5	324.0	+ 14.9	63.3	269.3	- 8.5	75.5
7	Tikhaya Bay (B.T.)	71.5	153.3	- 32.2	80.3	52.8	- 0.8	75.3
8	Bear Islands (M.O.)	71.1	124.5	- 37.9	74.5	19.2	- 5.1	72.1
9	Julisnensha (Yul.)	70.8	35.6	- 13.8	60.7	314.0	- 2.4	69.4
10	Fort Hae (F.H.)	69.0	290.9	+ 24.1	62.8	243.9	- 2.7	69.7
11	Point Barrow (P.B.)	68.6	241.2	+ 33.0	71.3	203.3	- 2.6	69.5
12	Tromsø (Tr.)	67.1	116.7	- 30.8	69.7	18.9	+ 0.3	66.7
13	Chelyuskin (Chel.)	66.3	176.5	- 3.2	77.7	104.3	- 6.3	73.3
14	Petsamo (Pet.)	64.9	125.8	- 27.6	63.5	31.2	0.0	67.0
15	Matochkin Shar (M.Sh.)	64.8	146.5	- 22.4	73.3	56.4	- 1.2	68.2
16	College, Fairbanks (K.F.)	64.5	255.4	+ 27.0	64.9	212.2	+ 2.0	65.0
17	Sodankylä (Sod.)	63.8	120.0	- 26.7	67.4	26.6	+ 2.4	64.6
18	Dickson Island (Dik.)	63.0	161.5	- 12.8	73.5	80.4	- 1.0	68.0
19	Lerwick (Ler.)	62.5	88.6	- 23.6	60.1	358.8	+ 6.2	60.8
20	Kandalaksha (Kan.)	62.5	124.2	- 25.0	67.1	32.4	-	-
21	Dombas (Dom.)	62.4	100.2	- 23.6	62.1	350.9	+ 6.5	61.5
22	Minuk (Min.)	61.8	301.0	+ 17.2	54.6	246.7	+ 3.8	63.2
23	Uellen (Uel.)	61.8	235.9	+ 24.5	66.2	190.2	+ 4.4	62.6
24	Sitka (Si.)	60.0	275.4	+ 21.4	57.0	224.7	+ 5.5	61.5
25	Eskdalemuir (Esk.)	58.5	82.9	- 20.4	55.3	356.8	+ 10.5	56.5
26	Lovo (Lov.)	58.1	105.8	- 22.1	59.4	17.8	+ 9.7	57.3
27	Slutsk (Sl.)	56.0	116.3	- 20.6	59.9	30.5	10.2	56.8
28	Rude Skou (R.S.)	55.0	98.5	- 20.6	55.8	12.4	12.7	54.7
29	Agincourt (Azh.)	55.0	347.0	+ 3.8	43.8	280.7	11.5	55.5
30	Abinger (Ab.)	55.0	83.3	- 18.4	51.2	359.6	14.8	52.2
31	de Bil (D.B.)	53.8	89.6	- 18.9	52.1	5.2	15.4	51.6
32	Srednikan (Sred.)	53.2	210.5	+ 12.7	62.6	152.3	9.5	57.5
33	Moscow (Mos.)	52.2	120.3	- 17.0	55.5	37.3	14.3	52.7
34	Paris - Val Joyeux (V.Zh.)	51.3	84.5	- 17.5	48.0	2.0	19.7	47.3
35	Yakutsk (Ynk.)	51.0	193.8	+ 5.8	62.0	129.7	10.8	56.2
36	Svidler (Sv.)	50.6	104.6	- 18.3	50.1	21.2	17.8	49.2
37	Cheltenham (Chelt.)	50.1	350.5	+ 2.4	38.7	283.2	16.5	50.5
38	Kazan' (Kaz.)	49.3	130.4	- 15.7	55.8	48.8	15.9	51.1
39	Sverdlovsk (Sver.)	48.8	140.7	- 13.3	56.7	61.1	15.9	51.1
40	Zuy (Irkutsk) (Ir.)	41.0	174.4	- 1.8	52.5	104.0	18.6	48.4
41	San Fernando (S.Fer.)	41.0	71.3	- 13.6	36.5	353.8	24.8	42.2
42	Tucson (Tuk.)	40.4	312.2	+ 10.1	32.2	249.2	24.6	42.4
43	South Sakhalin (Toyohara) (Toy.)	36.9	203.5	+ 6.7	47.0	142.8	22.4	44.6
44	Thilisi (Th.)	36.7	122.1	- 13.2	42.1	44.7	29.7	37.3
45	Mayann (Mt.)	32.4	198.3	+ 4.9	43.2	132.3	27.2	39.8
46	Tashkent (Tash.)	32.4	143.7	- 9.0	41.3	69.3	31.6	35.4
47	San Juan (S.Zh.)	29.9	3.2	- 0.7	18.4	293.9	37.3	29.7
48	Teoloyucan (Teo.)	29.6	327.0	+ 6.6	19.8	260.8	35.6	31.4
49	Helwan (Hel.)	27.2	106.4	- 12.7	29.9	31.3	40.0	27.0
50	Kakroka (Kak.)	26.0	206.0	+ 6.2	36.2	140.2	35.4	31.6
51	Honolulu (Hon.)	21.1	266.5	+ 12.3	21.3	201.9	45.4	21.6
52	Zu-se (Z.Z.)	20.0	189.1	+ 2.1	31.3	121.0	42.7	21.1
53	Hong Kong (G.K.)	11.0	182.9	+ 0.6	22.4	114.0	49.7	17.3
54	Alibag (Bombay) (Dom.)	9.5	143.6	- 7.2	18.6	72.9	54.8	12.2
55	Manila (Antipolo) (An.)	3.3	189.8	+ 2.0	14.6	121.2	57.8	9.2
56	Imancayo (Khuan.)	- 0.6	353.8	+ 1.3	- 12.0	284.7	-	-
57	Elizabethville (Vel.)	- 12.7	94.0	+ 11.7	- 11.7	27.5	-	-
58	Apia (Ap.)	- 16.0	260.2	+ 11.7	- 13.8	188.2	-	-
59	Batavia (Bat.)	- 18.0	175.6	- 0.9	- 6.6	106.8	-	-
60	Pilur (Pil.)	- 20.2	4.6	- 1.1	- 31.7	296.1	-	-
61	Mauritius (Mav.)	- 26.6	122.4	- 10.3	- 20.1	57.6	-	-
62	Cape Town (K.T.)	- 32.7	79.9	- 13.7	- 33.9	18.5	-	-
63	Watheroo (Wat.)	- 41.8	185.6	+ 1.3	- 30.3	115.9	-	-
64	Tonlaug (Tul.)	46.7	220.8	+ 9.5	- 37.5	145.5	-	-
65	Amberley (Amb.)	47.7	252.5	+ 15.1	- 43.5	172.7	-	-
66	South Orkney Islands (Ork.)	50.0	18.0	- 7.2	- 60.8	315.1	-	-

error involved in this assumption is not greater than ± 2 hours, since in the majority of cases the storms begin simultaneously with an accuracy of 1 hour. The calculation of D_{st} was performed by the method proposed in his day by Moos. The hourly values of the magnetic elements were entered for each storm on a separate line, and the resultant Table was averaged by columns corresponding to the hours of the time, reckoned from the beginning of the storm. This averaging eliminates the irregular fluctuations and the systematic S_p -variations, provided only that the beginnings of the storms are distributed with sufficient regularity among the hours of the day. The distribution of the 65 storms selected by me revealed a marked predominance of storms beginning in the morning hours. In view of this fact, I excluded 11 storms beginning a 4-7^h Universal Time from those selected by me. The final list of the 54 storms, used as the basis for the calculations, is given in Table 2.

The D_{st} -variations of the three elements were calculated for 34 hours: from the 4th hour before the onset of the storm to the 30th hour after the onset. The calculation of the D_{st} of the declination, or of the Y-component, showed that neither in the high nor in the low latitudes was it possible to discern any regularity in the variations of these elements during the course of the storm. Since the previous literature also contained references to the absence of distinct D_{st} -variations of the declination, the data on the accumulation were not included in the consideration, and I assumed that the horizontal component of the field strength of D_{st} lies roughly (at least in the low and middle latitudes) in the plane of the magnetic meridian.

The D_{st} -variations of the H and Z components for the individual observatories are shown in Figs. 12 and 13. The time indicated on the diagram is the time reckoned from the onset of the storm; the observatories are located in the order of decreasing geographic latitudes. Our attention is struck by the mobility and irregularity of many curves, which is particularly marked on comparison of Figs. 12 and 13 with the well-known D_{st} graphs of Chapman (Bibl. 40). An explanation of the presence of random fluctuations on the graphs of Figs. 12 and 13 might in all probability be

Table 2

List of Moderate and Great Magnetic Storms for 1931-1934

No. of Storm	Date	Onset	No. of Storm	Date	Onset	No. of Storm	Date	Onset	No. of Storm	Date	Onset
	1931 r										
1	16/I	3 h	14	3/II	2 h	29	15/X	4 h	43	5/VIII	4 h
2	24/II	0	15	3/III	12	30	20/X	6	44	8/IX	14
3	1/VI	11	16	10/III	6	31	15/XI	13	45	7/XI	11
4	20/VIII	1	17	28/III	5	32	14/XII	7	46	9/XII	9
5	30/IX	18	18	I/IV	10						
6	2/X	5	19	13/IV	8						
7	12/X	9	20	22/IV	7		1933 r			1934 r	
8	5/XI	13	21	23/IV	2	33	19/I	10	47	I/I	4 h
9	8/XI	1	22	25/IV	10	34	19/II	7	48	8/II	13
10	26/XI	7	23	27/IV	10	35	20/II	4	49	4/III	10
11	2/XII	5 h	24	2/V	16	36	21/II	8	50	30/III	15
			25	4/V	13	37	19/III	11	51	29/VII	23
			26	29/V	7	38	22/III	21	52	24/IX	2
	1932 r		27	26/VIII	8	39	24/III	0	53	7/XI	11
			28	5/IX	22	40	17/IV	6	54	7/XII	16
12	25/I	5 h				41	12/VI	16			
13	27/I	4				42	23/VII	6			

explained by the insufficient experimental material and the absence of any smoothing process. A consideration of D_{st} at the polar observatories ($\Phi > 65^\circ$) shows that the averaging of the data for 54 storms eliminated neither the irregular part of the field nor the S_D -variations. The influence of the S_D -variations is manifested in the marked diurnal periodicity of the curves presented, which is particularly strong

for the observatories at Dickson Island, Matochkin Shar, Tromso, Petsamo, and Sodankyla. Thus, the curves presented confirm the assertion made in the preceding Chapter to the effect that the D_{st} -variations in the polar regions cannot be calculated

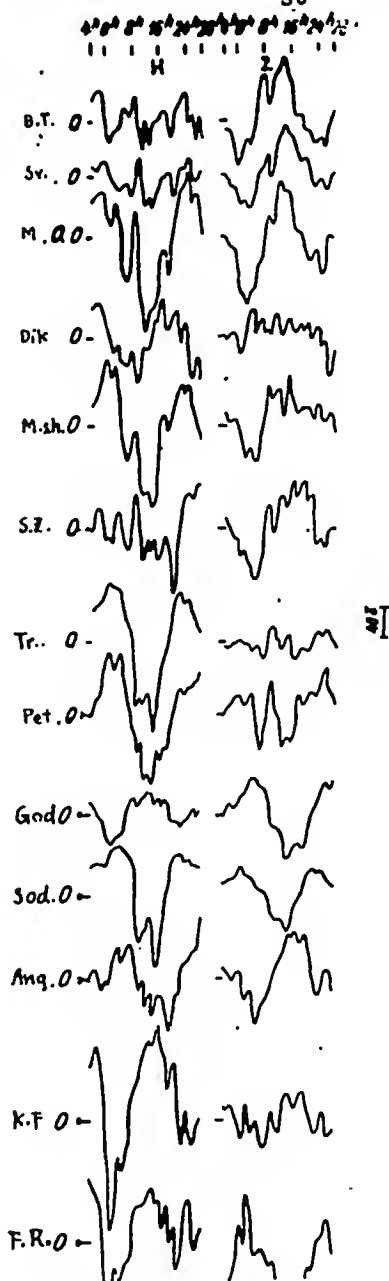


Fig.12 - D_{st} -Variations (Polar Observatories) *

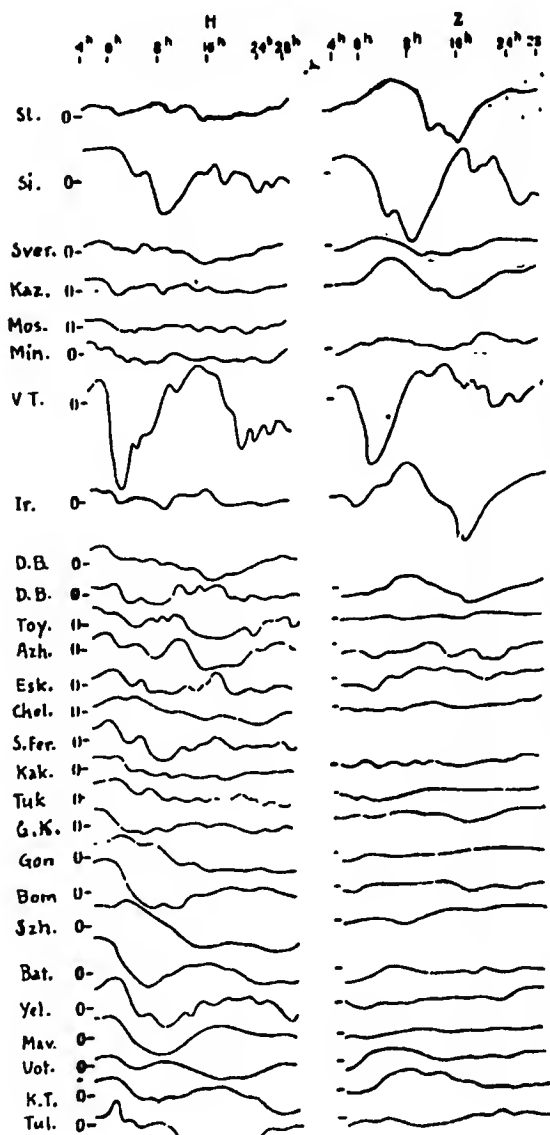


Fig.13 - D_{st} -Variations (Middle-Latitude Observatories)

* Translator's note: For meaning of abbreviations in diagram, see Table 1.

by the Moos-Chapman method. In the polar regions, the irregular fluctuations (D_1), the Polar storms (P), and the S_D -variations are so great that a simple averaging of the material does not eliminate them. In view of this fact it appeared to be inadvisable to use the data of the polar observatories given in Fig.12 in calculating the potential function of the D_{st} field, characterizing the course of the disturbance over the entire earth.

A consideration of the D_{st} -variations of the H and Z components of the middle-latitude observatories ($\Phi < 62^\circ$) allows us to draw the following conclusions:

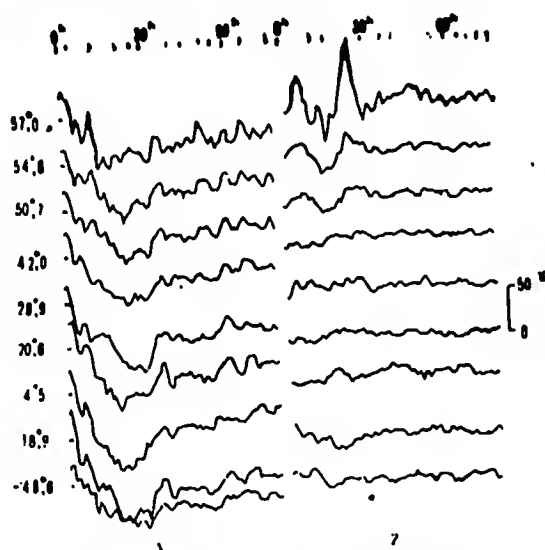


Fig.14 - The D_{st} -Variations
(After Vestine)

1. The principal feature of D_{st} is the lowering of the H component which is well perceptible at all latitudes, and is less in value than the increase in the Z component.

2. The D_{st} -variations of the H component are so similar in the northern and southern hemispheres, both in form and in sign, that it may be assumed that the distribution of H is symmetric with respect to the geomagnetic equator. The distribution of the Z component, on the other hand,

is asymmetric with respect to the equator.

3. The D_{st} -variations of observatories lying at the same geomagnetic latitudes, on the whole, resemble one another. Thus, it may be assumed that, in first approximation, the D_{st} field depends on two arguments: the geomagnetic latitude Φ and ψ the time elapsed from the beginning of the storm.

4. A more detailed consideration of Fig.13 shows that the D_{st} -variations of the observatories of the western hemisphere differ from those of the eastern hemisphere. A difference is also noted between the observatories of the same hemisphere (for

example, Irkutsk-de Bilt, Cape Town-Toolangi, etc.). It follows from the examples given that the field of D_{st} likewise contains longitudinal terms which, at one time, were found in the S_q -variations (Bibl.9).

The first phase of the storm (increases of the H component), noted by many investigators, was found to be vague on many curves of Fig.13. The possibility is not excluded that the absence of the first phase is connected with a certain inaccuracy in the determination of the time of onset of the storm, which might occur in cases when the storms begin gradually. To verify this assumption, I considered the data on the storms with sudden onsets (S_c). The D_{st} -variations obtained by averaging 13 S_c storms during the same interval of time, are given in Fig.14, constructed from materials furnished by Vestine (Bibl.62). Each curve of Fig.14 represents the mean for several observatories located at the corresponding latitude. A comparison of Figs.13 and 14 shows the great regularity in the distribution of the curves of Fig.14 and the presence of a distinct initial phase in them. The remaining conclusions enumerated by us with respect to the form and distribution of the D_{st} -variations are fully confirmed by Fig.14.

Section 2. Spherical Analysis of the D_{st} -Variations

In all possible types of calculation of a theoretical nature it is more convenient to operate not with the observed elements of the magnetic field H, D, Z, but with rectangular components. The geomagnetic components of the field of variations, X' , Y' , Z' are connected with the variations of D, H, Z by the following relations:

$$X' = H \cos(D_0 - \psi) - H_0 \sin(D_0 - \psi) \sin I' D', \quad (1)$$

$$Y' = H \sin(D_0 - \psi) + H_0 \cos(D_0 - \psi) \sin I' D', \quad (2)$$

$$Z' = Z,$$

where D_0 and H_0 are the mean annual values of these elements, and ψ is the angle between the geographical meridian of a given place.

In our case (absence of substantial and regular fluctuations in D), the second terms of eqs.(1) and (2) were rejected and it was shown that the variations of Y'

are small in comparison with X' . Thus the rectangular components of the D_{st} field were reduced to a calculation of X' by the formula $X' = H \cos (D_0 - \psi)$, the variations of X' so obtained proving to be very similar to those of the H component.

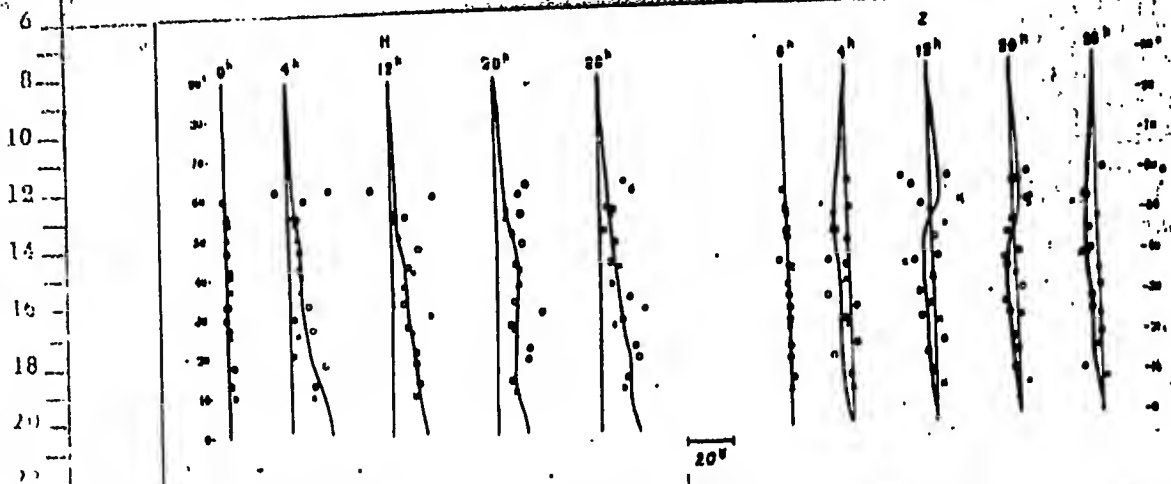


Fig.15 - Latitudinal Distribution of H and Z Components of the D_{st} -Variations
 x = Northern hemisphere; o = Southern hemisphere; not taken into account
 in calculating the mean.

Figure 15 gives graphs of the dependence of X' and Z on ϕ for a few stormtimes. The data of the southern and northern hemispheres are presented together, allowing for the symmetry of the H component and the asymmetry of the Z component. The D_{st} -variations of the individual observatories (Fig.13) were first averaged by groups in accordance with the value of ϕ , and the mean data were then entered in Fig.15. The dispersion of the points on both graphs is relatively low, and, in particular, there is absolutely no detectable systematic difference between the data of the northern and southern hemispheres,

Since we abandoned the use of the D_{st} -variations calculated from the observations for the polar observatories, the curves of X' and Z were extrapolated to the high latitudes, and, in accordance with the considerations made in Chapter II, it was assumed that, at the pole, $X' = 0$ and $Z \approx X'$ equiv. The comparatively simple form of the dependence of X' and Z on ϕ allowed us to use the method of spherical

analysis for the analytic representation of the field.

Neglecting the longitude-dependence of D_{st} , the potential of the field may be represented, for a fixed instant of time t , by a series of Legendre polynomials:

$$V = R \sum_n \left[I_n \left(\frac{R}{r} \right)^{n+1} + E_n \left(\frac{r}{R} \right)^n \right] P_n(\cos \theta), \quad (3)$$

where, as usual, the terms E_n are responsible for that part of the field due to sources external to the earth's surface, while the terms I_n are responsible for the internal part of the field.

On the earth's surface, $r = R$, and

$$V = R \sum_n g_n P_n(\cos \theta), \quad (4)$$

where

$$g_n = E_n + I_n. \quad (5)$$

Hence it follows that the rectangular components of the field in geomagnetic coordinates, for $r = R$, will be as follows:

$$X' = \frac{1}{R} \frac{\partial V}{\partial \theta} = \sum_n g_n \frac{dP_n(\cos \theta)}{d\theta}, \quad (6)$$

$$Z' = \frac{\partial V}{\partial r} = \sum_n j_n P_n(\cos \theta), \quad (7)$$

where

$$j_n = nE_n - (n+1)I_n. \quad (8)$$

The identity $Y = 0$ completely corresponds to the absence of systematic D_{st} -variations noted by us in the D and Y elements. The calculation of the potential of the D_{st} field was performed independently for 56 moderate storms (analysis I) and for 13 storms with sudden onset (analysis II). The method of calculation in both cases was one and the same. To find the coefficients of g_n on the basis of the graphs of the dependence $X'(\Phi)$ (the heavy curve in Fig.15), I calculated the curves $F(\theta) = X' \sin \theta$ which, in turn, were represented by Fourier series in θ

$$F(\theta) = \sum_k \beta_k^* \sin k\theta. \quad (9)$$

On the basis of the coefficients β_k , I used the Schuster-Schmidt formulas (Bibl.6, 9) for calculating the constants g_n , whose values are given in Tables 3

and 4. The constants j_n (also see Tables 3 and 4) were found by the Schuster formula by direct expansion of Z into a Fourier series in θ

$$Z = \sum_k \beta_k^x \sin k\theta. \quad (10)$$

Table 3

Analysis I

τ	g_1^Y	g_2^Y	g_3^Y	j_1^Y	j_2^Y	j_3^Y
4 h	24.93	-1.23	3.19	6.70	-5.11	0.23
12	21.74	-3.56	0.79	1.36	-6.21	1.79
20	23.14	-0.61	-0.14	0.84	-4.65	2.38
28	27.80	-3.16	0.16	6.44	-4.49	0.63

The coefficients of the expansion of the potential into series of spherical harmonics were repeatedly calculated by the Schuster method (Bibl.6, 9, 15), but nevertheless the application of this method requires certain explanations. The Schuster method is based on the replacement in the expression

$$\begin{aligned} & \sum_n \sum_m (g_n^m \cos m\lambda + h_n^m \sin m\lambda) = \\ & = \sum_m \left[\cos m\lambda \sum_{n=m}^q g_n^m P_n^m + \sin m\lambda \sum_{n=m}^q h_n^m P_n^m \right] \end{aligned} \quad (11)$$

of the series

$$k^m(\theta) = \sum_n g_n^m P_n^m \text{ и } l^m(\theta) = \sum_n h_n^m P_n^m$$

by the series

$$k^m(\theta) = \sum_s a_s \cos s\theta; \quad l^m(\theta) = \sum_s a_s \cos s\theta \quad (12)$$

or

$$k^m(\theta) = \sum_s \beta_s \sin s\theta; \quad l^m(\theta) = \sum_s b_s \sin s\theta \quad (13)$$

and on the calculation of g and h in terms of α_s, a_s or β_s, b_s . For $m = 2t$, Schuster recommends using eq.(13), and for $m = 2t + 1$, eq.(12). In these cases, the equations connecting g, h, c, α or β, b , are rather simple and convenient for calculation.

Table 4
Analysis II

τ	g_1^Y	g_2^Y	g_3^Y	j_1^Y	j_2^Y	j_3^Y
1 h	-33.3	-0.54	1.15	-0.98	-6.19	-
10	44.1	-2.05	-0.63	3.20	-15.5	-6.6
20	81.8	-0.90	-1.55	-1.20	-35.80	6.6
30	69.3	-0.66	-1.32	15.8	-12.84	-0.7
40	47.8	-0.54	-2.01	10.7	-11.41	2.46
60	32.8	-1.63	-1.24	9.36	-9.92	1.10

However, the representation of the function $k^m(\theta)$ (m being odd) known in the interval from 0 to π , by the series $\sum_s \beta_s \sin s\theta$ imposes on it the conditions of asymmetry with respect to $\theta = \pi$ and of its vanishing at the points $\theta = 0$ and $\theta = \pi$. If the empirical function being studied satisfies these conditions, then the application of the Schuster method is theoretically irreproachable, and in practice assures high accuracy in the computation of the coefficients g, h . If, however, $k^m(\theta)$ differs substantially from 0 at the poles, then the use of the Schuster method distorts the distribution of the function in the polar caps and may introduce substantial errors. It follows that an application of this method to the calculation of the coefficients of an expansion in spherical harmonics of the Z component of the earth's permanent magnetic field, of the D_{st} field, or of the noncyclic variations (i.e., of functions in the representation of which the terms P_1, P_3 , etc., play the principal role) is not completely successful, and, in any case, should be accompanied by an estimate of the error to be expected. Accordingly, the calculation of the co-

efficients j_n in eq.(7) for one instant of time ($\tau = 12$ hours) were calculated both by the Schuster method and the method of least squares. The good agreement between the results of the two methods (discrepancy of the order of 1%) and also a comparison of the initial curves of $Z(\theta)$ with those calculated by eq.(7) (cf. Table 5) showed that we could calculate j_n by the Schuster method without great danger. Table 5 shows that the deviation of the calculated curve of $Z(\theta)$ from the empirical curve is significant only in the polar regions, where, all the same, we do not know the true distribution of the field.

It follows from the symmetry of X' and the asymmetry of Z with respect to the equator ($\theta = \pi/2$) that, in the expression for the potential, eq.(4) must contain only odd polynomials.

The numerical values of the constants g and j in analyses I and II (Tables 3, 4) differ somewhat but are still in good agreement. In both cases, the first harmonic has the greatest weight, having a coefficient g_1 of the order of 20-30 γ in the first case and 50-80 γ in the second. The larger values of the coefficients in analysis II may possibly be explained by the fact that almost all the storms making up the 13 S_c -storms selected were great storms, while most of the storms among the 54 storms of analysis I belong to the category of moderate storms. The coefficients g_1 calculated for D_m by McNish and for D_{st} by Chapman and Whitehead (Bibl.40), lie within these same limits (30-50 γ). The sign of g_1 is everywhere positive, except for the first hour in analysis II, corresponding to the first phase of a magnetic storm. The sign of the coefficient of the third harmonic g_3 is negative, while the values of g_5 include both positive and negative quantities. Of the coefficients representing the expansion of Z , the greatest is j_3 , characterizing the stable negative values.

It will be seen from a comparison of the coefficients g and j at different instants of time that the storm reaches its maximum development at the end of the first day or the beginning of the second. The calculation by eqs.(5) and (8) of the coefficients of the internal and external fields of E and I separately gave the re-

sults shown in Table 6. In all cases, except for one, the absolute value of the external field is greater than that of the internal field.

Table 5

D_{gt} -Variations of the Z Components, in

	$\tau = 4 \text{ h}$		$\tau = 20 \text{ h}$	
	Observed	Calculated	Observed	Calculated
70°	3	4	-2	-2
50	7	8	-2	-3
30	5	4	5	7
10	3	3	2	3

The ratio I/E (Table 7) is very stable for the first harmonic (mean value 0.40 ± 0.07 and 0.39 ± 0.10). Within wide limits, the ratio fluctuates for the third harmonic (-0.17 ± 0.12 and -0.61 ± 0.18) and is not very regular for the fifth

Table 6

τ	E_1^Y	E_3^Y	E_5^Y	I_1^Y	I_3^Y	I_5^Y
4 h	18.8	-1.4	1.3	6.1	0.2	1.4
12	14.9	-1.8	0.6	6.8	0.2	0.2
20	15.7	-1.0	0.2	7.4	0.4	-0.3
28	20.7	-1.6	0.2	7.1	0.0	0.0
1	-22.2	-1.2	-	-11.1	0.7	-
10	30.5	-3.4	-	13.6	1.3	-
20	54.1	-5.6	-	27.7	4.8	-
30	51.4	-2.2	-	17.8	1.7	-
40	35.4	-1.9	-	12.4	1.4	-
60	25.0	-2.3	-	4.5	0.7	-

harmonic. The value of I_5/E_5 for $\tau = 20$ hours in absolute magnitude is > 1 and differs in sign from the corresponding ratio for other instants of time. This increase of the scatter of $1/E$ for P_3 , and especially for P_5 , finds its natural explanation in the fact that the absolute magnitude of these harmonics is considerably smaller, and consequently, the relative errors are larger, than with the first harmonic.

The systematic change of sign of the ratio is a point of interest

$$\frac{I_1}{E_1} > 0; \quad \frac{I_3}{E_3} < 0; \quad \frac{I_5}{E_5} > 0,$$

and the very good agreement of the results obtained in analyses I and II will be noted. Table 7 also gives other data known in the literature on the separation of the perturbation field into an external and an internal part, which are likewise in good agreement with our results. The mean values of 0.39 and 0.40 obtained by us for g_1 , D_{st} agree exactly with the ratio calculated by McNish for D_m . If, furthermore, we bear in mind that I_1/E_1 for D_{st} (according to the data by Chapman and Whitehead) varies within the range of 0.36-0.42 and, for the noncyclic variations, is equal to 0.30 (McNish) or 0.23 (Dolginov), then it may be considered as proved that the external part of the first harmonic is equal, on the average, to 0.30-0.40 of the value of the external part. The negative value of I_3/E_3 is confirmed by the data of McNish for D_m , and in part by the data of Chapman and Whitehead for D_{st} . The numerical values of $1/E$ will be discussed in greater detail below, in Chapter X, devoted to the discussion of the inductive origin of the internal part of the fields of variations.

Section 3. Ionospheric System of Currents of the D_{st} -Variations

It was stated above (Chapter II) that two versions of the explanation for the external part of the D_{st} -variations were proposed: one based on an ionospheric system of currents, the other on an extra-ionospheric ring current. We used the data of our analysis to calculate both these proposed current systems.

Assume that the magnetic field whose potential on the earth's surface is repre-

sented by the series of spherical functions

$$V = R \sum_n \sum_m (g_n^m \cos m\lambda + h_n^m \sin m\lambda) P_n^m,$$

is caused by a current layer located on a sphere having a radius of a ($a > R$). Then

Table 7

	τ	$\frac{I_1}{E_1}$	$\frac{I_2}{E_2}$	$\frac{I_3}{E_3}$	$\frac{I_4}{E_4}$
D_{st} Analysis I	4	0,32	-0,16	0,78	
	12	0,46	-0,11	0,33	
	20	0,47	-0,40	-1,60	
	28	0,34	0,00	0,00	
Mean		0,40	-0,17		
D_{st} Analysis II	1	0,50	-0,58		
	10	0,45	-0,38		
	20	0,51	-0,86		
	30	0,35	-0,77		
	40	0,35	-0,75		
	60	0,18	-0,34		
Mean		0,39	-0,61		
D_{st} acc. to Chapman and Whitehead	1	-5/-11	-0,5/-0,5	-1/0	
	3	-2/-6	-1/1	-2,5/-1,5	
	6	3/11	-2/2	-3,0/-1,0	
	12	10/26	1/1	-1/0	
	18	10/28	0/0	-1/0	
	24	11/26	-2/-1	0/-0,5	
	30	9/24	0/1	-1/-1	
	36	9/23	1/-1	0/-1	
	42	7/21	0/1	-1/-1	
	48	7/20	1/-1	-0,5/-0,5	
D_m acc. to McNish . .		0,39	-1,12	0,27	-0,80
nch acc. to Dolginov . .		0,28	0,20	0,86	1,46
nch { 1923		0,23			
acc. to McNish { 1926		0,37			

Note. nch = Noncyclic variations

the distribution of the current function in the layer can be calculated by the Bidlingmayer formula

$$I = -\frac{10}{4\pi} \sum_n \sum_m \frac{2n+1}{n+1} \left(\frac{a}{R}\right)^n (g_n^m \cos m\lambda + h_n^m \sin m\lambda) P_n^m \frac{A}{cM^2}.$$

In our case

$$I = -\frac{10}{4\pi} \sum_n \left(\frac{R+h}{R}\right)^n E_n P_n \frac{A}{cM^2}. \quad (14)$$

Since the most probable region of concentration of the currents responsible for the magnetic disturbances is the F_2 layer of the ionosphere, we assumed $h = 300$ km and calculated, from the coefficients E_n of analysis I, the current density for τ equal to 4, 12, 20, 28 hours.

As an example, Fig.16 represents the current systems for τ equal to 12 and 28 hours. Since the potential of the D_{st} field is represented only by zonal harmonics,

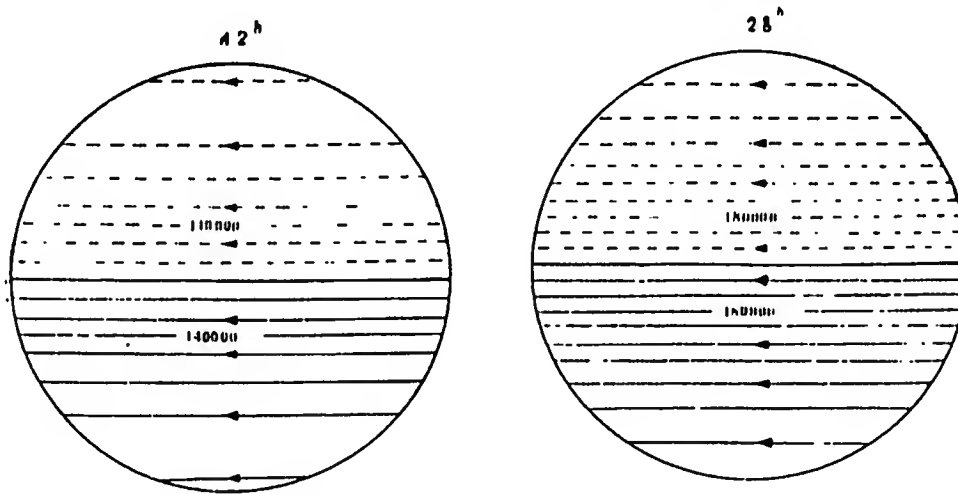


Fig.16 - Electric Currents of the D_{st} -Variations; a Current of 20,000 amp Flows Between Two Adjacent Lines

_____ Positive values of current function; - - - Negative values

it is natural that the lines of current shown in the diagram should be parallel circles. Since only the odd polynomials (P_1, P_3, P_5) entered the expression for the potential, it follows that the configuration and intensity of the currents in the northern and southern hemispheres are identical, but that the sign of the current function is different. In the northern hemisphere, $V > 0$ and $I < 0$ (the lines of current are given by broken lines) while in the southern hemisphere $V < 0$ and $I > 0$ (solid current lines). The Chapman current system (Fig.4a) does not allow for the change in sign of the current function on crossing the equator, in view of which fact, the current systems in Figs.4a and Fig.16 differ in their outward

forms*.

The lines of currents in Fig.16 are so drawn that a current of 20,000 amp flows between two adjacent lines. The intensity of the currents in the two systems is about the same. The total value of the current flowing from east to west between the pole and the equator is equal to 180,000 (for the system constructed by us). The current density $\rho = \frac{\partial I}{\partial s} = 0.0002$ amp/cm. The direction of the current in Fig.16 is determined according to the rule that current flows around I_{\min} clockwise and around I_{\max} counterclockwise. Thus in both hemispheres the current flows westerly during the main phase of a storm.

A comparison of the current systems (Figs.4a and 16) will show the increased density of the current lines in the polar regions in the Chapman current system, corresponding to the intensification postulated by him for the D_{st} field in the high latitudes. This densification of the current lines is absent from the systems constructed by us. Conversely, a certain densification of the lines in the equatorial regions can be noted, which expresses the well-known fact that the amplitude of D_{st} increases in the low latitudes. The current density varies from $\rho = 0.0001$ amp/cm at latitudes ϕ from 50 to 60°, to $\rho = 0.0003$ amp/cm near the equator. A comparison of the current calculated for 12 and 28 hours shows that during a storm the configuration of the current system hardly changes and that only its intensity varies. Only in the prolongation of the first phase of the storm ($\tau = 1$ hour in analysis II) is the direction of the currents opposite (from west to east). The systems of D_{st} curves in Fig.16 correspond to a mean decrease of I in the temperate latitudes, by 40-50 %. During certain storms, this decrease reaches 1000 %, so that the intensity of the currents equivalent to these storms should increase to $3-4 \times 10^6$ amp, and the density of the current should be $\rho = 0.0004$ amp/cm.

* The figure of the D_{st} -currents given in Mitra's monograph (Bibl.50), also shows that the current function is of opposite sign in different hemispheres.

Section 4. The Equatorial Current Ring

Leaving the discussion of the question as to the actual existence of the resultant system for later (cf. Chapter VIII), let us now turn to a calculation of the equatorial current ring, which presents an alternate explanation for the D_{st} -variations of the magnetic elements. As is generally known, the potential of the magnetic field of a linear ring current whose center lies on the axis $\theta = 0$, may be represented by the following series of spherical functions:

$$V_p = 2\pi i \left[1 - \cos \theta_0 + (1 - \cos^2 \theta_0) \sum_n \frac{1}{n} P_n(\cos \theta) P'_n(\cos \theta_0) \left(\frac{R}{a} \right)^n \right].$$

Here i denotes the current strength in the ring, θ_0 and a are the polar distance and radius of the ring, respectively, while θ and θ_0 are spherical coordinates of the point P . If the ring lies in the plane $\theta = 90^\circ$ (the plane of the equator), then $\cos \theta_0 = 0$, and

$$V_p = 2\pi i \left[1 + \sum_n \frac{1}{n} P_n(\cos \theta) P'_n(0) \left(\frac{R}{a} \right)^n \right]. \quad (15)$$

Confining ourselves to the first three terms of the sum and substituting numerical values of $P'_n(0)$ in eq. (15), we have

$$V_p = 2\pi i \left[1 + \frac{R}{a} P_1 - \frac{3}{2} \left(\frac{R}{a} \right)^3 P_3 + \frac{15}{8} \left(\frac{R}{a} \right)^5 P_5 \right]. \quad (15')$$

Let us likewise confine ourselves to three terms in the expression for the external part of the D_{st} potential. For the earth's surface ($r = R$), we have

$$V_e = R [E_1 P_1 + E_3 P_3 + E_5 P_5]. \quad (16)$$

Equating the potential V_e , calculated from the observations, to the potential of the magnetic field of the ring, an equation will be obtained by which the param-

eters of the ring can be evaluated. Equating eqs.(15') and (16), we have *

$$\left. \begin{aligned} RE_1 &= 2\pi i \frac{R}{a} \\ RE_2 &= -2\pi i \frac{3}{2} \left(\frac{R}{a}\right)^3 \\ RE_3 &= 2\pi i \frac{15}{8} \left(\frac{R}{a}\right)^5 \end{aligned} \right\} \quad (17)$$

Combining eqs.(17) pairwise, we obtain the following three equations:

$$\left(\frac{a}{R}\right)^2 = -\frac{3}{2} \frac{E_1}{E_2}; \quad \left(\frac{a}{R}\right)^4 = -\frac{5}{4} \frac{E_2}{E_3}; \quad \left(\frac{a}{R}\right)^6 = \frac{15}{8} \frac{E_1}{E_3}, \quad (18)$$

which lead to the numerical values of a/R given in Table 8. As will be seen from the Table, the values of a/R fluctuate within relatively narrow limits. The calculations of a/R on the basis of E_3/E_5 in E_1/E_5 indicate the systematic increase of the radius of the ring during the development of a storm. But the data for E_1/E_3 , which should be most trustworthy of all, do not display this increase. The mean value $a = 3.8R \pm 0.8R$ is in good agreement with the views of Chapman, Forbush, and Kalinin that have been discussed above. Thus both theoretical arguments and empirical data from the field of terrestrial magnetism and cosmic rays lead to a magnitude of the ring of the order of 3-5 earth radii. It goes without saying that the ring may be considerably larger than this during individual storms, but all the same Stoermer's hypothesis of a ring with a radius of several hundred earth-radii must be rejected. The current strength in the ring corresponding to the D_{st} -variation of 56 moderate storms is equal to

$$i = \frac{aE_1}{2\pi} = 7 \times 10^6 \text{ A},$$

* The term $2\pi i$ in eq.(15') denotes a part of the potential that is the same for the entire surface of the earth. There is no analogous term in eq.(16), since eq.(16) determines the field potential with accuracy to a constant.

and that corresponding to 13 S_c storms, equal to $i = 20 \times 10^5$ amp. This estimate, too, is in good agreement with the ideas of Chapman and Ferraro on the current ring.

Table 8

	τ	$\frac{E_1}{E_3}$	$\frac{E_3}{E_5}$	$\frac{E_1}{E_5}$	Mean
Analysis I	4 Hours	4.5	-	2.1	3.3
	12	3.6	2.0	2.7	2.8
	20	5.0	2.5	3.6	3.7
	28	4.5	3.3	3.8	3.9
	Mean	4.4	2.6	3.1	3.4 ± 0.8
Analysis II	1 Hour	-	-	-	-
	10	3.8	-	-	-
	20	3.8	-	-	-
	30	5.9	-	-	-
	40	5.2	-	-	-
	60	4.0	-	-	-
	Mean	4.6 ± 1.0	-	-	-

CHAPTER IV

CALCULATION OF ELECTRIC CURRENTS BY THE METHOD OF SURFACE INTEGRALS

Section 1. The Vestine Method of Separating the Observed Field into an External and an Internal Part

Spherical analysis, applied by us in the preceding Chapter to the study of the field of the D_{st} -variations, was long the only method for calculating the potential from the magnetic elements observed at a number of points of the earth's surface. It has been repeatedly used with great success in the representation of the permanent field and the S_q variation, and has allowed the solution of a number of major problems of the nature and structure of these fields. It has also been used in considering the secular and annual variations, and, as we have seen above, of certain parts of the field of variations: D_{st} , D_m , and nch . But the use of spherical analysis is limited by the requirement that the field studied must possess spherical symmetry and that it can be successfully represented by the first few terms of the series. If, however, the field has a rather complex structure and requires a large number of terms for its representation, then the labor needed in calculating the coefficients is immeasurably increased, and the series so obtained ceases to be convenient for various practical or theoretical applications. Accordingly, the spherical analysis of the S_p -variations, which characterize a complex geographical distribution, would seem a priori to be doomed to fail, and Chapman, Vestine, and other authors who have studied S_p , have abstained from any analytic representation of the field at all. In 1941, Vestine (Bibl.57a, b) proposed a new method of mathematical

analysis which, according to the author's idea, was to replace spherical analysis in the case of rather complex fields. This method, based on the representation of the potential of the field by the aid of surface integrals, allows a separation of the potential into a part of internal origin and one of external origin, from the components of the field as observed on the surface of the sphere. Since it imposes no restrictions whatever on the configuration of the field, I decided to apply this method to the calculation of the potential of the S_D -variations. For the purpose of our work, however, as for many questions of geomagnetism, it is necessary not only to separate the field into an external and an internal part, but also to calculate the electric currents whose field is equivalent to the observed field. The calculations performed by us showed that this problem, too, is successfully solved by the aid of surface integrals.

Since the method of surface integrals is here used in geomagnetic practice for the first time*, its mathematical foundations and practical methods will be discussed in the present Chapter, while the description of the calculations of the currents of the S_D -variations will be reserved for the next Chapter.

The theory of the method is very simple. Let the volume v be surrounded by a closed surface S , and let there be, both within and without the surface S , sources exciting the magnetic field. If U and V are functions with continuous first derivatives in the region v and on the surface S , and continuous second derivatives in the volume v , then Green's fundamental theorem indicates that

$$\int_v (U \Delta V - V \Delta U) dv = \int_S \left(U \frac{\partial V}{\partial n} - V \frac{\partial U}{\partial n} \right) ds, \quad (1)$$

* In Vestine's note (Bibl.57b) the calculation of the potential of the geomagnetic field at one instant of time is given as an example, and the work by Vestine and Davies (Bibl.61) on the interpretation of magnetic anomalies contains several formulas based on the solution of two-dimensional problems by the aid of surface integrals.

where n denotes the direction of the external normal. Let us assume that $U = 1/r$ (r = distance from a fixed point P outside S to the variable point M , in v or on S) and

$$V = \bar{V}_e + V_i, \quad (2)$$

where V_e is the potential of the field of the sources external with respect to S , and V_i is the potential of the field of sources internal with respect to S ; we then have

$$\int_v \left(\frac{1}{r} \Delta V - V \Delta \frac{1}{r} \right) dv = \int_s \left(\frac{1}{r} \frac{\partial V}{\partial n} - V \frac{\partial \frac{1}{r}}{\partial n} \right) ds. \quad (1')$$

For any point of the volume v

$$\Delta \frac{1}{r} = 0, \Delta V_e = 0 \text{ and } \Delta V_i = -4\pi\mu_i$$

(μ_i = density of the internal magnetic masses). Consequently, the left side of eq.(1') gives

$$\int_v \frac{1}{r} \Delta V dv = -4\pi \int_v \frac{\mu_i}{r} dv = -4\pi V_i;$$

and the potential at the external point P_e of the field of internal sources yields

$$V_i = -\frac{1}{4\pi} \int_s \left(\frac{1}{r} \frac{\partial V}{\partial n} - V \frac{\partial \frac{1}{r}}{\partial n} \right) ds. \quad (3)$$

By similar reasoning we get the result that the potential at the internal point P_i of the field of external sources reads as follows:

$$V_e = \frac{1}{4\pi} \int_s \left(\frac{1}{r} \frac{\partial V}{\partial n} - V \frac{\partial \frac{1}{r}}{\partial n} \right) ds. \quad (4)$$

Let the points P_e and P_i be located on the external and internal normals to S passing through the point of the surface P , where both $P_e \rightarrow P$ and $P_i \rightarrow P$.

Then, taking $\frac{1}{4\pi} \int \frac{1}{r} \frac{\partial V}{\partial n} ds$ as the potential of a single layer of the density

$\rho = -1/4 \frac{\partial V}{\partial n}$, and $\frac{1}{4\pi} \int_S V \frac{\partial \frac{1}{r}}{\partial n} ds$ as the potential of a double layer of the density $\rho = \frac{1}{4\pi} V$, and allowing for the known properties of the potentials of single and double layers, we get the result that

$$\begin{aligned} V_i|_{P_+} &= \int_S \frac{\sigma}{r} ds + \left[\int_S \rho \frac{\partial \frac{1}{r}}{\partial n} ds + 2\pi\rho_p \right] = \\ &= -\frac{1}{4\pi} \int_S \frac{1}{r} \frac{\partial V}{\partial n} ds + \frac{1}{4\pi} \int_S V \frac{\partial \frac{1}{r}}{\partial n} ds + \frac{1}{2} V_p, \end{aligned} \quad (5)$$

$$\begin{aligned} V_e|_{P_-} &= -\int_S \frac{\sigma}{r} ds - \left[\int_S \rho \frac{\partial \frac{1}{r}}{\partial n} ds - 2\pi\rho_p \right] = \\ &= \frac{1}{4\pi} \int_S \frac{1}{r} \frac{\partial V}{\partial n} ds - \frac{1}{4\pi} \int_S V \frac{\partial \frac{1}{r}}{\partial n} ds + \frac{1}{2} V_p, \end{aligned} \quad (6)$$

where P_+ and P_- denotes that the approach to the point was from the side of the external and internal normals. Hence,

$$V_e - V_i|_p = \frac{1}{2\pi} \int_S \left(\frac{1}{r} \frac{\partial V}{\partial n} - V \frac{\partial \frac{1}{r}}{\partial n} \right) ds. \quad (7)$$

Knowing the distribution of the surface S of the total potential V and its normal derivative $\partial V / \partial n$, $V_e - V_i$ may be calculated for any point of the surface; then, by combining eqs.(2) and (7), the value of V_e and V_i can be separately determined.

It must be noted, however, that the potential V_0 of any uniform double layer of a density of ρ_0 , located on the closed surface S , equals zero outside the surface and $-4\pi\rho_0$ inside it. For this reason, if, to the postulated double layer with a density of $1/4\pi V$, we add a layer of uniform density $\rho_0 = -V_0/4\pi$, then eq.(3) will remain without change, while eq.(4) will take the form

$$V_e = \frac{1}{4\pi} \int_S \left[\frac{1}{r} \frac{\partial V}{\partial n} - (V - V_0) \frac{\partial \frac{1}{r}}{\partial n} \right] ds + V_0, \quad (8)$$

whence

$$V_e|_{P_-} = \frac{1}{4\pi} \int_S \left[\frac{1}{r} \frac{\partial V}{\partial n} - (V - V_0) \frac{\partial \frac{1}{r}}{\partial n} \right] ds + \frac{V - V_0}{2} + V_0. \quad (9)$$

Instead of eq.(5) we will now have

$$V_i|_{P_+} = -\frac{1}{4\pi} \int_S \left[\frac{1}{r} \frac{\partial V}{\partial n} - (V - V_0) \frac{\partial \frac{1}{r}}{\partial n} \right] ds + \frac{V - V_0}{2} \quad (10)$$

and, consequently,

$$V_e - V_i = \frac{1}{2\pi} \int_S \left[\frac{1}{r} \frac{\partial V}{\partial n} - (V - V_0) \frac{\partial \frac{1}{r}}{\partial n} \right] ds + V_0. \quad (11)$$

It follows from eqs.(9) - (11) that, if the potential V on the surface S is known only with an accuracy to an additive constant, then the values of $V_e - V_i$ and V_e may be found only with an accuracy to a constant, while the values of V_i will be calculated exactly. Besides the above general formulas, Vestine also gave formulas applicable to cases when the surface S is a sphere or a plane. In spherical coordinates with the pole coinciding with the point P (cf. Fig. 17a), the distance between the points P and M ($r_0 \varphi$) is equal to

$$r = 2R \sin \frac{\theta}{2} = 2R \sin \psi, \quad \psi = \frac{\theta}{2},$$

$$\frac{\partial \frac{1}{r}}{\partial n} = -\frac{1}{r^2} \cos \alpha = -\frac{\sin \psi}{r^2} = -\frac{1}{4R^2 \sin \psi}.$$

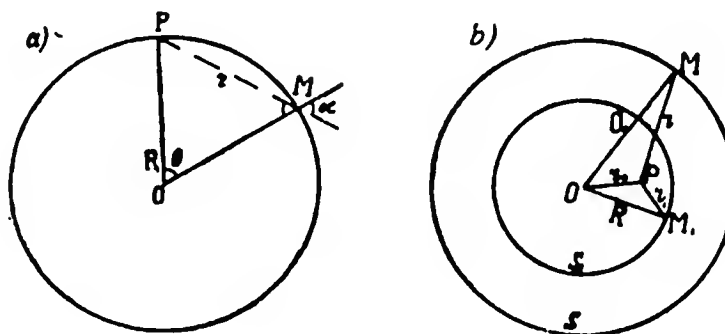
Denoting $\partial V / \partial n$ by Z , let us now transform eq.(7) into

$$V_e - V_i = \frac{1}{2\pi} \int_0^{2\pi} \int_0^{\frac{\pi}{2}} (V + 2RZ) \cos \psi \, d\psi \, d\varphi \quad (12)$$

or

$$V_e - V_i = \frac{1}{2\pi} \int_0^{2\pi} \int_0^{\frac{\pi}{2}} (V - V_0 + 2RZ) \cos \psi \, d\psi \, d\varphi, \quad (13)$$

It was eq.(12) that I used to separate the potential of the S_D -variations into an external and an internal part.



The solution of the two-dimensional problem leads to still simpler formulas.

In cylindrical coordinates r, φ, z , whose origin is placed at the point P, $PM = r$, and

$$V_e - V_i = \frac{1}{2\pi} \int_0^\infty \int_0^{2\pi} \left(\frac{1}{r} Z - V \frac{\partial}{\partial z} \frac{1}{r} \right) r dr d\varphi = \frac{1}{2\pi} \int_0^\infty \int_0^{2\pi} Z dr d\varphi, \quad (14)$$

Section 2. Practical Methods of Calculating the External and Internal Potentials

The fundamental difficulty in performing practical calculations of the difference $V_e - V_i$ by eq.(13) is that it is given in coordinates connected with the position of the point P, for which we seek the value of $V_e - V_i$. The transformation of the equation to any fixed coordinate at all (for instance, geographic or geomagnetic) by means of the usual formulas for the transformation of coordinates, leads to a complex expression inconvenient for mass calculations. In view of this fact I adopted the following technique:

If we denote by \bar{V} and \bar{Z} the mean values of V and Z on the circle of latitude $\psi = \text{const}$, then eq.(12) is transformed into

$$V_e - V_i = \int_0^{\frac{\pi}{2}} (2R\bar{Z} + \bar{V}) \cos \psi d\psi. \quad (15)$$

In order to calculate the integral of eq.(15), we must find, for each point P on the surface of the sphere, the mean values \bar{Z} and \bar{V} along the circles of latitude (P being taken as the pole of the coordinate system). For this purpose, the formulas of transition from one system of spherical coordinates (fixed pole) to another

(with the pole at P) were used for preparing overlays on which the lines $\psi = \text{const}$ were plotted. The formulas for calculating the overlays were obtained from the solution of the spherical triangles NDQ and PDQ (Fig.18). The figure uses the following notation: N, pole of the fixed system of coordinates. In this system, P(θ_0, Λ_0). In coordinates with the pole P, the point Q is determined by the polar distance θ and

the longitude λ . On dropping from Q a perpendicular to the prolongation of the arc NP and denoting the arc ND by k, we have

$$\text{tg } k = \text{tg } \theta \cos (\Lambda - \Lambda_0), \quad (16)$$

$$\text{tg } \lambda = \frac{\text{tg } QD}{\sin PD},$$

$$\text{tg } QD = \sin k \text{tg } (\Lambda - \Lambda_0),$$

whence

$$\text{tg } \lambda = \frac{\text{tg } (\Lambda - \Lambda_0)}{\sin (k - \theta_0)}. \quad (17)$$

From ΔPQD it follows that

$$\text{ctg } \theta = \text{ctg } (k - \theta_0) \cos \lambda. \quad (18)$$

By combining eqs.(17) and (18), we get

$$\text{ctg}^2 \theta = \frac{\cos^2 (k - \theta_0)}{\text{tg}^2 (\Lambda - \Lambda_0) \sin^2 k + \sin^2 (k - \theta_0)}. \quad (19)$$

Equations (17) and (19) give an expression for the coordinates of an arbitrary

point Q in the system with the pole P, in terms of the coordinates of the points P and Q in the system with the pole N. By eq.(19) we calculated the curves of $\psi = 0/2 = \text{const}$ for various values of θ_0 , and λ_0 , and plotted them on the coordinate net $\theta_0 = 20^\circ$

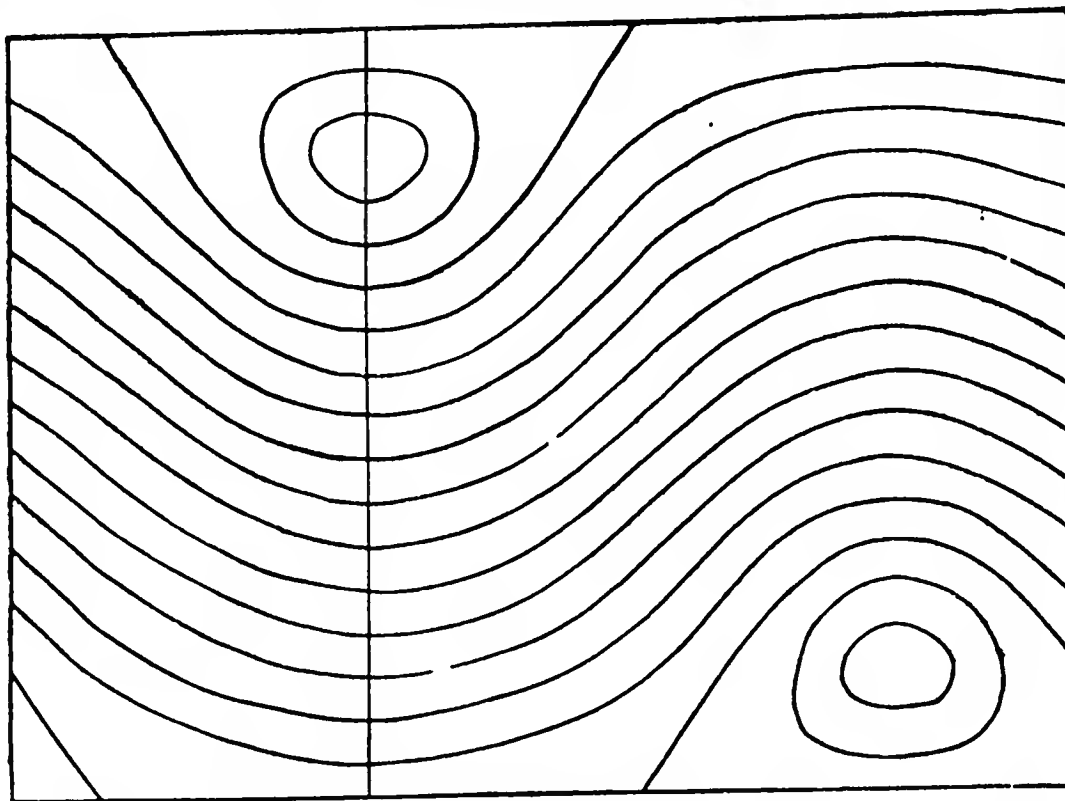


Fig.19 - The Overlay

θ, λ . By the aid of the overlays so obtained, the process of calculating V_e and V_i at the point $P(\theta_0, \lambda_0)$ reduces to the following:

1. From the components observed on the earth's surface, we must calculate (for instance, by integration of the X component) the potential V for a number of points covering the entire earth with a uniform net.
2. Plot the value of the potential and the Z component on the coordinate net θ, λ . For brevity we will, in the following, call a coordinate net with plotted values of any element a cartogram.
3. Placing on the cartograms of Z and V the overlay traced on transparent paper on the same scale and calculated for θ_0, λ_0 , take off the values of V and Z along

4. Calculate for each value of ψ the binomial $(2R\bar{Z} + \bar{V})$, and, by means of num-

[illegible]

5. Knowing $V_p = V_e + V_i$ and $V_e - V_i$, find V_e and V_i separately. As an example, Fig.19 and Tables 9 and 10 give cartograms of the Z and V of the S_D -variations and an overlay for $P(\theta_0)$ with $\theta_0 = 20^\circ$. The geomagnetic coordinates have been taken as the fixed coordinate system; the overlay and cartogram are given in cylindrical projection, while the isolines of ψ are drawn at intervals of 5° . For one and the same values of θ_0 , but different values of Λ_0 , one overlay can be used, by shifting it in proper manner on the cartogram. With preliminarily prepared cartograms and

overlays, the calculation of $V_e - V_i$ for each point is not so laborious.

Section 3. Calculation of the Electric Currents by the Integral Method

For calculating the currents whose field correspond to the external and internal parts of the observed magnetic field, the method of integral equations was selected. As is commonly known, the solution of potential problems is one of the

Table 10

S_D -Variations $V \times 10^{-3}$ CGS

	2	4	6	8	10	12	14	16	18	20	22	24
90	0	10	10	0	0	0	0	0	0	0	0	0
80	28	32	23	11	12	-11	-24	-37	-20	-18	3	18
70	64	64	49	0	14	14	41	78	42	35	11	32
60	90	90	76	4	24	-18	-57	-95	-64	-52	-22	38
50	80	80	48	15	24	26	30	50	24	43	37	15
40	23	4	-24	-37	-26	-13	1	5	29	18	14	5
30	3	-30	-49	-11	-32	-12	-11	-19	-45	-47	-37	-14
20	7	-34	-52	-17	-32	-12	12	21	48	50	38	15
10	7	-34	-50	-44	-30	-12	10	20	45	49	37	15
0	6	-31	-40	-40	-27	-10	8	18	40	44	34	15
-10	5	-28	-40	-36	-22	9	7	15	31	40	31	14
-20	5	-24	-35	-31	-18	8	6	12	29	31	27	12
-30	5	-21	-30	-27	-14	4	5	8	24	29	23	9
-40	4	-18	-26	-23	-10	-2	4	7	20	24	19	9
-50	2	-15	-22	-18	-8	1	3	6	16	20	15	8
-60	2	-11	-17	-14	-6	0	3	5	13	15	10	7
-70	2	-8	-12	-9	-3	0	2	4	10	11	8	6
-80	2	-4	-5	-4	-2	0	1	2	5	6	4	3
-90	0	0	0	0	0	0	0	0	0	0	0	0
90	0	0	0	0	0	0	0	0	0	0	0	0
80	2	8	12	9	5	0	-2	-4	-10	-11	-8	-2
70	2	11	17	14	6	0	-3	-5	-13	-15	-10	-4
60	2	15	22	18	8	1	-5	-8	-16	-20	-15	-7
50	4	18	26	23	10	2	-4	-7	-20	-24	-18	-9
40	5	21	30	27	14	4	-5	-8	-24	-29	-23	-11
30	5	24	35	31	18	8	-6	-12	-29	-34	-27	-12
20	5	28	40	36	22	9	-7	-15	-35	-40	-31	-14
10	6	31	46	40	27	10	-8	-18	-40	-44	-34	-15
0	6	34	50	44	30	12	-10	-20	-45	-49	-37	-15
-10	7	34	52	47	32	12	-12	-21	-48	-50	-38	-15
-20	7	34	49	45	32	12	-11	-19	-45	-47	-37	-14
-30	3	30	49	45	32	12	-11	-19	-45	-47	-37	-14
-40	23	4	24	37	26	11	-1	-5	-29	-18	-14	-5
-50	72	80	48	15	24	26	30	50	24	41	37	15
-60	78	90	76	4	24	18	57	95	64	52	22	38
-70	64	64	49	0	14	14	41	78	42	35	11	32
-80	28	32	23	11	12	-11	-24	-37	-20	-18	3	18
-90	0	0	0	0	0	0	0	0	0	0	0	0
	0	2	4	-8	8	10	12	14	16	18	20	22
	0	2	4	-8	8	10	12	14	16	18	20	22

classical fields of application of integral equations. The internal Dirichlet problem for the sphere is reduced to the Fredholm equation of the second kind:

$$-W_{IP} = 2\pi v_P + \int \frac{\gamma_M \cos \alpha}{r^3} ds, \quad (20)$$

where v denotes the density of the double layer located on the sphere; W_1 are values of the potential assigned for the surface of the sphere ($\Delta W_1 = 0$ inside the sphere); and the values of r and α are the same as in Section 1. Unfortunately, the conditions of our problem do not lead directly to this easily studied equation. The specific peculiarity of our problem resides in the fact that we know the function V_0 on the surface S_1 of a sphere of the radius R (on the earth's surface), satisfying the Laplace equation inside the sphere S_1 , while we desire to obtain distributions of the current function on the surface S of a sphere of a radius a , if $a > R$ (cf. Fig. 17b). Since the magnetic potential of a current layer with a current density of v is equivalent to the potential of an inhomogeneous magnetic layer of a density of v , it follows that we can replace derivation of the current function by derivation of the density of the double layer.

Let $M(\theta, \varphi)$ be a variable point of the sphere S ; and let $M_1(\theta_1, \varphi)$ on S_1 and $P(\theta_0, \varphi_0, r_0)$ be a certain point inside the sphere S_1 or on its surface. Then,

$$V_M = \int_S v_M \frac{\partial}{\partial n} \frac{1}{r} ds, \quad (21)$$

where $r = PM$. Since the values on the surface S_1 are assigned, it follows that the expression V_P for $r_0 \leq R$ may be found by the aid of the Poisson integral

$$V_P = \frac{R^2 - r_0^2}{4\pi R} \int_{S_1} \frac{V}{r_1^3} ds, \quad (22)$$

where $r_1 = PM_1$. By equating the right sides of eqs. (21) and (22), we get the Fredholm integral equation of the first kind:

$$\frac{R^2 - r_0^2}{4\pi R} \int_{S_1} \frac{V}{r_1^3} ds = \int_S v_M \frac{\partial}{\partial n} \frac{1}{r} ds. \quad (23)$$

for $r_0 = R$

$$V_{M_1} = \int_S v(\theta, \varphi) \frac{\partial}{\partial n} \frac{1}{r} ds. \quad (24)$$

It is generally known that the solution of Fredholm equations of the first kind in the general form is very complex and requires the core of the equation and the free term to satisfy certain conditions. This compels us to dispense with its solution. In order to reduce the determination of the density to the solution of eq.(20), the function V_0 , which is harmonic within the sphere, must be extrapolated, by some method, to the external space. But this is extremely difficult, since V_0 in the external space is an irregular function. I therefore decided to take another path. Namely, knowing the function V_0 at any point within the sphere S_1 , the fictitious density v is calculated for certain surfaces $\rho \leq R$, and then the values of v are extrapolated to $\rho = a$. This procedure is legitimate in principle, since v is a function regular throughout the entire space. In order to show that this method assures the accuracy necessary for many geophysical problems, we present two examples.

I. Let, on the sphere R , the potential of the external sources be assigned as

$$V = RgP_2^1(\cos \theta) \cos \varphi \left(\frac{\rho}{R}\right)^2.$$

Everywhere, for $\rho \leq R$, we have $\Delta V = 0$, and therefore V may be analytically continued on any $\rho < R$. For

$$\rho = R_1 \quad V = gRP_2^1 \cos \varphi \left(\frac{R_1}{R}\right)^2,$$

$$\rho = R_2 \quad V = gRP_2^1 \cos \varphi \left(\frac{R_2}{R}\right)^2,$$

$$\rho = R_3 \quad V = gRP_2^1 \cos \varphi \left(\frac{R_3}{R}\right)^2.$$

Assume that we are on the sphere R_3 .

Then: 1) we know the field of V on the sphere R_3 ; 2) we know that it is of external origin; and 3) we do not know at what ρ ($\rho > R_3$) its sources are located. It may therefore be assumed that the field is located on the sphere R_2 , R_1 , R , etc, so that the current density can be calculated by the usual formulas. If the potential

on the sphere R_3 is represented by the function

$$V = R_3 \gamma_n^m P_n^m \frac{\cos m\varphi}{\sin m\varphi},$$

then the current density on the surface of ρ ($\rho > R_3$) will be

$$i = -\frac{10R_3}{4\pi} \frac{2n+1}{n+1} \left(\frac{\rho}{R_3}\right)^n P_n^m \frac{\cos m\varphi}{\sin m\varphi} \gamma_n^m.$$

In our case $\frac{2n+1}{n+1} = \frac{5}{3}$ and $R_3 \gamma = gR(R_3)^2$, whence

$$i = -\frac{25}{6\pi} \frac{\rho^3}{R} P_2^1 \cos \varphi.$$

Denoting $-\frac{25}{6\pi} P_2^1 \cos \varphi g$ by B , we have

$$\text{for } \rho = R_2 \quad i = B \frac{R_2^2}{R}; \quad \text{at } R_2 = 0.96R \quad i = 0.92B;$$

$$\text{for } \rho = R_1 \quad i = B \frac{R_1^2}{R}; \quad \text{at } R_1 = 0.98R \quad i = 0.96B;$$

$$\text{for } \rho = R \quad i = BR; \quad \text{at } R = 1.00R \quad i = 1.00B.$$

But in reality the current flows along the sphere $\rho > R$, where we do not know the value of V_e . Let us find i for $\rho > R$ by simple graphic extrapolation (Fig.20). Then, for $a = 1.02R$, we have $i = 1.04B$. Check: from the value of V on the sphere R we have, for $a = 1.02R$:

$$i = -\frac{25}{6\pi} P_2^1 \cos \varphi (1.02)^2 = 1.04B.$$

II. On a sphere of a radius of R , the potential

$$V = RgP_{10}^1 \cos \varphi.$$

is known.

On the sphere

$$\rho = R_1 \quad V = gRP_{10}^1 \cos \varphi \left(\frac{R_1}{R}\right)^{10},$$

$$\rho = R_2 \quad V = gRP_{10}^1 \cos \varphi \left(\frac{R_2}{R}\right)^{10},$$

$$\rho = R_3 \quad V = gRP_{10}^1 \cos \varphi \left(\frac{R_3}{R}\right)^{10}.$$

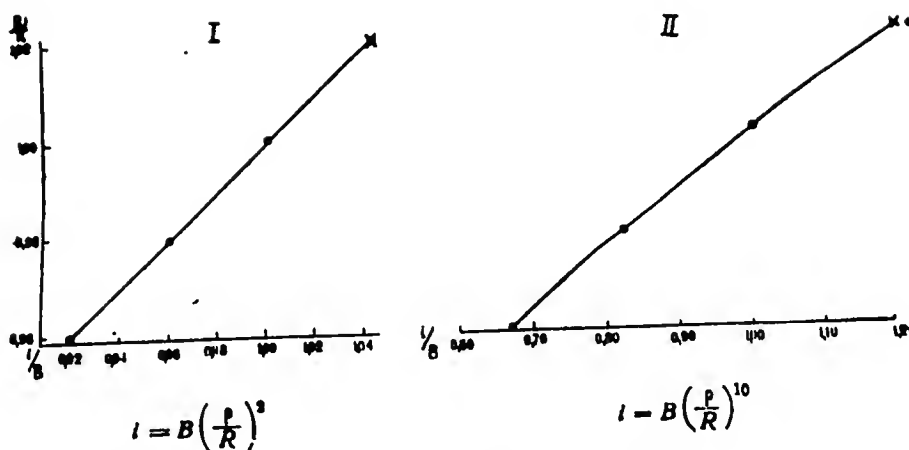


Fig.20 - Calculation of Current Density by Extrapolation

(. Calculated Values; x, Extrapolated Values)

Starting out from the values of V on the sphere R_3 , we have

$$i = -\frac{10R_3}{4\pi} \frac{21}{11} \left(\frac{\rho}{R_3}\right)^{10} P_{10}^1 \cos \varphi g \left(\frac{R_3}{R}\right)^9 = B \frac{\rho^{10}}{R^{10}},$$

where $B = -\frac{210}{44} g R P_{10}^1 \cos \varphi$.

$$\text{For } \rho = 0.96R \quad i = 0.67B,$$

$$\text{For } \rho = 0.98R \quad i = 0.82B,$$

$$\text{For } \rho = 1.00R \quad i = 1.00B.$$

Extrapolating on the graph of Fig.20 for $a = 1.02R$ will give $i = 1.20B$. Accord-

ing to the formulas of spherical analysis, $i = 1.22B$, i.e., the error is 2%.

Section 4. Finding the Current Density from an Assigned Potential on the Sphere.

Extrapolation of the Potential

After having thus reduced the solution of our problem to the classical problem of finding the density of a double spherical sheet from values of the potential assigned on the sphere, we must select a practically convenient method of solving eq.(20). Equation (20) is a special case of the equation

$$V_p = 2\pi v_p + \lambda \int_S v_M \frac{\cos \alpha}{r^2} ds \quad (25)$$

for $\lambda = +1$.

The usual method of solving an integral equation of the second kind by the aid of resolvents is inapplicable in this case, since the series expressing the resolvent becomes divergent at $\lambda = +1$. Two methods of solving eq.(25) are known in the literature. The first was given by Neumann in 1875, and the second by Bogolyubov and Krylov in 1926. Neumann's method (Bibl.14) reduces to the following: Since

$$2\pi = \int_S \frac{\cos \alpha}{r^2} ds,$$

then

$$2\pi v_p = \int_S \frac{v_p \cos \alpha}{r^2} ds$$

and

$$V_p = \int_S (v_M - v_p) \frac{\cos \alpha}{r^2} ds + 4\pi v_p.$$

This transformation is necessary in order to replace the integral $\int_S v_M \frac{\cos \alpha}{r^2} ds$, which has a singularity at the point K , coinciding with P , by a convergent integral that has no singularities as $K \rightarrow P$.

The equation

$$v_p = \frac{\lambda}{4\pi} \int_S \int (v_p - v_M) \frac{\cos \alpha}{r} ds + \frac{1}{4\pi} V_p \quad (26)$$

is solved by the aid of the series

$$v_p = \frac{1}{4\pi} [U_{0p} + \lambda U_{1p} + \lambda^2 U_{2p} + \dots + \lambda^n U_{np}], \quad (27)$$

which is convergent for $\lambda = +1$.

The functions U_n are determined successively through the recurrence formulas:

$$\left. \begin{aligned} U_{0p} &= V_p \\ U_{1p} &= \int_S (U_{0p} - U_{0M}) \frac{\cos \alpha}{r^2} ds \\ &\dots \dots \dots \\ U_{np} &= \int_S (U_{n-1,p} - U_{n-1,M}) \frac{\cos \alpha}{r^2} ds \end{aligned} \right\} \quad (28)$$

This method is convenient since the value of the n^{th} term depends on the first $(n-1)$ terms and does not depend on the $(n+1)^{\text{th}}$ and subsequent terms. Thus, in order to pass from the n^{th} approximations to the $(n+1)^{\text{th}}$ approximation, it is necessary to add, to the sum of n terms, an $(n+1)^{\text{th}}$ term without changing the first n terms.

On transforming eq.(28) into a form convenient for our calculations, we have

$$U_{1p} = \frac{1}{4\pi} \int_S (V_p - V_M) \frac{\cos \alpha}{r^2} R^2 \sin \theta d\theta d\lambda. \quad (29)$$

Denoting the angle between the radius vector of the points M and P by δ , we have

$$r = 2R \sin \frac{\delta}{2}, \quad \alpha = \frac{\pi}{2} - \frac{\delta}{2},$$

where $\cos \delta = \cos \theta \cos \theta_0 + \sin \theta \sin \theta_0 \cos (\lambda - \lambda_0)$, if the coordinates of P are θ_0, λ_0 and the coordinates of M are θ, λ .

Whence

$$U_P = \frac{1}{16\pi} \int_0^{2\pi} \int_0^\pi (V_P - V_M) \operatorname{cosec} \frac{\delta}{2} \sin \theta \, d\theta \, d\lambda. \quad (30)$$

We remark that, for $M \rightarrow P$, $\operatorname{cosec} \delta/2 \rightarrow \infty$, but since $V_P - V_M \rightarrow 0$, it is easy to show that $(V_P - V_M) \operatorname{cosec} \frac{\delta}{2}$ remains finite.

If, in calculating U_1 , we take for each point P its own system of coordinates with the pole P , then $\delta = \theta$ and

$$U_{1P} = \frac{1}{8\pi} \int_0^{2\pi} \int_0^\pi (V_P - V_M) \cos \frac{\theta}{2} \, d\theta \, d\lambda. \quad (31)$$

Introducing $\theta/2 = \psi$ and $\bar{V}_P = \bar{V}_M = \frac{1}{2} \int_0^{2\pi} (V_P - V_M) \, d\lambda$ (the mean value of $V_P - V_M$ from the parallel circle), we have

$$U_{1P} = \frac{1}{2} \int_0^{\frac{\pi}{2}} (\bar{V}_P - \bar{V}_M) \cos \psi \, d\psi \quad (32)$$

and in general

$$\begin{aligned} U_{nP} &= \frac{1}{2} \int_0^{\frac{\pi}{2}} (U_{n-1,P} - U_{n-1,M}) \cos \psi \, d\psi \\ &= \frac{1}{2} U_{n-1,P} - \frac{1}{2} \int_0^{\frac{\pi}{2}} \bar{U}_{n-1,M} \cos \psi \, d\psi. \end{aligned} \quad (33)$$

Thus in zero approximation, the function of current density is $v_P = -1/4\pi V_P$ and, in first approximation,

$$v_P = -\frac{1}{4\pi} \left[\frac{3}{2} V_P - \frac{1}{2} \int_0^{\frac{\pi}{2}} \bar{V}_P \cos \psi \, d\psi \right] \quad (34)$$

etc.

These formulas very clearly show that, in zero approximation, the current density is equal to the potential with an accuracy to a constant coefficient. Therefore, for a rough estimate of the configuration of a current system, it is sufficient to construct the isolines of potential. In first approximation, as will be clear from

eq.(34), the value of the current density is determined by the inequality:

$$\left| \frac{1}{4\pi} V_p \right| < |v_p| < \left| \frac{1}{4\pi} \frac{3}{2} V_p \right|. \quad (35)$$

Equation (34), serving to calculate the current density, allows us again to use the overlays described in the preceding paragraph.

Let us now turn to the question of extrapolating the values of V_e for $\rho < R$. Since we obtain V_e on the earth's surface not in an analytical but in a numerical form, the most convenient method of extrapolating V_e within the sphere is the Poisson integral. If the variable point of the surface of the sphere is $M(R, \theta, \varphi)$ and the internal point at which we desire to calculate the potential is $P(\rho, \theta_0, \varphi_0)$, then

$$U_p = \frac{R^2 - \rho^2}{4\pi R} \int_S U_M \frac{ds}{r^3}, \quad (36)$$

where U_M denotes the surface value of the potential. For convenience in practical computation, we will perform certain transformations.

Since

$$r^2 = R^2 + \rho^2 - 2R\rho \cos \delta,$$

where δ is the angle between OM and OP, then

$$U_p = \frac{R(R^2 - \rho^2)}{4\pi} \int_0^{2\pi} \int_0^\pi \frac{U_M \sin \theta d\theta d\varphi}{(R^2 + \rho^2 - 2R\rho \cos \delta)^{3/2}}. \quad (37)$$

If we again place the pole of the coordinate system at P, then

$$U_p = \frac{R(R^2 - \rho^2)}{4\pi R^3} \int_0^\pi \frac{\sin \theta}{\left(1 + \frac{\rho^2}{R^2} - 2\frac{\rho}{R} \cos \theta\right)^{3/2}} \int_0^{2\pi} U_M d\varphi d\theta = \int_0^\pi \bar{U}(\theta) K(\theta) d\theta, \quad (38)$$

where $\bar{U} = \frac{1}{2\pi} \int_0^{2\pi} U_M d\varphi$ denotes the mean value of U_M for the circle of latitude

and

$$K(\theta) = \frac{1}{2} \left(1 - \frac{\rho^2}{R^2}\right) \frac{\sin \theta}{\left(1 + \frac{\rho^2}{R^2} - 2 \frac{\rho}{R} \cos \theta\right)^{3/2}}. \quad (39)$$

Thus the extrapolation of V_e to any spherical surface $\rho < R$ may be performed by means of the same overlays that were used in calculating the difference $V_e - V_1$.

Section 5. Practical Methods. Conclusions as to the Suitability of the Method

In accordance with the above, the calculation of the external electric currents from geomagnetic elements known at the earth's surface reduces to the following steps:

- 1) Calculation of the potential V_e at the earth's surface;
- 2) Calculation of the potential V_e on spheres of radii ρ_1 and ρ_2 ;
- 3) Calculation of the current density v for three spheres of radii ρ_1 , ρ_2 and R ;
- 4) Calculation of the current density for a sphere of radius a ($a - R$ is the height of the currents above the earth's surface) by means of graphic extrapolation of v_{ρ_2} , v_{ρ_1} , and v_R .

We succeeded in turning all three laborious operations (calculation of $\int_0^{\pi/2} (2R\bar{Z} + \bar{V}) \cos \psi d\psi$, $\int_0^{\pi} \bar{U}(\theta) K(\theta) d\theta$ and $\int_0^{\pi/2} \bar{U}_{n-1} \cos \alpha d\alpha$) into operations of a single type which could easily be performed by the aid of overlays. The total volume of computation work in this case is comparable with the work for spherical analysis.

In this way, we calculated the electric currents responsible for the S_H -variations. The experience in actual calculations showed the method to be completely applicable to the study of magnetic fields with a complex geographic distribution.

These equations permit calculating the electric currents responsible for the external part of the potential. Formulas interpreting the internal part of the potential may be obtained by an entirely analogous method. The basic method in this case will be the solution of the external problem of Dirichlet by means of the

Fredholm equation

$$V_p = 2\pi v_p - \int_S \frac{v_M \cos \alpha}{r^3} ds \quad (40)$$

V_p in this equation denotes the values, known on the surface of the sphere, of the potential satisfying the Laplace equation outside the sphere. It must be taken into account here that the corresponding homogeneous equation

$$2\pi v = \int_S \frac{v \cos \alpha}{r^3} ds \quad (41)$$

has a solution other than zero ($v = \text{const}$) in view of which certain complications arise in the solution of the external problem of Dirichlet. In courses on mathematical physics, however, it is shown that this problem can be solved for any distribution of V_p . It is true, of course, that the values of v will be found with an accuracy to a constant. Thus, in both cases (finding the external currents responsible for V_e and the internal currents responsible for V_i), the problems are not solved with complete accuracy. In the former case, V_e is determined from the observed distribution of the geomagnetic components with an accuracy to a constant, while in the latter case the current density v_i is found from the calculated distribution V_i with an accuracy to a constant. But these limitations are negligible in considering the variations with time or space of the geomagnetic field. In studying the variable magnetic field or magnetic anomalies, we may reconcile ourselves to the fact that no uniform system of currents related to the permanent part of the potential is being calculated.

The extrapolation of the values of V_i known on the surface of the sphere K to external space may likewise be accomplished by means of the Poisson integral which, in this case, will be of the form

$$U_{p_e} = \frac{\rho'^3 - R^3}{4\pi R} \int_S \frac{\overline{U}_i}{r'^3} ds, \quad (42)$$

where ρ' is the radius vector of the point P_e , and r' is the distance between the point P_e and a variable point on the sphere. Thus the practical methods of calculating the internal currents may likewise be of entirely of the same type.

A consideration of the question of accuracy (for more details, cf. Section 5, Chapter V), has shown that the error of any operation of computation may be made as small as desired, and thus the accuracy of the results obtained is completely determined by the accuracy and completeness of the initial empirical data. Exactly as with spherical analysis, the integral method requires a knowledge of the geomagnetic components over the entire surface of the sphere. If the data do not cover the entire earth and are absent over large areas, then the formal calculation of the potentials and the calculations of the currents still remains possible, but the values so obtained will represent the phenomenon well for regions with abundant data and, possibly, represent it poorly for regions for which there are no data. A shortcoming of the method is the fact that it does not yield a compact analytic expression for the potential and for the current function: the final results are obtained in graphical or tabular form. Nevertheless, the fundamental problems (separation of the parts of external and internal origin from the observed field and calculation of the sources of the field, whether electric currents or magnetic masses) are solved by means of surface integrals. The method described above is therefore completely capable of replacing spherical analyses in cases of complex fields, in the consideration of a number of problems of geomagnetism, and possibly of other branches of geophysics as well. For example it would seem advisable to use this method in studying magnetic disturbances, the secular march representing a rather local phenomenon, a field of magnetic anomalies, etc.

A certain limitation of the method must also be pointed out. The extrapolation of the current density v , gives an accuracy which is sufficient for practical purposes if the current-carrying layer is not too far from the surface in which the distribution of potential is known. In the opposite case, however, an extrapolation may

lead to great errors. Thus, in the second example of Section 3 of the present Chapter, the extrapolation of v to a sphere with a radius of $1.20R$ gives an error of the order of 10%. If the sources of the magnetic field, however, are far enough from the surface at which the observations are made, then the field will not be characterized by great complexity of geographic distribution, and, consequently there will be nothing to prevent the use of spherical analysis for studying the field. But in all cases of complex geophysical fields (magnetic anomalies, magnetic storms, and a number of others), which do not allow the use of spherical analysis, it may be assumed that the sources of the field are located not more than $0.1R - 0.2R$ away from the earth's surface, at which the extrapolation required by the method of surface integrals is entirely allowable.

CHAPTER V

The S_D -VariationsSection 1. Basic Data

As stated above in Chapter II, the second portion of the field of magnetic storms, the disturbed diurnal variations S_D , is rather well represented by the difference between the diurnal march on disturbed days (S_d) and on quiet days (S_q). The differences $S_D = S_d - S_q$, averaged over the year, were calculated for the 61 stations enumerated in Table 1. Since the S_D -variations vary markedly with the 11-year cycle of solar activity (Chapter VII), the observations for the Second International Polar Year (II MPG) were used as in the study of D_{st} , in order to assure uniformity of the starting data for most of the observatories. The list of quiet and disturbed days for these years, established by the International Association for Terrestrial Magnetism and Electricity on the basis of the magnetic characteristics of a worldwide net of observatories, is given in another paper (Jibl.40). The characteristics of magnetic activity on these days show that the disturbed days were days of moderate and great magnetic disturbances, while the quiet days were completely quiet. Thus the difference $S_d - S_q$ can be completely characterized by the additional diurnal fluctuations which, on stormy days, are superimposed on the normal S_q variations. From seven observatories which are of great interest because of their geographic location, we did not have the data for the Second International Polar Year at our disposition. In view of this, we used the 1944 observations for three of them (Yakutsk, Tbilisi, and Tashkent). A comparison of the S_D -variations for 1944 and 1933 for a

number of observatories showed that both form and amplitude of the S_D in these years closely resembled each other. The data of four observatories (Chelyuskin, Uelen, Kakioka, and Apia) relate to 1935, but to "reduce" them to the Second International Polar Year, the amplitudes of S_D were decreased in accordance with the change in the S_D -variations from 1933 to 1935 at the other observatories. To reduce the first two of these four stations, we used the series of observations at Tikhaya Bay and Dickson Island, and to reduce the last two we used Watheroo.

It is well known that the field of S_D displays more symmetry with respect to the geomagnetic coordinates than to the geographic. In view of this, we calculated the geomagnetic component X' , Y' , Z for each observatory from the observations of the variations of H , Z , and D . A summary of these components is given in Fig.1 for the 44th observatory listed in Table 1. The time on the diagram is local geomagnetic time. The local geomagnetic time t_M was derived in 1936 by McNish (Bibl.9) by analogy to local mean solar time. Without allowing for small seasonal fluctuations, it is assumed that

$$t_M = T + \Lambda - 69^\circ;$$

$T - 69^\circ$ denotes the time of the zero geomagnetic meridian. In the middle latitudes, $\Lambda - 69^\circ$ differs little from the geographic longitude of the locality λ , and therefore the difference between the local geomagnetic and geographic times is slight.

Before proceeding to calculating the potential of the field of S_D -variations and the construction of the current systems corresponding to it, it seems advisable to make a qualitative examination of the collected material with the object of elucidating certain questions of the morphology of the field. The most substantial of these questions are as follows: 1) dependence of S_D on local and universal time; 2) geographic distribution of S_D and selection of a system of coordinates convenient for the execution of the computational work; 3) choice of a working hypothesis as to the sources of the S_D -variations.

Section 2 of the present Chapter is devoted to the first two of these questions.

Section 3 is devoted to the third question, while an exposition of the results of the calculation of the potential and electric currents of S_D is given in the next four Sections.

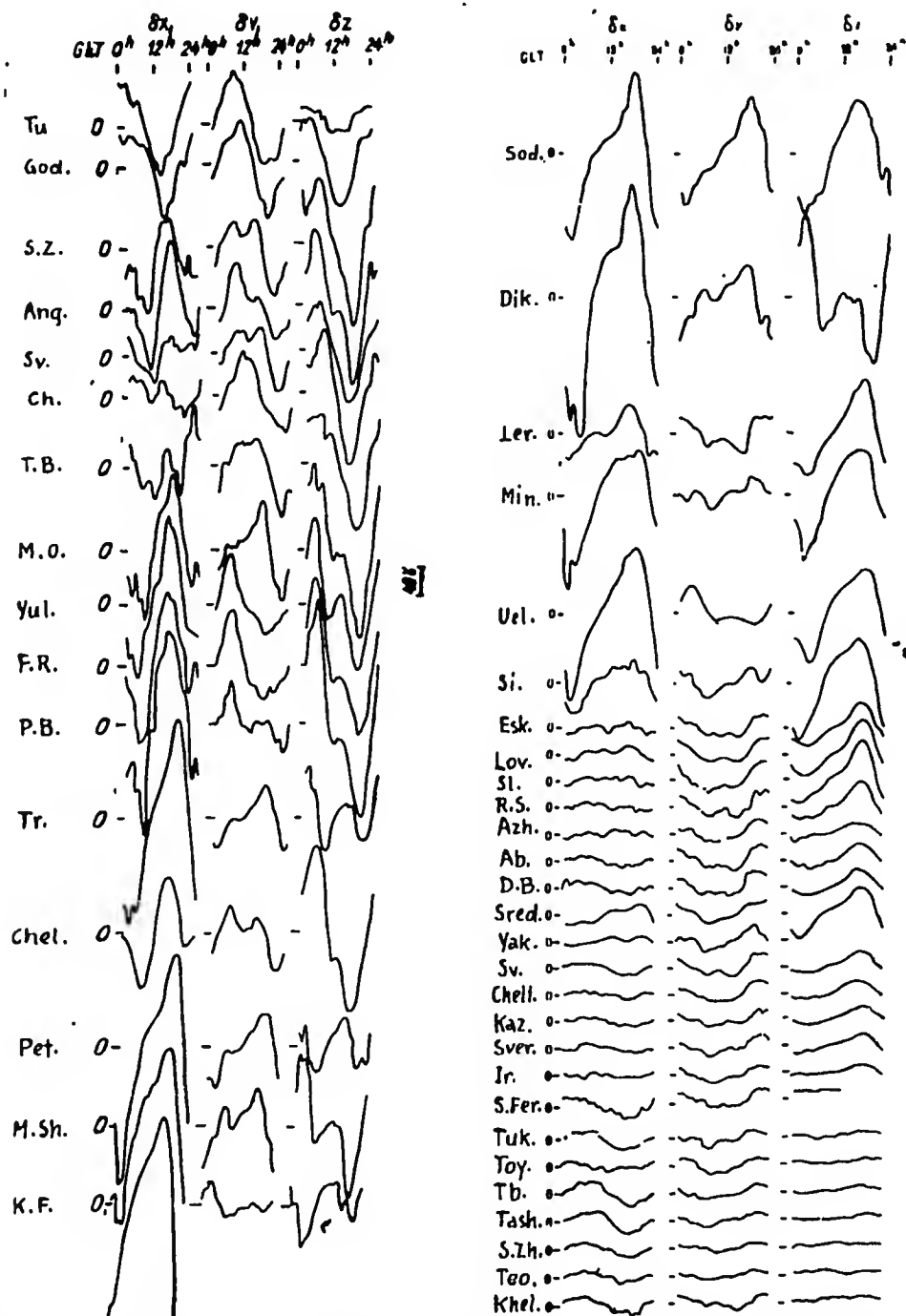


Fig.21 - S_D -Variations. The Observatories are Arranged in Order of Decreasing Geomagnetic Latitude (ϕ)

Section 2. Dependence of the S_D -Variations on Local and Universal Time.

The S_D -Variations in the Polar Regions

The graph in Fig.21 discloses the rather evident dependence of S_D on t_M and Φ . It still seems necessary to verify whether the position of the principal (or, perhaps, of the secondary) extreme values is tied to Universal Time, since the question of the influence of Universal Time on the diurnal variations has been repeatedly raised in the literature. K.K.Fedchenko, studying the diurnal variations of declination (for all days) has shown that the location of the diurnal maximum of D in the high latitudes is governed by Universal Time. A.P.Nikol'skiy (Bibl.26) makes analogous assertions with respect to the maximum of disturbance. According to him, there are two independent maxima in the diurnal march of the disturbance, one of which occurs in the evening hours of local time, and the other toward 17^h of Universal Time (noon at the magnetic axis pole). Since the correlation between the S_D -variations and the diurnal march of disturbance (S_a) is a priori very probable, and since in addition, in the high latitudes the S_D -variations are very close to the diurnal march for all days, these assertions force us to admit the possibility of the existence of two waves in the S_D -variations as well. The times of the principal and secondary maxima and minima of the Z component of the observatories of the northern hemisphere are noted on the diagram in Fig.22. Figure 22 shows the rather regular distribution of the extreme values as a function of the local geomagnetic time, while their distribution by Universal Time is completely random. The presence of two maxima in the S_D -variations is also found in the polar zone ($\Phi = 63 - 67^\circ$), over which, according to present ideas, the electric currents causing the strong disturbance of the high latitude must flow. For other latitudes, both at the center of the polar cap and in the middle latitude belt, the existence of two maxima is not characteristic. Thus Figs.21 and 22 compel us to consider that the S_D -variations over the entire earth are governed primarily by local time. The Universal Time either has no influence at all on the distribution of S_D or exerts such an insignificant influence that it cannot

be detected without a special workup.

The existence of S_D -variations at the magnetic axis pole appears to be somewhat in contradiction with this conclusion. At the magnetic axis pole, the concept of local geomagnetic time loses its ordinary meaning (just as the concept of local time at the geographic pole has a special meaning, since the altitude of the sun does not vary in the course of the day). It would seem that, if a diurnal periodicity exists at all at this boreal pole, it would have to be due only to Universal Time. In fact, in the zone near the pole (cf. the data of the Thule Observatory) the S_D -variations of the X and Y components are rather distinct, and only the variations of the Z component are equal to zero. But this contradiction is merely an apparent one. It is not hard to show that the existence of diurnal variations of the horizontal component at the pole ($\theta = 0$) may be explained even without assuming the dependence of the field on Universal Time. Indeed, the potential V of the diurnal variations in the general case may be represented as a sum of Tesseral harmonics*:

$$P_n^m(\cos \theta) \frac{\cos mt}{\sin mt}, \quad m \neq 0.$$

From the definition

$$P_n^m(\cos \theta) = \sin^m \theta \frac{d^m P_n(\cos \theta)}{d(\cos \theta)^m}$$

it follows that, for $\theta = 0$,

$$P_n^m \equiv 0 \text{ and } V(0) = 0 \quad (m > 0)$$

Since

$$X = \frac{1}{r} \frac{\partial V}{\partial \theta} = \frac{1}{r} \left[m \sin^{m-1} \theta \cos \theta \frac{d^m P_n}{d(\cos \theta)^m} + \sin^m \theta \frac{d^{m+1} P_n}{d(\cos \theta)^{m+1}} \right] \frac{\cos mt}{\sin mt},$$

$$Y = -\frac{1}{r \sin \theta} \frac{\partial V}{\partial t} = \pm \frac{m}{r} \sin^{m-1} \theta \frac{d^m P_n}{d(\cos \theta)^m} \frac{\sin mt}{\cos mt},$$

$$Z = \frac{\partial V}{\partial r} = \sin^m \theta \frac{d^m P_n}{d(\cos \theta)^m},$$

* This reasoning is equally correct for geographic and geomagnetic coordinates.

then $Z(0) \approx 0$ for $m = 1$, but $X(0) \neq 0$ and $Y(0) \neq 0$, i.e., Y and X depend on $\sin t$ and $\cos t$, and the vector diagram in the horizontal plane of diurnal variations must

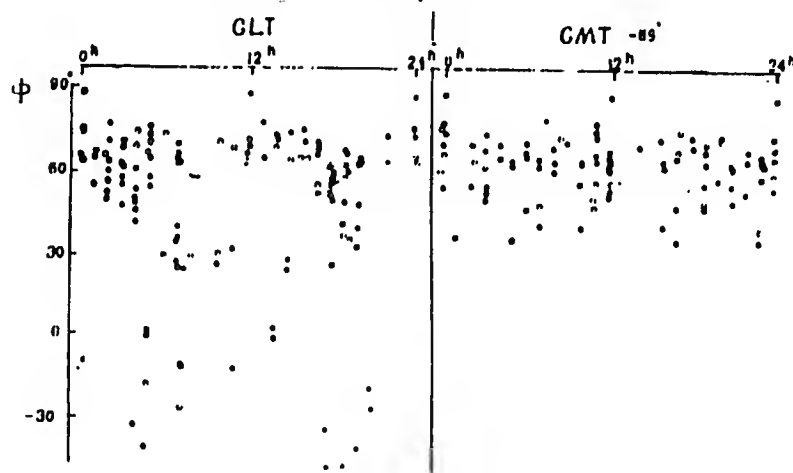


Fig.22 - Distribution of the Extremes of the (Z component of the S_D -Variations by Hours of the Day. O Time of Occurrence of Minimum;

● time of Occurrence of Maximum

have a circular form at the pole. The actual data on S_D at the poles are in complete agreement with these arguments. As a matter of fact, $S_D Z$ is very small at Thule, while the vector diagram of S_D in the XY plane for Thule, as for Cape Evans (an observatory near the south geomagnetic pole, cf. Bibl.40), is of circular form.

Here it is found that the vector of the horizontal component of S_D rotates with the variation of the azimuth of the sun (at the pole, the latitude of the sun does not vary throughout the course of the day, while its azimuth does vary). Thus, if viewed from the sun, the distribution of the vectors of the field of S_D remains constant, as is also the case for the S_q -variations.

Returning to a consideration of the graphs in Fig.21, we note that the dependence of S_D on ϕ in its general features may be described in the following way: The auroral zone ($\phi = 65 - 69^\circ$) is characterized by small amplitudes of X' and by an unstable two-wave form of Z . This is in agreement with the hypothesis that a linear current flows along the zone at the height of the ionosphere (or that the lines of

current of the surface current system are more closely spaced). North of the zone, Z has the form of a single wave with a minimum at noon, the greatest amplitude being

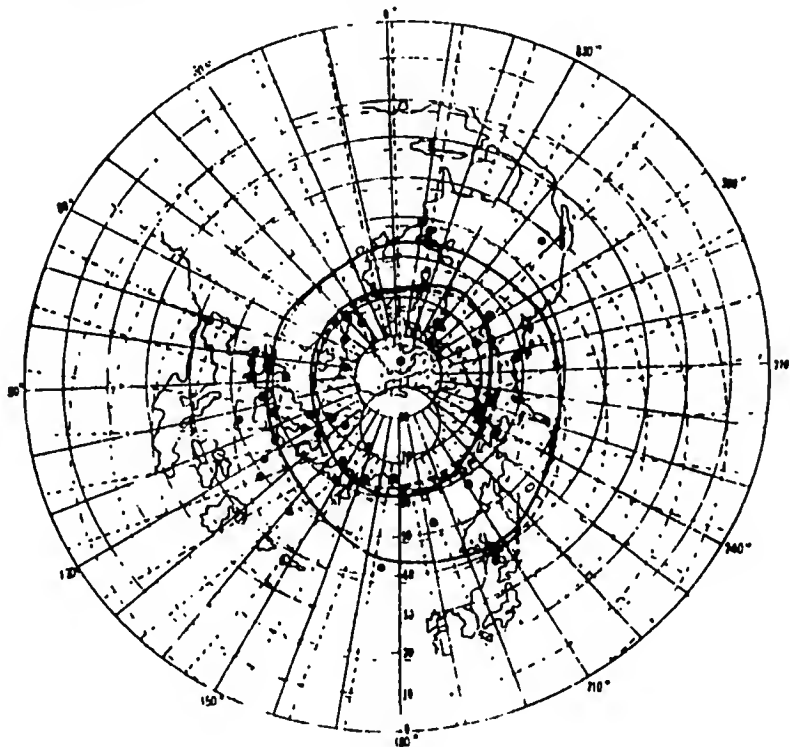


Fig.23 - The Auroral Zone and the Line of Centers of the Middle-Latitude Eddies of S_D -Variations (—— Position of Zone According to Vestline.

Coordinate Nets: —— Geomagnetic; ---- Geographic)

reached at latitudes 75° , north of which the amplitude again decreases. North of the zone, X' decreases in amplitude up to $\phi = 75^\circ$ where the phase is reversed. South of the zone, Z retains its form down to the very equator and only gradually decreases in amplitude, while X' decreases sharply in amplitude, resulting in still another phase reversal at latitude 40 to 50° .

However, there are a number of cases (Angmassalik, Chelyuskin, Sodankyla, etc.) which indicate a longitudinal asymmetry in the incidence of the variations. Vestline has pointed out that the asymmetry is considerably decreased if, instead of ϕ as the argument in the geographical distribution of S_D we take η , which is the distance to the zone of the hypothetical linear current. He determined the position of this zone

from the data of the magnetic variations and compared it with the maximum isochasm (the Vestine zone is shown by the broken line in Fig.23).

The data collected by us for the Second International Polar Year have allowed the position of the zone to be pin-pointed (the solid line in Fig.23), bringing it somewhat further south on the territory of the USSR. To determine the position of this zone, maps of the isoamplitude of $S_D X'$ were prepared, and the zone indicated in Fig.23 is the isoline of maximum amplitude of $S_D X'$. The second line in the diagram, lying between 40 and 50° , indicates the latitude at which the S_D -variations of X' change their phase*.

In columns 3 and 9 of Table 1 for each observatory, the values of η expressed in degrees and the values of ϕ' are given (ϕ' is the geomagnetic latitude corrected for the deviation of the zone from the circle of latitude $\phi_0 = 67^\circ$; $\phi' = 67^\circ - \eta^\circ$). The arrangement of the graphs of S_D in accordance with ϕ' (Fig.24) leads to an almost complete destruction of the anomalies in the distribution of S_D , especially in the high latitudes. In the low latitudes, the replacement of ϕ by ϕ' is insubstantial, and a consideration of the middle and low latitude portions of Figs.21 and 24 shows the same absence of any clearly anomalous observatories.

In this connection, the complete normality of the S_D at Huancayo and other observatories of the equatorial region is of great interest in this connection. Since the S_q - and L -variations of Huancayo are abnormally great, the absence of anomalies in S_D and D_{st} is an indication that the current systems of the disturbances and of the quiet variations are located in different layers of the ionosphere.

The close relation between S_D and ϕ' stands out most vividly on the graphs in Fig.25, which give the "meridian" of X' , Y' , Z corresponding to 0, 6, 12, and 18^h local geomagnetic time. The dispersion of the points, mapping the relation $X'(\phi')$ and $Z(\phi')$, is small. The dispersion of the curve of $Y'(\phi')$ is considerably

* As we will see later, the centers of the middle latitude eddies of S_D -variations are located at this latitude.

greater. This indicates that Y' , like D , depends to a greater extent on the value of D_0 .

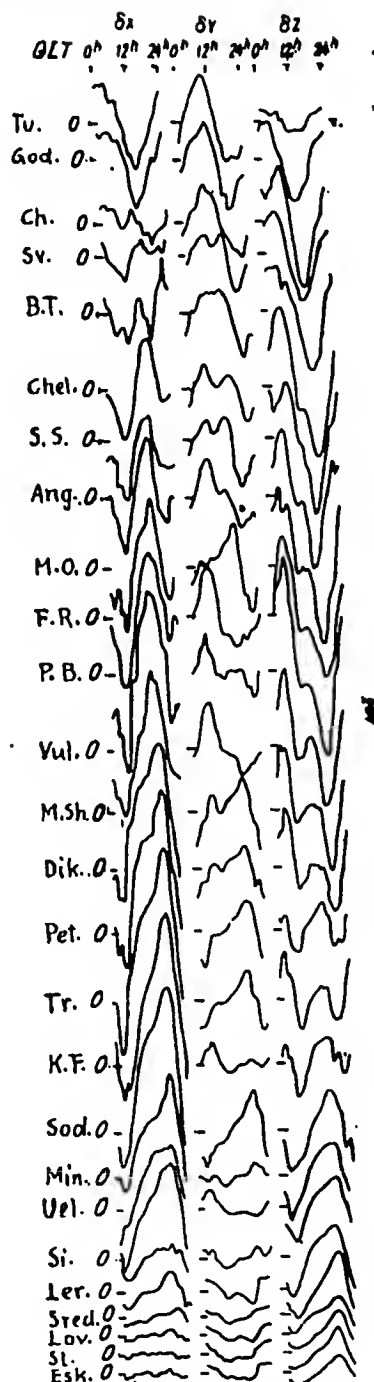


Fig.21 - The S_D -Variations; Observatories are Arranged in Order of Decreasing Corrected Geomagnetic Latitude (ϕ')

A comparison of Fig.25 with the corresponding graphs of Vestine (Bibl.58) discloses certain differences. The most substantial of these is that, according to Vestine X' in the auroral zone has extreme values at 6 and 18^h, and Z at 0 and 12^h, while according to our data the extreme values of X' are shifted to 4 and 16^h, respectively.

In concluding this discussion of the geographic incidence, let us describe the distribution of the field in the southern hemisphere. The data collected by us show a similarity in the behavior of X' , Y' and Z' in the low-latitude portions of the northern and southern hemispheres. The values Z' and Y' are opposite in sign in the different hemispheres and are equal to zero on the equator. The value X' is symmetric in the two hemispheres and has its maximum amplitude on the equator. Unfortunately we lack observations of high-latitude stations of the southern hemisphere for the Second International Polar Year, which would allow us to judge whether this symmetry in the two hemispheres persists at all latitudes. The literature contains only one attempt to determine the zone of magnetic activity from the data of the S_D -variations in the southern hemisphere (the work by Vestine and Snyder (Bibl.63), but the results of this work do not

seem trustworthy. The authors found that the polar zone in the southern hemisphere also has an elliptical form with its focus at the magnetic axis pole, except that it

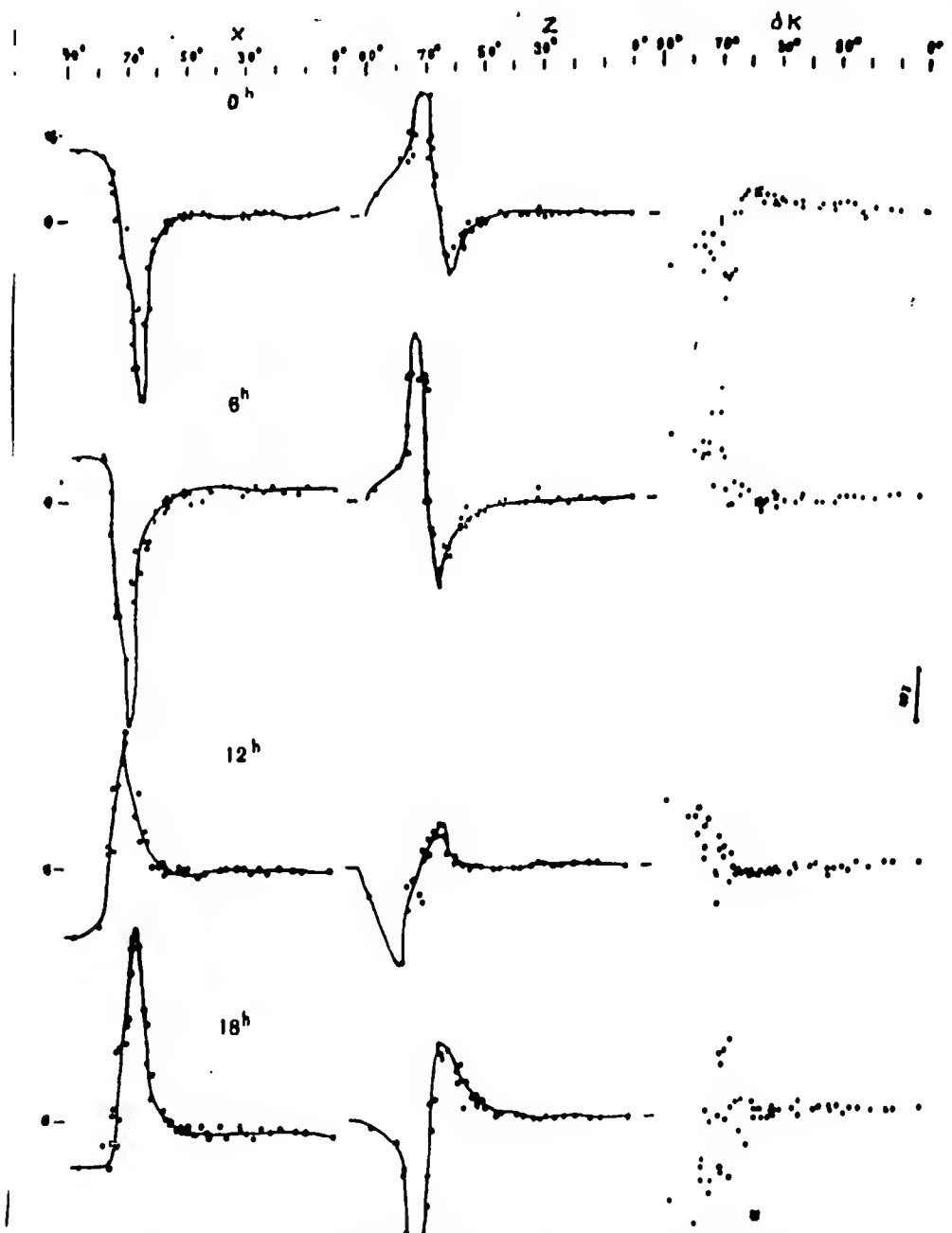


Fig.25 - Latitudinal Distribution of S_D -Variations

is not located symmetrically to the northern zone but is elongated on the side opposite the south geographic pole. This conclusion is based on extremely scanty and nonuniform material - observations of 1882, 1903, 1911, 1933, 1941 are used. Since

S_D varies considerably (cf. Chapter VII) with the 11-year cycle, the use of these observations without an appropriate reduction might give erroneous results. In view of the impossibility, at the present time, of making the position of the southern zone of magnetic activity more precise, we used only the data of the northern hemisphere in the analytic representation of the field, considering that, although only in rough approximation, the potential of S_D is the same in magnitude, but opposite in sign in the northern and southern hemispheres.

These arguments on the geographic distribution of the S_D -variations compel us to consider that, in calculating the potential, the field of S_D may be assumed to depend on two arguments, the geomagnetic latitude ϕ and the geomagnetic time t_M . In this case, however, the longitudinal terms will be rather great. The longitudinal asymmetry will be considerably less if the corrected value ϕ' is taken instead of ϕ as the first argument, i.e., $S_D = S_D(\phi', t_M)$. The replacement of ϕ by ϕ' corresponds to the replacement of the actual auroral zone by an arbitrary circular zone.

Section 3. Selection of the Type of the Current System

The selection of the method of calculating the currents responsible for the magnetic variations depends to a large extent on our a priori opinion as to the form of the current system. It is well known that the problem of finding the distribution of the currents from an assigned geomagnetic field on a sphere is in practice many-valued; for this reason all investigators desiring to evaluate the intensity and configuration of the currents have adopted in advance some hypothesis with respect to their distribution. We have already shown in Chapter II that, from this point of view, all investigators of magnetic storms are divided into two groups. The works of the first group assume that the magnetic disturbances are due to linear currents or relatively narrow current belts in the auroral zone. The second group embraces the works of Chapman and his colleagues, who consider that the currents of magnetic storms encompass the earth as a whole, forming a spherical current layer. To check these hypotheses, we calculated the geographical distribution of the fields of linear cur-

rents and compared them with the actually observed distribution of the field of S_D -variations. Figure 26 shows the latitudinal distribution of the X-component of the

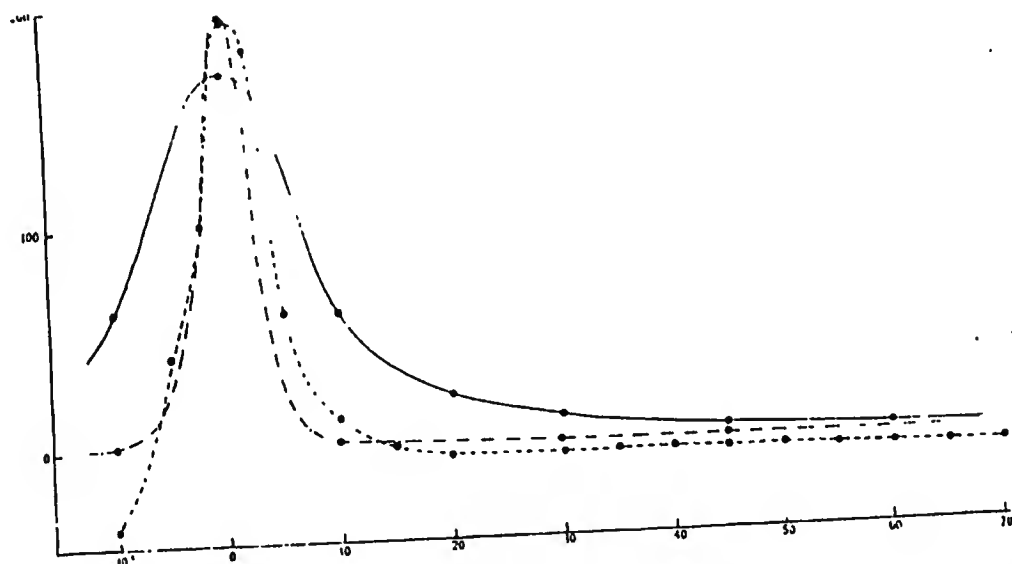


Fig. 26 - Comparison of S_D -Variations with the Field of the Linear Electric Current. Along the horizontal, the distance in degrees to the zone of linear current (the auroral zone) is plotted, and along the verticals, the field intensity in gammas (---, amplitude of night minimum of X component of S_D -variations; —, X component of field of vertical current (according to Gnevyshev); -.-.-, X component of field of horizontal current (according to Birkeland))

field of vertical current (according to Gnevyshev), and of the horizontal current (according to Birkeland). In reading the figure, the vertical linear current is conceived as flowing in the direction OZ from infinity to a height of 30 km, while the horizontal current flows at a height of 100 km in a direction perpendicular to the plane of the paper. The graph of the X' component of the S_D -variations is distinguished from the two theoretical curves by its asymmetry with respect to OZ and by its negative values of X' at a certain distance from OZ . Obviously the theoretical curves will be unable to approximate sufficiently well to the observed curve, no

matter what parameters are selected. The same non-correspondence is observed between the curves of latitudinal distribution of the field of linear currents and the S_D -variations of other components and at other hours of the day.

The hypothesis of a spherical inhomogeneous current layer is more general and, as shown by sample calculations of Chapman, it is able to explain the complex structure of the field of S_D . The above arguments forced us likewise to adopt the hypothesis of a spherical current layer, and, without making any further assumptions with respect to the configuration of the current lines, to calculate them from the observed geomagnetic elements, using the method of surface integrals.

Section 4. Calculation of External and Internal Potential

The values of the potential V , corresponding to the S_D -variations observed on the earth's surface were obtained by integration of the X' component. It follows from the symmetry of the X' and the asymmetry of Z with respect to the equator (cf. supra) that the potential should be antisymmetric and should vanish at the equator.

The values of $V(0, t_M)$ (for the northern hemisphere) were calculated from the graphs of Fig. 25 by the formula

$$V = - \int_0^{\frac{\pi}{2}} X' d\theta + V_{\theta=\frac{\pi}{2}} = - \int_0^{\frac{\pi}{2}} X' d\theta.$$

The calculations were made for 216 points at intervals of 2 hours in longitude and 5° in latitude. The integration along various meridians led to the following values of $V_0 = V = 0^\circ$:

Time, hours	0	2	4	6	8	10	12	14	16	18	20	22
$V_0 \times 10^{-3}$	2	14	14	12	-13	-19	10	20	3	0	-13	2

Since, as already noted, the potential of the diurnal variations not depending on Universal Time, must assume zero values at the pole, the values of V_0 from the annexed table would have to serve as an indication of the value of the calculation errors. But in reality the values of V_0 exceed the mean error of analysis, equal

to 3×10^{-3} CGS (for more details on the accuracy of analysis, see later). The existence of a potential-free part in the field of S_D -variations might be an explanation for this discrepancy. The existence of a potential-free part (1) in the permanent field of the earth and of the S_Q -variations has been detected by a number of authors. But since such a part requires the existence of vertical electric currents 10^3 to 10^4 times higher than the currents that can be observed by the methods of atmospheric electricity, the reality of the N field has always been subject to doubt. The vertical currents necessary to explain the N field of S_D -variations, calculated by the formula $i = \oint H ds$, should not exceed 0.5×10^{-14} CGS and should, as shown by calculations, be concentrated in the polar latitudes. The observations of the vertical current in Franz Josef Land by Scholtz and at Chelyuska by Gerasimenko (Sib1.10) have shown that the mean value of the currents fluctuates about $2-3 \times 10^{-16}$ CGS, while individual values often reach 1×10^{-15} CGS, which is only 5 times less than the values calculated for the N part of the S_D -variations.

Without discussing the question as to the reality and possible causes of the vertical currents (to which an extensive literature is devoted), we may say that it would be extremely desirable to repeat the observations in high latitudes on stormy days, which would help to solve the problem finally.

Since the magnitude of the potential-free field (if it exists) is small in comparison with the potential part, it proved possible in first approximation to neglect it, by assuming that integration along all meridians leads to one and the same value of V_0 , equal to zero. The errors of closure (i.e., of the values of V_0 obtained by integration) were distributed proportionally over all the latitudes, so as not to violate the condition that the algebraic sum of the 24 values of V along each parallel of latitude should be equal to zero. This last condition is dictated by the fact that the S_D -variations should be represented by deviations from the mean diurnal values of the magnetic elements. The values of the potential V obtained in the result of the above corrections are given in the cartogram of Table 10. This cer-

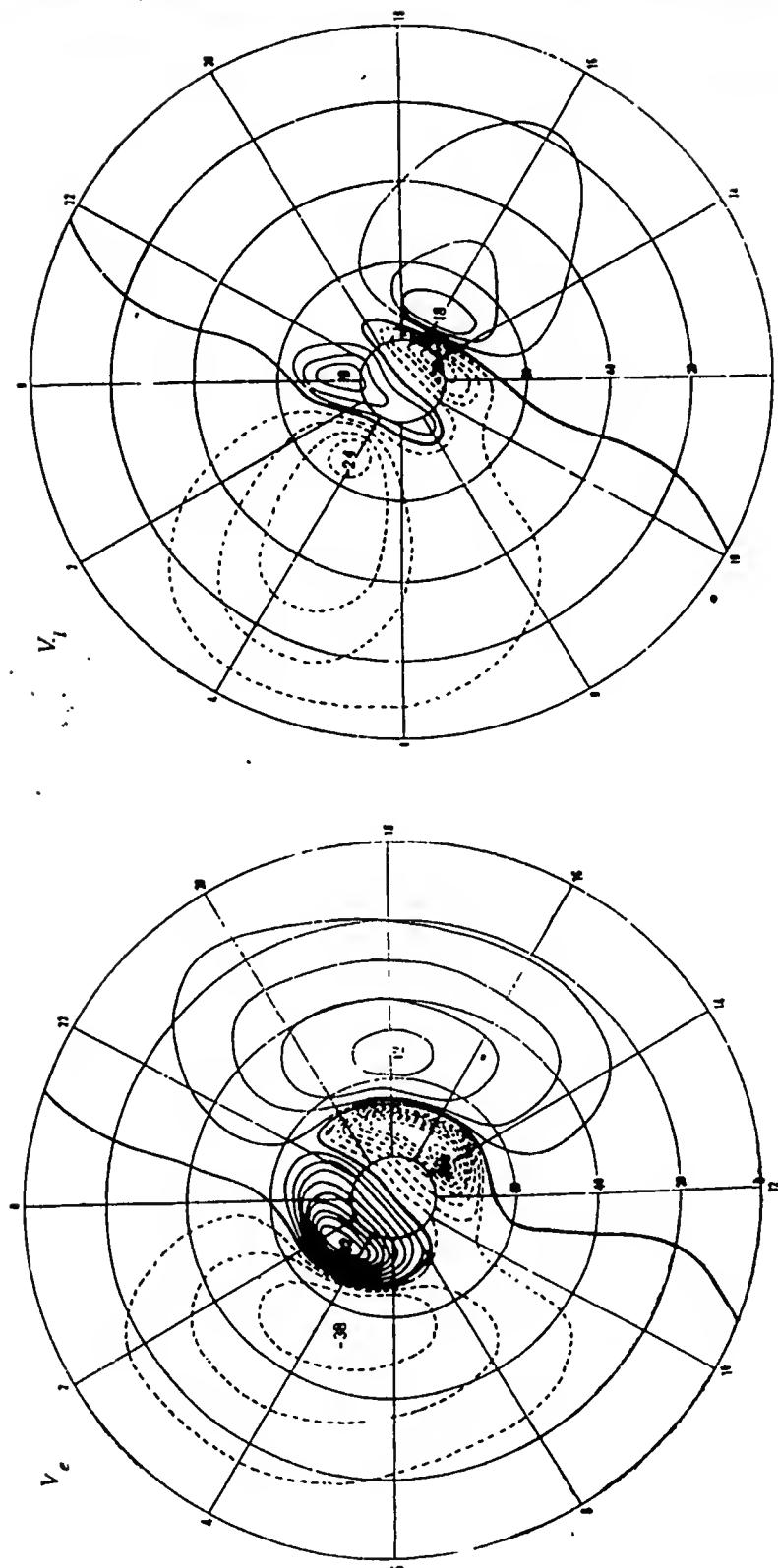


Fig.27 - Isolines of External(V_e) and Internal(V_i) Part of the Potential of the Variations
 (--- Negative Values of Potential; --- Positive values. Coordinate Net, Geomagnetic
 Latitude and Geomagnetic Time. Units of Potential, 10^3 CGSM. Isolines drawn at Intervals
 of 10^4 CGSM.)

gram and the analogous one (Table 9) for the Z component (prepared from the graphs of Fig.25) served as the starting material for calculating the external and internal parts of the potential, V_e and V_i . The calculations were performed by the method described in the preceding Chapter; the values of V_e and V_i were found for 108 points, at intervals of 10° in latitude and 2 hours in longitude. Figures 27 and 28 are

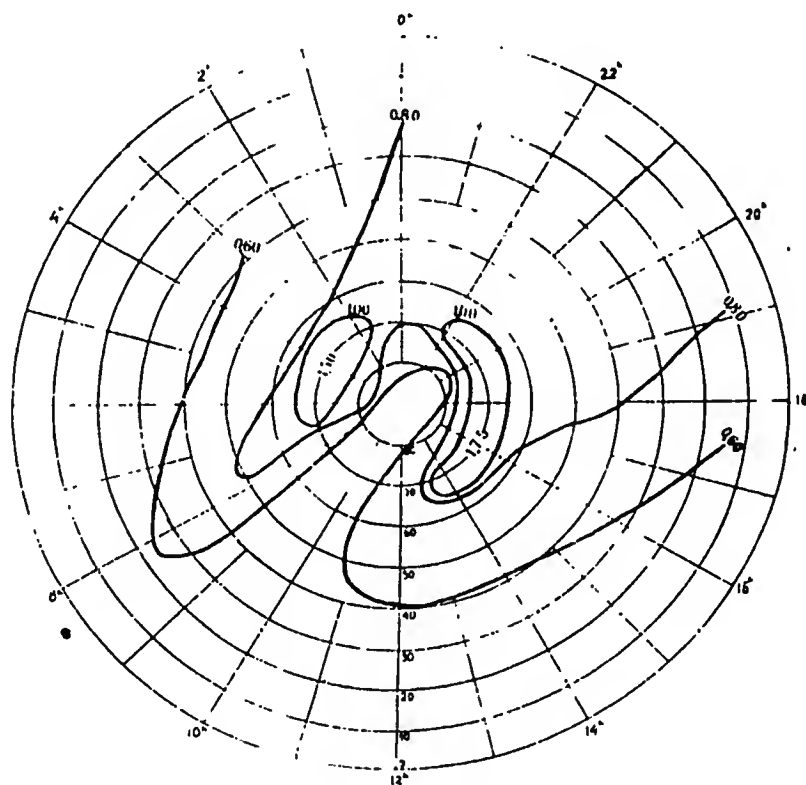


Fig.28 - The S_D -Variations. Ratio of External Part of Potential to Observed Potential (V_e/V)

maps of the potentials V_e , V_i and the ratio V_e/V . The isolines of V_e and V_i are drawn at intervals of 10^4 CGS. As will be seen from the diagram, the values of the potentials for V_e range from 92×10^3 CGS to -90×10^3 CGS, and for V_i from -29×10^3 CGS to 19×10^3 CGS, and the signs of the potentials are different on the morning and evening sides of the earth. The distributions of the isolines of V_e and those of V_i differ considerably. It is true that the distributions of both V_i and V_e are characterized by four extremes (two polar and two middle latitude), but the form of

the isolines on the V_e map is more elongated in a longitudinal direction. There is a shift in longitude which is particularly great for the morning polar maximum. The regularity of the distribution of V_e and V_i compels us to consider the results obtained as plausible.

In absolute magnitude, V_e considerably exceeds V_i , confirming the proposition that the principal sources of the field are located outside the earth's surface. The value of V_e/V varies over a wide range, from 0.55 to 1.75. For three points, $V_e/V > 1$ (1.50, 1.11, and 1.75). A regularity in the latitudinal distribution of V_e/V is noted: the mean value of V_e/V for the entire earth is 0.83; for the low-latitude belt ($\Phi \leq 50^\circ$) $V_e/V = 0.79$; and for the high-latitude cap ($\Phi > 50^\circ$), $V_e/V = 0.89$. The figures so obtained differ considerably from the value $V_e/V = 0.60$, adopted by Chapman, by analogy with the S_q -variations. It is not possible at the present time to give a trustworthy explanation of the latitudinal dependence found for V_e/V . Two hypotheses may, however, be advanced: 1) The variation in V_e/V with the latitude indicates the unequal conductivity of the earth at different latitudes; 2) it is possible that the height of the current layer is different at different latitudes, which would seem to be entirely plausible in view of our present knowledge as to the heights of the ionospheric layers.

Section 5. Discussion of the Accuracy of the Method

Let us now dwell on the question of the accuracy of the integral method of representing the field. First of all let us evaluate the error in the calculation of V . On replacing integration by summation, we have $V = R\Delta\theta \sum X$, where the X , for simplicity, are denoted by X' .

The error in V is evaluated as follows:

$$\delta V = R\Delta\theta \sum \delta X,$$

where δX is the error in X .

For $\Delta\theta = 5^\circ$, $R = 0.4 \times 10^3$ and $\delta\lambda = 1, 5$, and 10γ , we find that the maximum

error accumulated up to the pole δV_{\max} is 12×10^3 , 12×10^4 , and 60×10^4 CGS, respectively. The mean error $\delta V = 1/n \delta V_{\max}$ is 0.5×10^3 , 3×10^3 , and 6×10^3 CGS. At latitude 55° , the maximum error for $\delta X = 2\gamma$ will be $\delta V_{\max} = 14 \times 10^3$ and the mean error $\delta V = 1 \times 10^3$ CGS. If the accuracy of X is lower in the polar cap ($\phi \geq 55^\circ$), for instance $\delta X = 10\gamma$, then the errors $\delta V_{\max} = 6 \times 10^4$ and $\delta V = 3 \times 10^3$ will accumulate up to the pole. Judging from the graphs of Fig.25, the accuracy of the observed data of X in the middle latitudes is actually of the order of 2γ , while in the polar latitudes it is of the order of 10γ ; thus the accuracy of V observed can be evaluated as 1×10^3 CGS in the middle latitudes and 3×10^3 CGS at the pole. Since the observed value of the potential reaches 100×10^3 , the error would appear to be allowable.

The error accumulated in the calculation of $V_e - V_i$ may be evaluated as follows: On replacing the integral expression eq.(12, IV) by the summation expression, we have

$$V_e - V_i = \frac{1}{2\pi} \Delta\psi \Delta\theta \sum \sum (2RZ + V) \cos \psi.$$

For $\Delta\psi = \Delta\theta = 5^\circ$, $\cos \psi = 0.5$, we have

$$\delta(V_e - V_i) = \frac{0.5 \times 10^{-2}}{6.3} \sum \sum (2R\delta Z + \delta V).$$

The accuracy of observation of Z is lower than that of X ; the calculations have been made under the assumption of a δZ equal to 2, 5, 10, and 20γ (table 11).

In this calculation we assumed a mean error δV for the entire earth, since in calculating $V_e - V_i$ the values of V for the entire earth enter the integrand expression. The number of terms in the expression $\delta(V_e - V_i)$ is 2600. The small table presented shows that 1) the error $\delta(V_e - V_i)$ is due more to the inaccuracy of Z than to the inaccuracy of X ; 2) the mean error $\delta(V_e - V_i)$ is one or two orders smaller than the error of the observed V , even under the least favorable assumptions as to δZ . Thus the practical accuracy of V_e is the same as the accuracy of V .

In the calculations presented we did not take into consideration the errors of the mathematical operations themselves (integration, etc.), since these may be performed with a very high accuracy, much higher than the accuracy of the initial data.

Table 11 *

δZ	2×10^{-5}	5×10^{-5}	10×10^{-5}	20×10^{-5}
$2R\delta Z$	2.5×10^4	0.5×10^4	13×10^4	26×10^4
δV	0.3×10^4	0.3×10^4	0.3×10^4	0.3×10^4
$\delta(V_e - V_i)_{\max}$	3×10^4	7×10^4	13×10^4	26×10^4
$\delta(V_e - V_i)_{cp}$	24	56	104	208

These evaluations of the errors indicate that the integral method is able to provide adequate accuracy. In practice its accuracy is completely determined by the accuracy of the observed experimental material. By the accuracy of the observed data, of course, we mean not only the accuracy of the observations themselves, but also the stability and representative nature of the mean data and the distribution of observation points over the earth's surface.

Section 6. The Current System of Sp-Variations

From the values of V_e calculated by the integral method, a distribution of the current density in a spherical layer of radius $a = 1.05 R$ ($0.05 R = 313$ km) was constructed, corresponding to the height of the F_2 layer of the ionosphere, to which it is most probable that the currents of the magnetic disturbances can be referred. The current system so obtained (Fig. 29) like the above-described Chapman system, consists of four current eddies, of which the two more intense are located on the morning and evening sides of the polar cap, and the other two in the middle latitudes. The signs of the current functions are different: the polar evening and middle-latitude morning eddies have a positive sign for the current function, the polar

* All values given in Table 11 are in the CGSM system.

morning and middle-latitude evening eddies a negative sign. The centers of the polar current eddies are located on the 2 and 15 hour meridians, those of the middle-latitude eddies on the 4 and 16 hour meridians. The evening and morning eddies are unequal in intensity: the morning polar eddy is more intense than the evening eddy, while the evening middle-latitude eddy is more intense than the morning eddy. In the zone $\phi = 67 - 70^\circ$ (the auroral zone) the current lines are closely spaced, giving us the right to liken this part of the current system to the linear current flowing eastward on the evening side of the earth and westward on the morning side. It is this crowding of the lines of force that is responsible for the specific peculiarity of the course of magnetic and ionospheric phenomena in the zone.

The picture so constructed for the currents allows us to interpret in the following manner the pattern of geographic distribution of S_y described by us in section 2.

2. In each hemisphere, there are four characteristic types of S_y -variations:

I. Circumpolar type, characterizing the daily minimum in the λ' and λ components; the amplitude of λ is very small. This type corresponds to the center of the polar cap, over which the currents flow in the uniform layer in the direction of the 20 - 3 hour meridian.

II. Polar type, observed between the zone of close spacing of the current lines at the latitude $67 - 70^\circ$, and the latitude of the centers of the polar eddies ($\phi = 75^\circ$). It is characterized by the afternoon maximum in λ' and by the daytime minimum in λ . The amplitude of both components is high.

III. Middle-latitude type, observed between the auroral zone and the latitude over which the centers of the middle latitude eddies are located ($\phi = 55^\circ$). It is characterized by an evening maximum in λ' and λ .

IV. Low-latitude type (between the latitude of the centers of the middle-latitude eddies and the equator) with an evening minimum of λ' and an evening maximum of λ . The amplitudes of both components, especially of λ , are small.

Directly over the latitudes of the centers of the eddies ($\phi = 75^\circ$ and $\phi = 55^\circ$)

and under the zone of crowding of the current lines, transitional forms are observed, characterized by the change in sign of the X' variations and the maximum increase in the amplitude of Z in the former cases and by the change in sign of Z and an increase

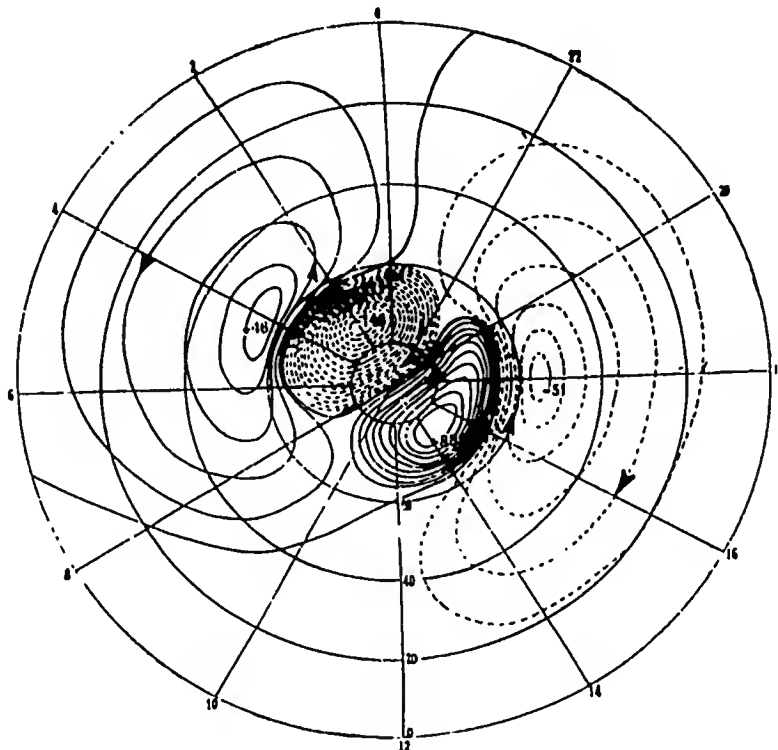


Fig.29 - Current System of S_D -Variations. Intensity of current given in thousands of amperes. A current of 10,000 amp flows between two successive lines of current. The coordinate net is the geomagnetic latitude and geomagnetic time (———, positive values of current functions; - - - - negative values)

in the amplitude of X' in the latter case.

The location of the centers of the middle-latitude and polar eddies at the various meridians is in full agreement with the well-known fact that the time of occurrence of the extreme values of S_D is different in the middle and polar latitudes. The unequal intensity of the morning and evening extreme values is likewise understandable if we bear in mind that the height of the evening maximum of S_D in the

middle latitudes is greater than the depth of the morning maximum. In reality, as pointed out above, the auroral zone (or the zone of linear current) is not a true parallel circle. For this reason, the boundaries of the regions corresponding to the various types of S_D will likewise deviate from the parallel.

A comparison of the system of currents of S_D calculated by us, which we shall hereafter term the IILZM* system) with the Chapman system (cf. Fig. 4b) discloses a number of substantial differences. First, in the Chapman sum of S_D -currents, as in his D_{ST} -system, the signs of the current function are not indicated. Obviously, the difference in sign of the current eddies discovered by us must be of significance in the construction of a quantitative theory of the S_D -variations.

The second difference of the IILZM system is the shift of the centers of the polar eddies, that of the morning eddy to 2^h of magnetic time, that of the evening eddy to 12 - 14^h, while in the Chapman system both eddies are centered symmetrically at 6 and 13^h. Because of this displacement of the eddy centers, the currents in the polar cap have a direction perpendicular to the 6 - 14 hour meridian, which well explains the S_D -variations of the horizontal components at Thule and Godhavn, with the minimum of X^1 at 14^h. According to the Chapman system, a minimum of X^1 at 13^h and a zero value at 12^h might be expected at these observatories.

The position of the morning middle-latitude eddy likewise does not agree in the two systems, and the absolute values of the intensity of the polar eddies is different. In the Chapman system, the total intensity of the current flowing through the polar cap is 450,000 amp, while in the IILZM system it is 200,000 amp. In the Chapman system, moreover, the intensity of the morning and evening eddies is the same.

However, it does seem that all these differences (except for the difference in the signs of the current function) are due not so much to the different method of calculation as to the difference in the starting data used. An approximate evaluation of the intensity of the currents from our data gave the following results:

* Terrestrial Magnetism Research Institute

As is commonly known, the density of a uniform current layer of sufficiently great extent is $i = \frac{F_e}{2\pi}$, where F_e is the field induced by this layer on the surface of the earth, perpendicular to the direction of i . Assuming that the ratio of the external field to the observed field (F) is equal to k , we have $i = \frac{kF}{2\pi}$. If the width of the belt of current is l_{cm} , then the total current is $I = \bar{i}l$, where \bar{i} is the mean value of the flux density which, without great error, can be taken as equal to $2/3 i_{max}$, if parabolic distribution of the density in the flux is assumed. It follows from this that

$$I = \frac{kF^2}{2\pi^3} / \text{CGS.} \quad (1)$$

Applying this approximate formula to the observed variations at Thule ($X'_{max} = 60\gamma$), setting the width of the flux at 32° , and replacing the value of the coefficient $k = 0.6$, adopted by Chapman, by the value $k = 0.9$ found by us for the polar cap, we have

$$I = \frac{0.9 \times 10 \times 10^{-5}}{6.3} \times \frac{2}{3} \times 32 \times 1.1 \times 10^7 \text{ CGS} = 22 \times 10^4 \text{ A.}$$

Thus a rough estimate of the current likewise leads to eddy intensities half as great as those given by Chapman. As for the directions of the parallel currents flowing through the polar cap, as we have already noted, it follows directly from the observations at Thule and Godhavn that the currents must be parallel to the 1 - 20 hour meridian instead of to 0 - 12 hour meridian, as is the case in the Chapman system. Thus the absence of a good agreement between the polar value of the S_D -currents in the Chapman system and the observed variations is explained simply by the inadequacy of the observational materials that were available to him. The calculations presented above show that the approximate method of estimating the intensity and direction of the currents gives very good results. Of course, the approximate method does not make it possible to separate the internal and external parts from the

observed field, to obtain the numerical values of the potential, to determine the signs of the current function, nor to elucidate the details of the configuration of the currents, etc., but it is simply sufficient to obtain a rough picture of the currents as necessary for a qualitative discussion of various problems.

Section 7. The Polar Part of the S_D -Currents

The distribution of the S_D -currents in the auroral zone shown in Fig. 29 was also compared by us with the parameters of the current obtained under the assumption of linearity of the current. As stated in Chapter 1, the calculations of the intensity, height, and position of the linear current in the auroral zone has been carried out by a number of authors from observations of a pair of stations or of several pairs, yielding different results, depending on the materials used. Accordingly, we repeated our calculations using the same data we used in constructing the system of surface currents.

The distribution of the vectors of the magnetic field of the linear electric current is schematically represented in Fig. 30. In considering this figure we must

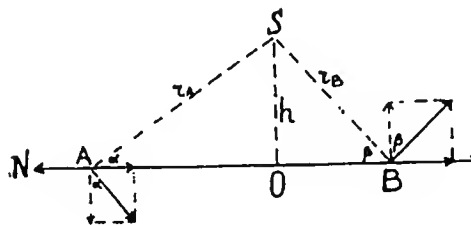


Fig. 30 - Pattern of Magnetic Field of Horizontal Linear Current

imagine the current to flow perpendicular to the plane of the paper in the direction from the paper toward the observer, and assume h to be the height of the current above the earth's surface, while A and B are two points at which the vectors of the magnetic field are known. On the drawing, they are located at different sides of O ,

the projection of the current onto the earth's surface. It follows from the drawing in Fig. 30 that:

$$\left. \begin{aligned} AO &= h \operatorname{ctg} \alpha \\ BO &= h \operatorname{ctg} \beta \end{aligned} \right\} \quad (2)$$

observed field, to obtain the numerical values of the potential, to determine the signs of the current function, nor to elucidate the details of the configuration of the currents, etc., but it is amply sufficient to obtain a rough picture of the currents as necessary for a qualitative discussion of various problems.

Section 7. The Polar Part of the Sp-Currents

The distribution of the Sp-currents in the auroral zone shown in fig.29 was also compared by us with the parameters of the current obtained under the assumption of linearity of the current. As stated in Chapter 1, the calculations of the intensity, height, and position of the linear current in the auroral zone has been carried out by a number of authors from observations of a pair of stations or of several pairs, yielding different results, depending on the materials used. Accordingly, we repeated our calculations using the same data we used in constructing the system of surface currents.

The distribution of the vectors of the magnetic field of the linear electric current is schematically represented in fig.30. In considering this figure we must

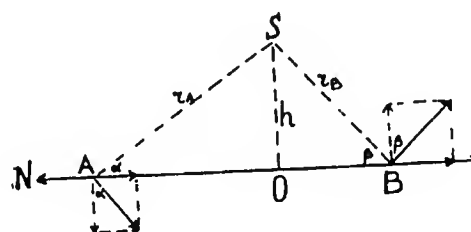


Fig.30 - Pattern of Magnetic Field of Horizontal Linear Current

imagine the current to flow perpendicular to the plane of the paper in the direction from the paper toward the observer, and assume h to be the height of the current above the earth's surface, while A and B are two points at which the vectors of the magnetic field are known. On the drawing, they are located at different sides of O ,

the projection of the current onto the earth's surface. It follows from the drawing in fig.30 that:

$$\left. \begin{aligned} AO &= h \operatorname{ctg} \alpha \\ BO &= h \operatorname{ctg} \beta \end{aligned} \right\} \quad (2)$$

$$h = \frac{AB}{\operatorname{ctg} \alpha \cdot \operatorname{ctg} \beta}, \quad (3)$$

$$\operatorname{tg} \alpha = \frac{X_A}{Z_A}, \quad (4)$$

$$\operatorname{tg} \beta = \frac{X_B}{Z_B}, \quad (5)$$

$$\Phi_0 = \Phi_B + h \operatorname{ctg} \beta = \Phi_A - h \operatorname{ctg} \alpha, \quad (6)$$

if Φ_0 is the latitude of point O (in our case of the auroral zone) and Φ_A and Φ_B are the latitudes of points A and B.

The vector of the magnetic field created by the infinite linear current I at the distance r is equal to

$$H = \frac{2I}{r}.$$

Consequently, if H is expressed in gauss, I in amperes and r in kilometers, then

$$I = 5rH = 5 \frac{h}{\sin \alpha} \frac{X_A}{\sin \alpha} = 5 \frac{h}{\sin \beta} \frac{X_B}{\sin \beta}$$

or

$$I = 5hX_A(1 + \operatorname{ctg}^2 \alpha) = 5hX_B(1 + \operatorname{ctg}^2 \beta). \quad (7)$$

For the case where both points A and B are located on the same side of the projection of O, we have

$$h = \frac{AB}{\operatorname{ctg} \beta - \operatorname{ctg} \alpha}, \quad (3')$$

$$\Phi_0 = \Phi_B + h \operatorname{ctg} \beta = \Phi_A + h \operatorname{ctg} \alpha. \quad (6')$$

Equations (3), (3'), (6), (6'), and (7) allow us to calculate all the parameters of the current if we know the distance between two observatories whose observations are available to us.

A consideration of Fig. 23 shows that the most convenient pairs located near the

POOR ORIGINAL

the height of the current may be considered to exist in reality. The most reliable height determinations appear to be those in the night and early morning hours (0-6) and in the afternoon hours (14-20) when the replacement of the surface current by the linear current is most logical. In these hours, all stations give results in agreement with each other (increase from 250 to 500 km in the period 4 to 6^h and decrease from 600 to 250 km in the period from 16 to 20^h), which are very close to those of ionospheric measurements. At the end of the day (20-24^h) and at noontime, the values of the heights are very diverse. The calculated values often appear absurd; $h > 1000$ km or $h < 0$ km (cf. omissions in the height column of Table 12). The poor results during this period are entirely understandable if we bear in mind that in these hours there is no crowding of the current lines (cf. Fig. 29) which might be compared to the linear current.

Owing to the relatively great dispersion of the values of h , no systemic difference in the values calculated for different pairs of stations is found. It can only be noted that the calculation of h for the pair IV gave the worst results, which most probably can be explained by the fact that the Pikhaya Bay Observatory is located far from the zone of linear current and is in the region of action of the surface current flowing in meridional direction through the polar cap.

Thus the determination of the height of the current in the polar zone by the above-presented formulas, as rough as it may be, still does indicate that in the high latitudes the current system of S_D can likewise be referred to the level of the F_2 layer, and that we did not commit a great error in adopting the height of the system $h = 0.05 R$ for the entire earth as an average. In more detailed calculations, which would be outside the scope of the present work, the diurnal fluctuations and the latitudinal variations of the height of the current layer should also be taken into account.

The variations in the geomagnetic latitude of the linear current zone (Φ_0) give a still more regular picture. All stations agree in indicating an increase in

the northward shift of the linear current during the daytime hours and a southward shift in the night hours, which is full agreement with the position of the zero current line on Fig. 29. The unexpected drop in the value of Φ_0 at 10^h and the great scatter at $20-24^h$ is explained, as in the case of the calculation of heights, by the absence of crowding of the current lines in these periods of the day. There is a notable systematic difference in the values $\Phi_{0 I}$, $\Phi_{0 II}$, $\Phi_{0 III}$, and $\Phi_{0 IV}$. Two pairs of stations, Inuk-Fort Rae and Point Barrow-Ullon give about the same values, fluctuating in the morning and evening hours about $\Phi_0 = 66^\circ$, which is in complete agreement with the position of the zone on Fig. 23, which we have drawn along the isoamplitudes of HS_D . As should have been expected on the basis of Fig. 23, the pair Pikhaya Bay-Matichkin Shar and Dickson indicate the southernmost position of the zone ($\Phi_0 = 63 - 64^\circ$). There is a certain lack of correspondence between Fig. 23 and the values of Table 12 only for the pair Petsamo-Joar Islands ($\Phi_0 = 65^\circ$) along the isoamplitudes and $\Phi_0 = 67^\circ$ for the morning and evening hours of Table 12. Thus the calculation of the latitude of the zone of linear current on the average is in very good agreement with the position of the zero current line in the system of surface currents and allows the position of the zone to be made more precise at various longitudes.

A comparison of the intensity of the linear current with that of the surface current flowing in the belt $60-70^\circ$, indicates good agreement, both in order of magnitude and in diurnal distribution. The systematic difference in $I_I \dots I_{III}$ again indicates the existence of the longitudinal asymmetry in the distribution of S_D , repeatedly noted by us. For obvious reasons, there is no special point in attaching any particular significance to the scattered values of I_{IV} .

The above-described parameters of the linear current, calculated by us from the S_D -variations for the Second International Polar Year, agree in part with the parameters from the calculations of Sucksdorff and (Sibl. 55) and Harang (Sibl. 44). In particular, the diurnal variations of altitude and density are about the same for

POOR ORIGINAL

all three studies. We did not, however, discover the existence of two branches of the current on one and the same meridian, which would follow from Harang's work. We likewise fail to find even indications of the existence of the "almost vertical" linear current calculated by Sucksdorff. On the contrary, the idea obtained by us as to the parameters of the linear current is in full agreement with the system of surface currents, which is more objective, and has been calculated without a priori assumptions as to the configuration of the current.

F-TS-3974/V

132

CHAPTER VI

POLAR STORMS

Section 1. Expansion of the Field Potential and Electric Currents into Series of Cylindrical Functions

As has been stated above, during the time of a polar storm (P), the fluctuations in the magnetic elements in the high latitudes reach great amplitudes, often exceeding 1000 γ , while in the low latitudes a polar storm manifests itself in the form of small bay-shaped disturbances. It follows from Figs. 7a and 6b that the field of a P storm for $\phi < 55^\circ$ is so small by comparison with the field in the polar cap that, without great error, a field that vanishes at $\theta = 50^\circ$ may be adopted, and the distribution of vectors considered only on the spherical segment $\phi \leq 40^\circ$. In this case, taking the spherical segment as a portion of a plane, the potential of a P storm may be represented by a series of Bessel functions. The approximation will of course be very rough and will give particularly great distortions along the edges of the regions considered, but it will still enable us to separate from the field observed on the earth's surface that part due to ionospheric sources, and to form an idea on the configuration and intensity of the currents flowing in the ionosphere. In the central part of the polar segment, we have $\theta \leq 45^\circ$, and it is here that the most intense fluctuations of the magnetic field are concentrated, while the distortions introduced by the replacement of the spherical surface by a plane surface are relatively small.

In view of the fact that the expansion of Bessel functions is here used for the

first time in investigations of the variable magnetic field of the earth, we will in this section derive the necessary formulas and will devote the next section to a description of the current system obtained for the P storms.

After selecting a system of cylindrical coordinates r, φ, z such that its origin coincides with the magnetic axis pole, that the plane $z = 0$ corresponds to the earth's surface, and that the positive axis z is directed toward, let us represent the potential of the storm at some fixed instant of time T by the Fourier-Bessel series:

$$V = \sum_n \sum_m (a_{nm}^e \cos n\varphi + b_{nm}^e \sin n\varphi) e^{-\frac{\lambda_n^m}{2} z} J_n(\lambda_n^m \frac{r}{\rho}) + \sum_n \sum_m (a_{nm}^i \cos n\varphi + b_{nm}^i \sin n\varphi) e^{\frac{\lambda_n^m}{2} z} J_n(\lambda_n^m \frac{r}{\rho}). \quad (1)$$

The first half of the series converges in the half-space $z > 0$, below the surface of the earth, and represents the potential due to external sources (V_e). The second half of the series converges for $z < 0$ and represents the potential of the field due to external sources (V_i). Here λ_n^m denotes the m th root of the Bessel function of the n th order, and eq. (1) vanishes on the surface of the cylinder of radius $r = \rho$.

Since we have assumed that $V = 0$ for $\theta \geq 40^\circ$, the numerical value of ρ in our analysis equals the length of the segment of the meridian included between $\theta = 0^\circ$ and $\theta = 40^\circ$, i.e., 111×40 km, or 4.5×10^3 cm. The field intensity is

$$F = -\text{grad } V \text{ in } R = -\frac{\partial V}{\partial r}, \quad Z = -\frac{\partial V}{\partial z}, \quad (2)$$

where X denotes the component of the horizontal vector directed along the geomagnetic meridian. Since the direction toward the pole is usually considered positive in geomagnetic measurements, while r increases with increasing distance from the pole, we have, from eq. (1),

$$X = -R \frac{\partial V}{\partial r}. \quad (2')$$

From eq.(1) we also have

$$Z = \sum_n \sum_m \frac{\lambda_n^m}{\rho} (x_{nm}^e \cos n\varphi + x_{nm}^i \sin n\varphi) e^{\frac{\lambda_n^m}{\rho} r} J_n \left(\lambda_n^m \frac{r}{\rho} \right) - \sum_n \sum_m \frac{\lambda_n^m}{\rho} (x_{nm}^e \cos n\varphi + x_{nm}^i \sin n\varphi) e^{-\frac{\lambda_n^m}{\rho} r} J_n \left(\lambda_n^m \frac{r}{\rho} \right). \quad (3)$$

on the earth's surface, $r = 0$ and

$$V = \sum_n \sum_m (a_{nm} \cos n\varphi + b_{nm} \sin n\varphi) J_n \left(\lambda_n^m \frac{r}{\rho} \right), \quad (4)$$

$$Z = \sum_n \sum_m (c_{nm} \cos n\varphi + d_{nm} \sin n\varphi) J_n \left(\lambda_n^m \frac{r}{\rho} \right), \quad (5)$$

where

$$a_{nm} = \alpha_{nm}^e + \alpha_{nm}^i, \quad c_{nm} = \frac{\lambda_n^m}{\rho} (\alpha_{nm}^e - \alpha_{nm}^i),$$

$$b_{nm} = \beta_{nm}^e + \beta_{nm}^i, \quad d_{nm} = \frac{\lambda_n^m}{\rho} (\beta_{nm}^e - \beta_{nm}^i).$$

If $\alpha_{nm}^e \dots \beta_{nm}^i$ are known, then $e_{nm} \dots i_{nm}$ may be calculated by the formulas

$$\alpha_{nm}^e = \frac{1}{2} \left(a_{nm} + \frac{\rho}{\lambda_n^m} c_{nm} \right); \quad \alpha_{nm}^i = \frac{1}{2} \left(a_{nm} - \frac{\rho}{\lambda_n^m} c_{nm} \right), \quad (6)$$

$$\beta_{nm}^e = \frac{1}{2} \left(b_{nm} + \frac{\rho}{\lambda_n^m} d_{nm} \right); \quad \beta_{nm}^i = \frac{1}{2} \left(b_{nm} - \frac{\rho}{\lambda_n^m} d_{nm} \right). \quad (7)$$

The values of c_{nm} and d_{nm} are easily obtained by expanding into series $J_n \left(\lambda_n^m \frac{r}{\rho} \right)$ the properly work-up data of the variations of the Z component of the geomagnetic field. For the calculation of a_{nm} and b_{nm} it is more convenient to make use of the data of the variations of the X component. From eq.(2) it follows, for $r_0 > r$, that

$$V_{r_0} - V_r = \int_r^{r_0} X dr = V - \int_r^{r_0} X dr + V_{r_0}.$$

Taking $r_0 = \rho$, we have

$$V = - \int_r^{\rho} X dr, \quad (8)$$

since, by hypothesis, $V_{\rho} = 0$.

On finding, by numerical integration of the X' component, the value of V for all the region $r < \rho$, we may find the coefficients a_{nm} and b_{nm} of the expansion of eq. (4).

From the distribution of the potential V_0 found on the surface $z = 0$ it is not difficult to pass to the distribution of the currents responsible for it. Let the potential V_0 known on $z = 0$ be due to a plane layer of currents lying at the level $z = -z_0$. Denoting the value of the potential for the lower surface of the layer by V_- , and that on the upper layer by V_+ , we have, under the condition that the normal derivative is continuous,

$$\frac{\partial V_+}{\partial z} = \frac{\partial V_-}{\partial z}. \quad (9)$$

Since the current layer is equivalent to a double magnetic sheet, the second

equation

$$V_+ - V_- = 4\pi I, \quad (10)$$

where $I(r, \varphi)$ is the density of the current layer, will also hold for the level $z = -z_0$. On expanding V_+ , V_- and I into a series of Bessel functions, we have

$$V_- = \sum_n \sum_m (\alpha_{nm}^- \cos n\varphi + \beta_{nm}^- \sin n\varphi) e^{\frac{\lambda_n^m}{\rho}(z+z_0)} J_n\left(\lambda_n^m \frac{r}{\rho}\right) \text{ as } |z| < z_0, \quad (11)$$

$$V_+ = \sum_n \sum_m (\alpha_{nm}^+ \cos n\varphi + \beta_{nm}^+ \sin n\varphi) e^{\frac{\lambda_n^m}{\rho}(z+z_0)} J_n\left(\lambda_n^m \frac{r}{\rho}\right) \text{ as } |z| > z_0, \quad (12)$$

$$I = \sum_n \sum_m (s_{nm} \cos n\varphi + \tau_{nm} \sin n\varphi) J_n\left(\lambda_n^m \frac{r}{\rho}\right) \text{ as } |z| = z_0. \quad (13)$$

Substituting eqs.(11) - (13) in eqs.(9) and (10), and equating the coefficients of the same $\overline{\cos n\varphi} J_n$, we have

$$\sin n\varphi \quad \alpha_{nm}^+ = -\alpha_{nm}^-; \quad \alpha_{nm}^+ - \alpha_{nm}^- = 4\pi s_{nm}, \quad (14)$$

$$\beta_{nm}^+ = -\beta_{nm}^-; \quad \beta_{nm}^+ - \beta_{nm}^- = 4\pi \tau_{nm}, \quad (15)$$

whence

$$s_{nm} = -\frac{1}{2\pi} \alpha_{nm}^-; \quad \tau_{nm} = -\frac{1}{2\pi} \beta_{nm}^-. \quad (16)$$

For $z = 0$, we have the two identical expressions:

$$V_- = \sum_n \sum_m (\alpha_{nm}^- \cos n\varphi + \beta_{nm}^- \sin n\varphi) e^{-\lambda_n^m \frac{z_0}{\rho}} J_n \left(\lambda_n^m \frac{r}{\rho} \right), \quad (17)$$

$$V_+ = \sum_n \sum_m (\alpha_{nm}^+ \cos n\varphi + \beta_{nm}^+ \sin n\varphi) J_n \left(\lambda_n^m \frac{r}{\rho} \right). \quad (18)$$

On equating them, we have

$$\left. \begin{aligned} \alpha_{nm}^- &= \alpha_{nm}^+ e^{\lambda_n^m \frac{z_0}{\rho}}; & \beta_{nm}^- &= \beta_{nm}^+ e^{\lambda_n^m \frac{z_0}{\rho}} \\ s_{nm} &= -\frac{\alpha_{nm}^+}{2\pi} e^{\lambda_n^m \frac{z_0}{\rho}}; & \tau_{nm} &= -\frac{\beta_{nm}^+}{2\pi} e^{\lambda_n^m \frac{z_0}{\rho}} \end{aligned} \right\} \quad (19)$$

where z_0 is the modulus of the height of the currents postulated by us.

Section 2. Starting Material. Results of the Analysis

As our starting material for calculating the currents responsible for polar storms, we used the data collected and worked up by Silsbee and Vestine (Bibl.54). Polar storms are so diverse in form and in intensity that the formal averaging of series of observations cannot give such good results as it gives with the S_q or S_D variations. Nevertheless, the statistics of a large number of storms for certain

observatories given by these authors do show that there is a definite regularity in the distribution of storms by hours of the day. The relation between the number of storms and the time of day given in Table 13 shows that the positive storms (i.e., deviation in H, $\Delta H > 0$) and the negative storms ($\Delta H < 0$) are usually encountered at different times of the day, the diurnal march of the bays depending on the latitude of the point of observation. The list of observatories used in the work of Silsbee and Vestine, and the number of bays registered, are given in Table 14.

Table 13
Diurnal March of Frequency of Bay-Shaped Disturbances
(Number of days in 5)

ϕ° from - to	ΔH	Hours																							
		1	2	3	4	5	6	7	8	9	10	11	12	13	14	15	16	17	18	19	20	21	22	23	24
38	+	4	4	3	5	6	5	3	3	7	8	8	5	3	2	4	3	4	7	5	3	5	5	4	4
70 - 63	+	0	0	0	0	0	0	0	0	0	0	0	0	0	0	1	1	2	3	2	1	1	1	0	0
	-	14	11	10	9	8	6	4	3	2	1	1	1	0	0	0	0	0	0	1	3	4	6	8	10
43 - 40	+	8	6	4	3	2	1	0	0	0	0	0	0	0	0	0	0	0	1	1	3	6	6	9	10
	-	0	0	0	0	0	0	1	1	2	3	3	3	4	5	5	4	3	2	2	2	1	0	0	0
3 - 16	+	9	6	5	3	2	2	1	0	0	0	0	0	0	0	0	0	0	1	3	6	8	8	9	9
	-	0	0	0	0	0	0	1	1	1	2	3	2	2	2	2	3	4	4	3	3	2	2	1	0

A consideration of the form and intensity of the bay-shaped fluctuations for all three elements enabled me to construct for each observatory a picture of the mean (or more exactly, idealized) bays by averaging the disturbances encountered at one and the same hours of local time. These mean bays were different for different hours of the day of the local day, but resembled each other for observatories located at the same latitude. In other words, I found that the storm field depends on the local time and the latitude. As in Chapter V, allowance was made, in averaging, for the local geomagnetic time and the geomagnetic latitude. Figure 31 gives the distribution of the field of an idealized bay for 0^h Universal Time. The coordinate net on

Table 14

Group	Observatory	ϕ	Λ	Number of Days
1	Thule	83° 0	0° 0	204
2	Julianahob	70.8	35.6	227
	Fort Rae	69.0	290.9	243
	Fromsø	67.1	116.7	99
	Colle, e, Alaska	64.5	255.4	146
	Dickson	63.0	161.5	103
3	Tucson	40.4	312.2	191
	Ebro	43.9	79.3	147
	Watheroo	-41.3	135.6	173
4	Antipolo	3.3	139.8	117
	Huancayo	-0.6	353.8	98
	Mogadiscio	-2.7	114.3	124
	Apia	-16.0	260.0	72

the map is formed by the geomagnetic parallels and meridians. On the edge of the diagram, the local geomagnetic time of the meridians corresponding to 0^h Universal Time is shown. In preparing the diagram, I used not only the values of the vectors for the 13 enumerated observatories for 0^h, but also for 21^h and 3^h, the latter values being placed on the meridians corresponding to 21^h + Λ - 69° and 3^h + Λ - 69° geomagnetic time. The horizontal component of the storm field is represented by the vector, the vertical component by the digit at the origin of the vector. It will be clear from the figure that the vectors of H are directed primarily along the geomagnetic meridians, that the vectors reach their maximum values in the zone $\phi = 60 - 65^\circ$, and that, at latitudes lower than 50° they are negligibly small. The representation of the field of a polar storm shown in Fig.31 by a series of Bessel functions was accomplished in the following manner: The data of the Z components were interpolated for

various latitudes (ϕ equal to 90, 70, 67, 64 and 50°). For each latitude I calculated the coefficients of the expansion of Z into the Fourier series:

$$Z = \sum (p_n \cos n\varphi + q_n \sin n\varphi),$$

where the argument φ corresponds to the geomagnetic longitude Λ . For a satisfactory representation of Z it proved to be sufficient to confine myself to $n = 0.1$ and 2.

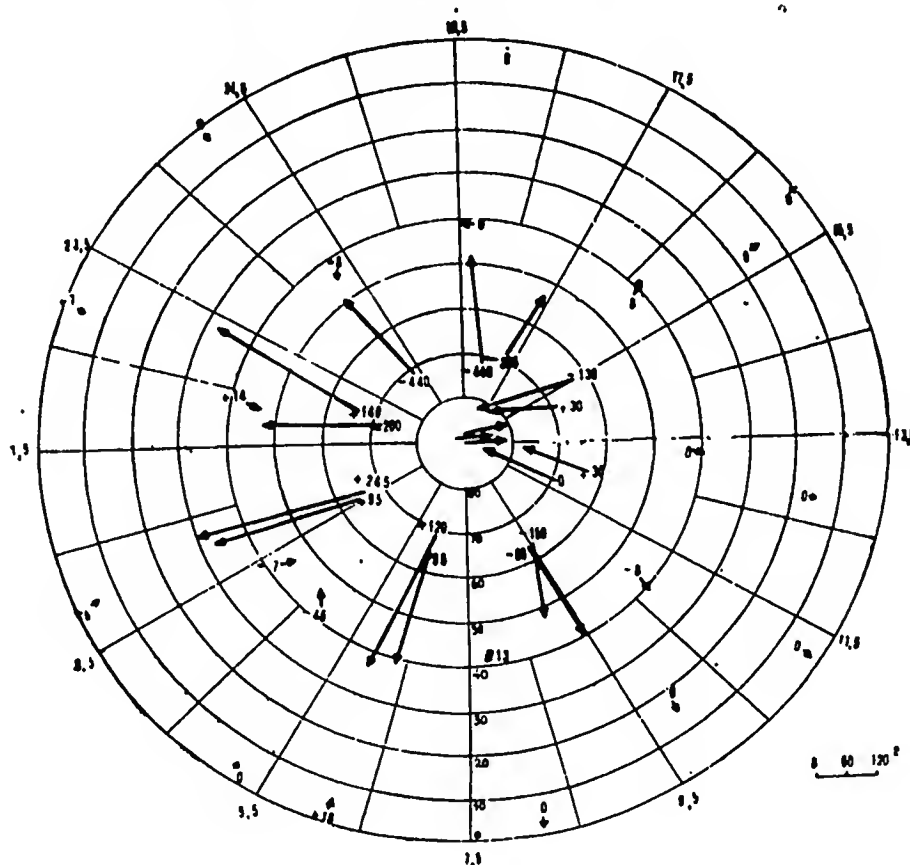


Fig.31 - Field of Polar Storm (According to Vestine). The horizontal component of the field is shown by an arrow, the vertical by numerals (in gammas). The coordinate net is the geomagnetic latitude and the geomagnetic time

Then p_n and q_n were represented by a series of Bessel functions of the n^{th}

order

$$p_n = \sum_m c_{nm} J_n \left(\lambda_n^m \frac{r}{\rho} \right),$$

$$q_n = \sum_m d_{nm} J_n \left(\lambda_n^m \frac{r}{\rho} \right).$$

while c_{nm} and d_{nm} were found by the well-known formulas

$$c_{nm} = \frac{2 \int_0^1 r \rho_n(r) J_n \left(\lambda_n^m \frac{r}{\rho} \right) dr}{[J_{n-1}(\lambda_n^m)]^2},$$

$$d_{nm} = \frac{2 \int_0^1 r q_n(r) J_n \left(\lambda_n^m \frac{r}{\rho} \right) dr}{[J_{n-1}(\lambda_n^m)]^2}.$$

The values of the H component, as indicated above, were first integrated to obtain the value of the potential V, and then a_{nm} and b_{nm} were calculated by means of eq.(4).

Table 15 gives a summary of the coefficients $a_{nm} \dots d_{nm}$ so obtained.

Table 15 *

m	1	2	3	4	5
c_0	-32	-39	53	46	-50
c_1	-51	-77	-6	60	-30
d_1	27	-81	-84	73	-34
c_2	-26	-64	-18	25	1
d_2	-31	-7	8	-2	-12
a_0	3.47	1.66	-0.60	0.02	-0.09
a_1	—	—	—	—	—
b_1	3.28	3.66	-1.48	-0.25	1.04
a_2	1.03	1.36	0.18	0.09	0.11
b_2	—	—	—	—	—

Equations (4) and (5) satisfactorily represent the initial observed data, as indicated in Table 16 which gives the calculated and observed values of V (in CGSN) and

* In Table 15 the values of the coefficients are given in units of 10^{-5} CGS. The values of a_1 and b_2 do not exceed a few units of the fifth decimal place.

of Z (in γ) for four points.

The separation of the potential into portions of external and internal origin by means of eqs.(6) and (7) showed (Table 17) that the external potential V_e consid-

Table 16

Φ	Λ	Z_{obs}	Z_{calc}	V_{obs}	V_{calc}
$30^{\circ 1}$	0°	-170	-140	5×10^{-5}	5×10^{-5}
80	90	- 60	- 90	5	6
66	0	120	100	2	2
66	90	180	200	2.5	2.5

erably exceeds the internal potential V_i . For a quantitative estimate of the ratio of the external to the internal fields it is more convenient to represent V in the form

$$V = \sum_n \sum_m \left(E_n^m e^{-\lambda - i(n\gamma + \tau_n^m)} + e^{\lambda - i(n\gamma + \zeta_n^m)} \right) I_n^m(\lambda r), \quad (20)$$

where

$$\begin{aligned} E_n^m &= V(\alpha_{nm}^e)^2 + (\beta_{nm}^e)^2; \quad \text{tg } \tau_n^m = -\frac{\beta_{nm}^e}{\alpha_{nm}^e}, \\ I_n^m &= V(\alpha_{nm}^i)^2 + (\beta_{nm}^i)^2; \quad \text{tg } \zeta_n^m = -\frac{\beta_{nm}^i}{\alpha_{nm}^i}. \end{aligned} \quad (21)$$

Table 17 gives the value of $E_n^m \dots \tau_n^m$ and also of $f = I/E$ and $\delta = \gamma - \zeta$.

This table shows that in two cases $f > 1$ and in one case f could not be calculated, because of the smallness of the initial coefficients. In Chapter X, we will show that the values obtained for f and δ are in agreement with the hypothesis that the internal part of the field is of inductive origin. The mean value $f = 0.86$ is the same as that obtained for the polar cap from the data of the S_D -variations ($V_i/V_e = 0.89$), which indicates the plausibility of these values. The value $f = 0.86$ - - 0.89 considerably exceeds the corresponding values for the S_q - and D_{st} -variations

CHAPTER VII

SEASONAL AND 11-YEAR VARIATIONS OF THE D_{st} AND S_D CURRENTSSection 1. The 11-Year and Seasonal Variations of the D_{st} Currents

The present Chapter is devoted to a discussion of the variations that the mean pictures of the electric currents described by us undergo with the seasons of the year, and with the 11-year cycle. It is not possible to collect the observational data for a series of years from the wide net of observatories that is necessary for the mathematical calculation of the currents. I therefore confined myself to the study of the 11-year and annual variations of the D_{st} and S_D variations from individual base stations, on the basis of which I then drew my conclusions as to the variations of the current system as a whole. As my basis I selected observatories with long series of observations whose variations are characteristic for the corresponding regions.

Let us first turn to the 11-year fluctuations of the D_{st} currents. The dependence of the degree of magnetic disturbance on the level of solar activity is widely known: the coefficient of correlation between the annual numbers of the u-measure of magnetic activity and the relative sunspot number may go as high as 0.9. Since with increasing solar activity, the number and mean intensity of the disturbances also increases, it may be expected that in the 11-year cycle the mean characteristic of the D_{st} variations will vary and, consequently, the intensity of the system of currents equivalent to it will also vary. Instead of the very laborious calculation

POOR ORIGINAL

in whose analysis the data from the entire earth were used. The possibility is not excluded that this discrepancy is not fortuitous, and that it indicates the anisotropy of the deep parts of the earth (for more details, see Chapter X).

Table 17 *

External Field					
<i>m</i>	1	2	3	4	5
<i>a</i> ₀	2,33	0,99	-0,44	-0,10	0,03
<i>a</i> ₁	0,30	0,25	0,01	-0,10	0,04
<i>β</i> ₁	1,48	2,09	-0,55	-0,25	0,56
<i>a</i> ₂	0,63	0,85	0,12	0,00	0,06
<i>β</i> ₂	0,14	0,02	0,00	0,00	0,02
<i>E</i> ₁	1,51	1,96	0,55	0,32	0,57
<i>γ</i> ₁	284	277	89	92	274
<i>E</i> ₂	0,65	0,85	0,10	0,00	0,06
<i>γ</i> ₂	348	359	0	90	342

Internal Field					
<i>m</i>	1	2	3	4	5
<i>a</i> ₀	1,02	0,72	-0,16	-0,07	-0,12
<i>a</i> ₁	-0,30	-0,25	-0,01	0,10	-0,04
<i>β</i> ₁	1,80	1,57	-0,92	0,00	0,48
<i>a</i> ₂	0,40	0,51	0,08	0,08	0,06
<i>β</i> ₂	-0,14	-0,02	0,00	0,00	-0,02
<i>γ</i> ₁	1,82	1,59	0,92	0,10	0,50
<i>γ</i> ₁	260	261	91	0	265
<i>γ</i> ₂	0,42	0,51	0,06	0,08	0,06
<i>γ</i> ₂	20	3	0	0	18

Ratio of Internal and External Fields					
<i>m</i>	1	2	3	4	5
<i>f</i> ₁	1,21	0,81	1,67	0,31	0,88
<i>f</i> ₂	0,65	0,60	0,60	—	1,00
<i>δ</i> ₁	24	16	-2	92	9
<i>δ</i> ₂	-32	-4	0	90	-36

The ionospheric currents whose field is identical with the field of the idealized polar storm were calculated by eqs.(13) and (19). The disturbances of the polar ionosphere, as a rule, extend to heights of 100-30 km. Down to these same heights the lower boundaries of the aurora usually descend. This forces us to consider that the most probable height of the currents of polar storms is the region of the E layer of the ionosphere, i.e., 90-120 km. The highly local character of the course of these storms, when the form and intensity of the disturbance varies considerably over a distance of a few hundred kilometers, likewise prevents us from referring these currents to great heights. These assumptions forced us to use $z_0 = 100$ km in eq.(19). The

* In Table 17, the values of α , β , E , and I are given in gammas and those of ζ , δ , and γ in degrees.

of the D_{st} variations for different years, I limited myself to the consideration of the quantity $D_m = H_d - H_q$. A consideration of D_m is entirely adequate for judging the geographic distribution or time fluctuations of the field of D_{st} , since, as noted above, D_m is approximately equal to the mean value of $D_{st}H$ on the two first days of a storm.

From Fig.33, showing the relation of D_m and ϕ , it will be seen that the geographic distribution of D_m in the middle latitudes ($\phi \leq 50^\circ$) varies little during the course of the 11-year cycle: the curves of $D_m(\phi)$ in the years of high activity (1938) and low activity (1933) almost parallel each other. In the high latitudes ($\phi > 50^\circ$) there is a considerable change in the form of the curve of $D_m(\phi)$. However, as repeatedly pointed out, the \tilde{D}_m of high latitudes are due mainly to polar storms and do not characterize the D_{st} field. In view of this it can be considered that, from year to year, there is little change in the configuration of the D_{st} current system, but that there is considerable change only in its intensity.

In the preceding Chapters we have pointed out that the approximate method of evaluating the intensity of currents gives good results, close to those of the exact mathematical methods. Thus, for example, the intensity of the D_{st} current flowing west along the parallels of latitude in each hemisphere, according to the data of spherical analysis, is $I = 180,000$ amp, while the approximate estimate, based on the value of D_m at Huancayo, gives $I = 176,000$ amp. Starting out from this good correspondence, the current strength of D_{st} was calculated from the Huancayo observations for 1922 - 1944. As will be seen from Fig.34* the current strength undergoes great fluctuations, from 12×10^4 amp in years of low solar activity to 40×10^4 and 50×10^4 amp in years of high activity. Corresponding to this, the mean current density varied from 1.2×10^5 to 5.0×10^5 CGSM. Just as in the consideration of the

* The values of I for 1919 - 1922 are calculated from the values of D_m at Watheroo, and for 1945 to 1950 from D_m at Zuy. The values of D_m at Watheroo and Zuy were multiplied by the factor 1.2 to reduce them to the values at Huancayo.

coefficients s and τ (in amperes) calculated under this hypothesis are given in Table 18, and the resultant system of currents is given in Fig.32. A comparison of

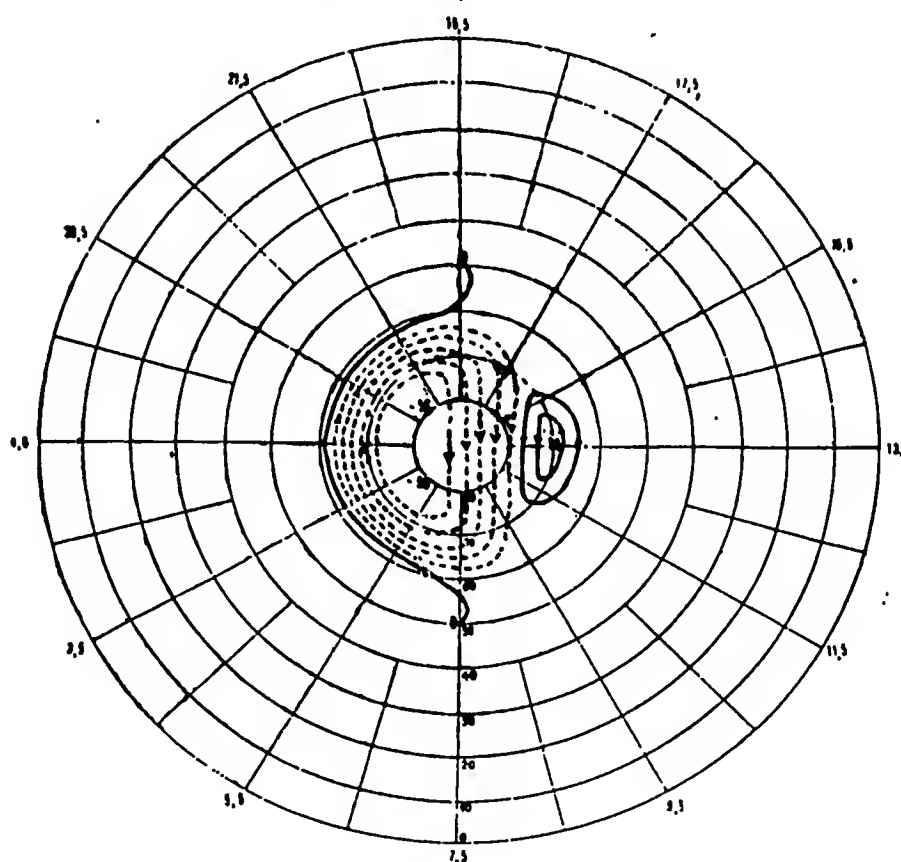


Fig.32 - Current System of Polar Storms; Intensity of Current in 10,000 Amperes. The current flowing between two adjacent lines of current is 10,000 amp. The coordinate net is the geomagnetic latitude and geomagnetic time. (— positive values of current function; - - -negative values)

the current system of Fig.32 with the Silsbee - Vestine system, constructed on the basis of these same data, but by an approximate method, indicates their great resemblance. This is still another confirmation of the conclusion drawn by us in Chapter V to the effect that the approximate method gives a good idea of the configuration and intensity of the current lines, and can be successfully used in cases where a qualitative idea of the current system must be obtained without great expenditure of

11-year cycle of other magnetic characteristics, a lag of the magnetic maxima behind the solar maxima is noted in good agreement with the corpuscular nature of magnetic

disturbances.

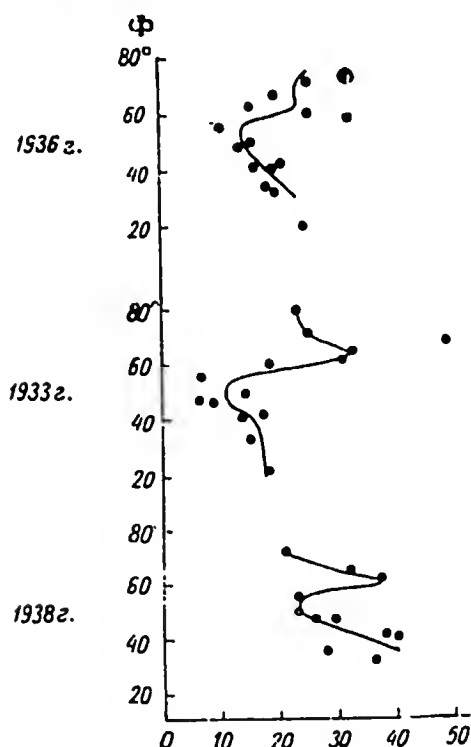


Fig.33 - Dependence of $D_m = H_q - H_d$ (in γ) on the Geomagnetic Latitude

In the work of Chynk (Bibl.41), cited in Chapter I, it has been established that D_m has systematic seasonal fluctuations. Besides the double wave with maxima at the epoch of the equinoxes and minima at the epoch of the solstices, which is inherent in all measures of magnetic activity, a simple sinusoidal wave with a maximum in the winter for each hemisphere and a minimum in the summer may also be separated from the annual march of D_m . At Huancayo, located close to the geomagnetic equator ($\phi = -0.6^\circ$; $\varphi = 12^\circ S$), the value of D_m is about equal at the December and June solstices (cf. Fig.35, which gives the values of D_m for the years 1922 - 1944). This compels the assumption that in the epoch of the solstices the

lines of zero value of the current function are not deflected far from the geomagnetic equator, in contrast to what happens in the case of the S_q variations. The intensity of the current (in 10^4 amperes) in the northern hemisphere, (calculated from the $D_m H$ of Zuy Observatory) and the southern hemisphere (calculated from the $D_m H$ of Watheroo Observatory) is shown in Table 19. The mean values for 1938 - 1944 of the intensity of the D_{st} current are given separately in Table 20 for the northern and southern hemispheres.

Thus the seasonal fluctuations of D_{st} actually do have a maximum at the epoch of the equinox and a minimum at the epoch of the solstice. The summer minimum is

labor.

The system of currents represented in Fig.32 consists of two eddies in which the current flows in opposite directions. This explains the fact, illustrated by Figs.9 and 31, that at polar stations located in different hemispheres the storms are usually observed simultaneously but have different signs for the H component. The current eddy located on the morning side of the polar cap is considerably weaker than the evening eddy: The total current in it reaches 16,000 amp, while on the evening side it is 55,000 amp.

The system so described is completely different from the currents postulated to explain the polar storm by Birkeland, but, conversely, it does resemble the polar part of the currents of the S_D -variations. This resemblance is entirely understandable if we bear in mind the fact that the polar disturbances, which everywhere accompany worldwide storms, make the greatest contributions to the S_D -variations.

Table 18

m	1	2	3	4	5
s_0	$-32 \times 10^3 A$	$-17 \times 10^3 A$	$8 \times 10^3 A$	$23 \times 10^3 A$	$1 \times 10^3 A$
s_1	-26	-40	11	5	13
s_2	-11	-16	-2	0	-1
τ_2	$-$	$-$	$-$	$-$	$-$

deeper in both hemispheres than the winter minimum.

Table 19

Year	a)			Year	a)			b)		
	c)	d)	e)		c)	d)	e)	d)	c)	e)
1919	12	18	26	1935	12	16	22			
1920	10	15	31	1936	17	19	28			
1921	10	39	16	1937	15	25	38			
1922	9	13	21	1938	35	34	49	45	26	51
1923	5	8	21	1939	26	45	48	29	39	44
1924	5	19	11	1940	18	25	64			
1925	15	17	16	1941	25	40	42	27	31	43
1926	18	23	41	1942	21	15	28	23	10	29
1927	4	20	28	1943	18	29	28	23	20	27
1928	13	28	22	1944	21	14	22	22	11	20
1929	30	19	22	1945				17	11	20
1930	26	29	28	1946				24	25	63
1931	13	16	14	1947				42	30	56
1932	13	17	19	1948				25	25	34
1933	16	16	19	1949				38	35	44
1934	9	16	15							

a) Watheroo; b) Zuy; c) Summer; d) Winter; e) Equinox

Section 2. 11-Year Variation of the Middle-Latitude Part of the S_D Currents

The 11-year and seasonal fluctuation of the S_D variations are considerably more complex. The mean annual S_D variations were calculated for a number of observatories for all years for which the data was available to us. As an example, the S_D variations for three observatories (Dombas, Slutsk and Huancayo) are given in Tables 21 - 23. A consideration of the materials collected by us has shown a very systematic variation of the S_D variations from year to year. In many cases these changes are expressed in the increase of the amplitudes with the increase of solar activity. But in a number of cases, changes of form and a shift in the time of the extreme values is observed (thus, for example the S_{DH} of Slutsk, the S_{DZ} of Uellen and Matochkin Shar, etc). At different latitudes, the cyclic variations of S_D proceed differently. The peculiarities noted in the variations of S_D force us to assume that the intensity, location and dimensions of the four current eddies making up the current system of S_D vary during the course of the cycle, the variations in the polar

and middle-latitude eddies being unequal. In this Section we shall discuss the fluctuations of the middle-latitude eddies responsible for the course of the S_D variations in the belt of $\pm 60^\circ$ geomagnetic latitude.

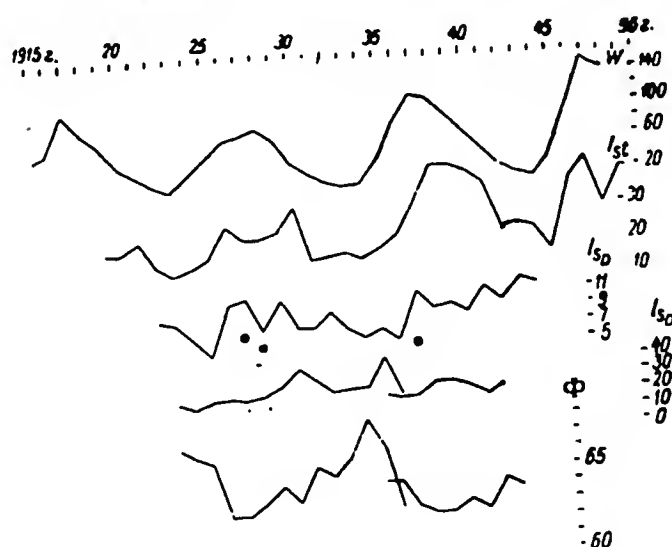


Fig.34 - Cyclical Fluctuation of Electric Currents of D_{st} and S_D Variations (W - relative sunspot number; I_{st} - intensity of D_{st} current; I_{SD}^1 - intensity of middle-latitude eddy of S_D current). The dots indicate the intensity of the additional eddies. J_{SD} - intensity of polar eddy. Units of intensity -10^4 amp. Φ - geomagnetic latitude of auroral zone (from 1922 to 1936, from data of the S_D variations at Sitka observatory, from 1934 to 1943, from data of the S_D variations at Uellen Observatory)

Table 20

Hemisphere	Equinox	Winter	Summer
Northern	36×10^4	28×10^4	23×10^4
Southern	40	28	23
Middle	38	28	23

The variation of the S_D variations at the low latitude observatories during the 11-year cycle are small (for example, the S_D variations at Huancayo, Watheroo and Paris), and manifest themselves mainly in variations of amplitudes. In the equatorial zone, the $S_D Z$ components differ little from zero, while the H components of the contrary are rather distinct. At the latitudes of the centers of the current eddies ($\phi = \pm 40^\circ - 50^\circ$), the S_D variations of the X components are faint while those of the

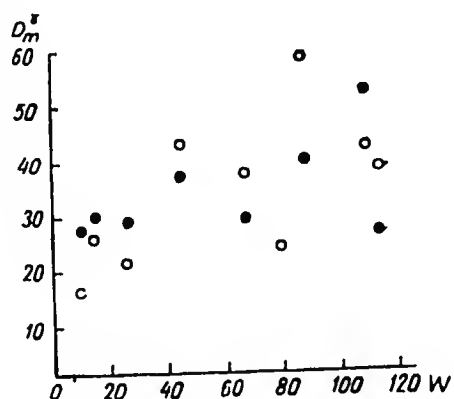


Fig.35 - Values of $D_m = H_q - H_d$ from Huancayo Data for 1922 - 1935 (o - I, II, XI, XII months; • - V, VI, VII, VIII months; W - Relative Sunspot Numbers)

Z components are distinct. In view of this fact, it is more convenient to select the amplitude of $S_D H$ (or X) at the equatorial stations (R_H) and the amplitude Z at the middle-latitude stations, as our index of intensity of the S_D variations. The values of R_H and R_Z given in Table 24 for Huancayo, Watheroo, Paris, and other observatories show that there is no exact parallelism between the march of the amplitude and the annual relative sunspot numbers; but still the periods of elevated activity (1925 - 1931, 1936 - 1942) are likewise marked by an increase of amplitude at

all observatories. A certain shift of the maxima is noted (a lag of the maxima of the S_D amplitudes behind W), which is entirely absent in the S_q amplitudes (for comparison we also give in the Table the $R(S_q H)$ for Watheroo and the u-measure of activity). Particularly characteristic in this respect is the maximum of the cycle 1923 - 1933 which occurred in solar activity and S_q variations in 1928, and in S_D in 1930 (see the very sharp increase of RS_D at Watheroo). The march of the RS_D numbers is less smooth than the march of RS_q , the u-measure and W. The cyclical variations depends on the latitude: at Paris, the RS_D are greater than at Watheroo and Huancayo.

The observatories located in the zone of the center of the middle-latitude eddy ($\lambda = 40 - 50^\circ$), display not only considerable fluctuations in the amplitudes of S_D , but also a variation in the form. This indicates that the position of the center of the middle-latitude eddy varies in latitude from year to year.* Thus, according to the data of the S_d at Slutsk (cf. Table 22) it is very clear that in 1924, 1931, 1933, and 1935 the center of the eddy was at the latitude of Slutsk, in 1932 and 1934 somewhat north of Slutsk, and in the remaining years south of Slutsk. In the first years of those enumerated, the S_{DH} hardly deviates from the zero line, in the following group of years the form of S_{DH} approaches the low-latitude type (with a minimum in the afternoon hours), and in the years of the last group, the form of S_{DH} is typically middle-latitude, with a clear maximum in the evening hours. The same variations in the phase of S_{DH} takes place at Sverdlovsk, Kazan', de Bilt, and Zuy. To give a more impressive idea of the fluctuations of the center of the middle-latitude eddy, Fig. 36 shows the position of the center of this eddy in 1932 - 1933, 1938 - 1939, 1941, 1944, and 1948. The position of the center in the II International Polar Year is plotted from the most complete data of all. It will be seen from the figure that it represents, like the zone of magnetic activity, an ellipse which, in very coarse approximation, is confocal with the zone of magnetic activity. This is evidence for the view that the asymmetry of S_D , which was mentioned in Chapter V, also exists in the middle latitudes, but to a lesser degree. On the territory of the USSR the line of the center of the eddy passes through Slutsk, north of Sverdlovsk and Kazan', somewhat north of Zuy, and considerably to the north of Toyohara, South Sakhalin. In another year of minimum (1944), in which the value of W was almost identical with its 1933 value, the S_{DH} at Zuy is close to that of 1933, but at

* There is also a small shift of the center of the eddy during the hours of the day, which is manifested, for example, in the shift of the maximum of S_{DZ} at Slutsk from 19 hours in 1932 to 1730 hours in 1939. But this shift is very small by comparison with the variation of the latitude of the center of the eddy.

Sverdlovsk and Kazan' S_{pH} is almost of transitional type, which compels us to plot the line of centers in 1944 somewhat to the north of these observatories. In the years of high activity, the line of centers plainly descends to low latitudes, but

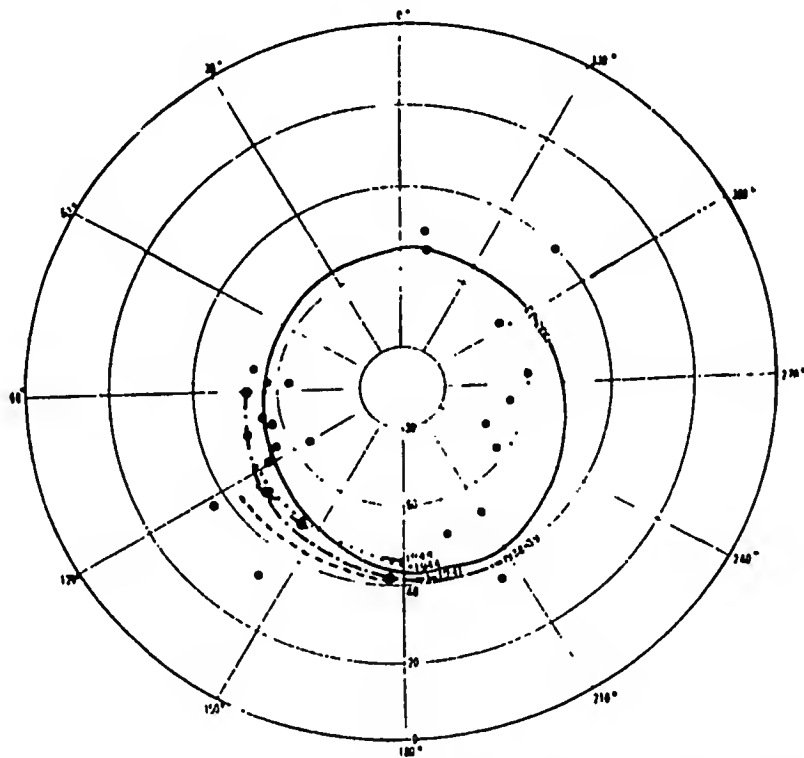


Fig.36 - Position of Line of Centers of Middle-Latitude Eddies in Different Years of the Solar Cycle. The Coordinate Net is Geomagnetic

this movement is not parallel in the entire sector we are discussing. The fact that in a year of exceptionally high activity (1948), the position of the lines according to the data of Kazan', Sverdlovsk, and Zuy was almost the same as in 1944, appears to be somewhat surprising. Thus the conclusion may be drawn that the fluctuations of the line of the center of the middle-latitude eddy are very complex, and that the data of observatories located at different longitudes must be used for their study.

Considering however, that on the average, with increasing activity, the lines of the centers descend by $5 - 6^\circ$, I calculated the intensity of the current of the evening eddy ($I_{S_D}^1$) for 1922 - 1944, based on the value of the evening minimum of S_D at Huancayo and using the above described approximate formula. It was found that

Table 21
S_D - Variations
Dom bas

Universal Time

Year	Hours																										
	0	1	2	3	4	5	6	7	8	9	10	11	12	13	14	15	16	17	18	19	20	21	22	23	24		
D - Declination (in min)																											
1916	-6.5	-4.0	-3.8	0.0	0.5	4.4	3.3	3.7	3.0	2.8	1.5	1.5	1.1	1.1	-0.1	0.0	-2.5	-3.5	-3.5	-3.5	-6.0	-6.0	-7.5	-7.5	-6.7		
1917	-5.3	-6.0	-5.0	-3.4	-1.6	0.4	2.0	2.0	1.5	0.5	0.4	-0.2	0.2	1.4	1.9	3.2	2.4	1.3	1.3	-0.1	-0.9	-3.9	-7.0	-7.8	-6.6		
1918	-9.8	-7.8	-6.7	-4.5	-1.1	1.8	2.2	1.8	1.1	0.6	1.2	1.8	1.4	2.2	3.8	3.8	3.2	0.7	0.7	-2.2	-5.1	-7.8	-9.1	-10.9	-10.2		
1919	-6.6	-6.8	-5.3	-2.4	1.4	1.5	1.2	-3.0	-7.3	-9.0	-6.8	-2.2	3.3	7.4	10.5	7.7	4.5	1.4	1.4	-2.3	-4.4	-5.7	-7.7	-10.7	-8.6		
1920	-6.4	-6.6	-6.2	-4.4	-1.1	1.5	1.6	1.1	-0.1	-1.1	-1.0	0.9	2.5	3.8	4.6	3.5	2.6	1.5	1.5	-0.9	-5.3	-6.7	-9.8	-10.4	-8.9		
1921	-2.8	-2.4	-3.2	-2.3	-1.8	0.3	1.5	1.0	1.2	1.4	2.2	2.4	2.9	3.6	3.1	2.4	1.6	-0.4	-3.6	-5.8	-6.4	-6.7	-6.6	-3.6	-4.7		
1922	-3.3	-3.6	-2.6	-2.2	-0.2	2.2	3.4	3.9	3.4	2.7	2.4	1.7	1.5	1.6	1.2	1.8	-0.6	-4.1	-4.1	-7.7	-9.7	-8.8	-7.2	-4.7	-4.7		
1923	-3.7	-2.5	-1.2	-1.0	0.4	1.3	1.2	1.0	0.9	0.4	0.8	1.2	1.7	1.2	1.5	1.4	0.2	-0.2	-0.2	-2.0	-4.0	-5.8	-6.8	-5.4	-5.4		
1924	-3.9	-3.2	-2.0	-0.9	-0.4	0.6	1.2	1.1	0.7	0.1	1.2	1.4	1.6	2.2	2.4	3.0	2.5	0.9	0.9	-1.1	-2.4	-4.9	-6.2	-4.7	-3.4		
1925	-4.2	-3.3	-2.0	-1.1	0.5	1.4	2.1	2.9	2.6	1.4	2.1	2.4	2.5	2.5	2.5	2.5	2.5	0.9	0.9	-1.0	-3.5	-5.6	-7.3	-4.7	-3.4		
1926	-7.7	-7.4	-4.9	-2.6	-0.1	2.2	4.2	3.7	2.6	1.0	1.0	1.4	1.3	0.9	1.1	1.0	1.2	-0.8	-0.8	-1.4	-4.1	-6.8	-7.1	-6.8	-7.5		
1927	-4.7	-3.6	-1.7	-0.8	-0.2	2.7	3.4	2.1	2.1	1.3	0.7	0.6	1.7	1.9	2.1	1.6	0.8	-0.4	-0.4	-3.0	-6.5	-6.8	-7.8	-7.4	-5.6		
1928	-5.5	-4.6	-4.2	-2.0	-0.2	0.7	2.3	1.4	0.2	-0.8	0.0	0.4	1.3	1.8	1.8	1.7	2.5	0.4	-1.4	-2.9	-6.3	-7.6	-8.9	-8.1	-8.1		
1929	-6.9	-5.3	-4.3	-3.0	0.1	2.2	2.9	2.1	0.8	0.2	0.8	0.1	0.3	0.8	1.0	-0.5	-1.0	-1.6	-1.6	-3.3	-6.0	-7.6	-10.6	-9.7	-8.4		
1930	-7.1	-5.9	-3.9	-2.6	0.8	2.9	4.6	5.4	4.0	1.5	1.2	1.6	2.1	0.6	0.8	0.1	-1.0	-1.4	-3.3	-3.3	-7.3	-8.1	-9.6	-8.5	-5.0		
1931	-3.3	-2.8	-2.2	-2.1	0.0	1.6	1.5	1.4	1.5	1.2	1.6	2.1	0.6	0.8	0.1	1.1	0.1	-1.6	-4.3	-7.5	-8.7	-9.6	-11.0	-7.9	-5.8		
1932	-3.9	-3.4	-2.9	-2.2	-0.2	1.7	3.4	3.2	1.9	0.9	0.6	0.5	0.2	1.1	1.1	1.8	1.1	0.7	-1.6	-5.0	-6.4	-8.3	-8.8	-7.0	-5.6		
1933	-3.5	-1.9	-2.3	-2.5	-0.2	2.8	3.5	2.7	0.7	-0.2	0.6	0.7	0.4	1.2	1.5	1.7	1.3	-0.8	-3.1	-4.9	-7.5	-7.5	-5.8	-3.0	-3.0		
1934	-2.1	-2.3	-3.2	-2.1	-1.3	1.6	3.2	2.9	2.3	1.4	1.0	1.3	1.8	1.8	1.5	1.7	1.7	0.4	-0.8	-3.1	-4.9	-7.5	-7.5	-5.8	-3.0		
1935	-6.4	-4.8	-4.9	-3.1	-1.2	1.1	2.3	2.1	2.9	2.3	2.2	2.6	2.4	1.9	1.6	1.6	0.4	-0.6	-1.8	-4.1	-4.7	-7.2	-8.7	-9.2	-7.9		
1936	-6.6	-6.0	-5.2	-4.0	-2.0	0.2	1.8	1.2	1.9	1.7	1.8	2.8	2.2	2.2	2.1	2.2	1.8	1.8	1.8	0.8	-2.2	-6.0	-7.6	-8.3	-7.2		
H - Component (in γ)																											
1916	-20	-17	-18	-11	-7	-4	-3	-1	-1	-1	0	4	6	8	8	8	10	6	4	2	0	-6	-10	-15	-12		
1917	-14	-13	-12	-8	-6	-4	-3	-2	-2	0	2	5	8	11	14	16	16	15	12	7	2	-4	-12	-12	-13		
1918	-29	-24	-19	-15	-8	-4	-4	-3	-2	-1	2	5	9	16	16	16	16	15	14	12	5	-6	-15	-21	-23		

D - Declination (in min)

H - Component (in γ)

1916	-20	-17	-18	-11	-7	-4	-3	-1	-1	-1	0	4	6	8	8	8	10	6	4	2	0	-6	-10	-15	-12
1917	-14	-13	-12	-8	-6	-4	-3	-2	-2	0	2	5	8	11	14	16	16	15	12	7	2	-4	-12	-13	-13
1918	-29	-24	-19	-15	-8	-4	-4	-3	-2	-1	2	5	9	16	16	16	16	15	14	12	5	-6	-15	-21	-23

0

F-TS-8974/V

Table 22
SD - Variations
Slutsk

Year	Hours																								Universal Time
	0	1	2	3	4	5	6	7	8	9	10	11	12	13	14	15	16	17	18	19	20	21	22	23	24
D - Declination (in min)																									
1923	1.1	0.0	-0.2	-1.1	-1.5	-1.5	-1.7	-1.4	-1.1	-1.4	-1.5	-1.1	-1.4	-1.6	-1.1	-1.1	-0.8	-0.2	0.9	1.3	2.9	2.5	3.1	2.5	2.9
1924	1.1	0.8	-0.2	-0.7	-1.5	-1.4	-1.9	-1.7	-1.4	-0.8	-0.3	-0.3	-0.8	-1.1	-1.6	-1.1	-1.4	-1.2	-0.2	1.3	1.8	3.4	1.7	2.5	2.9
1925	2.1	1.5	0.3	-0.3	-2.6	-3.0	-2.5	-2.2	-1.3	-1.7	-1.2	-1.1	-1.3	-1.0	-1.5	-0.9	-0.9	0.0	0.0	0.3	1.8	2.9	5.2	3.8	3.9
1926	4.1	3.4	3.1	0.7	-0.5	-2.1	-2.8	-2.5	-2.2	-1.3	-1.5	-1.1	-1.5	-2.0	-2.6	-2.4	-3.2	-1.6	0.0	0.4	1.9	2.6	4.8	3.6	3.5
1927	1.5	1.0	0.6	0.2	-2.8	-1.2	-1.3	-2.2	-1.4	-1.4	-1.9	-1.2	-0.8	-2.3	-1.9	-1.1	-1.6	-0.2	1.4	1.4	3.3	3.1	4.8	3.9	3.9
1928	2.2	0.7	1.7	0.2	0.0	-0.7	-0.6	-0.6	-1.2	-0.5	-0.8	-1.5	-1.8	-1.9	-2.6	-1.6	-1.7	-0.4	0.2	3.3	3.1	1.7	2.4	3.5	2.6
1929	1.0	-0.1	-1.7	-3.4	-3.8	-3.8	-3.5	-2.9	-2.1	-1.8	-0.9	-1.3	-1.6	-2.2	-0.8	1.5	2.1	3.6	4.0	4.1	3.1	1.7	2.4	3.2	3.5
1930	-0.7	-1.3	-1.5	-2.9	-3.1	-2.8	-2.2	-2.2	-1.5	-0.9	-1.3	-1.5	-0.5	-0.8	-0.8	1.5	2.1	3.6	4.0	4.1	4.3	4.3	3.1	2.5	2.5
1931	-0.1	-0.5	-1.2	-1.8	-2.4	-2.3	-2.3	-2.3	-1.2	-1.4	-0.9	-1.1	-1.3	-1.4	-0.3	1.5	2.0	2.9	2.9	3.6	3.5	2.8	2.3	0.6	0.6
1932	-0.4	-0.5	-1.1	-2.3	-2.5	-2.8	-2.4	-1.7	-1.3	-1.2	-1.2	-1.6	-1.5	-2.2	-0.7	1.5	1.2	3.4	4.0	3.3	2.6	2.5	1.0	0.9	0.9
1933	-0.2	-0.8	-0.8	-1.4	-2.2	-2.5	-2.6	-1.8	-1.1	-1.3	-0.7	-0.9	-1.0	-0.8	-0.3	0.5	1.6	3.2	3.8	3.1	3.9	2.9	1.4	0.9	0.9
1934	1.0	0.6	-0.2	-1.8	-2.2	-2.1	-1.7	-1.7	-1.6	-1.6	-1.6	-1.8	-1.7	-2.5	-2.3	0.2	1.5	2.0	3.6	3.6	2.4	1.9	1.4	1.1	1.1
1935	1.4	1.1	0.0	-0.9	-1.5	-1.3	-1.3	-1.4	-1.4	-1.5	-1.3	-2.1	-2.4	-3.0	-2.3	-1.0	-0.2	1.4	2.3	2.5	3.0	3.0	3.0	2.9	2.9
1936	1.8	0.1	-1.4	-2.4	-2.5	-2.7	-2.5	-2.0	-1.6	-1.6	-1.3	-1.3	-1.0	-3.6	-2.4	-2.3	0.6	1.8	2.3	3.7	4.6	5.0	5.6	5.3	4.1
1937	3.1	2.6	-0.8	-2.7	-2.3	-1.8	-1.3	-2.1	-1.9	-2.2	-2.1	-2.6	-3.7	-4.6	-3.1	-2.3	0.1	1.0	2.9	3.4	4.8	6.2	5.5	5.5	4.1
H - Component (in T)																									
1923	2	1	1	-1	-1	0	-1	-1	-3	-3	-2	-2	-3	-1	0	3	5	0	6	3	-1	0	1	1	1
1924	0	1	2	1	-5	-2	0	0	-2	-2	0	-3	-4	-1	0	2	2	3	2	5	1	-3	3	-2	0
1925	1	-2	3	2	-3	1	-1	-4	-5	-7	-2	-4	0	1	-3	3	6	5	6	3	2	0	-5	-2	0

1926	-18	-13	-13	-10	-12	-16	-16	-14	-9	-6	-1	-3	10	11	13	21	26	26	29	17	0	1	-13	-19
1927	-6	4	-1	-3	-12	-3	-2	-13	-10	-7	-6	-1	-4	6	8	15	10	12	4	-1	-5	-3	-8	-8
1928	-1	-4	-2	-7	-9	-2	-7	-12	-7	-7	-8	-5	-3	4	7	16	12	14	10	8	2	2	-6	-2
1929	-1	-1	-6	-8	-10	-9	-10	-9	-11	-4	0	2	8	11	12	20	16	14	7	2	-4	-3	-6	-9
1930	4	4	4	1	0	1	1	-2	-5	-5	-6	-4	-2	2	4	7	2	5	1	2	-3	-4	-6	-3
1931	1	0	-2	0	1	-5	-4	-3	-3	-7	-5	-6	-2	1	0	4	2	3	3	0	-3	-3	-6	-5
1932	2	2	0	-2	-1	-3	-2	-1	2	0	-1	-2	-3	0	-1	4	5	1	2	2	1	-5	-4	-4
1933	-4	-3	-3	-3	-3	-7	-7	-6	-8	-9	-8	-10	-11	-11	-9	-7	-6	-7	-13	-11	-10	-11	-10	-10
1934	5	5	5	4	3	2	0	-5	-5	-3	2	0	2	2	5	2	3	0	-2	-6	-5	-7	-3	-7
1935	5	5	4	0	-1	-4	-7	-6	-4	-2	0	3	8	8	8	5	1	0	-3	-4	-5	-10	-8	-8
1936	-14	-5	-3	1	2	-5	-5	-3	1	5	8	15	24	32	30	32	24	10	-5	-9	-23	-42	-42	-29
1937	2	-4	-3	-7	-3	-10	-14	-10	-4	1	6	13	28	37	45	42	27	11	3	-15	-34	-43	-29	-29

Z-Component (int)

1923	-18	-16	-13	-15	-13	-19	-7	-3	0	1	3	5	6	9	13	15	18	20	15	11	3	-2	-8	-17
1924	-12	-14	-16	-16	-13	-13	-9	-7	-4	-1	2	4	7	8	13	16	19	18	15	13	7	1	-6	-12
1925	-20	-25	-22	-20	-18	-18	-11	-7	-3	1	3	7	10	15	17	19	22	24	23	16	9	0	-9	-17
1926	-34	-34	-50	-43	-34	-23	-18	-11	-5	2	9	16	19	23	33	38	44	41	39	26	15	-8	-18	-30
1927	-22	-23	-23	-24	-26	-17	-12	-11	-7	-3	2	7	13	21	28	35	35	34	26	14	0	-10	-16	-20
1928	-27	-28	-29	-25	-25	-18	-13	-9	-5	-3	2	7	10	15	20	28	27	27	25	11	0	-6	-13	-18
1929																								
1930																								
1931																								
1932	-27	-29	-26	-20	-13	-8	-3	0	4	8	13	16	21	28	32	32	34	24	12	1	-13	-23	-31	-30
1933	-19	-18	-16	-16	-13	-9	-5	-2	2	4	7	9	15	21	30	35	30	21	11	-6	-16	-23	-24	-28
1934	-16	-15	-12	-10	-8	-7	-5	-4	-1	1	3	6	11	17	19	24	22	17	7	-2	-6	-11	-16	-19
1935	-21	-21	-20	-17	13	-10	-6	-6	-1	3	7	13	18	24	31	31	28	20	11	3	-7	-16	-26	-27
1936	-26	-25	-23	-20	-18	-12	-7	-2	2	6	8	15	22	30	35	34	26	20	12	1	-8	-17	-22	-24
1937																								
1938	-49	-49	-46	-39	-28	-20	-11	-7	1	13	17	26	40	49	59	62	56	48	21	6	-24	-38	-45	-30
1939	-50	-50	-49	-43	-32	-20	-12	-3	3	13	22	31	44	59	66	62	56	40	18	-8	-20	-37	-50	-47

F-TS-8974/V

Table 23
SD - Variations
Huancayo

		Universal Time																								
		Hours																								
Year		0	1	2	3	4	5	6	7	8	9	10	11	12	13	14	15	16	17	18	19	20	21	22	23	24
1922	D - Declinations(in tenth of a minute)	-2	-1	-1	-1	-1	-1	-1	-1	-1	-1	-1	-1	-1	-1	-1	-1	-1	-1	-1	-1	-1	-1	-1	-1	-1
1923		-1	-1	-1	-1	-1	-1	-1	-1	-1	-1	-1	-1	-1	-1	-1	-1	-1	-1	-1	-1	-1	-1	-1	-1	-1
1924		-1	-1	-1	-1	-1	-1	-1	-1	-1	-1	-1	-1	-1	-1	-1	-1	-1	-1	-1	-1	-1	-1	-1	-1	-1
1925		-1	-1	-1	-1	-1	-1	-1	-1	-1	-1	-1	-1	-1	-1	-1	-1	-1	-1	-1	-1	-1	-1	-1	-1	-1
1926		-1	-1	-1	-1	-1	-1	-1	-1	-1	-1	-1	-1	-1	-1	-1	-1	-1	-1	-1	-1	-1	-1	-1	-1	-1
1927		-1	-1	-1	-1	-1	-1	-1	-1	-1	-1	-1	-1	-1	-1	-1	-1	-1	-1	-1	-1	-1	-1	-1	-1	-1
1928		-1	-1	-1	-1	-1	-1	-1	-1	-1	-1	-1	-1	-1	-1	-1	-1	-1	-1	-1	-1	-1	-1	-1	-1	-1
1929		-1	-1	-1	-1	-1	-1	-1	-1	-1	-1	-1	-1	-1	-1	-1	-1	-1	-1	-1	-1	-1	-1	-1	-1	-1
1930		-1	-1	-1	-1	-1	-1	-1	-1	-1	-1	-1	-1	-1	-1	-1	-1	-1	-1	-1	-1	-1	-1	-1	-1	-1
1931		-1	-1	-1	-1	-1	-1	-1	-1	-1	-1	-1	-1	-1	-1	-1	-1	-1	-1	-1	-1	-1	-1	-1	-1	-1
1932		-1	-1	-1	-1	-1	-1	-1	-1	-1	-1	-1	-1	-1	-1	-1	-1	-1	-1	-1	-1	-1	-1	-1	-1	-1
1933		-1	-1	-1	-1	-1	-1	-1	-1	-1	-1	-1	-1	-1	-1	-1	-1	-1	-1	-1	-1	-1	-1	-1	-1	-1
1934		-1	-1	-1	-1	-1	-1	-1	-1	-1	-1	-1	-1	-1	-1	-1	-1	-1	-1	-1	-1	-1	-1	-1	-1	-1
1935		-1	-1	-1	-1	-1	-1	-1	-1	-1	-1	-1	-1	-1	-1	-1	-1	-1	-1	-1	-1	-1	-1	-1	-1	-1
1936		-1	-1	-1	-1	-1	-1	-1	-1	-1	-1	-1	-1	-1	-1	-1	-1	-1	-1	-1	-1	-1	-1	-1	-1	-1
1937		-1	-1	-1	-1	-1	-1	-1	-1	-1	-1	-1	-1	-1	-1	-1	-1	-1	-1	-1	-1	-1	-1	-1	-1	-1
1938		-1	-1	-1	-1	-1	-1	-1	-1	-1	-1	-1	-1	-1	-1	-1	-1	-1	-1	-1	-1	-1	-1	-1	-1	-1
1939		-1	-1	-1	-1	-1	-1	-1	-1	-1	-1	-1	-1	-1	-1	-1	-1	-1	-1	-1	-1	-1	-1	-1	-1	-1
1940		-1	-1	-1	-1	-1	-1	-1	-1	-1	-1	-1	-1	-1	-1	-1	-1	-1	-1	-1	-1	-1	-1	-1	-1	-1
1941		-1	-1	-1	-1	-1	-1	-1	-1	-1	-1	-1	-1	-1	-1	-1	-1	-1	-1	-1	-1	-1	-1	-1	-1	-1
1942		-1	-1	-1	-1	-1	-1	-1	-1	-1	-1	-1	-1	-1	-1	-1	-1	-1	-1	-1	-1	-1	-1	-1	-1	-1
1943		-1	-1	-1	-1	-1	-1	-1	-1	-1	-1	-1	-1	-1	-1	-1	-1	-1	-1	-1	-1	-1	-1	-1	-1	-1
1944		-1	-1	-1	-1	-1	-1	-1	-1	-1	-1	-1	-1	-1	-1	-1	-1	-1	-1	-1	-1	-1	-1	-1	-1	-1
1922	H - Component (in γ)	8	7	3	6	6	6	6	6	6	6	6	6	6	6	6	6	6	6	6	6	6	6	6	6	6
1923		0	3	5	7	8	8	8	8	8	8	8	8	8	8	8	8	8	8	8	8	8	8	8	8	8
1924		1	5	6	6	6	6	6	6	6	6	6	6	6	6	6	6	6	6	6	6	6	6	6	6	6
1925		4	4	4	4	4	4	4	4	4	4	4	4	4	4	4	4	4	4	4	4	4	4	4	4	4

1926	2	9	4	1	8	3	4	2	4	1	1	6	2	3	6	1	1	1	3	4	1	2	1	4	1	3	8	1	8	4	16	4	9	6
1927	1	1	1	1	1	1	1	1	1	1	1	1	1	1	1	1	1	1	1	1	1	1	1	1	1	1	1	1	1	1	1	1	1	
1928	8	2	3	4	4	1	1	0	1	3	5	10	6	3	8	3	4	5																
1929	9	3	2	4	3	5	4	1	3	5	6	15	2	5	0	1	3	6	3															
1930	13	1	5	7	6	3	8	1	3	7	6	17	6	5	1	2	1	2																
1931	24	0	7	10	24	7	8	6	3	7	6	13	7	4	3	0	3	1																
1932	11	5	9	5	3	11	5	1	9	4	14	14	7	4	3	0	3	1																
1933	11	3	9	10	11	12	7	4	6	6	14	13	10	10	5	4																		
1934	12	0	9	18	12	12	7	4	3	6	14	13	10	10	5	4																		
1935	15	4	7	18	10	12	7	4	3	6	14	13	10	10	5	4																		
1936	16	1	1	13	6	9	7	6	5	6	4	5	5	6	10	13	11	11																
1937	5	10	1	1	8	5	5	5	4	5	8	5	5	12	13	22	14	9	13															
1938	12	20	9	4	10	6	3	3	3	1	14	1	17	15	17	14	5	16																
1939	12	14	0	10	1	12	4	0	6	3	2	0	4	1	15	2	2	3																
1940	18	12	3	11	5	7	0	2	6	1	6	5	12	1	9	1	1																	
1941	19	1	8	9	2	5	6	1	7	9	7	13	0	2	7	1	1																	
1942	14	5	4	13	2	7	3	9	1	5	10	16	8	1	10	0	9																	
1943	14	7	2	13	7	11	5	9	5	8	9	11	12	16	5	10	6	9																
1944	14	11	10	12	10	6	9	7	9	8	5	9	13	24	13	12	9	10																

Z-Component (in T)

1922	0	0	0	1	2	9	1	0	0	1	0	0	0	1	0	0	2	2	1	2	8												
1923	0	0	0	1	2	9	1	0	0	0	1	0	0	1	0	0	2	2	1	1	0												
1924	0	1	1	1	0	1	0	0	1	1	0	0	0	0	2	2	1	0															
1925	1	1	1	1	0	0	2	1	1	0	0	1	0	0	1	0	0	2	2	1													
1926	0	0	0	0	1	0	1	1	0	1	1	0	1	1	0	9	1	2	1	1	1												
1927	0	0	1	0	0	0	1	1	0	1	1	0	1	0	1	0	2	2	1	0													
1928	1	1	1	1	0	0	2	1	1	0	0	1	0	0	1	0	0	2	2	1													
1929	0	0	0	0	1	0	1	1	0	1	1	0	1	1	0	1	0	2	1	0													
1930	1	0	1	0	2	0	2	0	2	0	2	0	2	0	1	2	2	2	1	0	1												
1931	3	1	2	1	2	0	3	2	3	2	3	1	3	3	1	4	3	3	1	2	2												
1932	2	1	3	0	2	3	3	5	3	1	4	3	3	1	4	3	3	0	1	4	2												
1933	1	2	2	0	3	0	2	7	3	2	3	4	2	4	0	2	4	1	1	2	4												
1934	1	3	1	0	3	2	1	6	2	1	2	2	1	4	1	0	2	0	2	4	2												
1935	0	2	0	2	3	2	1	4	1	0	2	3	0	1	0	1	3	3	0	2	1												
1936	1	0	0	4	2	2	1	2	1	1	1	2	1	0	1	2	1	6	4	3	0	0											
1937	2	0	2	3	0	0	1	1	1	0	4	0	3	2	0	4	2	7	5	0	1												
1938	3	1	3	3	0	4	2	4	0	4	0	3	0	5	5	8	5	4	2	3	3												
1939	3	1	2	3	4	1	3	4	3	1	5	2	2	3	2	7	4	6	5	4	2	4											
1940	1	1	1	3	2	1	1	3	3	1	3	2	0	2	3	3	2	1	2	1	2												
1941	1	0	2	0	3	1	0	2	3	1	2	1	1	1	1	1	1	0	0	1	1												
1942	1	0	1	0	2	0	0	1	2	1	2	1	0	1	0	1	1	1	2	1	1												
1943	1	0	1	0	2	0	0	1	1	0	1	1	1	0	0	1	0	2	2	1	0												
1944	0	0	1	1	2	0	2	1	1	0	1	1	0	0	0	0	1	2	2	0	1												

the march I_{SD}^1 is completely parallel to the march of R_H at Huancayo. It follows that S_D depends almost completely on the value of X and depends little on the extension of the eddy along the meridian. Consequently, the error of $\pm 4^\circ$ which may possibly have been made in estimating the position of the center of the eddy will distort the value of I_{SD}^1 only slightly.

Table 24

a)	b)	c)	d)	e)	f)	g)	h)	i)	j)	W	S_H
	R_Z	R_Z	R_Z	R_Z	R_Z	R_Z	R_Z	R_H			
1916							28			56	
1917							28			104	
1918							43			80	
1919	20						48		1,2	64	23,2
1920	18						30		1,1	38	15,8
1921	20						18		1,0	26	12,4
1922	18						20	16	0,7	14	14,2
1923	14		35	75			10	15	0,6	6	12,4
1924	12		30	72			7	11	0,7	26	15,0
1925	15		50	98			15	8	0,8	44	14,4
1926	22		100	125			45	24	1,2	64	19,6
1927	24		60	120			30	26	1,0	70	22,2
1928	19		65	125			30	15	1,0	78	23,0
1929	24			155			35	25	1,0	65	19,5
1930	32			240	200		50	15	1,0	36	14,8
1931	16			120	130		23	18	0,7	21	14,0
1932	17		60	115	160	15	20	11	0,7	11	14,4
1933	18		57	110	140	13	18	9	0,7	6	13,2
1934	15		40	80	100	5	13	12	0,7	8	16,8
1935	21		58	110	135	20	20	9	0,8	36	15,0
1936	22	22	60	117	130	30	20	24	0,9	80	18,0
1937	23	24			112	50		19	1,4	114	25,4
1938	31	38	105			77		21	1,4	110	23,6
1939	32	40	110			95		18	1,3	89	24,2
1940	27	47				77		24	1,3	68	18,4
1941	30	49				85		19	1,2	46	20,0
1942	21	26				35		24	0,9	27	17,0
1943	26	28				30		22	0,9	15	18,4
1944	20	22				20			0,8	10	16,1
1945		20				15			0,9	35	
1946		52							1,4	92	
1947									1,4	152	
1948										136	

a) Year; b) Watheroo; c) Paris; d) Slutsk; e) Sitka; f) Tromso; g) Lovo;
h) Dombas; i) Huancayo; j) u-Measure

The following features must be noted in the march of I_{SD}^1 (cf. Fig. 34):

1. The values of I_{SD}^1 vary by a factor of almost 3 from the year of maximum ac-

tivity to the year of minimum activity (3.8 in 1925 and 11.0 in 1927 and 1943).

2. After 1938 the values of $I_{S_D}^1$ continue to rise almost monotone, reaching very high values in the years of the minimum (1943 and 1944). Since material for only two cycles is available to us, it is difficult to give an explanation for this phenomenon.

3. In some years (years of high solar activity: 1927, 1928, 1937) the center of the eddy splits into two parts, that is two maxima are found in the S_D at Huancayo. The secondary maxima are marked by dots on Fig.34.

4. The agreement between the cyclical variations of $I_{D_{st}}$ and $I_{S_D}^1$ is small. Thus, for example, the sharp drop in $I_{S_D}^1$ in 1928 corresponds to a smooth march of $I_{D_{st}}^1$, and, on the other hand, the maximum of $I_{D_{st}}^1$ in 1930 corresponds to a minimum in $I_{S_D}^1$. The fluctuations $I_{S_D}^1$ are less regular than the fluctuations of $I_{D_{st}}$; the latter follow the cyclical variations of W considerably more closely. The march of $I_{S_D}^1$ displays no tendency to a lag in the time of the maxima with respect to W , and, on the other hand, a certain lag of the epochs of the minimum does appear. The relatively poor correspondence between $I_{D_{st}}^1$ and $I_{S_D}^1$ becomes particularly interesting if we bear in mind the fact that the intensity in both systems of current is calculated from one and the same empirical data of the X component at Huancayo Observatory. This poor correspondence, it seems to us, is one of the indications of the different nature of these two current systems, the D_{st} currents being more directly correlated with the intensity of solar activity, while the S_D currents may possibly be affected by other factors as well.

Section 3. The 11-Year Variation of the Polar Part of the S_D Currents

For studying the fluctuations of the polar eddies, the S_D variations of the observatories at Dombas, Lovo, Sitka, Godhavn, Sodankyla and other Arctic Observatories were calculated by me. The fluctuations of S_D at the polar observatories from year to year are considerably greater than at the middle-latitude observatories. The cyclical variations of the amplitude of S_D reach their maximum value in the im-

mediate vicinity of the auroral zone (observatories at Tromso, Sitka, etc). At the observatories with the circumpolar type of variations (Godhavn, and, in part, Tikhaya Bay) the variation of the amplitude is again considerably smaller. Since all the above enumerated observatories are far from the centers of the current eddies, the S_D variations of the horizontal component are of the same type as to form in all years, and differ only in amplitude. A change in form is observed in the S_D of the observatories located beneath the zone of the hypothetical linear current: Sodankyla, Matochkin Shar, Dickson. In the Second International Polar Year, a transitional type of Z variations was observed at these observatories: at Sodankyla, it was close to the middle-latitude type, while at Matochkin Shar and Dickson it was close to the polar type. This indicates that the zone of linear current, (or of strong concentration of surface currents) must pass to the north of Sodankyla and to the south of Matochkin Shar and Dickson. In years of high activity, the S_D variations of Z at all three observatories take on a distinctly polar form, which confirms the well known fact of the descent of the zone to lower latitudes with the growth of activity.

To obtain the numerical data on the location of the zone and the intensity of the current in different years of the 11-year cycle, I calculated the value of I and ϕ_0 , using the formulas for the linear current (cf. Chapter V), from the data of few observatories, assuming that the height of the current during the entire 11-year cycle did not substantially vary from that of 1933. The replacement of the surface system of currents by linear system as we have seen in Chapter V, allows a rather good estimate to be made of the position of the auroral zone. The assumption of the invariability of h does not of course correspond to the actual behavior of the heights of the ionospheric layers, and this produces a certain element of the arbitrary in my results. But whatever scanty information on the 11-year fluctuation of the height of the F_2 layer in the polar latitudes is today available indicates that these fluctuations are not large. The calculations made separately for the morning and evening hours (cf. Table 25) show that the latitude of the zone and the intensity

Table 25

Year	Time of Day	Sitka		Dombas	
		Φ_0°	$I \times 10^4 \text{ A}$	Φ_0°	$I \times 10^4 \text{ A}$
1920	a)			66,4	-9
	b)			68,2	5
1921	a)			67,1	-7
	b)			70,3	6
1922	a)			68,5	-10
	b)			67,8	6
1923	a)	67,4	-18	68,5	-5
	b)	65,7	16	69,6	3
1924	a)	66,8	-16	68,9	-5
	b)	65,2	13	71,5	11
1925	a)	66,0	-19	67,1	-6
	b)	65,2	18	68,2	4
1926	a)	62,7	-19	65,3	-9
	b)	62,2	19	65,3	6
1927	a)	62,7	-19	66,4	-7
	b)	62,2	17	64,6	4
1928	a)	63,5	-23	66,7	-9
	b)	63,0	16	66,0	6
1929	a)	64,6	-28	65,6	-8
	b)	63,8	24	66,4	7
1930	a)	63,3	-42	65,3	-10
	b)	63,2	31	65,7	7
1931	a)	67,2	-32	69,7	-11
	b)	63,2	24	68,9	5
1932	a)	64,6	-23	67,8	-10
	b)	64,6	19	68,9	5
1933	a)	65,7	-23	68,2	-9
	b)	65,4	20	68,6	5
1934	a)	69,8	-28	69,3	-7
	b)	66,2	18	68,9	4
1935	a)	68,0	-65	69,0	-8
	b)	64,6	17	66,4	4
1936	a)	62,7	-20	69,0	-10
	b)	62,7	15	66,8	5

Year	Time of Day	Chelyuskin		Dickson		Matochkin Shar		Uellen	
		Φ_0°	$I \times 10^4 \text{ A}$	Φ_0°	$I \times 10^4 \text{ A}$	Φ_0°	$I \times 10^4 \text{ A}$	Φ_0°	$I \times 10^4 \text{ A}$
1933	a)			61,0	-30	61,9	-33		
	b)			62,9	17	64,1	18		
1934	a)			60,2	-27	61,8	-26		
	b)			62,1	17	64,3	13		
1935	a)	45,5	-100	60,8	-34			64,6	-21
	b)	59,5	44	61,9	22			64,0	15
1936	a)	51,4	-121	60,4	-32			65,0	-19
	b)	59,1	55	61,8	22			63,4	15
1937	a)			60,1	-39	61,5	-42	62,6	-19
	b)			60,9	30	62,7	31	62,7	16
1938	a)			59,1	-55	59,6	-72	62,3	-27
	b)			59,3	48	59,6	76	62,1	23
1939	a)	56,7	-79	59,7	-46	59,5	-39	62,6	-31
	b)			59,3	53	59,8	50	62,0	19
1940	a)	49,7	-123	60,7	-43	60,3	-45	63,0	-26
	b)	47,4	150	60,6	34	61,5	41	62,9	19
1941	a)	54,3	-106	59,3	-50	55,6	-65	62,3	-17
	b)			59,9	36	61,4	29	62,6	17
1942	a)	54,6	-76	60,3	-37			64,6	-29
	b)	52,8	78	60,9	26			63,6	18
1943	a)	56,1	-96	59,0	-45			64,2	-22
	b)	49,6	-148	60,5	33			63,0	25
1944	a)	56,7	-61						
	b)	46,4	124						

a) morning b) evening

of the current vary about equally in the two halves of the day during the course of these years. No systematic difference whatever was found in the cyclical variations of I or ϕ_0 at various times of the day, as should have been the case if the morning and evening disturbance were due to different solar agents (cf. Chapter I).

In view of the fact that the fluctuations of the parameters of the current, from the data of observatories located south of the auroral zone, lead to similar results for all those stations, Fig. 34 gives the mean values for I and ϕ_0 of the morning and evening hours at the Sitka Observatory for 1920 - 1926 and the Uellen Observatory for 1933 - 1943.* The southward shift of the auroral zone was distinctly manifested during the course of both maxima: this shift amounted to 4.5° in the 1923 - 1933 cycle, and to 3.5° in the 1933 - 1944 cycle. But the return to the high latitudes after the 1938 maximum was not immediate. In 1943, already characterized by low values of the solar activity, the position of the zone was only slightly north of its 1937 position. There is a strikingly good correlation between the position of the zone and the intensity of the zonal current, which is notable not merely in the general tendency of the variations during the 11-year cycle, but also in the oscillations in individual years (for example, the increase of ϕ_0 and the decrease of I in 1940, in 1942, etc). The absence of parallelism between the 11-year fluctuations of the intensity of the current in the polar zone and the middle latitude current eddy indicates that possibly the mechanisms exciting them may be somewhat different. The curve of annual values of the intensity of the polar currents would appear to display two maxima each in the course of an 11-year cycle, of which one is located on the branch of rising activity, and the other on the branch of falling activity (cf. years 1930, 1935, 1938, 1939).

The variations, with the solar cycle, of the position and intensity of the polar current, according to the data of observatories situated in the zone itself or

* The absolute values of I and ϕ_0 , as already stated in Chapter V, differ somewhat between the different observatories.

north of it, are less regular. Thus, for example, according to the data of the Dickson Observatory, the southern position of the zone connected with the maximum of 1938 was maintained until 1943 inclusive. The fluctuations of the position of the zone, from the data of the Matochkin Shar and Chelyuskin Observatories, according to the extremely fragmentary information represented by the data of Table 25, appear to be entirely random. The intensity of the polar current, according to the Chelyuskin data had maxima in 1940 and 1943, but according to the Matochkin Shar data, in 1937. It is possible that the results obtained may be interpreted as follows: during the 11-year cycle the width of the auroral zone varies. Its southern boundary is regularly shifted southward in the years of high magnetic activity and northward in the years of low activity. The northern edge of the zone is either little shifted at all during the 11-year cycle or is shifted according to certain peculiar and still imperfectly elucidated laws of its own. These facts are in good agreement with the view of auroral investigators to the effect that the cyclical fluctuations of the auroral frequency in the zone and in the polar cap are different from those at lower latitudes. Thus Vegard denies any existence whatever of a regular cyclical behavior in the auroral frequency. Tromhold indicates a cyclical march inverse to the march of solar activity. On the polar cap, the 11-year oscillations have 2 maxima each (on the branches of falling and rising activity), and in the zone itself the 11-year march has a transitional form. Pushkov and Brunkovskaya (Bibl.28) have found that the southward displacement of the auroral zone on days with elevated magnetic activity does not involve the weakening of the auroral displays to the north of the zone, which once again indicates the possible expansion of the zone with increasing activity.

The question as to the position of the zone of linear current and of its fluctuations in the 11-year cycle is of great importance in calculating the working frequencies of radio waves over routes passing through high latitudes, since this zone is at the same time the zone of maximum absorption. In view of this fact it appears

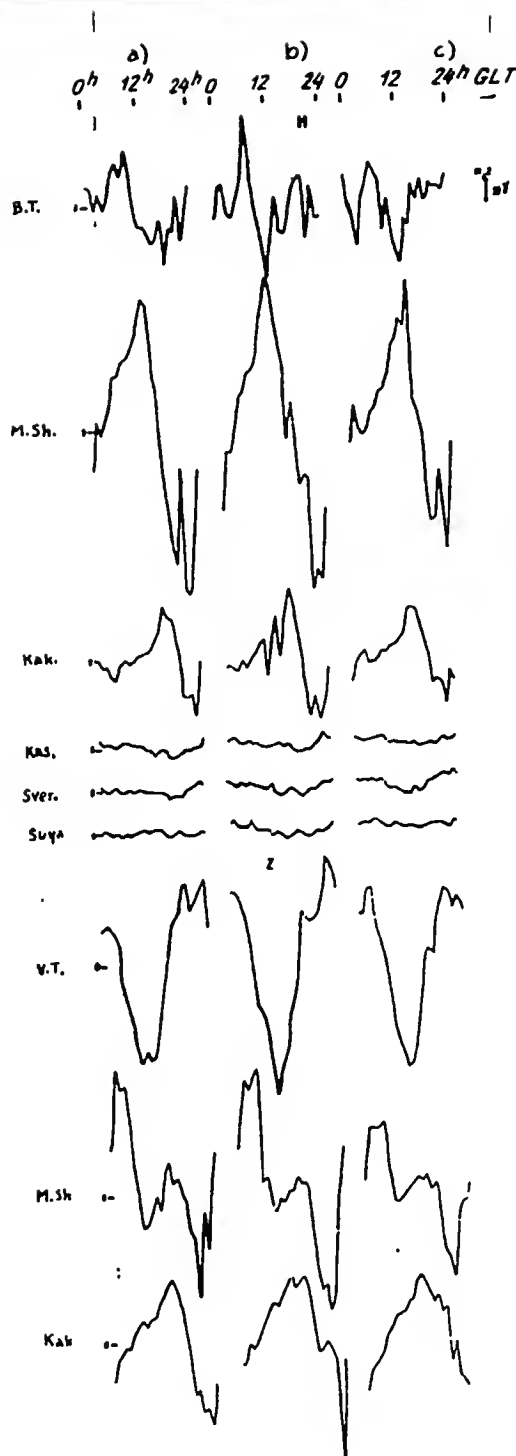


Fig.37 - The S_D Variation of the H and Z Components of the Magnetic Field in 1932 - 1933 from USSR Observatories
a) Winter; b) Equinox; c) Summer

to be necessary to continue the accumulation of material on magnetic disturbances and their auroral displays, which will help to pinpoint the position of the zone.

The material on the S_D variations considered by us allow us to draw two conclusions: first, that the study of the S_D variations can yield useful information on the diurnal march, on the 11-year fluctuations, and on other peculiarities of the zone, and second, that the presently available data from observatories situated inside the zone are insufficient for the formulation of any reliable picture of the displacement of the northern edge of the zone.

Section 4. Seasonal Variations of the S_D Currents

Let us now consider the seasonal variations of the current systems of the S_D variations. The literature summaries of the S_D variations (Bibl.4, 6, 61) show that the seasonal variations of the S_D of all three elements are small, especially in the middle and low latitudes. As in the case of the 11-year fluctuations, the character of the variation of the components with the seasons is completely de-

terminated by the position of the observatory with respect to the current eddies. At observatories far from both the centers of the eddies and the zone of linear current, the seasonal variations reduce, on the whole, to an increase or decrease of the amplitudes. Observatories near the centers of the eddies often note an inversion of the the phase of X , while observatories located in the neighborhood of the polar current note an inversion of the phase of Z . Figure 37 gives the S_D variations of a few observatories for the Second International Polar Year, which give a clear idea of the seasonal variations characteristic for different types of S_D . The amplitude of the variations is greatest at all latitudes in the epochs of the equinox and is smallest in the winter period. Their position of the centers of the middle-latitude eddies does not remain constant throughout the year, descending southward in the summer months and ascending northward in the winter. From the S_D variations of the horizontal component at Zuy Observatory, at the latitude of which the centers of the eddies were located during the Second International Polar Year, it is clear that in summer the middle-latitude type of S_D is observed, while in winter the type observed is low-latitude. In the equinox, when the lines of centers occupy an intermediate position, the S_D at Zuy are of transitional type with very small and irregular oscillations during the course of the day.

At observatories close to the auroral zone (Dickson, Matochkin Shar) the middle-latitude type of S_D variations is observed in summer and the high latitude type in the equinox (cf. the $S_D Z$ components) while in the winter the $S_D Z$ components have a characteristically transitional form. This indicates that the fluctuations of the auroral zone are similar to the fluctuations of the line of centers, more specifically, that zone occupies an intermediate position in winter, descending to the south in the equinox and ascending to the north in the summer months. The position of the line of centers of the middle-latitude eddies and of the auroral zone, calculated from the data of the whole net of observatories, is shown in Fig. 38a. The broken lines in the sector 180 to 270° denote the absence of data for these longitudes.

The intensity of the middle-latitude eddies (I) and of the high-latitude eddies (II) (in amperes), calculated by approximate formulas for the surface current, are given in Table 26.

Table 26

	a)		1938-1939	
	I	II	I	II
b)	3	12	4	16
c)	5	18	7	26
d)	4	16	5	21
e)	4	15	5	21

Note. The values in Table 26 are given in 10^4 amp.

a) Second International Polar Year; b) Winter; c) Equinox;
d) Summer; e) Year

The seasonal fluctuations differ in years of different solar activity: in the years of high activity they are considerably sharper. Figure 38b gives the position of the line of centers and of the polar zone for 1938 - 1939. The character of the displacement of the line of centers and of the zone remains the same as in the years of the minimum, but the value of the shift is considerably greater. It will be seen from Table 26 that in the year of the maximum the seasonal fluctuations of the intensity of the currents likewise increased.

Summarizing all that has been said in the present Chapter, the following conclusions may be drawn: the seasonal and 11-year fluctuations of the D_{st} and S_D variations, which differ in character and amplitude at different observatories and for different elements, find their explanation in the changes undergone by the systems of electric currents responsible for these variations. The 11-year fluctuations of the D_{st} currents follow the 11-year cycle of solar activity most closely of all,

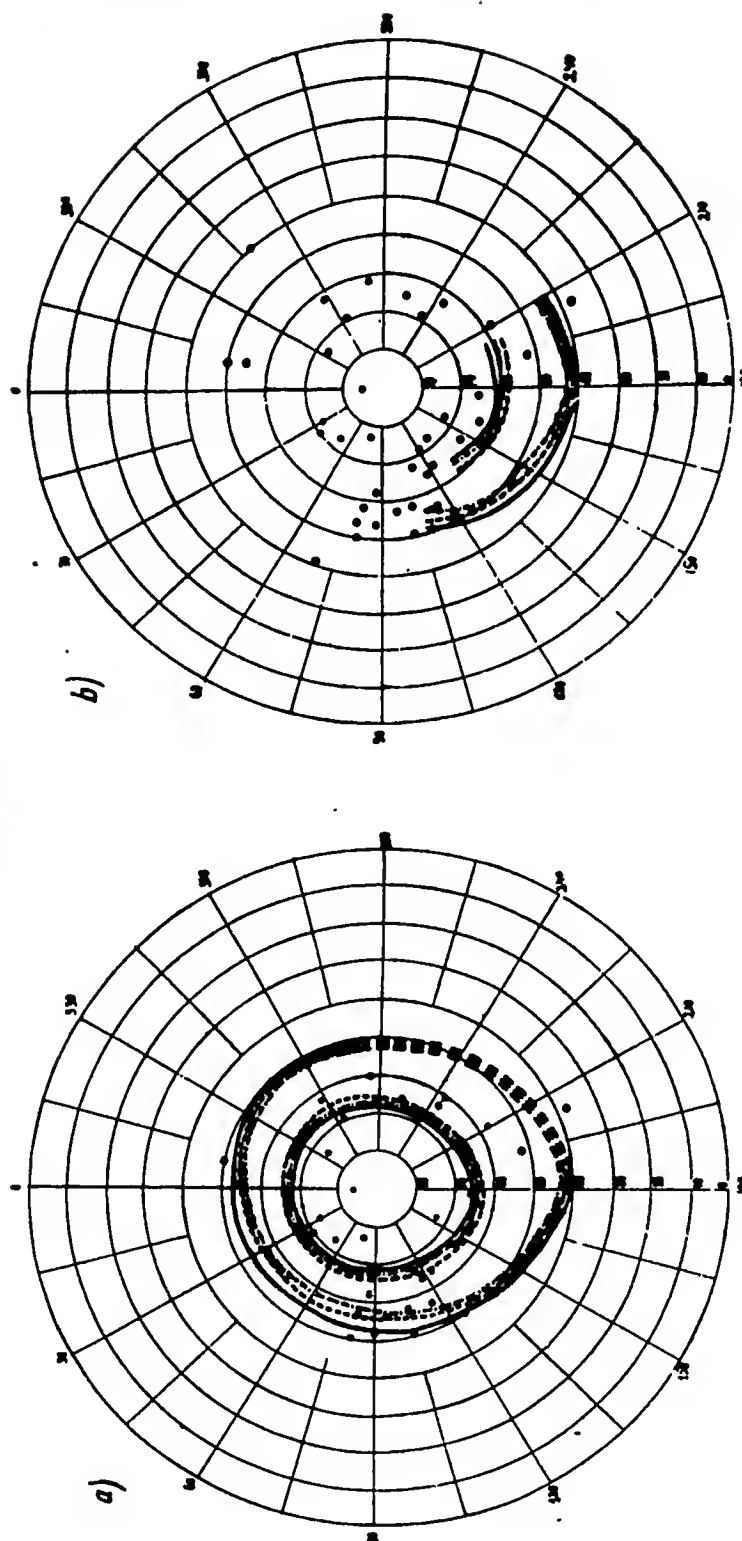


Fig.38 - Position of Auroral Zone and Lines of Centers of Middle-Latitude Eddies

(a - 1932 - 1933; b - 1938 - 1939; - - - Equinox, ——— Summer; -.-.- Winter.

The Points Mark the Position of the Magnetic Observatories. The Coordinate Net

Used is Geomagnetic)

with the lag that is characteristic for geophysical phenomena due to corpuscular radiation. The seasonal march of D_{st} has the pronounced equinoctial maxima which likewise confirm the corpuscular nature of the phenomenon, amplitude and also have an annual march of small amplitude with extreme values at the epoch of the solstices. This second annual wave likewise may be explained within the frame of the corpuscular theory, if we bear in mind that it is not only the heliographic latitude of the earth that varies during the course of the year (Corti effect) but also the angle between the magnetic axis of the earth and the line sun-earth. As stated by Bartels, the variation of this angle during the course of the year changes the direction and magnitude of the field on which the charged particles coming from the sun impinge and, Consequently, also modifies the conditions of the course of the disturbances. The 11-year and seasonal variations of the currents of the S_D variations are much more complex. The correlation between the 11-year fluctuations of solar activity and the intensity of the S_D currents is not so close, and is different for the middle-latitude and polar currents. It would seem that the fluctuations of the S_D currents are not due only to fluctuations in the intensity of the corpuscular radiation, but also to the condition of the upper layers of the atmosphere. This latter differs in different latitudes, depends on the solar radiation of both types (photon and corpuscular), and obeys its own more complex regularities.

CHAPTER VIII

MORPHOLOGY OF THE DISTURBED IONOSPHERE AND THE CURRENT SYSTEMS
OF MAGNETIC STORMSSection 1. Ionospheric Disturbances

In the preceding Chapters we have described the calculation of the electric currents corresponding to the external part of the field of magnetic storms, and we have discussed the properties and peculiarities of these currents. But since we used only geomagnetic data in studying these currents, many questions still remained obscure: the distance of these currents from the surface of the earth, the actual physical conditions in the medium in which, as we postulate, the currents are located; whether the current layer can be identified with one ionospheric layer or another; and so on. We have seen in Chapter I that the discussion of these questions in the literature is only beginning. In order to give answers, though only provisional ones, to these questions, it is necessary to formulate an idea as to the variations that take place in the ionosphere during the time of magnetic disturbances. In the present Section we shall briefly set forth certain information of the morphology of ionospheric disturbances, taken from literature sources, and other data obtained as a result of the work up of the data from a number of ionospheric stations.

The first investigators of ionospheric disturbances were Bulatov, Berkner and Wells and Seaton (Bibl.3, 40) whose works give a detailed description of magnetic storms from observations at Tomsk, and in South America and Great Britain. The au-

thors noted the basic features of the behavior of the disturbed ionosphere: the lowering of the critical frequencies of the F_2 layer and the increase in its heights, the appearance of a sporadic layer at the level of the E layer, the fused and scattered reflections, indicating the inhomogeneous, cloudlike structure of the ionosphere, and the increase of absorption. These features were further confirmed by a number of works of Soviet and foreign authors, and a description of them may be found in modern surveys of ionospheric physics (Bibl.1, 2). One of the latest works devoted to the description of the individual disturbances is the paper by Burkhard (Bibl. 39) on the magnetic ionospheric storm of 15 March 1948. The data of about 30 ionospheric observatories were available to Burkhard, who calculated the value for each observatory of $\Delta = \frac{f^{0z} - f_n^{0z}}{f_n^z}$ where f^0 = critical frequency of F_2 layer on day of storm and f_n^0 = corresponding value for a normal day. The latitudinal distribution of Δ discloses obviously decreased values of $f_{F_2}^0$ in the high latitudes and increased values in latitudes near the equator. The dispersion of values is relatively small, which forces us to accept, without doubt, the relation found. A work by Yu. D.Kalinin (Bibl.22) is also devoted to the morphology of an ionospheric disturbance. To elucidate the regularities of the behavior of the ionospheric layers, he used statistical methods common to the methods used in geomagnetism. He studied the D_{st} and S_D variations of the critical frequencies and the heights of the ionospheric layers for two ionospheric observatories, Leningrad and Tomsk. An analysis of the material showed that the parameters of the E layer remained in fact normal during the time of magnetic disturbances. This conclusion is in full agreement with the well known fact that usually, in the middle latitudes, the disturbance affects only the F region and only in the strongest storms does the disturbance penetrate down to the underlying layers and disturb their structure. In the variations of height of the F_2 layer and particularly of the critical frequencies of that layer, a regular part could be detected. The D_{st} variations of $f_{F_2}^0$ are characterized by an increased in-

index of f^oF_2 in the first hours of a storm, followed by a decrease in the subsequent hours of the storm. The S_D variations of f^oF_2 differ for the winter and summer months and are not the same at Tomsk and Leningrad. A consideration of the materials for two years for two stations is, under all circumstances, inadequate for any judgment as to the geographic incidence of the disturbed variations, or even as to how much the variations change from year to year. Nevertheless the work has shown that statistical methods are fully applicable to the study of the ionosphere of ionospheric disturbance.

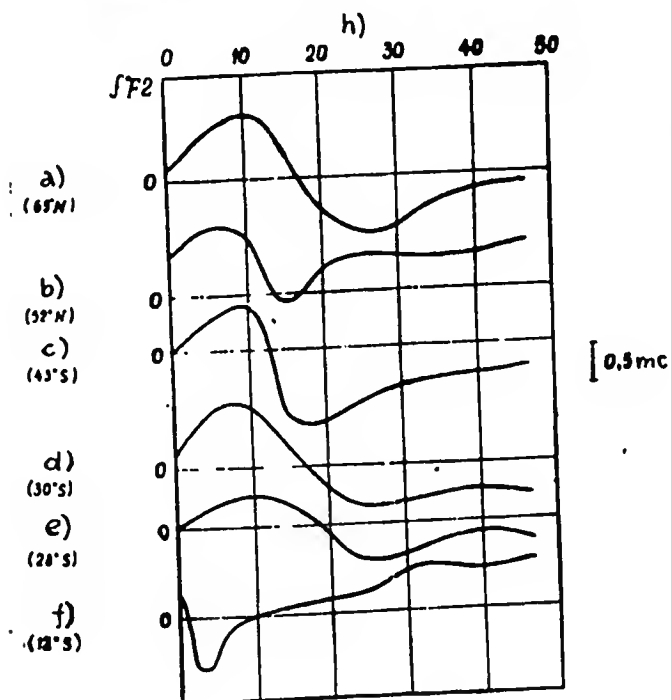


Fig.39 - D_{st} Variations of the Critical

Frequencies of the F_2 Layer

- a) Alaska; b) Slough; c) Hobart;
d) Watheroo; e) Brisbane; f) Huan-
cayo; g) 0.5 mc; h) Hours

Analogous results have been published by Appleton and Piggott (Bibl. 36) in 1950 on the question of the correlation between magnetic and ionospheric disturbances. After working up the data on the F_2 layer of a number of observatories located at different latitudes, the authors concluded that in the middle latitudes ionospheric disturbance usually

take the following course: during a few first hours of the magnetic storm an increase in the critical frequencies of the F_2 layer is observed. This is the positive phase, which is replaced afterwards by the negative phase, in which the decrease of f^oF_2 in absolute value considerably exceeds its increase during the first phase. The negative phase lasts considerably longer than the positive phase. The return to the normal state of the F_2 layer is slow, dragging out to a few days, as

occurs with the phase of restoration of the D_{st} variations of the magnetic field. The negative values of f^0F_2 are observed during the entire magnetic storm. In the high latitudes, on the contrary, the ionospheric disturbances as a rule have only a negative phase, commencing immediately together with the magnetic disturbance. The negative disturbances of the f^0F_2 of the high latitudes differ substantially from the negative phase of the middle-latitude disturbances. But it is precisely the restoration of the normal state of the F_2 layer after the polar disturbance that occurs very rapidly, without a long drawn-out period of after-effect. This fact, it seems to us, is responsible for the negative disturbances in the F_2 layer that accompany polar geomagnetic storms. There are indications in the literature that by now the D_{st} and S_D variations of f^0F_2 have been calculated for many ionospheric observatories, but more detailed data on the results of such calculations are not available to us.* The papers devoted to the variation of the critical frequencies and the heights of the regular layers during the time of a disturbance have been enumerated above. In addition to works of this kind, there have also been a large number of other investigations with respect to special types of disturbances (for example sudden ionospheric disturbances due to outbursts of ultraviolet radiation), formation of additional layers at various heights during storms, the correlation of E sporadic with the degree of magnetic disturbance, the nonuniformity of the ionosphere, etc. In view of our basic object, to elucidate the ionospheric conditions of a typical magnetic storm, these studies are of less interest for us. Indeed, the existence of an E_s layer of corpuscular origin, related to and correlated with the degree of magnetic disturbance, is very probable. However, in the middle latitudes, in a large number of cases, E_s is observed with a completely quiet field, and E_s is often absent during a storm. There is therefore no reason to consider that its formation leads

* This question is also considered in the papers by Martin, Louis Waldo, and Appleton and Martin, published before the completion of the present work (cf. Proc. Roy. Soc. and Journ. Atm. Terr. Phys., 1952 and 1953).

to the formation of the electric currents responsible for the regular parts of the field of magnetic storms.

This applies to an even greater extent to the appearance of additional high lay-

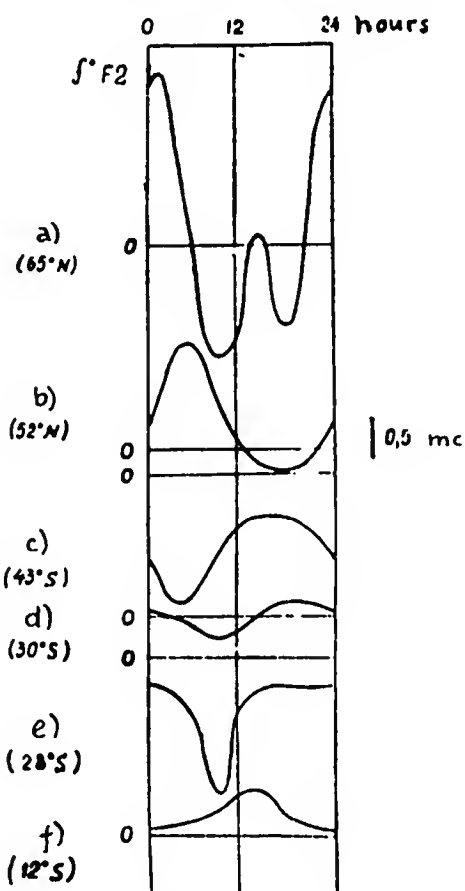


Fig.40 - S_D Variations of the Critical Frequencies of the F_2 Layer

- a) Alaska; b) Slough; c) Hobart;
d) Watheroo; e) Brisbane;
f) Huancayo; g) Hours; h) 0.5 mc

ers during the time of a disturbance. Additional and sporadic layers at the level of the F_2 layer and above it are not invariably observed during the time of magnetic disturbances, and it is not probable that they are connected with the regularly originating currents.

On analyzing similarly the other manifestations of an ionospheric disturbance, it may be concluded that the regular parts of the field of a magnetic storm are most likely to be related to such processes in the ionosphere as variations of density or circulations of large scale. Starting out from these considerations, in the present survey we have touched only on a few investigations devoted to the consideration of precisely these questions.

The additional statistical treatment of the ionospheric data performed by us leads to the following results (Figs.39 and 40):

1. The D_{st} variations of f^oF_2 have a two-phase character at all latitudes: in the high and middle latitudes, the first phase is positive and the second negative. In the low and equatorial latitudes, on the contrary, the first phase is negative and the second positive. Thus the geographic distribution of the D_{st} variations of

the magnetic field and f^0F_2 do not resemble each other.

2. The S_D variations of f^0F_2 vary strongly, depending on the season and on the level of solar activity. Nevertheless certain regularities in the geographic distribution of S_D can be established: the amplitude of $S_D f^0F_2$ is smallest in the equatorial regions and greatest in the polar latitudes; the time of the extreme values likewise varies with the latitude: in the low latitudes the minimum is observed in the forenoon hours, and the maximum in the afternoon hours, while in the high latitudes, on the contrary, the minimum occurs in the second half of the day and the maximum in the first half. It follows from this that the geographic distribution of $S_D f^0F_2$ is analogous to that of the S_D variations of the magnetic elements.

3. The D_{st} and S_D variations of f^0F_2 are considerably less regular than the corresponding variations of the magnetic elements.

No regular disturbed variations of the E layer are detected, either at low latitudes or in the polar regions.

Section 2. Conductivity of the Ionospheric E and F Layers, and the Dynamo Effects in the F_2 Layer

As we have seen in the preceding paragraph, the density of ionization of the F_2 layer undergoes variations during the time of a disturbance, depending on the storm-time (D_{st} variations) and on the time of day (S_D variations). Our task is to elucidate the question whether these variations can cause the rise of the electric currents responsible for the D_{st} and S_D variations of the geomagnetic field. In order to compare the quantitative characteristics of the ionosphere (for example the density of ionization or the velocity of motion) with the intensity and configuration of the electric currents, it is necessary to have some working hypothesis about the mechanism of excitation of these currents. The hypotheses in the literature as to the causes for the origin of the currents of magnetic disturbances may be divided into two main groups. The first of these groups includes the hypotheses related to the assumption of the deep penetration of solar corpuscles into the earth atmosphere

(to the level of the F region and lower). As we have already shown, this hypothesis has recently been confirmed by auroral spectroscopy, and thus there should be no doubt of the penetration of corpuscles down to the very lowest layers of the ionosphere in the polar latitudes. But the question as to the penetration of corpuscles into the ionosphere of the middle latitudes still remains unsolved. Eckersley (Bibl. 42), Burkhard (Bibl. 39), and a number of other authors consider it possible that the corpuscles penetrate in all latitudes, and explain, by the direct action of the corpuscles, those variations that are observed in the ionosphere and the magnetic field of the earth during the time of a disturbance.

According to Eckersley, the positive ions penetrate somewhat deeper into the atmosphere than the electrons, and the vertical electrostatic field thereby formed is the prime cause of the drift of charged particles and of the excitation of the electric currents responsible for magnetic storms. Without making it my task here to give a complete critical discussion of Eckersley's work, I may say that an electric vertical field should in my opinion prevent the further invasion of the corpuscles into the atmosphere, and thus, the process of a disturbance, as soon as it began, should at once thereafter die out, without leading to the formation of stable current systems.

According to Burkhard, the entrance of corpuscles into the ionosphere leads, in some manner (the author does not specify precisely in what manner) not to the increase of ionization but to its decrease. The corpuscles emitted by the sun during quiet periods penetrate the earth atmosphere at all latitudes and reduce the ionization of the F₂ layer due to ultraviolet radiation. During the time of disturbances, the parameters of the particles vary in such a way that the particles are collected toward the polar regions of the earth, without reaching the low latitudes. Accordingly, there is a particularly strong decrease in the density of ionization in the high latitudes, while in the low latitude there is an increase, connected with the disappearance of the negative corpuscular effect. We have cited Burkhard's reason-

ing in order to show to what absurd conclusions the speculative idea of the deionizing action of the corpuscular stream, developed without any connection with experimental data, can lead. Not only is the course of the arguments of Eckersley and Burkhard erroneous, in our opinion, but the very penetration of particles into the lower latitudes would appear to be contradicted by a number of facts. First, the geographic distribution of the aurora is such that, at relatively low latitudes, ($\phi = 30 - 40^\circ$), it is observed only during exceptionally strong magnetic storms, while the ordinary moderate and great magnetic storms are accompanied by a shift of the isochasms by only $5 - 6^\circ$ toward lower latitudes, from their mean position ($\phi_0 = 67^\circ$). The calculation of the paths of the particles in the magnetic field and the determination of the zone of their penetration into the ionosphere that have been made by a number of authors, with various objects in view (Störmer, Bugoslavskiy, Vallarta, Alfven, Martin, and others) are likewise all in agreement that the approach of particles to the earth in the low latitudes is impossible if the velocity of the particles is less than the velocity of light (for instance about 1000 km/sec). It goes without saying that particularly great active formations on the solar surface emit corpuscles at high velocities (about 3000 km/sec and perhaps even higher) which are little deflected by the magnetic field, and produce the aurora in the middle latitudes, while the intensifying the ionization in the high layers of the ionosphere or the (more energetic) lower layers of the ionosphere (cf. work of N.V. Mednikova (Bibl. 24)). But such powerful processes are relatively rare, and consequently, we should not take them as a basis for discussing the possible mechanism of excitation of the electric currents of the regular variations, flowing around the earth during moderate and small magnetic storms.

The following argument against the approach of the corpuscles to the earth surface is provided by the morphology of the magnetic disturbances. The great but smooth deviations from the normal values in the march of the magnetic elements, and the absence of a local character in the course of storms in the equatorial latitudes,

all speak for the view that the fluctuations of the magnetic field are due to stable current systems encompassing the earth as a whole, which are not disturbed by the invasion of streams of charged particles.

It follows from this that it is more advisable to assume that the middle-latitude parts of the currents of the magnetic variations are excited in the ionosphere, if they can be referred to the height of the ionosphere at all, without direct entrance of additional charges into the ionospheric layers.* The authors of the works placed by us in the second group share this viewpoint. In Chapter I we have already mentioned the investigators (Yu.D.Kalinin, S.M.Matsushita, Khiroiyama) who have attempted to explain the currents of magnetic storms by a dynamo effect in the ionosphere. In addition, the thought has been expressed that with the existence of an external extra-ionospheric primary field varying with time, the currents in the ionosphere would be excited owing to electromagnetic induction, and would make their contribution to the observed disturbance field. These thoughts have been developed in the paper by Ashour and Price (Bibl.37), and in certain papers by Sugiura (Bibl.55). But the dynamo and induction effects are not the only methods for the excitation of currents. It is well known that the excitation of currents in an ionized gas by the combined action of two fields of force on the particles (magnetic and gravitational fields, or magnetic and electric fields) is also possible. The current so excited (drift current) has been used to explain the S_q variations and the regular field of the sun. A number of considerations, which we shall present below, compels us to consider the drift also as a possible cause of the formation of the currents of magnetic disturbances. It is to the discussion of the dynamo, drift and induction me-

* The literature sometimes gives as an argument for the penetration of corpuscles into the ionosphere the so-called "geomagnetic effects" in the F_2 layer (the dependence of ionization density on the geomagnetic latitude, etc). But it would appear to be more plausible to explain these effects by the redistribution of the charges already in the layer under the action of the earth magnetic field.

mechanisms of excitation of ionospheric currents that this and the following Sections of the present will be devoted.

The question of the excitation of electric currents in plasma and of the evaluation of its conductivity has been discussed with great vigor in the literature of recent years. The works of Pedersen, Tamm, Cowling et al (Bibl.23) show that the value of the conductivity of an ionized gas depends substantially on the magnitude and direction of the magnetic and electric fields acting on the particles, on the length of the free path, and on the parameters of the particles; the motion of the particles in the plasma will be completely different from that in the case of a rarefied gas, the interaction between whose particles may be neglected, and which has been considered in their time by Störmer and Chapman. In the works of Tamm and Cowling, the conductivity of an ionized gas is considered specially in its application to the earth atmosphere. Tamm assumes the ionosphere to be completely ionized and gives approximate expressions for the conductivity, one of which expressions is true for regions of short free paths and the other for regions of long paths. Cowling considers the ionosphere as a ternary gas composed of electrons, positive ions, and neutral molecules, and obtains more general expressions for its conductivity. It is not hard however, to show that the conclusions of Tamm and Cowling do not contradict each other. If the charged particles of the plasma are under the action of a magnetic field (\vec{H}), an electric field (\vec{E}) and a gravitational field (acceleration of gravity \vec{g}) and, is also undergoing motion of translation under the action of certain other forces, at the velocity \vec{w} , then according to Tamm, the density of the current formed by the translation of particles of one kind will be:

$$j = eN \left\{ \vec{w} + \frac{4\lambda V_m}{3\sqrt{2\pi kT}} (\vec{g} + \frac{e}{m} \{ \vec{E} + [\vec{w}\vec{H}] \} - \frac{kT}{m} \frac{\nabla N}{N} - \frac{k}{2m} \nabla T) \right\} \quad r \gg \lambda, \quad (1)$$

$$j_{\perp} = eN\vec{w} + \frac{1}{H^2} [\{ Nm\vec{g} + Ne(\vec{E} + [\vec{w}\vec{H}]) - \text{grad}(kTN) \} \vec{H}] \quad r \ll \lambda. \quad (2)$$

Here the density of the given gas (N) and the temperature (T) are not assumed to be uniform, r is the radius of vortex motion of the particles about the lines of

force of the magnetic field, and λ = free path of the particles. The component of density of the current parallel to \vec{H} in the field of the long free paths ($r \ll \lambda$) is likewise described by eq.(1). If we have a binary gas ($n_+ \approx n_- = N$), then, from eq.(1), neglecting the temperature gradient and density gradient, we get

$$j_{\perp} = \sigma_0 (\vec{E} + [\vec{w}\vec{H}]) \quad r \gg \lambda, \quad (3)$$

where

$$\sigma_0 = \frac{2e^2 N}{3\sqrt{2}\pi kT} \left(\frac{\lambda_+}{v_{m_+}} + \frac{\lambda_-}{v_{m_-}} \right) = \frac{Ne^2 \lambda_+}{m_+ v_+} + \frac{Ne^2 \lambda_-}{m_- v_-} = \frac{Ne^2}{m_+ v_+} + \frac{Ne^2}{m_- v_-} \quad (4)$$

is the conductivity of the gas in the absence of a magnetic field. Here v = kinetic velocity of molecules, and ν = number of collisions per second ($\lambda v = v$). The current described by eqs.(3) and (4) is the dynamo current used by Schuster and Chapman to explain the S_q variations.

According to Cowling, in an ionized gas under the action of the crossed, mutually perpendicular electric and magnetic fields \vec{E} and \vec{H} , an electric current of density

$$j = \sigma^I \vec{E}' + \sigma^{II} \frac{[\vec{H}\vec{E}']}{H}, \quad (5)$$

is excited, where \vec{E}' must be understood as meaning not only the proper electrostatic field \vec{E} of some external origin, but also the electric field arising as a result of the motion of the mass of gas in the field \vec{H} at velocity \vec{w} , that is

$$\vec{E}' = \vec{E} + [\vec{w}\vec{H}], \quad (6)$$

and, consequently,

$$j = \sigma^I (\vec{E} + [\vec{w}\vec{H}]) + \sigma^{II} \left(\frac{[\vec{H}\vec{E}]}{H} + \vec{H}\vec{w} \right). \quad (7)$$

The first term in the expression for j denotes the Schuster-Chapman dynamo effect, while the second indicates the formation of a current in the direction of the velocity of motion of the gas \vec{w} , or in a direction perpendicular to the crossed mag-

netic and electric fields. The expression σ^I , according to Cowling, is equal to

$$\sigma^I = \frac{\sigma_0}{1 + \omega^2 \tau^2}, \quad (8)$$

where τ = time of free path ($\tau = v^{-1}$), and ω = angular velocity of precession of the particle ($\omega = \frac{eH}{mc}$, $v_{\perp} = r\omega$). It is identical with the expression for the conductivity of a gas in a direction perpendicular to the magnetic field, introduced into the literature by Pedersen:

$$\sigma_{\perp} = \frac{\sigma_0 v^2}{v^2 + \omega^2}. \quad (8')$$

For a region of short free paths ($\frac{r}{\lambda} = \frac{v}{\omega} \ll 1$) neglecting the value of ω^2 , we have $\sigma_{\perp} \approx \sigma_0$, as is put in the Tamm equations. The conductivity σ^{II} is determined by the expression

$$\sigma^{II} = \frac{\sigma_0 \omega \tau}{1 + \omega^2 \tau^2}. \quad (9)$$

In the field of short free paths,

$$\sigma^{II} \approx \sigma_0 \frac{\omega}{v} \text{ and } \sigma^{II} \ll \sigma^I. \quad (10)$$

Consequently, Tamm did not make a large error by neglecting the current in the direction of \vec{w} (or perpendicular to \vec{H} and \vec{E}) for this region. In the region of long free paths ($v/\omega \ll 1$)

$$\left. \begin{aligned} \sigma^I &\approx \sigma_0 \frac{v^2}{\omega^2}, & \sigma^{II} &\approx \sigma_0 \frac{v}{\omega} \\ \sigma^I &\ll \sigma^{II} & \ll \sigma_0 \end{aligned} \right\} \quad (11)$$

and, consequently, the current in the direction of \vec{w} is considerably greater than the current in the direction of \vec{E} . It is therefore entirely natural that in the approximate equation of Tamm, out of the terms describing the dependence of the current on \vec{H} and \vec{E} , only the term $\frac{Ne}{11^2} [(\vec{E} + [\vec{w}\vec{H}]) \cdot \vec{H}]$ should be retained.

The scalar Coefficient $\frac{Ne}{11^2}$ is the same as the coefficient $\frac{\sigma^{II}}{11}$ in eq.(5).

In fact,

$$\frac{\sigma^{II}}{H} \approx \frac{Ne^2 v}{m v H \omega} = \frac{Ne^2}{m H} \frac{m}{e H} = \frac{Ne}{H^2}.$$

Thus eqs.(1) and (2) of Tamm and eq.(5) of Cowling do not contradict each other.

Let us see now to what extent the identification of this or that ionospheric layer with the region of long or short free paths is correct. The angular velocity of motion of a particle ($\omega = \frac{eH}{m}$) depends only on the parameters of this particle and the magnitude of the magnetic field. Neglecting the variation of the earth magnetic field with height for the region of the ionosphere, we find that for all ionospheric layers the velocity of an electron $\omega_e = 5 \times 10^6$ and the velocity of an ionized oxygen molecule $\omega_i = 10^2$. The number of collisions in the ionosphere has been repeatedly determined from the experimental data on the absorption (Bibl.1), and has also been calculated by the formulas (Bibl.11):

$$\left. \begin{aligned} v_m^e &= \frac{4\pi a^2}{3} N_m \bar{v} \\ v_i^e &= \frac{\pi e^4}{(kT)^2} N_i \bar{v} \ln \left(0,37 \frac{kT}{e^2 N_i^{1/2}} \right) \\ v_m^i &= \frac{16\pi}{3} \bar{v}^2 a^2 N_m \bar{v} \\ v_i^i &= \frac{\pi \bar{v}^2 r^4}{(kT)^2} N_i \bar{v} \ln \left(0,37 \frac{kT}{e^2 N_i^{1/2}} \right) \end{aligned} \right\} \quad (12)$$

Here v_m^e denotes the frequency of collision of electrons with neutral molecules, v_i^e with positive ions, v_m^i the number of collisions of ions with molecules, and v_i^i of ions with ions; a = effective diameter of a particle (for air the value $\pi a^2 = 7 \times 10^{-16}$ is usually taken); \bar{v} = kinetic velocity of the particles. The collisions of electron with electron and ion with ion with the same sign may be neglected in evaluating the total number of collisions, and therefore the term v_i^i will have a substantial value only in those regions where there is a sufficient number of both positive and negative ions. Radio methods enable us to determine directly only the effective ionization density N_{ef} , while the actual number of charged particles $N = N_{ef} \frac{m_i}{m_e}$ remains unknown. But a number of supplementary considerations (the magneto-ionic splitting of a deflected radio signal, etc) allow us to judge the ratio between electrons and negative ions in the layer $1 = \frac{n_-}{n_e}$. There is no doubt today

that the conductivity of the F_2 and F_1 layers is due primarily to electrons ($n_- < n_e$). It is also probable that, in the E layer as well, the conductivity is determined mainly by the electrons, since in the D layer the number of free electrons is in all probability small. The first columns of Table 27 give the values of N_{ef} adopted in the modern literature for all layers, together with the possible values of l ; the following columns give the values of n_e , n_- , n_+ and the most probable values of n_m , all calculated on the basis of N_{ef} and l . Columns 7 - 12 give the values of $v_e \dots v_i^i$ calculated by eq.(12), as well as the total number of collisions for particles of a given kind, v^e or v^i . Column 13 gives the value of v determined from experimental data. It will be seen from the tables that in the D layer, the total number of collisions is determined by the collision of charged particles with neutral particles, and none of the three assumptions as to the value of l contradicts the order of the observed v_{ef} . For the E and F_1 layers, as will be seen from the table, the data on v_{ef} agree only with the assumption $l = 0$, that is, with absence of any substantial number of negative ions. The value of n_m for the F_2 layer is determined only indirectly, namely on the basis of the number of collisions. For an ionization density of the order of 10^6 ions/cm³ and the assumption that ionization in the layer is due to electrons and positive ions ($l = 0$), this number of collisions corresponds to the effective number of collisions between electrons and ions (cf. Table 4, p.97, of the Ginzburg monograph Bibl.11). About the same number of collisions takes place for electrons and neutral molecules, if the molecular density $n_m \approx 10^{11}$. From this it is concluded that the number of neutral molecules in the F_2 layer does not exceed 10^{11} molecules/cm³. It is true that the literature also contains hypotheses of the complete ionization of the F_2 layer, particularly in the daytime.

The data of Table 27 show that the D layer is a region of short paths of both ions and electrons, that the E layer is a region of short paths for the ions and long ones for the electrons, and that the F_1 and F_2 layers are a region of long free paths for particles of both kinds. The conductivity σ^I which determines the dynamo

effect has the smallest value in the D layer and rises for the higher layers just as the conductivity σ^{II} does. In the D layer $\sigma^{II} \ll \sigma^I$, while in the overlying layers σ^I and σ^{II} are of comparable value, and σ^{II} is even somewhat greater than σ^I . Evaluating the integral conductivity of the R region, Cowling shows that it is possible that the conductivity of this region is considerably less, since the presence of current in the magnetic field leads to the excitation of ponderomotive forces $[wH]$ which retard the further motion of the charged particles, that is, it is as though they decreased the value of the conductivity. Thus the current that arises should be damped after the time $\frac{\rho}{\sigma^{II}}$ (where ρ is the density of the mass), which amounts to 45 days for the E layer, $3\frac{1}{2}$ hours for the F_1 layer and 20 min for the F_2 layer. The damping of the currents does not occur if the particles are under the constant action of a force, that is, if the motion of the particles is accelerated, or if under the action of the magnetic field a polarization of the gas occurs, neutralizing the retarding force $[wH]$, or if currents screening the internal parts of the volume from the action of the magnetic field are induced on the surface of the moving mass of gas.

In accordance with the above, Cowling considers that the conductivity* of the F_2 layer in reality does not exceed $\sigma^I = e \times 10^{-9}$, and that the conductivity of the E layer is practically constant (for instance, $\sigma^I = 10^{-7}$ for $l = 25$). Cowling concludes from this that the total conductivity of the entire ionosphere must be within the range from 10^{-7} to 10^{-8} and must be due primarily to the charged particles of the E layer.

The values of $\int \sigma^I dh$ given in Table 27 force us to apply the following corrections. Since the more probable value of the conductivity for the E layer would seem to be $\int \sigma^I dh = 10^{-9}$, then the integral conductivity of the entire ionosphere, causing the dynamo effect, is probably not more than 10^{-9} , while both layers of E and F

* Under the condition that the motion takes place under the action of tidal forces. From what has been said it follows that the conductivity differs for different kinds of motion of the gas.

possibly yield equal contributions to the value of the conductivity. The conclusions drawn as to the conductivity of the E and F layers are based on the values of the ionization density for a normal day. On a disturbed day, however, (cf. Chapter II), the order of magnitude of the ionization density remains the same and, consequently, the order of magnitude of the conductivity should likewise not differ markedly from that of a normal day.*

It follows from Chapter III and VII of the present work that the D_{st} variations of the geomagnetic field may cause ionospheric currents flowing westward along the parallels of latitude and having a density of about 3×10^{-9} CGS in a year of moderate solar activity. If these currents are attributed to the action of the dynamo effect, then it would be necessary to assume the presence in the ionosphere of a stable wind of meridional direction with a speed of the order of

$$w = \frac{3 \times 10^{-5}}{0.3 \times 10^{-9}} = 10^6 \text{ cm/sec.} = 1 \text{ km/sec.}$$

* After the present work had been completed, I learned of the paper by J.K. Csada, Acta Phys. Acad. Sc. Hungaricae I (3) 235 - 246, 1952, which considers the variation of the electromagnetic parameters of a gas under the influence of turbulent processes. It is shown that the local magnetic field formed in presence of turbulence lead to an increase of magnetic permeability and to a decrease of the electric conductivity of the gas. The turbulent processes occurring in stellar atmospheres may, according to Csada's calculations, reduce the conductivity of the atmospheric gas by several orders of magnitude. During magneto-ionospheric disturbances, it is generally known that turbulent processes also develop in the ionosphere. However, as shown by rough preliminary calculations, owing to the low temperature and the low degree of ionization of the ionosphere of the earth, the turbulent processes in it cannot lead to such great changes of the electromagnetic parameters as occur in stellar atmospheres.

A number of experiments in recent years (cf. Bibl. 2, 3, and 27) indicate the existence of horizontal movements of the clouds in the ionosphere in both its lower layers and the F_2 layers. In most cases, however, the authors give lower values for the velocities. Thus, according to the data of Australian stations, a systematic displacement of clouds in the F_2 layer, having a meridional direction and a velocity of 80 - 400 m/sec, has been found. Observations at Slough have shown displacement from time to time, of the F_2 layer as a whole (or of parts of it) at velocities of 120 m/sec in east-west direction. Velocities of the order of one kilometer a second are noted considerably less often. Thus, for example, from the observations in Australia the usual rates of motion of the clouds of the F_2 layer (of the order of 400 - 500 m/sec) increase, sometimes to 1800 m/sec, during magnetic storms. It would thus appear that the dynamo-excitation of the D_{st} currents requires somewhat higher rates of motion in the ionosphere than those usually observed. A still more weighty argument against the dynamo hypothesis of the D_{st} variations is the configuration of the current system, which is a latitudinal distribution of the current lines from eastward during the first phase of the storm and westward during the second stage. To explain such a form it would be necessary for the D_{st} variations of conductivity (and, consequently, of the critical frequency of the F_2 layer) to be of a very regular character, which would be the same over the entire earth, with an increase of $f^0_{F_2}$ in the first phase of a storm and a decrease in the second phase. However, as will be seen from Chapter II of the present work, the D_{st} variations of $f^0_{F_2}$ only have such a form in the middle latitudes, while in the low latitudes, their form, on the contrary, is negative in the first phase of the storm and positive in the second phase. The irregularity and instability of the D_{st} variations of $f^0_{F_2}$, which is particularly striking on a comparison with the D_{st} variations of the magnetic field, compels the definitive recognition of the impossibility of explaining the latter by the dynamo currents flowing in the F_2 layer of the ionosphere. These same considerations as to the dissimilarity of the D_{st} variations of $f^0_{F_2}$ and of the magnetic

POOR ORIGINAL

Table 27

Layer	ϵ_0	ϵ_1	ϵ_2	ϵ_3	ϵ_4	ϵ_5	ϵ_6	ϵ_7
D	10^8	1	0.5×10^8	2.5×10^7	2×10^7	—	1.5×10^8	$10^7 - 10^8$
	—	20	5×10^7	5×10^7	$10^8 - 10^9$	—	—	$10^7 - 10^8$
	—	—	5×10^7	5×10^7	—	—	—	$10^7 - 10^8$
E	3×10^8	0	3×10^8	—	3×10^8	—	2×10^8	10^8
	—	1	1.5×10^8	7.5×10^8	7.5×10^8	10^8	2×10^7	10^8
	—	80	6×10^8	1.5×10^{10}	1.5×10^{10}	—	—	10^8
F1	5×10^8	0	5×10^8	—	5×10^8	10^{11}	2×10^8	10^8
	—	1	2.5×10^8	1.2×10^{10}	1.2×10^{10}	—	4×10^7	10^8
F2	2×10^8	0	2×10^8	—	2×10^8	$10^{10} - 10^{11}$	—	$10^8 - 10^9$

Layer	ϵ_0	ϵ_1^I	ϵ_2^{II}	ϵ_3^I	ϵ_4^{II}	$\frac{3}{2} y_m$
D	10^{-17}	1.2×10^{-18}	6×10^{-20}	10^{-17}	10^{-22}	2×10^8
	2.5×10^{-16}	5×10^{-20}	2.5×10^{-21}	2.5×10^{-16}	2.5×10^{-21}	2×10^8
	2.5×10^{-16}	—	—	2.5×10^{-16}	2.5×10^{-21}	2×10^8
E	2.5×10^{-16}	3×10^{-16}	1.5×10^{-14}	2.5×10^{-16}	2.5×10^{-18}	2×10^8
	—	—	—	—	—	—
	—	—	—	—	—	—
F1	4×10^{-14}	10^{-17}	2.4×10^{-14}	1.5×10^{-14}	2×10^{-14}	7.5×10^8
	—	—	—	—	—	7.5×10^8
F2	3×10^{-13}	2×10^{-16}	1×10^{-13}	3×10^{-14}	10^{-13}	1.5×10^7

Note. In this Table the values of N_{ef} , n , and ν are given in $1/\text{cm}^3$, σ in the CGS-system, and y_m in cm, while l and $\frac{\omega}{\nu}$ are dimensionless quantities.

Table 27 (cont.)

v_0	v_1	v_m	v_l	v_d	$\frac{v_0}{v_1}$	$\frac{v_0}{v_l}$	$\frac{v_0}{v_d}$
10^8	2×10^8	6×10^8	10^7	—	5×10^{-2}	10^{-5}	1.3×10^{-12}
10^8	5×10^8	6×10^8	10^7	10^8-10^7	5×10^{-2}	10^{-5}	3×10^{-10}
10^8	5×10^8	6×10^8	10^7	—	5×10^{-2}	10^{-5}	—
10^8	—	6×10^8	10^4	—	50	10^{-2}	7.5×10^{-13}
10^7	5×10^8	6×10^8	—	10^8	—	—	—
5×10^7	1×10^8	6×10^8	—	—	—	—	—
2×10^3	—	60	60	10^8	4×10^4	1.7	6.2×10^{-11}
4×10^7	7×10^8	60	—	—	—	—	—
1×10^4	—	6-60	30	10^8-10^4	5×10^8	3.3	5×10^{-11}

$\int \sigma_e^I dh$	$\int \sigma_e^{II} dh$	$\int \sigma_l^I dh$	$\int \sigma_l^{II} dh$	$\int \sigma^I dh$	$\int \sigma^{II} dh$
2.4×10^{-12}	1.2×10^{-13}	2.0×10^{-11}	2×10^{-16}	2×10^{-11}	1×10^{-13}
1.0×10^{-13}	5×10^{-15}	5×10^{-10}	5×10^{-15}	5×10^{-10}	5×10^{-15}
—	—	5×10^{-10}	5×10^{-15}	5×10^{-10}	5×10^{-15}
6.0×10^{-9}	3×10^{-8}	5×10^{-10}	5×10^{-12}	6×10^{-9}	3×10^{-8}
—	—	—	—	—	—
—	—	—	—	—	—
7.5×10^{-11}	2×10^{-7}	1×10^{-7}	1.5×10^{-7}	10^{-7}	10^{-7}
—	—	—	—	—	—
3×10^{-9}	1.5×10^{-6}	4.5×10^{-7}	1.5×10^{-6}	4×10^{-7}	10^{-6}

field also force us to abandon other possible mechanisms of excitation of the ionospheric currents, although these, too, may not lead to any quantitative contradictions with respect to conductivity or motion in the ionosphere.

Let us consider in greater detail the possibility of current originating in the ionosphere in the direction of motion of the gaseous masses. It follows from Table 27 that the conductivity $\int \sigma^{II} dh$ of the F_2 layer in the direction of motion is one order of magnitude greater than the conductivity $\int \sigma^I dh$. Moreover, in the case of the formation of a current in the direction of motion of the retarding mechanical force $\sigma^{II} H^2 w$, which arises as a result of the motion of charged particles in a direction transverse to the magnetic field, would cause not a decrease in conductivity as with Cowling's examination of the dynamo effect, but the excitation of a Hall current of perpendicular direction. Thus the value of the conductivity $\int \sigma^{II} dh$ in the F_2 layer would hardly be much less than 10^{-9} , and, consequently, if there are any displacements of ionized masses or winds in the layer, they would lead to the excitation of currents of relatively high intensity in the direction of these motions. It follows from eq.(7) that to explain the D_{st} variations, very low velocities would be sufficient:

$$w = \frac{3 \times 10^{-5}}{0.3 \times 10^{-6}} \approx 1 \text{ m/cek.}$$

The presence of such small motions in a latitudinal direction would appear not to be in contradiction with the empirical data. Nevertheless, as we have already pointed out, it would hardly be possible to explain the origin of the D_{st} currents in this way, since the fluctuations in the ionization density of the F_2 layer during storms does not satisfy the necessary requirements.

The density of the drift current produced by the combined action of a magnetic field and, for instance, of the gravitational field, on the charges, in exactly the same way should be proportional to the ionization density (for further details see below), and, consequently, the drift currents which have been repeatedly used by in-

investigators to explain the disturbances (Hulburt, Eckersley) are likewise unable to explain the regular character of the D_{st} variations of the magnetic field. Thus a consideration of the D_{st} variations of the ionospheric parameters and a survey of the possible mechanisms of excitation of currents forces us to consider that the most plausible explanation of the D_{st} variations of the magnetic field would be an extra-ionospheric ring current. The great radius of the ring by comparison with the ionosphere (3 - 4 R according to our calculations) well explains the regularity and the absence of local anomalies in the D_{st} variations, which are very difficult to explain if the distance between the earth and the current-carrying layer is assumed to be short.

Section 3. Explanation of the S_D Variations of the Magnetic Field by Drift Currents

In the brief survey of the literature presented in Chapter I we stated that the S_D variations of the magnetic field might be explained either by means of an extra-ionospheric ring, assuming it to be elliptic, or by the aid of ionospheric current systems. Most of the arguments, however, are in favor of the ionospheric system. The S_D variations of the parameters of the F_2 layer which we have just described likewise do not contradict the attribution of the S_D currents to the height of the F_2 layer. The fundamental facts supporting this point of view, it seems to us, may be considered to be the similarity of the geographic distribution and of the 11-year fluctuations of the S_D variations of the magnetic field and of the ionization density of the F_2 layer. From the example of the D_{st} variations that we have discussed we have seen that the quantitative relations between the current density necessary to explain the magnetic disturbances and the possible values of the conductivity, and these relations between that current density and the possible motions in the ionosphere, lead to promising results. The current density of the S_D variations in the temperate latitudes (between $\phi = \pm 50^\circ$) amounts, in years of moderate magnetic activity, to a few units of 10^{-4} amp or of 10^{-5} CGS. At latitudes $\phi = 50 - 67^\circ$, the

current density is 3 to 4 times as great, that is, it reaches 10^{-4} CGS. Thus, to excite currents of the necessary density in the F_2 layer, the existence of systematic displacements of masses at a velocity of several meters a second would be sufficient, the direction of the current coinciding, on the whole, with the direction of the wind. In the light of experiments disclosing the motion of ionized gases at velocities of tens and hundreds of meters a second, the existence of such small velocities is very possible. Moreover it seems to us that arguments may be adduced according to which the formation of such storms during magnetic storms would be very plausible from the theoretical point of view as well. These arguments are as follows. Since we have recognized that the formation of an equatorial ring current is the most probable explanation of the D_{st} variations, the influence of the field of this ring current on the electromagnetic processes in the ionosphere must be examined. We have already mentioned one possible effect of the ring current, the electromagnetic induction of currents in the ionosphere under the action of the alternating field of the ring. As we shall show below (Section 3), this effect could hardly be of major importance for the formation of the S_D currents. In this Section we shall turn to a different type of the action of the ring on the ionosphere. Since the ionosphere participates in the diurnal rotation of the earth about its axis, while the field of the equatorial ring may be considered in sun-bound coordinates, as constant or slowly varying, it follows that it is necessary to consider the problem of the rotation of a conducting spherical layer in a quasi-constant field H . Let us simplify our problem by considering, at first, the rotation in the magnetic field H of an individual charged particle of mass and charge e . If this particle is bound to the earth (of mass M) by the forces of gravitational attraction, then its motion, in fixed coordinates, will be described by the equation

$$\frac{kmM}{R^2} + eR\omega H = mw_n, \quad (13)$$

where $\frac{kmM}{R^2}$ = force of gravitation; mw_n = centripetal force; $eR\omega H$ = Lorentz force

acting on a charge moving at velocity ωR in the field H ; and ω = initial velocity of rotation. On introducing a new system of coordinates rotating at velocity $\Delta\omega$, it is easy to show (Bibl.33) that the motion of the charge in the new system will be as follows:

$$mw_n = \frac{mkM}{R^3} + eR\omega H + 2mR\omega\Delta\omega + mR(\Delta\omega)^2. \quad (14)$$

If $\Delta\omega$ is selected such that

$$eR\omega H + 2mR\omega\Delta\omega + mR(\Delta\omega)^2 = 0, \quad (15)$$

then it will be found that the charge will continue to move along its orbit, but with a changed velocity equal to $\omega + \Delta\omega$. If the motion of our charge were governed only by eq.(13), then the quantity $\Delta\omega$ would be found to be so great for an electron and an ion that they would practically not participate at all in the diurnal rotation of the earth, but would obey only electromagnetic forces. However, as soon as the charge begins to move with respect to earthbound coordinates, it will be under the action of the geomagnetic field H_0 , which considerably exceeds the field of the ring H . The resultant motion under the action of the fields H and H_0 is described by the equation:

$$\frac{kmM}{R^3} + eR[(\omega + \Delta\omega)H + \Delta\omega H_0] + 2mR\omega\Delta\omega + mR(\Delta\omega)^2 = mw_n. \quad (16)$$

By an appropriate choice of $\Delta\omega$, we get

$$eH\omega + eH\Delta\omega + eH_0\Delta\omega + 2m\omega\Delta\omega + m(\Delta\omega)^2 = 0, \quad (17)$$

whence, neglecting the small terms,

$$\Delta\omega = -\frac{H}{H+H_0}\omega. \quad (18)$$

Taking $H = 10^{-3}$ CGS, $H_0 = 0.3$ CGS, $\omega = 7 \times 10^{-5}$, we have $\Delta\omega \approx -3 \times 10^{-3}$ and the linear velocity $w_n \approx 1 - 2$ m/sec, which is the same for charges of both signs. It

goes without saying, of course, that these arguments are not entirely correct, since the collisions between particles will disturb the regular drift of particles in the westward direction. Nevertheless, owing to the low molecular density of the atmosphere at the F_2 level, it may be considered that the interaction between the field of the ring and the main field of the earth will lead to a certain mean displacement of the charges in a latitudinal direction. If this displacement, all the same, should amount to centimeters or meters a second, it would still be sufficient to produce a current of density 10^{-5} CGS in latitudinal direction. This current would have a maximum density at the equator and a minimum density at the poles. Its role in the deformation of the S_D variations could therefore be substantial only in the middle latitudes.

The inductive influence of the extra-ionospheric current ring, however, is not the only cause leading to the formation of stable currents. A consideration of the drift of particles in the F_2 layer likewise leads us to the formation of an analogous current of latitudinal direction. It follows from eq.(2) that, in the region of long free paths, a drift of particles under the action of the gravitational and magnetic fields will occur, provided that the force of gravity per unit volume $\vec{g}Nm$ is not balanced completely by the partial pressure grad kTN . Since, in Tamm's opinion, there is a rule a disturbance of the equilibrium distribution by a barometric law in the ionosphere, the term $[(\vec{g}Nm - \text{grad } kTN) \vec{H}]$ may play a substantial role in the formation of the S_q variations. Cowling gives the following expression for the density of the drift current:

$$j = \frac{1}{H^2} \left[\vec{H} \left(2 \frac{\partial p_e}{\partial r} - \frac{p_e}{p} \frac{\partial p}{\partial r} \right) \right]. \quad (19)$$

Here p_e is the partial pressure of electrons, p = pressure of gas as a whole, and r = radius vector.

For a layer whose molecular density obeys the barometric law, and whose ionization density obeys the Kryuchkov-Chapman law,

$$p_e = P_e \left(\frac{p}{P} \right)^{\frac{1}{2}} e^{\frac{1}{2} \left(1 - \frac{p}{P} \right)} \quad (20)$$

and

$$j = \frac{1}{H^2} H \frac{P_e}{P} \left(\frac{p}{P} \right)^{\frac{1}{2}} e^{\frac{1}{2} \left(1 - \frac{p}{P} \right)} \frac{\partial p}{\partial r}. \quad (21)$$

Here P_e = value of P_e at level of maximum electron density, while P = corresponding value of p .

Integrating eq.(20) over the entire thickness of the ionosphere, and putting $P_e = 2.5 \times 10^{-7}$ CGS, Cowling obtains the result for the equator $j = 3 \times 10^{-6}$ CGSM, that is, a quantity smaller by one order of magnitude than what we need to explain the disturbance field. But if we bear in mind that the actual distribution of molecular or electron density may differ strongly from both the Chapman law and the barometric law, then a calculation by eq.(20) leads to other results. At the present time experiments do not yield so great a material on vertical motions in the ionosphere as we have on horizontal winds, but still it is possible to find certain opinions on this subject in the literature. First of all, investigators have several times succeeded in noting a variation in the height of the level reflecting a radio signal, deducing such variation from the Doppler shift of the frequency. The velocity of the displacement so revealed was found to be of the order of meters per second. A consideration of the behavior of the active heights of the F_2 layer during disturbances shows that H often varies by 100 - 150 km in one or two hours, which makes 10 - 20 m/sec.* This can also be noted both in the analysis of individual

* We shall not dwell here on the tidal motions of the F_2 layer experimentally found and theoretically considered in a number of works by Martin and other authors. The existence of horizontal vertical motions connected with tidal effects is today beyond all doubt, but it would still seem to be more advisable to correlate them with the geomagnetic variations in discussing the normal diurnal march S_q instead of the disturbances.

cases and in calculating the mean parameters. At the present time we have no opportunity to establish whether these changes in the height of the reflecting layer constitute actual displacements of air masses or wavelike fluctuations of density. But, under either of these assumptions, we should have a deviation of density from the barometric equilibrium and, consequently, a drift term that does not vanish in eqs. (2) and (19). It is very probable that the disequilibrium is intensified on days of magnetic disturbances, when the scattered and diffused reflections and the appearance of additional layers speak for the cloudlike structure and motions in the layer. If we assume that the fluctuations with density with height may be by a factor of several times (2, 5, 10), then the order of the term $\bar{g}Nm - \text{grad } kTN$ is the same as the order of $\bar{g}Nm$. Then, as follows from eq.(2), the density of the drift current:

$$j = \frac{10^3 \times 3 \times 10^6 \times 5 \times 10^{-23} \times 10^7}{0.3} = 5 \times 10^{-6} \text{ CGS}$$

is half an order of magnitude smaller than the density of the S_D currents. The vector of densities of the drift current must be perpendicular to the magnetic and gravitational field, that is, directed according to latitude. Thus both the influence of the equatorial ring current discussed by us, and that of the drift charges under the combined action of the gravitational and magnetic fields, should lead to the formation of currents of latitudinal direction and density 10^{-5} to 10^{-6} CGS. Let us now consider whether these currents could lead to the formation of the current system of the S_D variations. The mathematical formulation of the theory of drift currents of the S_q variations proposed in 1920 by Chapman has not been carried to completion and gives only a qualitative scheme of the formation of the S_q currents, instead of a quantitative calculation, which the dynamo theory does give. Nevertheless, this aspect of the work, the possibility of the formation of currents of the necessary configuration, has not evoked objections either from Tamm or from critics of this theory. I therefore deemed it possible to transfer this qualitative scheme of the formation of the S_q currents to the formation of the S_D currents as well.

The fundamental proposition of Chapman's theory of the S_q variations is as follows: the interaction of the gravitational and magnetic fields leads to the formation of a drift current in an easterly direction. The mean diurnal value of this drift, I_0 , corresponding to the mean diurnal density of ionization of N_0 , makes a contribution to the main field of the earth, somewhat increasing the H component. In the noon hours there is an excess of ionization ΔN , to which there likewise corresponds an excess current of easterly direction ΔI . To the deficit of ionization in the night hours there corresponds the negative current $-\Delta I$. As a consequence of these additional currents, there is an accumulation of positive charges on the evening side of the earth and of negative charges on the morning side. Since the conductivity of the ionosphere along the lines of force of the magnetic field is very great, these charges will tend to be displaced toward the higher latitudes along the lines of force, and will form two current eddies: a more intense one on the daylight side of the earth and a less intense one, negative in sign, on the night side of the earth. In its application to the S_D variations, this scheme must be modified as follows.

If we assume that: 1) the S_D variations of the ionization density of the F_2 layer are responsible for the S_D currents; and 2) the vector $\vec{g}_{Nm} - \text{grad } kTN$ is directed vertically upward,* then an additional current will begin to flow in westerly direction on the evening side of the low latitudes (0 to 45°), while an easterly current

* Since only the term \vec{g}_{Nm} , directed vertically downward, entered into the Chapman drift theory, this predetermined the formation of the current I_0 of easterly direction. Following Tamm, we assume that the drift is determined by the difference vector $\vec{g}_{Nm} - \text{grad } kTN$, which may be either positive or negative. The assumption of a $\vec{g}_{Nm} - \text{grad } kTN$ directed downward leads to signs of currents opposite those obtained from geomagnetic data. The assumption $\vec{g}_{Nm} - \text{grad } kTN$ directed upward leads to the formation of a westerly mean current I_0 , which, being superimposed with the western current, due to the effect of the equatorial ring, gives the necessary signs of ΔI on the morning and evening sides in the low and middle latitudes.

will begin to flow on the morning side. In the middle latitudes (45 to 60°) the direction of the currents on the evening and morning sides will be opposite, and the closure of the currents along the lines of force of the magnetic field leads to the formation of a negative eddy on the evening side and positive eddy on the morning side, the centers of the eddies being located at the latitudes $40 - 50^\circ$, where we have an inversion of the phase of $S_D f^0 F_2$. This scheme of formation is a rough one, intended merely to show that the explanation of the S_D variations by ionospheric current is possible in principle with respect to both the order of magnitude and configuration of the current lines. Which of these two mechanisms we have discussed, the influence of the equatorial ring or of the drift current, yields the greater contribution to the formation of the S_D currents at one latitude or another, remains obscure without performing exact mathematical calculations. The question as to whether these effects are capable of explaining all features of the S_D variations likewise remains unanswered. To elucidate these and other questions that may arise in connection with the explanation of the S_D variations, a detailed development of the theory would be necessary. The above presented reasoning is but an attempt to determine the direction in which this theory can be developed.

Section 4. Currents in the Ionosphere Induced by the External Field

In this Section we shall discuss the role of the currents induced in the ionosphere by the alternating magnetic field of the equatorial ring current. Let us denote the field external with respect to the ionosphere (that is, the field of the equatorial ring) by the letter E , and the field of internal origin (with respect to the outer edge of the ionosphere) by the letter I . The field I is made up of fields induced by the external field in the conducting layer of the earth and the ionosphere. Let us assume for simplicity, an ionosphere beyond the homogeneous conducting spherical layer of conductivity σ_d (σ = specific conductivity, d = thickness of layer). Then, denoting the external and internal fields observed directly under the

current layer by E' and I' , we have, by the Whitehead formulas:

$$\left. \begin{aligned} E' &= E - \frac{C_0}{n} \frac{d}{dt} [nE - (n+1)I] \\ I' &= I - \frac{C_0}{n+1} \frac{d}{dt} [nE - (n+1)I] \end{aligned} \right\} \quad (22)$$

where $C_0 = \frac{4\pi a_0}{2n+1}$ and a_0 = radius of the conducting spherical layer. Let us estimate the influence exerted on the E and I fields by the currents induced in the ionosphere, that is, in other words, let us estimate the differences $E' - E$ and $I' - I$. Considering only the first harmonic of the series representing the fields E and I , and assuming the terms E and I to be expressed by exponential term of the form

$$E = A_e e^{-\alpha_e(t-t_{0e})}, \quad I = A_i e^{-\alpha_i(t-t_{0i})}, \quad (23)$$

we have

$$\left. \begin{aligned} \frac{dE}{dt} &= -\alpha_e E, \quad \frac{dI}{dt} = -\alpha_i I, \\ E' &= E - C_0 \frac{d}{dt} (E - 2I), \quad I' = I - \frac{C_0}{2} \frac{d}{dt} (E - 2I), \\ E' &= E(1 + C_0 \alpha_e) - 2C_0 \alpha_i I \\ I' &= I(1 - C_0 \alpha_i) + \frac{C_0 \alpha_e}{2} E \end{aligned} \right\} \quad (24)$$

The quantities E and I are completely unknown to us, while the values of E' and I' may be judged on the basis of the field of D_{st} variations observed on the earth surface. Thus, eq.(24) enables us to determine the values of E and I if we only make definite assumptions as to the conductivity of the ionosphere. After eliminating I from eq.(24), we have

$$E = \frac{E'(1 - C_0 \alpha_i) + 2C_0 \alpha_i I'}{1 + C_0 \alpha_e - C_0 \alpha_i}, \quad (25)$$

whence

$$E - E' = \frac{2C_0 \alpha_i I' - C_0 \alpha_e E'}{1 + C_0 \alpha_e - C_0 \alpha_i}. \quad (26)$$

It follows from a consideration of table 27 that if αd is understood to mean

The conductivity even of the entire first half of the ionosphere, it would even hardly be reasonable to evaluate β_p as a quantity greater than 5×10^{-7} CGS. Hence the approximate quantity

$$C_0 \approx \frac{12.5 \times 6.4 \times 10^8}{3} 5 \times 10^{-7} \approx 1.5 \times 10^3.$$

The numerical values of α_e and α_i are unknown to us, but an idea of their order of magnitude can be formulated in the following way. Let us assume that the field of the equatorial ring during two days (the mean duration of a moderate storm) falls to 0.1 of its greatest value observed at the instant t^0 . In that case it follows, from eq.(23), that

$$0.1A_e = A_e e^{-\alpha_e 48 \times 3600} \text{ and } \alpha_e \approx 10^{-5}.$$

If the storm dies away still more slowly, then the value of α_e is even less. The coefficient α_i is of an analogous order of magnitude. Thus,

$$C_0 \alpha \approx 1.5 \times 10^{-2}.$$

and

$$E - E' \approx 1.5 \times 10^{-2} (2I' - E'). \quad (27)$$

The values of E' (that is, the field of the equatorial ring, allowing for the influence of the currents induced in the ionosphere) and of I' (the field of the currents induced in the earth) are known to us, not directly "under" the current layer, but on the earth surface. It follows from eq.(3 III), however, that the value of the field at the earth surface and at the level of the lower edge of the ionosphere ($h = 100 - 300$ km) are little different from each other, and, thus, the value of the difference eq.(27) can be estimated from the values of I and E in Tables 7. Thus, for instance: for $\tau = 20$ hours, $E' - E = 1.5 \times 10^{-2} (54\gamma - 28\gamma \times 2) \approx 0$; for $\gamma = 30$ hours, $E' - E = 1.5 \times 10^{-2} (51\gamma - 17\gamma \times 2) \approx 0.3$.

From these results the difference $I - I'$ was calculated.

For more rapid fluctuations (for example weakening of the storm to 0.1 of its initial value in 12 hours or, on the other hand its development at the beginning of

the magnetic field), the value of ΔB is also increased (about 5×10^{-4}), but for no values whatever of ΔB and ΔI (cf. Table 7), will they exceed 1 - 2%. It follows from the examples given that the currents induced in the ionosphere by variations as slow as D_{31} cannot exert any substantial influence on the magnetic field on the earth surface and, in any case cannot be called upon for an explanation of the S_D variations. They can likewise in our opinion not be used to explain the seasonal fluctuations of D_m , either (cf. Chapter VII, Section 1). On the other hand, in studying the rapid-course fluctuations (pulsations or aperiodic fluctuations of the type of sudden commencements), the current induced in the ionosphere may furnish a substantial contribution to the observed variations.*

The discussion of the dynamo, drift, and induction mechanisms of current excitation given in Sections 4 and 5 had the object of explaining the origin of the middle-latitude part of the S_D variations. The formation of the polar part of the S_D currents and of the currents of the P-storms may possibly originate in entirely different ways. First of all, in the polar regions, the direct penetration of charged particles occurs, and it goes without saying that this cannot but affect the conditions of the electromagnetic field. Then, as we have pointed out above, the disturbances of the polar ionosphere as a rule are accompanied by a sharp increase of ionization in the lowest layers of all (the D and E layers). Thus it may be assumed that the current systems disturbing the normal geomagnetic field are formed in these layers as well, and not only in the F_2 layer, as is the case in the middle latitudes. A discussion of the electromagnetic processes in the polar regions would go beyond the scope of the present work, since any opinions on this question would have to be based on a special study of magnetic and ionospheric material that are unavailable

* It is easy to show by analogous calculations that the induction produced in the E layer by the magnetic fields of currents flowing in the F_2 layer, is likewise very slight.

to me. It would, however, appear advisable to say the following. It is very probable that the S_D currents in the polar latitudes flow, as in the middle latitudes, at a great height (the height of the F_2 region). This is indicated both by the geomagnetic data (determination of the height of the linear current, cf. Chapter V) and the great influence of the disturbances on the F_2 layer (the decrease in the ionization of the F_2 layer in the high latitudes, as we have seen, is far more substantial than in the middle latitudes). The penetration of corpuscles down to the lower layers of the ionosphere, resulting in an elevated ionization at the level of the D and E layers, may possibly be responsible for the origin of polar storms. This proposition is based on the statistics given by Wells and a number of other authors, disclosing the correlation between the appearance of the E_s , the aurora, the bay-shaped disturbances, and the disruption of radio communication, as well as the highly local nature of the course of P-storms, which does not allow us to refer the S_D current to great heights. All determinations of the height of the current of the P-storms, under the assumption of the linearity of the current, may lead, as we have seen in Chapter I, to heights of the order of 100 - 120 km, or less. As for the mechanisms of excitation of the P-currents in the low layers of the ionosphere, it would appear not impossible that the dynamo effect plays a great role in their formation. If, as follows from Nagata's work (Bibl.52), the ionization density of the lower levels increases tenfold during a disturbance, then the conductivity σ^I of the D and E layers may reach such a value (about 10^{-6}), that the displacement of ionized masses at relatively low velocities is able to produce currents of the necessary intensity.

But conduction currents are not the only possible cause of the polar storms. In the light of the modern theories of the aurora, which have been developed with particular success by the Soviet scientist A.I. Lebedinskiy, it would appear more probable that the storm field is induced by currents of the discharge type.

CHAPTER IX

CURRENT SYSTEMS OF INDIVIDUAL STORMS

Section 1. Polar Storms

The preceding Chapters of this work have been devoted to the discussion of the average features of the field of magnetic disturbance and to the description of the average current systems. The few attempts to construct the system of currents corresponding to individual storms (cf. Chapter I) have shown that the individual systems are of the same character as the average systems. The task of the present Chapter is to check this proposition on a large amount of empirical material.

A calculation of the external current systems of the S_D and D_{st} variations and of the P-storms, performed by rigorous analytic methods, showed that the approximate method of constructing currents gives good results both with respect to the configuration of the currents and to their intensity. This conclusion must be understood to the effect that with a given relatively sparse distribution over the earth surface of points with observed values of the magnetic elements, the analytic and approximate methods give a similar and rather coarse picture of the currents. With a more complete starting material, the analytic methods, of course, would yield more accurate results, while the accuracy of the approximate methods would not be increased. In the present case, the consideration of the individual disturbances, the number of observatories whose materials can be used proves to be still smaller than the number used by us in our study of the average features of the field. For this

reason it seems advisable to construct the individual current systems by the approximate method, estimating the current density by the Biot-Savara law (cf. eq.(1.V)). The ratio between the external part of the field E and the observed field was assumed, in accordance with the results of an analysis of the S_D variations, to be 0.8 for the middle latitudes and 0.9 for the high latitudes.

The current systems are calculated for 26 separate instants of polar and worldwide storms. The current systems of two polar and one worldwide storm are given as an example in Figs.41 - 43.

All the figures were constructed of exactly the same type. The legend under the drawings indicates the Universal Time, and the local time for the various meridians corresponding to that Universal Time is indicated at the edge of the coordinate net. The coordinate net composed of solid lines is formed by the geomagnetic parallels and meridians, while the net composed of dashed lines is formed by the geographic parallels and meridians. The negative values of the current function (the current flows clockwise about the extremum) are indicated by dashed lines, while the positive values (the current flows counter clockwise around the extremum) by solid lines. The horizontal component of the vector of the disturbance field is shown by an arrow. The current lines are so drawn that a current of 10,000 amp flows between adjacent lines. The legend under each drawing gives the intensity of the largest current eddy.

Let us turn at first to a consideration of the current systems of polar storms. In order best to bring out the characteristic features of the P-storms, all the examples were selected on quiet days, when one disturbance is not piled on top of the other. Figures 41a and 41b represent the maps of the currents for two consecutive instants of the polar storm of 9 October 1932.* The vectors plotted on the maps correspond to the mean hourly values of the magnetic elements. On both figures the

* The starting data for the disturbances of 9 October 1932 and 23 February 1933 have been taken from Vestine (Bibl.62).

current system consists of two pairs of eddies. The eddy with the current of positive direction is located on the evening hours of the polar latitude, while the eddy with the negative current is located on the morning hours. In the middle-latitude pair of eddies, the signs are opposite. On Fig.41a, corresponding to the greatest development of the storm, the polar eddies considerably exceed the middle-latitude eddies in intensity. The intensity of the morning and evening eddies is not the same. Of the polar eddies, the most intense is the morning eddy, of the middle latitude eddies, the most intense is the evening eddy. Figure 41b shows the end of the polar disturbance, when the values of the magnetic elements have almost returned to the normal state. The form of the current lines and their location with respect to the local time persists in both figures. A comparison of Figs.41a and 41b with Fig.32 shows that the distribution of currents during the disturbance of 9 October 1932 is very much like the currents of the idealized P-storm, both with respect to the sign and position of the current eddies, and to the configuration of the current lines. It is true, of course, that it is necessary to note that the centers of the eddies on the idealized picture are located at earlier morning hours than in all instances of the disturbance of 9 October 1932. The second example (Fig.42) yields a picture of a more intense polar storm. The intensity of the current in the polar cap reached one million amperes at 1400 hours, 23 February 1933. The current strength in the middle latitudes in this case remains very small. The general form of the current lines and the distribution of the signs of the current function are the same as in the first example. Our attention is attracted by the strong asymmetry in the intensity of the morning and evening polar eddies: the morning eddy is 5 times as intense as the evening eddy. Such asymmetry in the distribution of currents gives the impression that the storm is observed only in a narrow longitudinal sector of the Arctic over North America. Since in many cases the distribution of the degree of disturbance in a polar storm is also characterized by such asymmetry, an uncritical consideration of the material has led many investigators to the conclusion that

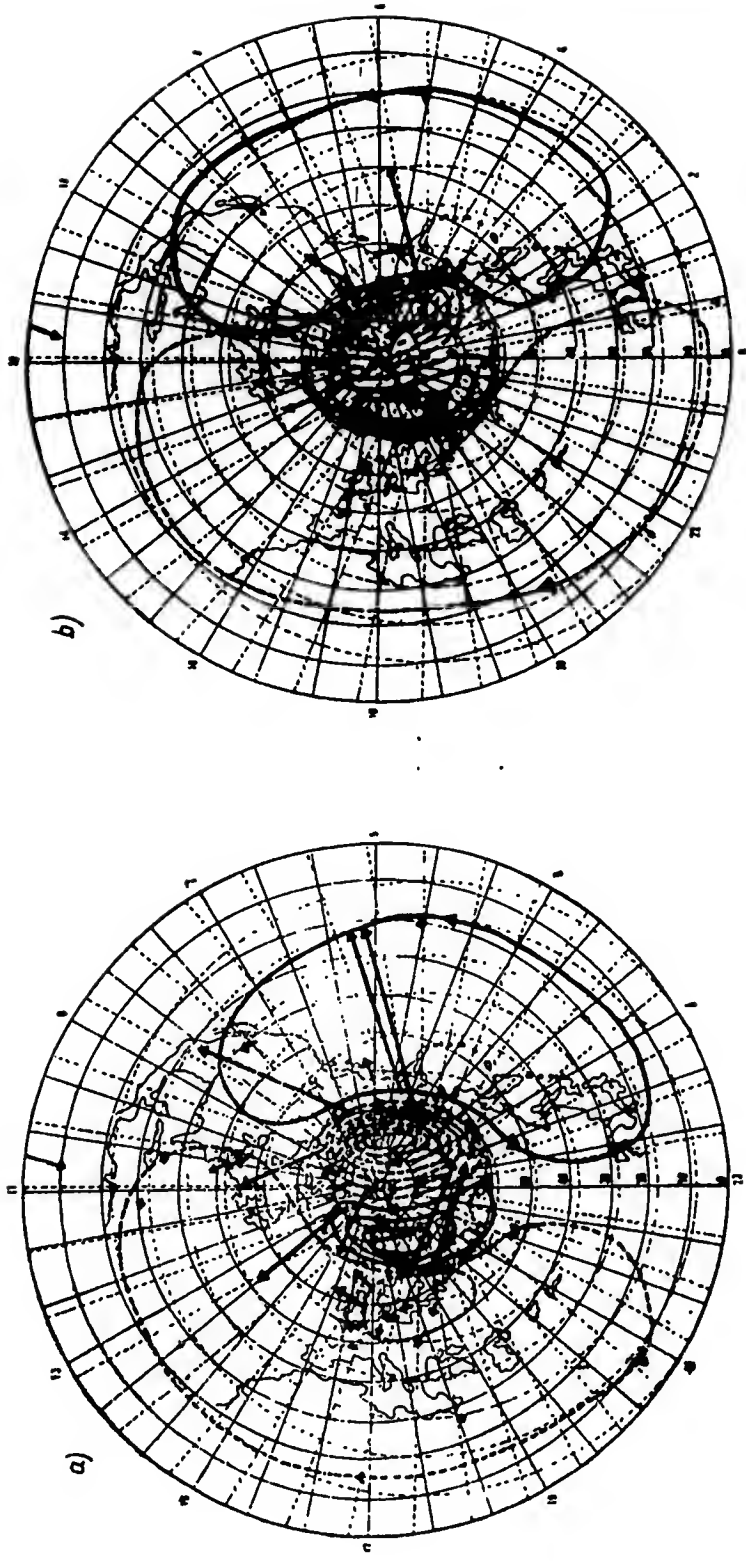


Fig.41 - Polar Storm of 9 October 1932
(a - 1500 Hours, $I = 70 \times 10^4$ amp; b - 1600 Hours, $I = 40 \times 10^4$ amp)

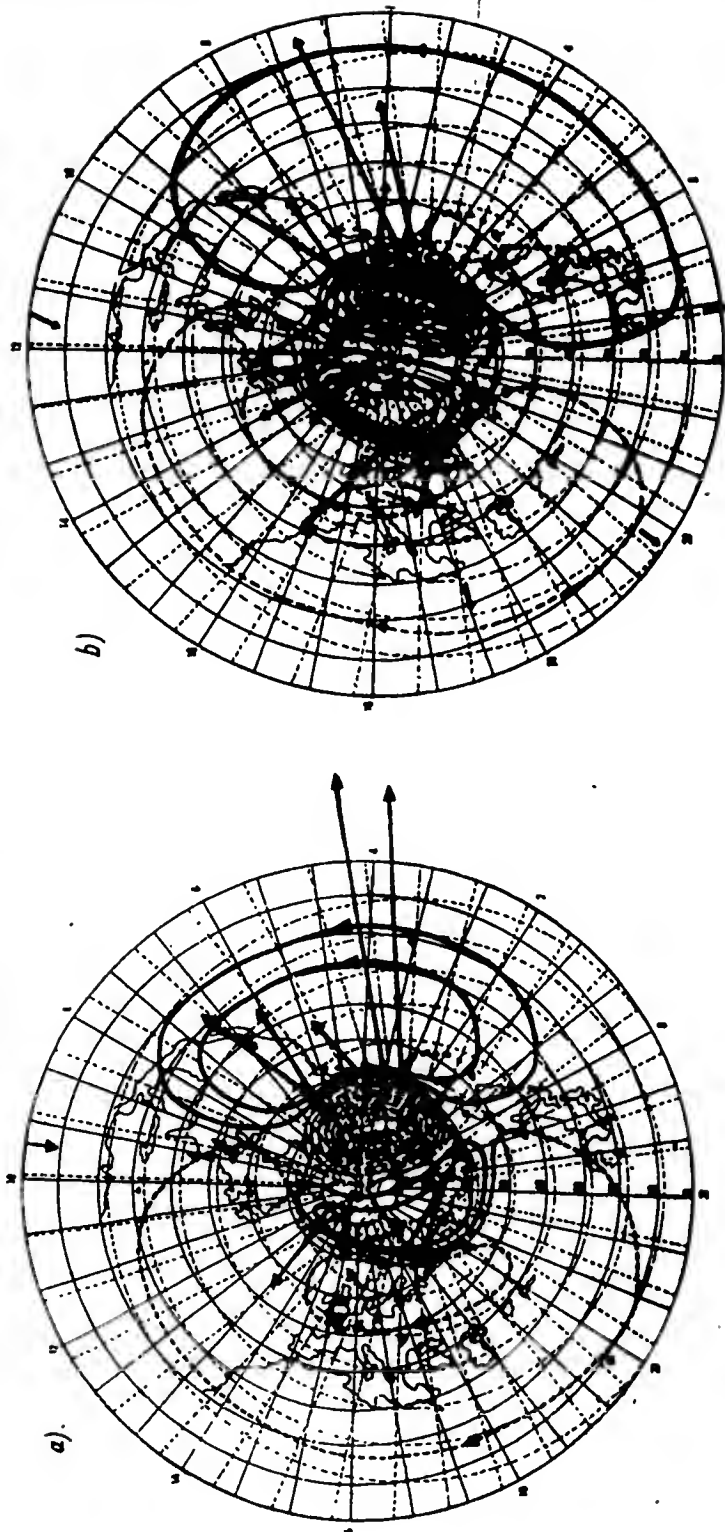
POOR ORIGINAL

Fig. 42 - Polar Storm of 23 February 1933

(a - 1400 Hours, $I = 100 \times 10^4$ amp; b - 1600 Hours, $I = 60 \times 10^4$ amp)

polar storms are local in character, that is, that a polar storm usually covers only a small longitudinal sector. The examples of polar storms we have considered show, on the contrary, that an intense negative disturbance on one side of the earth is always accompanied by a small positive disturbance on the other side. Thus the current system of a polar storm always consists of a pair of current eddies of different sign and intensity. The disturbance of 23 February 1933 vividly illustrates still another property of the current system of a P-storm: the current system is fixed with respect to the sun but not with respect to the earth. During the two hours that elapsed between 1400 and 1600 hours, 23 February, the centers of the current eddies were so displaced with respect to the earth that at both 14 and 16 hours the center of the main polar eddy remained at 4 hours local time.

The vectors represented on Figs. 41 and 42, as already mentioned, represent the mean hourly values of the elements. They show that the smoothed course of the individual polar storms, as represented by the mean hourly values, is in good agreement with the typical picture of the polar storm described in Chapter VI. For other polar storms, the diagrams of instantaneous values of the vectors have been constructed and the current systems corresponding to them have been drawn.

A typical polar disturbance was observed on 7 March 1946. The magnetograms of the Sitka and Tucson Observatories revealed a barely perceptible curvature of the quiet march of the magnetic elements at the Tucson Observatory, while at Sitka the amplitude of the fluctuations reaches 200 γ . The first diagram of the currents corresponding to maximum deviation of the H and Z components from normal (that is, to the moment of maximum development of the disturbance) shows a negative current eddy of considerable strength on the morning side of the polar cap ($I = 170 \times 10^4$ amp) and a weak eddy on the evening side. The middle-latitude eddies, positive on the morning side and negative on the evening side, are developed relatively well, but there are no currents flowing along the parallels of latitude and responsible for the D_{st} variations. At 14 hours the current strength in the polar and middle

latitude eddies weakened, and the polar eddy shifted to the night hours. The signs of the current eddies remained the same as at 123 hours. Thus the instantaneous distribution of the field of the polar storm is likewise in good agreement with the field of the averaged storm. The same picture of currents typical for polar storms is shown by the disturbances of 14 March and 4 July 1946. In all cases (except one), the polar part of the system consists of two eddies, a positive on the evening side and a negative on the morning side. The exception is the current system for 14 March 1946, 20 hours, on which the negative eddy moved over to the evening side. The morning eddy, as a rule is more intense than the evening eddy and is usually extended to the central part of the polar cap. Only in two cases (12 hours and 1530 hours, 4 July) did the evening eddy prove to be more intense. The middle latitude eddies have the opposite sign to the polar eddies: the morning is positive and the evening is negative. In intensity they are either both the same, or the evening eddy is stronger. In almost all cases the intensity of the middle latitude eddy is considerably less than the intensity of the polar eddies, and only at the beginning, or, on the contrary on the extinction of the disturbance, do the middle latitude and polar eddy become comparable in power. It was not possible in even a single case to draw even a single current line along the parallel, which would be due to a vector of disturbance equal for all meridians (D_{st} variations).

The form of the current lines, the intensity and locations of the centers of the eddies, fluctuate from instant to instant, and from storm to storm, within wide limits. Thus the center of the morning polar eddy is sometimes observed at 7 hours and is sometimes shifted to 2 - 3 hours. The position of the center of the evening eddy fluctuates within just as wide limits (from 15 to 19 hours). The line of maximum crowding together of the current lines is in all cases located between $\phi = 60^\circ$ and $\phi = 70^\circ$, regularly shifting to the lower latitudes with increasing disturbance. The greatest current intensity registered, $I = 170 \times 10^4$ amp (1230 hours, 7 March 1946) is about three times as intense as the current of the average bay (Chapter VI).

But the storm of 7 March 1946 is not particularly great; stronger disturbances are often encountered with a current strength probably much exceeding this amount. It follows from all that has been said that the penetration of corpuscles in the high latitudes always lead to the formation of a current system of a definite type. The most characteristic features of this system are: the formation of a powerful negative eddy on the morning side and in the central part of the polar zone, and the formation of a weaker positive eddy on the evening side. The fluctuations in the intensity, form, and position of these current eddies results in an infinite diversity of disturbances. But with all the multiplicity of the currents of the P-storms, the fundamental features of the system always persist, which is evidence of the definite regularities which the formation of these currents obeys.

Section 2. Worldwide Storms

The storm of 8 April 1947 is a moderate storm. The currents calculated for 22 and 23 hours, 8 April, characterized the first phase of the storm in elevated values of H . The current encircling the earth along the circles of latitude is directed eastward in both cases. At 22 hours, both polar eddies of the S_D variations show up rather distinctly on the diagrams, while, of the pair of middle latitude eddies, only the positive morning eddy still persists. During the course of an hour, the position of the eddies was considerably modified, and the polar evening eddy spread out to the middle latitudes as far as 40° , while the polar negative eddy occupied the central part of the polar cap. Three consecutive instants of the disturbance (7, 11, and 17 hours, 9 April, Fig.43) were selected in the negative phase of the storm, during which the D_{st} current was directed westward. From the current system of the S_D variations, two polar and the negative evening middle latitude eddy persisted for all these three instants.

The storm of 8 August 1946 is a small magnetic storm (with amplitudes $R_H = 70$ gammas at Sitka and $R_H = 25$ gammas at Honolulu) without great irregular fluctuations.

All the three instants of time for which the current systems were constructed are in the second phase of the storm. The system of currents of 22 hours, 8 August, consists of three current eddies in the polar cap and a current flowing along the circles of latitude in the middle and low latitudes. The negative eddy in the morning hours of the latitude zone 60 - 70° is the most intense; the weaker eddy of positive

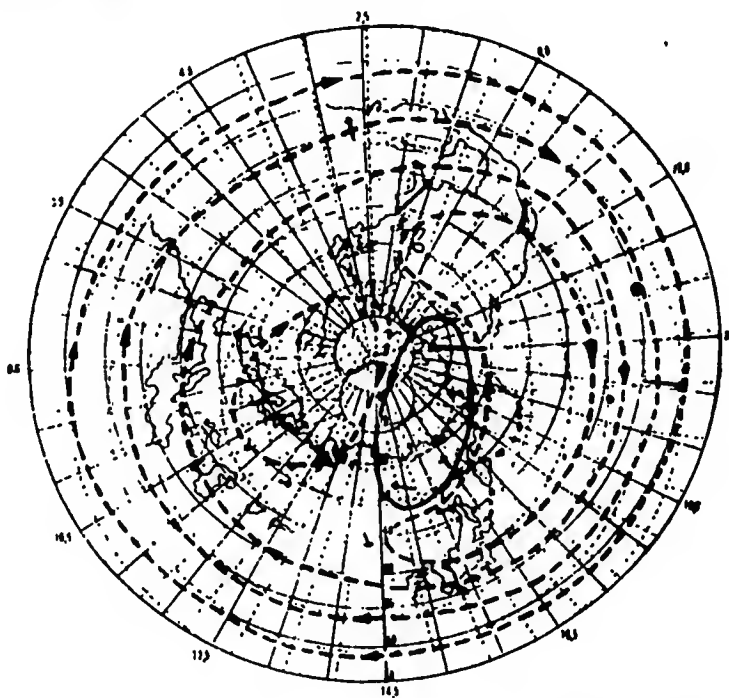


Fig.43a - The Worldwide Storm of 9 April 1947
0700 Hours

current is located at the center of the polar zone. In these eddies the pair of polar eddies of the S_D variations may be recognized. The third negative eddy on the afternoon side of the earth is in all probability the evening eddy of the middle latitude part of the S_D variation. The positive eddy on the morning hours paired with it is absent, neutralized by the negative current girdling the entire earth. This last current (presented on the basis of two stations, Honolulu and San Juan) gives an indication of the existence of D_{st} currents symmetrical with respect to the earth axis. For three instants of the storm of 8 August 1946, the D_{st} current is weak

($I \sim 10^4$ amp) and is noted only in the low latitudes. The configuration of the current lines varies considerably from hour to hour, but the general character of the distribution persists. From this hasty description it follows that the current lines of the storms of 8 April 1947 and 8 August 1946 may be considered as the result of the composition of the S_D and D_{st} systems.* The direction of the current, the ratio

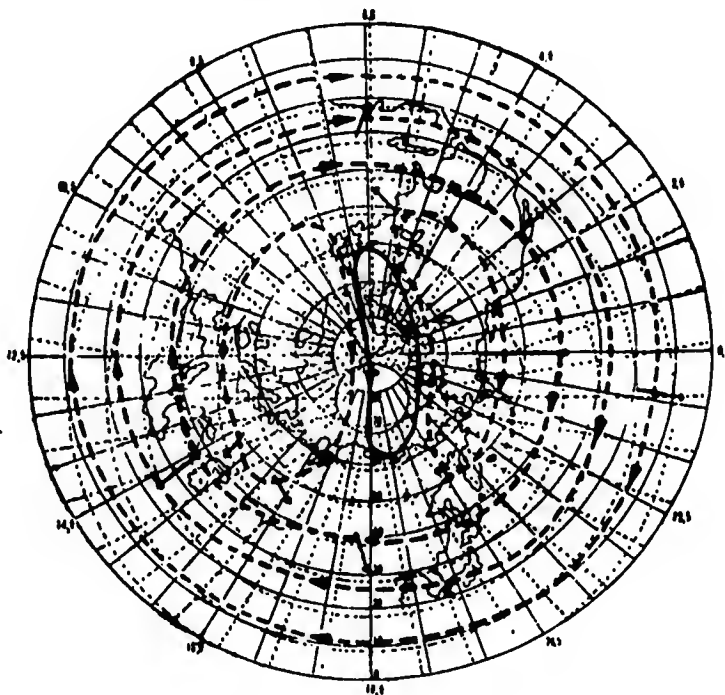


Fig.43b - Worldwide Storm of 9 April 1947

1100 Hours

of the corresponding intensities of the eddies, and the location of the centers of the eddies - all these features of the current system of a given disturbance find

* The current systems of Fig.43 have been calculated, for convenience, under the assumption that all the current flows in a spherical layer at the height of the ionosphere. However, as follows from the preceding, it is more probable that the D_{st} currents form an equatorial ring several earth-radii in size. For this reason the current maps that we have described are arbitrary, and they must not be considered as a proof that all the current actually does flow at one level.

explanation in the fluctuations of the current systems of the average D_{st} and S_D variations.

The principal features of the D_{st} and S_D current systems are likewise manifested in two other examples of disturbances discussed, 17 April and 5 June 1947. These storms are great storms and the intensity of the currents during them reaches 60 and 70×10^4 amp. The variation in the configuration of the current lines and the variation of the current intensity from hour to hour in both cases are very great, but the general character of the system remains unchanged.

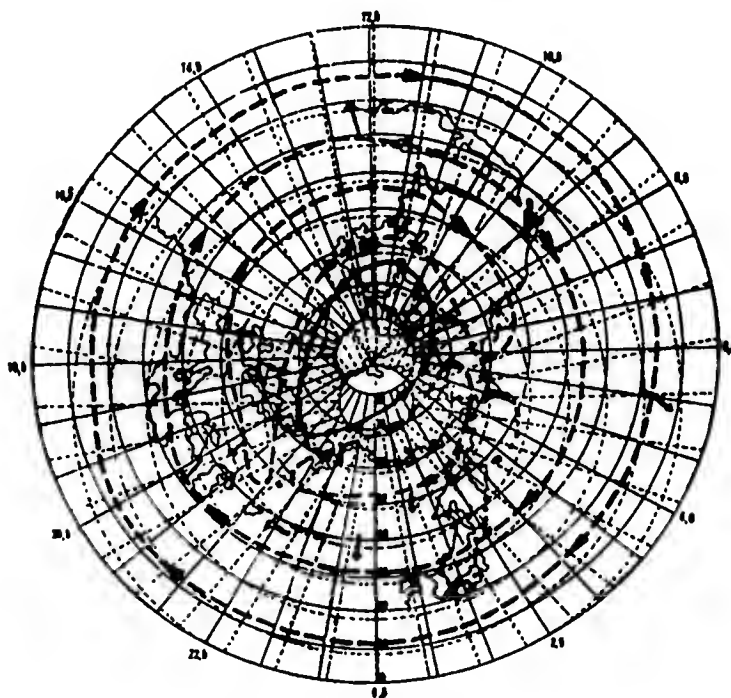


Fig.43c - The Worldwide Storm of 9 April 1947

1700 Hours

It follows from the four examples we have discussed that, in spite of the very complex and outwardly random course of worldwide magnetic storms, the field of disturbance, even at individual instants of time, obeys definite regularities which are well described by the average D_{st} and S_D variations. The multiplicity of the fluctuations of the magnetic elements during a storm is explained by the fluctuations of

POOR ORIGINAL

the parameters of these current systems and the superimposition on them of polar disturbances, the piling up of which gives an irregular and grotesque form to the variations of the magnetic elements. A comparison of diagrams for successive instants of one and the same storm clearly shows how the current systems are deformed (their configuration and intensity both vary), thereby producing the variations of the geomagnetic field.

CHAPTER X

THE INTERNAL PART OF THE DISTURBANCE FIELD

Section 1. The Inductive Origin of the Inner Part of the Field. Survey of the Results Obtained

It appears beyond question today that the part of the field of magnetic variations whose sources are located inside the earth is not independent; its existence is due to currents induced by the alternating field in the conducting regions of the earth. The study of this internal part is of great interest, since it is still the only source of our knowledge of the electromagnetic properties of the deep parts of the earth. The idea on which the induction theory of the internal part of the magnetic variations is based is very simple. Every external alternating magnetic field $E(t)$ induces, in a conductor of conductivity κ and magnetic permeability μ , magnetization (magnetic induction) and a certain distribution of currents (electromagnetic induction). The field of these currents (I') and of inductive magnetization (I'') can be calculated theoretically if the function $E(t)$ and the parameters κ and μ of the medium are known, that is,

$$I' + I'' = I(E, \kappa, \mu). \quad (1)$$

On the other hand, by substituting in eq.(1) the values of the external and internal fields known from the experimental data, the parameters κ and μ can be expressed in terms of E and I . In practice, however, the finding of $I(E, \kappa, \mu)$, and all the more the solution of the inverse problem, to find κ and μ from observations of

E and I on the earth surface, encounters great mathematical difficulties. The problem has been solved only for a few very special cases. Thus, Lamb (Bibl.40), developed a theory of electromagnetic induction in a sphere of uniform conductivity ($\kappa = \text{const}$) for the case when the field of $E(t)$ is a periodic function. Lamb's formulas, used by a number of authors (see (Bibl.9) for more details) in the analysis of the solar-diurnal variations (S_q), show that the earth could be represented as consisting of a conducting core ($\frac{\kappa}{\mu} = 10^{-12} - 10^{-13}$ CGSM), surrounded by a nonconducting shell 200 - 400 km thick.* A consideration of the diurnal variations does not enable us to determine the values of κ and μ separately, but it appears unlikely that μ in the deep parts of the earth should differ much from unity. To verify this proposition, Chapman and Whitehead undertook a qualitative investigation of the slow D_{st} variations. The potential of the field of induced magnetization (I'') should be expressed by the same harmonic as the induced field $E(T)$, and the ratio of the harmonic coefficients of the internal field to the external not depending on the rate of change of $E(t)$ (for more details, see Section 6). Therefore on the 5th to 10th day of a storm, when the variations of D_{st} are extremely slow, and, consequently, the influence of electromagnetic induction is very slight, I'' should exert most of the influence on the field observed at the earth surface. This influence decreases H and increases the Z component of the E field. For example, for $\mu = 10$, the expected effect should be equal to $\frac{3}{4} E$ in H and $\frac{3}{2} E$ in Z. During the first days of a storm, with rapid variation of D_{st} , the field of electromagnetic induction I' should have a great weight. This field, as is commonly known, is expressed by the same harmonics, but with reversed sign, that is, increasing H and decreasing Z. But Chapman and Whitehead (Bibl.40) found no substantial difference in the ratio of the observed H and Z of the D_{st} field on the first and subsequent days of a storm, which is evidence that magnetic induction plays a small part in the establishment of the inter-

* The term "core" here employed is not identical with the notion, generally adopted in geophysics, of the earth core, with a radius of $0.6R$.

nal field.

The rigorous solution of the inductive problem for an aperiodic field (for example the D_{st} field) involves major computational difficulties. For a sphere $\kappa = \text{const}$ this problem has been solved by Price, who found that to explain the ratio of E and I of the first harmonic of the D_{st} field it is necessary to assume different parameters for the earth, namely a thickness of 400 km for the nonconducting layer, and $\kappa = 4 \times 10^{-12}$. The most probable explanation of this disagreement would appear to be the phenomenon of the skin effect. Let us assume for simplicity that the field E is proportional to $\sin pt$. Then the magnetic flux f through any contour at a certain level in the earth will be proportional to $\sin pt$, that is, $f = f_0 \sin pt$, and the electromotive force due to it, $\varepsilon = -\frac{df}{dt} = -pf_0 \cos pt$, whence it follows that the current induced in this layer is proportional to p and κ . The field I' created by this current will neutralize the inducing field E and will prevent it from penetrating into deeper layers. The depth at which the full screening of the internal region from the field E takes place will be inversely proportional to the intensity of I' or ε , that is, proportional to $\frac{1}{\kappa p}$. Consequently the more rapid fluctuations of $E(t)$ will induce currents concentrated in a thinner surface layer of the earth, while to the slow fluctuations will correspond currents extending to great depths. Thus the increased value of κ and the increased depth of the nonconducting shell for D_{st} indicates that the currents of D_{st} penetrate deeper within the earth, and that increases toward the center of the earth. Accordingly, Lahiri and Price (Bibl.47) have made calculations for a model of the earth with a core of nonuniform conductivity, $\kappa = \kappa_0 \sigma^{-s} (\sigma = \frac{r}{a}$, where a = radius of core), which explains the ratio of the fields $\frac{I}{E}$ for both the S_q and the D_{st} variations. Calculations showed that for a depth of the order of 600 km, the κ differs little from the κ of dry rocks, i.e., it is 10^{-14} to 10^{-15} CGSM, and that below that level it strongly increases with the depth.

A number of authors have attempted to evaluate the field of currents induced in

the oceans and upper conducting layers of the earth crust. They have succeeded in finding that a uniform layer of seawater, 1.5 km thick, markedly changes the ratio $\frac{I}{E}$ observed on the earth surface (for instance, for P_3^2 , from 0.4 to 0.5). But the continents, alternating with the mainlands, reduce the effectiveness of the currents in the oceans, and as a result it may be considered that the internal parts of the S_q and D_{st} fields are almost entirely due to currents flowing in the deep parts of the earth. It goes without saying that for the more rapid variations of the magnetic field the influence of the surface currents is greater, and, in the case, for instance, of the pulsations, which are periodic fluctuations with a period of a few seconds, the upper conducting layers may possibly completely screen the conducting core.

S.Sh.Dolginov (Bibl.15) has obtained interesting results by using the spherical analysis of the noncyclical variations to evaluate the earth conductivity. Considering the noncyclical variations as the derivative of D_{st} and using the approximate Chapman-Whitehead formulas, Dolginov confirmed the value $\kappa = 4 \times 10^{-13}$ for a radius of the conducting core from 0.88R to 1.00R which had been obtained by Chapman from S_q data.

In 1949, A.N.Tikhonov (Bibl.31) found a new possibility of estimating the conductivity of the earth by using simultaneous observations of the geomagnetic variations and the earth currents. The equations relating the variations of the magnetic and electric vectors at a given point permit the determination of the conductivity and the thickness of the earth crust for different regions of the earth, and thereby yield material that is valuable for geotectonics and geology.

All the authors mentioned by us, except S.Sh.Dolginov, started out from one and the same experimental material, the spherical analysis of the D_{st} field performed by Chapman and Whitehead. Only the first term of the spherical series, the harmonic P_1 , was examined in this case. In view of this fact, the literature has repeatedly pointed out the necessity of repeating the evaluation of the parameters, using new

experimental materials. We performed such work on the basis of the separation of the disturbance field into E and I parts, as described in the preceding chapters, and the results of this work are given below.

Since the theory of induction in the form developed in the works of Lamb and Price can be successfully used only in cases when the E and I parts of the field are represented by series of special functions, the data on the S_D variations remained unused. It proved possible to employ only the D_{st} variations and the polar storms for the evaluation of κ . In the calculations based on D_{st} we used the formulas of Price for a homogeneous sphere and of Lahiri and Price for a sphere of nonuniform conductivity. Since the field of a polar storm was represented by a series of Bessel functions, the induction problem was solved in cylindrical coordinates in order to make the use of these data possible. For convenience, the exposition of the solution of this problem has been placed in a separate section (Section 2), while Sections 3 - 6 are devoted to the calculation of the conductivity from the data of D_{st} , and the results are discussed in Section 7.

Section 2. Solution of the Induction Problem in Cylindrical Coordinates

Assume that the earth, beginning at a certain depth z_1 , has the constant conductivity κ . The upper half-space (the upper layers of the earth and the atmosphere) constitute an ideal dielectric. Then the magnetic field may be described in the dielectric by the scale of potential v , and in the conductor by the vector potential \vec{A} , which, as shown by Lamb, satisfies the equations:

$$\Delta \vec{A} - a^2 \frac{\partial \vec{A}}{\partial T} = 0 \quad (2)$$

and

$$\text{div } \vec{A} = 0. \quad (3)$$

Here $a^2 = 4\pi\kappa\mu$, and T , as before, denotes Universal Time. The condition of continuity of the tangential components of the field H and of the radial component of

induction B at the surface of separation of the two media ($z = z_1$) enables us to find the constant a entering into the expression for vector potential, and thus to evaluate κ and μ . It is therefore necessary first of all to solve the system of equations (2) and (3), and, from the vector potential so found, to calculate the components of the vectors of induction and field intensity.

Putting $\vec{A} = R(r)\Phi(\varphi)(z)T(T)$, we may, without prejudice to the generality of the solution assume that $T(T) = e^{-inT}$, where in the case of aperiodic variations n is a real number, for aperiodic variations an imaginary number, and in the general case, a complex number. Denoting $R(r)\Phi(\varphi)Z(z)$ by \vec{A}_0 , we have

$$\left. \begin{aligned} \vec{A} &= \vec{A}_0 e^{-inT} \\ \frac{\partial \vec{A}}{\partial T} &= -\vec{A}_0 in e^{-inT} \end{aligned} \right\} \quad (4)$$

and

$$\Delta \vec{A}_0 + k^2 \vec{A}_0 = 0, \quad (5)$$

where

$$k^2 \cong in4\pi\kappa\mu = ina^2. \quad (6)$$

In curvilinear coordinates, the meaning of the symbol Δ of the vector is defined by the identity $\text{rot rot } \vec{F} = \text{grad div } \vec{F} = \Delta \vec{F}$, from which it follows that

$$\text{rot rot } \vec{A}_0 - k^2 \vec{A}_0 = 0. \quad (7)$$

In cylindrical coordinates, the r, φ, z components of eq.(7) are written as follows:

$$-\frac{1}{r^2} \left(\frac{\partial^2 A_\varphi}{\partial \varphi \partial r} - \frac{\partial^2 A_r}{\partial \varphi^2} \right) + \frac{\partial^2 A_z}{\partial z^2} + k^2 A_r = 0, \quad (8)$$

$$\frac{\partial^2 A_\varphi}{\partial z^2} + \frac{\partial}{\partial r} \left(\frac{1}{r} \frac{\partial r A_\varphi}{\partial r} \right) - \frac{\partial^2}{\partial r \partial \varphi} \frac{1}{r} A_r + k^2 A_\varphi = 0, \quad (9)$$

$$\frac{1}{r} \frac{\partial^2 r A_r}{\partial r \partial z} + \frac{1}{r} \frac{\partial^2 A_\varphi}{\partial \varphi \partial z} = 0. \quad (10)$$

Here A_φ and A_r denote the respective components \vec{A}_0 and $A_z = 0$, which corresponds

to the fact that the induced currents are assumed to be parallel to the plane $z = 0$.
Setting $R(r)\psi(\varphi) = Y(r, \varphi)$, $A_r = ZY_r$ and $A_\varphi = ZY_\varphi$, we have, from eq.(8):

$$-\frac{Z}{r^2} \left(\frac{\partial^2 Y_\varphi}{\partial \varphi \partial r} - \frac{\partial^2 Y_r}{\partial \varphi^2} \right) + Y_r Z'' + k^2 Y_r Z = 0$$

and

$$\frac{Z'}{Z} + k^2 - \frac{1}{r^2 Y_r} \left[\frac{\partial^2 Y_\varphi}{\partial \varphi \partial r} - \frac{\partial^2 Y_r}{\partial \varphi^2} \right] = 0,$$

whence

$$\frac{Z''}{Z} + k^2 = \lambda^2, \quad (11)$$

$$-\frac{1}{r^2 Y_r} \left[\frac{\partial^2 Y_\varphi}{\partial \varphi \partial r} - \frac{\partial^2 Y_r}{\partial \varphi^2} \right] = -\lambda^2. \quad (12)$$

Introducing the notation $\lambda^2 - k^2 = f^2$, we have

$$Z'' = f^2 Z \text{ and } Z = e^{-fz}. \quad (11')$$

Equation (10) is equivalent to the identity

$$\frac{\partial r Y_r}{\partial r} + \frac{\partial Y_\varphi}{\partial \varphi} = 0. \quad (10')$$

On replacing $\frac{\partial Y_\varphi}{\partial \mu}$ in eq.(12) by $\frac{\partial r Y_r}{\partial r}$, we have

$$\frac{r}{R} \frac{\partial^2 R_r}{\partial r^2} + \frac{1}{R} \frac{\partial r R_r}{\partial r} + \lambda^2 r^2 = -\frac{1}{\Phi_r} \frac{\partial^2 \Phi_r}{\partial \varphi^2} = \text{const} = h^2. \quad (13)$$

It follows from the right side of eq.(13) that

$$\Phi_r = \sin(h\varphi + \epsilon). \quad (14)$$

Putting $rR_r = \mathcal{Q}$ and $\lambda_r = \rho$ in the left side, we obtain after several transformations,

$$\rho^2 \mathcal{Q}'' + \rho \mathcal{Q}' + (\rho^2 - h^2) \mathcal{Q} = 0. \quad (15)$$

Equation (15) is the Bessel equation of order h , whose integral

$$\mathcal{Q} = c J_h(\rho) \text{ and } R_r = \frac{c}{r} J_h(\lambda r), \quad (16)$$

where c is a constant coefficient. It follows from eqs.(11', 14, and 16) that

$$A_r = ce^{-fz} \sin(h\varphi + \epsilon) \frac{1}{r} J_h(\lambda r). \quad (17)$$

Substituting eq.(17) and eq.(10"), we get

$$A_{\varphi} = \frac{c}{h} e^{-fz} \cos(h\varphi + z) \frac{\partial J_h(\lambda r)}{\partial r}. \quad (18)$$

From eq.(17) and eq.(18), which completely determine the vector \vec{A}_0 , we find the components of the magnetic induction $\vec{B} = \text{rot } \vec{A}$. For $T = 0$

$$B_r = -\frac{\partial A_{\varphi}}{\partial z} = \frac{c}{h} f e^{-fz} \cos(h\varphi + z) \frac{\partial J_h(\lambda r)}{\partial r}, \quad (19)$$

$$B_{\varphi} = \frac{\partial A_r}{\partial z} = -c f e^{-fz} \sin(h\varphi + z) \frac{1}{r} J_h(\lambda r), \quad (20)$$

$$B_z = -\frac{c\lambda^2}{h} e^{-fz} \cos(h\varphi + z) J_h(\lambda r). \quad (21)$$

It follows from eqs.(19) - (21) that the components of the vector $B(T)$ are the real parts of the expressions

$$B_r = \text{Re} \frac{cf}{h} e^{-fz - i(h\varphi + z) - inT} \frac{dJ_h(\lambda r)}{dr}, \quad (22)$$

$$B_{\varphi} = \text{Re} - i h \frac{cf}{h} e^{-fz - i(h\varphi + z) - inT} \frac{1}{r} J_h(\lambda r), \quad (23)$$

$$B_z = \text{Re} - \frac{c\lambda^2}{h} e^{-fz - i(h\varphi + z) - inT} J_h(\lambda r). \quad (24)$$

The field of the polar storm discussed in Chapter VI is a function of the local time t . Putting $h = n$ and $T + \varphi = t$ in eqs.(22) - (24), we have, for $Z = Z_1$:

$$H_r = \mu B_r = \frac{cf}{n} \mu e^{-fz_1 - i(n t + z)} \frac{dJ_n(\lambda r)}{dr}, \quad (25)$$

$$H_{\varphi} = \mu B_{\varphi} = -in \frac{cf}{n} \mu e^{-fz_1 - i(n t + z)} \frac{1}{r} J_n(\lambda r), \quad (26)$$

$$B_z = -\frac{c\lambda^2}{n} e^{-fz_1 - i(n t + z)} J_n(\lambda r). \quad (27)$$

In the nonconducting half-space, the potential of the field satisfies the Laplace equation and consequently may be represented, under the condition $h = n$, by the series

$$V = \text{Re} [E e^{-z\lambda - i(n t + \tau)} + I e^{z\lambda - i(n t + \tau)}] J_n(\lambda r), \quad (28)$$

where E , I , γ and ζ are known constants (cf. Table 17, Chapter VI). From eq.(28), for $Z = Z_1$:

$$H_r = \mu [Ee^{-z_1\lambda - i(n\gamma + \gamma)} + Ie^{z_1\lambda - i(n\gamma + \gamma)}] \frac{dJ_n(\lambda r)}{dr}, \quad (29)$$

$$H_\phi = -in\mu [Ee^{-z_1\lambda - i(n\gamma + \gamma)} + Ie^{z_1\lambda - i(n\gamma + \gamma)}] \frac{1}{r} J_n(\lambda r), \quad (30)$$

$$B_z = \lambda [-Ee^{-z_1\lambda - i(n\gamma + \gamma)} + Ie^{z_1\lambda - i(n\gamma + \gamma)}] J_n(\lambda r). \quad (31)$$

From the condition of the continuity of H_r or H_ϕ for $Z = Z_1$, we get, by equating eq.(22) and eq.(17), or eq.(22) and eq.(23), and putting $\mu = 1$:

$$\frac{c}{n} \sqrt{\lambda^2 - ina^2} e^{-\sqrt{\lambda^2 - ina^2} z_1 - i\epsilon} = Ee^{-z_1\lambda - i\gamma} + Ie^{z_1\lambda - i\gamma}. \quad (32)$$

From the condition of continuity of B_z on $Z = Z_1$, we have

$$-\frac{c}{n} \lambda e^{\sqrt{\lambda^2 - ina^2} z_1 - i\epsilon} = -Ee^{-z_1\lambda - i\gamma} + Ie^{z_1\lambda - i\gamma}. \quad (33)$$

On dividing eq.(32) by eq.(33) to eliminate the unknown constants c and ϵ , we have

$$-\frac{\sqrt{\lambda^2 - ina^2}}{\lambda} = \frac{Ee^{-z_1\lambda - i\gamma} + Ie^{z_1\lambda - i\gamma}}{-Ee^{-z_1\lambda - i\gamma} + Ie^{z_1\lambda - i\gamma}}. \quad (34)$$

Equation (34), connecting these complex quantities with each other, is entirely sufficient for the determination of the constants a^2 and Z_1 in which we are interested. Introducing the notation

$$\frac{I}{E} e^{2z_1\lambda} = x \text{ and } \frac{na^2}{\lambda^2} = \alpha,$$

we get

$$1 - i\alpha = \frac{(1 + xe^{i\delta})^2}{(1 - xe^{i\delta})^2}. \quad (35)$$

Separating the real and imaginary parts in eq.(35), we get

$$1 = \frac{(1 - x^2)^2 - 4x^2 \sin^2 \delta}{(1 - 2x \cos \delta + x^2)^2}, \quad (36)$$

$$-a = \frac{4x(1-x^2)\sin\delta}{(1-2x\cos\delta+x^2)^2} \quad (37)$$

It is easy to obtain a computational expression for x from eq.(36):

$$x = \frac{1 + \sin\delta}{\cos\delta} \quad (38)$$

From eq.(37) we have

$$x = \frac{x(x^2-1)\sin\delta\lambda^2}{\rho^2\pi\epsilon(1+x^2-2x\cos\delta)^2} \quad (37')$$

The coefficient $\epsilon = \frac{2}{24 \times 60 \times 60} = \frac{1}{1.5} \cdot 10^{-4}$ is introduced in connection with the fact that the time t is indicated in eqs.(25) - (31) not in angular measure but in seconds. The numerical value of the coefficient ρ (cf. Chapter VI) is 4.5×10^3 km, or 4.5×10^8 cm.

From eq.(37') and eq.(38) the quantities x and z_1 may be found, if the field observed on the earth surface is separated into an external and an internal part. Thus the solution of the induction problem in cylindrical coordinates leads to very simple formulas which are entirely convenient for practical calculations. *

The values of x and z_1 calculated from the data of Table 18 are presented in Table 28. For five terms I did not succeed in getting a reasonable value of the conductivity, owing to negative values of the numerator in eq.(37), but in evaluating the results it must be borne in mind that the values of the coefficients E and I for a few terms would hardly exceed the margin of accuracy of the analysis.

The results obtained are discussed in more detail in Section 7.

* After these calculations had been completed, I learned of the work by Yu.D. Kalinin (Bibl.17) in which the plane problem is solved in rectangular coordinates, and still simpler formulas for determining x and z_1 are obtained. Kalinin's formulas, however, are applicable only in the case where the field depends on a single argument.

Table 28

	$n \backslash m$	1	2	3	4	5
χ , CGSM	1	$8 \cdot 10^{-13}$	$14 \cdot 10^{-13}$	—	$1 \cdot 18 \cdot 10^{-14}$	$2 \cdot 10^{-12}$
z , KM	1	144	256	—	198	45
χ , CGSM	2	—	—	$7 \cdot 10^{-15}$	—	—
z , KM	2	—	12!	103	—	81

Section 3. Determination of the Earth Conductivity from the Data of the First Harmonic of D_{st} (the Lamb Model)

If the alternating magnetic field of origin external to the earth surface is represented by the sum of terms of the form

$$RE_n^{mh} (1 - e^{-\frac{r}{R}}) \left(\frac{r}{R}\right)^n S_n^m, \quad (39)$$

then, under the condition that the conductivity of the earth is uniform, to each term E_n^{mh} will correspond a term in the inductive field, represented by the same harmonic:

$$I_n^{mh}(t) = \left(\frac{r}{R}\right)^{-n-1} E_n^{mh} \varphi_n^{mh}(t) S_n^m. \quad (40)$$

Here $\varphi_n^{mh}(t)$ is a function expressing the time dependence of I_n^{mh} and represented by the infinite series

$$\varphi_n^{mh}(t) = -\frac{nq^{2n+1}}{n+1} 2(2n+1)(k_n^{mh})^2 \times \sum_{s=1}^{\infty} \frac{e^{-\frac{r}{R_{ns}} t} - e^{-\frac{r}{R} t}}{(k_{ns}^{mh})^2 [(k_n^{mh})^2 - (k_{ns}^{mh})^2]}. \quad (41)$$

The constants k^2 and α are connected with each other by the relation

$$k^2 = -4\pi\alpha \quad (42)$$

and $q = \frac{a}{R}$, where a is the radius of the conducting core. The constants k_{ns}^{mh} and α_{ns}^{mh} are not arbitrary, but satisfy the following conditions:

$$-(k_{ns}^{mh})^2 q^2 a^2 = (\alpha_{ns}^{mh})^2 = 4\pi\alpha_{ns}^{mh} q^2 a^2 \quad (43)$$

and

$$\int_{n-\frac{1}{2}}^J (x_{ns}^{mh}) = 0. \quad (44)$$

The terms containing $e^{-\alpha_{ns}^{mh} t}$ are introduced in the expression for $\varphi(t)$ by Price in accordance with the fact that the equations describing the boundary conditions (analogous to eq.(30) and eq.(31) of Section 2) have solutions even in the absence of the induced field ($E_n^{mh} = 0$). These solutions indicate the existence of free electric systems which are damped by an exponential law.

In considering the periodic fluctuations, which do not require the satisfaction of initial conditions, the free systems may be left out of consideration, but in solving the problem of induction by aperiodic variations, these systems must be included in the equations of the initial conditions. The failure to allow for the free systems led Chapman and Whitehead to erroneous conclusions.

The imposition of initial conditions (vanishing of the total field for $t = 0$) causes the terms containing $e^{-\alpha_s t}$ to obey eq.(43) and eq.(44).

For convenience in calculating series eq.(41), Price proposed selecting, for the representation of the induced field, the constants α_n^{mh} , equal to a certain α_s satisfying the conditions eq.(43) and eq.(44). In that case, putting $\alpha_n^{mh} = \alpha_p$, we must omit the term $s = p$ from the sum eq.(41) and add the term

$$\frac{nq^{2n+1}}{n+1} \frac{2(2n+1)te^{-\alpha_p t}}{q^2 a^{24\pi x}}.$$

Fixing our attention on one term of eq.(40), and omitting the indexes n , m , and h in eq.(41), we have

$$\begin{aligned} \varphi_p(t) &= \frac{2n(2n+1)}{n+1} q^{2n+1} \left[\frac{te^{-\alpha_p t}}{4\pi x q^2 a^2} - \sum_{s=1}^{\infty} \frac{\alpha_p (e^{-\alpha_s t} - e^{-\alpha_p t})}{\alpha_s q^2 a^2 (k_p^2 - k_s^2)} \right] = \\ &= \frac{2n(2n+1)q^{2n+1}}{n+1} \left[\frac{At}{\pi^2} e^{-\alpha_p t} - x_p^2 \sum_{s=1}^{\infty} \frac{e^{-\alpha_s t} - e^{-\alpha_p t}}{x_s^2 (x_s^2 - x_p^2)} \right], \end{aligned} \quad (41')$$

$$\text{where } A = \frac{\pi}{4\pi x q^2 a^2}$$

Chapman and Price performed their calculations for the case $n = 1$, for which eq.(44) is transformed into

$$I_{\frac{1}{2}}(x) = \frac{\sin x}{\sqrt{\pi x}} = 0 \text{ and } x = s\pi, \quad (45)$$

where s takes on the series of successive values 0, 1, 2...

Under this condition, on the basis of eq.(43), we have

$$k_s^2 = -\frac{s^2\pi^2}{q^2a^2}; \quad \alpha_s = \frac{s^2\pi}{4\pi q^2a^2} = s^2A \quad (46)$$

and

$$\varphi_p(t) = \frac{3q^2}{\pi^2} \left[\left(At + \frac{9-2p^2\pi^2}{12p^2} \right) e^{-p^2At} - p^2 \sum_{s=1}^{\infty} \frac{e^{s^2At}}{s^2(s^2-p^2)} \right]. \quad (47)$$

To solve our problem, which is to find κ and q , we must calculate the value of $\varphi(t) = \frac{I(t)}{E}$ from values of I and E known on the earth surface, and must then by

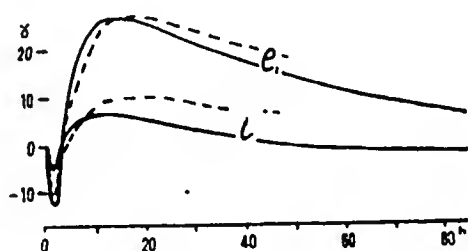


Fig.44 - Coefficients of Spherical Analysis of the D_{st} Variations (after Chapman)

— observed value;
---- calculated values

some numerical or graphical method determine q and κ from eq.(47). In view of the extreme complexity of this method, Chapman and Price attempted to satisfy the observed values of $\frac{I(t)}{E}$ calculating $\varphi(t)$ from the values of q and κ found on the basis of the S_q variations ($q = 0.96, \kappa = 4 \times 10^{-13}, A = 5.7 \times 10^{-6}$). The poor agreement between the calculated and observed values of $I(t)$ (cf. Fig.44) forced them to assume that to the D_{st} variations correspond greater depths of

penetration of the currents ($q = 0.94$) and greater values of the conductivity ($\kappa = 44 \times 10^{-13}$). Evaluating α and q from the data of the spherical analysis of D_{st} performed by us, we considered it more advisable to begin the tests of the calculation of $I(t)$ with the values of κ and q proposed by Chapman. For $\kappa = 4 \times 10^{-12}$ CGSM,

we found the value $\Lambda = 5 \times 10^{-17}$, or, if t is expressed in hours, then $\Lambda \approx 2 \times 10^{-3}$. The time dependence of E_1 so obtained (cf. Table 6, Chapter III and Fig. 45) was approximated by four terms of the form $a_s(1 - e^{-s^2 t})$, whose coefficients a_s are pairwise equal, i.e.,

$$E_1(t) = -a_{1,2}(e^{-s_1^2 \Lambda t} - e^{-s_2^2 \Lambda t}) + a_{3,4}(e^{-s_3^2 \Lambda t} - e^{-s_4^2 \Lambda t}), \quad (48)$$

where $s_1 < s_2$, $s_3 < s_4$, and $s_4 < s_1$. Such a selection of constants assures the representation by eq. (48) of the first and second phases of the magnetic storm (the terms s_1 and s_2 being mainly responsible for the first phase and s_3 and s_4 for the second).

The most favorable numerical values of s and a were found in the following way. Denoting the value of $E(t)$ for $t > 5$ hours by E_{II} , we have

$$E_{II} \cong a_{3,4}(e^{-s_3^2 \Lambda t} - e^{-s_4^2 \Lambda t}), \quad (49)$$

$$\frac{dE_{II}}{dt} = a_{3,4}(-x\Lambda e^{-x\Lambda t} + y\Lambda e^{-y\Lambda t}), \quad (50)$$

where $x = s_3^2$ and $y = s_4^2$. E_{II} reaches its maximum value $E_{II \max} = 55$ at $t = 20$ hours, whence we have the two equations:

$$x\Lambda e^{-20\Lambda x} = y\Lambda e^{-20\Lambda y}, \quad (51)$$

$$55 = a_{3,4}(e^{-20\Lambda x} - e^{-20\Lambda y}). \quad (52)$$

As the third equation necessary for the unique determination of x , y , and $a_{3,4}$, let us take the value of E_1 at $t = 40$ hours:

$$35 = a_{3,4}(e^{-40\Lambda x} - e^{-40\Lambda y}). \quad (53)$$

It follows from eqs. (51) - (53) that the pair $x = 16$ and $y = 36$ will be most favorable, whence $s_3 = 4$ and $s_4 = 6$; the $a_{3,4}$ corresponding to them is 190. The coefficients $a_{1,2} = 200$, $s_1 = 13$ and $s_2 = 18$ were found in a completely analogous way.

The formula so obtained

$$E_1 = 200 (e^{-0.34t} - e^{-0.05t}) + 190 (e^{-0.032t} - e^{-0.072t}) \quad (54)$$

approximates the observed relation $E_1(t)$ rather well. The observed values of $E_1(t)$ are shown on Fig.45 by the solid lines, while those calculated by eq.(54) are shown

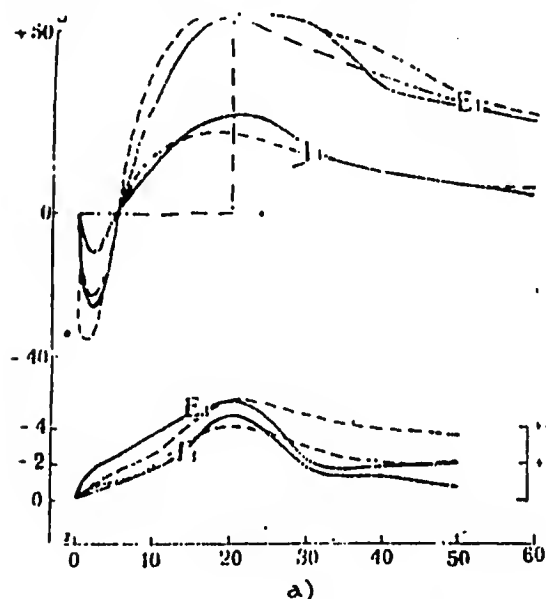


Fig.45 - Coefficients of Spherical

Analysis of D_{st} Variations

(Analysis II)

a) Hours

by the dashed lines.

The calculations of the induced field of I_1 , corresponding to the field E_1 , thus led to the calculation of four functions by eq.(47): $\varphi_4(t)$, $\varphi_6(t)$, $\varphi_{13}(t)$, and $\varphi_{18}(t)$.

The calculations were made with accuracy to the eight term of the series, which provided the fifth place in the value of $\varphi(t)$. The resulting function

$$I_1(t) = -a_{18,13}(\varphi_{18} - \varphi_{13}) + a_{6,4}(\varphi_6 - \varphi_4) = 200(\varphi_{13} - \varphi_{18}) + 190(\varphi_6 - \varphi_4) \quad (55)$$

is shown on Fig.45 by the dashed curve. It corresponds to the observed I_1 (the solid curve) considerably better than the analog-

ous curve calculated by Chapman and Whitehead (cf.Fig.44).

Thus the calculations above presented confirm Chapman's hypothesis that the values $q = 0.94$ and $\kappa = 4 \times 10^{-12}$ well correspond to the first harmonic D_{st} .

Section 4. Determination of the Constants q, s, κ_0 (Lahiri Model)

The values found for q and κ are in good agreement with those previously calculated by us on the basis of the S_q variations (Bibl.9) $q \cong 0.935$ and $\kappa = 5 \times 10^{-12}$. But this agreement can hardly be regarded as an argument in favor of the correctness of the assumption of a uniform conductivity for a core of radius qR . An explanation

of this agreement might rather be that in both cases variations of about the same velocities were investigated (in the case of S_q , the gradients were of the order of $2 - 3 \gamma$ an hour, in the case of D_{st} , 3γ an hour on the first day of the storm and 1γ an hour on the second day), and consequently gave information about one and the same layers of the earth. In view of this it appeared advisable to evaluate the earth conductivity in accordance with the Lahiri model ($q, \kappa = \kappa_0 \rho^{-s}$). Lahiri and Price (Bibl.47) selected the constant coefficients q, κ_0, s such that they satisfied the ratio of the amplitudes and phase difference of the harmonic $P_3^2 S_q$, and then separated, from the series so obtained, those values best corresponding to the ratio $\frac{1}{E}$ for $P_1 D_{st}$. In contrast to this method of calculation, we made simultaneous use of the data of several harmonics of S_q and $P_1 D_{st}$, which enabled us to set up the number of equations sufficient for the determination of all the coefficients.

It follows from the Lahiri formulas that if the inducing part of the periodic field is represented by the expression

$$E(t) = E_n^m e^{i(\omega_m t + \phi_n^m)}, \quad (56)$$

and the induced part by

$$I(t) = I_n^m e^{i(\omega_m t + \phi_n^m)}, \quad (57)$$

then (omitting the indexes n and m), we have

$$\frac{I}{E} = \text{mod } N(i\alpha), \quad (58)$$

$$j - \epsilon = \arg N(i\alpha), \quad (59)$$

where

$$N(i\alpha) = \frac{nq^{2n+1}}{n+1} \frac{\Gamma(1-\nu)}{\Gamma(1+\nu)} \left(\frac{x}{2}\right)^{2\nu} \left(\cos \frac{\nu\pi}{2} + i \sin \frac{\nu\pi}{2}\right), \quad (60)$$

$$\nu = \frac{2n+1}{s-2}, \quad (61)$$

$$x = \frac{4Rq \sqrt{\pi \kappa_0 a_m}}{s-2}, \quad (62)$$

$$a_m = m^2$$

and

$$\xi = \frac{2\pi}{24 \cdot 60 \cdot 60} \quad (63)$$

Equation (60) is approximate, and is true for $\nu < 1$ and small enough values of κ . Denoting $\frac{l_n^m}{l_n^m}$ by f_n^m , we have

$$f_n^m = \frac{nq^{2n+1}}{n+1} \frac{\Gamma(1-\nu)}{\Gamma(1+\nu)} \left(\frac{x}{2}\right)^{2\nu} = \frac{nq^{2n+1}}{n+1} \frac{\Gamma(1-\nu)}{\Gamma(1+\nu)} \left(\frac{2Rq\sqrt{\pi x_0 m \xi}}{s-2}\right)^{\frac{2(2n+1)}{s-2}} \quad (64)$$

Selecting from among the coefficients of the expansion of S_q to a series in spherical functions, two terms with the same indexes n and different orders m_1 and m_2 , we obtain, on the basis of eq.(64):

$$\frac{f_n^{m_1}}{f_n^{m_2}} \dots \left(\frac{m_1}{m_2}\right)^{\frac{2n+1}{s-2}} \quad (65)$$

Equation (65) allows us to evaluate s from known $f_n^{m_1}$ and $f_n^{m_2}$. From Table (15) of the above cited work (Bibl.9), it follows that $f_2^1 = 0.43$, $f_3^1 = 0.38$, $f_2^2 = 0.53$, $f_3^2 = 0.43$.

Thus,

$$\frac{f_2^1}{f_2^2} = \frac{1}{2} \frac{s}{s-2} \text{ and } \frac{f_3^1}{f_3^2} = \frac{1}{2} \frac{7}{s-2} \quad (66)$$

The first of the eq.(66) leads to the value $s \approx 23$, the second to the value $s \approx 33$, which allows us to take the mean value $s \approx 26$.

Putting in eq.(64), $n = 2$, $m = 1$, $f_2^1 = 0.43$ and $\nu = 0.21$, we obtain the following equation connecting the unknown q and κ_0 with each other:

$$\lg \kappa_0 = -13.27 - 25.70 \lg q. \quad (67)$$

To obtain the second equation for the determination of q and κ_0 , let us turn to $P_{1D_{st}}$. The formulas obtained by Lahiri are sufficiently convenient only in the case where the external, inducing field is approximated by an exponential function and

the unique Heaviside function*

$$E(t) = Ae^{-\alpha t} H(t), \quad (68)$$

where $H(t) = 0$ for $t < 0$, and $H(t) = 1$ for $t \geq 0$.

In this case the function $\varphi(t)$ (for its definition, see Section 3) is represented by the infinite series

$$\begin{aligned} \varphi(t) = & \frac{nq^{2n+1}}{(n+1)\Gamma(1+\nu)} \left\{ \left(\frac{\tau}{4t}\right)^\nu M_{-\nu}(at) + 2\left(\frac{\tau}{4t}\right)^{1+\nu} M_{-1-\nu}(at) + \dots + \right. \\ & \left. + \frac{2[\Gamma(1-\nu)]^2}{\Gamma(2+\nu)\Gamma(1-2\nu)} \left(\frac{\tau}{4t}\right)^{1+2\nu} M_{-1-2\nu}(at) + \dots \right\}, \end{aligned} \quad (69)$$

where $\tau = \frac{16\pi\eta^2 q^2 \kappa_0}{(s-2)^2}$ and $M_{-\lambda}$ is the confluent hypergeometric function

$$M_{-\lambda}(at) = 1 - \frac{at}{1-\lambda} + \frac{(at)^2}{(1-\lambda)(2-\lambda)} - \dots \quad (70)$$

The series eq.(69) and eq.(70) are convergent for small values of $\frac{\tau}{4t}$ and at . For the calculation of $\varphi(t)$ by eq.(69), the observed curve of $E_1(t)$ was replaced by the curve

$$E_1(t) = Ae^{-\alpha(t-20)} H(t),$$

repressed in Fig.45 by the dashed (dash-dot) line.

Here $H(t) = 0$ for $t < 20$; $H(t) = 1$ for $t \geq 20$ hours.

Starting out from the values $E_1(20 \text{ hours}) = 55$ and $E_1(60 \text{ hours}) = 25$, the numerical values of the parameters were found: $A = 55$ and $\alpha = 0.02$ (if t is expressed in hours).

The approximate formula so obtained

$$E_1(t) = 55e^{-0.02(t-20)} H(t) \quad (71)$$

(the broken line in Fig.45) satisfactorily represents the observed curve for $t > 20$

* For convenience of exposition, the notation in the Lahiri formulas has been modified, and in addition, the misprints have been corrected.

hours. The replacement of the smooth variation of the values of E_1 during the first phase of the storm by a sudden increase at the moment of the maximum should not, in Lahiri's opinion, strongly distort the subsequent results. For assigned values $n = 1$, $s = 26$ and $\alpha = 0.02$, we get, for the instant $t = 30$ hours (that is, $t - t_0 = 10$ hours) the following numerical values of the quantities entering into eq.(69):

$$\tau = 3,5 \cdot 10^{16} q^2 x_0, v = 0,12, M_{-1,12} = 2,33, M_{-0,12} = 0,795, M_{-1,24} = 1,828, \frac{\tau}{4(t-t_0)} = 0,25 \cdot 10^{18}.$$

Confining ourselves in eq.(69) to three terms of the series, and bearing in mind that $\Phi(30 \text{ hours}) = \frac{18}{55} = 0.33$, we have

$$0,62 = 9,8 x_0^{0,12} q^{3,24} + 2,72 \cdot 10^3 x_0^{1,12} q^{5,24} + 4,58 \cdot 10^{14} x_0^{1,24} q^{5,48}. \quad (72)$$

By graphic solution of eq.(67) and eq.(72) we get $q = 0.925$ and $x_0 = 4.0 \times 10^{-13}$.

If the data for the term $P_2^2 S_q$ are used in eq.(64), then $q = 0.909$ and $x_0 = 4.0 \times 10^{-13}$.

Thus an investigation of the D_{st} and S_q variations has shown that if we start out from the Lahiri model of the earth, then the conductivity of the core varies by the law

$$x = 4,0 \cdot 10^{-13} \rho^{-26}, \quad (73)$$

Its radius is $0.91R - 0.92R$, and the thickness of the nonconducting upper shell $d = 500 - 600 \text{ km}$.

Section 5. Allowance for the Upper Conducting Layer

As stated in Section 1, Whitehead and Lahiri considered the question how much the parameters of the core would be modified if we allow for the effect of the currents induced in the upper conducting layers of the earth (oceans and wet soil). They found the following formulas. If the conductivity of the upper spherical shell is κ_1 , the radius of its lower surface is q_1 and its thickness $\partial = (1 - q_1)R$, then the field in the nonconducting layer under the shell ($q_1 > \frac{r}{R} > q$) is connected with

POOR ORIGINAL

the field of the earth surface by the equations:

$$\left. \begin{aligned} E_i &= E - \frac{C_0}{n} \frac{d}{dt} [nE - (n+1)I] \\ I_i &= I - \frac{C_0}{n+1} \frac{d}{dt} [nE - (n-1)I] \end{aligned} \right\} \quad (74)$$

Here E_i denotes the field of origin external with respect to the surface $q_1 R$, I_i the internal field, E and I , as before, respectively the external and internal fields observed on the surface $r = R$, and

$$C_0 = \frac{4\pi R}{2n+1} \partial x_1. \quad (75)$$

The parameters of the core may be calculated in this case by the formulas of Section 4, if the values of E_i and I_i are used instead of the quantities E and I . We give below the calculations of the errors introduced in allowing for the upper conducting layers in the evaluations of s , q , and κ_0 , obtained by us.

If the field observed on the earth surface is a periodic function of time (cf. eq.(56) and eq.(57),

$$E(t) = E_n^m e^{i(\epsilon_m t + \epsilon_n^m)}; \quad I(t) = I_n^m e^{i(\epsilon_m t + \epsilon_n^m)},$$

then eqs.(74) are reduced to the form:

$$E_i = E e^{i(\epsilon_m t + \epsilon)} - \frac{C_0 i \epsilon_m}{n} \{ n E e^{i(\epsilon_m t + \epsilon)} - (n-1) I e^{i(\epsilon_m t + \epsilon)} \}, \quad (76)$$

$$I_i = I e^{i(\epsilon_m t + \epsilon)} - \frac{C_0 i \epsilon_m}{n+1} \{ n E e^{i(\epsilon_m t + \epsilon)} - (n+1) I e^{i(\epsilon_m t + \epsilon)} \}. \quad (77)$$

Here, to save space, the indices n and m after the quantities ϵ and j are omitted.

Equation (76) allows us, after several transformations, to calculate, from assigned values of $f = \frac{I}{E}$ and $\epsilon - j$, the values of $f_i = \frac{I_i}{E_i}$ and $\epsilon_i - j_i$. We give below the values of f_i for four harmonics obtained under the assumption that the conducting shell consists of a continuous ocean, 1 km deep, of conductivity $\kappa_1 = 5 \times$

$\times 10^{-11}$ CGS ($\kappa_1 \partial = 5 \times 10^{-6}$ and $C_0 \alpha_m = 4\pi R \kappa_1 \partial \xi \frac{m}{2n+1} = 1.3 \frac{m}{2n+1}$):

m, n	1,2	2,3	2,2	1,3
f_i	0,42	0,40	0,43	0,34

A comparison of the values f_i so obtained with the initial values of f shows that allowing for the conductivity of the oceans in all cases decreases the ratio $\frac{1}{E}$.

The evaluation of the parameter s from corrected data, performed as described in Section 4, yielded the following results: from a comparison of f_3^2 and f_3^1 , $s = 30$; from f_2^1 and f_2^2 , $s > 100$.

The latter value was rejected owing to the unreliable value $j_2^2 - \epsilon_2^2 = -15^\circ$, and for convenience of calculations, $s = 32$ was taken. A recalculation of eq.(64) with the new values of the constants:

$$v = 0,17, \frac{x}{2} = 0,62 \cdot 10^6 q \sqrt{x_0}, f_2^1 = 0,42,$$

$$v = 0,23, \frac{x}{2} = 0,89 \cdot 10^6 q \sqrt{x_0}, f_3^2 = 0,40$$

gave the following relations:

$$\left. \begin{aligned} \text{for } P_2^1 \lg x_0 &= -13,31 - 31,41 \lg q \\ P_3^2 \lg x_0 &= -13,61 - 32,44 \lg q \end{aligned} \right\} \quad (78)$$

Allowance was made for the influence of the surface currents on the D_{st} variations in the following manner. The internal part of the first harmonic was represented by the approximate formula

$$I_1 = 25e^{-0,04(t-20)} \quad (79)$$

(time in hours).

For $n = 1$,

$$\begin{aligned} D &= \frac{d}{dt} [nE - (n+1)I] = \frac{dE_1}{dt} - 2 \frac{dI_1}{dt} = \\ &= 3,1 \cdot 10^{-4} e^{-0,02(t-20)} + 5,6 \cdot 10^{-4} e^{-0,04(t-20)}, \\ C_0 &= 1,34 \cdot 10^6, \end{aligned}$$

$$C_0 D = 4,2 e^{-0,02(t-20)} + 7,5 e^{-0,04(t-20)}.$$

For $t = 20$ hrs $C_0 D = +3,3$ $E_i = 55 - 3,3 = 52,$
" $t = 30$ hrs $C_0 D = +1,6$ $E_i = 45 - 1,6 = 43,$
" $t = 60$ hrs $C_0 D = -0,4$ $E_i = 25 + 0,4 = 25.$

Whence E_i may be approximated by the expression

$$E_i = 52 e^{-0,018(t-20)}. \tag{80}$$

The revised value of $\varphi(t)$ for $t = 30$ hours is completely identical with the previous value. Indeed, for $t = 30$ hours, $I_i = 18 - 0.8 = 17$, and $\varphi(30 \text{ hours}) = \frac{17}{52} = 0.33.$

For the new values of the constants ($\nu = 0.1, \alpha = 0.018, \tau = 2.3 \times 10^{-16} \kappa_0 q^2$), the numerical quantities entering into eq.(69) are somewhat modified, and q and κ_0 are connected with each other by the following equation:

$$0,67 = 10,8 \kappa_0^{0,1} q^{3,2} + 1,04 \cdot 10^{13} \kappa_0^{1,1} q^{5,2} + 9,14 \cdot 10^{13} \kappa_0^{1,2} q^{5,4}. \tag{81}$$

On solving eq.(81) in turn by the first and second equation of eqs.(78), we get the following results:

	P_2^1	P_3^2
$q \dots \dots \dots$	0,949	0,921
$\kappa_0 \dots \dots \dots$	$2,5 \cdot 10^{-13}$	$3,7 \cdot 10^{-13}$

Since the mean value of κ_0 for the upper layers of the earth is obviously less than the value 5×10^{-6} CGS taken by us, the most probable values of the parameters q and κ_0 may be expected to lie between the above values and those calculated in the preceding Section.

Section 6. External and Internal Parts of the Harmonic P_3 of the D_{st} Field

In the present Section we shall discuss the application of the Lamb-Price induction theory to the third order harmonic of the D_{st} field. From eq.(42), which

holds for the case $\mu = 1$, it follows that $\varphi(t) > 0$, since all terms of the series

$$\sum_{s=1}^{\infty} \frac{e^{-\alpha_s t} - e^{-\alpha_p t}}{x_s^2 (x_s^2 - x_p^2)}$$

are always < 0 .

Indeed: for $s < p$, $\kappa_s^2 < \kappa_p^2$, and $\alpha_s < \alpha_p$, consequently $e^{-\alpha_s t} - e^{-\alpha_p t} > 0$, and $\kappa_s^2 - \kappa_p^2 < 0$; for $s > p$, $\kappa_s^2 > \kappa_p^2$ and $\alpha_s > \alpha_p$, consequently $e^{-\alpha_s t} - e^{-\alpha_p t} < 0$, and $\kappa_s^2 - \kappa_p^2 > 0$.

From this it follows that each term of the potential of the induced fields $I_n^{mh}(t)$ will be of the same sign as the term of the inducing field $E_n^{mh} (1 - e^{-\alpha_n t})$ corresponding to it, and the ratio $\frac{I_n^{mh}}{E_n^{mh}}$ for any instant t must lie within the limits*

$$0 < \frac{I_n^{mh}}{E_n^{mh}} < 1.$$

Accordingly, the negative ratio $\frac{I}{E}$ for the harmonic P_3 (cf. Table 8) is very surprising. The data obtained earlier by other authors (cf. Table 8), however, do not contradict our results. It will be seen from the Table that the negative values of $\frac{I}{E}$ for the harmonics P_3 and P_7 are also obtained by Mc.Nish in the spherical analysis of D_m . The values of the coefficients E and I for the third and fifth harmonics in the Chapman-Whitehead analysis are at the limit of accuracy of the analysis. But all the same it does seem possible to assume that with these authors $\frac{I_3}{E_3} < 0$, while $\frac{I_5}{E_5} > 0$. A positive sign for $\frac{I_3}{E_3}$ was obtained only once by S.Sh.Dolginov, in the analysis of the noncyclical variations. Thus the four spherical analyses of the aperiodic part of the storm field, made by different authors and from different starting ma-

* The erroneous assertion of Chapman and Whitehead that $\frac{I}{E}$ can vary within any limits from $-\infty$ to $+\infty$ is connected, as was shown later by Chapman and Lahiri, with the failure to allow for the free damping currents, which has already been mentioned in Section 1 of the present Chapter.

terials, all speak in agreement in favor of the alternating sign of the ratio $\frac{I}{E}$:

$$\frac{I}{E} > 0 \text{ for } P_1 \text{ and } P_5; \quad \frac{I}{E} < 0 \text{ for } P_3 \text{ and } P_7.$$

For the harmonics $P_3 D_{sf}$, as for P_1 , we calculated the internal field I_3 corresponding to the external field E_3 . For $n = 3$, eq. (42) assumed the form:

$$\varphi_p(t) = \frac{42}{4} q^7 \left[2 \cdot 10^{-4} t e^{-\alpha^2 t} - x_p^2 \sum_{s=1}^{\infty} \frac{e^{-2 \cdot 10^4 x_s^2 t} - e^{-2 \cdot 10^4 x_p^2 t}}{x_s^2 (x_s^2 - x_p^2)} \right], \quad (82)$$

where $\alpha^2 = \frac{\kappa_s^2 \Lambda}{\pi^2}$ and x_3 is a root of the equation

$$J_{2,5}(x_s) = \frac{1}{\sqrt{\pi x}} \left[\left(\frac{3}{x^2} - 1 \right) \sin x - \frac{3}{x} \cos x \right] = 0. \quad (83)$$

From the tabulated values of the roots of Bessel equations we selected values of α_p satisfactorily representing the observed function $E_3(t)$ (see the solid curve in Fig. 45): $\alpha_4 = 0.035$ and $\alpha_6 = 0.074$.

The approximate curve so obtained:

$$E_3 = 80 (e^{-0.035t} - e^{-0.074t}) \quad (84)$$

(t in hours) is given on this same figure by the dashed line.

The internal induced field corresponding to E_3

$$I_3 = 80 (\varphi_6 - \varphi_4), \quad (85)$$

while computational expressions for φ_4 and φ_6 are given by the series eq. (82).

Figure 45 also gives the observed field of $I_3(t)$ (solid line) and the calculated field (dashed line). It will be seen from the figure that the calculated values of I_3 plotted with reversed sign very satisfactorily represent the observed I_3 . Our attention is struck by the very high agreement in the course of the curves $E_3(t)$ and $I_3(t)$, which forces us to the conclusion that the Lamb-Price induction theory well explains the ratio of the external and internal field of the third harmonic of D_{st} in absolute value, but cannot explain the negative sign of this ratio.

The negative sign of $\frac{1}{E}$ is possible under the condition that the medium in which the currents are induced possesses a high magnetic permeability' ($\mu \gg 1$). In this case, eq.(42) is of the form

$$\varphi_{\mu}(t) = \frac{nq^{2n+1}}{n+1} \left[-\frac{(n+1)(\mu-1)}{n\mu+n+1} (1 - e^{-\alpha t}) + \right. \\ \left. + 2(2n+1)\mu k^2 \sum_{s=1}^{\infty} \frac{e^{-\alpha n_s t} - e^{-\alpha t}}{[n(\mu-1)(n\mu+n+1) - k_{ns}^2 q^2 a^2] (k^2 - k_{ns}^2)} \right], \quad (86)$$

where the terms containing $\mu - 1$ express the magnetic induction. If the inducing field does not depend on the time ($\alpha = 0$), then eq.(6) is transformed into the ratio, mentioned in Section 1, between the inducing and induced permanent magnetic fields

$$-\frac{nq^{2n+1}(\mu-1)}{n\mu+n+1}.$$

Beginning at certain sufficiently large values of t , the terms expressing the electromagnetic induction and containing the exponential functions $e^{-\alpha t}$ become small, and $\varphi(t)$ passes into the region of negative values. But such an explanation of the negative sign of $\frac{I_3}{E_3}$, expressed at one time by McNish, appears to be implausible, since:

- 1) the ratio $\frac{I_3}{E_3}$ gives no indications whatever that $\mu \gg 1$;
- 2) $\frac{I_3}{E_3}$ maintains an almost constant negative value beginning at $t = 0$ hours to the end of the storm ($t = 60$ hours). McNish's other assumption as to the role of the nonuniform conductivity of the surface conducting layers appears to be equally unfounded. The nonuniform conductivity of the medium leads to the result that to one harmonic of P_n^m in the inducing field there correspond a considerable number of harmonics in the induced field, with coefficients depending on the law of distribution of the conductivity of the medium. This argument at one time was used by me to explain the great variations of $\frac{1}{E}$ in the longitudinal terms of the field of S_q (Bibl.9). However, as shown by the calculation described in Section 5, the influence of the surface layers, even under an exaggerated assumption as to the conductivity

POOR ORIGINAL

value of κ , according to this material, ranges from 10^{-14} to 2×10^{-12} , while d ranges from 45 to 250 km. Still, if we leave out of consideration the considerably aberrant point $d = 45$ km, $\kappa = 2 \times 10^{-12}$, we shall note a tendency for the conductivity to increase with the depth. Still smaller values of κ follow from the Chapman data on $P_3^2 S_q$ ($\kappa = 0.37 \times 10^{-12}$, $d = 250$ km, curve I).

Such differences in the values of κ and d , calculated from different experimental material, would tend to indicate the arbitrary nature of any sharp boundary between the conducting core and the nonconducting shell. The curves showing the increase of conductivity with depth appear more plausible. The two curves calculated by me for the model q, κ_0, s , that is, without allowing for the surface currents (cf. the curves 5 and 6 on Fig.46) are in good agreement. Both of them indicate the low values of κ ($\sim 10^{-12}$ CGS) at depth of 400 - 700 km, and the sharp increase of κ for $d = 900 - 1100$ km. In still deeper layers a further increase of κ is found, but the data from depths over >1500 km, obtained from short-period variations, must be considered unreliable. According to Chapman's calculations, in a sphere of uniform conductivity, 70% of the induced currents corresponding to the harmonic P_2^1 and 77% of the currents corresponding to P_3^2 are concentrated in the peripheral shell of the sphere, $0.9Rq < r < Rq$, that is, with our values of q , at depths of 400 - 1100 km. The increase of κ with depth, of course, also increases the downward propagation of the currents, but still, a substantial part of the currents would hardly be induced at levels deeper than 1300 - 1500 km.

The allowance for the currents induced in the upper layers of the earth crust, as would be expected from simple physical reasoning, increased the values of κ (see curves 7 and 8). Thus, for example, at depth 1100 km, the value of κ increased from $50 - 65 \times 10^{-13}$ to $70 - 110 \times 10^{-13}$. In the upper layers of the conducting core ($d < 700 - 800$ km), however, the corrected values of κ are somewhat smaller than the uncorrected values.

From the series of curves of $\kappa(d)$, calculated by Lahiri, Fig.46 gives the two

that he considers the most probable. Curve 9 is calculated on the assumption $\kappa_0 = 4 \times 10^{-14}$ CGS, $q = 1$, $s = 37$, and $\kappa_1 \partial = 2 \times 10^{-6}$ CGS. Curve 10 assumes $\kappa_0 = 2.3 \times 10^{-13}$, $q = 0.903$, $s = \infty$, and $\kappa_1 \partial = 5 \times 10^{-6}$. Both curves indicate the shallow

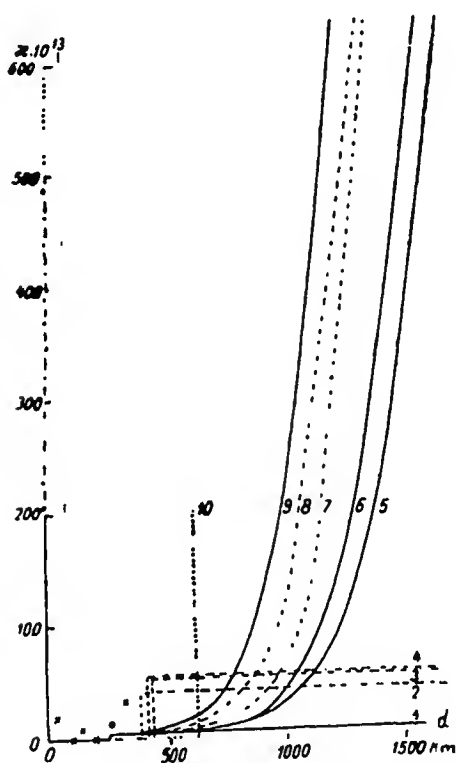


Fig.46 - Conductivity of the Earth (κ) from the Data of Geomagnetic Variations

depth of the level at which κ increases ($d \approx 600 - 700$ km). The discrepancy between the curves 7, 8, and 9, 10 can be explained not only by the different starting materials, but also by the different method of calculation. One of the Lahiri curves (not given on the figure) is calculated under the assumption $\kappa_0 = 4 \times 10^{-11}$, $q = 1$, and $s = 30$ (without allowing for the conductivity of the oceans) coincides almost completely with our own curve 7. Thus a consideration of Fig.46 shows that the following distribution with depth is the most probable. The surface layers (mainly on account of the oceans, which occupy 0.7 of the earth surface with a mean depth of 4.2 km) have a very high conductivity. The action of the ocean may be taken as

equivalent to a spherical layer of conductivity $\kappa, \partial = 2 - 5 \times 10^{-6}$. The conductivity of the first 200 km is roughly the same as that of the dry rocks on the earth surface, that is, it does not exceed 10^{-14} CGS. The induction of currents at these depths may be practically disregarded. A substantial increase of conductivity begins at depths 200 - 300 km, while a sharp rise is located at $d \approx 900 - 1000$ km, and a still steeper ascent of the curves is found at depths 1100 - 1200 km. The calculation of a model with a sharp surface of separation gives a moderate value of the conductivity. It is naturally greater than the actual value in the upper layers of

the conducting core, and smaller than the actual value in the deep parts.

The distribution of conductivity so obtained does not contradict the modern idea on the structure of the earth. As will be seen from a comparison of Figs. 47 and 46, the region of the earth crust (to a depth of 60 - 80 km), is characterized by very low values of the conductivity which, in all probability, is connected with the anisotropic state of matter, and with the predominance of rocks with low iron content. A slight increase of conductivity begins from the upper layers of the outer shell downward, and a more substantial increase occurs in the lower layers of the shell, which are characterized by a change of chemical composition, an increase in the metallic content, and an increase in density and temperature.

A certain analogy is noted between the curves of $\kappa(d)$ and the dependence of the velocity of longitudinal waves p on the depth. The second-order discontinuities of Repetti ($d = 950$ km) and Gutenberg ($d = 1200$ km) find their reflection in the curve of $\kappa(d)$ as well: at these depths, as already remarked, $\kappa(d)$ appreciably changes its direction. Thus the modification of the physical properties of matter at a depth of 900 - 1200 km, on the transition from the lithosphere to the barysphere, may be considered a confirmation of the change in the electric characteristics of the earth. It is true that the analogy between the curves of $\kappa(d)$ and $p(d)$ noted by us does not by any means indicate any parallelism of the curves. On the contrary, the increase of the gradient of the function $\kappa(d)$ at depths of 900 - 1200 km is related to the decrease in the gradient of $p(d)$. The curve of temperature distribution given in Fig. 47 for comparison (T_G for Gutenberg and T_D for Jeffreys) and of density (P_1 according to Gutenberg, and P_2 according to Bullen) also confirm the changes in the physical properties of matter with depth.

This conclusion as to the variation of conductivity with depth may be considered a first approximation. The solution of the question of the negative sign of the third harmonic, and the more detailed study of the polar storms and other forms of local disturbances may possibly introduce substantial corrections in the conclusions

so obtained. In order to judge of the nonuniformity of the deep layers it would seem advisable to apply the formulas of the plane problem to disturbances of local type

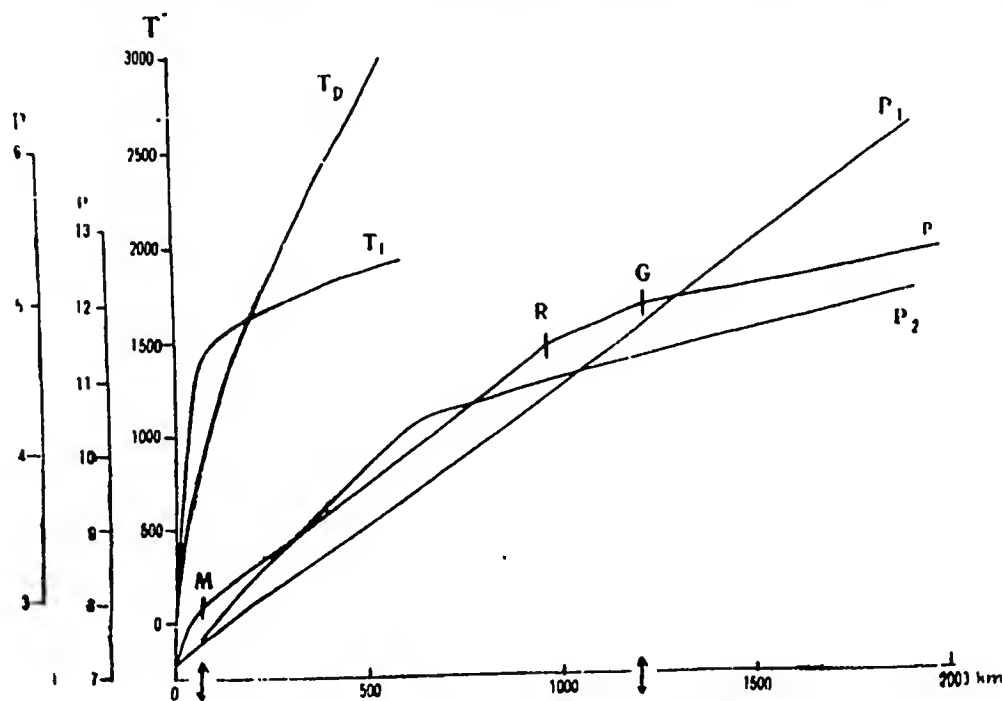


Fig.47 - Internal Structure of the Earth

(bays, pulsations). In this way it will be possible to obtain an extensive material on the conductivity of various depths and various areas of the earth.

Conclusion

Section 1. It follows from all the above that the primary object of the present work, the construction of the electric currents causing the magnetic disturbances, has been accomplished. The calculations we have made are based on a sufficiently extensive empirical material (65 observatories) which allows us to expect that the field of calculated currents will be a good approximation to the field of observed variations. A consideration of the morphology of the disturbances, which preceded the calculation of the currents, shed light on certain questions of the structure and geographic distribution of the field. The most substantial of them are as follows:

1. The classification of magnetic storms and the separation of the storm field

into its component parts. It appears to be most correct to divide storms into two main categories, worldwide and polar. Polar storms reach their maximum intensity in the auroral zone, and manifest themselves in the middle latitudes in the form of small bay-shaped disturbances. The field of polar storms depends on the local time and has no aperiodic part symmetric with respect to the earth axis, just as it has no prolonged after-effect.

The data on worldwide storms collected by us have confirmed the advisability of the separation of the regular parts, the D_{st} and the S_D variations, from the disturbance field, as proposed by Chapman. Worldwide storms, in our opinion, are always accompanied by polar storms superimposed on each other, and therefore the field of a worldwide storm should be divided by the means of the four-term formula

$$D_{st} + S_D + P + D_i.$$

2. The worked-up data on the D_{st} variations of a worldwide net of observatories have confirmed the fundamental features of the structure of the field described earlier by other investigators (position of the vector of the disturbance in the plane of the magnetic equator, low dependence of the field on the longitude, form of the D_{st} fluctuations of H and Z in the temperate latitudes). A more detailed examination of the question, however, by means of an evaluation of an estimate of the values of H and Z for the quiet intervals on days of worldwide storms, has shown that the D_{st} field does not have a sharp increase in the auroral zone, and varies smoothly from equator to the poles.

3. The S_D variations, on the other hand, do have a sharp increase in the auroral zone, and the form of S_D is determined primarily by the distance from that zone and by the local time. The S_D variations of the magnetic elements have been used to pinpoint the position of the zone. The data used by me have compelled me to place the position of the zone considerably further south than the Vestine zone. No dependence of the S_D variations on Universal Time was detected. The form and amplitude

of the variations in the region near the pole have been elucidated.

4. It has been established that if the D_{st} field is considered as a function of ϕ and τ , and S_D as a function of ϕ' and t_M , then there are no substantial anomalies in the geographic distribution of D_{st} and S_D . In particular, the complete normality of the disturbed variations at Huancayo has been specially noted.

5. A consideration of the geographical distribution of the S_D variations has shown that the linear current flowing in the auroral zone cannot explain the middle-latitude part of the field. For this reason it has been shown to be more correct to take the S_D system of currents as a system of surface spherical currents.

The currents of the polar disturbances have likewise been taken as surface currents, but extending only over the polar cap down to latitudes $\phi = 50^\circ$.

Section 2. The extensive starting materials used made it advisable to calculate the currents of the disturbances by analytical methods.

The D_{st} currents were calculated on the basis of a spherical analysis of the D_{st} variations. For calculating the currents I used an expansion of the storm potential into a series of Bessel functions. The complexity of the geographic distribution of the S_D variations preventing me from using spherical analysis, and forced me to turn to the method of surface integrals. The method of calculating the external and internal parts of the potential from values of the potential and Z component, assigned on the surface of a sphere, proposed in 1941 by Vestine, has been further developed in the present work. A method has been given for calculating the density of the surface currents from the potential assigned on the surface of the sphere. The method is based on the extrapolation of the values of the external potential for points inside the sphere, the calculation from it of the current density from it (by solving a Fredholm equation of the second kind, to which the external Dirichlet problem leads), and extrapolation of the function of current density for external points at the distance of the hypothetical current layer. An analogous method of solution may be applied to the calculation of the internal current systems. All the laborious

POOR ORIGINAL

operations in the course of the calculations of the currents by the integral method are now reduced to a single type and allow use of the very same overlays to facilitate the calculations. A consideration of the accuracy of the method has shown that the errors of the mathematical operations themselves are considerably less than the accuracy of the initial geomagnetic data. The accuracy obtained as a result of the calculations performed is sufficient for the construction of a general picture of the currents.

The method can yield good results only in the case where the radius of the current-carrying layer differs little from the earth radius. But since in most geomagnetic problems, both for the main and irregular fields, this condition is satisfied, it follows that the method may be recommended for the investigation of a number of questions, as for example the construction of the currents responsible for the secular variations, the study of magnetic anomalies, and the like. The possibility is not excluded that the integral method may also find application in other branches of geophysics, replacing spherical analysis in the case of fields of rather complex structure.

Section 3. The current system of the D_{st} variations consists of current lines parallel to the circles of latitude. It differs substantially from the well known system of Chapman by the fact that there is no crowding of lines in the polar zones, and by the different signs of the current functions in the northern and southern hemispheres. On the basis of spherical analysis of the D_{st} variation, I also made a calculation of the equatorial ring current, which yielded the following results: radius of ring $a = 3.8R \pm 0.8R$; current strength $I = 7 \times 10^5$ amp. These values were calculated on the basis of the ratio between the harmonic coefficients of terms of different orders and is in good agreement with the ideas of other authors on the ring current.

The current systems of S_D variations, like the corresponding Chapman systems, consists of four current eddies. The intensity and location of the polar currents proved to be different from what would follow from the Chapman data. The signs of

POOR ORIGINAL

the current functions, which are different in each pair of eddies, also constitute a substantial difference.

The current system of the P-storms resembles the polar part of the S_D currents. A calculation of the linear current flowing along the zone from the data of the S_D variations is in good correspondence with the crowding of the current lines on the map of surface S_D currents. A calculation of the linear current, based on four pairs of Arctic stations, allowed me to establish the fluctuations of the height of the linear current, of its intensity, and of its position throughout the course of the day. The results proved somewhat different from the analogous results of other investigators.

In this work the seasonal and 11-year fluctuations of the S_D and D_{st} currents have been considered. It has been found that the intensity of the D_{st} currents varies rather regularly throughout the 11-year cycle, displaying the lag in the epochs of the maxima by 1 to 2 years with respect to the solar maxima, which is characteristic of all phenomena due to corpuscular radiation. The seasonal fluctuations of the D_{st} current can likewise be explained from the point of view of the corpuscular origin of the ring current: the maxima in the equinoctial epoch may be explained by the Corti effect, the additional maximum in summer by the Bartels effect.

The fluctuations of the S_D currents are much more complex, and are different at different latitudes: the 11-year fluctuations in the intensity of the middle-latitude eddies do not display a good correspondence with the march of the solar indexes. Small displacements of the lines of the centers of the middle-latitude eddies have been found. The 11-year fluctuations of the polar eddies are considerably greater with respect to their intensity and to the position of the auroral zone in years of high activity, there is a marked increase in the intensity of the currents, and there is also a shift in the position of the zone toward lower latitudes. The seasonal fluctuation of the middle latitude eddies are small, while those of the polar eddies are considerable. An intensification of the current in the equinoctial months and

F-TS-8974/V

244

summer has been found, together with a shift of the zone from higher latitudes in the summer to lower latitudes in the equinox.

Section 4. The current systems calculated for individual instants of individual storms are in good correspondence with the average pictures depicting the regular part of the disturbance field. The 26 individual cases considered showed that in all cases the position and signs of the current eddies are the same as in the average systems. It is true that the form of the current lines and the intensity of the currents varies not only from storm to storm, but also from hour to hour within wide limits. But all the same the consideration of the individual storms confirmed the physical reality of the concept of a stable current system embracing the entire earth, and causing the magnetic disturbances.

Section 5. Data on the disturbed-day structure of the ionosphere have been adduced to judge the location of the currents of magnetic storms. A calculation of the D_{st} and S_D variations of the ionospheric parameters has shown that the greatest and most regular variations take place in the F_2 layer. The D_{st} variations of ionization density of the F_2 layers display a two-phase character at all latitudes; in the high and middle latitudes, the first phase is characterized by an increase in ionization density, the second by a decrease. In the equatorial latitudes, on the contrary, the first phase is negative, the second positive. This lack of correspondence between the D_{st} variations of the magnetic field and f^0F_2 , and also the great regularity of the D_{st} of the magnetic elements - which is absent in the D_{st} of the ionospheric parameters, forces complete abandonment of any possibility of explaining the D_{st} variation by ionospheric processes, and, on the contrary, supports the hypotheses of an extra-ionospheric ring current.

The S_D variations of f^0F_2 are similar in their geographical distribution to the S_D variation of the magnetic elements: at latitudes higher than $\phi = 40^\circ$, S_D represents a simple wave with a maximum in the evening and a minimum in the morning, while in the low latitudes, this relative position of the extreme values is reversed.

~~POOR ORIGINAL~~

This resemblance makes it possible to explain the S_D variations by currents in the F_2 layer. The possible mechanisms of formation of these currents have been investigated. The values of the conductivity of individually layers of the ionosphere in the direction of the magnetic field (σ_0) and in two directions perpendicular to it (σ^I and σ^{II}) have been reviewed, and it has been found that for the F_2 layer, the conductivity along the velocity of the mechanical displacement of the gaseous masses (σ^{II}) is greater than the conductivity of the dynamo effect (σ^I). Thus it would appear that the dynamo effects can hardly have the decisive role in the formation of the S_D currents. The currents induced in the ionosphere by the alternating magnetic field of the equatorial ring current are likewise very small. In all probability the greatest part in formation of the current is played by the currents of latitudinal direction which either arise owing to the drift effect or owing to the motion of the earth in the field of the ring. The experimental data known from the literature as to the vertical motions or the vertical gradients of the ionization density in the F_2 layer, which are particularly increased during the time of a disturbance, allow us to consider that the drift of charges under the action of the magnetic and gravitational fields is not eliminated, owing to the equilibrium between the force of gravity and the partial pressure in the gas, and consequently, may be adduced for the explanation of the magnetic variations. I have schematically shown here that, owing to the S_D variations of the ionization density of the F_2 layer, currents of latitudinal direction may lead to the formation of current systems resembling the middle-latitude part of the S_D currents.

Section 6. The separation of the observed potential of the D_{st} , S_D - variations, and P-storms into an external and an internal part led to the following results.

The ratio $\frac{I}{E}$ for the first harmonic of the D_{st} field is about 0.40. Considering the internal field to arise by induction from the external field, I calculated by the Lamb-Price formula that the conductivity of the earth core (corresponding to $\frac{I_1}{E_1} = 0.40$) $\kappa = 4.4 \times 10^{-12}$ CGS, and that its radius is 0.94R. If the influence of

the superficial conducting layers is taken into account, however, and the conductivity is assumed to increase with depth by the exponential law:

$$\kappa = \kappa_0 \left(\frac{r}{\rho} \right)^{-S},$$

then

$$S = 26, \rho = 0.31R \text{ and } \kappa_0 = 4 \cdot 10^{-13}.$$

The curve relating κ to the depth, calculated by this formula, discloses the sharp rise of κ at the depth 900 - 1200 km at which Gutenberg and Repetti found discontinuities in the variation of the velocity of longitudinal seismic waves. Thus the information on κ obtained from magnetic data does not contradict the modern idea of the structure of the Earth.

The mean ratio $\frac{E}{E+1}$ for P-storms was found to be 0.86. To use these data to judge the structure of the Earth, I solved the Lamb problem in cylindrical coordinates. The numerical values of κ according to the data of the $\frac{I}{E}$ of various terms of the P-storm potential ranges between 10^{-12} and 10^{-14} . In spite of the great scatter of the values of κ , these values do not contradict the conclusions drawn from the first harmonic of the D_{st} variations.

The ratio $\frac{I}{E}$ for the third harmonic of the D_{st} variations was found to be negative. Comparison of this conclusion with the data of other authors compels belief in its authenticity, but it does not appear to be possible to verify it from the viewpoint of the induction theory (under the assumption of the spherical symmetry of κ). The possibility is not excluded that this result may indicate the existence of great nonuniformities of conductivity in the depths of the Earth. At the present time, however, this question still remains open. The ratio $\frac{E}{1+E}$ for the S_D variations ranges from 0.79 for the middle latitudes to 0.89 for the high latitudes.

This value differs appreciably from that adopted by Chapman for the entire Earth,

$\frac{E}{1+E} = 0.6$. The latitudinal dependence of $\frac{E}{1+E}$ for the S_D current may similarly be considered as an indication of the absence of spherical symmetry in the dis-

POOR ORIGINAL

tribution of κ .

Section 7. All the arguments of morphological and physical character advanced in the present work compel us to accept the following mechanism of formation of magnetic storms. A powerful corpuscular stream arriving from the Sun acts in several ways on the geomagnetic field. First, interacting with the geomagnetic field, it leads to the formation of an equatorial ring of currents, whose field produces the D_{st} variations of the magnetic elements. Second, as a result of the drift of charges, or of some other mechanism, electric currents are generated in the upper part of the ionosphere at both high and low latitudes. Since the conditions in the ionosphere are substantially related to the solar altitude, a characteristic property of these currents is their dependence on the local time (the S_D variations). And third, a certain part of the particles, becoming detached from the body of the ring (or from the corpuscular stream itself), are directed under the action of the magnetic field toward the polar regions, where they penetrate deep into the Earth atmosphere (to the levels of the E and D layers of the ionosphere), causing auroral displays and intense magneto-ionospheric disturbances there. The polar magnetic storms connected with the immediate processes in the ionosphere are of very local nature, and their course is governed by local time.

Thus the field of world-wide storms always contains three components: the D_{st} variations, the S_D variations, and the P-storms. The fluctuations of the D_{st} and S_D systems, and the superimposition of P-storms differing in form and intensity, gives the fluctuation of the magnetic elements a complex, random character during world-wide storms. The storm field also has smaller irregular fluctuations (D_i), which may perhaps be connected with some ionospheric processes of more local type.

Less energetic solar streams do not lead to the formation of an equatorial ring nor of ionospheric currents. The particles of such streams, detaching themselves immediately from the body of the stream, proceed to the Polar regions and cause Polar storms there. Thus the P-storms can be observed even in the absence of world-

wide storms.

It goes without saying, of course, that this work does not answer all questions connected with the construction of the current systems of magnetic storms. The possible investigations in the domain of the morphology of the disturbance field and of the disturbed ionosphere have not been exhausted, and no physical explanation of the origin of the currents has been worked out. In this work we have only considered the macro-structures of the disturbances in the geomagnetic field and in the ionosphere, and we have merely marked out paths along which the solution of the questions of the formation of the currents may be sought.

In studying the morphology of the field of magnetic storms in the future particular attention must be paid to the individual fluctuations, to the irregular part of the field D_1 on which the present work has no bearing. It is necessary by elucidating the statistical regularities, or by analyzing the individual phenomena to confirm, on a large amount of material, the proposition here enunciated to the effect that the individual fluctuations during worldwide storms, noted on the magnetograms in the middle latitudes, are the result of the superimposition of polar storms piled one on top of the other.

In the present work we have collected a large amount of factual material on the regular variations, and have given a representation of it in the form of current systems. This material, it seems to us, may be of great use in the solution of the following practical questions: reduction of the magnetic observations to the middle of the year, and short-term magnetic forecasting. The methods of reduction existing at the present time, for days that are not magnetically quiet, are very imperfect, and are particularly unsuitable for high latitudes. The systematization of the regular disturbed variations, and the calculation of the current systems, will help to evaluate the possible deviations, during a disturbance, of the values of the magnetic elements from the normal, and to interpolate (or extrapolate) the observatory data for the points of observation. It also seems to us that the representation of the

POOR ORIGINAL

average current system of a magnetic storm will help to increase the accuracy of the geographical distribution of the degree of disturbance by time of day, and to evaluate the amplitude of the possible fluctuations, both of which accomplishments are necessary for short-time forecasting. Thus it is desirable to continue the consideration of the morphology of disturbance presented in this work, and to give it a form convenient for utilization in practical problems.

To a still greater extent it is necessary to continue the study of the morphology of the disturbed ionosphere. The regular variations of D_{st} and S_D of the disturbed ionosphere that have been considered in this work should be calculated for the largest possible number of years and points of observation. The study of the morphology of the disturbed ionosphere is not only of theoretical value but is also of great practical value for the maintenance of shortwave radio communication through the ionosphere. In view of this fact it is inadequate to have merely a schematic representation of the geographical distribution or time fluctuations of S_D and D_{st} , but it is necessary to have a distinctly elucidated picture of each observatory separately. Of particularly great interest is the study of the polar ionosphere, the processes in which are the cause of the polar magnetic storms and of the high-latitude part of the S_D variations.

As for the method of calculating the current systems from the data of geomagnetic variations, the integral method developed in this work has enabled us to obtain the numerical values of the external and internal potential, and of the current function, with sufficient accuracy. In future, however, in cases where it may be sufficient to obtain only a rough picture of the distribution of currents, or when the sparsity of data makes it impossible fully to utilize all the advantages of the method, it will still be possible to use an approximate method employing the analytical technique for solving the fundamental problems of geomagnetism on the basis of an extensive empirical material.

The question of the mechanisms of excitation of electric currents in the iono-

POOR ORIGINAL

sphere may be considered as having merely been posed in the present work.

I shall consider my object achieved if the present work attracts attention to the study of magnetic storms and thereby encourages the further development of the theory of geomagnetic variations.

Bibliography

1. Al'pert, Ya.L. - Propagation of Radio Waves in the Ionosphere, Gostekhizdat, Moscow, 1947.
2. Al'pert, Ya.L. - The Present State of the Question of the Investigation of the Ionosphere, Parts I, II. Usp.fiz.nauk 34 (2), (1948); 36(1) 1948.
3. Al'pert, Ya.L. - The Present State of the Question of the Investigation of the Ionosphere, Part III. Ibid 38(3) 1949.
4. Al'fven, Kh. (Alfven, H.) - Cosmic Electrodynamics. Publishing House for Foreign Literature, Moscow, 1952.
5. Afanas'yeva, V.I. - Regular Geomagnetic Variations in the USSR. Trudy NIIZM, No.3(13) 1948.
6. Afanas'yeva, V.I. - Spherical Harmonic Analysis of the Geomagnetic Field of Epoch 1945. Izv.An SSR, ser.geog. i geofiz. 11(1) 1947.
7. Afanas'yeva, V.I. - Results of observations by Magnetic Observatories for 1938, 1939, 1941 and 1942. Trudy NIU GUGMS, ser.VI, No.3 1946.
8. Afanas'yeva, V.I. - The Diurnal and Annual March of Bay-Shaped Disturbances at Zaymishche (Kazan'). Inform.sborn. po zemn. magn. i elektr. No.5, issue 2, Leningrad 1940.
9. Ben'kova, N.P. - Quiet Solar-Diurnal Variations of Terrestrial Magnetism. Trudy NIU GUGMS, ser.VI, No.1 1941.
10. Gerasimenko, V.I. - Atmospheric Electricity Observations at Cape Chelyuskin in 1934 - 35. Inform.sborn. po zmn. magn. i elektr. No.3, Leningrad 1936.

11. Ginzburg, V.L. - Theory of Propagation of Radio Waves in the Ionosphere.
Gostekhizdat, Moscow, 1949.
12. Gnevyshev, M.N. - The Nature of Solar Corpuscles. Astron.zhur. 25(2) 1948.
13. Gnevyshev, M.N. - The Nature of Geomagnetic and Ionospheric Disturbances. Trudy
NIIZM, No.1(11) 1947.
14. Gursa, E. (Edward Coursat) - Course in Mathematical Analysis. GtTI, Moscow
Leningrad 1933.
15. Dolginov, S.Sh. - The Noncyclical Variations of the Elements of Terrestrial
Magnetism. Trudy NIIZM, No.2(12) 1948.
16. Kalashnikov, A.G. - A New Method of Studying Weak Variations of the Earth Magnet-
ic Field. Izv.AN SSR,ser.geog.i geogiz. 12(2) 1948.
17. Kalinin, Yu.D. - Theory of Geomagnetic Disturbed Diurnal Variations. Dok,AN
SSSR 58(8) 1946.
18. Kalinin, Yu.D. - On the Determination of the Earth Electrical Conductivity from
Observations of the Variations of the Magnetic Field of the Earth in a
Bounded Region. Trudy NIIZM, No.8(18) 1952.
19. Kalinin, Yu.D. - The Equatorial Ring Current Arising During Magnetic Storms.
Met. i gidrol. No.10 - 11 1939.
20. Kalinin, Yu.D. - The u-Measure of Magnetic Activity. Inform.sborn. po zemn.
magn. i elektr. No.5, issue 2, Leningrad 1940.
21. Kalinin, Yu.D. - Experience in Study of Magnetic Disturbance by the Method of
Graphic Integration. Probl.Arktiki No.12 1940.
22. Kalinin, Yu.D. - Technique of Calculating the Working Waves for Communication
Under Conditions of Magneto-Ionospheric Disturbance. Trudy NIU GUGMS,
ser.VI, No.3 1946.
23. Kouling, T.G. (Cowling) - Contemporary Problems of Astrophysics and Heliophysics.
Collection of Papers. Publishing House for Foreign Literature, Moscow 1951.
24. Mednikova, N.V. - Ionospheric Disturbances of a Peculiar Type. Dok.AN SSSR

- 59(3) 1948.
25. Mikhalkov, V.N. - Bay-Shaped Disturbances at Tashkent-Keles. Trudy TGO, No.4, Leningrad 1950.
 26. Nikol'skiy, A.P. - The Nature of Geomagnetic Disturbances. Priroda 1947.
 27. - Problems of Modern Physics. Propagation of Radio Waves and the Ionosphere. Publishing House for Foreign Literature, ser.3, No.6, Moscow 1951; No.XII 1952.
 28. Pushkov, N.V. and Brunkovskaya, N.S. - Comparison of Magnetic Activity and Auroral Displays from Observations of a Large Number of Magnetic and Meteorological Stations. Inform.sborn.po zemn. magn. i elektr. issue 5, No.2, Leningrad 1940.
 29. Rozenberg, G. - Direct proof of the Cosmic Origin of the Hydrogen in the High Layers of the Atmosphere. Usp.fiz.nauk 44 1951.
 30. Svyatskiy, D.O. - The Northern Lights in Russian Literature and Science from the 10th and 18th Centuries. Trudy inst.gist.nauki i tekhn. AN SSSR, ser.I, No.4 1934.
 31. Tamm, I.Ye. - The Currents in the Ionosphere Causing the Variations of the Earth Magnetic Field. Izv.AN SSSR,ser.fiz. 8(2) 1944.
 32. Tikhonov, A.N. - Determination of the Electrical Characteristics of the Deep Layers of the Earth Crust. Dok.AN SSSR 23(2) 1950.
 33. Frish, S.E. and Timoreva, A.V. - Course in General Physics. GITTL, Moscow 1951.
 34. Eygenson, M.S. et al. - Solar Activity and its Geophysical Manifestations. GITTL Moscow-Leningrad 1947.
 35. Yanossi (Janossy), L. - Cosmic Rays. Publishing House for Foreign Literature, Moscow 1950.
 36. Appleton, E. and Piggott, W. - World Morphology of Ionospheric Storms. Nature, 165, No.41, 87, 1950.
 37. Ashour, A.A. and Price, A.T. - The Induction of Electric Currents in a Nonuni-

- form Ionosphere. Proc. Roy. Soc., A, 195 London, 1948.
38. Birkeland, Kr. - Norwegian Aurora Polaris Expedition 1902 - 1903.
Christiania, 1, Pt. I, 1908; I, Pt.2, 1913.
39. Burkard, O. - Studies on World-Wide Ionosphere Disturbances of 15 March 1948.
Arch. f. Meteor. Geoph. and Bioklimat. Bd. II, Ht. 2 - 3, 1950.
40. Chapman, S. and Bartels, J. - Geomagnetism. Oxford, 1940.
41. Cynk, B. - Variation in the Disturbance Field of Magnetic Storms. Terr.
Magn., 44. No.1, 1939.
42. Eckersley, T.G. - Differential Penetration Theory. Terr. Magn., 52, No.3;
No.4, 1947.
43. Forbush, S.E. - On Cosmic Ray Effects, Associated with Magnetic Storms.
Terr. Magn., 43, No.2, 1938.
44. Harang, L. - The Mean Field of Disturbances of Polar Geomagnetic Storms.
Terr. Magn., 51, No.3, 1946.
45. Hasegawa, M. - A Suggestion for the Electric Conductivity of the Upper Atmos-
phere from an Analysis of the Diurnal Variation of Terrestrial Magnetism.
Intern. Association of Terrestrial Magnetism and Electricity, Oslo
Assembly, August, 1948.
46. Hayakawa, S., Nagata, T., Nishimura, J. and Sugiura, M. - Note on the Effect
of the Equatorial Ring Current on Cosmic Ray Intensity. Journ. Geoph.
Res., 55, No.2, 1950.
47. Lahiri, B.N. and Price, A.T. - Electromagnetic Induction in Nonuniform Con-
ductors and the Determination of the Conductivity of the Earth from
Terrestrial Magnetic Variations. Philos. Trans. Roy. Soc. London,
A, 237, 1939.
48. Martyn, D.T. - The Theory of Magnetic Storms and Auroras. Nature, 1951,
167, No.4238, 1951.
49. McNish, A.G. - Heights of Electric Currents Near the Auroral Zone. Terr.

- Magn., 43, No.1, 1938.
50. Mitra, S.N. - The Upper Atmosphere. Calcutta, 1947.
51. Nagata, T. - Development of Magnetic Storms: The Southward Shifting of the Auroral Zone. Journ. Geoph. Res., 55, No.2, 1950.
52. Nagata, T. - The Auroral Zone Current. Rep. Ionosph. Res. Japan, 4, No.2, 1950.
53. Rikitake, T. - The Electrical State of the Earth's Interior as Inferred from Variations in the Earth's Magnetic Field. Internat. Association of Terrestrial Magnetism and Electricity. Transaction of Oslo Meetings, 1948. Bull. No.13, 1950.
54. Silsbee, H.B. and Vestine, E.H. - Geomagnetic Bays, Their Frequency and Current-Systems. Terr. Magn., 47, No.3, 1942.
55. Sucksdorff, E. - Variations of Electric Currents in High Atmosphere. Terr. Magn., 52, No.2, 1947.
56. Sugiura, M. - The Shielding Effect of the Ionosphere. Rep. Ionosph. Res. Japan, IV, No.1, 1950.
57. Vestine, E. - a) On the Analysis of Surface Magnetic Fields by Integrals. Terr. Magn., 46, No.1, 1941.
b) Note on Surface-Field Analysis. Transactions of 1940 of the Amer. Geoph. Union, 1941.
58. Vestine, E. - The Assymmetrical Characteristics of the Earth's Magnetic Disturbance Field. Terr. Magn., 43, No.3, 1938.
59. Vestine, E. - The Geographic Incidence of Aurora and Magnetic Disturbance. Northern Hemisphere. Terr. Magn., 49, No.2, 1944.
60. Vestine, E. and Chapman, S. - The Electric Current System of Geomagnetic Disturbance. Terr. Magn., 43, No.4, 1938.
61. Vestine, E. and Davids, A. - Analysis and Interpretation of Geomagnetic Anomalies. Terr. Magn., 50, No.1, 1945.
62. Vestine, E., Lange, I. and Others - The Geomagnetic Field, Its Description and

Analysis. Department of Terrestrial Magnetism, Carnegie Institution of Washington, publ. 580, 1947.

63. Vestine, E. and Snyder, E. - The Geographic Incidence of Aurora and Magnetic Disturbance, Southern Hemisphere. Terr. Magn. 50, No.1, 1945.

64. Wells, H.W. - Polar Radio Disturbances During Magnetic Bays. Terr. Magn., 52, No.3, 1947.

65. Budden, K.G. and Yates, G.G. - A Search for Radio Echoes of Long Delay. Journ. Atmos. Terr. Phys., 2, No.5, 1952.

POOR ORIGINAL

TABLE OF CONTENTS

	Page
Introduction	1
Section 1. General Discussion of the Theories of Magnetic Storms	2
Section 2. The Electric Current Systems of Magnetic Storms	5
Section 3. Content of This Report	9
Chapter I. Survey of the Literature	13
Section 1. Basic Properties of Magnetic Storms. The Works of Birkeland	13
Section 2. Chapman's Investigations and Their Revisions	18
Section 3. Analytical Representation of the D_{st} -Variations	26
Section 4. Position of the Points of Magnetic Storms. The Equatorial Ring	27
Section 5. Electric Currents of the Auroral Zone	33
Section 6. Penetration of Corpuscles Into the Earth's Atmosphere. The Alfven Theory	36
Section 7. Dynamo Theory of Magnetic Storms	42
Section 8. Bay Disturbances	44
Section 9. Current Systems of Individual Bays	45
Section 10. Irregular Part of the Storm Field	46
Section 11. Conclusions	48
Chapter II. Division of the Field of Magnetic Storms	50
Section 1. Classification of Storms. Polar Storms	50
Section 2. Worldwide Storms. D_{st} -Variations	53
Section 3. S_D -Variations	58
Section 4. Division of the Field of Magnetic Storms	60
Chapter III. The D_{st} -Variations	63
Section 1. The Starting Materials	63
Section 2. Spherical Analysis of the D_{st} -Variations	68

POOR ORIGINAL

	Page
Section 3. Ionospheric System of Current of the D_{st} -Variations	75
Section 4. The Equatorial Current Ring	79
Chapter IV. Calculation of Electric Currents by the Method of Surface Integrals	82
Section 1. The Vestine Method of Separating the Observed Field into an External and an Internal Part	82
Section 2. Practical Methods of Calculating the External and Internal Potentials	87
Section 3. Calculation of the Electric Currents by the Integral Method	91
Section 4. Finding the Current Density from an Assigned Potential on the Sphere. Extrapolation of the Potential	96
Section 5. Practical Methods. Conclusions as to the Suitability of the Method	100
Chapter V. The S_D -Variations	104
Section 1. Basic Data	104
Section 2. Dependence of the S_D -Variations on Local and Universal Time The S_D -Variations in the Polar Regions	107
Section 3. Selection of the Type of the Current System	114
Section 4. Calculation of External and Internal Potential	116
Section 5. Discussion of the Accuracy of the Method	120
Section 6. The Current System of S_D -Variations	122
Section 7. The Polar Part of the S_D -Currents	127
Chapter VI. Polar Storms	133
Section 1. Expansion of the Field Potential and Electric Currents into Series of Cylindrical Functions	133
Section 2. Starting Material. Results of the Analysis	137
Chapter VII. Seasonal and 11-Year Variations of the D_{st} and S_D Currents ...	142
Section 1. The 11-Year and Seasonal Variations of the D_{st} Currents	142
Section 2. 11-Year Variation of the Middle-Latitude Part of the S_D Currents	145

	Page
Section 3. The 11-Year Variation of the Polar Part of the S_D Currents ..	157
Section 4. Seasonal Variations of the S_D Currents	162
Chapter VIII. Morphology of the Disturbed Ionosphere and the Current Systems of Magnetic Storms	167
Section 1. Ionospheric Disturbances	167
Section 2. Conductivity of the Ionospheric E and F Layers, and the Dynamo Effects in the F2 Layer	172
Section 3. Explanation of the S_D Variations of the Magnetic Field by Drift Currents	187
Section 4. Currents in the Ionosphere Induced by the External Field	194
Chapter IX. Current Systems of Individual Storms	199
Section 1. Polar Storms	199
Section 2. Worldwide Storms	206
Chapter X. The Internal Part of the Disturbance Field	211
Section 1. The Inductive Origin of the Inner Part of the Field. Survey of the Results Obtained	211
Section 2. Solution of the Induction Problem in Cylindrical Coordinates	215
Section 3. Determination of the Earth Conductivity from the Data of the First Harmonic of D_{st} (the Lamb Model)	221
Section 4. Determination of the Constants η , s , χ_0 (Lahiri Model)	225
Section 5. Allowance for the Upper Conducting Layer	229
Section 6. External and Internal Parts of the Harmonic P_3 of the D_{st} Field	232
Section 7. Variation of Conductivity with Depth and the Internal Structure of the Earth	236
Conclusion	240
Bibliography	251

TAB B

Explanation of Exemptions

Freedom of Information Act:

- (b)(1) exempts from disclosure information currently and properly classified, pursuant to an Executive Order;
- (b)(2) exempts from disclosure information which pertains solely to the internal personnel rules and practices of the Agency;
- (b)(3) exempts from disclosure information that another federal statute protects, provided that the other federal statute either requires that the matters be withheld, or establishes particular criteria for withholding or refers to particular types of matters to be withheld. The (b)(3) statutes upon which the CIA relies include, but are not limited to, the CIA Act of 1949;
- (b)(4) exempts from disclosure trade secrets and commercial or financial information that is obtained from a person and that is privileged or confidential;
- (b)(5) exempts from disclosure inter-and intra-agency memoranda or letters that would not be available by law to a party other than an agency in litigation with the agency;
- (b)(6) exempts from disclosure information from personnel and medical files and similar files the disclosure of which would constitute a clearly unwarranted invasion of privacy;
- (b)(7) exempts from disclosure information compiled for law enforcement purposes to the extent that the production of the information (A) could reasonably be expected to interfere with enforcement proceedings; (B) would deprive a person of a right to a fair trial or an impartial adjudication; (C) could reasonably be expected to constitute an unwarranted invasion of personal privacy; (D) could reasonably be expected to disclose the identity of a confidential source or, in the case of information compiled by a criminal law enforcement authority in the course of a criminal investigation or by an agency conducting a lawful national security intelligence investigation, information furnished by a confidential source; (E) would disclose techniques and procedures for law enforcement investigations or prosecutions if such disclosure could reasonably be expected to risk circumvention of the law; or (F) could reasonably be expected to endanger any individual's life or physical safety;
- (b)(8) exempts from disclosure information contained in reports or related to examination, operating, or condition reports prepared by, or on behalf of, or for use of an agency responsible for regulating or supervising financial institutions; and
- (b)(9) exempts from disclosure geological and geophysical information and data, including maps, concerning wells.

April 2012

(b)(3)

On Forecasting the Annual Cycle of Critical Ionosphere
Frequencies and Magnetic Storms

by G. M. Bartenev

Izvestiya Akademii Nauk SSSR, Otdeleniye Tekhnicheskikh
Nauk, No 9, pp 1153-1173, Russian Mo per, Sep 1947

(b)(3)

(b)(1)
(b)(3)

ON FORECASTING THE ANNUAL CYCLE OF CRITICAL IONOSPHERE
FREQUENCIES AND MAGNETIC STORMS

G. M. Bartenev

Presented by academician B. A. Vvedenskiy.

The numerous observations of the critical frequencies and the actual altitudes of the ionosphere during the course of the current 11-year cycle of solar activity make it possible to draw conclusions on the character of the variation in the ionization of the atmospheric layers during the course of the annual period. The ultimate object of this paper is to obtain computational formulae for forecasting the critical frequencies, as well as the number of magnetic storms, during which the quality of radio communication considerably deteriorates or is even completely interrupted.

Thanks to the large number of observations, it may now be considered as established that the ionization of the E and F₁ layers is primarily due to the ultraviolet rays of the sun, except in cases of abnormal sporadic ionization, which remains unchanged during the course of the night, when the influence of ultraviolet radiation is excluded.

According to Chapman's law [1], for a layer of the atmosphere ionized by monochromatic radiation of the sun, the critical frequency of the ionized layer at noon varies with the zenith angle of the sun in the following way:

$$f_{cr} = A \cos^{\frac{1}{4}} \theta$$

where A is a constant

This law satisfactorily describes the variations in the diurnal and seasonal ionization of the E and F_1 layers, but the behavior of the F_2 layer is not entirely subject to Chapman's law. This has been shown by ionosphere observations made at Huancayo, Peru [2], and also at Washington and Watheroo, Uoteru, published in the investigations of Berkner and Wells [3].

The ionization of the F_2 layer at noon in the northern hemisphere is less in midsummer than in winter, in December, when according to the law $\cos \theta$ the ionization in June should be greater, since the zenith angle of the sun is less at this time.

In midsummer the density of ionization in the F_2 layer is lower at noon than at 1000 hours, and there is a second maximum at 1800 to 2000 hours. Thus instead of a single noon maximum there are 2 maxima; this indicates that more than a single cause is responsible for the ionization of the F_2 layer.

Before the session of the International Scientific Radio Union in September, 1934, Appleton suggested that the cause of this anomaly might be found in the considerable variation in the molecular temperature of the higher layers of the ionosphere. In consequence of the low molecular density of the air at the altitude of the F_2 layer, a considerable heating of the medium by the solar radiation may be assumed.

Appleton and Naismith [4] suggest that as a result of this heating, the altitude of the uniform atmosphere H is increased, since

$$H = \frac{kT}{mg}$$

where T is the absolute molecular temperature, k is Boltzmann's constant, m is the mean molecular mass, and g the acceleration of gravity.

This reduces the density ρ in the region where maximum ionization takes place, since according to Chapman

$$\rho = \frac{\cos x}{A H} \quad (3)$$

where A is the absorption coefficient of radiation, x is the zenith distance of the sun, determined by the expression

$$\cos x = \sin \delta \cos \theta + \cos \delta \sin \theta \cos \Phi \quad (4)$$

δ is the sun's declination of the sun, θ is the zenith angle, Φ is the local time after noon, expressed in radians αt_{sec} or the longitude of the point, measured towards the east from the noon meridian at the moment of time t (time in seconds) that is

$$t = \frac{86,400 \Phi}{2\pi} = 1.37 \cdot 10^4 \Phi \quad (5)$$

whence

$$\Phi = 0.73 \cdot 10^{-4} t,$$

The reduction in ρ the density of the atmosphere, produced by the heating, reduces the maximum electron density N_{max} , since the full ionization attained at each definite level is now distributed over a greater thickness H of the ionized layer in question. [5]

The reduction in the noon ionization in midsummer is attributed by Appleton and Naismith to this circumstance [5].

Simultaneous and coordinated studies of ionization in the northern hemisphere (Washington, $\phi = 39^\circ$ N) and the southern hemisphere (Watheroo, $\phi = 30^\circ$ S), conducted by Berkner and Wells [4], demonstrated the untenability of the hypothesis seeking to explain the summer behavior of ionization in the F_2 layer by the heating of the ionosphere.

According to the observations at Washington and Watheroo, located almost symmetrically with respect to the equator, no summer effect on ionization of the F_2 layer is observed. The summer effect in the northern hemisphere proves to be general and simultaneous throughout the entire earth, and is thus observed in the southern hemisphere in winter, when the possibility of applying the heating hypothesis is excluded.

Moreover, according to the theory of Appleton and Naismith, the ratio of summer ionization density N_s to that in winter N_w is equal to

$$\frac{N_s}{N_w} = \left[\frac{\sin(\theta + \delta)}{\sin(\theta - \delta)} \left(\frac{T_w}{T_s} \right)^{\frac{1}{2}} \right]^{\frac{1}{2}} \quad (6)$$

Here T_w and T_s are the winter and summer molecular temperatures, taken as proportional to the electron temperature. On applying this expression to the Washington observations, we obtain a ratio of the summer molecular temperature to the winter, i.e. $\frac{T_s}{T_w}$, equal to 300, while according to the Watheroo observations this ratio is 2. Thus the temperature in the ionosphere over Washington

would be roughly 150 times higher than in the ionosphere over Watheroo, which is improbable.

The ionosphere observations at Washington and Watheroo, conducted by Berkner and Wells from 1933 to 1937 make it possible to reach the conclusion that there is an additional ionizing component, of period equal to one year, with a December maximum, and moving in phase for both hemispheres of the earth. This component has so great an amplitude that the seasonal variations in the ionosphere are completely masked.

Megacycles

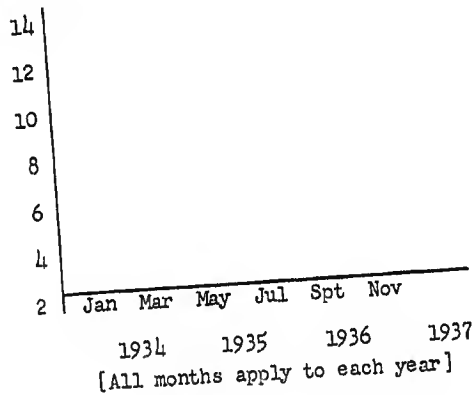


Figure 1

On the basis of the same experimental material from 1934 to 1938, T. L. Eckersley [5] held the detailed analysis of the F_2 layer ionization curves conducted by Berkner and Wells, disassociating them into secular, annual and seasonal components, to be well-founded, and turned his attention to the circumstance that in winter there is not one maximum but two, which are appreciably advanced towards the equinoxes (Figure 1).

In the course of his own detailed analysis, Eckersley came to the conclusion that there is also a half-year period in the ionization of the F_2 layer, due to the existence of active zones on the sun (at the average latitude of $\pm 15^\circ$ at the time of the maximum) and to the fact that the sun's axis of rotation is inclined to the plane of the ecliptic. In consequence of this, the earth on its orbit passes on 5 March and 7 September through those sectors most subject to solar radiations, and, conversely, passes in June and December through those sectors of its orbit that are least subject to solar radiation.

The existence of more complete experimental data than those at the disposition of Berkner and Wells, and likewise of Eckersley and others, now allows development of the work commenced by them up to the limit at which it will be possible to obtain computational formulae for forecasting the optimum frequencies of radio communication.

If the results of the ionosphere observations made at Washington from 1933 to 1945 are represented on a diagram $f_{kp} = \varphi(t)$, we obtain the curves shown on Figure 2. This figure shows the behavior of the critical frequencies for the E and F_2 layers, day and night, during the course of each month and year of the 11-year cycle; and in addition the flat curve characterizes the mean annual values of the critical frequencies f_E , $f_{F_2}^{-d}$, f_{F_2} and $f_{F_2}^{-M}$. As may be seen from the curve of noon values for the critical frequencies $f_{F_2}^{-d}$ of the F_2 layer, the peculiarities noted by Berkner and Wells, and likewise by Eckersley and others, in the behavior of the noon critical values are of systematic character throughout the entire 11-year cycle, which permits us to speak with great confidence of the

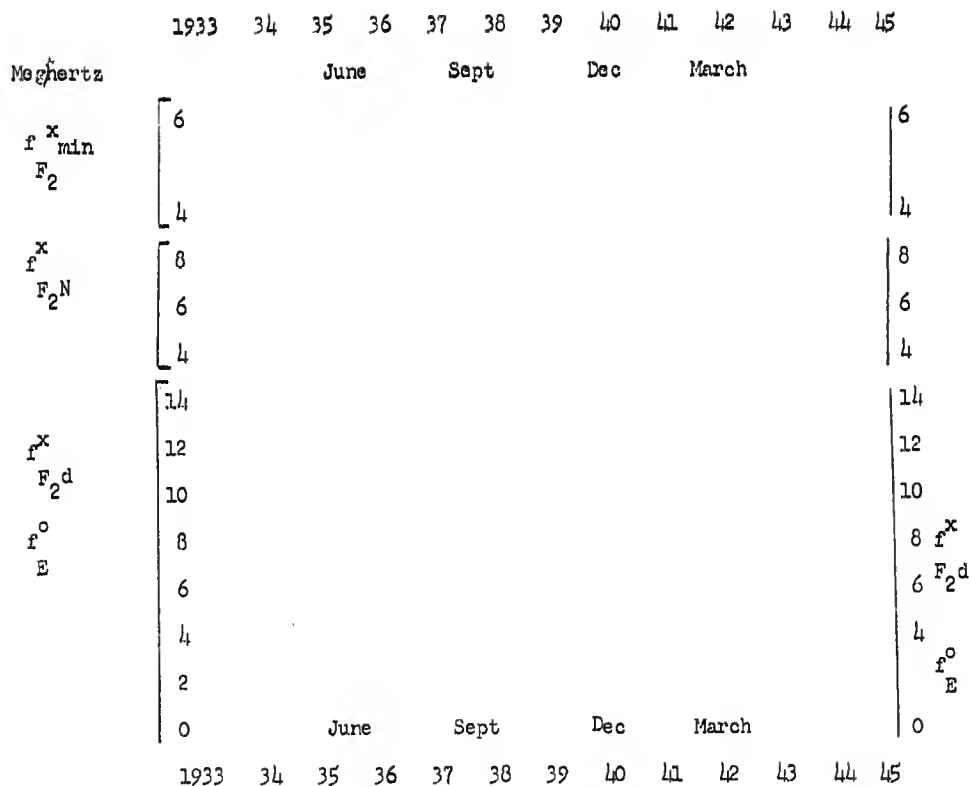
causes that produce variation in the march of the critical frequencies. Eckersley [5] has expressed the opinion that the causes producing these variations do not depend on the number of sunspots and have no connection whatever with any of the solar radiations. If the cause of the annual effect were the ultraviolet radiation of the sun, it would only be observed by day, but if it were due to causes not depending on the sun, and arising, for example, in stellar radiation, then the maximum effect would obviously be determined not by solar time but by sidereal time. Thus besides the noon maximum in December and January - for the northern hemisphere - there should also be a nocturnal maximum in June and July.

[See Figures 2 and 3 on next page]

Eckersley confirmed this opinion of his by the observations of the march of nocturnal ionization of the F_2 layer made at Tokio and published in the paper of Maeda, Tukada and Kamochida [6] (Figure 3).

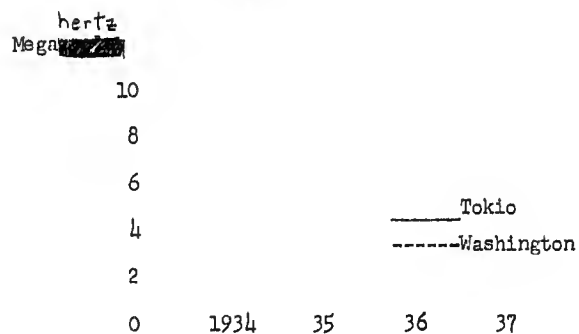
The observations of the Japanese were quantitatively inadequate to dispose definitely of the discussion provoked by Eckersley's hypothesis of the galactic origin of the ionization component responsible for the annual cycle.

The results of the observations of the critical frequencies $f_{F_2}^N$ of the F_2 layer at night, and of the minimum critical frequencies $f_{F_2}^M$ in the early morning hours at Washington, as shown on the top of Figure 2, confirm Eckersley's hypothesis, since the maximum ionization effect in these layers on a summer night represents a regular phenomenon over the course of every 11-year cycle.



[All months at top and bottom
apply to each year]

Figure 2



[All months apply to each year]

Figure 3

This phenomenon may be even more sharply emphasized by re-presenting in polar coordinates the observations shown in Figure 2, as we have done in Figure 4, and then, after calculating the monthly means for the noon night and minimum critical frequencies, for the year, over the entire 11-year cycle, also representing them in polar coordinates. (Figure 5).

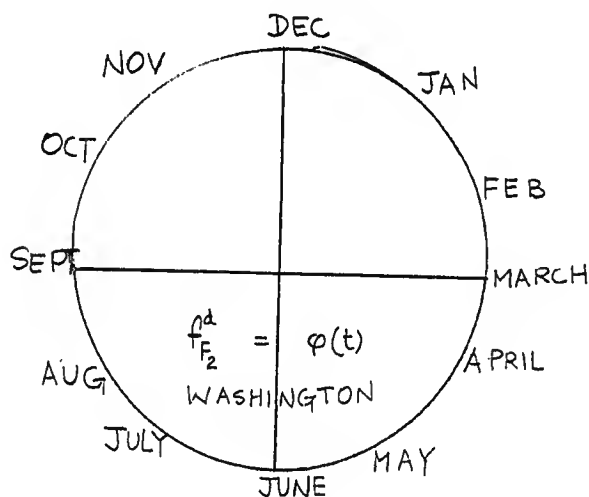
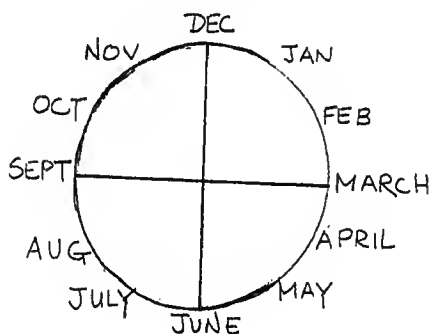


Figure 4



WASHINGTON
1934-1944

o - $\bar{f}_{F_2}^d$
 Δ - $\bar{f}_{F_2}^h$
 x - $\bar{f}_{F_2}^m$
 • - \bar{f}_E

Figure 5

This comparative diagram of the general annual march of the critical frequencies, on which the maximum effect has been taken as unity, vividly emphasizes that the annual-march component, which has a single maximum in December-January, is due to radiation of non-solar origin, since it depends on the march of sidereal time.

Eckersley [5] has suggested that the amplitude of the annual-fluctuation component of the ionization should be equal to the difference between the summer and winter ionization minima. Having available experimental material only for the first half of the solar cycle, he found, on eliminating the component of seasonal fluctuation, that the mean value of this amplitude was ± 20 per cent of the level of the mean annual value of the secular (11 year) march in the variation of atmospheric ionization.

Since we now ^(1.6 18 00.0) dispose of more complete material, covering the whole cycle, (Figure 5), we can now proceed to draw the same conclusion on the magnitude of the mean amplitude of the annual component, in the fluctuation.

Thus one of the components of the general curve (Figure 5) of the annual march $f^d \varphi = (t)$ is a curve that does not depend on the 11-year cycle of sunspot variation, with an amplitude ± 20 per cent of the level of that secular cycle. Eckersley assumed this curve to be an ordinary sine-curve, but this is not entirely correct.

Assuming that, the annual variation in the critical frequencies is dependent, as Eckersley claims, on galactic radiation, that the orbit of the earth is a true circle and that the stream of galactic radiation falling on the edge of the earth's orbit represents a parallel pencil, we determine the character of the variation in the noon

critical frequency for the F_2 layer of the atmosphere during the course of the annual period, as the path of a point on a circle of contracted radius, intimately connected with the earth's orbit and rolling, without sliding along a line of constant intensity of galactic radiation. This line of constant intensity we take for the axis of abscissae and plot on it the time by months of the year,

(Figure 6). Here the circle of radius r_1 , represents the orbit of the earth. If this circle rolled along the axis of abscissae without sliding, we would obtain an ordinary cycloid. But, if we limit the annual summer-winter fluctuation in the ionization of the F_2 layer by day, to ± 20 per cent which corresponds to the actually observed fluctuations in the critical frequencies, it is necessary to consider the rolling of a circle with the smaller radius r_2 ; this circle is intimately linked with the above-mentioned circle (the orbit of the earth). The locus of a point lying on the circumference of this smaller circle with radius r_2 as the circle rolls without sliding, represents a contracted cycloid, or what is termed a trochoid, rather than a simple curve, as Eckersley assumed in first approximation.

Taking as parameter the angle $QOP = \varphi$, which corresponds on the axis of abscissae to the segment traversed by the earth during its rolling along the orbit, we find how the ordinate QR , which is proportional to the value of the frequency $f_{F_2}^{-d}$, varies during the course of a year.

It is clear from Figure 6 that

$$f_{F_2}^{-d} = QR = OP - ON$$

But since

$$OP = r_1,$$

$$ON = r_2 \cos \varphi,$$

then

$$f_{F_2}^{-d} = QR = r_1 - r_2 \cos \varphi,$$

where ϕ is an angle proportional to the season of the year.

We find the numerical expressions for r_1 and r_2 on the basis of experimental data.

Berkner and Wells [4], and also Eckersley [5], have estimated in detail the various components of the annual march at atmospheric ionization. According to Eckersley the amplitude of the component of annual fluctuation amounts to ± 20 per cent. This figure remains true, on the average, throughout the entire cycle. Thus the radius of the smaller circle r_2 will be equal to 0.2.

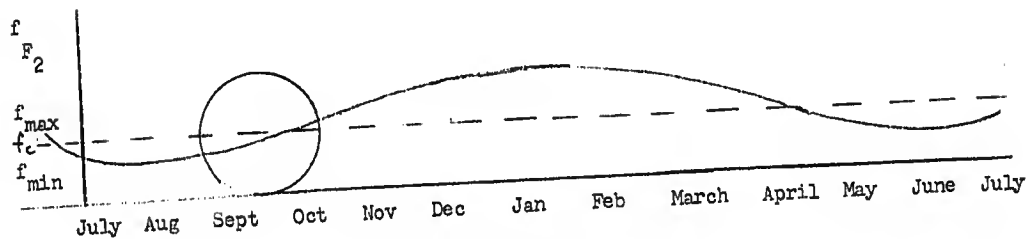


Figure 6

The value of r_1 is equal to the ordinate of the small circle (Figure 6), if it is taken as constant throughout the year. The component of annual fluctuation r_2 will vary during the course of the 11-year cycle as shown on Figure 7.

In fact, the component r_1 is not constant throughout the 11-

year (secular) cycle, and varies proportionately to the variation in the mean annual value of the critical frequencies.

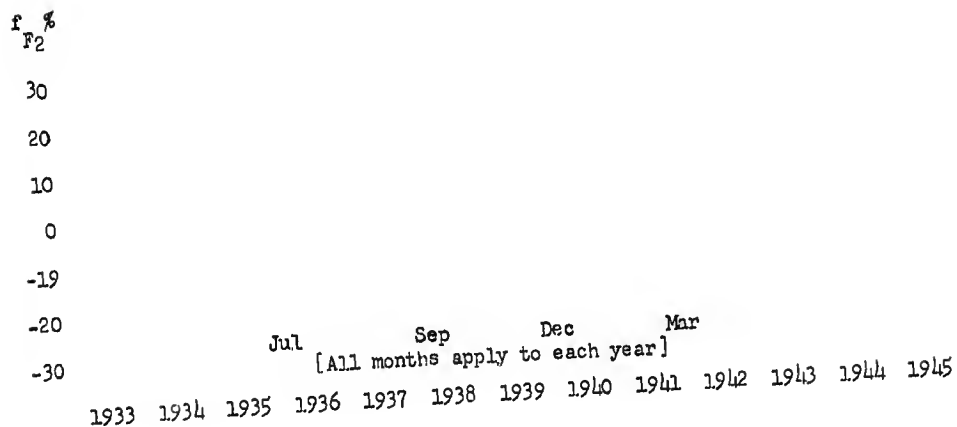


Figure 7

The value of r_1 thus corresponds to the critical frequency of the secular march, i. e.

$$r_1 = \frac{f_d}{F_2} \quad \text{secular}$$

Substituting now for the angle ϕ its value for each month, of the year, i. e.

$$\phi^\circ = \frac{2\pi}{12} t = (30t)^\circ$$

(where $t = 1, 2, \dots, 12$),

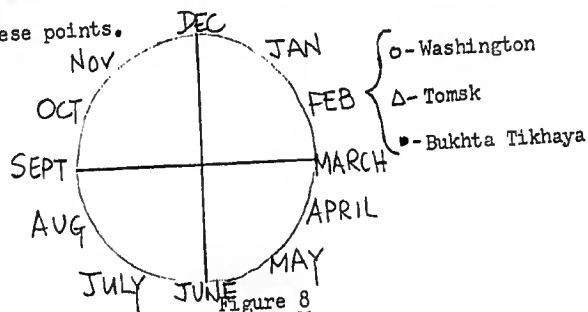
we shall have instead of (7):

$$\bar{f}_{F_2}^d = \bar{f}_{F_2}^d \text{ SECULAR} - 0.2 \cos(30t)^\circ \quad (8)$$

where $t = 1, 2, \dots, 12$ corresponds to January, February, etc. to December.

We now proceed to the determination of the semiannual component. The second principal component that enters into the general annual cycle of variation in the ionization of the atmosphere is the semiannual component.

If we consider from year to year the spiral curve shown on Figure 4, we shall note that as the 11-year cycle of ionization develops, the individual curves for each year, which at first are of epicycloidal character, change their form, and become deformed during the winter months (December to January), thanks to which cusps are formed at the time of the autumn and spring equinoxes. As the rate of solar activity falls, the annual curves again resume their original shape. This deformation of the epicycloids, which reaches its greatest extent during the time of maximum solar activity, is shown on Figure 8. The observations in Washington and Tomsk in 1937 and in Bukhta Tikhaya in 1939 [7] (Figure 8) clearly illustrate these points.



In addition to this, study of the catalog of magnetic storms according to the data of the Slutsk observatory of the period from 1878 to 1914 enables us to reach the conclusion that there is a sharply expressed semiannual march of the number N of magnetic storms, with spring and fall maxima (cf. table of distribution of the number of magnetic storms by months).

[See Table on following page]

Figure 9 is a polar diagram of the distribution of the number of geomagnetic storms, by months, for the period from 1878 to 1914. The radius-vector of this diagram is the number of magnetic storms taking place in the given month during the period from 1878 to 1914, while the argument is the time of year.

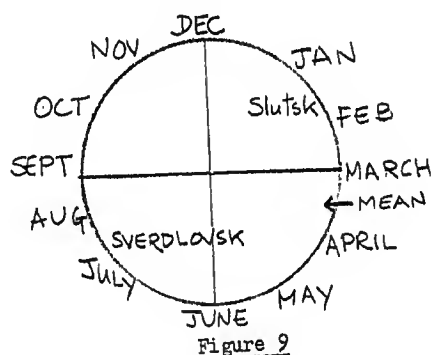


Figure 9

The construction of this diagram confirms the existence of a semiannual wave in the curves of geomagnetic activity as well. This phenomenon, known by the term Corti effect, subsequently termed Corti-

TABLE OF DISTRIBUTION OF THE NUMBER OF MAGNETIC STORMS BY MONTHS

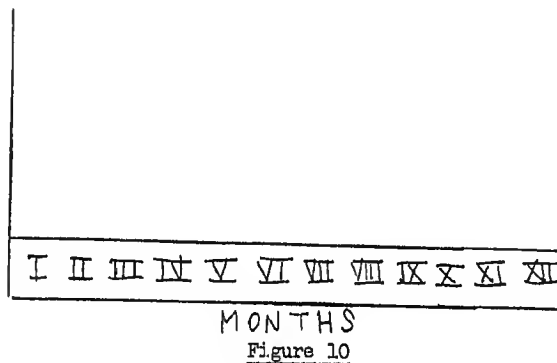
	JAN	FEB	MAR	APR	MAY	JUN	JUL	AUG	SEPT	OCT	NOV	DEC
Number of Magnetic Storms	61	81	86	68	65	49	52	63	73	72	65	48
Number of Magnetic Storms Related to Spring Maximum	0.71	0.94	1	0.79	0.755	0.57	0.605	0.73	0.85	0.838	0.755	0.56

Felitsyn effect (after Felitsyn [8] refuted the doubts of Yu. Bartels as the existence of the effect), arises in consequence of the fact that the geographic latitude (breadth) of the earth's equator does not coincide with the latitude of the sun's equator as we have already pointed out.

The diagram of magnetic-storm statistics (Figure 9) indicates to the same extent the existence of a definite zonal character in the active areas on the sun, to the same extent as on the diagrams of atmospheric ionization, and confirms the view that the direction of the stream of solar corpuscular radiation which produces geomagnetic storms, is primarily normal to the surface of the sun and has a small solid angle, which according to the investigations of M. N. Gnevishew and A. I. Ol, is equal to 8 or 9°.

On the lines of radio communication studied in 1944 according to the operating data of a number of radio lines, the semiannual march of geomagnetic disturbance in the ionosphere is likewise strongly reflected, as is well shown in Figure 10. The curves characterize the operation of the main radio lines under investigation during the day when the magnetic characteristic is equal to

$$M = 0, \quad M = 0.5, \quad M > 1.$$



The time, by months in 1944, is laid off along the axis of abscissae, and along the ordinates is plotted an expression, in percent, of communication interrupted equal to

$$K\% = \frac{t - t'}{t} \times 100, \quad (9)$$

where t is the scheduled operating time, and t' is the actual time operated.

These points may be even more clearly illustrated if the curve $M=0$ (Figure 10) is taken out of the curve for $M > 1$ and the curve IV so obtained is plotted on the diagram of Figure 9 (curve K). Here, by means of subtracting the ordinate of the curve $M=0$ from the ordinates of the curve $M > 1$, we eliminate the influence of the various factors that interfere with radio communication, other than the influence of magnetic disturbances in the ionosphere.

The predominance, in all seasons, of the geoactive indices of solar activity in the corresponding hemisphere of the sun (which results in the inequality of the ordinates of autumn and spring maxima) has been pointed out by Felitsyn [8] on the basis of a study of the march of the prominences. We see the same thing in Figure 9 with respect to the number N of magnetic storms as well. The spring wave of magnetic storms according to the Slutsk catalogue is dominant over the autumn wave. The march of the magnetic storms according to the Sverdlovsk catalogue is shown by dotted lines on Figure 9 as the mean value of the number N of magnetic storms during the four cycles from 1901 to 1945. The continuous thin line shows the mean value of magnetic storms according to the Slutsk catalogue.

Christy and Carrington [10] first directed attention to the zonal character of the active zones on the surface of the sun, which produce the semiannual wave in the march of atmospheric ionization (Figure 8) and in the march N of the number of magnetic storms (Figure 9). Subsequently Sporer [11] established his law of the movement of the active zones during the 11-year cycle. The accumulation of new data after the investigations of these astronomers now makes it possible to construct a diagram (Figure 11), on which the march of

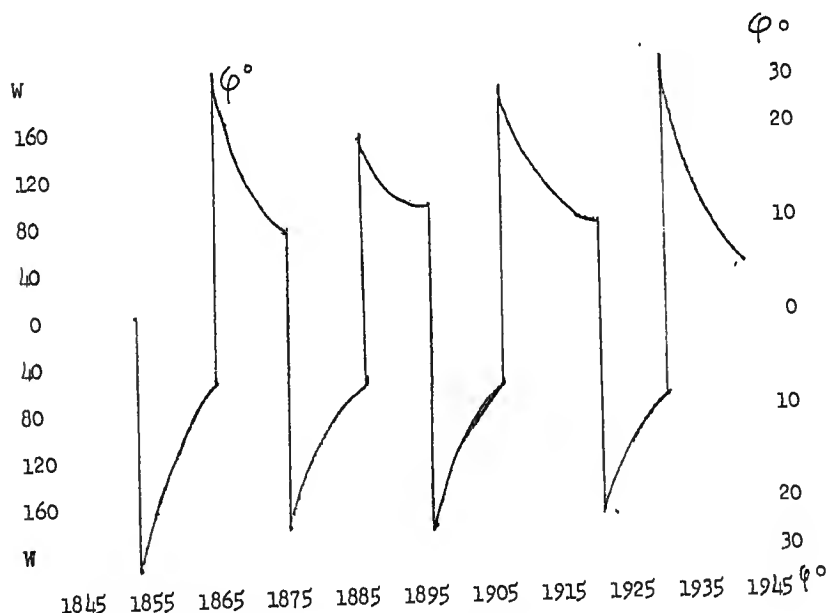


Figure 11

the active zones on the surface of the sun are shown, for the 8 cycles from 1855 to 1945 by their direction from the high solar latitudes ϕ towards the equator, together with the variations in the Wolf numbers W. This diagram gives a clear idea of the facts that

Diagram illustrating the Earth's tilt and the resulting seasons. The Earth is tilted on its axis. The top hemisphere is labeled 'June' and the bottom hemisphere is labeled 'December'. The top hemisphere is tilted towards the sun, and the bottom hemisphere is tilted away from the sun. The top hemisphere is labeled 'J', 'A', 'S', 'O', 'N', 'D' and the bottom hemisphere is labeled 'J', 'F', 'M', 'A', 'M', 'J'.

Figure 13

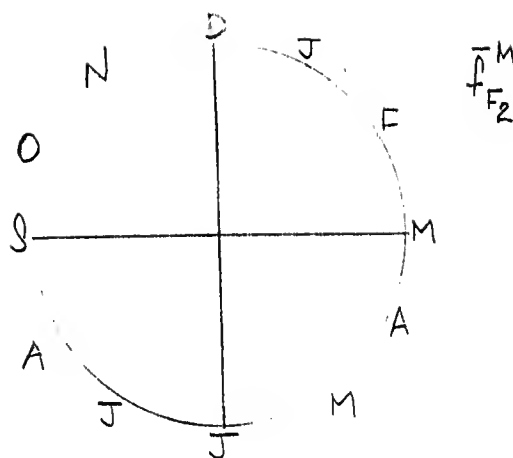


Figure 16

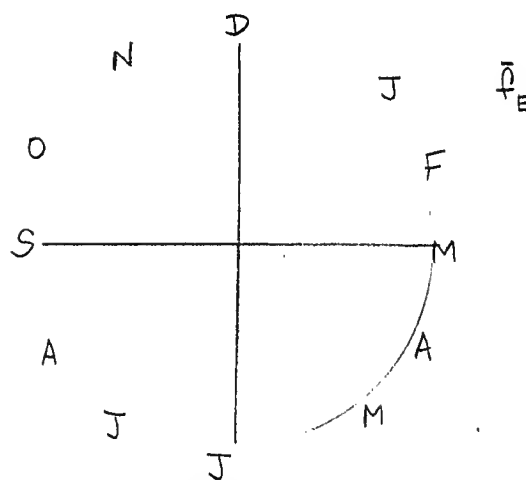


Figure 17

To give a graphic representation of the picture of variation in the intensity of solar activity throughout the 11-year cycle, the dependence of "W" on φ^0 (solar latitude) is shown in polar coordinates on Figure 12, for the minimum, mean and maximum intensity of the cycle.

The curve $W = f(\varphi^0)$ (Figure 12) may be generalized by an enveloping curve, known by the term "rose", expressed as follows in polar coordinates:

$$\rho = \rho_0 \sin(n\varphi) \quad (10)$$

where ρ is the radius-vector, varying from $-\rho$ to $+\rho$ as $n\varphi$ varies from 0 to 360 degrees.

Expression (10) may be transformed into a formula serving to forecast the Wolf numbers (1) [(1) See the author's dissertation "On the forecasting of radio communications".)], as follows:

$$W = W_0 \sin^m \varphi, \quad (11)$$

where

$$m = p_0 + p_1 t + p_2 t^2 + \dots + p_n t^n$$

Here t is the time by year of the cycle, and P_0, P_1, P_2 are constants determined for each individual cycle.

Thus, considering as we do that the existence on the sun of zones of maximum activity emitting a more or less directional radiation is indisputable, it is possible for us to propose the following method of forecasting the semiannual component in atmospheric ionization and the semiannual march of geomagnetic disturbance and disruption of radio communication.

The diagram of the 11-year march of radiation from the active zones, as shown on Figure 12, is represented by the congruent petals of a rose. In consequence of the symmetry of the radiation with respect to the axes of rotation of the Sun, the petals of the rose form a figure of rotation, the maximum radiation (radius-vector) of which is oriented, on the average, towards the angle ≈ 15 degrees of south and north solar latitude. This radius-vector, which symbolizes the magnitude and direction of the radiation, coincides with the normal to the solar surface at those places which most actively emit corpuscular and ultraviolet radiation during the epoch of maximum activity (Figure 13).

The sun's axis of rotation is inclined to the plane of the ecliptic at an angle of 7.2 degrees. The figure of rotation of the rose around the sun's axis, subjected to section at this angle, may be taken in its lowest part as the paraboloid of rotation with axis z , expressed by the following equation:

$$\frac{x^2}{p} + \frac{y^2}{p} - 2z = 0. \quad (12)$$

The equation of the plane so cutting the paraboloid of rotation at the angle of 7.2 degrees, and passing through the origin of coordinates, is:

$$-x \cos \alpha + z \cos \gamma = 0 \quad (12')$$

This plane is located in such a way that a line lying upon it and coinciding with the diameter of the ecliptic is located along the y axis perpendicular to the plane of the upper part of the drawing (Figure 13).

Equations (12) and (12') yield

$$y^2 = x \left(2p \frac{\cos \alpha}{\cos \gamma} - x \right). \quad (13)$$

This is the equation of a circle with the origin of coordinates lying on it, and the radius of which is determined by the expression

$$r = p \frac{\cos \alpha}{\cos \gamma}$$

and is located along the x axis.

In polar coordinates expression (13) takes the following form:

$$\rho = 2r \cos \psi. \quad (14)$$

The curve presented on the lower part of Figure 13 is a section of the northern and southern paraboloids of rotation and is a lemniscatoid with the following equation:

$$\rho^2 = 4r^2 \cos 2\psi$$

This curve belongs to what is termed the class of sinusoidal spirals, for which the general expression is of the form

$$\rho^m = 2r^m \frac{\sin}{\cos} (m\psi).$$

If we compare the curves that characterize the march of the critical frequencies at their maxima (Figure 4), and the values of the march of the number of magnetic storms obtained as the mean of the data of the Slutsk and Sverdlovsk catalogs (Figure 9, curve marked "mean") with the curve in Figure 13 (lower part), which is expressed by Equation (15), by superimposing the curves on the same chart (Figure 14), we see that equation (15) does not accurately characterize the distribution of magnetic storms.

For $\psi = 90$ degrees or $\psi = 270$ degrees, ρ will be zero by Equation (15), while on the diagram (cf. Figure 9) we have a value for ρ , at these angles, which is not less than 0.56 of the maximum December value of N and not less than 0.57 of the maximum June critical frequencies.

On the diagram of Figure 14, besides the lemniscatoid and the distribution curve for the magnetic storms, curves belonging to the same class of sinusoidal spirals are also plotted -- Cassini ovals. On comparing the curve of distribution of storms with these ovals it is clear that the distribution of storms (denoted by dots) can be well expressed by the equation of the Cassini oval, which represents the locus of points separated from two given points F_1 and F_2 by a constant distance τ^2 , equal to the product of the distance of these two points to the point sought on the Cassini oval. These given points F_1 and F_2 are separated from each other by the distance $2r$.

Since (by Figure 14)

$$\begin{aligned}\rho_1^2 &= \rho^2 + r^2 - 2\rho r \cos \psi, \\ \rho_2^2 &= \rho^2 + r^2 + 2\rho r \cos \psi,\end{aligned}$$

then

$$\begin{aligned}\rho_1^2 \rho_2^2 &= (\rho^2 + r^2)^2 - 4\rho^2 r^2 \cos^2 \psi = \tau^4, \\ \rho^4 + r^4 + 2\rho^2 r^2 \cos^2 2\psi &= \tau^4.\end{aligned}$$

Whence we have, as the general equation of the Cassini ovals,

$$\rho = r \sqrt{\cos 2\psi \pm \sqrt{\cos^2 2\psi + \frac{a^4}{r^4} - 1}} \quad (16)$$

The Cassini ovals corresponding to the three basic conditions

$$a > r, \quad a = r, \quad a < r$$

are plotted on Figure 14.

The first case -- curve I -- is expressed by Equation (16);
the second case -- curve II -- is the Bernoulli lemniscate expressed
by

$$\rho = r \sqrt{2 \cos \psi}$$

the third case -- curve III -- is expressed by the equation

$$\rho = r \sqrt{\cos 2\psi \pm \sqrt{\cos^2 2\psi - \cos^2 2\alpha}}$$

$$\text{where } \frac{a^2}{r^2} = \sin 2\alpha.$$

On this net of sinusoidal spirals (Figure 14), we plot the
curve of the annual march of the mean values for the number of mag-
netic storms obtained by averaging the statistical data published
in the Slutsk and Sverdlovsk catalogs of magnetic storms (Figure
9, curve of mean values).

Judging by the coincidence of the curve of magnetic storms
indicated by dots on Figure 14, with curve I of the Cassini ovals,
it may perhaps be considered that the annual march of magnetic
storms is well described by Equation (16). But since we are only
interested in the actual values, we shall have, instead of Equation
(16)

$$\rho = r \sqrt{\cos 2\psi + \sqrt{\cos^2 2\psi + \beta}} \quad (17)$$

where the parameter

$$\beta = \frac{r^4}{N_w^4} - 1 \quad (A)$$

depends on the value of h , which is, on a certain scale, proportional to the secular march of N_w , the number of magnetic storms, which number is readily determined on the basis of the good correlation of N_w with the Wolf numbers W ⁽¹⁾ [(1) See other paper by the author in this journal.]

Thus instead of parameter (A) we may write

$$\beta = \frac{r^4}{N_w^4} - 1.$$

The value of

$$r^2 = p_1 p_2$$

within this parameter, is constant for the correct Cassini oval [Equation (17)]. The numerical expression for r^2 may be determined by the method of quadratic approximation of periodic functions, using trigonometric polynomials.

Placing, for convenience, $\frac{r^2}{r^2}$ (Figure 14), or, what amounts to the same thing, $\frac{r^2}{N_w^2} = \sec 2\alpha$, we obtain, instead of the expression (17)

$$f(\psi) = \rho = N_w \sqrt{\cos 2\psi + r \sqrt{\frac{\cos^2 2\psi \cos^2 2\alpha - 2\cos^4 \alpha}{N_w^4}}} \quad (18)$$

Since (16) is a real function and applies to all real axes $-\infty < \psi < +\infty$ and has the period 2π , we may start out, in order to approximate it, from the polynomials,

$$T_n(\psi) = a_0 + \sum_{m=1}^n (a_m \cos m\psi + b_m \sin m\psi),$$

where the coefficients a_m and b_m are real numbers.

Regarding the function $\varphi(\psi)$ given within the period $(-\pi \leq \psi \leq \pi)$ as an integral weight, we set the task of reducing to a minimum the integral

$$\int_{-\pi}^{+\pi} [T_n(\psi) - f(\psi)]^2 d\varphi(\psi), \quad (19)$$

which by Weierstrass's second theorem [13] approaches zero as n increases without limit.

In consequence of the fact that the functions

$$\begin{aligned} \delta_0(\psi) &= 1, \quad \delta_1(\psi) = \cos(\psi), \quad \delta_2(\psi) = \sin(\psi), \quad \delta_3(\psi) = \cos 2\psi \\ \delta_4(\psi) &= \sin 2\psi \end{aligned}$$

etc., form a linearly independent system, it becomes possible as the only method, to select a system of trigonometric polynomials, orthogonal within the period $(-\pi, +\pi)$ with respect to the weight $\varphi(\psi)$.

By means of trigonometric polynomials of first, second and higher degree, the function $f(\psi)$ was aligned to the twelve successive ordinates corresponding to the months of the year, on the basis of which it was found that the value \uparrow has a mean value of 0.784 with an error not exceeding 7 percent.

On substituting the numerical value of \uparrow in the parameter β in Formula (17), and replacing the expression φ by N_T

and r by N_w , we finally obtain the following expression for forecasting the annual march of the number of magnetic storms

$$N_r = N_w \sqrt{\cos 2\psi + \sqrt{\cos^2 2\psi + \frac{0.787^4}{N_w^4} - 1}}, \quad (20)$$

where $\psi = (30t)^\circ$ ($t=1,2,3,\dots,12$ -- the months of the year).

In deriving Equation (20), which defines the annual march of magnetic storms, we confine ourselves to the only physically existing cause that disturbs the smooth secular march of magnetic storms and is responsible for the spring and fall maxima.

But we have no right to limit ourselves similarly in studying the annual march of atmospheric ionization. While in the case of magnetic disturbances taking place as the result of non-stationary phenomena on the surface of the sun, such as the appearance and disintegration of sunspots in the neighborhood of the central meridian, we still could confine ourselves to the mere statistical number N of magnetic storms, it is necessary, in studying the annual march of ionization, as we have already seen, to take account of the continuously acting causes that produce variation in the total amount of ultraviolet and corpuscular radiation falling on the earth.

It will be clear from the foregoing that in considering the variation in the march of ionization during the course of a single year, we may confine ourselves to three components. The annual component, with a maximum in December-January, has the character of a trochoid. The semiannual components with maxima in spring and

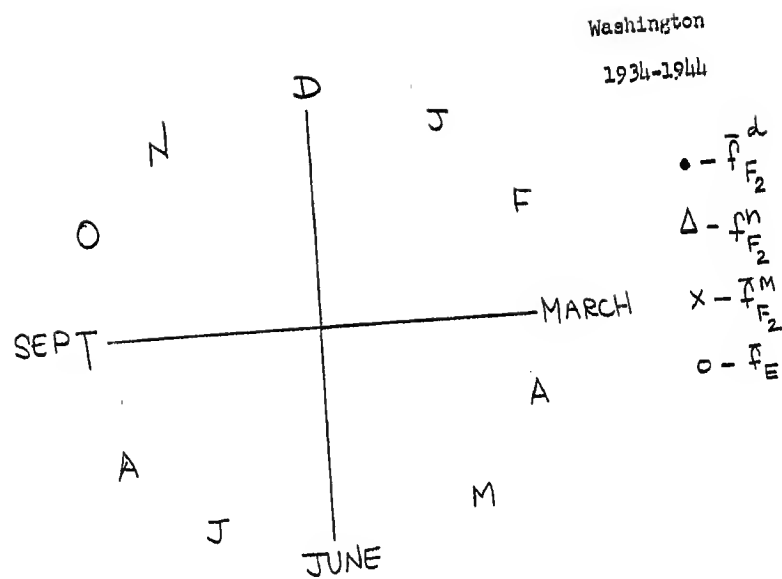


FIGURE 18

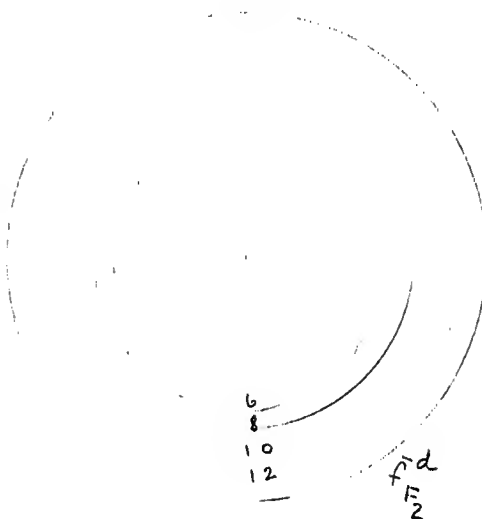


FIGURE 19

fall could be well represented by a Cassini oval, if it were not for the galactic corpuscular radiation postulated by Eccersley, which changes the shape of the ionization curve from a Cassini oval into an epicycloid, as may be seen from Figure 5, which represents the annual curves of the march of ionization of the layers of the ionosphere, averaged over the eleven years of the current cycle. Finally, the seasonal component, due to the inclination of the earth's axis to the plane of the ecliptic, has its maximum in June.

The curve of the seasonal march of ionization, as is clearly seen for the E layer (cf. Figure 5), can also be classified, in first approximation, as an epicycloid. For greater reliability in determining the character of the curves of the general annual march of the variation of ionization in the upper layers of the atmosphere, we have represented in megacycles (Figures 15, 16 and 17) the march of the critical frequencies by years of the 11-year cycle, at noon, for the F_2 layer (Figure 15), the march of the early morning minimum values -- half an hour before sunrise -- for the F_2 layer (Figure 16), and the march of the critical frequencies in the E layer at noon (Figure 17). To avoid complicating the picture, the whole 11-year cycle is not plotted on these diagrams. Each cycle, indicated by a spiral, corresponds to a single year.

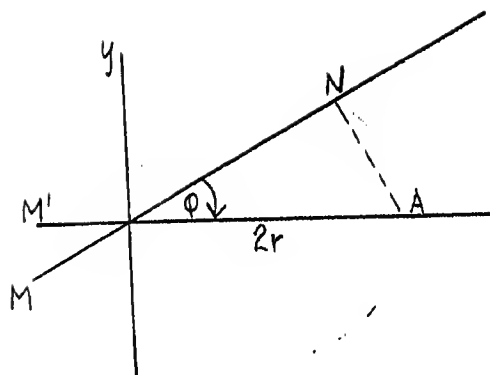


FIGURE 20

For the analytical determination of the shape of the curves in general form, we present in Figure 18 the mean values of the annual march of critical frequencies for 11 years for the F_2 layer (noon, midnight, and the minimum values) and for the E layer (noon values).

The curves thus obtained recall the cardioid, with its point of inflection for the curve $\bar{f}_{F_2}^d = \varphi(t)$ in June and for the other curves in December (Figure 18), but a cardioid may belong to any of three classes of curves, epicycloids, sinusoidal spirals, and "helices". The cardioid has a singular point at the origin of coordinates, which also constitutes a point of inflection. This cannot be said, however, of the critical-frequency curves we have derived (Figure 18), since the origin of coordinates in this case is the isolated point O.

We shall first investigate only a single curve, namely $\bar{f}_{F_2}^d = \varphi(t)$. This curve does not possess polar symmetry, inasmuch as the value of the critical frequency in December does not coincide with the value in June. But if the center be advanced to Point 2 (on Figure 19), then these values do coincide. We pass rays through the center O, joining the points of the curve derived, thus dividing each ray into the two equal parts $b_1 = b_2$ (Figure 19) and join the points that divide each ray. It then appears that the locus of these points represents a curve of almost circular shape and a diameter (O-2), equal to 2 megacycles (Figure 19). We now find that analytical expression of the values $\bar{f}_{F_2}^d$ which represents the radius-vector of the curve (19) in polar coordinates. For this purpose we represent separately, on an enlarged scale, the central part of Figure 19 (shown separately in Figure 20), where the circle of diameter 2r constitutes the above mentioned locus of the points dividing the rays in half.

We now determine the length of the radius-vector $\bar{f}_{F_2}^d = OL$.

Since

$$OL = 2r \cos \varphi + b,$$

then

$$\bar{f}_{F_2}^d = 2r \cos \varphi + b. \quad (21)$$

The curve obtained represents the polar equation of Pascal's helix, with a center which is an isolated singular point, since $b > 2r$.

In order to maintain the location of the curves which we have adapted (Figures 18 and 19), when the axis of abscissae coincides with the spring and fall equinoxes, we transform expression (21) as follows:

$$\bar{f}_{F_2}^d = 2r \sin \varphi + b.$$

Assuming, as in equation (8) that $\varphi = 30t = \frac{\pi}{6} t$, where t equals 1, 2, 3, ..., 12 for January, February etc., we shall finally obtain:

$$\bar{f}_{F_2}^d = 2r \sin \frac{\pi}{6} t + b$$

On making a similar study of the curves

$$\bar{f}_{F_2}^n = \varphi(t), \quad \bar{f}_{F_2}^m = \varphi(t), \quad \bar{f}_E = \varphi(t),$$

we find that they are also well described by the equation of Pascal's helix with an isolated singular point, namely:

$$\bar{f}_{F_2}^n = 2r_1 \sin \frac{\pi}{6} t^0 + b_1, \quad (23)$$

$$\bar{f}_{F_2}^m = 2r_2 \sin \frac{\pi}{6} t^0 + b_2, \quad (24)$$

$$\bar{f}_E = 2r_3 \sin \frac{\pi}{6} t^0 + b_3. \quad (25)$$

The numerical estimation of r , b , r_1 , b_1 , r_2 , b_2 , r_3 , and b_3 in equations (22), (23), (24), and (25) for the 11-year summer mean of the annual cycle (from 1933 to 1944), may be carried out as follows.

On superimposing the radius-vector $\vec{r}_{F_2} = OL$ on the axis of abscissae, which is the line joining the points of the summer and winter solstices (Figure 20), we see that

$$b = AL' = \frac{OL' + OM'}{2}$$

On the other hand,

$$2r = OA = \frac{OL' - OM'}{2}.$$

On substituting for the segment OL' in these equations the value of \bar{f}_{\max} of the critical frequencies in the F_2 layer at noon (for the time of the December solstice), which is proportional to that segment, and substituting for the segment OM the value of \bar{f}_{\min} , we have

$$b = \frac{\bar{f}_{\max} + \bar{f}_{\min}}{2}$$

(26)

$$2r = \frac{\bar{f}_{\max} - \bar{f}_{\min}}{2}$$

We obtain similar expressions b and $2r$ for the critical frequencies of the F_2 layer (night-time and early morning hours), and for the critical frequencies of the E layer, with the single difference that the maximum values for the frequencies of these layers will be in June, and the minimum values in December.

Using the mean values for the annual march of critical frequencies observed at Washington, putting their maximum value as unity, and applying expressions (26) and (27), we have

$$\bar{f}_{F_2}^d = 2 \sin \frac{\pi}{6} \tau + 9,$$

$$\bar{f}_{F_2}^n = 0.85 \sin \frac{\pi}{6} \tau + 4.92$$

$$\bar{f}_{F_2}^m = 0.375 \sin \frac{\pi}{6} \tau + 4.325$$

$$\bar{f}_E = 0.345 \sin \frac{\pi}{6} \tau + 3.295$$

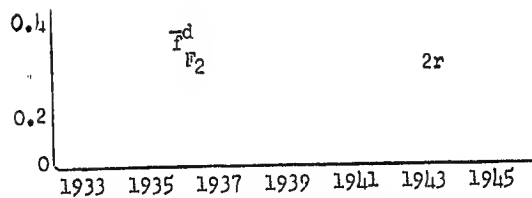


Figure 21

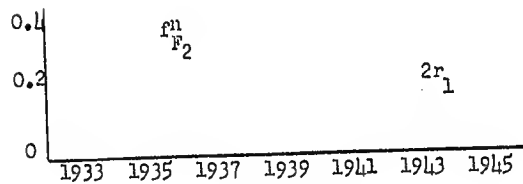


Figure 22

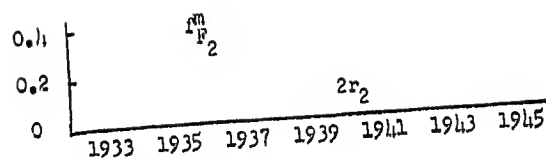


Figure 23

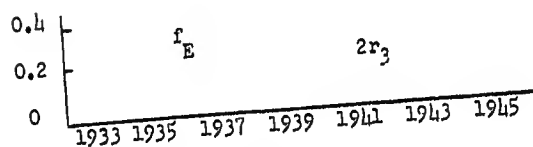


Figure 24

Here the values for the critical frequencies are expressed in megacycles. Estimation of the errors, carried out by comparison of the theoretical curves with the experimental, (Figure 19), shows the maximum deviation of the radius-vector of the curve of noon values for the F_2 layer from that obtained by calculation does not exceed 5 percent.

In the general case the following expressions may be used for forecasting purposes. In these expressions the mean annual values for the critical frequencies,

$$\bar{f}_{F_2W}^d, \bar{f}_{F_2W}^n, \bar{f}_{F_2W}^m, \text{ and } \bar{f}_{EW},$$

determined by the correlation equations, (1) [1. See other paper by this author in same number of this journal.] have been substituted for b, b_1, b_2, b_3 (Formulae (22) to (25)),

$$f_{F_2}^d = 2r \sin \frac{\pi}{6} t + f_{F_2W}^d, \quad (32)$$

$$f_{F_2}^n = 2r_1 \sin \frac{\pi}{6} t + f_{F_2W}^n, \quad (33)$$

$$f_{F_2}^M = 2r_2 \sin \frac{\pi}{6} t + f_{F_2W}^M, \quad (34)$$

$$f_E = 2r_3 \sin \frac{\pi}{6} t + f_{EW}^6. \quad (35)$$

The values of r , r_1 , r_2 and r_3 are determined by formula (27) where there is an experimental value for the December value f_{\max} or the June value f_{\min} .

The character of the variation in r , r_1 , r_2 and r_3 during the past cycle in the areas of their maximum values is depicted on Figures 21-24.

It may be seen from studying these diagrams that the course of the curves differ. The variation in the value $2r$ agrees with the march of the cycle; the same may be said of the variation in $2r_1$ (Figure 22) and $2r_2$ (Figure 23), but $2r_3$ varies only slightly with the development of the cycle. The more precise forecasting of the critical frequencies is limited by the inadequate accumulation of experimental data, which still requires considerable supplementation to render possible the verification and elaboration of our conclusions.

Section of scientific treatment
of problems of radio technology
of the Academy of Sciences USSR

Received by the editors
4 June 1947

BIBLIOGRAPHY

1. Chapman, S. Proc. Phys. Soc., 43, 1931.
2. Berkner, L. and Wells, H. Terr. Magn. and Atm. El. 43, No. 1
March 1938.
3. Berkner, L. and Wells, H., Terr. Magn. and Atm. El. 39, 215 1934.
4. Appleton, E. and Naismith, R., Proc. Roy. Soc. Ser. A 150, July 1935.
5. Eccersley, T. L., Terr. Magn. and Atm. El. 45, No. 1, 1940.
6. Maeda, H., Fukada, T. and Kamochida, T. Rep. Radio Res. Japan,
7, 109-119, 1937.
7. Arkhangel'skiy, B. F. Bulleten' ionosfernykh solnechnykh i
geomagnitnykh dannikh Soveta po radiofizika i radiotekhnike
AN SSR (Bulletin of ionospheric, solar and terrestrial mag-
netism data of the Council on Radio Physics and Radio Tech-
nology of the Academy of Sciences USSR), VIII-IX, 1940.
8. Felitsyn, F. I. Astronomicheskii Zhurnal (Astronomical Journal)
17, 21, 1.
9. Gnevishew, M. N. and Ol, A. I., Terr. Magn. and Atm. El. 51
No. 2, 1946.
10. Carrington, J.M.N., 19, 1, 1858.
11. Sporer, H., Publ. Astrophys. Obs. Potsdam, 11, Tafel (Table) 32,
1881.
12. Waldmeier, M. Astronomische Mitteilungen, (Astronomical Commu-
nication Nr. CXXXVIII, 1939.
13. Goncharov, V. L. Teoriya interpolirovaniya i priblizheniya
funktsiy (Theory of Interpolation and Approximation of
Functions), ONTI-GTTI, 1934.
14. Whittaker, E. (Uittek) and Robinson, G., Matematicheskaya obrabotka
rezultatov nablyudeniya (The mathematical treatment of observational
results). GTTI, 1933.

12/24
B-4/11/66
INFORMATION REPORT INFORMATION REPORT
CENTRAL INTELLIGENCE AGENCY

This material contains information affecting the National Defense of the United States within the meaning of the Espionage Laws, Title 18, U.S.C. Secs. 793 and 794, the transmission or revelation of which in any manner to an unauthorized person is prohibited by law.

C-O-N-F-I-D-E-N-T-I-A-L

13553-195

COUNTRY Czechoslovakia

REPORT NO. [redacted] (b)(3)

SUBJECT Bohumila Bednarova-Novakova/Czechoslovakian
Work on the Origin of Geomagnetic Storms/
Role of Solar Filaments/Prediction of
Solar Flares

DATE DISTR. 24 December 1964

NO. PAGES 2

REFERENCES

DATE OF
INFO.

December 1964 and earlier

PLACE &

DATE ACQ. -- - December 1964 and earlier

THIS IS UNEVALUATED INFORMATION

[redacted] 59 page article, in English, entitled, "On the Problems of the Origin of Geomagnetic Storms," co-authored by Bohumila Bednarova-Novakova, Vaclav Bucha, Jaroslav Halenka, and Majmir Konecny, all of the Czechoslovakian Academy of Science's Geophysical Institute, Prague

UNCLASSIFIED]

1. Above listed on file item is one of the more complete works in a long series of booklets, pamphlets, articles, letters, etc, authored by herself and other members of the institute, [redacted] over the years on the subject of solar magnetic storms and their predictability by the examination of filaments. [All these items are available on loan] (b)(3)
2. With some of her statements, such as that claiming solar flares are essentially unimportant to the study of geomagnetic storms, Madam Bednarova [redacted] complete disagreement. Other aspects of the work, however, are convincing enough [redacted] there should be some US investigations along similar lines. (b)(3)
3. Much US work has been done on solar filaments, but not as Bednarova has, on their use as a means of predicting solar geomagnetic activity. [redacted] some prediction is possible by her method, [redacted] unconvinced of the extent she claims for it. Like so many of the other Soviet and East European scientists, she accepts a few agreeable phenomena as "proof" of her thesis and thus tends to build much of her later work on a poor foundation. Never the less, her work has continued to become more precise and complex over the years; she continues in her efforts, and now claims a prediction time of several days. (b)(3)
4. Several recent US filament studies have failed to support Bednarova's claims. In support of her reply, however, [redacted] the US work was based on filaments in general, and lacked the sophisticated selection of type that she states is necessary. Although there is little support for her system in this country, [redacted] there may be some sound basis for her claim and that it merits further examination. (b)(3)

C-O-N-F-I-D-E-N-T-I-A-L

GROUP 1
Excluded from automatic
downgrading and
declassification

U-NO

S-NO

STATE ARMY NAVY AIR FBI AEC

INFORMATION REPORT INFORMATION REPORT

CONTROLLED DISSEM

NO DISSEM ABROAD

NO FOREIGN DISSEM

The dissemination of this document is limited to civilian employees and active duty military personnel within the intelligence component of the USIB member agencies, and to those senior officials of the member agencies who must act upon the information. However, unless specifically controlled in accordance with paragraph 8 of DCID 1/7, it may be released to those components of the departments and agencies of the U. S. Government directly participating in the production of National Intelligence. IT SHALL NOT BE DISSEMINATED TO CONTRACTORS. It shall not be disseminated to organizations or personnel, including consultants, under a contractual relationship to the U.S. Government without the written permission of the originator.

Approved for Release 2005/05/05 UNCLASSIFIED C06131746

~~CONFIDENTIAL~~

-2-

(b)(3)

5. Bednarova has worked in this field for many years now, seemingly with increasing prominence. [redacted] fail, however, to find any indication of USSR, or other, direction or support to back up space communication or man-in-space programs.

(b)(3)

-end-

C-O-N-F-I-D-E-N-T-I-A-L

5
4
3
2
1

CONTROLLED DISSEM

NO DISSEM ABROAD

NO FOREIGN DISSEM

PRÁCE GEOFYSIKÁLNÍHO ÚSTAVU ČESKOSLOVENSKÉ AKADEMIE VĚD
ТРУДЫ ГЕОФИЗИЧЕСКОГО ИНСТИТУТА ЧЕХОСЛОВАЦКОЙ АКАДЕМИИ
НАУК

TRAVAUX DE L'INSTITUT GÉOPHYSIQUE DE L'ACADÉMIE
TCHÉCOSLOVAQUE DES SCIENCES

No 192

GEOFYSIKÁLNÍ SBORNÍK 1963

ON THE PROBLEMS OF THE ORIGIN OF GEOMAGNETIC STORMS

Bohumila Bednářová-Nováková, Václav Bucha, Jaroslav Halenka,
Mojmír Konečný

Geophysical Institute Czechosl. Acad. Sci., Prague

Contents

Introduction	408
I. Events on the Sun	409
1) Sunspots	411
2) Flares	413
3) Filaments (prominences)	414
4) Relations between spots, flares and filaments.	415
II. Conditions in interplanetary space and exosphere.	416
III. Geomagnetic activity	418
1) Time variations of geomagnetic field	418
2) Classification of geomagnetic storms	421
3) Attempt at new classification of sc-storms	423
IV. On the question of the mechanism of geomagnetic storm development	428
1) Basic classification of geomagnetic storm	428
2) Types of geomagnetic storms from aspect of their geographic expression.	429
3) On the theory of the causes and origin of geomagnetic storms.	431
V. Connection between processes on the Sun and geomagnetic activity	437
1) Solar activity — Phases of development of active centre	437
2) Geomagnetic activity and sunspots.	438
3) The question of the geoactivity of flares	441
4) Filaments and corona — their geoactive effects	446
5) Deductions — On the problem of geomagnetic storm prognosis	454
Conclusion	456

407

INTRODUCTION

The study of questions concerning the origin of geomagnetic storms represents a very topical problem of a wide scientific and practical range; for this reason relatively great attention is at present devoted to it. The aim of the present paper, apart from some new conclusions, is to give a comprehensive interpretation of the results obtained by us when studying the connection between geomagnetic and solar activity and to contribute towards an evaluation of the knowledge obtained hitherto in this field of research. In investigating the relations between the two effects the paper starts out with a brief discussion of solar events and the mechanism of geomagnetic storms, which is included in order to clarify the dependences given. The paper tries to point out the complexity of the problems solved.

Geomagnetic storms, which according to the character of their expression can be divided into several groups, are caused essentially by processes taking place on the Sun. A neutral cloud of ions and electrons of solar origin approaches the region of the Earth, where it is influenced by the latter's magnetic field. At such a mutual effect of the dynamic and magnetic factors an electrical current system is induced in the cloud. This leads to the compression of the Earth's magnetic field and thus to the origin of the first phase of a geomagnetic storm. As is seen, a relatively complicated mechanism marks the actual process of the formation of a storm. This mechanism can be divided into several partial stages as a function of the place and the conditions in which these processes take place.

The basic source of all geomagnetic disturbances of the external field are processes taking place on the solar surface and in the corona. It is well known that the active regions on the Sun exhibit relatively strong magnetic fields which influence the movements of glowing solar matter on the surface and in the neighbourhood of the Sun. The forms of such flow and the movement of matter differ and also the expressions of such events, as observed on the solar disc, have a quite definitely defined character. An important object of present-day research is to clarify which of these processes may be geoeffective.

It is thus important to study the composition of solar corpuscular streams, and particularly to determine whether they can maintain and carry with them part of the magnetic field from the Sun. The study of this question may contribute towards explaining the fact that some magnetic storms are not followed by a storm of cosmic radiation.

Another open question is how corpuscular streams behave in the space between the Sun and the Earth before they reach the region of the geomagnetic field and to what extent they are braked by the interplanetary gas.

Another field of research deals with the space in the neighbourhood of the Earth, where complex processes take place due to the motion of particles in the magnetic field. The hydromagnetic processes obviously taking place here are certainly strongly dependent on the conditions and physical composition of the outer atmosphere. The

questions of the laws of interaction between magnetic fields and fluid-motion are also very important despite the fact that many new results have been obtained by observations using satellites.

The basic material for studying geomagnetic storms are their expressions as recorded at magnetic observatories. If, however, we wish to explain their physical causes and the influences to which they are subject during their formation and to contribute towards explaining the mechanism of their formation and their prognoses, the results of studying processes taking place on the Sun, which are the primary cause of geomagnetic storms, must be taken into consideration.

The above-mentioned partial problems show the whole sequence of data from the initial impulse on the Sun up to the expression of the geomagnetic storm on the Earth's surface.

The present paper also aims at contributing, at least along basic lines, towards explaining some of the above questions, particularly as regards processes taking place at the formation of geoactive processes on the Sun and as regards the classification of magnetic storms and the relations between solar and geomagnetic phenomena.

Questions of the magnetic fields on the Sun and the hydrodynamic processes taking place there are discussed. An evaluation is made of the different events on the Sun with regard to whether they may be considered as sources of disturbances in the geomagnetic field. Chapter II contains some brief notes on the conditions in interplanetary space.

It is well known that a whole series of geomagnetic disturbances occur which differ from one another. This question of the classification of storms is dealt with in Chap. III.

Chapter IV gives some data on processes taking place at the interaction of corpuscular streams with the geomagnetic field.

In Chap. V the authors sum up their results of studying the dependence of magnetic storms on solar activity. An evaluation is also made of the results obtained up to now from which some interesting conclusions are drawn as to the causes of magnetic disturbances.

The conclusion contains an evaluation of present-day knowledge as well as describing the main tasks to be solved in the immediate future.

I. EVENTS ON SUN

The processes, which take place on the solar surface and which are connected with the interaction of the motion of glowing matter and the magnetic fields are very complicated and heterogeneous. However, one can find among them a series of processes exhibiting a certain system in their occurrence and form. It is found that magnetic fields on the Sun have a great influence on the production of different solar formations. Although it cannot yet be deduced whether parts of the magnetic fields are transferred

from the Sun to the Earth with the corpuscular stream and whether they influence the magnetic field of the Earth directly, in any case these fields play a role in the ejection of particles from the solar region. The importance of studying them is therefore obvious.

Analogously as for the Earth, there exists a total magnetic field of the Sun which can be modelled by means of dipoles. Although the intensity found for the total field reaches relatively small values compared with the magnetic fields accompanying some other solar effects, its dimensions show its decisive influence on the formation of a corona of so-called minimum type. If regions of strong local fields occur then they greatly disturb the total field in the neighbourhood of the Sun, which, due to their high intensity, loses its dipolar character.

From the geoactive point of view the formations occurring in connection with sun-spots as well as the spots themselves are important; the effects are included under the concept of a centre of activity. The development of such a centre is governed by certain laws while the lifetime of the phenomena which occur is not the same. The whole cycle of development of such a region has been described in detail in [1].

We are interested in those formations about which it can be assumed that they might be the causes of geomagnetic storms. Opinions held hitherto on this question have varied a lot and have been far from giving a clear answer. They can be divided into three groups:

a) The causes of geomagnetic storms have been ascribed to the occurrence of spots on the Sun. Earlier statistical comparisons, which paid no attention to other processes occurring in the spot regions, showed a certain connection particularly for average values from annual intervals; however, the degree of correlation between the two effects decreases with decreasing length of the intervals. At shorter intervals the connection between the two effects can no longer be proved [2]. A more detailed analysis of the solar situation during the occurrence of spots showed that certain connections are apparent between geomagnetic activity and spots of large dimensions. They depend to a great extent also on the mutual arrangement of the spots. The correlation improves [3] if spots with a high flare activity are used in the analysis.

b) For this reason relatively great attention was paid to the occurrence of flares. Certain relations have been found between the occurrence of geomagnetic storms and strong flares. At present flares are regarded in the world as the source of geomagnetically effective corpuscular streams. However, as regards medium and weak flares, no laws were found. For this reason increased attention is paid in this paper to the question of the geoactivity of flares.

c) It has also been shown [4] that the occurrence of filaments in the neighbourhood of the central meridian (CM) results, in approximately 3 to 5 days, in a magnetic disturbance. One might deduce from this that filaments are the source of corpuscular radiation. Coronal rays above filaments were regarded as an even more likely cause of storms [5]. A profounder set of laws was found on the basis of a detailed investigation into filaments and their relation to the coronal formations [6, 7]. The question

4

from the Sun to the Earth with the corpuscular stream and whether they influence the magnetic field of the Earth directly, in any case these fields play a role in the ejection of particles from the solar region. The importance of studying them is therefore obvious.

Analogously as for the Earth, there exists a total magnetic field of the Sun which can be modelled by means of dipoles. Although the intensity found for the total field reaches relatively small values compared with the magnetic fields accompanying some other solar effects, its dimensions show its decisive influence on the formation of a corona of so-called minimum type. If regions of strong local fields occur then they greatly disturb the total field in the neighbourhood of the Sun, which, due to their high intensity, loses its dipolar character.

From the geoactive point of view the formations occurring in connection with sun-spots as well as the spots themselves are important; the effects are included under the concept of a centre of activity. The development of such a centre is governed by certain laws while the lifetime of the phenomena which occur is not the same. The whole cycle of development of such a region has been described in detail in [1].

We are interested in those formations about which it can be assumed that they might be the causes of geomagnetic storms. Opinions held hitherto on this question have varied a lot and have been far from giving a clear answer. They can be divided into three groups:

a) The causes of geomagnetic storms have been ascribed to the occurrence of spots on the Sun. Earlier statistical comparisons, which paid no attention to other processes occurring in the spot regions, showed a certain connection particularly for average values from annual intervals; however, the degree of correlation between the two effects decreases with decreasing length of the intervals. At shorter intervals the connection between the two effects can no longer be proved [2]. A more detailed analysis of the solar situation during the occurrence of spots showed that certain connections are apparent between geomagnetic activity and spots of large dimensions. They depend to a great extent also on the mutual arrangement of the spots. The correlation improves [3] if spots with a high flare activity are used in the analysis.

b) For this reason relatively great attention was paid to the occurrence of flares. Certain relations have been found between the occurrence of geomagnetic storms and strong flares. At present flares are regarded in the world as the source of geomagnetically effective corpuscular streams. However, as regards medium and weak flares, no laws were found. For this reason increased attention is paid in this paper to the question of the geoactivity of flares.

c) It has also been shown [4] that the occurrence of filaments in the neighbourhood of the central meridian (CM) results, in approximately 3 to 5 days, in a magnetic disturbance. One might deduce from this that filaments are the source of corpuscular radiation. Coronal rays above filaments were regarded as an even more likely cause of storms [5]. A profounder set of laws was found on the basis of a detailed investigation into filaments and their relation to the coronal formations [6, 7]. The question

of the causes of geomagnetic storms has still not been convincingly explained, however. As is clear from the above, there are considerable differences in opinion as to the identification of the actual sources of geoeffective corpuscular radiation.

Let us now deal in greater detail with the most important solar phenomena from the point of view of the processes which take place during them and with the possible mechanism of their origin.

1) Sunspots

It is well known that sunspots have a very strong field, attaining an intensity up to 4500 Oe, compared with the total field of the Sun. It can therefore be assumed that this property plays a considerable role in the equilibrium of sunspots. The mechanical forces appearing during such phenomena are balanced by magnetic pressures. The magnetic flux passing through the sunspot region can be expressed by the relation [8]

$$(1) \quad \Phi = \int H d\sigma$$

where σ is the surface element, H the magnetic field. It is seen that a change in flux takes place in approximately the same way as the formation of a sunspot region. We can therefore assume [9] that the field already existed in the deeper parts below the surface of the Sun before the spot became visible and that it is brought to the surface by the action of some mechanism. This is confirmed by the relatively long-term existence of solar centres of activity while the sunspots characterizing the time maximum of the field have a much shorter life. In the interior of the Sun, on the assumption of strong convection, torsional oscillations may be produced. As a consequence of the uneven rotation of the Sun certain parts of the mass may be exposed to oscillations in longitude and latitude; they begin to get near to the surface of the Sun and cause considerable distortion of the lines of force (Fig. 1). The pre-condition for this process is a relatively high degree of magnetic rigidity. For a non-uniformly rotating Sun, having a magnetic field, one may consider that it has lines of force frozen into its matter. Its field can be constant on the assumption that it is symmetrical around the axis of rotation.

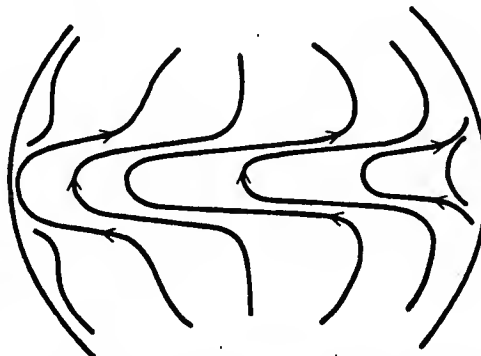


Fig. 1. Distortion of magnetic lines of force near to solar surface at approach of torsion wave to equator.

According to the law of isorotation [10] it holds that

$$(2) \quad \partial \mathbf{H} / \partial t = (\mathbf{H} \cdot \text{grad}) \mathbf{v} - (\mathbf{v} \cdot \text{grad}) \mathbf{H}$$

where \mathbf{H} is the magnetic field, \mathbf{v} the velocity of motion of the mass.

In cylindrical coordinates R, Φ, z , where R is the distance from the axis of rotation, Φ the corresponding angle and z the distance from the equatorial plane, the above equation can be resolved into components. Let ω be the angular velocity so that $\mathbf{v} = R\omega$. If the stationary state of rotation is disturbed as a result of the azimuthal removal of part of a body, the disturbance is equivalent to a torsional magnetohydrodynamic wave propagated along the lines of force. Let the motion be defined by

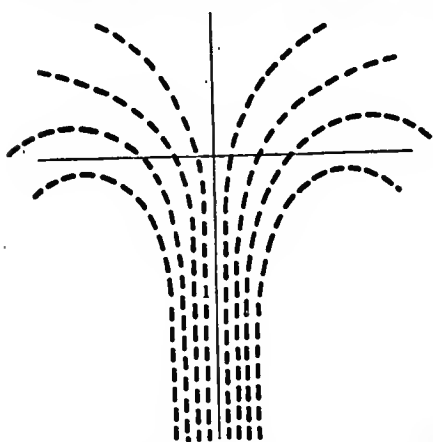


Fig. 2. Hypothetical distribution of magnetic lines of force at their exit from spots on surface of Sun (vertical cross-section of spot).

the component of the undisturbed angular velocity ω_0 and the component ω' as a result of the disturbance. Analogously, let the field \mathbf{H} be composed of the undisturbed component \mathbf{H}_0 and the disturbance field \mathbf{h} . Then we obtain

$$(3) \quad \partial h_\Phi / \partial t = R(\mathbf{H}_0 \cdot \text{grad}) \omega'$$

In the component Φ of the equation of motion there then appears only the electromagnetic force $\mu[\mathbf{j} \times \mathbf{H}]$ so that this component reduces to

$$(4) \quad 4\pi \rho R^2 (\partial \omega' / \partial t) = \mu(\mathbf{H}_0 \cdot \text{grad}) R h_\Phi$$

The permeability μ , about which it is assumed that it is equal to one, is usually left in the expressions to facilitate transformation. Expressions (3) and (4) form important relations in the theory of magnetohydrodynamic waves. They can be used on the

assumption that the disturbance field \mathbf{h} is much larger than the field \mathbf{H}_0 and thus the torsional oscillations may form a large azimuthal field \mathbf{h} from the small field \mathbf{H}_0 in the meridional planes [9]. Strong convection may then cause a decrease in angular velocity in the interior of the Sun. This fact then causes the torsional magnetohydrodynamic wave to propagate along the lines of force in the direction of the surface (Fig. 1). It may be considered that this torsional wave proceeds against the equator. If it gets close to the surface the lines of force there form a band around the Sun. On penetration to the surface two regions with reversed magnetic polarity may then be formed; in one the lines of force intersect the surface in the outwards direction and in the other they return inwards. These regions can then be regarded as a pair of sunspots with reverse magnetic polarity.

Due to the high values of the magnetic field in the spots the magnetic pressure ($\mu H^2 / 8\pi$) here reaches relatively high values of the order of 1.6×10^5 dyne/cm². This

magnitude causes the mass in the regions around the spots to be pressed back and the lines of force lose their original vertical direction. They are detained in the sub-surface layers and above the surface, as is seen from Fig. 2.

Due to the relatively strong magnetic fields in the spots and in their immediate neighbourhood solar matter can hardly be released outside the region of the Sun; the movements of the mass here are governed by their magnetohydrodynamic laws. Spots can therefore hardly be regarded as a direct source of geomagnetic disturbances.

2) Flares

Flares appearing as short-term sudden effects in the neighbourhood of sunspots are fundamentally characterized by a strong light increase in part of the floccular field and not by the ejection of matter. In a period of strong solar activity flares occur very frequently, of the order of once in two hours. They do not usually appear at distances larger than 100 000 km from a group of spots but always inside a facular region. It is often observed that in a period of flare occurrence existing filaments change or even disappear, new filaments and surges are formed even at large distances from the flare. Sometimes, of course, the filaments closely neighbouring a flare remain without change. It was found [11, 12] that solar flares appear in the region of zero line of the magnetic field dividing off the places with opposite magnetic polarity.

Although the temperature of the spots is relatively low much higher temperatures are found in their neighbourhood during flares. These are very probably electromagnetic in origin. During the motion of solar mass in the magnetic field of a spot it can be assumed that the electrical fields produced here may be the cause of electrical currents and the latter are then the source of tremendous temperature effects. Their sudden origin in the form of a light increase may then be apparent as a solar flare.

Large flares are usually conjugate with spots having irregular polarity; in this case they usually have a complicated shape.

During theoretical considerations an investigation was made into the question of the formation of a corresponding discharge in ionized gas considered as the probable physical mechanism of the flare and the connection between flares and the surrounding formations was studied.

During motion in an electric field the electrons collide with the ions [13]. At such collisions the fast electrons lose relatively little energy. On the other hand, during their motion they obtain energy from the electric field present. But with increasing temperature the number of collisions decreases which leads to a further increase in the energy of the electrons. For a strong electric field this increase may continue without limitation and there thus occurs an effect analogous to an electric discharge.

Let the mean velocity v , the electric field E of which acts on an electron, be given by

$$(5) \quad v = -eE \cdot V,$$

8

where V is the velocity of the electrons passing through the solar mass. Then the change in energy of the electrons

$$(6) \quad dW_e/dt = -eEV - 2m_e v(W_e - W_i)/m_i.$$

The second term on the right-hand side represents the energy loss of the electrons on collision with the ions, where v is the frequency of collision, m_e and m_i the masses of the electrons and ions. On certain assumptions, when the electric field is perpendicular to the magnetic field present, we obtain

$$(7) \quad \frac{dW_e}{dt} = \frac{2m_e v}{m_i} \left(W_i - W_e + \frac{m_i e^2 E^2 W_e^3}{2m_e^2 a n_i + W_e} \right),$$

where a is a value defining the magnetic field present and n_i gives the number of collisions. The expression in brackets is negative for large values of W_e , which may lead to an unlimited escape of electron energies. It thus follows that the discharge takes place along the lines of force; this is also obvious from the fact that on motion across the lines of force the mechanical force $\mu[\mathbf{j} \times \mathbf{H}]$ would rapidly change the motion of the mass.

As regards the place of origin, on the one hand we considered the region of zero fields between the spots and on the other hand we assumed the discharge motion inside the flare to be along the lines of force of the magnetic fields of the spot, the shape of which is very irregular at turbulent motions of solar matter. The complexity of the phenomenon under investigation, however, requires further detailed study.

While flares rise to relatively very low heights above the solar surface, eruptive surges are often produced in their neighbourhood. These appear as bright short-term prominences rising to relatively great heights, up to 10^5 km.

3) Filaments (Prominences)

Filaments appear on the solar surface as relatively stable formations in the shape of long dark ribbons. In some opinions, coronal matter condenses in them along the magnetic lines of force. It can be deduced from this that the stability of the filamentary arch-like shapes is to a great extent influenced by the magnetic fields and the relatively high magnetic rigidity. The density of a filament is approximately 100 times greater than the surrounding corona; the temperature corresponds to $\frac{1}{200}$ [1]. A magnetic field acts not only on prominences but also on the corona while there often exists a close relation between these two formations. A convenient grouping of the fields may then cause a rise in a certain part of or the whole prominence from the Sun while, at the same time, part of the corona may be expected to flow out above the rising prominence [14].

A satisfactory theoretical explanation of the origin of filaments has not yet been given. At present the existence of filaments is relatively well explained in the theory of

magnetic arcs [15]. It is assumed that a filament lies along a line of force of a magnetic field. The weight of the filament mass is compensated by the forces due to the distortion of the lines of force, defined by the factor K . Then the magnetic pressures can be converted to the forces $K\mu H^2/8\pi$, which must be equivalent to the expression ρg (product of density and gravity) if equilibrium is to be ensured. For this it is necessary that for the corresponding values of ρg and K there be present a field H of an order of at least 50 Oe. Such a value H can be quite easily assumed in the neighbourhood of spots; the long-term duration of the existence of prominences can then be explained by magnetic rigidity. The mass of a filament sometimes appears as though it were wedged into a shallow depression in the beam of surrounding lines of force. Such a favourable grouping of the magnetic field contributes towards the filament remaining suspended above the solar surface for a long time. A solution of the magnetohydrodynamic equation

$$(8) \quad 0 = -\text{grad } p + \rho g + \mu[\mathbf{j} \times \mathbf{H}]$$

has already been found as applied to this case, where p is the pressure, ρ the density of the medium and the term $\mu[\mathbf{j} \times \mathbf{H}]$ expresses the force of electromagnetic origin [15]. The equation of the corresponding lines of force in a prominence is given in the form

$$(9) \quad f = \exp [(z - z_0)/\lambda]$$

where z gives the vertical height, λ a certain constant. The shape of the lines of force is seen in Fig. 3.

However, such a theoretical conception expresses the carried prominence only in rough outlines and isolated from all the surrounding influences; the theory of the origin of filaments will therefore have to be elaborated further.

The theory of jet streams [16] is based on the assumption that a filament is the trace of electric currents, analogously as in a discharge tube. It is seen, however, that with such a mechanism the required stability, which is normal for filaments, cannot be ensured. For this reason the preceding theory seems more favourable for the explanation.

4) Relations Between Spots, Flares and Filaments

The laws governing the formation of an activity centre and its further development prove that phenomena occurring during the different phases may be related to and influence one another. Although the characteristic features of the different phenomena are quite different, as regards their duration, form, temperature and place of occurrence, some connections have been found although not always proved. The magnetic

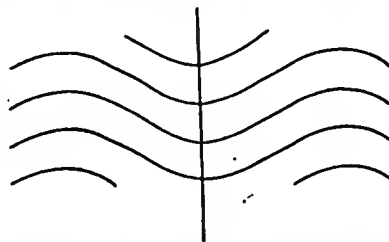


Fig. 3. Course of magnetic lines of force according to Menzel's theory.

fields are seen here to have a very strong effect; then, as a function of their grouping, the partial effects may influence one another. Some scientists even assume that the magnetic fields are the direct causes of spots, flares and the corona. As regards the connection between them, it has not yet been decided for certain whether the flares activate the filament or whether the two phenomena are different results of the same cause (change in magnetic field). Here the influences of structure of the magnetic field present and not only the mechanical forces obviously play a role.

During activation the filament may also disappear but often, particularly in regions of strong fields, it reappears in its original form after a short time. In the solar atmosphere there is a connection between the motion of the mass and the magnetic fields and current systems. This is very strong in the region of sunspots which have large magnetic fields. Therefore the corona above the group of spots is also strongly deformed by local magnetic fields. Sudden changes in their grouping may then result in the deformation of the corona.

It follows from the above that all the events in the activity centres are fundamentally influenced by the occurrence of magnetic fields and their relatively strong effect on the corona and coronal formations. Particular attention must therefore be devoted to these questions.

II. CONDITIONS IN INTERPLANETARY SPACE AND EXOSPHERE

An important factor in the propagation of corpuscular streams after their ejection from the solar region is the space between the Earth and the Sun, the physical properties of which may to a great extent influence the behaviour of a moving cloud of corpuscular particles. Definite conclusions have not been reached in determining the density and temperature of interplanetary mass. It is assumed that the density is approximately 10^3 particles/cm³.

Different models have been proposed for the interplanetary magnetic field. While earlier the field was regarded as negligible, it has been found that in this space there exist regions with a rapid flow of plasma, obviously moving in different directions [17]. Many scientists assume that the magnetic field is produced here and that it is maintained by the ejection of parts of the magnetic field of the Sun, caught on the corpuscular radiation from the active solar regions. The value of the interplanetary magnetic field is approximately 2.5×10^{-5} Oe. Fresh data along these lines are provided by investigations into the paths of cosmic rays which are influenced and guided by this field. It can be assumed that there exists a relatively continuous transition between the geomagnetic and the interplanetary magnetic fields.

A great contribution towards explaining the conditions in interplanetary space and the exosphere has been made by material obtained by means of satellites and cosmic rockets. The discovery of two radiation belts (van Allen) [18] surrounding the Earth, at distances from 700 km to 60 000 km from the Earth, in which the very intense ra-

diation of high-energy particles plays a role, has meant the finding of a further important link in the chain of events beginning with activity on the Sun and ending with a geomagnetic storm. The charged particles are caught by the magnetic field of the Earth. From the equatorial regions they move along the lines of force towards the poles and cause an increase in magnetic intensity. As a result of the vertical component of the geomagnetic field the motion and oscillation of the particles about the lines of force is damped. The inhomogeneous geomagnetic field causes the particles to move in the longitudinal directions on the surface of the level, forming two ring-shaped regions of maximum radiation intensity (Fig. 4).

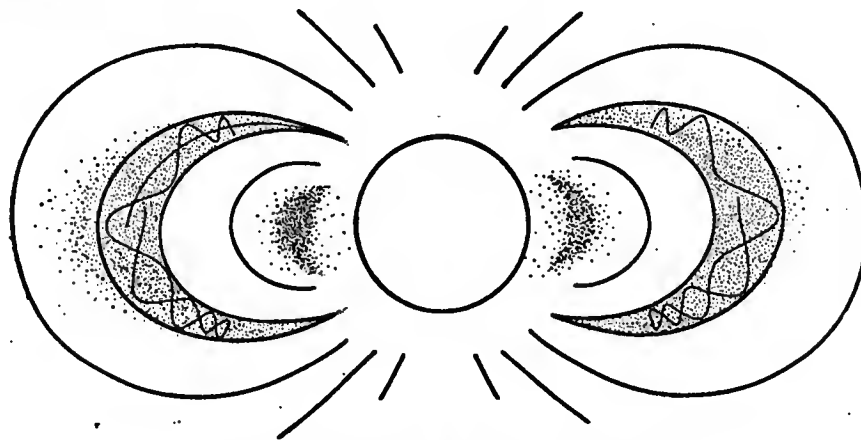


Fig. 4. Distribution of radiation (van Allen) belts.

The composition of the particles is not the same in the two radiation belts. In the outer belt the energy of the electrons fluctuates between 40 keV and 5 MeV, while for protons it reaches a maximum of 200 keV. On the other hand, the energy in the inner belt is quite different; for electrons it reaches a maximum value of 600 keV while for protons it has a much higher value (from 10 to 200 MeV).

The density of the radiation belts is not always the same. Solar geoactivity apparently causes an increase in the concentration of particles in the belts; however, calculation shows that the lifetime of protons of the inner belt is limited to a maximum of a few weeks. The outer belt would also disappear in a short time (a few hours) if it were not for the effect of a certain source of particles and the mechanism working inside the magnetic field which keeps the particles in its domain although they no longer have a high energy.

There are relatively few data available on the character of interplanetary space and the exosphere so that conclusions as to the conditions reigning there are far from being complete. A further study of the phenomena, particularly in radiation belts, could contribute towards explaining the conditions necessary for the motion and behaviour of high-energy particles.

III. GEOMAGNETIC ACTIVITY

1) Time Variations of Geomagnetic Field

It is already quite clear that the basic cause of geomagnetic activity is solar radiation. Since geomagnetic storms are only one, although the most pronounced, form of the set of time variations of the geomagnetic field which must be taken into consideration when investigating their connection with solar phenomena, it will be expedient to make a few brief remarks of a broader aspect on the time variations of the geomagnetic field in general. On the other hand, the solar radiation itself represents a wide sphere of fundamentally different wave and corpuscular components so that one can quite obviously expect different effects and mechanisms of expression, and this is actually the case.

If we disregard the secular variation of the geomagnetic field, which is fundamentally given by the processes taking place under specific conditions deep in the body of the Earth, and is thus outside our sphere of interest, all the other time variations are conditioned directly or indirectly by solar radiation. This conditional state may be understood as "static" if a certain time variation of the geomagnetic field is excited just by the mere existence, more or less permanent and constant, of the appropriate component of solar radiation, or as "dynamic" if the time variation is excited only at sudden and substantial increases in the corresponding components of solar radiation.

A typical example of "static" conditions is the variation of the geomagnetic field on quiet days S_q , and from the sphere of "dynamically" conditioned variations, a geomagnetic storm. These examples concern direct conditions. The purest form of variations from the sphere of indirect conditions is the variation caused by tidal influences of the Moon — lunar variation L .

On the basis of a detailed analysis of the above types of variations we proposed the scheme given in Tab. I where the most important variations and processes in the geomagnetic field are drawn up, taking into consideration the character of solar radiation.

Before analyzing it, however, a few remarks must be made on solar radiation. The geomagnetically effective parts, particularly of the short-wave component of solar radiation (X-rays and ultra-violet region) as well as of the corpuscular component (electrically charged particles with energy up to an order of 10^5 eV), are already quite well known. It should merely be emphasized that in the corpuscular component a strict distinction should be made between *geomagnetically effective* radiation and other *geoactive* radiation (the solar component of cosmic radiation with particles having an energy of the order of 10^9 eV). Here there are deviations both at emission from the Sun and during interaction with the geomagnetic field: on the one hand, one cannot deduce from the emission of one kind of radiation the simultaneous emission of another kind, and, on the other hand, the interaction of geomagnetically effective corpuscular radiation with the geomagnetic field can be understood as a hydromagnetic process while

the penetration of the solar component of cosmic radiation through the geomagnetic field can be interpreted by Störmer's theory [19] (Fig. 5).

We shall not take into consideration below the time variations and processes in the geomagnetic field which are subject to wave radiations and which in their mechanism and results lie outside our sphere of interest.

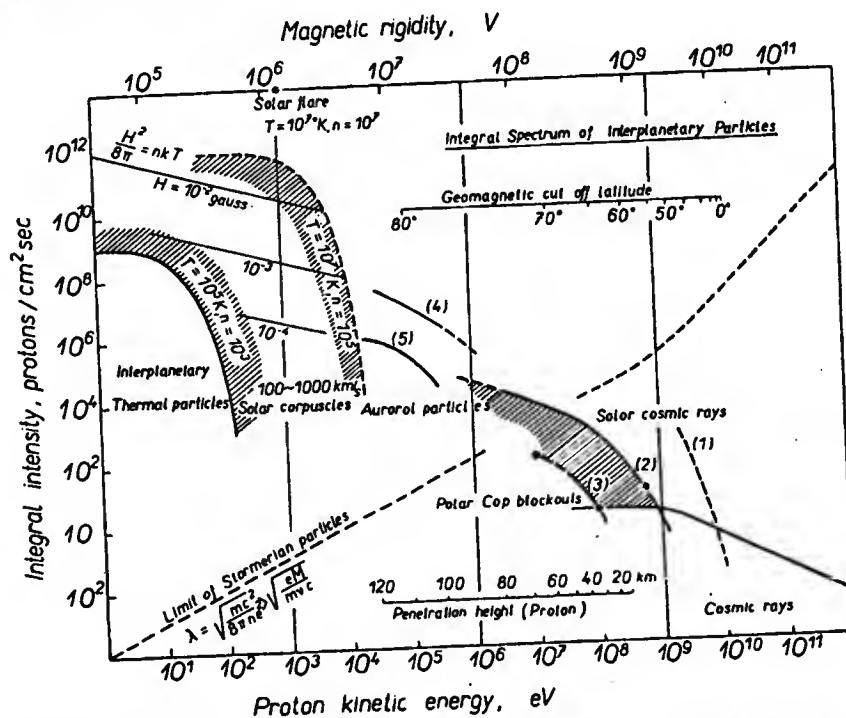


Fig. 5. Survey of basic types and characteristics of corpuscular radiation in space between Sun and Earth (after [19]).

As regards the classification of the time variations of the geomagnetic field subject to corpuscular radiation*) in Tab. I, mention should be made of the following:

Geomagnetic storms: The classification is quite obvious. These very pronounced disturbances, some of the characteristics of which will be dealt with in greater detail presently (Chap. IV), are, however, practically always accompanied by the following variations:

Sudden impulses: These appear as small changes in the geomagnetic field. Their classification is clear as long as the impulses can be interpreted (after [20]) as a certain "more moderate" analogy to sudden commencements of geomagnetic storms ssc. This is probably the interaction between the more pronounced density inhomogeneities in a constant inflow of charged particles from the Sun ("solar wind") and the Earth's

*) In the following text corpuscular radiation always means geomagnetically effective solar corpuscular radiation.

T4

Table I

Plot of dependence of basic variations and events in geomagnetic field on solar radiation (inside square corresponds to corpuscular component of geomagnetically effective solar radiation)

Condition	"Static"	"Dynamical"
direct	variations Sq sudden impulses	solar flare effects sc and g storms, bays
indirect	pulsations pc variations L	bays, pulsations pt

magnetosphere. From the point of view of solar events this interpretation can be accepted since a number of processes in the solar chromosphere and corona can be mentioned which might excite the inhomogeneities; these are particularly changes in the floccular fields, small flares, surges and changes in the structure of filaments.

Pulsations: In this field of small changes with periods of the order of 1 – 100 sec one can consider two classifications. Apart from the well-known conceptions that the cause of pulsations are hydromagnetic oscillations of the plasmatic medium of the Earth's magnetosphere, excited by the interaction of the solar wind with the surface of the magnetosphere [21], we can also take into consideration the conception that in some cases the occurrence of pulsations is facilitated by the increase in conductivity of the ionosphere at a bay disturbance [22]. As regards solar causes, for the excitation of oscillations one must probably again assume density inhomogeneities in the solar wind and thus also similar causes as in the case of sudden impulses. We have, however, preliminarily pointed out some specific features, apparent in the fact that day-type pulsations *pc* [23] exhibited a tendency to more frequent occurrence after the passage of active solar regions with flare activity through the central solar meridian while pulsations of the night type *pt* showed a tendency to greater occurrence after the passage of regions with probably "quieter" emission of corpuscular radiation [24].

Bays: With these disturbances of a regional character we are also forced to make a double classification. The direct condition is obvious, particularly for those bays which actually form some geomagnetic storms and disturbances with a gradual commencement (g-storms) and it also follows from the possibility of the prognoses of such bays on the basis of the character of the solar situation (see Chap. V). Other bays, particularly those which substantially participate in the daily variation of geomagnetic activity with maximum in the evening hours local time [25], lead rather to the conception that in periods of increased inflow of corpuscular radiation, the surplus of particles caught in the Earth's magnetosphere penetrate to the region of polar zones [26].

2) Classification of Geomagnetic Storms

When classifying geomagnetic storms, necessary *inter alia* for a more detailed research of their dependence on solar activity, one can use the quantitative and morphological features of the storms. A quantitative classification makes use of both the course of the geomagnetic storm found directly and that expressed by means of a suitable index of geomagnetic activity.

In the first case the scheme in Tab. IIa is commonly used. The classification is in relation to the energy of the geomagnetic storm, the boundaries are obviously purely conventional and here the well-known dependence of the geomagnetic activity on the geomagnetic latitude is clear. In the second case the *K*-index is used. The scheme, whose boundaries are also conventional, is given in Tab. IIb.

Table II

Quantitative classification of geomagnetic storms

a		b		
ΔH (γ)	Storm	Max. <i>K</i>	Storm	
<150	small	5	m	moderate
150—300	medium	6—7	ms	medium severe
>300	large	8—9	s	severe

ΔH (γ) maximum amplitude of horizontal component of geomagnetic field during storm,
max. *K* maximum three-hour index *K* during storm.

From the point of view of solar influences it should be emphasized in connection with the above classification that here there is no simple dependence of the severity of storms on the importance of visible expressions of solar activity, which come into

Bays: With these disturbances of a regional character we are also forced to make a double classification. The direct condition is obvious, particularly for those bays which actually form some geomagnetic storms and disturbances with a gradual commencement (g-storms) and it also follows from the possibility of the prognoses of such bays on the basis of the character of the solar situation (see Chap. V). Other bays, particularly those which substantially participate in the daily variation of geomagnetic activity with maximum in the evening hours local time [25], lead rather to the conception that in periods of increased inflow of corpuscular radiation, the surplus of particles caught in the Earth's magnetosphere penetrate to the region of polar zones [26].

2) Classification of Geomagnetic Storms

When classifying geomagnetic storms, necessary *inter alia* for a more detailed research of their dependence on solar activity, one can use the quantitative and morphological features of the storms. A quantitative classification makes use of both the course of the geomagnetic storm found directly and that expressed by means of a suitable index of geomagnetic activity.

In the first case the scheme in Tab. IIa is commonly used. The classification is in relation to the energy of the geomagnetic storm, the boundaries are obviously purely conventional and here the well-known dependence of the geomagnetic activity on the geomagnetic latitude is clear. In the second case the *K*-index is used. The scheme, whose boundaries are also conventional, is given in Tab. IIb.

Table II
Quantitative classification of geomagnetic storms

a		b		
$\Delta H(\gamma)$	Storm	Max. <i>K</i>	Storm	
<150	small	5	m	moderate
150-300	medium	6-7	ms	medium severe
>300	large	8-9	s	severe

$\Delta H(\gamma)$ maximum amplitude of horizontal component of geomagnetic field during storm,
max. *K* maximum three-hour index *K* during storm.

From the point of view of solar influences it should be emphasized in connection with the above classification that here there is no simple dependence of the severity of storms on the importance of visible expressions of solar activity, which come into

consideration as sources of corpuscular radiation. It is often observed that from the point of view of solar activity insignificant events are followed by important geomagnetic storms and, vice versa, some very important expressions of solar activity remain without a response in the geomagnetic field. (An interpretation of this effect is given in Chap. V.) It seems that much better agreement can be obtained from the quantitative aspect if solar radio outbursts are also taken into consideration [28, 29].

From the morphological aspect geomagnetic storms are commonly classified according to the time sharpness of the onset of a storm and are divided into two types: storms with sudden commencement (sc-storms) and storms with a gradual commencement (g-storms). It can be expected that these two types differ primarily in the magnitude of the density gradient of the particles in the front of the corpuscular stream or even at the side of the stream if the Earth meets a stream which has already lasted for some time. Differences in velocities cannot play such a role here nor do our results show them to be so important as is usually deduced (Chap. V).

From the point of view of solar influences the situation in this method of morphological classification of geomagnetic storms is much clearer than in the preceding case. It follows from the above that sc-storms are preceded by sudden changes in the solar situation connected with the short-term emission of corpuscular radiation or a short-term favourable direction of the emitted corpuscular radiation. On the other hand, g-storms occur after slow changes in the solar situation, accompanied by long-term emissions of corpuscular radiation.

The classification based on the dependence of the character of geomagnetic disturbances on the geomagnetic latitude can also be regarded as a certain type of morphological classification corresponding in a heightened degree to the physical mechanism of the origin of geomagnetic storms as a whole [30]. It is seen that in the belt of low latitudes, up to about 45° , the disturbance takes place synphasically on large regions of the Earth's surface (S-type), in the middle and upper latitudes roughly between 45° to 70° the disturbances may be different even at places only a few hundred km away from one another (L-type), and finally in the polar regions, above 70° , disturbances take place on disturbed days more or less permanently and often occur also on days which are geomagnetically quiet in other belts (P-type).

The dependence of the type structure of a storm on its intensity is important. According to [30] geomagnetic storms with K_p max 7-9 consist of disturbances of the type S, L and P, have a pronounced storm variation D_{st} and begin suddenly. On the other hand storms with K_p max 3-6 consist only of L and P type disturbances, no D_{st} variations are seen and they begin with a gradual commencement.

It is possible that the relation between the intensities of S and L type disturbances, together with the possible latitude displacements of the boundary in the 45° latitude, is one of the causes of the occurrence of different types of geomagnetic storms for an otherwise special morphological classification, the results of which will now be mentioned.

3) Attempt at New Classification of Sc-storms

The gradual refinement of conceptions as to the connection between solar and geomagnetic activity has made it necessary, and also possible, to solve other special problems. One such problem, also of practical importance for forecasting geomagnetic activity, is the question whether some morphological peculiarities in the course of different geomagnetic storms can be at least partly derived from the morphological peculiarities of solar situations during the emission of the corresponding corpuscular stream. The results would also contribute towards determining to what extent the specific properties of the different corpuscular streams, assumed to be given by the different character of the solar situation, where they were emitted, are preserved, i.e. to determining the possible smoothing effect of the medium along the path of the corpuscular stream. The investigations made so far along these lines, the results of which will be given below (details will be published later), represent the first step in a broader attempt at a new classification of geomagnetic storms taking into consideration the character of the solar situation in question.

The records of 90 geomagnetic sc-storms on standard magnetograms from the geomagnetic observatory in Průhonice ($\lambda = 14^{\circ}33'$, $\varphi = +49^{\circ}59'$, $A = 97.5^{\circ}$, $\Phi = +50.1^{\circ}$) were used for the classification. The typical course of a storm, obtained as the average of all the cases by the usual method of the displacement of the epochs of storm commencements (storm variation D_{st}), is shown in Fig. 6. After a detailed evaluation of the different courses of geomagnetic storms as regards similarity and deviations from the typical course, the whole set of storms could be reliably divided into a number of special types according to exactly defined simple criteria. Here, for the sake of brevity, we give only the plots of the most pronounced representatives of the different types (Fig. 7) instead of the definitions used in the classification.

Type analysis showed that the majority of geomagnetic storms of the set in question has the expected "two-phase" course, both phases of which can be modified quite differently. It is interesting, however, that apart from this a not insignificant part of the set exhibits a definitely "one-phase" course, also differently modified. The small remainder is formed by some storms of a more complicated character which obviously

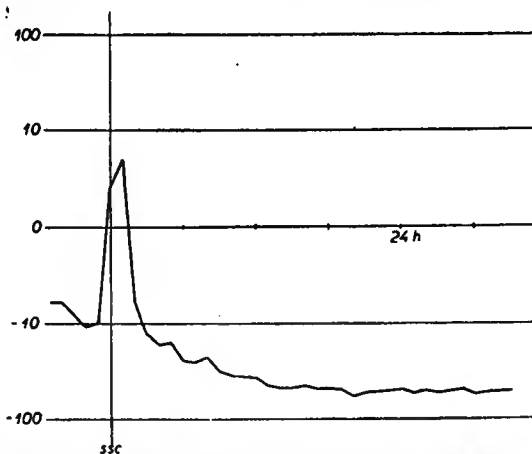
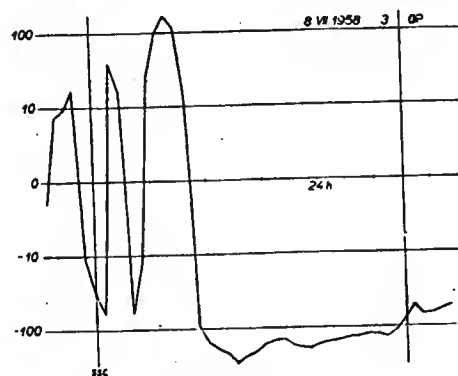
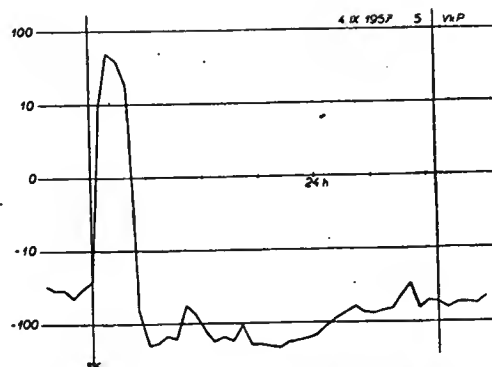
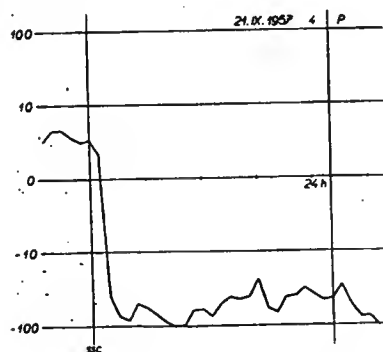
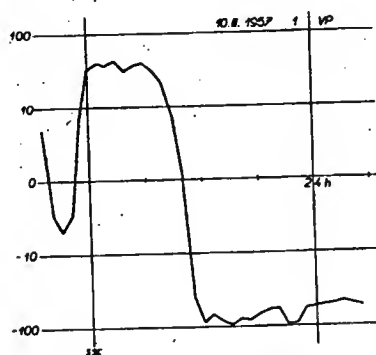


Fig. 6. Average time dependence of horizontal component of geomagnetic field for set of storms used in experiment on new classification of sc-storms. Vertical axis: $H_d - H_q$ (γ).

424



18

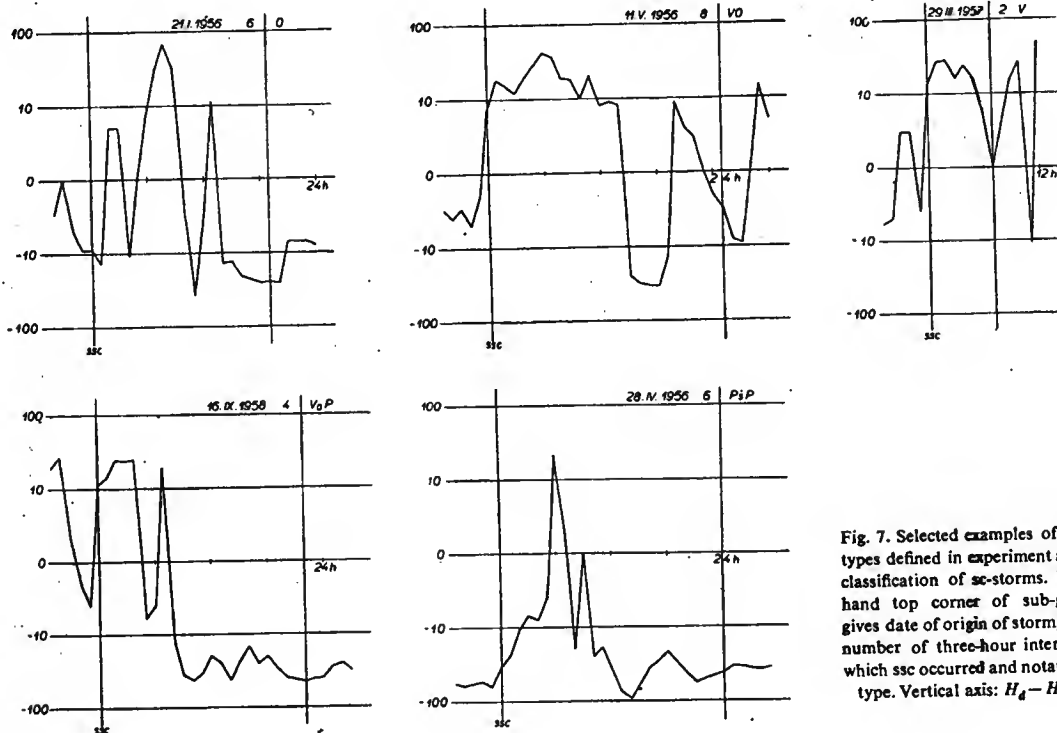


Fig. 7. Selected examples of basic types defined in experiment at new classification of sc-storms. Right-hand top corner of sub-graphs gives date of origin of storm, order number of three-hour interval in which ssc occurred and notation of type. Vertical axis: $H_d - H_q (y)$.

originated by the overlapping of two or more disturbances, as is also indicated by the length of their duration. The statistics of the occurrence of the different main types is given in Tab. III.

In order to decide whether the deviations of the different storm courses from the typical course cannot be caused inter alia also by the different time of day at which the storm occurred, the material was classified into partial sets according to the three-hour period in which the storm started.

The average storm courses of these partial sets, obtained by displacing the epochs, are on the whole similar (Fig. 8), which indicates that the possible influence of local time is very small. This is also supported, as was to be expected, by the random distribution of the points in Fig. 9, where all the investigated storms are plotted taking into

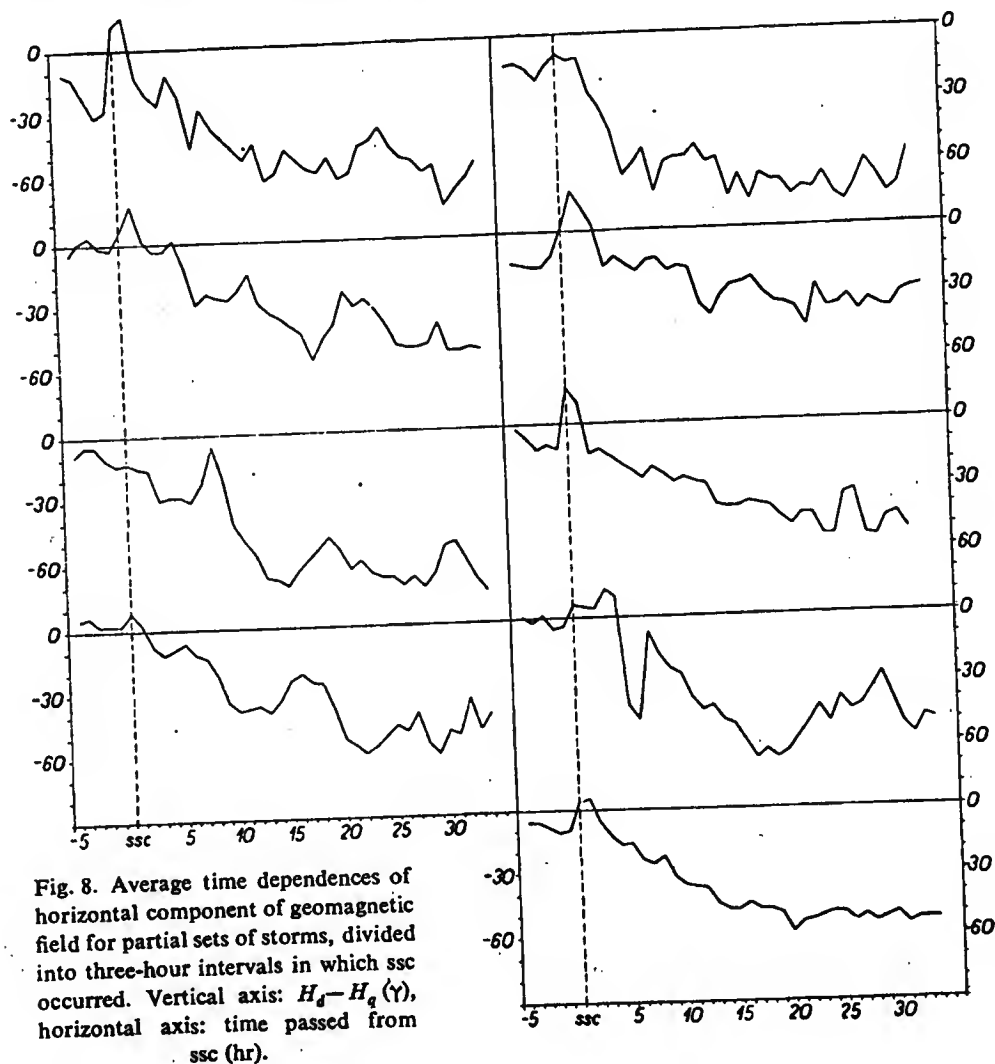


Table III
Statistics of occurrence of different main types of geomagnetic storms

Type	Number	%	Total	
			number	%
VP	36	40	54	60
OP	15	17		
PP	2	2		
V	1	1		
O	8	9	30	33
P	18	20		
VO	4	4		
more complicated	6	7	6	7

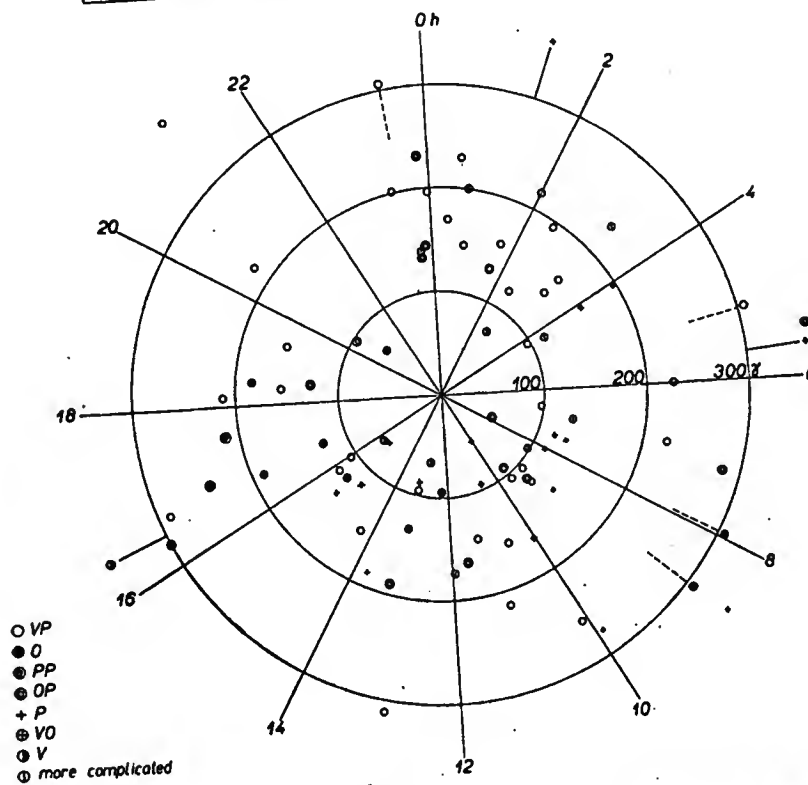


Fig. 9. Polar diagram of occurrence of geomagnetic storms used in attempt at new classification taking into consideration type of storm, moment of ssc and magnitude of maximum amplitude H .

consideration the type of storm, the instant of sudden commencement and the magnitude of the maximum amplitude of the horizontal component of the geomagnetic field during the storm.

On the other hand, if the occurrence of the different types is investigated separately, the P and O one-phase types show a tendency to occur only at a certain time of day (Fig. 10). This is also a proof that in the above classification not only possible local disturbing influences but also causes on a world-wide scale may play a part and that the classification of storms also has physical significance.

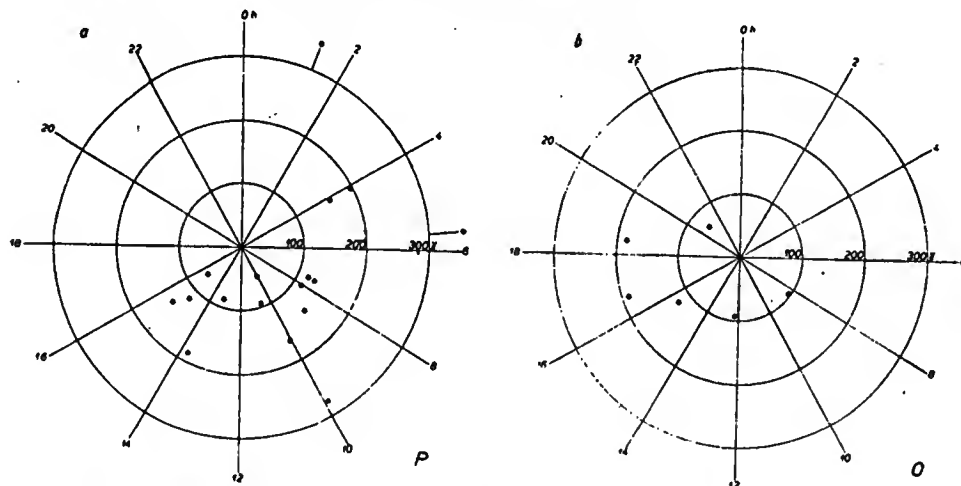


Fig. 10. Polar diagram of occurrence of one-phase geomagnetic storms a) type P, b) type O, taking into consideration moment of ssc and magnitude of maximum amplitude H .

IV. ON THE QUESTION OF THE MECHANISM OF GEOMAGNETIC STORM DEVELOPMENT

The classification of phenomena occurring within the framework of geomagnetic activity has shown that storms represent a very pronounced group of disturbances. In order to be able to make use of the laws governing the phases of storms for studying the connection between solar and geomagnetic activity, the most fundamental of them should be pointed out here. At the same time one must not forget a brief definition of the different types of storms from the point of view of structure and geographical expression together with their theoretical conceptions.

1) Basic Classification of Storms

Geomagnetic storms are distinguished by several pronounced features. If we study their time dependence (Fig. 11), it can be included in the general characteristics of storms [2]. These are:

a) Sudden commencement, which is characterized by a relatively rapid growth in the magnitude of the horizontal component of the geomagnetic field, especially in low latitudes. The value of this increase is on an average around 30γ and increases towards the equatorial region, where it attains maximum values. The rise time fluctuates around 2 minutes. However, the occurrence of a sudden commencement is not a rule for all storms. With so-called sc-storms it is observed all over the world but its magnitude varies from place to place. The sc also reaches higher values in the auroral zone on the illuminated side. At present the microstructure of the commencements of storms is the object of interest in a number of papers [31, 32].

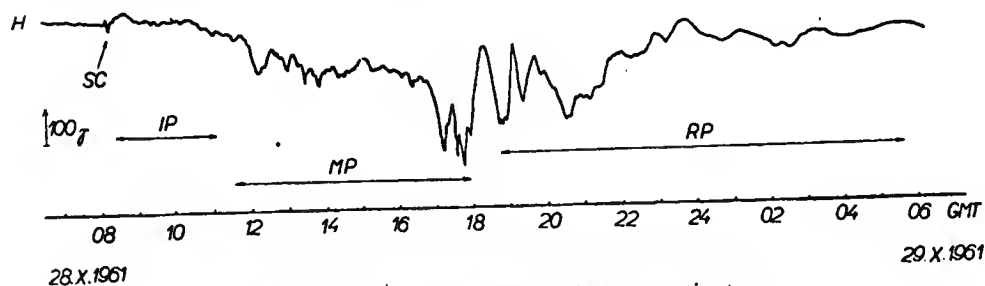


Fig. 11. Total time dependence of geomagnetic storm.

b) The initial phase of a storm is the interval lasting for approximately 2 to 8 hours after the sudden commencement. It is characterized by the fact that the H component maintains approximately its initial undisturbed value, slightly increased compared with the period before the storm.

c) The main phase is marked by a considerable decrease in the horizontal component compared with the initial undisturbed field. After reaching minimum the H component gradually returns but it is covered by strong storminess of the whole process; for a large part of this period, usually lasting 12–24 hours, there are large positive and negative changes which reach several hundred γ .

d) The return phase, as the last part of storm activity, is seen as a further gradual return of the H intensity to the original undisturbed value and a gradual quietening of activity (decrease in amplitudes of positive and negative changes). They last approximately 1–3 days while in the second part there is only a gradual return.

2) Types of Geomagnetic Storms from Aspect of their Geographic Expression

The records of the time dependence of the geomagnetic field confirm that geomagnetic storms can be divided into two basic types according to the laws governing their expression. The first group consists of world storms, which are accompanied by a general decrease (to a smaller extent an increase) in intensity of the geomagnetic field

24.

simultaneously over the whole Earth, both in the polar and in the equatorial regions. The second type are so-called polar storms or disturbances occurring both as negative and positive forms. Both types of storm are excited by the action of corpuscular radiation.

a) *World storms* are disturbances of the geomagnetic field of maximum intensity, where the fluctuation of the elements reaches values of up to thousands of γ . They take place over a period of several days. The main changes during a storm occur to a great

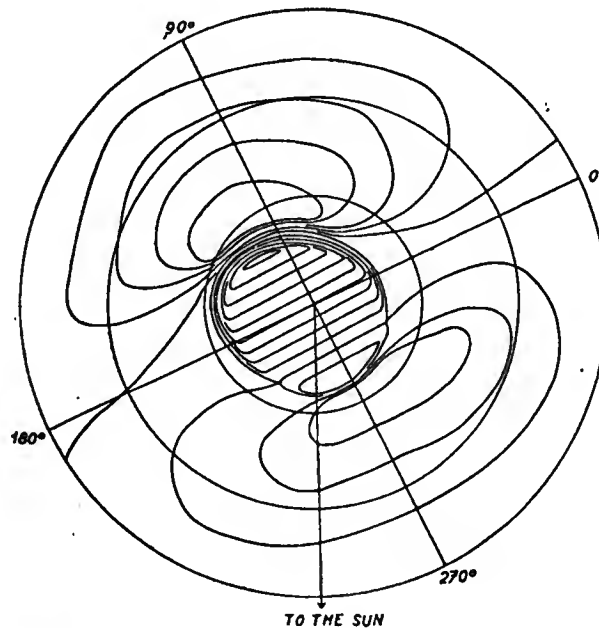


Fig. 12. System of streams produced in E-layer which formally explains field distribution during geomagnetic disturbance.

extent simultaneously and similarly over the whole surface but of course the total dependence is disturbed by disturbances of a local character, particularly in higher latitudes, where there is also an increase in the amplitudes of irregular fluctuations. A typical world storm begins with a sudden commencement (sudden sharp increase in horizontal component — ssc) observed in 1 minute synchronously over the whole surface of the Earth, with maximum amplitude in the equatorial regions. Here, too, the storms occur in their purest form.

After the sudden commencement the storms then develop in phases as described above.

The average course of the storm is given by the storm variation D_{st} , to which three

components of the disturbance field D contribute; the field is described by the expression [33]

$$(11) \quad D = DCF + DP + DR.$$

The DCF field is excited by the inflow of the corpuscular stream (sudden commencement + initial phase), DP is the disturbance field produced in the polar regions (sudden fluctuations during main phase) and DR represents the effect of a toroidal electric current.

b) *Polar storms* have maximum values not directly in the polar regions but in the zones of aurorae. This proves the connection between the two phenomena. Polar storms are characterized by the single occurrence or sequence of several sudden (increase or decrease) deviations from the undisturbed value, the most pronounced at the horizontal component. The intensity of the impulses decreases together with the distance from the polar regions in the direction of the equatorial region. In lower latitudes storms are apparent only in the form of a bay; for this reason they are sometimes called bay storms. Their annual time distribution has been found to be characterized by two maxima in periods of the equinox. The daily variation of the disturbances then exhibits interesting properties in that negative disturbances are produced during the night in auroral zones and positive disturbances during the day. However, many more negative disturbances occur than positive ones. In the middle latitudes this circumstance is not nearly so obvious.

The relatively rich material obtained for these disturbances permitted the proposal of a system of currents originating in the height of the ionospheric layer E [34] (Fig. 12), by means of which the observed field distribution during disturbances can be formally explained. The currents have a high density and flow along the auroral zones. While there exists only one current system above the polar regions, in the middle latitudes two vortices are formed; one runs anti-clockwise on the night and morning side of the Earth, and the other clockwise on the day and evening side. The absolute value of the current can reach up to hundreds of thousands of A.

3) On the Theory of the Causes and Origin of Geomagnetic Storms

The very complexity and irregularity in the course and other characteristic features of storm activity indicate that not even the finding of the actual physical conception of the model, which would satisfactorily explain all the natural phenomena taking place during storms, will be easy or without obstacles.

Research hitherto has basically followed two different lines, the difference consisting mainly in the conception of the properties of interplanetary space and of the charged particles moving along the Sun-Earth path.

α) The first conception is based on the assumption that in interplanetary space there exists no large magnetic field and that the ionized matter emitted from the Sun is not magnetic. This assumption is used in many theories starting out from hydromagnetic equations as well as in the classical theory of Chapman-Ferraro [35], which in addition assumed the negligible influence of interplanetary gas.

β) The second conception is based on the opinion that the ionized clouds emitted from the Sun are magnetized either by the total solar field or by local fields of the active regions. The particles move with a velocity of 10^8 cm/sec and the flux is also electrically polarized; the electric field is of an order of $1 - 100$ V/cm and is very important for the creation of magnetic storms. The theoretical procedure is then based on a study of the motion of the individual particles.

Difficulties arise in the first group of theories if it is required to explain how a corpuscular cloud penetrates into the magnetic field of the Earth; it is equally difficult to explain the formation of a toroidal current. Also the 27 daily variations of cosmic radiation are in conflict with the fact that interplanetary space has no magnetic field. The incorrectness of this opinion was proved by cosmic radiation measurements by means of satellites. The Forbush decrease in intensity of cosmic rays was recorded at large distances from the Earth due to the influence of the magnetic field present there, which is in considerable disagreement with the second conception.

Let us now deal with the basic features of some models which try to explain the different phases observed during storms. Recently theoretical research has taken into consideration the latest observational data on the state of interplanetary space and the exosphere, which has led to more exact physical models.

The starting point for all more recent theoretical models of geomagnetic storms is the assumption of an electrostatically neutral corpuscular stream propagating from the Sun to the Earth. However, opinions differ as to the effect of such a stream on the magnetic field and this has led to the elaboration of different models.

a) *The model based on the effect of a dipole magnetic field on the moving conducting medium* [35] assumes that a cylindrically shaped cloud of corpuscular gas with sharp boundaries approaches the geomagnetic field. If the medium is conductive, then by its approach to the magnetic field electric currents are induced in it which prevent the magnetic field from penetrating into the interior of the corpuscular cloud. In addition mechanical forces of a repulsive character are produced between the dipole and the conductive medium and try to prevent the cloud from further movement. Since the conductive medium is not rigid, these forces cause the surface of the corpuscular stream to begin to deepen and a cavity to be formed in it. The lines of force between the Earth and the front of the cavity densify results in an increase in the horizontal component of the geomagnetic field, observed during the initial phase of the geomagnetic storm. The increase in the horizontal component ΔH at a sudden commencement, which is related to the dimensions of the cavity and the flux moment nmv^2 , is described by the expression $H_0/8z^3$, where H_0 is the equatorial value of the

horizontal component on the surface and $z = (H_0^2/8\pi E)^{1/6}$ represents the distance between the peak of the cavity and the centre of the Earth. Further, the energy $E = H^2/8\pi = nmv^2$, where H is the geomagnetic field in the peak of the cavity, n the density of the particles, m the mass and v the velocity of the corpuscles. The main phase, seen as a decrease in the horizontal component, can be explained by the production of a closed toroidal electric current around the Earth, flowing in the equatorial plane. This current is formed as a consequence of the electric field produced by volume charges which collect on the evening and morning side of the cavity as a result of the separation of the charged particles by the geomagnetic field. Only protons are of importance for the current due to their large gyration radius.

b) *The model explaining the origin of geomagnetic storms by the effect of the electric field of a corpuscular cloud* [36] is based on the assumption that the particles of electrically polarized gas emitted by the Sun carry with them the magnetic field frozen into a highly conductive medium. When the beam of ionized gas moves an electric field is produced described by the relation $E = - (1/c) [\mathbf{v} \times \mathbf{H}]$, where \mathbf{v} is the velocity of motion of the beam and \mathbf{H} is the field frozen into the beam. When the flux reaches the Earth's magnetic field and the separation of the positive and negative particles begins, the influence of the electrons flowing round the Earth in the eastern direction is seen in the form of a sudden commencement. The motion of particles in a combined electric and magnetic dipole field consisting of circular motion superposed on translational motion was calculated. The velocity of particles behaving in this manner is given by

$$(12) \quad \mathbf{v} = - (c/eH^2) [\mathbf{H} \times \{e\mathbf{E} - \mu \text{grad } H - m(d\mathbf{v}/dt)\}],$$

where μ defines the ratio of the kinetic energy of the particle to the magnetic field. The motion of particles forms a volume charge in certain regions, which leads to the creation of toroidal currents. When looking from the north pole the left-handed current forms a sudden commencement while the creation of the main phase of a geomagnetic storm is ascribed to the right-handed current (due to the eastern motion of the electrons).

The interval between the sudden commencement and the main phase of a geomagnetic storm was not explained by this model. The following model attempts to do this.

c) *The model taking into consideration a shock wave* in the origin of geomagnetic storms is based on the assumption that apart from the corpuscular stream a shock wave, which has its source in the ejection of particles from the Sun [37], also plays a role in the storm mechanism. Such a wave contributes to the separation of the charges and thus also to the causes of currents flowing in the atmosphere and manifest as a sudden commencement. It follows from the theory of strong shocks that the velocity of the gas borne along by this wave is only three-quarters of the velocity of the shock wave. Therefore, the corpuscular stream reaches the Earth with roughly a nine-hour

lag (Fig. 13). The particles of this stream can therefore penetrate into the depths of the geomagnetic field and thus also into the forbidden Störmer regions since they enter the field already disturbed by the wave. The particles caught in the geomagnetic field move primarily along the geomagnetic lines of force but simultaneously they drift according to their polarity to the east or west while an electric current is produced which flows in the western direction (main phase). This current gradually decays due

to the absorption of the particles in the Earth's atmosphere, which also explains the decay of the geomagnetic storm.

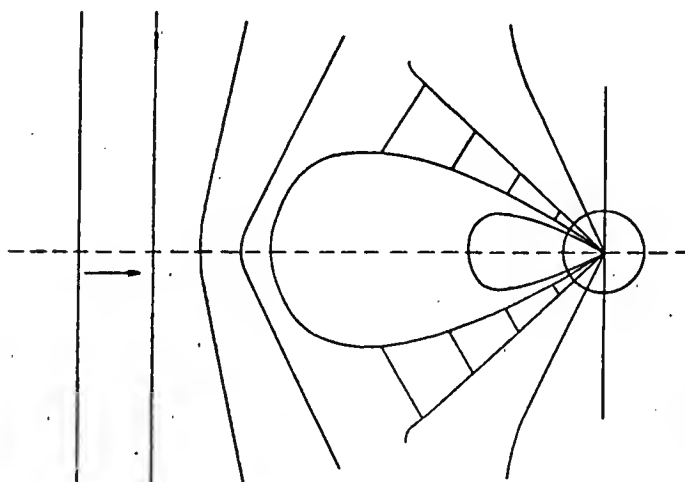


Fig. 13.

d) The hydromagnetic model is characterized by the interaction of solar plasma with the geomagnetic field and the method of propagating the effects towards the Earth. It is assumed that due to the influence of the pressure of solar plasma the Earth's dipole field is limited by regions up to a distance of approximately 10 Earth's radii [38], where the magnetic pressure is already lower than the pressure of the solar plasma. When

the plasma suddenly ejected from the Sun collides with the geomagnetic field processes occur which result in the geomagnetic storm on the Earth's surface. The sharp front of the solar plasma cloud is formed by the influence of the interplanetary magnetic field and the gas present there.

The basic hydromagnetic equation defining the relation between the velocity v of the particles, arriving at the region of the geomagnetic field on sudden ejection from the Sun, and the intensity of the magnetic field is given in the form [38]

$$(10) \quad \rho \, dv/dt = - (P_1 + P_2 + B^2/2\mu_0) + (B\nabla) B/\mu_0,$$

where P_1 gives the pressure of the tenuous plasma in the field B , P_2 is the equivalent pressure of the injected particles and $B^2/2\mu_0$ is the magnetic pressure. The different phases of the storm can then be ascribed, as has been elaborated in detail, to the partial expressions of the interaction resulting in the production of pressures propagating towards the Earth in the form of hydromagnetic waves.

The sudden commencement of a geomagnetic storm is ascribed to the impact of

solar plasma with the sharp front on the geomagnetic field. This disturbance propagates towards the Earth in the form of a hydromagnetic wave.

The initial phase of a storm is caused by the increase in pressure of the constantly inflowing solar wind on the magnetic field of the Earth. The main phase is obviously due to the pressures which are produced in the Earth's magnetic field by the trapped protons of solar origin. A considerable part of the pressure is caused by the centrifugal force of the trapped particles at their oscillation along the lines of force during passage through the equatorial plane (Fig. 14).

A geomagnetic storm ends with the phase of decay, which due to its limited duration requires the quietening of most of the trapped particles in a period of about one day. This process corresponds to the mechanism of charge exchange between the active protons and the neutral atoms of atmospheric hydrogen.

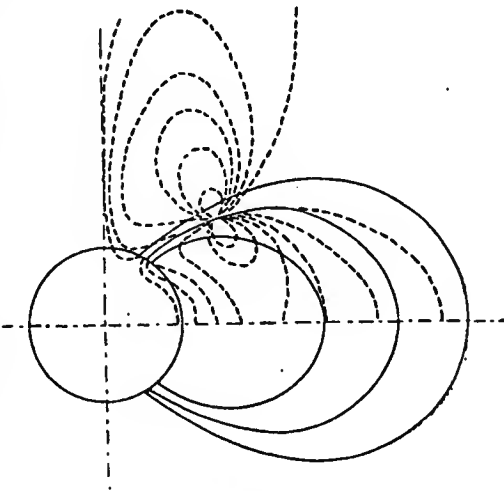


Fig. 14.

e) *The model of a geomagnetic storm, which is based on a combination of the effect of the homogeneous electric field of the volume charge and the system of irregular fields, aims at explaining the mechanism of the penetration of solar ions into the geomagnetic field [39].* Existing theories explaining the origin of geomagnetic storms by the effects of the corpuscular stream have in most cases not been able to explain how the particles can penetrate into the Earth's magnetic field. The increase in the horizontal component (at a sudden commencement) cannot be caused by a toroidal current outside the geomagnetic field but by a mechanical force acting on the electrically conductive gas at a distance of several Earth's radii in the direction of the Earth. On the other hand, during the main phase the mechanical force acts away from the Earth. The effect of such a force leads to hydromagnetic processes in regions at a distance of several hundred km from the earth due to the moving gas in the magnetic field. The consequence of such processes is that the lines of force of the magnetic field, frozen into the conductive medium, are borne away from the Earth and form an elongated cylindrically shaped formation, "a magnetic tail", on the unilluminated side of the Earth (Fig. 15). The continuous acceleration of the ions in this "tail" against the Earth by the electromagnetic forces leads to a total decrease in the horizontal component of the geomagnetic field — the main phase of the storm.

The theory is based on a study of the motion of two forms of gas — ion-electron plasma and neutral atomic gas. The application of such a study shows that at distances of several hundred km from the Earth's surface the disturbances are transported by

30

means of the hydromagnetic waves, while in lower regions the dispersion medium causes the disturbances to be transported by means of diffusion. This model permits an explanation of some important effects connected with the course of a geomagnetic storm, including processes in the radiation (Van Allen) belts, counter glow, daily variations in cosmic rays etc.

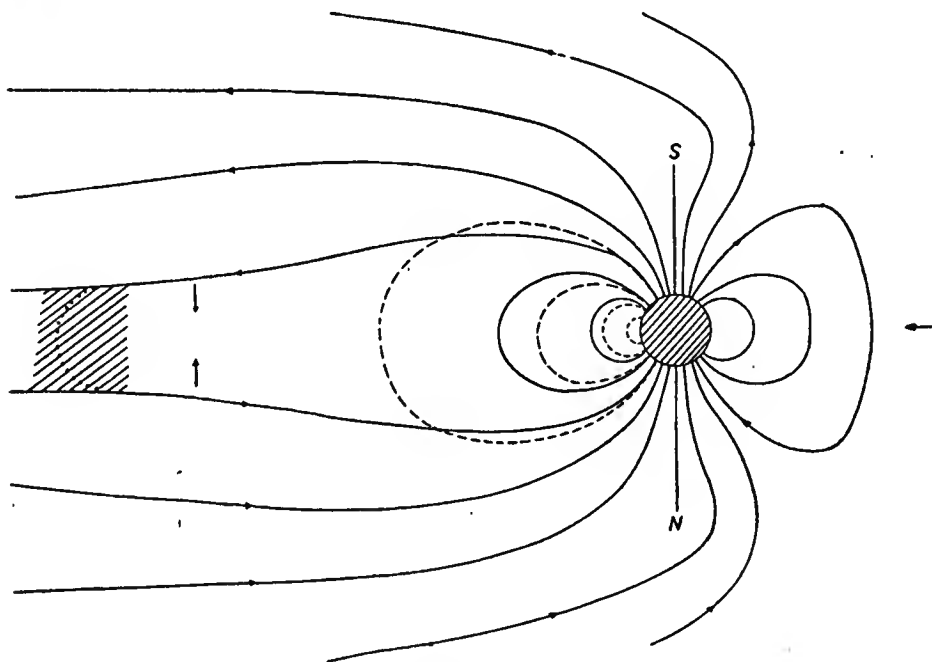


Fig. 15.

The principal conceptions of the above models represent a brief survey of the basic and latest theoretical conceptions as to the conditions necessary for the creation of the mechanism of geomagnetic storms. The very fact that a series of models exists in parallel, each of which is physically substantiated in a different way, indicates that it has not yet been possible to arrive at a completely satisfactory conception which would be in keeping with the physical nature of storms and would also explain their partial features and individual peculiarities. Greater uniformity could certainly be achieved by studying other parameters which have not yet been sufficiently investigated but which might play an important role in the correct physical conception of the model.

One important way of refining such parameters is indoubtably a study of the conditions and causes of the emission of solar geoactive corpuscular radiation. In this the above models differ quite considerably; some do not take the question of the emission mechanism into consideration at all and others make obviously very simplified as-

436

sumptions although it can be expected that the parameters by which the corpuscular stream enters into interaction with the geomagnetic field will to a great extent be given by the mechanism of its origin on the Sun. The determination of the correct relations between solar and geomagnetic activity is a contribution towards finding the most probable parameters.

V. CONNECTION BETWEEN PROCESSES ON SUN AND GEOMAGNETIC ACTIVITY

The connection between solar and geomagnetic activity has been known for more than a century but still no unified conception has been reached as to what is the source of geoactive corpuscular radiation. Different papers treating the various epochs of the solar cycle have dealt with all the expressions of solar activity and a definite but often unsatisfactory connection has been found. For this reason a detailed analysis of all the expressions of solar activity had to be made and their inter-relation determined when elaborating a method for the prognosis of geomagnetic storms.

Investigations into active centres consisting of successive expressions of solar activity have shown that on its passage through the central solar meridian (CMP) one and the same active region often has different consequences corresponding to its phase of development, and that the geoactivity (i.e. the following increase in geomagnetic activity excited by corpuscular radiation) depends on their instantaneous state at the time of the CMP. It was also found that the connection between active regions and geomagnetic storms is not a simple affair since it depends on the processes taking place in their surroundings and on the mutual configuration.

These questions became the object of our investigations. Here we give some of the most important conclusions with a view to contributing towards a clarification of the above relations which have been the object of geophysical research for a number of years. Our attention will successively be paid to all main phenomena occurring in active centres both as isolated effects and taken complexly.

Since the geoactivity of a solar active centre substantially depends on its phases of development, let us first deal briefly with the chronological sequence of events on the Sun from the point of view of their development.

1) Solar Activity – Phases of Development of Active Centre

Each active region is preceded by the formation of a local magnetic field. Bright small facular and floccular fields appear and gradually increase their extent. Then spots are formed but these accompany the life of the active region for a relatively short time. They gradually become larger and the magnetic field becomes complex. If the development of the group of spots reaches a certain degree flares and surges begin to occur

in it and filaments (prominences) appear. The chromospheric structure shows that in the chromosphere there is a very complex magnetic field which corresponds to a certain extent to the photospheric field. During flare activity in the active region more filaments are produced while those already existing here often change their direction and shape or even disappear (activation of filament). Others are "extracted" from the region, and straighten if they were previously arc-shaped. Sometimes these changes occur during flares while at other times this occurs in a broad time interval around the flare. For the filament to disappear it is not necessary that it be near to a flare. Distant filaments also often disappear. According to the mechanism explaining the existence of a filament, which was given in Chap. I, it can be assumed that their disappearance may occur when the magnetic field which kept them in equilibrium is at least temporarily compensated. Such compensation occurring in the period of changes in the magnetic field can be expected rather in those parts of the active region where the magnetic field strength is lower than that of weaker disturbing fields. It can be admitted [40] that filaments disappear as a consequence of changes in the local magnetic fields; one cannot, however, neglect the influence of the total field which adds up with the local fields.

In the next phase the filament moves away from the active region and different basic configurations can occur. From the behaviour of the free part of the filament we can deduce that it is under the influence of the magnetic fields of the surrounding spots. Sometimes the filament may decay [41] or join up with a neighbouring filament.

If so-called spot prominences are produced by the condensation of the coronal masses on the lines of force of the strong local magnetic fields already formed directly above the active centre, then the above interpretation of the disappearance of the filament due to compensation by the field can be applied.

Filaments often last much longer than the period of spot occurrence; they remain in the floccular field and are gradually shifted to higher heliographic latitudes. Finally, the floccular field disappears entirely and only the filament remains. Apparently the rotation causes the filament to turn into the approximately parallel direction while the filaments originally occurring in the spot zones had the meridional direction.

2) Geomagnetic Activity and Sunspots

When investigating the relations between these phenomena it was generally found that in the same way as the occurrence of sunspots falls into an eleven-year period so geomagnetic storms are subject to analogous laws. This fact has become the starting point for many scientists in their search for inter-relations. The average values of the main characteristics (number, area and relative number) of spots were primarily compared with different geomagnetic indices. It was found statistically that a few days after the CMP of the spots there exists a definite probability of the occurrence of geomagnetic storms. A comparison of the individual cases, however, showed that not

Figure 1 is a combined bar and line graph. The x-axis is labeled with the number of eggs per female (K) and has values 19, 22, 25, 28, 2, 5, 8, 11, 14, and 17. The left y-axis is labeled 'R' and ranges from 0 to 80 in increments of 20. The right y-axis is labeled 'K' and ranges from 0 to 20 in increments of 10. The bars represent the percentage of females (R) with a given number of eggs. The line with dots represents the number of females (K) with a given number of eggs. The data is as follows:

Number of eggs (K)	Percentage of females (R)	Number of females (K)
19	65	15
20	30	10
21	5	5
22	10	10
23	80	15
24	20	10
25	18	0
26	60	0
27	60	0
28	45	0
29	40	0
30	10	0
31	60	0
32	75	0
33	80	5
34	78	5
35	78	5
36	70	10
37	70	10
38	60	15
39	60	10
40	55	15
41	55	20
42	45	15
43	40	15
44	55	10
45	50	10
46	65	10
47	65	15

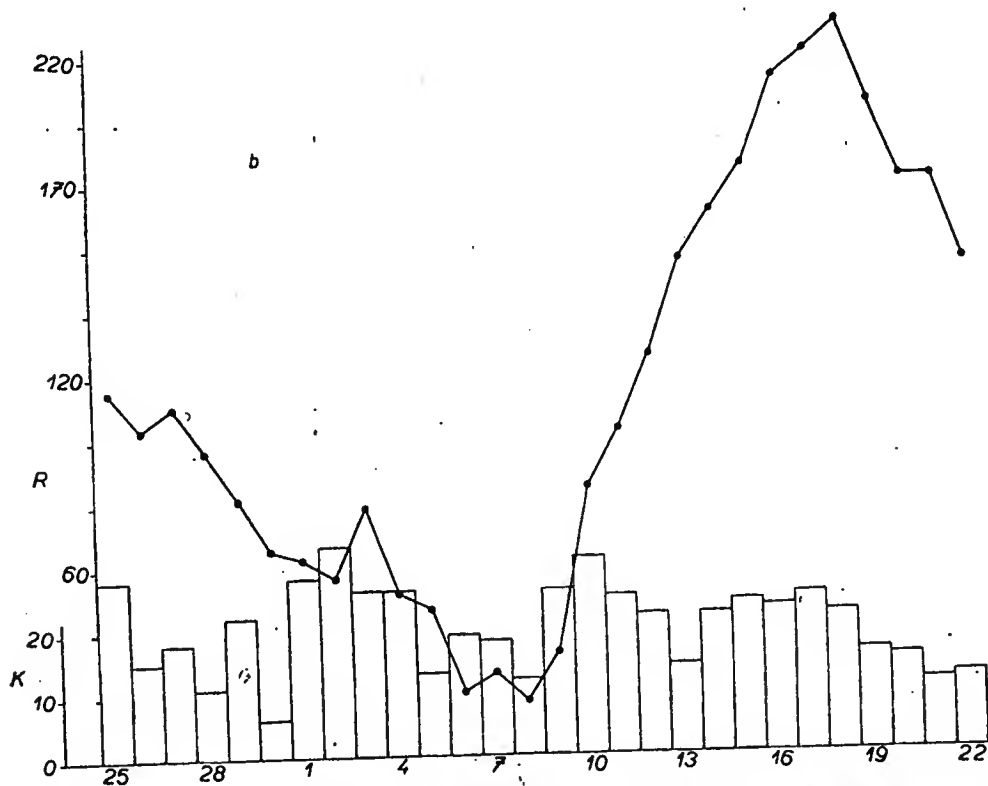


Fig. 16. Time dependence of relative number of sunspots R (line with points) and daily sums of K -index of geomagnetic activity in period a) 19. II.—17. III. 1952, b) 25. IV.—22. V. 1951.

Let us now deal in greater detail with the question of whether spots by themselves can be geoactive. We compared the curves of the daily values of the relative number of solar spots [43] and the daily sums of the K -indices [44], characterizing the geomagnetic activity [45]. In a number of cases it was clearly seen that geomagnetic disturbances are produced even in those epochs when spots did not occur on the Sun at all

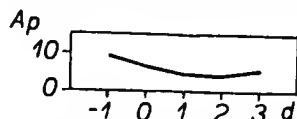


Fig. 17. Average time dependence of geomagnetic activity after CMP of groups of spots, which were not accompanied by central filament.

and, vice versa, there is often a decrease in geomagnetic activity even at large spot activity. Examples of the two above cases are plotted in Fig. 16. It is seen from Fig. 16a that in the epoch of zero relative number (25. II. to 4. III. 1952) there was an increase in the K -indices.

On the other hand, they decreased around 19. V. 1951 (Fig. 16b) when the relative number was very high.

Such investigations would not in themselves be proof because the relative number does not take into consideration the position of the spots on the solar disc.

However, due to the conception of the radial propagation of corpuscular radiation one can expect the distance between the group of spots and the centre of the disc to be the decisive factor. For this reason we investigated the chosen very quiet, internationally determined intervals of geomagnetic activity [46] for the years of a fall in solar activity (1950 to 1953) from the period when the zones of sunspot occurrence approach the equator and thus when the individual groups of spots may occur more frequently in the centre of the disc. A quiet interval can thus be expected when there is no geoactive source in activity on the Sun. Table IV shows, however, that in 90% of the cases the quiet intervals in 1950 were preceded by the CMP of sunspot groups [47], which is a quite convincing proof that spots cannot be geoactive. With the decrease in solar activity the percentage of quiet intervals preceded by the CMP of sunspot groups also decreases but this is the obvious consequence of a decrease in the number of sunspot groups in the direction of the minimum of solar activity. It thus follows that a large number of sunspot groups is followed by a pronounced decrease in geomagnetic activity, i.e. these spots cannot be the source of geoactivity.

Comprehensive material was elaborated by the method of superposed epochs during

Table IV
Very quiet intervals

Year	Number of intervals		%
	total	with preceding spots	
1950	19	17	90
1951	11	8	73
1952	13	7	54
1953	17	5	29

the 1937–1958 period in order to reach a definite decision on the question of the geoactivity of spots. Zero day was taken to be all the CMP of isolated groups of spots regardless of type, whether with or without flares; these groups were not accompanied by a filament passing through the centre of the solar disc. Altogether 110 cases were investigated to find the average course of the geomagnetic activity expressed by the values of the A_p -index [48] in the critical period after CMP (Fig. 17). It is obvious that the activity in this period is very low and, moreover, shows a slight decrease on the +1 and +2 days. Since it might be objected that this statistical treatment could smooth out the possible geoactivity of the most important sunspot groups, the set of most important and medium sunspot groups was treated individually. Not even in these most favourable cases did a geomagnetic disturbance occur, as is seen in Fig. 18. These results showed quite definitely that spots in themselves cannot be geoactive. The connection between spots and geomagnetic storms found by some earlier statistical papers can easily be explained by the fact that the methods used then did not take into account the occurrence of other expressions of solar activity in the spot regions.

3) The Question of the Geoactivity of Flares

Shortly after the discovery of flares the first conclusions were drawn that strong flares are connected with geomagnetic storms [49]. The values they gave for the velocity of propagation of corpuscular streams are still recognized. Later a statistical verification was made of the results where it was found that there is a certain dependence of the geoactivity of flares on the distance from the centre of the solar disc; according to this the angular aperture of the cone in which the corpuscular rays are emitted from the flare, would be roughly 90° [3, 50]. As material has accumulated great attention has been paid to this question in other papers. The results obtained for the direct connection between flares and geomagnetic storms, however, showed that the correlation is not convincing [51]. The question of why a large number (around 50%) of flares, even when conveniently situated, do not appear to be geoactive is still unanswered. Papers have also appeared which doubt any connection [52–54]. Sometimes the geomagnetic disturbance is ascribed to flares occurring on the edge of the disc.

In our work we concentrated on a detailed investigation of the main aspects of the connection between flares and geomagnetic activity.

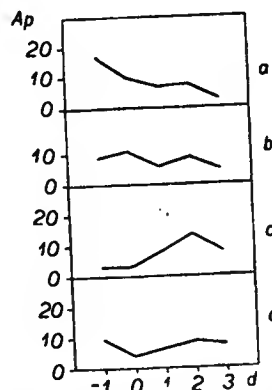


Fig. 18. Time dependence of geomagnetic activity after CMP of four selected largest groups of spots which were not accompanied by central filament. Date, type and heliographic latitude at CMP of group of spots: a) 12.VIII.1940, F, 7°N , b) 20.VIII.1940, F, 9°N , c) 14.IV.1943, E, 14°S , d) 17.VI.1958, E, 15°N .

36

The material from the IGY period was elaborated statistically using the method of superposed epochs [55]. We found that even the commonly used statistical methods produce results which cannot be satisfactorily explained by assuming a direct connection between flares and geomagnetic activity.

An analysis of the results led to the conclusion that the geoactivity of flares, particularly of those with smaller importance, should be understood as the geoactivity of the active regions in which these flares occurred. A statistical evaluation was then made by an analogous method [57] of all flares observed in 1937 to 1956 and contained in the Catalogue of large chromospheric flares [56].

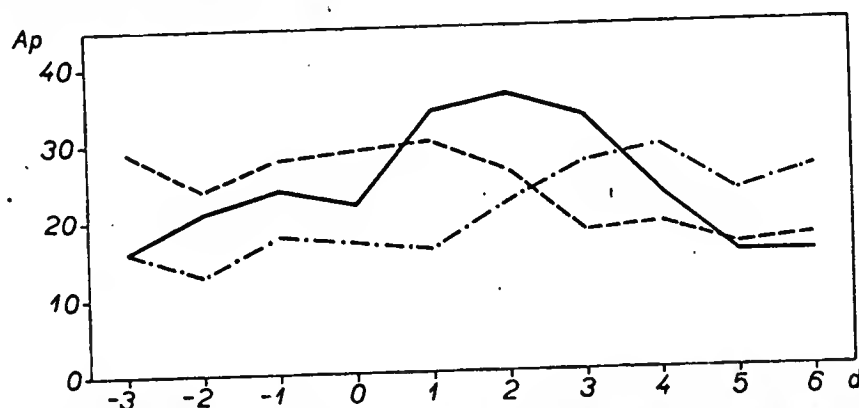


Fig. 19. Average time dependence of geomagnetic activity after flares $i = 3$, with regard to distance of flares from CM. Full line — central flare ($29^{\circ}\text{E} - 29^{\circ}\text{W}$), dashed line — western flare ($\geq 30^{\circ}\text{W}$), dotted-and-dashed line — eastern flare ($\geq 30^{\circ}\text{E}$).

Figure 19 shows that although medium flares are followed by a pronounced increase in geomagnetic activity the analogous increases for eastern and western flares are time displaced so that the maximum for western flares is earlier and that for eastern flares is later. This fact, together with other proofs, led to the above conclusion that there exists only an indirect connection between flares and geomagnetic activity. We also found that even if a direct connection is admitted, the value of the angular aperture is smaller than 60° .

It is also clear from [57] that the mean value of the time interval between a flare and the following geomagnetic storms has only formal significance and depends on the length of the period to which we confine ourselves in ascribing the geomagnetic storms to the different flares (Fig. 20). This indicates the random distribution of geomagnetic storms occurring after flares and does not give the typical mean value of the interval.

Two conceptions of how to understand the connection between flares and geomagnetic storms were proposed for a satisfactory explanation of all the dependences found statistically:

1) Flare activity in the active region, or any other source of geoactivity of the active region in which a large flare occurred, lasts for a long time, during which the active region may pass through the central meridian. If the conditions for the emission and direction of a corpuscular stream are fulfilled in this critical position, then this active region may be followed by an increase in geomagnetic activity with which the flare in question is not directly connected.

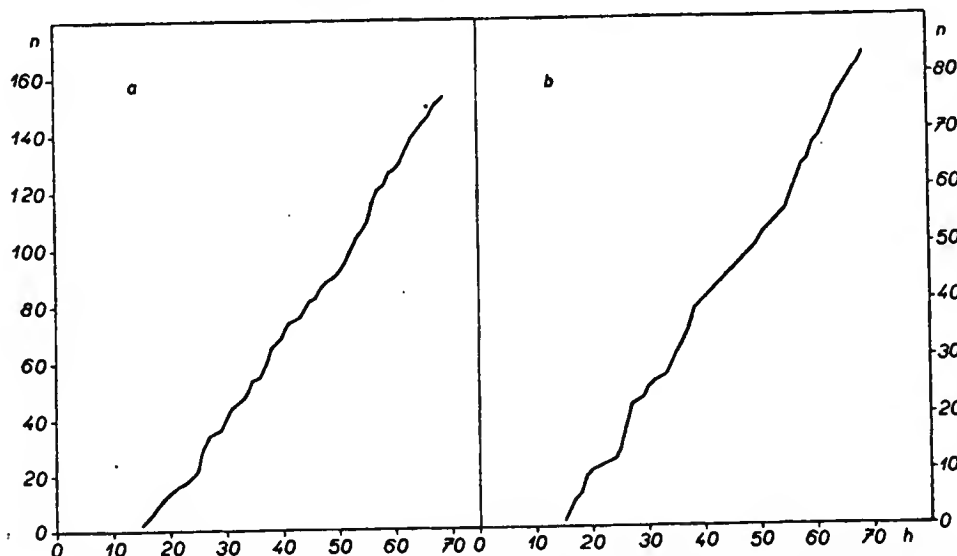


Fig. 20. Summation curves for set of time intervals between large flares and following geomagnetic storms. a) all flares, b) central flares (29°E–29°W).

2) The increase in chromospheric activity, which was seen inter alia as the occurrence of a large flare in some active region at a distance from the CM, need not remain limited only to this active region and its immediate neighbourhood but can appear more or less simultaneously in more distant parts of the solar surface. If such an increase takes place also in the active regions which are just on the CM, then such regions may be followed by an increase in geomagnetic activity with which the flare in question is not directly connected.

The above statistical results are in keeping with the individual investigations into the geoactivity of the different active regions with rich flare activity. Four isolated active regions were chosen (this means that during their passage over the solar disc practically no other flare activity occurred on the solar surface) and the results of observing flares in them were classified with the course of the geomagnetic activity during passage over the solar disc [58]. Despite the fact that throughout this time a series of large flares occurred in the active regions, the geomagnetic activity increased markedly only in the expected interval after the passage of the active region through the cen-

tral meridian (Fig. 21). From this it is clear, inter alia, that the influence of flares might be seen (if it exists) only in the immediate neighbourhood of the CM; thus conceptions ascribing geomagnetic storms to flares on the edge of the disc are quite unjustified.

Previous papers paid particular attention to how flares are reflected in geomagnetic activity; this means that the zero day in the method of superposed epochs was the day of occurrence of a flare. A possible connection can be verified, however, in the opposite direction, i.e. whether an increase in geomagnetic activity is preceded by a flare (zero day in the method of epoch displacement is the day of increased geomagnetic activity).

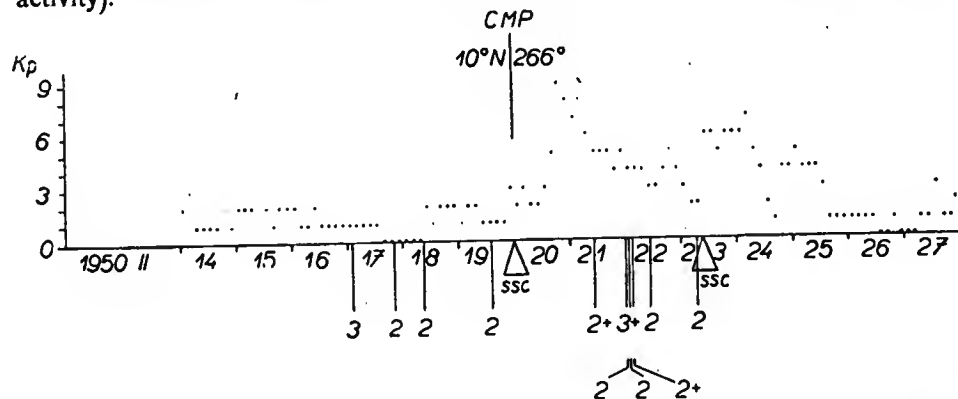


Fig. 21. Time dependence of geomagnetic activity (points) around CMP of active region with occurrence of strong flares (vertical lines with notation of flare importance).

With this in mind a statistical analysis was made of the solar situations preceding sudden commencements of geomagnetic storms (ssc), which also contains an elaboration of the occurrences of flares between these commencements in 1957-60 [40]. Only those ssc were chosen for which 100% observation of flares was ensured in an interval of 28 to 38 hours before an ssc. This 10-hour interval was chosen on the basis of the results of investigations which will be discussed in the next chapter. The investigations covered flares of all importances from 1- to 3+, which occurred in $\pm 10^\circ$ from the CM. The percentage of the number of cases when no such flare occurred before a sudden commencement was calculated. Table V shows that a geomagnetic storm occurred on an average in 45% of the cases without being preceded by a flare.

Due to the problematical character of the connection between flares and geomagnetic activity, which is clear from the statistical papers just discussed, it can be deduced that the increase in geomagnetic activity observed sometimes after flares could actually be explained by the geoactivity of other expressions of solar activity occurring in the active regions together with flares or possibly the geoactivity of expressions occurring on the CM synchronously with the flare which is at some distance from the CM.

A partly complex procedure was therefore adopted in investigating the influence of flares; not only flares but also filaments about whose connection with geomagnetic activity positive conclusions had been reached (see paragraph 4), were taken into consideration. The different configurations of flare and filament were thereby considered. Material was elaborated from 1950–1959 [59] for which the method of superposed epochs was used to determine the average variation of the A_p -indices around

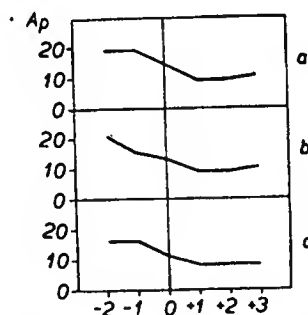


Fig. 22. Average time dependence of geomagnetic activity after occurrence of flare without presence of filament on centre of solar disc, taking into consideration distance of flare from CM, a) max. $\pm 45^\circ$, b) max. $\pm 20^\circ$, c) max. $\pm 10^\circ$.

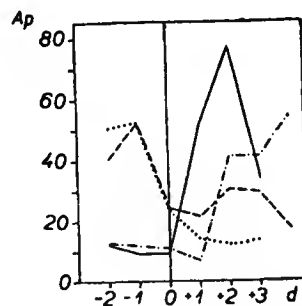


Fig. 23. Average courses of geomagnetic activity after occurrence of flares (max. $\pm 45^\circ$ from CM) in simultaneous presence of filaments.
— filament on disc centre on same day as flare; filament preceded (1–2 days); — . — . filament followed (1–3 days); — — — one filament preceded, other followed.

zero day (all days with the occurrence of a strong flare $i = 3$ or $3+$ at successive distances of 10° , 20° , and 45° from the CM were chosen as zero day), in all 48 cases without the occurrence of a central filament (i. e. one, of which a certain part would pass through the centre of the solar disc). It was found (Fig. 22) that after the occurrence of flares without the presence of a central filament no increase in geomagnetic

Table V

Year	Number of geomagnetic storms not preceded by any flare
1957	30
1958	54
1959	46
1st half 1960	50
mean value	45

activity occurred; on the contrary, a slight decrease is observed. This is proof that there was no geoactive source in activity at the time in question and therefore the flare itself is not geoactive.

Quite different results were obtained when zero day was taken to be the day on which there was a flare at a maximum distance of $\pm 45^\circ$ from the CM but a central filament occurred, as is dealt with below. On the basis of 23 cases we distinguished four basic situations as a function of the time configuration of the flare and filament:

a) the passage of the filament through the centre of the disc occurred on days of flare occurrence, b) the passage of a filament occurred just before a flare (roughly up to 1–2 days), c) the passage of a filament occurred just after a flare (max. 1 to 2 days), d) two filaments passed through the centre, just before and after a flare. The method of superposed epochs was used for all these four situations to obtain the average courses of the geomagnetic activity (Fig. 23) from which the following conclusions can be drawn:

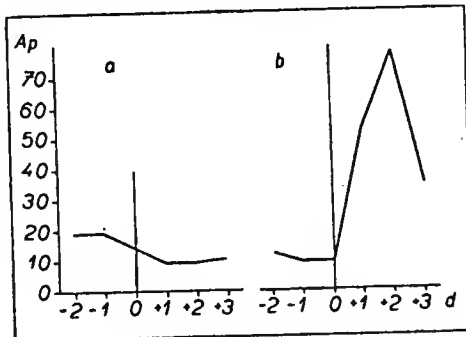


Fig. 24. Average time dependences of geomagnetic activity after occurrence of flares at max. distance of $\pm 45^\circ$ from CM a) without presence of filament on centre of solar disc, b) in presence of filament on centre of solar disc.

increase is time displaced in keeping with the time displacement of the passage of a filament from that of a flare. The geoactivity of the opposite solar situations is shown in Fig. 24.

Apart from this, individual investigations of the same question on a set of flares of homogenized importances gave analogous results [60] confirming the fact that flares are not the direct source of geomagnetically effective corpuscular radiation.

4) Filaments and Corona – Their Geoactive Effects

Filaments – prominences – occur in the external solar layers above the photosphere, in the chromosphere and in the inner and middle corona; in the case of rising filaments they sometimes penetrate to the outer corona. Since it can be assumed that they are produced by the condensation of coronal matter along the lines of force of the local magnetic fields, leaving the photosphere, the structure of such fields can be deduced from their shape. At the same time prominences give a conception of the arrangement of the magnetic fields in the direction perpendicular to the solar surface while

filaments and the fine structure of the chromosphere indicate the magnetic fields distributed parallel to the surfaces of the Sun.

On the basis of the relation of filaments to the surrounding magnetic fields we classified filaments into three groups [6, 61], which proved to be very useful in investigating the geoactivity of filaments. It was later found that this classification can be made in keeping with the development of filaments [6, 62] and therefore we give here the different types in the order of the phase development of the filament.

1) *Bound Filaments*. These are the youngest type of filaments occurring directly in the active regions and, as is clearly shown by their shape, they are under the influence of the local magnetic field. They persist in the active region without any great changes until they more or less suddenly become type 2 or gradually become type 3.

2) *Unstable Filaments*. Active, eruptive and disappearing filaments belong here, in the order according to the suddenness of the changes occurring in them. They occur again in active regions, not necessarily directly in the sunspot groups but always under the influence of the local magnetic field, the basic time changes of which are, we assume, the actual cause of instability of the filaments of this type.

3) *Free Filaments*. These include all filaments occurring clearly outside the active region which are thus not under the influence of local magnetic fields. They are filaments of the oldest phase of development which were produced in the active region as type 1 and outlasted the period characterized by sunspot and flare activity in which there occurred the strongest time changes in the magnetic field. In this period they begin to move gradually further away from the active region in the direction of the poles and to take up a position roughly in the direction of the solar parallels.

To the different types of filaments defined by our "magnetic" classification, one can ascribe*) different types of prominences according to the "motion" classification [63]

Table VI
Classifications of different types of filaments-prominences

Classification		
Magnetic	Motion	Morphological
1. Bound filaments	electromagnetic prominences	particularly prominences of type III a)-c) and less active type I a)-c)
2. Unstable filaments	eruptive prominences	particularly prominences of type II a)-b) and more active type of I a)-c)
3. Free filaments	chaotic prominences	some prominences of type V

*) If the filaments in question were observed on the solar limb as prominences.

or the classical "morphological" classification [64], based on quite different principles (Tab. VI).

The geoactivity of filaments — prominences — has already been investigated in a number of papers [65–67]. A certain connection between filaments and geomagnetic activity was statistically proved in the period before the minimum of solar activity, and this was explained by the fact that filaments could be the source of slower corpuscular streams exciting smaller geomagnetic storms with a gradual commencement, repeating after 27 days as a consequence of solar rotation. However, papers have also appeared which, on the basis of statistical methods, refute such a connection [68–71].

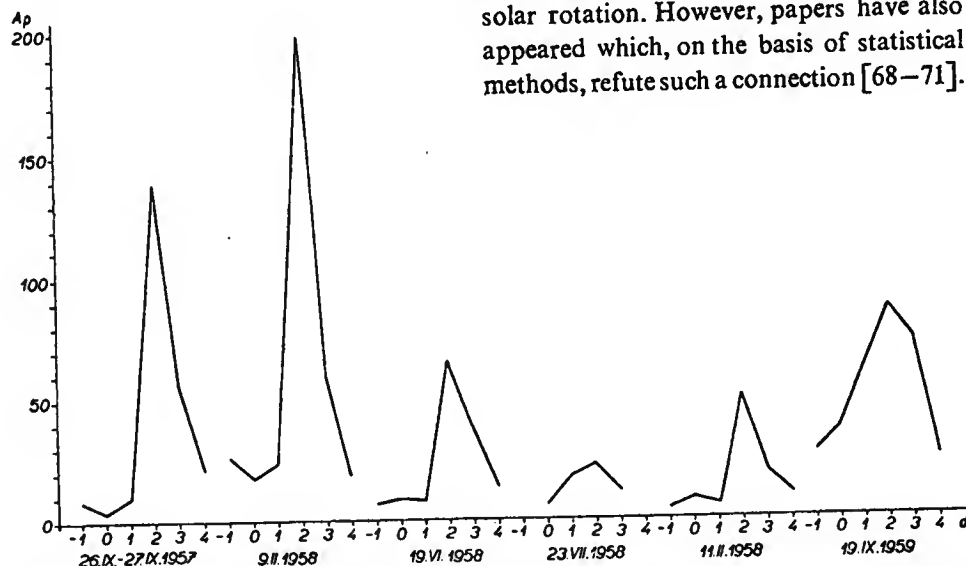


Fig. 25. Time dependences of geomagnetic activity after passages of unstable filaments through centre of solar disc.

The question of the geoactivity of filaments, however, requires a more detailed investigation using not only statistical methods but also methods of analyzing the individual cases [72–77] which led to the need for the elaboration of the above classification of filaments. It was on the basis of such a classification that we could prove that there only seems to be disagreement in the conceptions of the geoactivity of filaments because the different types of filaments have different results, as is seen below:

Bound filaments: The geoactivity of these filaments was investigated by comparing the course of the geomagnetic activity with the CMP of the filament [6, 7]. It was clearly shown that there is no increase in geomagnetic activity after the CMP of filaments of this type.

Unstable filaments: When investigating the geoactivity of filaments of this type we used different methods, chosen in keeping with the character of the problem to be solved, and arrived at the following conclusions [7]:

When these filaments pass through the centre of the solar disc (or its immediate neighbourhood — max. a few degrees), a geomagnetic disturbance, usually a strong storm, occurs in 100% of the cases (Fig. 25). An increase in geomagnetic activity occurs even after the CMP of some non-central filaments oriented in the direction of the meridian (Fig. 26). The value of the time interval between the CMP or between the disappearance of a filament and the commencement of the storm varies between 27 and 53 hrs and it seems that it might depend on the degree of activity of the filament (Tab. VII).

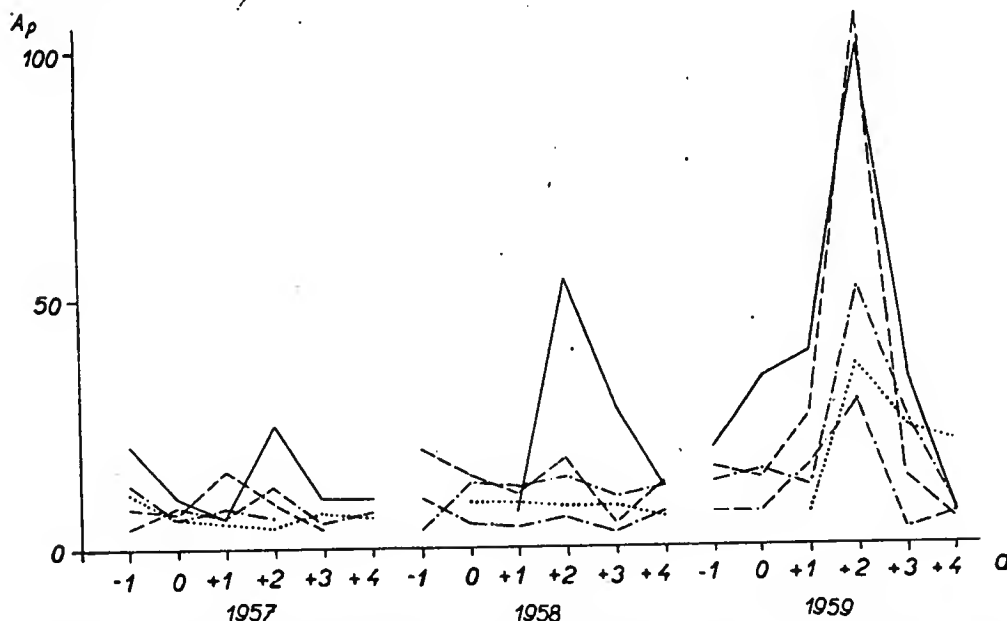


Fig. 26. Course of A_p -indices after CMP of non-central meridional filaments. The curves relate to the dates as follows: 1957: 14. V.; -.-.- 22. V.; --- 27. VII.; --- 8. VIII.; — 16. XI.; 1958: --- 1. X.; --- 9. X.; 16. X.; — 2. XII.; -.-.- 26. XII.; 1959: 8.-9. II.; --- 3. V.; --- 10. V.; -.-.- 22. V.; — 2. IX.

Free filaments: The indisputable geoactivity of filaments of this type was proved by an analysis of the different cases based on a comparison of the geomagnetic activity after the CMP of a filament in the periods before minimum solar activity [6]. It was found that as long as there is no local magnetic field between the free filament and the equator, then there is always an increase in geomagnetic activity after the CMP of the filament in a time interval comparable with the values for the unstable filaments [7]; thus the conception of the existence of corpuscular streams with very small velocity (interval of 4 or more days) is not confirmed [66, 78].

Here we give only the results valid for isolated filaments so that their geoactivity can be compared with that of other expressions of solar activity, discussed in the preceding paragraphs separately.

Table VII

Mean values of time interval for different sets according to degree of activity

	Maximum degree of activity		Medium degree of activity		Lowest degree of activity	
		No. of cases		No. of cases		No. of cases
time interval in hrs.	28.3 ± 0.6	2	37.9 ± 0.9	11	50.9 ± 0.8	7
velocity in km/sec	1500		1100		800	

The results given here lead one to think that, due to the practically 100% connection between suitably placed unstable and free filaments and the geomagnetic activity, it is these that are the expression of solar activity which is the direct source of geomagnetically effective corpuscular radiation. However, further investigations [59] showed that the question of determining the direct source is not so simple; the whole matter becomes clearer if the connection with the solar corona is taken into consideration.

The Corona and its Connection with Filaments

It is usually stated that the solar corona, changing markedly during the eleven-year cycle of solar activity, can be characterized by three basic types (Fig. 27):

- a) The minimum type occurs usually in the period of the minimum of sunspots. It

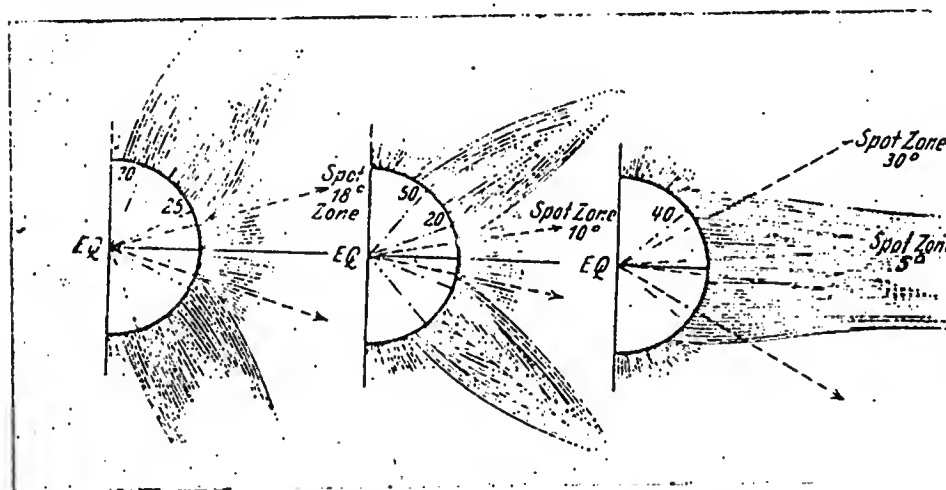


Fig. 27. Types of solar corona (maximum, intermediate, minimum) in relation to zones of prominences, marked by shorter radial lines (after [79]).

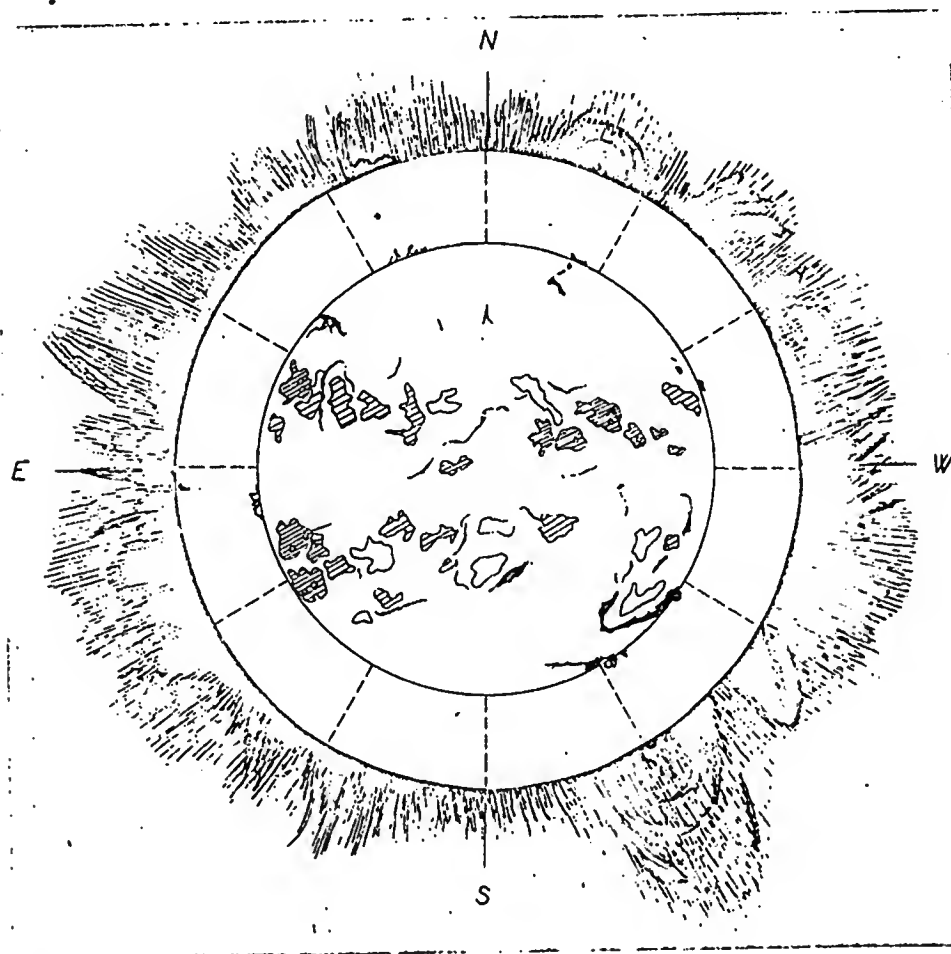


Fig 28. Comparison of structure of inner corona from 12. X. 1958 [80] with chromospheric situation according to solar map from Meudon. Since times of two observations do not exactly agree comparison is valid only for more permanent events.

is characterized by a particularly simple regular shape with long equatorial wings, without complex structures.

b) The intermediate type appearing in periods of medium solar activity is distinguished by a more complicated and less regular structure consisting usually of several coronal wings.

c) The maximum type, which is formed during high solar activity, usually has a very complicated ray-like shape with many coronal wings and streams.

The above types represent only the average idealized corona; in reality its instantaneous shape is given by the distribution of the different expressions of solar activity on the edge of the disc and thus also of the local magnetic fields. The best known and

most pronounced is the connection between coronal formations and prominences. A certain coronal wing is sometimes regarded as a large three-dimensional copy of a filament which is in the base of this wing [1].

If we take into consideration the distribution of filaments (prominences) given above, we see their close connection with the shape of the corona. To bound prominences, as long as they occurred in the region of simpler local magnetic fields, one can ascribe the arched structure occurring in the base of the elongated elements — "helmets" — from the Sun (Fig. 28). When they occur in strong more complicated fields (sunspot groups) only arched formations are found. As regards unstable prominences, we found [7] that they correspond to coronal streams of cylindrical shape (Fig. 29) usually ascribed to facular fields [81].

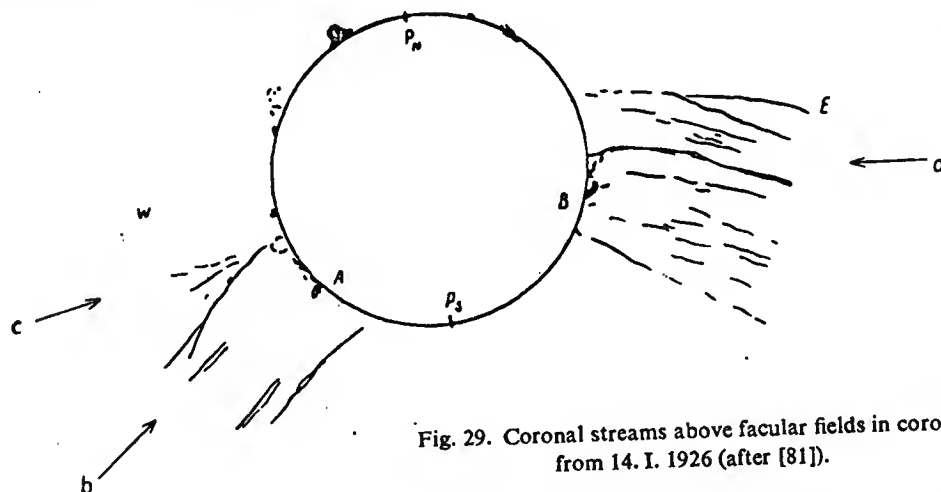


Fig. 29. Coronal streams above facular fields in corona from 14. I. 1926 (after [81]).

Free prominences are not seen in the corona above them by any corresponding formation.

We can now go on to explain the conditions for the emission of geomagnetically effective solar corpuscular radiation. The observed transformations of the bound (non-geoactive) filaments into the unstable type (geoactive) must obviously correspond to a change in the appropriate coronal formations above them. This, together with the minimum type of corona at free (also geoactive) filaments, permits the assumption that coronal formations represent the paths of corpuscular streams. The geoactivity of unstable filaments occurring on the centre of the solar disc, which has been proved quite definitely, is explained by a broad, favourably directed coronal stream rising above them, which in this case is pointed towards the Earth. The geoactivity of free filaments, which occurs if the filaments are high-latitude ones, can be explained by the concentration of the emitted corpuscles into the equatorial plane as a result of the effect of the total solar magnetic field, i.e. in the equatorial coronal wings which are aimed towards the Earth. In this way it was possible to explain the origin of geomag-

netic disturbances which are ascribed to hypothetical *M*-regions [6, 82–84]. If a local magnetic field appears between the free filament and the equator (non-geo-active sunspot group), the arrangement of the minimum corona is disturbed and the corpuscular radiation is deflected from its original direction — negative effect of spots occurs.

It remains to explain that in some cases a geomagnetic storm occurs even during the passage of non-central unstable filaments through the central meridian [7].

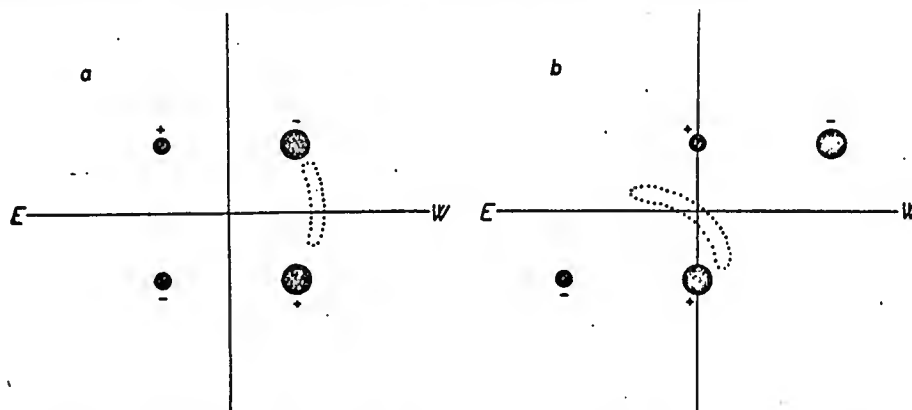


Fig. 30. Diagram of position of filament for different configuration of active regions.

It can be assumed that if the local magnetic field is temporarily compensated the corona may prematurely become the minimum type with equatorial wing pointing to the Earth and the emitted particles then move in the same way as in the case of free filaments. In this way one can obviously explain why there is no increase in geomagnetic activity after the CMP of active regions occurring symmetrically with respect to the equator but that after the passage of a pair of active regions somewhat displaced in heliographic longitude a magnetic disturbance sometimes occurs [85]. The explanation is obvious from the representation of the magnetic fields excited during simple configurations of idealized groups of spots [86]. It is seen from Fig. 30a that with a symmetrical arrangement of the sunspot groups the central filament, if it is formed, would be bound to the fields of both groups. In this case it is not very likely that there would be a synchronous change in both magnetic fields and, moreover, a change such as to cause the conversion of the filament into an unstable type. There is thus no reason for an increase in geomagnetic activity at such a configuration.

If, however, the arrangement shown in Fig. 30b occurs, then the central filament, if it occurs here, will try to take up a position along the boundary between the magnetic fields of the two groups of spots. In this case a change in magnetic field of only one-group with which the filament is connected is sufficient for the transition to the unstable type; this gives rise to a favourable situation for the origin of a geomagnetic disturbance.

5) Deductions – On the Problem of Geomagnetic Storm Prognosis

The analysis made above mainly concerned individual solar phenomena from the point of view of their geoactive effects. It is quite obvious, however, that for a satisfactory explanation of the emission of corpuscular radiation, particularly in connection with the prognoses of geomagnetic storms, one cannot confine oneself only to separate investigations into the geoactivity of the above phenomena.

The conceptions on the role of the corona in the emission of corpuscular particles, discussed above, permit filaments to be regarded as indicators of coronal formations; this is of great importance in forecasting geomagnetic activity since the corona has not yet been continuously observed in its whole extent.

On the Determination of the Direct Source of Corpuscular Streams

The question is, whether filaments contribute directly by their mass to the formation of corpuscular streams, as can be expected from the high percentage of cases when geomagnetic storms were preceded by filaments, or whether filaments merely determine the shape, position and change in the corresponding coronal formations which were themselves the source of corpuscular streams. If we take it that filaments are the source, then in the case of free filaments it should be possible to accept the conception according to which hydrogen masses escape from the filaments by diffusion into the surrounding corona [66], where they are quite ionized and the protons and electrons thereby released form the base of the corpuscular streams. This is also borne out by the slow weakening of the filaments which often lasts for several rotations. In the case of unstable filaments a larger amount of hydrogen atoms would get into the outer corona which, after ionization, would give rise to the possibility of the origin of important corpuscular streams.

The Geoactivity of the Active Region as a Function of its Phase of Development

Let us first assume for the sake of simplicity that the active region is isolated. In order to understand the character of its geoactivity the duration of the active region is substantially divided into two periods: the first period is limited by the instants of the formation and decay of the facular fields and the second is given by the existence of a filament which was produced in the active region and outlasts the first period without disappearing. This latter period lasts from the decay of the facular fields up to the gradual decay of the filament.

As regards the geoactivity of the active region, two quite different cases may occur in the first period according to the instantaneous situation in the active region during CMP. If the conditions for the emission of a geomagnetically effective corpuscular

stream, discussed in detail in the preceding paragraphs, are not satisfied a complete decrease in geomagnetic activity follows. In the opposite case a geomagnetic storm with sudden commencement occurs.

The geoactivity in the second period is clear as long as the region is isolated. After the CMP of the active region, which in this case reduces merely to a free filament, there follows a geomagnetic disturbance or storm with gradual commencement. This simple picture is of course complicated by the fact that not always only isolated active regions occur on the Sun. In the period around the maximum of solar activity, in particular, there is often a considerable concentration of different local magnetic fields in the immediate neighbourhood of the central meridian. It is therefore more difficult in periods of greater solar activity to determine in a simple way when a geomagnetic storm begins.

The negative effect of spots, causing the decay or temporary interruption of geomagnetic disturbances from the hypothetical *M*-regions, is the reason why these regions cannot be expressed otherwise than in the period of smaller solar activity, when there are less spots.

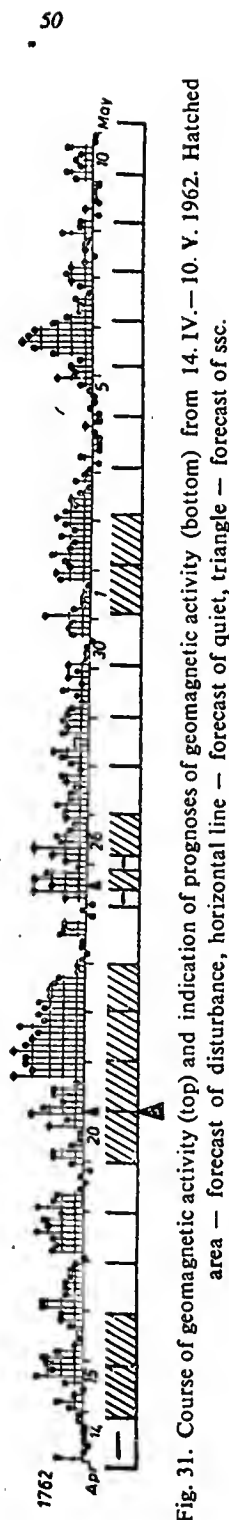
We proved of recurrent geomagnetic storms that they are produced by the joining up of several disturbances [82-84]. A disturbance with a sudden commencement, after the CMP of an active region through the centre of the solar disc, may be followed by disturbances with a gradual commencement after the CMP of high-latitude filaments.

Prognoses of Geomagnetic Activity

On the basis of the above results, to which special solar observations contributed to a great degree [87, 88], it was possible to elaborate a method for the prognosis of geomagnetic activity*) and also on the basis of our own solar observations to start issuing test forecasts.

In prognoses one must distinguish the degree of reliability of the solar bases, since this is reflected in the varying degree of accuracy of the prognoses. The most exact are prognoses of the first kind on the basis of changes seen directly in the central solar meridian; this, of course, requires continuous detailed observation of the Sun for forecasting the time dependence of the geomagnetic activity (i.e. of all geomagnetic storms and smaller disturbances as well as geomagnetically quiet periods), which cannot be ensured at one station on the Earth. Such a prognosis can be given for a maximum of two days ahead. At sudden changes a 28-38 hr interval is commonly used, the length of which is made more exact according to the estimated degree of suddenness of the change in the solar situation. Prognoses of this kind should agree practically 100% with reality within the limits of accuracy of the interval used since here one is mainly determining a certain phenomenon from a total of other phenomena on the basis of relations which in principle are known. High agreement of the

*) This will be published in detail later.



forecasts of the first kind with reality is actually observed in practice; of course, there are not many of them because data from continuous observation of the Sun are not available.

Prognoses of the 2nd kind differ from the first group in that the decisive changes were not observed directly but only the possibility of such changes was estimated from the character of the solar situation on the central solar meridian. The accuracy of prognoses of this kind, which are issued for the same period ahead and using the same time interval as for prognoses of the first type, is limited mainly by the degree of probability of extrapolating the development of the active region.

Less accurate are prognoses of the 3rd type, based on observations of the solar situation before the CMP, when extrapolation of the development of the active region must be made for a period of several days. These prognoses, which do not have to be made if data from continuous observation of the Sun are available, may be of greater importance only in periods of lower solar activity, when the starting point for prognoses are mainly long-term free filaments. In periods of greater solar activity they must be made as accurate as possible by prognoses at least of the 2nd type.

For illustration we give an example of a prognosis together with the course of geomagnetic activity for one 27-day period (Fig. 31). It is obvious that as long as solar observations were available, the prognoses could determine storms with a sudden commencement as well as several smaller disturbances and even the quiet periods.

Prognoses of geomagnetic activity based on the above principles, as long as our own solar observations were available, have been made since September 1959.

It is seen from the 135 prognoses issued so far that they agree with reality in 90% of the cases so that the above method can at present be regarded as very good; this is also borne out by the correctness of the conclusions based on our analysis of the connection between solar and geomagnetic activity.

CONCLUSION

The problem of the origin of geomagnetic storms, as discussed here, represents a relatively very broad complex of problems which are solved in this connection. In addition to

a general view of the partial phase of the general development of geomagnetic storms, our paper gives some new results of research, obtained recently, which contribute to the classification of storms and to clarifying the relations between geomagnetic and solar activity.

When classifying geomagnetic storms type analysis showed that the majority of storms has a two-phase course although one cannot neglect even that number of storms which exhibits a one-phase course. Such storms have a tendency to occur only in a certain period of the day.

A systematic investigation of the relations between solar and geomagnetic activity provided some important data contributing towards a decision on the causes of geomagnetic storms.

The relatively comprehensive material, on the basis of which the influence of sunspots on geomagnetic activity was determined, showed that the spots in themselves cannot be geoactive; a certain connection, found earlier in a number of papers, can be explained by the fact that other solar effects in the regions of spots were not taken into consideration.

An analysis of the results of observing flares, which was made in a number of papers both by statistical methods and for some individual cases, showed that flares might play a role in events which are followed by an increase in geomagnetic activity (in particular the occurrence of flares might disturb the shape of local magnetic fields on the Sun, if of course the flares themselves are not the consequence of the changes in these fields); it was found quite definitely, however, that flares are not the direct source of geomagnetically effective corpuscular radiation.

A study of filaments and the corona provided new results from the point of view of the causes of geoactivity. We made a new division of filaments into three groups and arrived at the conclusion that the filaments classified in unstable and free groups are very closely related to sources of geoactive radiation. However, it is not a simple problem to determine the direct source. It was found necessary to take into consideration phenomena occurring in the corona. An important role here is played by the approximately equatorial coronal streams or wings. The influence of the total magnetic field of the Sun is also very important in directing corpuscular radiation (particularly ejections connected with free high-latitude filaments).

The correctness of the conclusions we have derived is borne out by the reliability of the prognoses of geomagnetic activity based on our conceptions of the geoactivity of expressions of solar activity. The results obtained permit a unified interpretation of the connection between geomagnetic and solar activity throughout the solar cycle.

It is natural that it has not yet been possible to explain quite satisfactorily all the solar situations and the level of geomagnetic activity connected with them, on account of the very complicated conditions, sometimes reigning on the Sun. A number of other problems will have to be clarified for such purposes, particularly as regards the local magnetic fields of the Sun.

The results obtained hitherto are mostly of a qualitative character, as followed from an elaboration of the results of observations and the correlation of geomagnetic and solar phenomena. This phase in research was indispensable for ensuring a sufficient base of new experimental grounds; it contributed towards the discovery of a series of new laws and should be continued. However, the problems have not yet been solved from the quantitative point of view as regards the investigation of physical conditions and the interpretation of the causes of the effects, as they actually occur, by the proposal of suitable theoretical models. These questions will be the subject of further work.

The discussion of events on the Sun shows that a decisive role in their formation is played by the magnetic fields, their distribution and dynamics. It is therefore important to explain their role in connection with geoactive processes and thus in relation to the origin of geomagnetic storms. In this respect it will be expedient to use inter alia the results of research into the internal geomagnetic field (particularly of continental geomagnetic anomalies and isoporic expressions) at present being done in our department [89] and at the same time to carry out model experimental investigations of the general magnetic fields with the possibility of applying the conclusions derived to the study of solar magnetic fields. From the theoretical point of view one must concentrate on the application of magnetohydrodynamical laws in explaining the causes of magnetic fields.

It is well known that the hydromagnetic processes taking place in the Earth's interior, which to a certain extent participate in the formation and maintenance of the Earth's magnetic field, have a relatively great similarity to processes on other cosmic bodies, i.e. on stars and thus also on the Sun [90, 91]. It is therefore expedient to make use of the results obtained from research into solar phenomena for the study of the Earth's magnetic field and vice versa. This procedure, common at many laboratories throughout the world where questions of research into the geomagnetic field are solved, is quite logical. This is because while relatively much is known about the geomagnetic field and its dynamic expressions (whether external or internal) we are not able to study directly hydrodynamic events appearing as the magnetic field on the Earth's surface. It is therefore indispensable that, apart from an analysis of the surface expressions of the geomagnetic field, analogies should be sought for the hydromagnetic processes in the Earth's interior and studied in those places where the mechanisms of such events, i.e. particularly on the Sun, can easily be investigated.

Quite analogously, research into the external geomagnetic field, the structure of which is observed at geomagnetic observatories, must use data from studies of processes, which are the source of the above disturbances or at least influence them to a certain extent, to explain the causes of geomagnetic disturbances.

Research work will have to be carried out along such lines both from the point of view of obtaining new experimental data and as regards theoretical generalization.

Received 13. 4. 1963

Reviewer: A. Zátpek

REFERENCES

- [1] K. O. Kiepenheuer: The Solar Activity, The Sun. Ed. G. P. Kuiper, The Univ. of Chicago Press, Chicago 1954.
- [2] S. Chapman, J. Bartels: Geomagnetism. Oxford Univ. Press, London 1940.
- [3] H. W. Newton: Solar Flares and Magnetic Storms. MN, 104 (1944), 4.
- [4] K. O. Kiepenheuer: Sonnenzirkular. 1949.
- [5] C. W. Allen: Relation between Magnetic Storms and Solar Activity. MN, 104 (1944), 13.
- [6] B. Bednářová-Nováková: Солнечные волокна-протуберанцы а их связь с геомагнитными бурями. Studia geoph. et geod., 4 (1960), 54.
- [7] B. Bednářová-Nováková: Connection between Geomagnetic Storms in IGY and IGC and Occurrence of some Kinds of Filaments. Studia geoph. et geod., 5 (1961), 138.
- [8] T. G. Cowling: The Growth and Decay of the Sunspot Magnetic Field. MN, 106 (1946), 218.
- [9] C. Walén: On the Distribution of the Solar General Magnetic Field and Remarks Concerning the Geomagnetism and the Solar Rotation. Arkiv Mat. Astr. Fysik 33A, 18 (1946).
- [10] V. A. C. Ferraro: The Non-uniform Rotation of the Sun and its Magnetic Field. MN, 97 (1937), 458.
- [11] А. Б. Северный: Некоторые особенности движения плазмы в солнечных магнитных полях. Изв. Крым. астрофиз. общ., 25 (1960), 281.
- [12] В. Бумба: Связь хромосферных вспышек с магнитными полями групп солнечных пятен. Изв. Крым. астрофиз. общ., 19 (1958), 105.
- [13] R. G. Giovanelli: Chromospheric Flares. MN, 108 (1948), 163.
- [14] W. H. Ward: On the Origin of Terrestrial Particles from Solar Flares. Journ. of Atm. and Terr. Physics, 14 (1959), 296.
- [15] D. H. Menzel: Report of Conference on the Dynamics of Ionized Media. London 1951.
- [16] J. W. Dungey: A Semily of Solution of the Magneto-Hydrostatic Problem in a Conducting Atmosphere in a Gravitational Field. MN, 113, 1953, 180.
- [17] K. Saito: Equatorial Coronal Streamers of the Sun. Publ. Astr. Soc. Japan, 11 (1959), 234.
- [18] J. A. Van Allen: The Geomagnetically-trapped Corpuscular Radiation. J. Geophys. Res., 64 (1959), 1683.
- [19] T. Obayashi: Particle Precipitations and Geomagnetic Storms. Proc. Int. Conf. on Cosmic Rays and the Earth Storm, Kyoto, 4-15 Sept., 1961. I. Earth Storm, 201.
- [20] A. Nishide J. A. Jacobs: World Wide Changes in the Geomagnetic Field. Proc. Int. Conf. on Cosmic Rays and the Earth Storm, Kyoto, 4-15 Sept., 1961. I. Earth Storm, 39.
- [21] T. Obayashi: Geomagnetic Storms and the Earth's Outer Atmosphere. Rep. of Ion. Res. Japan, XII (1958), 301.
- [22] M. Konečný: Geomagnetic Pulsations at the Time of Bay Disturbances Observed by Induction Magnetometer at Observatory of Budkov. Travaux Inst. Geophys. Acad. Tchecosl. Sci. No 193, Geofysikální sborník 1963, NČSAV, Praha 1964.
- [23] J. Pěčová: Sur les variations rapides du champ électrotellurique à Budkov (Tchécoslovaquie). Studia geoph. et geod., 4 (1960), 158.
- [24] J. Halenka, J. Pěčová: Beitrag zur Frage des Zusammenhanges der Pulsationen des elektromagnetischen Feldes der Erde und der Sonnentätigkeit. Studia geoph. et geod., 4 (1960), 42.
- [25] J. Halenka: Další geomagnetické charakteristiky observatoře Průhonice. Results of the Geomagnetic Observations made at Průhonice Observatory near Prague in the Year 1955, NČSAV, Praha 1957, 9.
- [26] T. Nagata: On the Earth Storms I. General Introduction. Rep. of Ion. and Space Res. Japan, XIV (1960), 249.

REFERENCES

- [1] K. O. Kiepenheuer: The Solar Activity, The Sun. Ed. G. P. Kuiper, The Univ. of Chicago Press, Chicago 1954.
- [2] S. Chapman, J. Bartels: Geomagnetism. Oxford Univ. Press, London 1940.
- [3] H. W. Newton: Solar Flares and Magnetic Storms. MN, 104 (1944), 4.
- [4] K. O. Kiepenheuer: Sonnenzirkular. 1949.
- [5] C. W. Allen: Relation between Magnetic Storms and Solar Activity. MN, 104 (1944), 13.
- [6] B. Bednářová-Nováková: Солнечные волокна-протуберанцы и их связь с геомагнитными бурями. Studia geoph. et geod., 4 (1960), 54.
- [7] B. Bednářová-Nováková: Connection between Geomagnetic Storms in IGY and IGC and Occurrence of some Kinds of Filaments. Studia geoph. et geod., 5 (1961), 138.
- [8] T. G. Cowling: The Growth and Decay of the Sunspot Magnetic Field. MN, 106 (1946), 218.
- [9] C. Walén: On the Distribution of the Solar General Magnetic Field and Remarks Concerning the Geomagnetism and the Solar Rotation. Arkiv Mat. Astr. Fysik 33A, 18 (1946).
- [10] V. A. C. Ferraro: The Non-uniform Rotation of the Sun and its Magnetic Field. MN, 97 (1937), 458.
- [11] А. Б. Северный: Некоторые особенности движения плазмы в солнечных магнитных полях. Изв. Крым. астрофиз. общ., 25 (1960), 281.
- [12] В. Бумба: Связь хромосферных вспышек с магнитными полями групп солнечных пятен. Изв. Крым. астрофиз. общ., 19 (1958), 105.
- [13] R. G. Giovanelli: Chromospheric Flares. MN, 108 (1948), 163.
- [14] W. H. Ward: On the Origin of Terrestrial Particles from Solar Flares. Journ. of Atm. and Terr. Physics, 14 (1959), 296.
- [15] D. H. Menzel: Report of Conference on the Dynamics of Ionized Media. London 1951.
- [16] J. W. Dungey: A Semily of Solution of the Magneto-Hydrostatic Problem in a Conducting Atmosphere in a Gravitational Field. MN, 113, 1953, 180.
- [17] K. Saito: Equatorial Coronal Streamers of the Sun. Publ. Astr. Soc. Japan, 11 (1959), 234.
- [18] J. A. Van Allen: The Geomagnetically-trapped Corpuscular Radiation. J. Geophys. Res., 64 (1959), 1683.
- [19] T. Obayashi: Particle Precipitations and Geomagnetic Storms. Proc. Int. Conf. on Cosmic Rays and the Earth Storm, Kyoto, 4-15 Sept., 1961. I. Earth Storm, 201.
- [20] A. Nishide J. A. Jacobs: World Wide Changes in the Geomagnetic Field. Proc. Int. Conf. on Cosmic Rays and the Earth Storm, Kyoto, 4-15 Sept., 1961. I. Earth Storm, 39.
- [21] T. Obayashi: Geomagnetic Storms and the Earth's Outer Atmosphere. Rep. of Ion. Res. Japan, XII (1958), 301.
- [22] M. Konečný: Geomagnetic Pulsations at the Time of Bay Disturbances Observed by Induction Magnetometer at Observatory of Budkov. Travaux Inst. Geophys. Acad. Tchécosl. Sci. No 193, Geofysikální sborník 1963, NČSAV, Praha 1964.
- [23] J. Pěčová: Sur les variations rapides du champ électrotellurique à Budkov (Tchécoslovaquie). Studia geoph. et geod., 4 (1960), 158.
- [24] J. Halenka, J. Pěčová: Beitrag zur Frage des Zusammenhanges der Pulsationen des elektromagnetischen Feldes der Erde und der Sonnentätigkeit. Studia geoph. et geod., 4 (1960), 42.
- [25] J. Halenka: Další geomagnetické charakteristiky observatoře Průhonice. Results of the Geomagnetic Observations made at Průhonice Observatory near Prague in the Year 1955, NČSAV, Praha 1957, 9.
- [26] T. Nagata: On the Earth Storms I. General Introduction. Rep. of Ion. and Space Res. Japan, XIV (1960), 249.

- [27] J. Bartels, N. H. Heck, H. F. Johnston: The Three-Hour Range Index Measuring Geomagnetic Activity. *Terr. Magn. a. Atm. El.*, 44 (1939), 411.
- [28] J. Halenka: Kontrola účinnosti erupci z hlcdiska geomagnetického pomocí radiových vzplanutí. *Travaux Inst. Géophys. Acad. Tchécosl. Sci.* No. 31, *Geofysikální sborník 1955*, NČSAV, Praha 1956, 239.
- [29] H. Maeda, K. Sakurai, U. Ondoh, M. Yamamoto: Solar-Terrestrial Relationships during the IGY and IGC. *Proc. Int. Conf. on Cosmic Rays and the Earth Storm*, Kyoto, 4-15 Sept., 1961. I. Earth Storm, 45.
- [30] M. S. Bobrov: The Morphological Features of the Magnetic Storms observed during IGY-IGC. *Int. Conf. on Cosmic Rays and the Earth Storm*, Kyoto, Japan, Sept. 4-15, 1961. Preprints, Part I. Earth Storm, MS I-1-13.
- [31] J. Bouška: The Microstructure of ISc of Geomagnetic Storms. *Proc. Int. Conf. on Cosmic Rays and the Earth Storm*, Kyoto, 4-15 Sept., 1961. II. Joint Ses., 45.
- [32] J. Bouška: Commencement of Geomagnetic Storm. *Travaux Inst. Géophys. Acad. Tchécosl. Sci.* No 189, *Geofysikální sborník 1963*, NČSAV, Praha 1964.
- [33] S. Chapman: Magnetic Storms, Their Geometrical and Physical Analysis and their Classification. *Studia geoph. et geod.*, 5 (1961), 30.
- [34] E. H. Vestine, L. Laporte, T. Lange, W. E. Scott: The Geomagnetic Field, its Description and Analysis. Publ. 580, Carnegie Institution of Washington, Washington 1947.
- [35] S. Chapman, V. C. A. Ferraro: A New Theory of Magnetic Storms. *Terr. Magn. Atm. Electr.*, 36 (1931), 77.
- [36] H. Alfvén: On the Electric Field Theory of Magnetic Storms and Aurorae. *Tellus*, 7 (1955), 50.
- [37] S. F. Singer: A New Model of Magnetic Storms and Aurorae. *Trans. Am. Geophys. Un.*, 38 (1957), 175.
- [38] A. J. Dessler, E. N. Parker: Hydromagnetic Theory of Geomagnetic Storms. *J. Geophys. Res.*, 64 (1959), 2239.
- [39] J. H. Piddington: Geomagnetic Storm Theory. *J. Geophys. Res.*, 65 (1960), 93.
- [40] B. Bednářová-Nováková: Анализ солнечных ситуаций, предшествующих внезапно-му началу геомагнитных бурь. *Геомагнетизм и аэронавигация*, III (1963), 436.
- [41] M. et L. D'Azambuja: L'évolution et les mouvements d'ensemble des protubérances solaires. *Extrait de l'Astronomie* (1941).
- [42] И. С. Шкловский: Физика солнечной короны. ГИФМЛ, Москва 1962.
- [43] M. Waldmeier: Sonnenaktivität im Jahre 1951, im Jahre 1952. *Astr. Mitt. d. Eidg. Sternw.*, Zürich, No 180 u. 184.
- [44] M. Pavlučová: Sledování geomagnetické aktivity metodou K-indexu. *Travaux Inst. Geoph. Acad. Tchécosl. Sci.* No 8, *Geofysikální sborník 1953*, NČSAV, Praha 1954.
- [45] B. Bednářová: Srovnání sluneční a geomagnetické aktivity. *Travaux Inst. Geoph. Acad. Tchécosl. Sci.* No 11, *Geofysikální Sborník 1953*, NČSAV, Praha 1954.
- [46] J. Bartels, J. Veldkamp: Geomagnetic Indices K and C. *IATME Bull.* No 12f (1951), 12g (1952), 12h (1953).
- [47] B. Bednářová-Nováková: Negativní efekt skvrn (manuscript).
- [48] J. Bartels, J. Veldkamp: Geomagnetic Indices K and C, 1951. *IATME Bull.* No. 12e, Washington 1952, 136.
- [49] G. E. Hale: The Spectroheliograph and its Work, Part II. Solar Eruptions and their Apparent Terrestrial Effects. *Ap. J.*, 73 (1931), 379.
- [50] H. W. Newton, W. Jackson: Observations of Solar Corpuscular Radiation. VIIème rapport de la com. p. l'étude des relations entre les phénomènes solaires et terrestres. *Concil Int. des Un. Sci.*, Paris 1951, 113.

- [51] B. Bell: Major Flares and Geomagnetic Activity. Smithsonian Contr. Astrophys., Smithsonian Inst. Washington, D. C., 5 (1961), 69.
- [52] D. Van Sabben: Solar-Flare Effects and Magnetic Storms. J. Atm. Terr. Phys., 3 (1953), 270.
- [53] R. A. Watson: Magnetic Activity Following a Solar Flare. J. Atm. Terr. Phys., II (1957), 59.
- [54] O. M. Барсуков: Геомагнитная эффективность хромосферных вспышек по материалам 1957 г. Изв. АН СССР, сер. геофиз., № 11 (1959), 1690.
- [55] J. Halenka: The Connection between Chromospheric Flares and Geomagnetic Activity in the IGY. Studia geoph. et geod., 4 (1960), 361.
- [56] L. Fritzová, M. Kopecký, Z. Švestka: Catalogue of Great Chromospheric Flares and their Terrestrial Consequences. Astr. Inst. CAS Praha and Ondřejov, Publ. No. 35, 16.
- [57] J. Halenka: Geomagnetic Activity after Large Chromospheric Flares. Studia geoph. et geod., 5 (1961), 237.
- [58] B. Bednářová-Nováková: Une note sur la question de l'origine des orages géomagnétiques. Studia geoph. et geod., 4 (1960), 167.
- [59] B. Bednářová-Nováková: Analysis of Solar Situations during Flares and Geomagnetic Activity Afterwards. Travaux Inst. Geophys. Acad. Tchécosl. Sci. No 191, Geofysikální sborník 1963, NČSAV, Praha 1964.
- [60] B. Bednářová-Nováková: A Contribution to the Question of the Sources of Corpuscular Geomagnetically Active Solar Radiation. Studia geoph. et geod., 8 (1964), 63.
- [61] B. Bednářová-Nováková: Répartition des protubérances selon leurs effets géomagnétiques. BAC, VII (1956), 100.
- [62] B. Bednářová-Nováková: The Active Solar Region and its Relation to Geomagnetic Activity in the Period Around the Minimum of 1954. Travaux Inst. Geophys. Acad. Tchécosl. Sci. No 190, Geofysikální sborník 1963, NČSAV, Praha 1964.
- [63] А. В. Северин, В. Л. Хохлова: Исследование движений и свечения солнечных протуберанцев. Изв. Крымской Астр. Общ., X (1953), 9.
- [64] E. Pettit: The Properties of Solar Prominences as Related to Type. Ap. J., 98 (1943), 6.
- [65] M. Waldmeier: An Attempt at an Identification of the M-region. Terr. Magn. and El., 51 (1946), 538.
- [66] K. O. Kiepenheuer: Eine langsame Partikelstrahlung der Sonne. Naturwiss., 33 (1946), 118.
- [67] С. К. Всехсвятский: Сонячна активність, вплив сонця на земні явища. Наукові записки Т. V, В. 2 (1946), Київський Державний Унів.
- [68] D. E. Trotter, W. Roberts: Solar Prominences and Geomagnetic Disturbances. J. Atm. Terr. Phys., 6 (1955), 282.
- [69] H. S. Leighton, D. E. Billings: Solar H α Filaments and Geomagnetic Disturbances. J. Atm. Terr. Phys., 6 (1955), 249.
- [70] R. T. Hansen: Recurrent Geomagnetic Storms and Solar Prominences. J. Geoph. Res., 64 (1959), 23.
- [71] M. Dizer: Sudden Disappearance of Filaments and Geomagnetic Activity. Annales Géophys., 18 (1962), 388.
- [72] B. Bednářová: Sledování souvislosti mezi sluneční a geomagnetickou aktivitou. Travaux Inst. Géophys. Acad. Tchécosl. Sci. No 28, Geofysikální sborník 1955, NČSAV, Praha 1956.
- [73] B. Bednářová, M. Kárník: Pozorování slunečních protuberancí a jejich použití při studiu vnějšího pole geomagnetického. Travaux Inst. Géophys. Acad. Tchécosl. Sci. No 19, Geofysikální sborník 1954, NČSAV, Praha 1955.
- [74] B. Bednářová, M. Kárník: Pozorování slunečních protuberancí a jejich použití při studiu změn vnějšího pole geomagnetického v roce 1954. Travaux Inst. Géophys. Acad. Tchécosl. Sci. No 29, Geofysikální sborník 1955, NČSAV, Praha 1956.
- [75] B. Bednářová, M. Kárník: Pozorování slunečních protuberancí a jejich použití při studiu

- změn vnějšího pole geomagnetického v r. 1955. Travaux Inst. Géophys. Acad. Tchécosl. Sci. No 53, Geofysikální sborník 1956, NČSAV, Praha 1957.
- [76] B. Bednářová, M. Kárník: Pozorování slunečních protuberancí a jejich použití při studiu změn vnějšího pole geomagnetického v roce 1956 (manuscript).
- [77] B. Bednářová: Srovnání sluneční a geomagnetické aktivity z let 1950, 1951 a 1952, část II. Rozpravy ČSAV, Řada MPV, 65 (1955), No 12.
- [78] Э. Р. Мустель, О. Н. Митропольская: Сопоставление калыцевых флоккулов с геомагнитными и ионосферными возмущениями. Изв. Крымской Астрон. Общ., X (1958), 162.
- [79] G. Abetti: Solar Physics. Hdb. d. Astrophysik, Bd IV, Berlin 1929, 158.
- [80] M. Waldmeier: Die totale Sonnenfinsternis von 12. Okt. 1958. Die Sterne, 35 (1959), 176.
- [81] Е. Я. Бугославская: Структура солнечной короны. Труды госуд. Астр. Инст., Изд. Москов. унив. 1950.
- [82] B. Bednářová-Nováková: Recurrent Geomagnetic Storms and Solar Prominences. J. Geoph. Res., 65 (1960), 36.
- [83] B. Bednářová-Nováková: Recurrent Geomagnetic Storms and their Relation to Solar Activity. Travaux Inst. Geophys. Acad. Tchécosl. Sci. No 172, Geofysikální sborník 1962, NČSAV, Praha 1963.
- [84] B. Bednářová-Nováková: Рескуррентные геомагнитные бури и их связь с солнечной активностью. Studia geoph. et geod., 7 (1963), 71.
- [85] U. Becker: Über eine Beziehung zwischen erdmagnetischer Unruhe und der Anordnung der Sonnenflecken. Mitt. Fraunh. Inst. Freiburg Br. Nr. II (1953), 195.
- [86] A. Šťastná: Geomagnetic Activity after Passage of Two Different Configurations of Sunspot Groups through Central Meridian of Sun. Studia geoph. et geod., 8 (1964), 174.
- [87] J. Halenka: A New Solar Observing Station. Studia geoph. et geod., 3 (1959), 294.
- [88] A. Plešinger, J. Halenka: Combined Servoelectric Solar Telescope. SNTL, Technical Digest, IV (1962), 32.
- [89] V. Bucha: Dynamics of the Earth's Magnetic Field. Travaux Inst. Géophys. Acad. Tchécosl. Sci. No 170, Geofysikální sborník 1962, NČSAV, Praha 1963.
- [90] W. Elsasser: Hydromagnetic Dynamo Theory. Rev. Mod. Phys. 28 (1956), 135.
- [91] D. Inglis: Theories of the Earth's Magnetism. Rev. Mod. Phys., 27 (1955), 212.

Výtah

K PROBLEMATICE VZNIKU GEOMAGNETICKÝCH BOUŘÍ

Bohumila Bednářová-Nováková, Václav Bucha, Jaroslav Halenka,
Mojmír Konečný

Problematika vzniku geomagnetických bouří, jak je diskutována v předložené práci, představuje poměrně široký komplex úkolů, které jsou v této souvislosti řešeny. Kromě souhrnného pohledu na dílčí fáze celkového vývoje geomagnetických bouří jsou uvedeny některé nové výsledky výzkumu, námi dosažené za poslední období, které přispívají ke klasifikaci bouří a k objasnění vzájemných vztahů mezi geomagnetickou a sluneční aktivitou.

Při klasifikaci geomagnetických bouří typová analýza ukázala, že většina bouří má dvoufázový průběh, i když nelze zanedbat ani část, která ukazuje průběh jednofázový. U těchto bouří je patrná tendence výskytu pouze v určitém denním období.

Při systematickém vyšetřování vztahů mezi sluneční a geomagnetickou aktivitou byly získány některé důležité poznatky přispívající k rozhodnutí o příčinách vzniku geomagnetických bouří.

Poměrně rozsáhlý materiál, na jehož základě bylo provedeno posouzení vlivu slunečních skvrn na geomagnetickou aktivitu, ukázal, že skvrny samy o sobě nemohou být geoaktivní; určitou, některými pracemi dříve zjištěnou souvislost lze vysvětlit tím, že nebylo přihlíženo k výskytu dalších slunečních jevů v oblastech skvrn.

Rozbor výsledků pozorování erupcí, který jsme provedli v řadě prací jak statistickými metodami, tak pro některé jednotlivé případy, ukázal, že erupce by se mohly podílet na dějích, po nich může nastat zvýšení geomagnetické aktivity (zvláště tím, že výskyt erupcí by mohl narušovat a měnit tvar místních magnetických polí na Slunci, pokud ovšem samy erupce nejsou důsledkem změn těchto polí); bylo však námi zjištěno, že erupce nejsou přímým zdrojem geomagneticky účinného korpuskulárního záření.

Studium filamentů a korony přineslo některé nové výsledky z hlediska příčin geoaktivity. Provedli jsme nové rozdělení filamentů do tří skupin a došli k závěru, že filameny zařazené do skupin nestabilních a volných mají velice blízký vztah ke zdrojům geoaktivního záření. Určení přímého zdroje však není jednoduchý problém; ukázala se nutnost přihlídnout k jevům, které nastávají v koruně. Důležitou roli zde hrají přibližně ekvatorální koronální proudy nebo křídla. Velký význam při nasměrování korpuskulárního záření má též vliv celkového magnetického pole slunečního (zvláště při výronech souvisících s volnými filameny vysokošířkovými).

Pro správnost závěrů, jež jsme odvodili, mluví spolehlivost prognos geomagnetické aktivity, založených na našich představách o geoaktivitě projevů sluneční činnosti.

58

Získané výsledky umožňují jednotný výklad souvislosti geomagnetické aktivity se sluneční činností v celém období slunečního cyklu.

Je přirozené, že zatím nebylo možno vysvětlit zcela uspokojivě všechny sluneční situace a s nimi souvisící stav geomagnetické aktivity vzhledem k velice složitým podmínkám, které někdy na Slunci panují. Pro tyto účely bude třeba vyjasnění ještě dalších otázek zvláště pokud jde o lokální magnetická pole sluneční.

Dosud získané výsledky jsou většinou kvalitativního charakteru, jak vyplynuly ze zpracování výsledků pozorování a z korelace geomagnetických a solárních jevů. Tato fáze naší výzkumné činnosti byla nezbytně nutná pro zajištění dostačující báze nových základních materiálů z pozorování, přispěla k objevení řady nových zákonitostí a je nutno v ní pokračovat. Uvedená problematika však dosud nebyla řešena po stránce kvantitativní, pokud jde o vyšetřování fyzikálních podmínek a objasňování příčin zkoumaných jevů, jak ve skutečnosti probíhají, navržením vhodných teoretických modelů; tyto otázky budou předmětem další naší činnosti.

464

Резюме

К ПРОБЛЕМАТИКЕ ВОЗНИКНОВЕНИЯ ГЕОМАГНИТНЫХ БУРЬ

Bohumila Bednářová-Nováková, Václav Bucha, Jaroslav Halenka,
Mojmír Konečný

Проблематика возникновения геомагнитных бурь в том виде, как она рассматривается в настоящей работе, представляет собой сравнительно широкий комплекс заданий, решаемых в этой связи. Помимо общей характеристики отдельных стадий всего развития геомагнитных бурь здесь приводятся некоторые новые результаты исследований, полученные нами в последнее время и способствующие созданию классификации бурь и объяснению взаимных связей между геомагнитной и солнечной активностями.

При классификации геомагнитных бурь типовой анализ показал, что большинство бурь имеет двухфазный ход изменений, хотя частью бурь, имеющий однофазный ход изменений тоже нельзя пренебречь. У таких бурь обнаруживается тенденция к появлению лишь в известное время суток.

При систематическом обследовании связей между солнечной и геомагнитной активностями были получены некоторые важные сведения, способствующие нахождению причин возникновения геомагнитных бурь.

Сравнительно обширный материал, на основании которого была проведена оценка влияния солнечных пятен на геомагнитную активность, показал, что пятна сами по себе не могут быть геоактивными; ранее установленную в некоторых работах определенную связь можно объяснить тем, что дальнейшие солнечные явления в областях пятен не учитывались.

Анализ результатов наблюдений вспышек, проведенный в ряде работ с помощью статистических методов, и анализ отдельных явлений показали, что вспышки могут принимать участие в процессах, после которых может иметь место повышение геомагнитной активности (в частности таким образом, что появление вспышек может нарушать и изменять форму местных магнитных полей на Солнце, но три условия, что вспышки сами не являются следствием изменения этих полей); однако мы однозначно установили, что вспышки не являются непосредственным источником геомагнитно эффективного корпускулярного излучения.

Изучение волокон и короны принесло некоторые новые результаты с точки зрения причин возникновения геоактивности. Было проведено новое подразделение волокон на три группы и сделан вывод, что волокна, отнесенные к свободным и неустойчивым группам, находятся в весьма тесной связи с источниками геоактивного излучения. Однако определение непосредственного источника не

так уже просто; здесь обнаружилась необходимость учитывать явления, происходящие в короне. Важную роль притом играют примерно экваториальные корональные потоки или крылья. Большое значение для направленности корпускулярного излучения имеет также влияние общего магнитного поля на Солнце (в особенности при выбросах, связанных со свободными высокоширотными волокнами).

Правильность сделанных нами выводов подтверждается надежностью прогнозов геомагнитной активности, основанных на наших представлениях о геоактивности проявлений солнечной активности. Полученные результаты дают возможность однообразной интерпретации связи геомагнитной и солнечной активностей во всем периоде солнечного цикла.

Естественно, что пока еще не удалось вполне удовлетворительно объяснить все солнечные ситуации и с ними связанную геомагнитную активность из-за весьма сложных условий, создающихся иногда на Солнце. Для этих целей потребуются еще разрешить ряд дальнейших вопросов, в частности, что касается местных магнитных полей на Солнце.

Полученные до сего времени результаты имеют по большей мере качественный характер, так как они являются следствием обработки результатов наблюдений и корреляции геомагнитных и солнечных явлений. Такая стадия нашей исследовательской деятельности была необходима для обеспечения достаточной базы для новых основных материалов из наблюдений, так как она способствовала нахождению ряда новых закономерностей; поэтому такую работу следует продолжать. Однако приведенная выше проблематика не рассматривалась с количественной точки зрения, а именно, что касается исследования физических условий и объяснения причин возникновения исследуемых явлений так, как они протекают в действительности, а также проектирования пригодных теоретических моделей; этими вопросами мы будем заниматься в дальнейшей деятельности.

C06131786

UNCLASSIFIED

Approved for Release 2001/03/11 : C06131786

UNCLASSIFIED CONFIDENTIAL OFFICIAL USE ONLY		CONFIDENTIAL	SECRET
CENTRAL INTELLIGENCE AGENCY ROUTING AND CONTROL RECORD		DATE 26 October 1964	
TO: OSI [redacted]		#38 (b)(3)	
ATTN: [redacted] (b)(3)			
BUILDING	ROOM NO.		
TITLE			
[redacted] - Scientific Paper "A Contribution Towards Solving the Question of the Occurrence of Chromospheric Flares Before Geomagnetic Storms" (CZECHOSLOVAKIA) (b)(3)			
REMARKS			
RETAIN			
XXX RETAIN		<input type="checkbox"/> ON LOAN	
DOCUMENT(S) FOR RETENTION BY ADDRESSEE		DOCUMENT(S) MUST BE RETURNED TO CONTACT DIVISION [redacted] (b)(3)	
		BY (Deadline) [redacted] (b)(3)	
FROM: CONTACT DIVISION [redacted]		BRANCH [redacted] (b)(3)	
BUILDING 1717 H St		ROOM NO. 511	EXTENSION 2491 (b)(3)

Approved for Release 2001/03/11 : C06131786

UNCLASSIFIED

July 1964

A CONTRIBUTION TOWARDS SOLVING THE QUESTION OF THE OCCURRENCE OF CHROMOSPHERIC FLARES BEFORE GEOMAGNETIC STORMS.

by Bohumila Bednářová-Nováková

Geophysical Institute,
Czechosl. Acad. Sci., Prague

ABSTRACT

The incorrectness of the hypothesis according to which flares should be the source of corpuscular solar radiation, which is responsible for the origin of geomagnetic storms, is proved on the basis of determining the number of geomagnetic storms not preceded by any flares. Using the list of guaranteed large flares from the IGY of C.S. Warwick [14] and making an analysis of the solar situations occurring simultaneously with flares but on the CM or in the centre of the solar disc, it was shown why some flares were followed by a geomagnetic storm while after others, on the contrary, a period of absolute geomagnetic quiet set in.

Since it was shown that geomagnetic storms are preceded by changes in the magnetic fields in the solar chromosphere and because flares also occur during such changes, the question arises, what role do flares play here? Are they the cause of such changes or are they their product? It is deduced, and observations confirm this, that although flares are produced as a sort of consequence of changes in the photospheric fields, they can simultaneously be regarded to a certain degree as the cause of substantial changes in the chromosphere which lead to the annulling of the field at least in that component which is represented by chromospheric structure and filaments. Their relationship to geophysical effects of a solar corpuscular origin is, however, quite indirect and very limited.

The fact that after the first historically recorded observation of a flare on September 1, 1859, by Carrington and Hodson and also after the two consecutive flares on August 3 and 5, 1872, which were observed by Young, a strong geomagnetic storm always followed, led to the hy-

pothesis of a connection between flares and geomagnetic storms. This hypothesis was also supported by the classical observations of G.E. Hale, carried out from 1892, using the new instruments developed by him : a spectroheliograph and later by means of a spectrohelioscope. After the discovery of the radiotelescope and after it was found by means of it that in the period when a flare occurs on the Sun, radiation is sometimes magnified on some wave-lengths (much longer than the optical), it was hoped that this meant an indicator of an effusion of corpuscular radiation had been found, i.e. such radiation which is responsible for the origin of geomagnetic disturbances. It was only later that it was discovered that not even this fact can be used for example for prognoses etc.

From the hypothesis on the connection between flares and geomagnetic storms the opinion gradually developed that flares were the direct source of geoactive corpuscular radiation. However, flares in themselves are not high formations [1] and than they are observed on the edge of the solar disc, they do not exhibit any marked rise of matter to any great height [2]. They are often accompanied by rising prominences which, as will be seen later, may be conceived as the consequence of changes in the local magnetic field which occur often without flares and sometimes during a flare. It is this random simultaneity of the two effects which is the cause of frequent mistakes so that there are some authors who speak of flares but obviously have in mind rising prominences. That these are two quite different effects, which probably have no direct physical inter-relationship, is borne out by the fact that disappearing filaments-rising prominences occur ~~simultaneously with flares and sometimes only~~ very often in absence of flares. It seems that the two phenomena are likely the consequences of one and the same cause. Sometimes they occur simultaneously and other times only one of them appears.

Flares occur almost universally in active centres and are thus only one part of a complex of events which occur shortly after one another or at absolutely the same time. From the consequences occurring after either a shorter or a longer interval it is impossible to deduce a connection with the different effects separately. This is even more difficult with geomagnetic storms which exhibit a longer time lag after sudden changes occurring on the Sun. If, however, the mechanism of the effusion of corpuscular radiation and its propagation towards the Earth is to be found, it must first be determined whether such a phenomenon can be found among the known expressions of solar activity which, in each period and during the whole cycle of solar activity, would be reliable indicator of geomagnetic storms. It is also necessary to give physical reasons for each connection found. One must also take into consideration an explanation of the fact that sometimes no connection was found. As is clear from the many papers already published, it was found in the Geophysical Institute of the Czechoslovak Academy of Sciences that of all the known expressions of solar activity studied by optical methods the best indicators of the origin of geomagnetic storms are filaments and the fine chromospheric structure under certain circumstances. As will be seen below, in the period of greater solar activity, i.e. in the period of flare occurrence, these are eruptive and disappearing filaments, denoted in the Geophysical Institute by the one term - unstable α filaments - which, only if they are in a suitable position, safely indicate when a geomagnetic storm with ssc will occur [3]. This is because such phenomena, as will be seen later, provide direct information on changes in the magnetic field of the Sun. And it is then only these changes which are actually the direct indicators of changes in the corona and thus also of the origin of geomagnetic storms.

Doubts as to flares being the source of corpuscular radiation were raised by D. Van Sabben [4], R.A. Watson [5] and O.M. Barsukov [6]. The sta-

tistical paper by C.S. Warwick and R.T. Hansen [7] shows the not very high maxima of the Ap-indices after flares in the period of greater solar activity for flares nearer to the CM but does not give positive results for the period before the minimum. It can easily be supposed, and later this will be quite clearly proved, that the circumstance can be regarded as merely a statistical phenomenon, as is also clear from the table given in [8]: the more elements contained by the two series compared, the more frequently two of them are found which are either simultaneous or follow one another in a certain time interval. The effect is the same although one series is much more numerous than the other, as is the case when the number of flares greatly exceeds, particularly in periods of greater activity, the number of geomagnetic storms. It is seen from Tab. I. and even better from Fig.1 that a decrease in the number of flares after the maximum (1959-60) is followed not by decrease but by an increase in the number of geomagnetic storms whether flares of greater importance or whether ~~all~~ all, including those with the smallest importance, are used for the comparison. No connection can be observed even if one takes the number of ssc or the greatest storms which, according to accepted world opinion, should be connected with flares but which, as will be seen later, indicate no pronounced connection.

Table I Comparison between number of flares and number of geomagnetic storms.

Year	Imp.	number of flares				number of geomag. storms		
		3,3+	2	1	1-	total	all	ssc
						≥ 2 $\geq 1-$	$Kp \geq 5+$	
1957, 2nd half		25	203	-	-	228 5189	27	17
1958		24	327	-	-	351 9668	42	24
1959		30	239	2208	910	269 3387	50	22
1960		19	118	1490	541	137 2168	72	32
1961		10	38	787	294	48 1129	35	17

The results in the paper by ^{J.} Halenka [9], [10] also give rise to doubts as to the direct connection between chromospheric flares and geomagnetic storms.

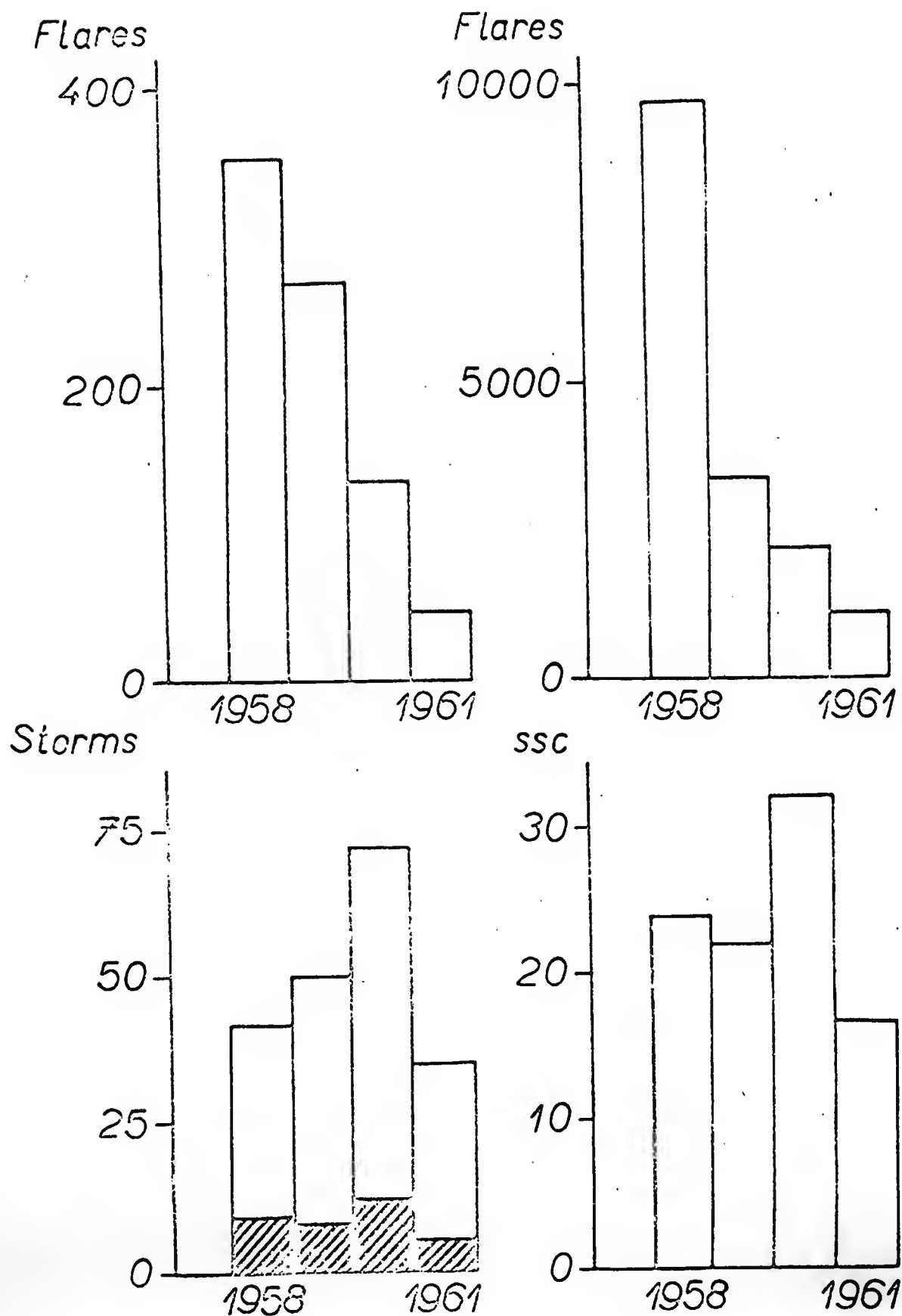


Fig. 1. Comparison of number of flares with number of geomagnetic storms in 1958-61 ; top left: flare ≥ 2 , top right: flare $\geq 1-$, bottom left: geomagnetic storm Kpmax. $\geq 5+$, dashed line - large geomagnetic storm Kpmax. $\geq 7+$, Kpmin. = 5-, bottom right: ssc.

as given in [11]. The author of the present paper showed [12] that when studying the flare activity of different active centres during the whole period of passage over the solar disc a geomagnetic storm occurred only after the CMP of the active centre in which flares occurred throughout the period. This means that flares outside the CM fell flat. This is in complete agreement with the results of O.M. Barsukov [6].

In 1961 a paper was published by B. Bell [13] from which it is clear that the connection between flares and geomagnetic storms is doubtful if it is guaranteed, and then only in the relatively long interval of three days, only to 50%. Not even a distribution according to the magnetic types of spots, in the neighbourhood of which the flares occurred, gives satisfactory results. Despite these facts flares are continually given in ^{real} relation with geomagnetic storms. But the question of theoretical opinions, in the same way as the question of prognoses, necessitates a detailed investigation. For this reason the author decided to supplement the work of B. Bell and to find, on the contrary, how great a percentage of geomagnetic storms is preceded by flares. This kind of research is part of the work of the heliogeophysical group of the geomagnetic department of the Geophysical Institute which aims at leaving no geomagnetic storm unexplained.

For this purpose the material from 30.VI. 1957 to the end of 1962 was investigated. Only material from these years, thanks to the IGY and IGC, can be regarded as practically complete as regards flares. The work was divided into several stages.

1) The percentage of geomagnetic storms for $Kp_{max} \geq 5+$ was found which were not preceded by any flares ≥ 2 in intervals of 10-48 hours, 10-60 hours, 10-72 hours. These are relatively long intervals. In an earlier paper the present author found shorter intervals, valid for disappearing filaments, i.e. 28-38 hours. Since, however on account of the small number of observations from which these values were derived they must be regarded as provisional. Since an interval of three days was used in the work of B. Bell, such longer time intervals were left in the present paper as well. Indeed

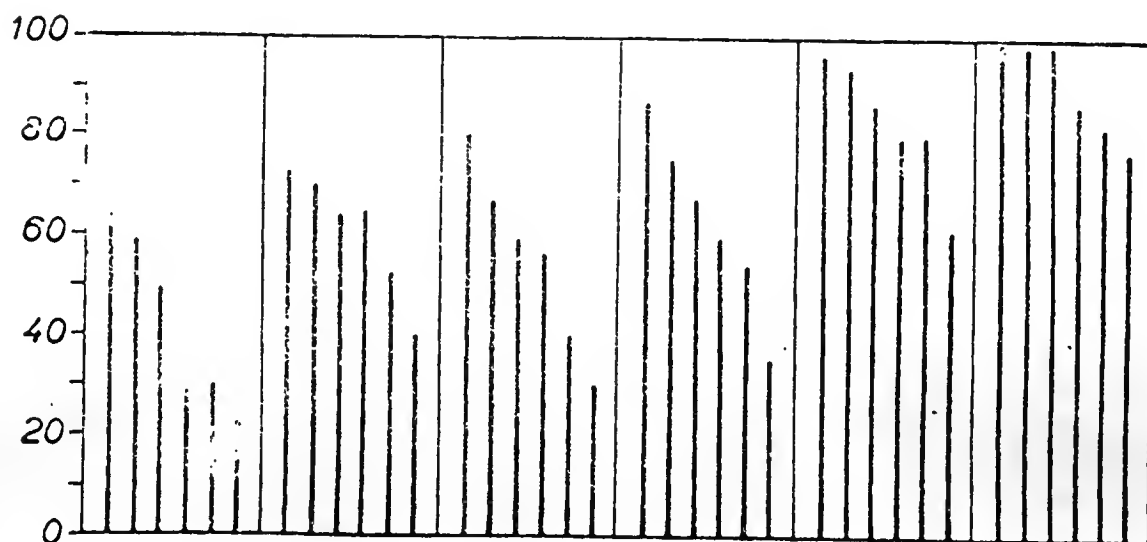
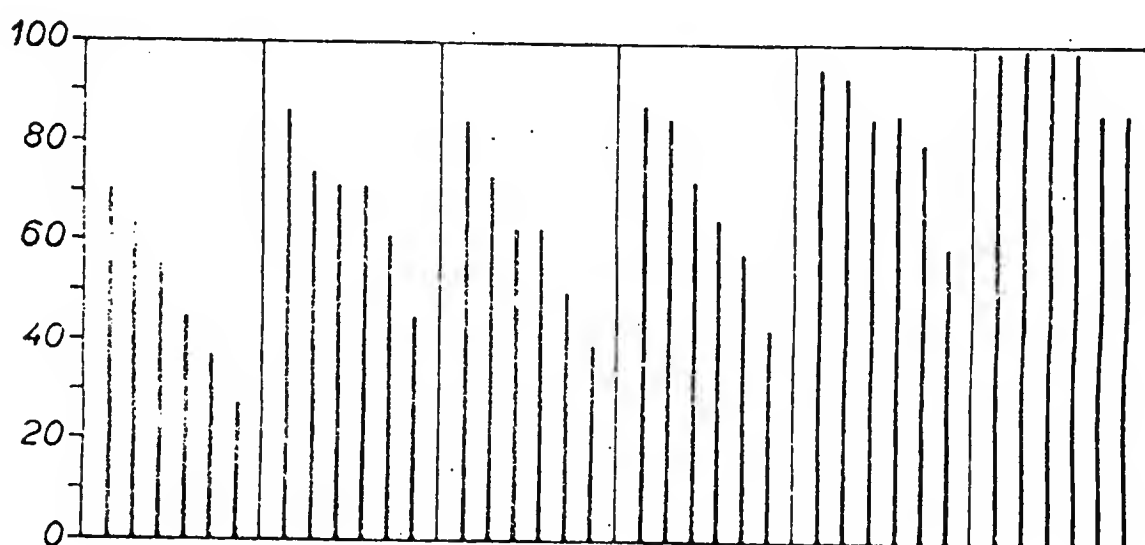
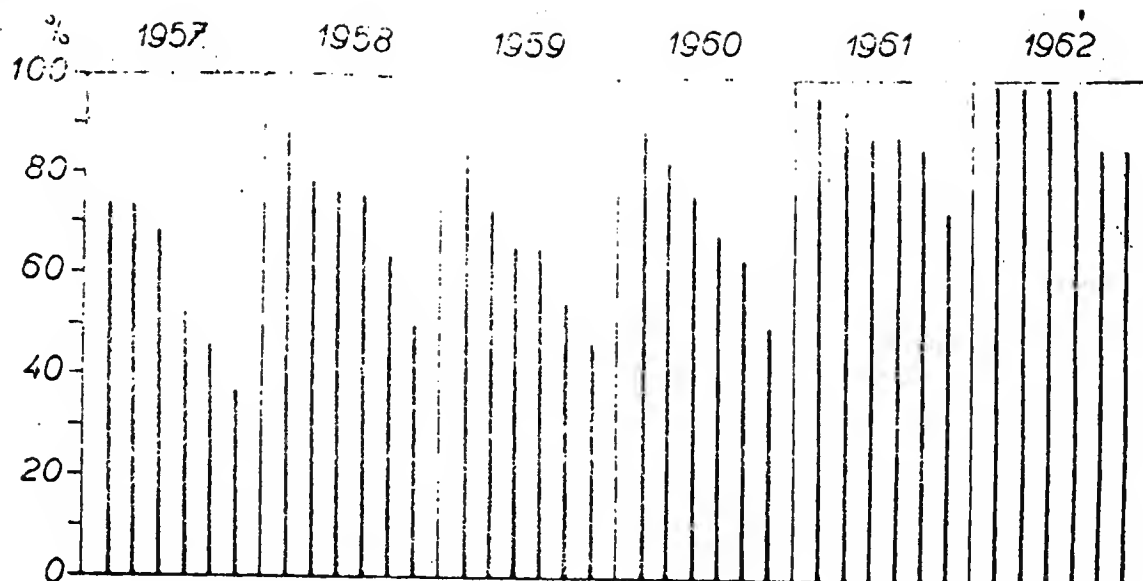


Fig. 2. Percentage of geomagnetic storms $Kp_{max} \geq 5+$ from 1957 (2nd half), 1958, 1959, 1960, 1961 and 1962. Vertical abscissae denote, from left right, magnitude of percentage for flares from spaces (with respect to CM) : $0^\circ - 10^\circ$, $0^\circ - 20^\circ$, $0^\circ - 30^\circ$, $0^\circ - 45^\circ$, $0^\circ - 60^\circ$, $0^\circ - 90^\circ$. From top to bottom with respect to commencement of geomagnetic storm for intervals of 10- Approved for Release 2001/05/14 C06131786 hours

if it is proved for such intervals, that there is no connection between flares and geomagnetic storms, this is even more likely to be for shorter intervals.

1) Altogether 248 geomagnetic storms, obtained from the graphs of K_p -indices from Göttingen, were investigated in the manner indicated. As regards flares, American catalogues [14], [15], [16], [17] were used. Only for 1962 was the Quarterly Bulletin from Zürich [18] used. The results are plotted in Fig.1, where the magnitude of the number of percentages is denoted by the vertical abscissa successively from left to right for the individual years and for flares considered in the areas defined by the distances from the CM: $0^\circ-10^\circ$, $0^\circ-20^\circ$, $0^\circ-30^\circ$, $0^\circ-45^\circ$, $0^\circ-60^\circ$ and $0^\circ-90^\circ$, and from the top downwards for the different time intervals, beginning with the shortest and ending with the longest, as given above.

It is seen that the height of the percentages of geomagnetic storms not preceded by a flare is considerable in all cases. Of the large number of flares e.g. in the period of sunspot maximum, there are less geomagnetic storms without flares than in other years when there were less flares (see Tab.I and Fig.1). The percentages of geomagnetic storms continually decrease with a gradual increase in flares, as the distance from ^{the} CM grows. They also decrease gradually and disproportionately as the length of the time interval increased which is again connected with a rise in the number of flares, the more likely one is to occur in the critical interval before a geomagnetic storm. However, such an occurrence need not indicate an interdependence. It is merely a statistical matter. If this fact is taken into consideration, it must be deduced from the graph in Fig.2 that the connection between flares and geomagnetic storms can be only random. Later this this conception will be made somewhat more exact and supplemented.

2) Since it might be objected that it is actually only large geomagnetic storms which are connected with flares, it was necessary to investigate the percentage of the number of geomagnetic storms with $K_{pmax} \geq 7+$ and $K_{pmin} \geq 5-$. In this part of work the Quarterly Bulletins [18] were used in

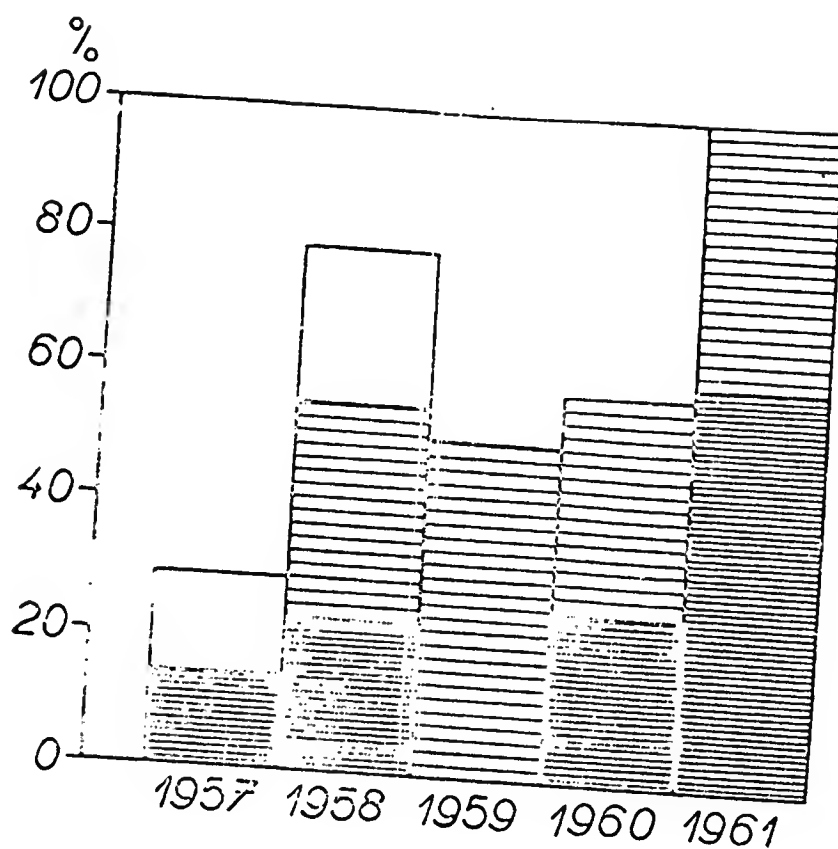


Fig. 3. Percentage of large geomagnetic storms ($K_{pmax.} \geq 7+$, $K_{pmin.} \geq 5-$) not preceded by flare at distances from 0° to 10° from CM. White strip : importance ≥ 3 ; lightly dashed strip : ≥ 2 ; dashed strip : $\geq 1-$. For 1959-61 white strip coincides with lightly dashed strip.

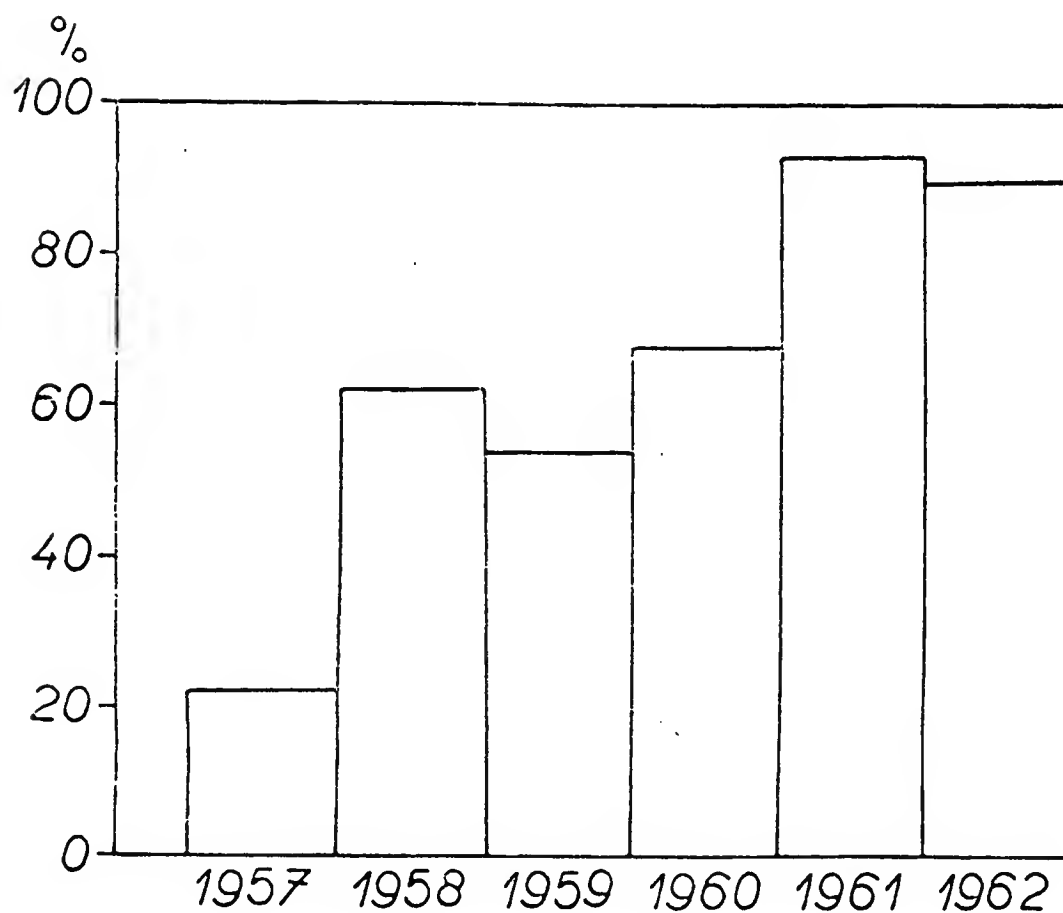


Fig.4. Percentage of geomagnetic storms with sudden commencement not preceded by flare (imp. ≥ 2) at distances from 0° to 10° from CM.

the hope that the number of flares would be as complete as possible and importances ≥ 3 , ≥ 2 and ≥ 1 - occurring between 0° to 10° from the CM in intervals of -3 days to -1 day with respect to the commencement of the geomagnetic storm (first part of Tab. II) were considered separately. The results are plotted in Fig. 2. Since there were no large geomagnetic storms in 1962, only material up to the end of 1961 was treated. It is seen that even for large geomagnetic storms the percentages of cases without preceding flares were considerable in 1958-61 not only for the largest flares but also when using flares ≥ 2 , when they were above 50%. Although the percentages of large storms without flares ≥ 1 - are zero for 1957 and 1959, in 1961 they already reach 60%. This circumstance can easily be explained on the conception of a large number of flares in the years around the maximum (see Tab. I).

3) For the investigation of geomagnetic storms in relation to flares to be complete, one must also consider ssc which are likely to be connected with sudden solar phenomena on the CM, such as flares etc. We investigated 128 ssc chosen from the graphs of prof. J. Bartels. In this part of the work flares of importance ≥ 2 which occurred in the interval from 0° to 10° from the CM were used. The heights of the percentages of geomagnetic storms with ssc from 1957-61 not preceded by flares are plotted in Fig. 4. Beginning with 1958 these are values above 50 %. The maximum is reached in 1961 (93%). It is seen that not even with geomagnetic storms with a sudden commencement is any connection found with flares in the neighbourhood of the CM.

Table II. Percentage of number of large geomagnetic storms ($K_{pmax} \geq 7+$, $K_{min} \geq 5-$), not preceded by any flare from 0° - 10° from CM.
Number of flares before storm.

Year	Number of storms without flares from -3 to							Number of flares								
	of storm	≥ 3	≥ 2	≥ 1	≥ 3	≥ 2	≥ 1	from -3 to -1 day	from 0 to +2 day	before	after	≥ 3	≥ 2	≥ 1		
1957	7	2	29	1	14	0	0	9	27	91	2	5	30	+7	+22	+61
1958	9	7	73	5	55	2	22	2	14	59	0	4	39	+2	+10	+20
1959	8	4	50	4	50	0	0	4	11	64	0	4	17	+4	+7	+47
1960	12	7	58	7	53	3	25	5	7	56	2	10	49	+3	-5	+7
1961	9	5	100	3	100	3	60	0	0	16	0	1	17	0	-1	-1

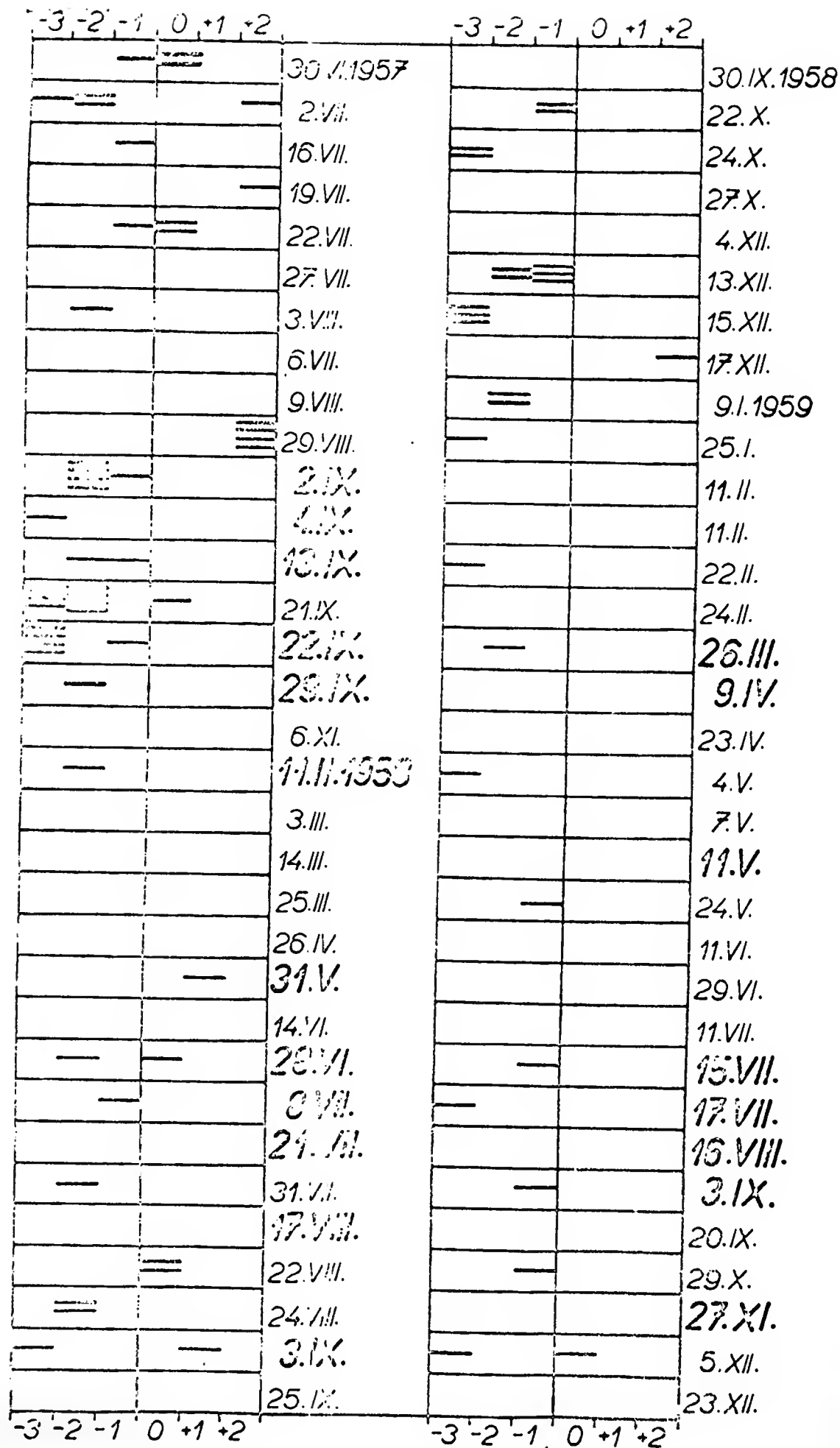


Fig.5a. Time distribution of occurrence of larger chromospheric flares ≥ 2 (denoted by horizontal abscissa on corresponding day), before (from -3 to -1 day) and after ssc (from 0 to +2 day), at distances from 0° to 10° from CM - in IGY and IGC - periods of greater solar activity. Data of strong storms are denoted by larger letters.

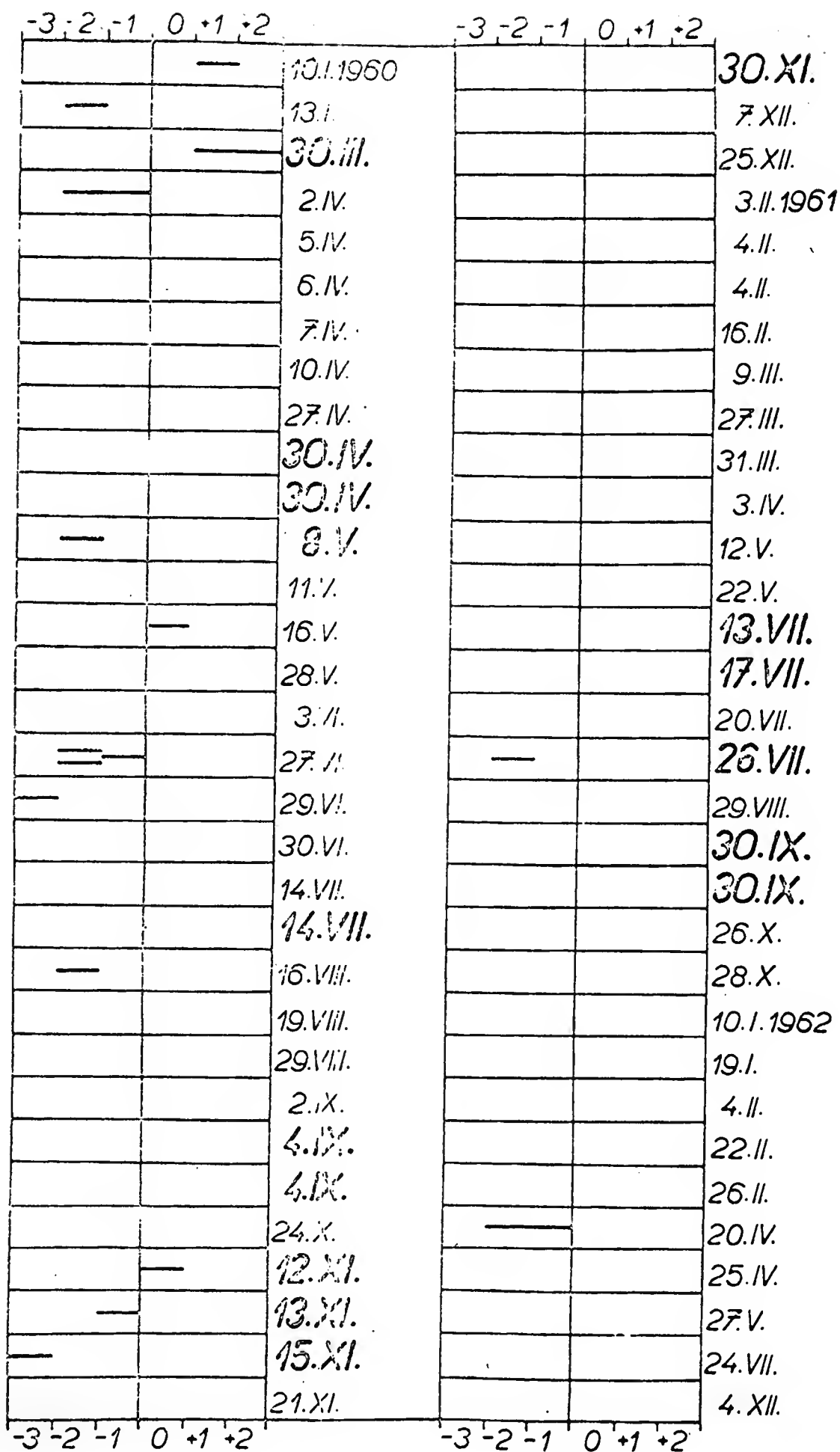


Fig. 5b. Time distribution of occurrence of larger chromospheric flares ≥ 2 (denoted by horizontal abscissa on corresponding day), before (from -3 to -1 day) and after ssc (from 0 to +2 day), at distances from 0° to 10° from CM - periods of smaller solar activity. Data of strong storms are denoted by larger letters.

The second part of Tab. II compares the number of flares occurring in the interval of one to three days before the geomagnetic storm (large storms and flares ≥ 5 , ≥ 2 and ≥ 1 -) with the number of flares not occurring until after the commencement of the storm up to the +2 day. The result is very instructive. The number of flares preceding is somewhat higher so that the difference in the two numbers gives positive numbers except for 1961. For medium and large flares it is zero in 1960. It is seen again, primarily for medium and large flares, that the value of the difference decreases with a decrease in the total number of flares. However, despite everything, there exists on the average a sort of predominance of the number of flares occurring ~~but~~ before compared with the number of flares occurring after the commencement of a geomagnetic storm. In order to determine this more exactly for a larger number of cases, a similar investigation was made for a set of all ssc. The results are plotted in Fig. 5 a and 5 b (all storms with ssc, apart from one large storm on 30.III. 1960, which had gradual commencement). It is seen that here, too, flares occur both before and after the commencement of a storm. If, however, we add up all the flares we obtain a higher number before storms (73) than after storms (21). If, in addition, we consider that this graph gives a high percentage of geomagnetic storms not preceded by any flares (68%) and simultaneously also a certain percentage when flares occurred only after the commencement of the storm (7%) then it be deduced that if there exists a connection between geomagnetic storms with ssc and flares it must be quite limited and indirect.

4) What ^{from} this interdependence may have, can be determined as follows. It was shown earlier that a geomagnetic storm occurred after a flare if an unstable filament or active centre with unstable filaments, surges etc., were simultaneously on the CM or even better in the centre of the solar disc [20], [21]. Since the opinion is still held that large flares are after all connected with geomagnetic storms, an investigation of the solar situations during the occurrence of large flares was made

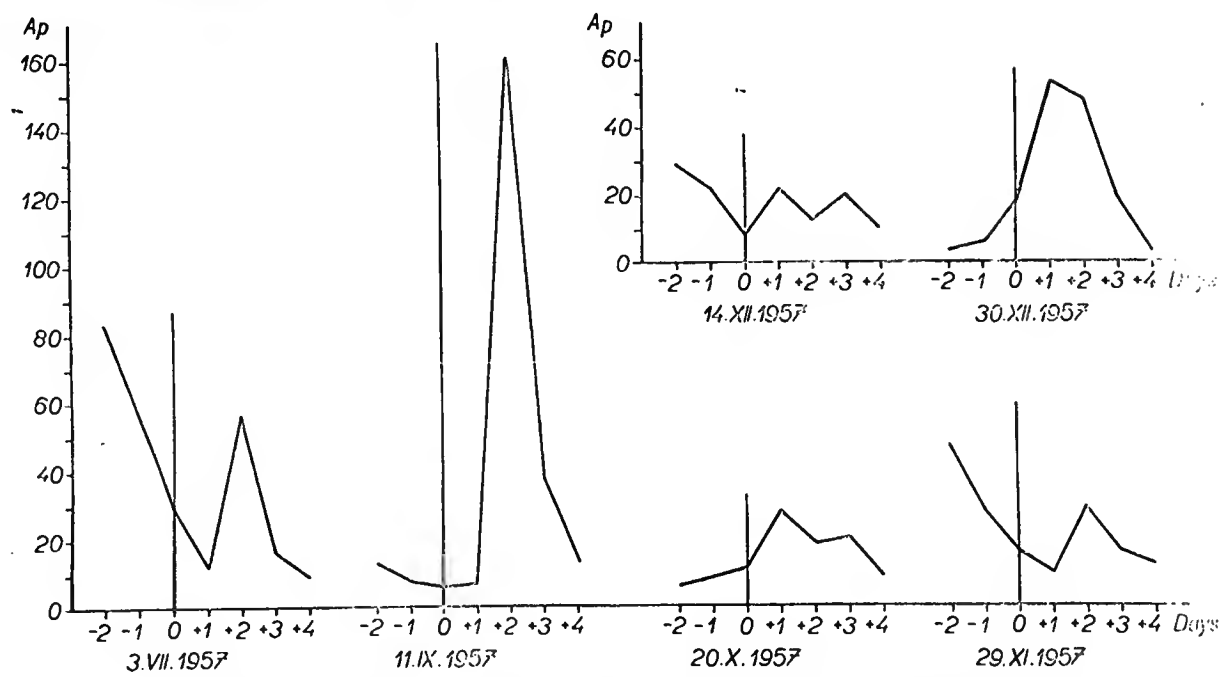


Fig. 6. Course of Ap-indices after large flare (imp. ≥ 3 -) during simultaneous presence of unstable filament in centre of visible solar disc (day of occurrence of flare is zero day) year 1957 (flare from corrected catalogue C.S.Warwick)

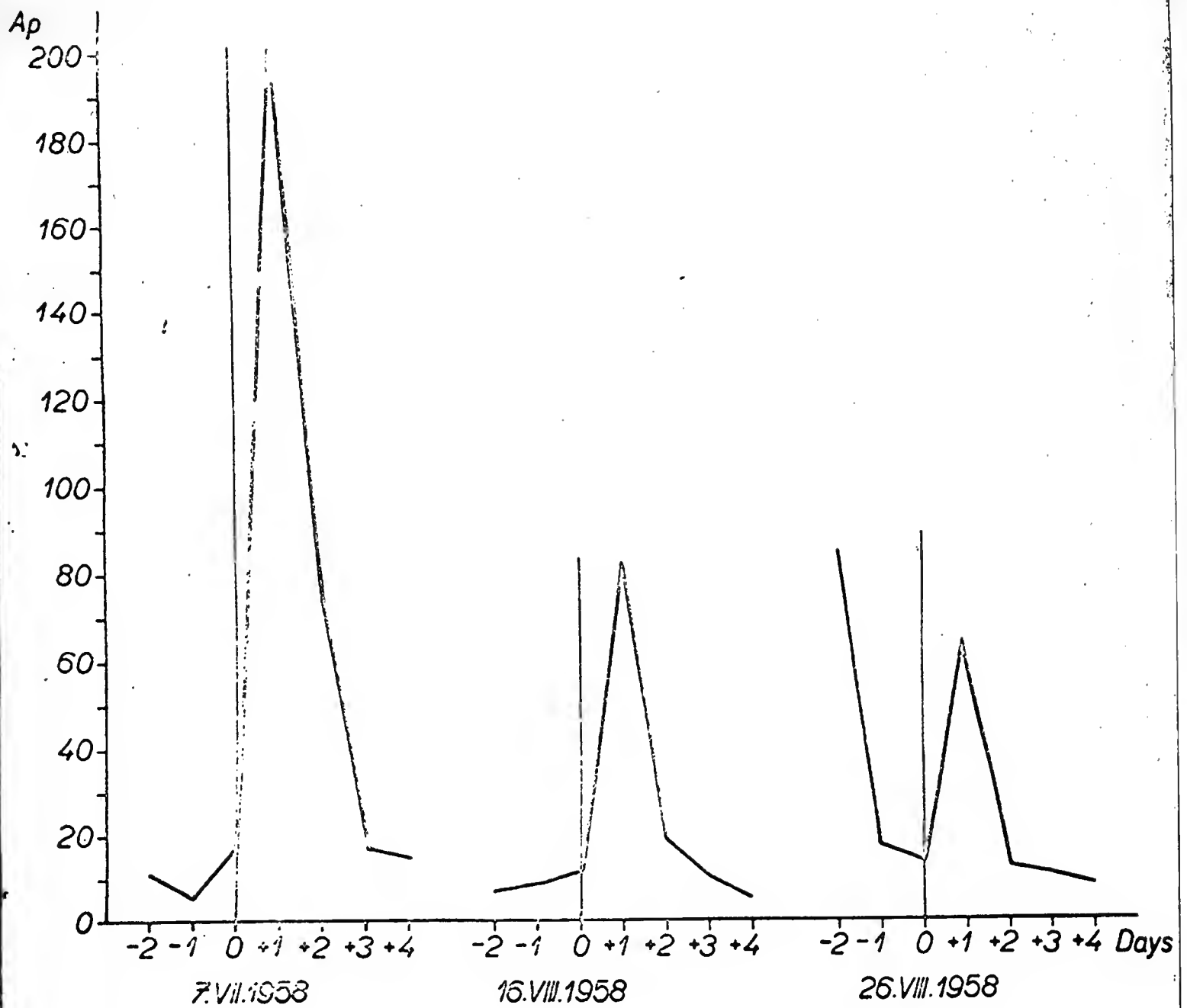


Fig.7. Course of AP-indices after large flare (imp. $\geq 3-$) during simultaneous presence of unstable filament in centre of visible solar disc (day of flare occurrence is zero day), 1958 (flare from corrected catalogue of C.S. Warwick).

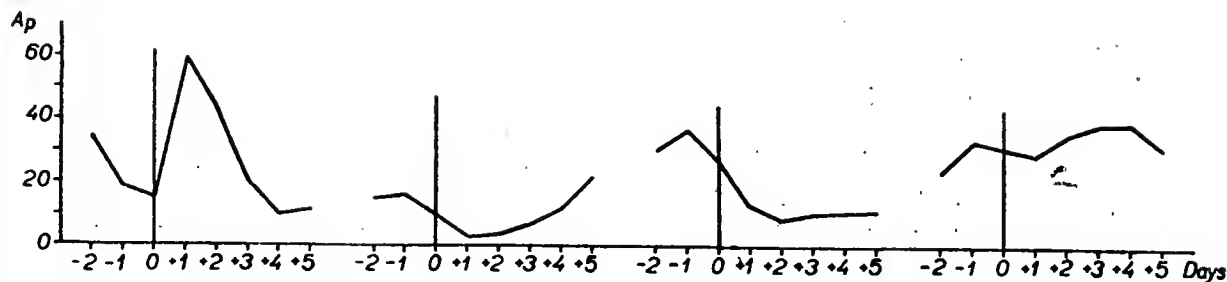


Fig. 8. Courses of average AP-indices (method of superposed epochs) after large flare in period of IGY. a) in presence of unstable filament (8 cases), b) during simultaneous CMP of active centre without essential changes (2 cases), c) in centre of solar disc no unstable filament or other phenomenon on day when flare occurred (10 cases), d) CMP of unstable filaments was not simultaneous with flare (23 cases).

at the suggestion of C.S. Warwick, who kindly supplied the reworked catalogue of large flares from the IGY. From the list of days on which large flares certainly occurred, the following groups were chosen: 1) with simultaneous occurrence (in the limits of one day) of filaments in the centre of the solar disc regardless of the position of the flare and its distance from the CM and also from the filament, 2) with simultaneous CMP of the active centre without flare activity, 3) without the presence of an unstable filament, and likewise in the absence of other phenomena, 4) the occurrence of unstable filaments was not simultaneous, the filament either preceded or followed the day when large flare occurred. The results are given in Figs 6-7 which show the course of the Ap-indices plotted for the different days characterized by the occurrence of at least one flare from 1957 (2nd half) and 1958 for group 1), i.e. for the cases when an unstable filament was present in the centre of the solar disc. Figures 8 a, b, c and d are valid successively for all above-mentioned groups; in them are plotted the courses of the average Ap-indices calculated on the basis of the method of superposed epochs. It is seen from all the graphs 6-8 that an unstable filament was necessary in order that a geomagnetic storm might occur; the presence of a flare was not decisive. If a filament was not present a decrease occurred in the Ap-indices after a flare. In Fig. 8 d the maxima are not pronounced and are displaced as a consequence of the uncorresponding and displaced passages of unstable filaments. In the case of Fig. 8 b the decrease is caused by the CMP of the active centre which does not vary very much. It is seen from all this that flares cannot be directly connected with the occurrence of geomagnetic storms. The slight trace of connection, based on the fact that there is a larger number of flares before the commencement of a storm than after it, may be the consequence only of an direct connection with which we shall deal in the analysis of the results.

Recapitulation and analysis of results.

It must be borne in mind that 1) a direct connection between flares and geomagnetic storms is disputable if it is considered that is obtained in only 50 % of the cases [13]; 2) if geomagnetic storms exist in periods when flares do not occur, a direct connection must be considered doubtful; 3) in no case did flares prove suitable as an indicator of geomagnetic storms in prognoses; 4) statistical papers dealing with the connection between flares and geomagnetic storms and giving results based on the average values of Ap-indices, exhibit low and unpronounced maxima [9], [10]. This fact in itself raises doubts as to the hypothesis on the direct connection between geomagnetic storms and flares [11]. 5) The fact that in the period before and after minimum no connection between flares and geomagnetic storms is obtained [7] is a confirmation of the incorrectness of the flare hypothesis. 6) Not the slightest connection between the importance of a flare and the occurrence of a geomagnetic storm was obtained in any convincing manner. There are many large geomagnetic storms preceded only by the weakest flare.

Apart from this there are also the results of the present paper where material from 30.VI. 1957 to the end of 1962 was used. It was found that 7) there exist high percentages of the number of geomagnetic storms before which not a single flare was observed even in relatively long intervals (up to three days before). The percentages decrease if the chosen interval is longer and more flares are taken into consideration, and increase with a decrease in the number of flares (they also depend on limitations as regards distance from CM and importance and on the period of the eleven-year cycle). It is thus clear that we have to do with only a statistical effect. The larger the number of elements being compared, the more frequently it happens that both fall simultaneously into the chosen time interval and this is even more likely if a longer interval is chosen. When there is a large number of flares (see Tab. I. Fig 1) it is more likely that one will occur by chance in the interval of three days before a geomagnetic storm beyond the maximum than

beyond or before the minimum, when the number of flares disproportionately falls, while the number of geomagnetic storms decreases much less. This fact was proved for all geomagnetic storms : from $Kp_{max} \geq 5+$, and for large storms: $Kp_{max} \geq 7+$ and $Kp_{min} \geq 5-$, and also for all, etc. If the percentages of sudden commencements without a flare are compared with other storms the latter are somewhat lower although they are still large. 8) The apparent connection between flares and geomagnetic storms can be explained by the simultaneous occurrence of other effects on the CM and possibly directly in the centre of the solar disc, as has been shown earlier [20], [8].

The somewhat larger number of flares occurring before geomagnetic storms compared with that following after the commencement of a storm indicates a slight connection, although this is limited compared with the high percentages of storm occurrence without a flare. This is just what can be found from the observations: that during a flare there is sometimes a greater probability of the occurrence of a geomagnetic storm although at other times this is not true at all. It seems that not always but only sometimes do flares have the tendency to precede the occurrence of a geomagnetic storm. And this is just what, as a consequence of point 8), is the cause of the rise in A_p -indices after a flare. The indirect connection can be explained by the presence of other affects. These are primarily unstable filaments ; their change from filaments of other types shows that not even here is there a simple connection but that a profounder significance must be ascribed to this circumstance. This means a completely new view of the relations between solar and geomagnetic activity: flares occur mostly in active centres. In such places there are strong magnetic fields, which are manifest, although with smaller intensity, also in the chromosphere and in the corona. The way in which such fields are distributed in the space above active centres is designed by the chromospheric structure and the shapes of the filaments-prominences. When changes occur in the local magnetic field a change takes place in the chromospheric and coronal structures and this

can be studied with great certainty on hydrogen masses above the active centre and its neighbourhood. Under certain conditions the filaments and chromospheric structure disappear altogether. It can be deduced from this that in such cases changes occurred in the given layers which had the result that the field was "disappear" there. This apparently, primarily concerns one of its components. It can occur suddenly or gradually, temporarily or permanently. During such changes flares often, though not always, occur. Since the "disappearance" of the local magnetic field in the centre of the solar disc - under certain conditions also outside the centre but on the CM - always means the advent of a geomagnetic storm [21], [22], [23] flares are also classified among processes which occur around the same time as the commencement of the geomagnetic storm appears on the Sun.

The question remains, what is important from the point of view of theoretical opinion as well as for practical use: are flares the cause of changes in local magnetic fields or their consequence? This will certainly be the subject of discussion for a long time to come, until the very nature of flares is known. A flare as the cause of a disturbance of magnetic field in the chromosphere is also considered by M.A. Ellison [24]. Perhaps this question could be answered by the conception of a combination of magnetic and electric conditions in the outer solar layers.

It is also necessary to explain some facts which, if incorrectly interpreted, might lead to controversies. This is primarily the question of changes and the possible annulling of chromospheric fields. These occur sometimes during a flare and at other times simply without it. Flares occur in the majority of cases above active centres with a complex structure of magnetic fields. It can be expected that a very effective interference will be required to annul chromospheric fields which in this case have considerable intensity. And it is during a flare (often regardless of the importance) that the disappearance of chromospheric structure and filaments can be observed in different places. On the other hand, if the fields ~~are~~ are very weak

such as those distributed above facular areas without sunspots a quite small change is enough to bring about such an effect. In such cases quite insignificant flares are usually present in the active region, or its surroundings or flares do not occur there at all.

It is certain, of course, that sometimes, after a certain time after a flare, the chromospheric structure is restored to what it was before and the filaments also appear as though they had not disappeared at all. This happens if it ^{is} in a region above strong photospheric fields. As soon as after a flare in the outer layers above the active centre is renewed the normal state, i.e. the state they had before, than the hydrogen masses, partly still unionized and partly already recombined, begin to rewind around the lines of force of the still existing magnetic field reaching here from the photosphere. This could explain the coronal origin of prominences considered by K.O. Kiepenheuer [25].

Another objection to considering flares as the cause of changes in magnetic fields might be the fact that the changes in local magnetic fields actually occur before the flares. But, according to our own subjective impressions obtained during observations, the changes before flares are of a different kind to those observed immediately after them. Before a flare there is an increase in intensity and extent of the field which becomes more and more complicated. Then surges and small filaments are produced. These are phenomena of short duration. It depends on the aspect from which we explain the process leading to the annulling of the field. In any case, however, we must admit that we have here the conditions for the superposition of fields and their temporary compensation, which is manifested differently in different places. These are changes appearing rather as isolated cases. While large and extensive changes occur only during the flare and after it. If an active centre is observed just after a flare, it can be said that a considerable and very striking simplification of the chromospheric structure has taken place and sometimes it completely disappears over large areas. Anyone who deals with the observation and study of fine

chromospheric structure and filaments can find this difference himself and there are certainly many who have already observed it.

However, there should be no misunderstanding. The question of whether a flare is the cause or consequence of changes in magnetic fields in the chromosphere cannot for the time being be decided even by the arguments given here. It should also be borne in mind that, whatever the case, one cannot in any case speak of a direct and universal connection between flares and geomagnetic storms. This might be permissible perhaps only in very limited cases when annulling of the fields occurred in the active centre just in the centre of the solar disc or under certain conditions on the CM and when flares also occurred just in this centre. But even then the connection would be indirect. The actual and nearest indicators of this fact are always unstable filaments. This can be explained by means of the known relation between filaments and coronal formations extending above them. As has already been shown [3] a geomagnetic storm occurs when some coronal formation is directed toward the Earth. The density of the coronal plasma, in other words the density ^{of the} corpuscular streams is apparently directly related to the magnitude of the geomagnetic storm and vice versa. A filament and the chromosphere obviously contribute by their masses so that after their ionization, which occurs in certain layers of the corona - apparently layers at heights to which the rising prominences reach - the coronal plasma becomes denser. As was to be expected perhaps, there definitely exists no simple relation between the size of a filament and the magnitude of a geomagnetic storm. This is natural since the main question here is to what percentage the atoms were ionized. It is not impossible, however, that the necessary parameters could be determined by a detailed study, e.g. by determining the amount of masses which returned to the chromosphere etc.

On the basis of the above considerations and whole series of working hypotheses and using the results of observations, a new method of fore-

casting geomagnetic activity, disturbances and quiet, was elaborated [26]. Its successful try-out in practice proves the correctness both of the method itself and of the corresponding hypotheses. In order to be able to forecast every geomagnetic storm with maximum accuracy, a correct and continuous observations of the Sun is required. Only in this way is it possible to record all sudden and of short duration phenomena which precede the occurrence of geomagnetic storms. And only in this way will it be possible to forecast each period of absolute geomagnetic quiet which follows after the CMP of an active centre in which ^{and also above which} the magnetic field was not annulled.

Table III. The connection between flares and some solar and geophysical phenomena as seen from the results obtained hitherto.

a) Immediate results :

1) disappearing filaments rising prominences	exist also without flares	no dependent directly on importance of flare	limited indirect connection
---	------------------------------	---	-----------------------------------

2) SFE	exist only with flare	dependent directly on importance of flare	possible direct connection
--------	--------------------------	--	----------------------------------

3) Dellinger effect	exist only with flare	dependent directly on importance of flare	possible direct connection
---------------------	--------------------------	--	----------------------------------

b) Later results:

4) geomagnetic storms	exist also without flares (high percentage well above 50%) not all flares are followed by geomagnetic storms (50%)	not directly dependent on importance of flare	limited indirect connection
-----------------------	--	--	-----------------------------------

5) polar aurorae are accompanying phenomenon of geomagnetic storms and the same holds for them as for storms.

To sum up, it must be explained what form the connection between flares and some solar and geophysical effects, has judging by what we have had the opportunity to observe. The analysis is given in Tab.III according to which the SFE and Dellinger effect begin immediately after a flare, depend on the magnitude of its importance and are thus directly related to it. Meanwhile, however, the disappearing filaments-rising prominences, despite the fact that they occur near to the flare in time - and often absolutely simultaneously [27] - are, like the effects occurring after it in a longer time interval, i.e. geomagnetic storms and polar aurorae, indirectly related to the flare. In order to supplement Tab.III the connection between flares and radio outbursts will have to be verified in a radical manner. According to the work of J. Halenka [28], one could deduce a certain dependence on the presence of a filament.

References.

- [1] J.W. Warwick: Hights of Solar Flares, Ap.J. 121, 1955, 376-384.
- [2] C.S. Warwick : Flare Hight and Association with SID' S, Ap.J. 121, 1955, 385-390.
- [3] B. Bednářová-Nováková: Connection between Geomagnetic Storms in IGY and IGC and Occurence of some Kinds of Filaments, Studia geoph. et geod. 5, 1961, 138-163.
- [4] D. Van Sabben: Solar Flare-Effects and Magnetic Storms. J. Atm. Terr. Phys. 3, 1952, 270
- [5] R. A. Watson: Magnetic Activity following a Solar Flare. J. Atm. Terr. Phys. 11, 1957, 59-61.
- [6] O.M. Barsukov : Геомагнитная эффективность хромосферных вспышек по материалам 1957г. Bulletin of the Academy of Sci., U.S.S.R., Geophysical Series, 1959, No. 11, 1690-1693.
- [7] C.S. Warwick and R.T. Hansen: Geomagnetic Activity following Large Flares. J. Atm. Terr. Phys. 14, 1959, 287-295.
- [8] B. Bednářová-Nováková: Analysis of Solar Situations During Flares and Geomagnetic Activity Afterwards, Travaux de l'Inst. géoph. de l'Acad. Tchecosl. des Sci, No. 191, Geofysikální Sborník 1963, MSAV, Praha, 399-405.
- [9] J. Halenka: The connection between chromospheric Flares and Geomagnetic Activity in the IGY, Studia geoph. et geod. 4, 1960, 361-377.
- [10] J. Halenka : Geomagnetic Activity after Large Chromospheric Flares, Studia geoph. et geod. 5, 1961, 237-255.
- [11] J. Halenka : On the Character of the Connection between Geomagnetic Activity and Chromospheric Flares. Studia geoph. et geod. 8, 1964 (in press)
- [12] B. Bednářová-Nováková: Une note sur la question de l'origine des orages géomagnétiques. Studia geoph. et geod. 4, 1960, 167-171.
- [13] B. Bell: Major Flares and Geomagnetic Activity, Smithsonian Contributions to Astrophysics, Vol. 5, No. 7, 1961, 67-83.
- [14] C.S. Warwick: National Bureau of Standards List of IGY Flares with Normalized Values of Importance and Area, IGY Solar Activity Report Series, Number 17, May 1, 1962, High Altitude Observatory University of Colorado, Boulder, Colorado.

- [15] H.W. Dodson and Ruth Hedemen: Mc Math-Hulbert Observatory Working List of Flares and Daily Flare Index For IGC-1959, IGY Solar Activity Report Series Number 15, June 26, 1961, High Altitude Observatory, Boulder, Colorado.
- [16] H.W. Dodson and Ruth Hedeman : McMath - Hulbert Observatory Working List of Flares and Daily Flare Index for 1960, IGY Solar Report Series Number 18, May 17, 1962, High Altitude Observatory, Boulder, Colorado.
- [17] H.W. Dodson and Ruth Hedeman : Mc Math - Hulbert Observatory Working List of Flares and Daily Flare Index for 1961, IGY Solar Report Series Number 21, March 15, 1963. High Altitude Observatory, Boulder, Colorado.
- [18] Quarterly Bulletin on Solar Activity Nos 118-138, Eidg. Sternwarte in zürich (1958-1963).
- [19] IAGA Bulletin Nos 12 1 and 12 m 1.
- [20] B. Bednářová-Nováková: A contribution to the Question of Sources of Corpuscular Geomagnetically Active Solar Radiation, *Studia geoph. et geod.* 8, 1964, 63-71.
- [21] B. Bednářová-Nováková: A Remark on the Relation between UM-Regions and Geomagnetic Disturbances (manuscript)
- [22] B. Bednářová-Nováková : Remarks on the Retrospective Investigation of the Interval of 13-30 September 1963, Proposed by Regional Centre of IQSY IZMIRAN (Manuscript)
- [23] B.Bednářová-Nováková, V.Bucha, J.Halenka, M.Konečný : On the Problems of the Origine of Geomagnetic Storms, *Travaux de l'Inst. Géoph. de l'Acad. Tchecosl. des Sci*, No 192, *Geofysikální Sborník* 1963, NČSAV, Praha, 1964, 407-466.
- [24] M.A. Ellison: Energy Release in Solar Flares, *The Quarterly Journal of the R.A.S.*, Vol.4, No 1, The R.A.S. Burlington House, London, W.1. 1963, 62-73.
- [25] K.O. Kiepenheuer: Über die Beziehung zwischen Protuberanzen und Korona. *Convegno di scienze fisiche matematiche e naturali* 14-19 sett. 1952, *Atti dei Convegni* 11, *Accad. Naz. dei Lincei*, Roma 1953, 148 -155.

- [26] B. Bednářová-Nováková: K charakteru souvislosti mizejících filamentů s geomagnetickými bouřemi (manuscript).
- [27] B. Bednářová-Nováková: A New Method of Forecasting Geomagnetic Activity and its Practical Application, Travaux de l'Inst. Géoph. de l'Acad. des Sci, No206, Geofysikální Sborník 1964, NČSAV 1965 (in presse)
- [28] J. Halenka: Kontrola účinnosti erupcí s hlediska geomagnetického pomoci radiových vzplanutí. Travaux de l'Inst. Géoph. de l'Acad. Tchécosl. des Sci. No 31, Geofysikální Sborník 1955, NČSAV, Praha, 1956, 239-248.

INFORMATION REPORT INFORMATION REPORT

CENTRAL INTELLIGENCE AGENCY

#12

This material contains information affecting the National Defense of the United States within the meaning of the Espionage Laws, Title 18, U.S.C. Secs. 793 and 794, the transmission or revelation of which in any manner to an unauthorized person is prohibited by law.

C-O-N-F-I-D-E-N-T-I-A-L

COUNTRY International / *Su. Technol.*
SUBJECT Papers to be Presented at the
International Conference on
Atmospheric and Space Electricity,
Montreux, Switzerland, 6-10 May 63

REPORT NO. []

DATE DISTR. 9 May 63

NO. PAGES 2

REFERENCES []

DATE OF INFO. 19 Apr 63 & prior

PLACE & DATE ACQ. -- 19 Apr 63 & prior

THIS IS UNEVALUATED INFORMATION

[]

[] listed below are the titled and authors of the
foreign papers to be presented at the International Conference on
Atmospheric and Space Electricity, Montreux, Switzerland, 6-10 May 1963:

- (a) "Atmospheric Electricity Research in the Far East" by H.
Hatakeyama
- (b) "Report on Atmospheric Electricity in Central Europe 1959-62"
by R. M. H. Leisen
- (c) "Atmospheric Electricity Research in Great Britain, Ireland,
Africa and New Zealand" by W. C. A. Hutchinson
- (d) "Electromagnetic Energy Radiated From Lightning" by Atsushi
Kikugawa
- (e) "The Concepts of Atmospheric Electricity as Applied to the
Ionosphere" by K. Maeda
- (f) "Geoelektrische Probleme der Blitzforschung" by Volker Fritsch
- (g) "Charge Generation in Thunderstorms" by J. Alan Chalmers
- (h) "Relations Between Lightning Discharges and Different Types
of Musical Atmosphericities" by Harald Norinder
- (i) "Problems of Fair Weather Electricity; Introducing Remarks"
by H. Israel
- (j) "Action of Radioactivity and of Pollution upon Parameters of
Atmospheric Electricity" by J. Bricard
- (k) "Generation of Electric Charges Outside Thunderclouds" by J.
Alan Chalmers

5
4
3
2
1

C-O-N-F-I-D-E-N-T-I-A-L

5
4
3
2
1

GROUP 1
Excluded from automatic
downgrading and
declassification

STATE ARMY NAVY AIR FBI AEC

INFORMATION REPORT INFORMATION REPORT

CONTROLLED

NO DISSEM ABROAD

NO FOREIGN DISSEM

DISSEM: The dissemination of this document is limited to civilian employees and active duty military personnel within the intelligence components of the USIB member agencies, and to those senior officials of the member agencies who must act upon the information. However, unless specifically controlled in accordance with paragraph 8 of DCID 1/7, it may be released to those components of the departments and agencies of the U. S. Government directly participating in the production of National Intelligence. IT SHALL NOT BE DISSEMINATED TO CONTRACTORS. It shall not be disseminated to organizations or personnel, including consultants, under a contractual relationship to the U.S. Government without the written permission of the originator.

(b)(3)

- (l) "Charge Generation in Thunderstorms" by B J Mason
- (m) "The Theory of Lightning" by D J Malan
- (n) "Types of Lightning" by N Kitagawa
- (o) "Lightning Protection" by D Miller-Hillebrand
- (p) "Whistlers as a Phenomenon to Study Space Electricity"
by N D Clarence

UNCLASSIFIED.]

- end -

~~C-O-N-F-I-D-E-N-T-I-A-L~~

(b)(3)

(b)(3)

SESSION 1.1

Atmospheric Electricity Research in the Far East

H. Hatakeyama

1. Atmospheric electric observations in the upper atmosphere.

Observations of the electrical conductivity and the electric field in the upper atmosphere were made twice a day during the World Meteorological Intervals in the IGY and ICG at four stations in Japan--Sapporo ($43^{\circ}03'N$, $141^{\circ}20'E$), Tateno ($36^{\circ}03'N$, $140^{\circ}08'E$), Hachijojima ($33^{\circ}07'N$, $139^{\circ}47'E$) and Kagoshima ($31^{\circ}38'N$, $130^{\circ}36'E$).

The results of observations were discussed by K. Uchikawa (1961) and ^{he} show that the mean vertical distribution of the conductivity obtained at respective stations are almost equal to each other from the ground up to 500 mb level and that the conductivity increases with the latitude in the upper troposphere and in the lower stratosphere as shown graphically in Fig. 1. This suggests that the conductivity in the free atmosphere is mainly under the control of cosmic ray intensity, because the total intensity of cosmic rays increases with the geomagnetic latitude.

Mean values of the potential gradient in the upper atmosphere obtained at four stations are shown in Fig. 2. Values of the potential gradient are large near the ground and decrease exponentially with an altitude. Above 100 mb level the value becomes lower than 5 V/m. However, as the accuracy of the measurement is ± 5 V/m, the electric field intensity above 100 mb level could not be measured precisely.

When the exchange layer develops, as shown in Fig. 3, the sudden decrease in the atmospheric electric field and relatively small sudden

increase in the electrical conductivity were observed at the top of the exchange layer as in other measurements in foreign countries. This marked decrease and increase disappear for several days after the low pressure or the cyclone passes through the observation point because the exchange layer fades away after the low pressure.

The conduction current in the exchange layer is about 1.3 times larger than that above the exchange layer. This means that the "Austausch" contributes to generate the conduction current in the exchange layer through the rapid production of ions.

Day to day variations of the electric field and the electrical conductivity in the upper troposphere were investigated. These variations are related to meteorological factors, such as the air mass, the upward or downward motion of the air, and the jet stream. For example the increasing rate of the electrical conductivity with respect to the latitude in case of a strong jet stream is larger than that in a weak jet.

The concentration of small ions was computed from the observed electrical conductivity. The vertical air currents in and around the jet stream were calculated using the time and space variation of the concentration of small ions. When the intensity of the jet stream is increasing, downward motions of the air predominate in and around the jet stream, only except the southern and lower part of it where upward motion exists. And vice versa when the intensity of the jet stream is decreasing. An example of which is shown in Fig. 4. These characteristics coincide qualitatively with those obtained thermodynamically from the time and

space variations of the air temperature.

At Poona in India, observations of the potential gradient using radio^sonde techniques have been made since 1953 and systematic observations were made during the IGY. The results of the observations were discussed by S. P. Venkiteshwaran and Anna Mani (1962).

During clear weather, in both winter and summer, the higher values of potential gradient are confined to a region extending from the ground to about 600-500 mb, above which height it either remains fairly constant, at about 20 V/m, or increase slightly with height. Within the exchange layer, there are appreciable diurnal variations in the potential gradient. They are at a minimum and almost constant during the hotter parts of the day and higher at other times.

The data obtained during the IGY 1957-59 have been classified into four groups, corresponding to the four main seasons -- (1) November-February (Winter), (2) March-May (Summer), (3) June-August (Monsoon season) and (4) September-October (when the monsoon is withdrawing and the skies are clear or partly covered with low clouds with a few thunderstorms). Examples of the results of observations are shown in Fig. 5.

In winter, high potential values are confined to a region from the ground up to about 600 mb (4.4 km), above which, which represents ^{to} the top of the austausch region, the potential gradient remains almost steady (about 10-40 V/m) with increasing height up to about 300 mb (9.7 km). Above which it again increases up to the highest levels studied, -- 50 mb (19 km),

suggesting an increase in the particle content of the atmosphere. The 300 mb region nearly corresponds to the altitude of the jet stream over India to the north of Poona. The increase in the potential gradient above 300 mb therefore suggests the existence of fine suspended particles, presumably of extra terrestrial origin, in a larger concentration just above the level where the extra-tropical stratosphere flows into the troposphere, through the region of the jet stream between the tropical and extra-tropical stratospheres.

The conditions over Poona in the summer season are as follows:

(a) The Austausch region extends up to 500 mb (5.8 km), about 1.4 km higher than in winter: (b) the region of maximum potential gradient lies very near the ground and the potential gradient generally decreases with height up to 500 mb: (c) above the Austausch region, the potential gradient is quite steady at the 500 mb value up to 150 mb (14.2 km) or above: and (d) the potential gradient above 500 mb is of the order of 20-30 V/m compared to 10-40 V/m during winter.

The observations during the monsoon month are again markedly different from those observed in either winter or summer. The potential gradient attains its highest values between 800 and 600 mb, which is the region of maximum cloudiness during the season. The upper limit of the region of high potential gradient (500 mb) also represents roughly the top of the clouds during this season. The most important difference is the steady fall in the potential gradient above 500 mb, from 20-60 V/m to about 20-40 V/m at 200 mb, and decreasing to less than 10 V/m at about 100 mb.

September and October is a transition period when the monsoon is withdrawing and winter conditions are setting in. The potential gradient values are characteristic of both seasons.

T. Sekigawa (1960) observed and discussed the atmospheric electric potential gradient at the summit of Mt. Fuji (3,776 m). Results are shown graphically in Fig. 6. In summer months (May-August), the potential gradient is large in later afternoon hours and small at about midnight. On the contrary, in winter months (November-February) it is large in early morning hours and small in later morning hours. In equino^{ct}xial months (March, April, September and October) the diurnal variation is double oscillation and maxima appear after midnight and in later afternoon hours and minima in the morning and in the evening hours.

The diurnal variation in winter corresponds to the universal change of potential gradient (9h L. M. T. = 0h U. T.). In summer months the top of the exchange layer exceeds the summit of Mt. Fuji, and the potential gradient is higher in afternoon hours and smaller in night hours. And in equino^{ct}xial months characteristic of both summer and winter appears.

2. Atmospheric electric elements near the ground.

Kondo (1959) discussed the secular change of atmospheric electric elements using the observational data at the Kakioka Magnetic Observatory for the period 1930-1957. He found that the potential gradient is decreasing and the electrical conductivity is increasing since 1953. He thought the cause of this decrease in the potential gradient and increase in the

electrical conductivity was the artificial radioactivity of fallouts due to the test explosions of nuclear bombs.

Secular variations of the potential gradient at Kakioka ($36^{\circ}14'N$, $140^{\circ}11'E$) and Memambetsu ($43^{\circ}55'N$, $144^{\circ}12'E$) are shown in Fig. 7. The curve of Kakioka is the deviation from the mean value 130 V/m for 1936-49, and that of Memambetsu is that from the mean value 124 V/m for 1950-53. In the fall of 1958 the test explosions were stopped and the potential gradient gradually recovered its normal value, but in the summer of 1961 the test explosions were again started and the potential gradient is decreasing speedily.

Hatakeyama and Kawano (1953) reported the diurnal change of the potential gradient at several places in Japan. In Tokyo we have observations of that in rather old time 1897-1903, which is shown in Fig. 8. We are making the observation of potential gradient in Tokyo since January, 1962. The mean diurnal variation January-August, 1962, is shown also in Fig. 8. This type of diurnal variation is usually seen in large cities.

In the upper part of Fig. 8, the mean diurnal variation at Kakioka for the period 1936-55 is shown. The distance between Tokyo and Kakioka is about 70 km and the type of the diurnal variation at Kakioka has never changed up to the present. Sixty years ago, the air at Tokyo was very clear and the type of the diurnal variation was rural.

Misaki (1950, 1961) devised a method for measuring the ion spectrum and discussed the relation between the ion spectrum and the electrical conductivity. According to his method the inner cylinder of aspiration

apparatus is divided into two parts. The value $\left(\frac{i_1}{C_1} - \frac{i_2}{C_2}\right)$ is observed and the characteristic curve is formed taking $\left(\frac{i_1}{C_1} - \frac{i_2}{C_2}\right)$ as ordinate and potential applied to the outer cylinder as abscissa (i_1, C_1, i_2, C_2 are current and capacity of each part respectively). Ion spectrum is obtained by deriving the first derivative of this characteristic curve and the second derivative is not needed.

He made experiments for obtaining the mobility spectrum of atmospheric ions in the mobility region between 3.0 and 0.2 $\text{cm}^2/\text{V}.\text{sec.}$ in 1960 in the polluted air at Tokyo and in the clear air at Karuizawa. Results of the diurnal series of observations made at both sites indicate some effects of pollution on the relation between the electrical conductivity and the mobility spectrum. In the polluted air, scores of per cent of the conductivity is attributed to the large or the intermediate ions while the conductivity in the clear air is practically attributed to the small ions only, as is generally believed.

The spectrum of the small ions does not shift on the mobility axis, maximum concentration lying in the interval 1.0-0.7 $\text{cm}^2/\text{V}.\text{sec.}$, regardless of the variations in the conductivity. On the contrary, the equivalent mobility, i. e. the ratio of the polar conductivity to the small ion concentration, changes with the variations of the conductivity in the intensely polluted air. An example of the results of observations are shown in Fig.

9.

The ionizations by α -, β -, γ - rays and β -, γ - rays and the

natural radioactive dust concentration in the atmosphere near the ground have been observed continuously with two ionization chambers and an electrostatic precipitator at Tanashi near Tokyo since April, 1958, by M. Kawano and S. Nakatani (1958, 1959). They discussed the results of observations.

On fine days the diurnal variation of the ionization by α -, β -, γ - rays is similar to that of the ionization by β -, γ - rays. As is shown in Fig. 10, the maximum value occurs in early morning (4-6 h), and the minimum in the daytime (11-13 h). On cloudy and rainy days the time variations are very irregular and the values are considerably larger than those on fine days. On fine days the values of $(\beta, \gamma)/(\alpha, \beta, \gamma)$ are about 2-5 per cent, being large in the daytime and small at night, but the values on cloudy and rainy days are considerably smaller than these on fine days.

The natural radioactive dust concentration is large at night and small in the daytime, and the diurnal variation being similar to that of ionization. But the amplitude of the diurnal variation curve of the dust concentration collected with the electrostatic precipitator is remarkably larger than that of the ionization by β -, γ - rays measured with an ionization chamber.

The results of simultaneous observations mentioned above seem to be important for the researches on the natural radioactivity and on the frequency distribution of the particle size of the radioactive dusts in the atmosphere.

M. Kawano and S. Nakatani (1961) studied the size distribution of dust particles suspended in the atmosphere near the ground which carry the

naturally occurring radioactive substances by the cascade impactor and autoradiography. The cascade impactor was used for classifying the dust particles into four groups by their particle sizes, and the autoradiography was used for counting the number of α -tracks of each class at 0 hrs and 18 hrs after collection by the impactor.

Table. Size distribution of dust particles which hold the α -activity.

Class	I	II	III	IV
Particle size (μ)	5.2-1.3	2.5-0.9	0.9-0.5	0.5-0.3
Number of α -tracks at 0 hrs after collection (per unit area)	1	10	13	200
Number of α -tracks at 18 hrs after collection (per unit area)	0	0	4	17

According to the results of measurements, as shown in the Table, a large part of naturally occurring radioactive dust was concentrated in the size range below 0.5μ , and the radioactivity was radiated almost solely from radon and thoron daughter products of short half lives.

M. Kawano (1957) pointed^{out} the abnormal increase of the ionization by α -, β -, γ - rays was found during the solar eclipse on April 19, 1958. As is shown in Fig. 11, the maximum value occurred at the time of maximum obscuration and was more than twice that on the other days.

3. Atmospheric electric elements during disturbed weather.

Ch. Magone and K. Orikasa (1960, 1961) and K. Orikasa (1962) made simultaneous observations of the surface electric fields, the charge on

raindrops and snow particles, the form of snow particles and the intensity of rainfall and snowfall from 1956 to 1960 at Sapporo. And the latter author made similar observations simultaneously at two stations 1.2 km apart each other.

Analysing the data of these records, the following conclusions were obtained. When the rainfall was light or steady, positive field relatively smaller than those of fine weather or negative field was observed, and when there was light or steady snowfall, positive field was observed. During continuous heavy rain or snowfall and during heavy rain shower or snow shower, wave patterns of the electric field were often observed.

In almost all the cases of positive or negative electric field and of the wave patterns of field, mirror image relations ^(continued) ~~held~~ generally between the sign of electric field and the sign of electric charge on rain or snow particles. But in the beginning of rain or snowfall and when the rapid increase in the intensity of rain or snowfall occurred, the sign of the electric field and the sign of electric charge on particles ^{was} ~~became~~ the same. An example of the observation is shown in Fig. 12.

To explain the mirror image relation mentioned above, the author considered that the rain or snow particles were mainly electrified in the cloud and ^{carried} ~~carried~~ electric charges down to the ground, consequently the cloud may be electrified to the sign opposite to the net charge which was carried down to the ground by the particles. The case of the same sign of both the electric field and the electric charge on rain or snow particles was explained hypothetically by considering the space charge due to charged

rain or snow particles.

Kikuchi and Magono (1961, 1961a) measured charges on natural snow crystals before and after their artificial melting during snowfall. It was found that the snow crystals obtained considerable positive charge when they were melted. This observation appears to explain the above mentioned general observational fact that in steady rainfall negative surface electric field is predominant and raindrops carry positive charge in most cases, while in steady snowfall positive surface electric field is predominant and most of the snow crystals are charged negatively.

T. Ogawa (1960) and T. Ogawa and S. Saga (1961) made the continuous observations of the electric current carried by rain drops, the rate of rainfall and the surface potential gradient. Providing the Wilson's theory of ion capture by water drops, ^{they explained,} the raindrop starts a cloud with a small charge in the same sign as the electric field and reverses its sign at a point between the cloud base and the ground. A quantitative representation between the rain current, the rate of rainfall and the potential gradient was assumed and a relation between the surface potential gradient and the potential gradient in the charging region of raindrops below the clouds was deduced. An example of the effect of splashing of raindrops at the ground was shown, in which the intensity of rainfall was 10 mm/hr or more the effect reduced the surface potential gradient in the value of about 2 V/cm toward negative.

Department of physics in the University of Singapore has plans to expand itself and a new Atmospheric Physics Laboratory will soon be

built. Last year and up to August of this year, under the supervision of Hon Yung Sen, J. Pakiam investigated the electrical conductivity of the atmosphere near the ground during the disturbed weather and some interesting results were obtained but they are not yet published.

References

- Hatakeyama, H. and M. Kawano (1953): On the Diurnal Variation of Atmospheric Potential Gradient in the Japan Archipelago, Pap. In Met. and Geophys. 4, 55-60.
- Kawano, M. (1957): The Result of Observation of the Rate of Ion Pair Production in the Atmosphere during the Solar Eclipse, Apr. 19, 1958, Journ. Geomag. and Geoelec. 9, 210-211.
- Kawano, M. and S. Nakatani (1958): The Results of Routine Observations of the Ionization and the Natural Radioactive Dust Concentration in the Atmosphere in Tokyo. Journ. Met. Soc. Japan, 36, 135-140.
- Kawano, M. and S. Nakatani (1959): The Absolute Measurement of the Concentrations of the Radioactive Substances in the Atmosphere in Tokyo, Journ. Geomag. and Geoelec. 10, 56-63.
- Kawano, M. and S. Nakatani (1961): Size Distribution of Naturally Occurring Radioactive Dust measured by a Cascade Impactor and Autoradiography, Geofis. Purk. e Appl. 50, 243-248.
- Kikuchi, K. and Ch. Magono (1961): On the Electrification of Snow Crystals by their Melting, Journ. Japanese Society of Snow and Ice, 23, 41-45.

- Kikuchi, K. and Ch. Magone (1961a): On the Electrification of Snow Crystals by their Melting, II, Journ. Japanese Society of Snow and Ice, 23, 155-158.
- Kondo, G. (1959): The Recent Status of Secular Variations of the Atmospheric Electric Elements and their Relation to the Nuclear Explosions, Memoirs of Kakioka Magnetic Observatory, 9, 2-6.
- Magone, Ch. and K. Orikasa (1960): On the Surface Electric Field During Rainfall, Journ. Met. Soc. Japan, 38, 182-194.
- Magone, Ch. and K. Orikasa (1961): On the Surface Electric Field Caused by the Space Charge of Charged Raindrops, Journ. Met. Soc. Japan, 39, 1-11.
- Misaki, M. (1950): A Method of Measuring the Ion Spectrum, Pap. in Met. and Geophys. 1, 313-318.
- Misaki, M. (1961): Studies on the Atmospheric Ion Spectrum (1 and 2), Pap. in Met. and Geophys. 12, 247-276.
- Ogawa, T. (1960): Electricity in Rain, Journ. Geomag. and Geoelec. 12, 21-31.
- Ogawa, T. and S. Saga (1961): Charge on Rain Drop, Journ. Geomag. and Geoelec. 12, 99.
- Orikasa, K. (1962): On the Disturbance of the Surface Electric Field Caused by Rainfall and Snowfall, Geophys. Bull. Hokkaido Univ. 9, 123-160.
- Sekigawa, T. (1960): Observation of Atmospheric Electricity at the Summit

of Mt. Fuji, Tenki, 7, 65-71 (in Japanese).

Uchikawa, K. (1961): Atmospheric Electric Phenomena in the Upper Air
over Japan (Part I and II), Geophys. Mag. 30, 617-672.

Venkiteshwaran, S. P. and Anna Mani (196?): Measurement of Electrical
Potential Gradient in the Free Atmosphere over Poona, Journ. Atm.
Sci. 19, 226-231.

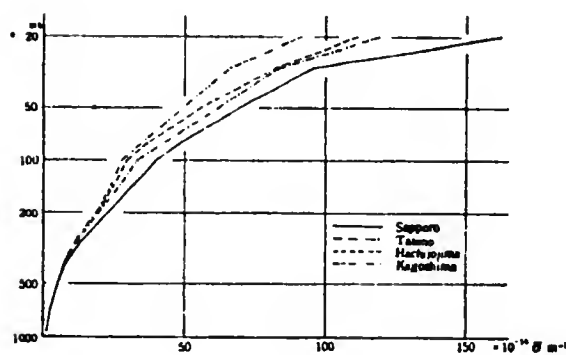


Fig. 1. Mean values of the negative polar conductivity.

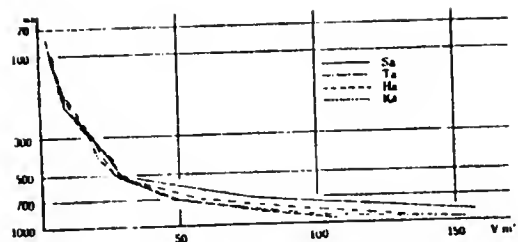


Fig. 2. Mean values of the potential gradient. Sa: Sapporo, Ta: Tateno, Ha: Hachijojima, Ka: Kagoshima

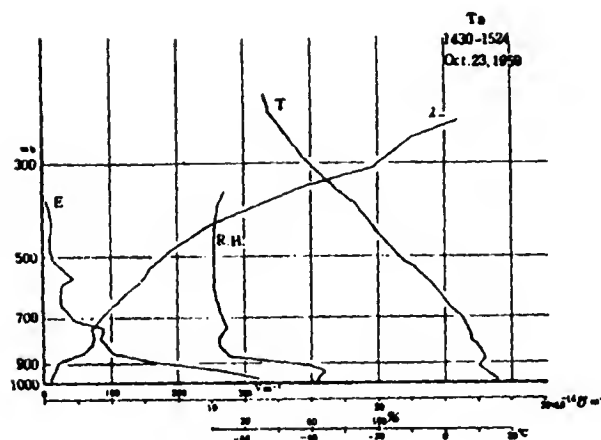


Fig. 3. Ascent curves of the negative polar conductivity (), The potential gradient (E), the temperature (T) and the relative humidity (R.H.) observed at Tateno.

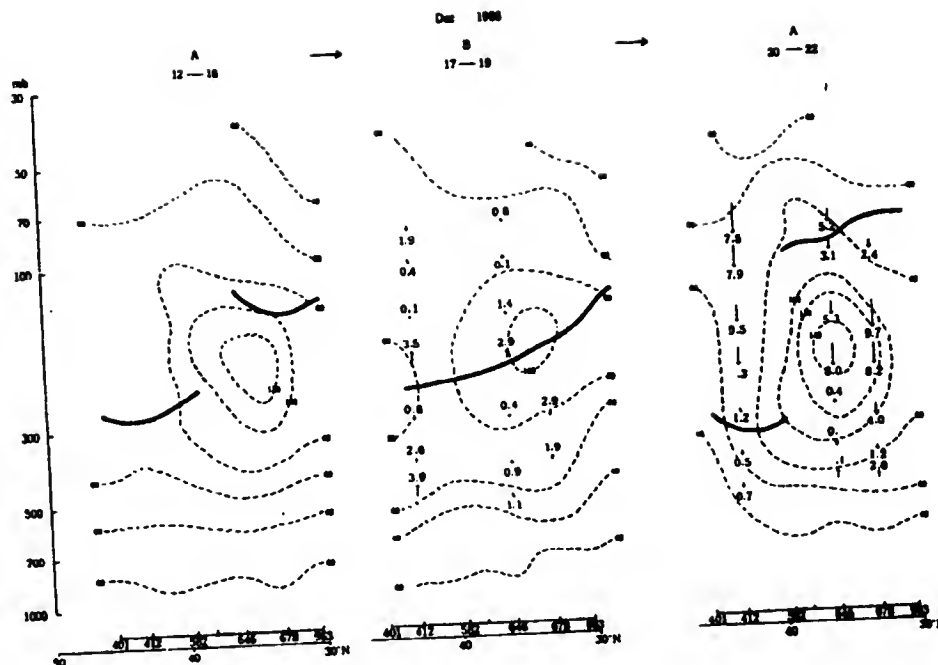


Fig. 4. Vertical air currents computed from the time and space variation of the concentration of small ions. Arrow: The direction of vertical motion (unit: cm/sec.). Broken line: Isotach (knots). Thick Line: tropopause.

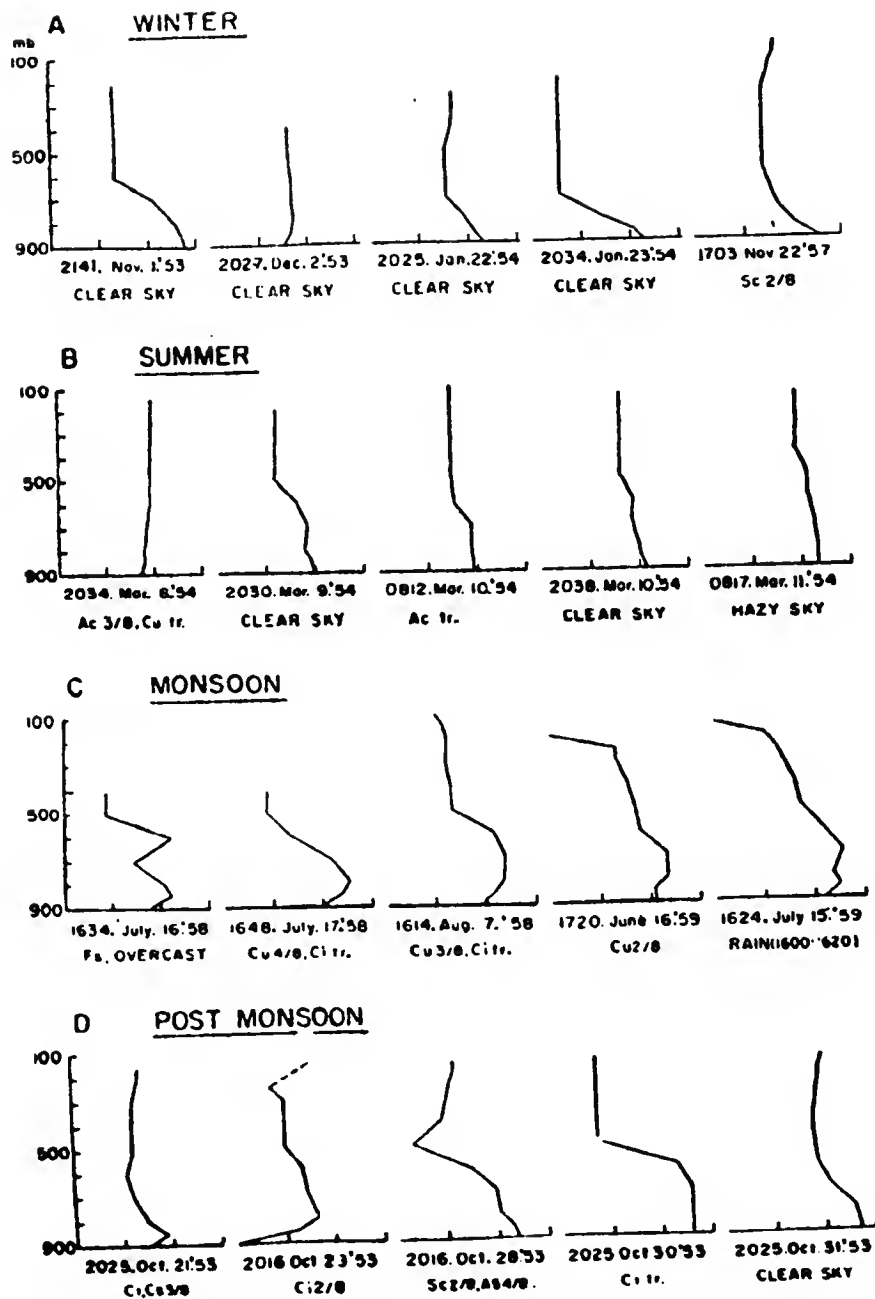


Fig. 5. Seasonal variation of potential gradient with height at Poona. The horizontal scale of each graph is logarithmic, with potential gradient by radiosonde from 1 to 1,000 V/M.

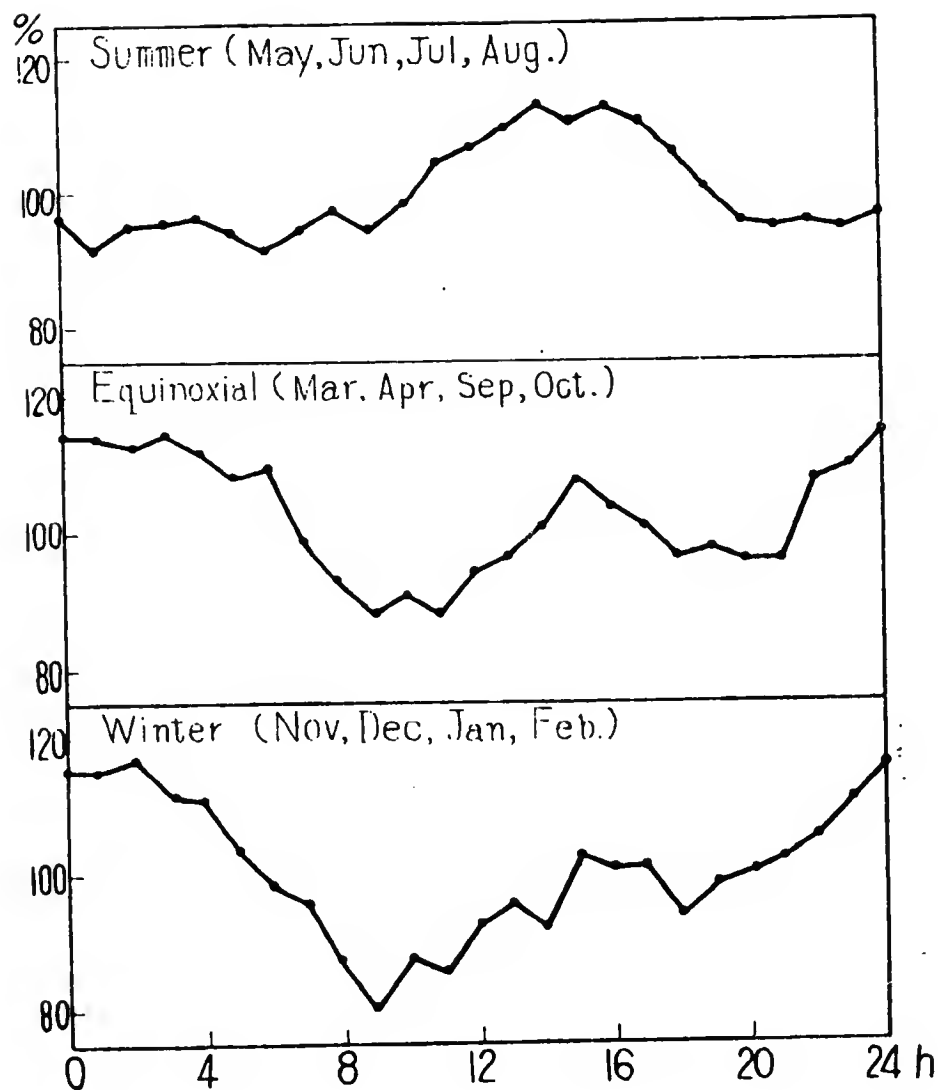


Fig. 6. Diurnal variation of the potential gradient at the summit of Mt. Fuji.

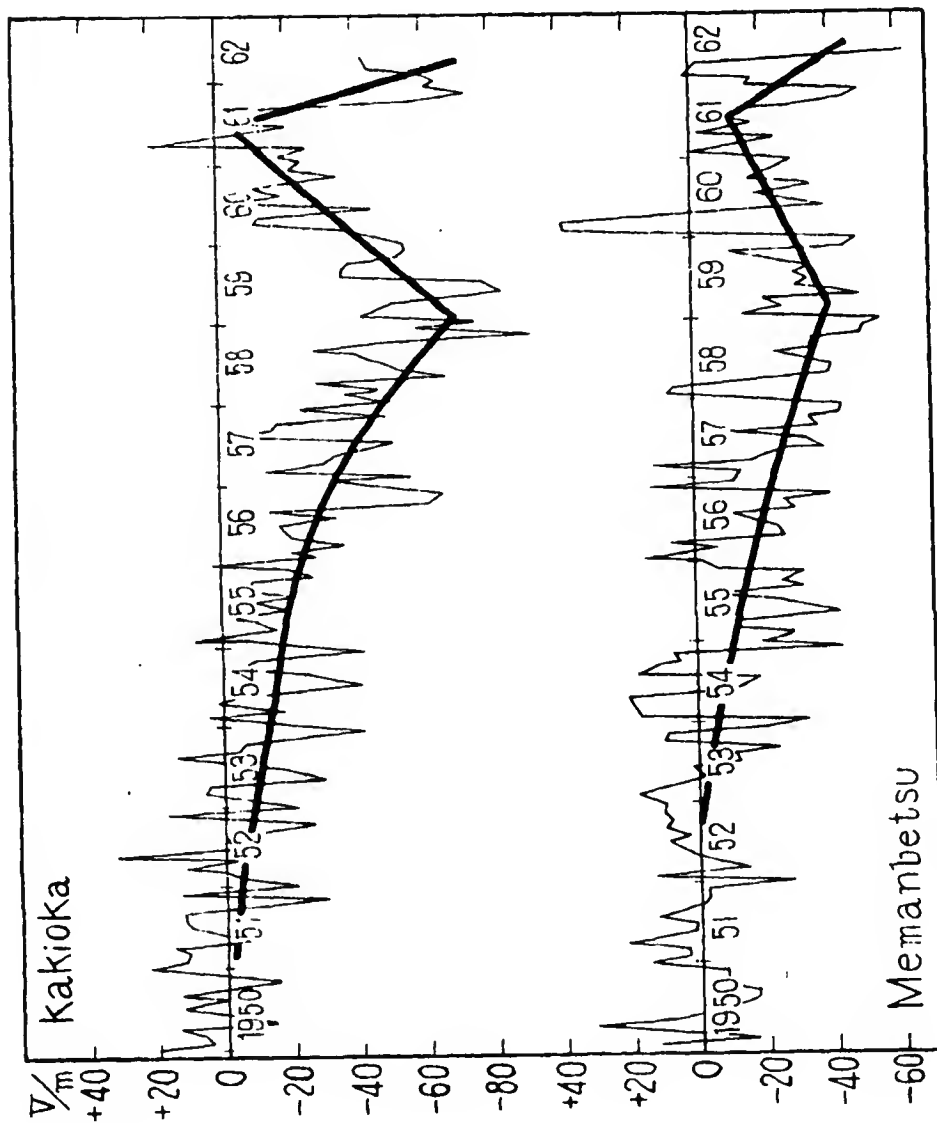


Fig. 7. Secular variation of the potential gradient at Kakioka and Memanbetsu.

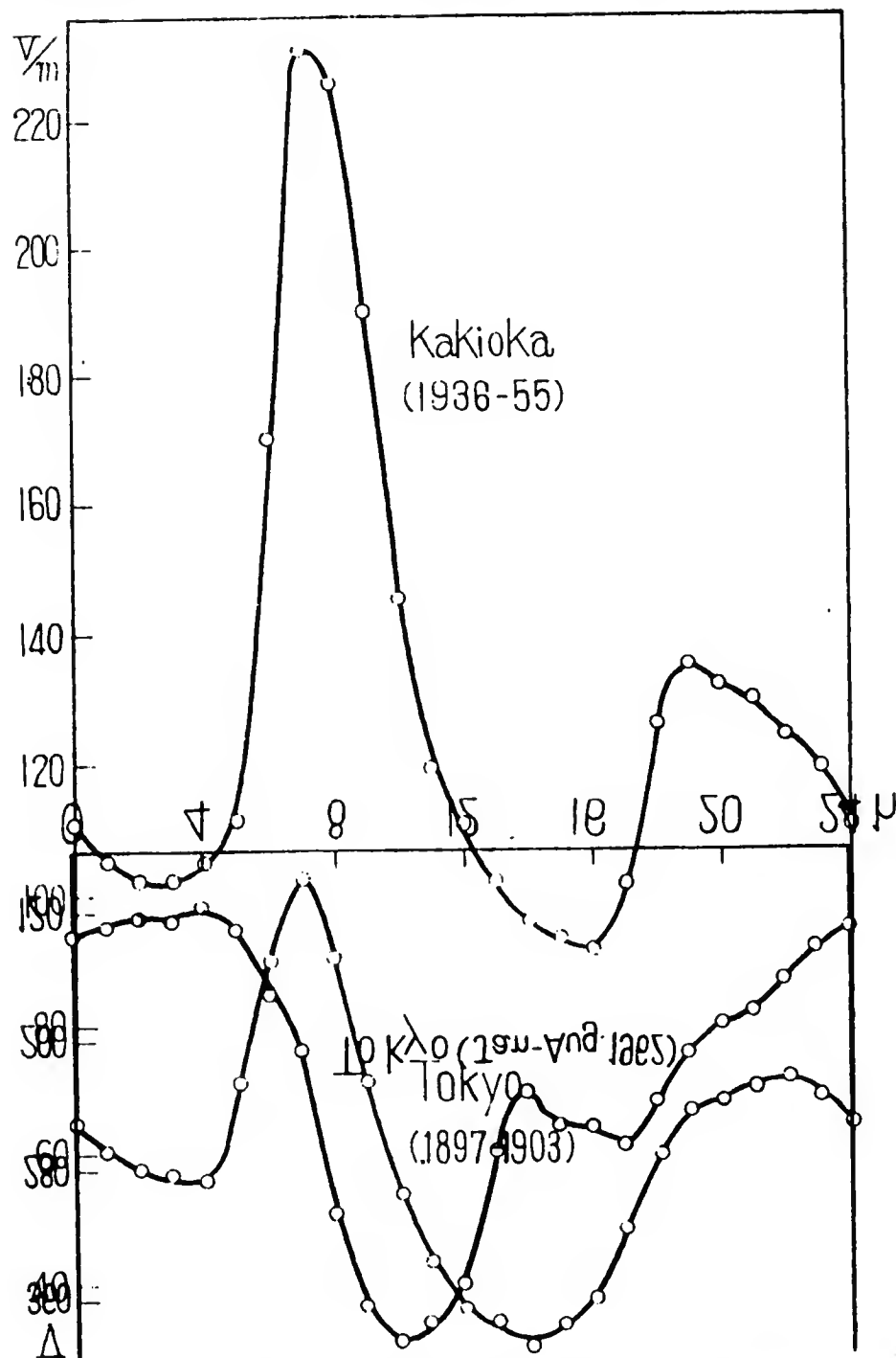


Fig. 8. Diurnal variation of the potential gradient at Kakioka and Tokyo.

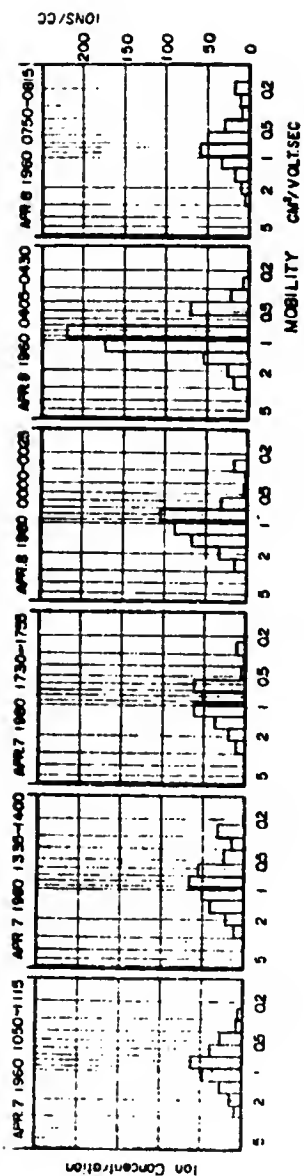


Fig. 9. Diurnal series of the Positive Ion Spectra (Tokyo)

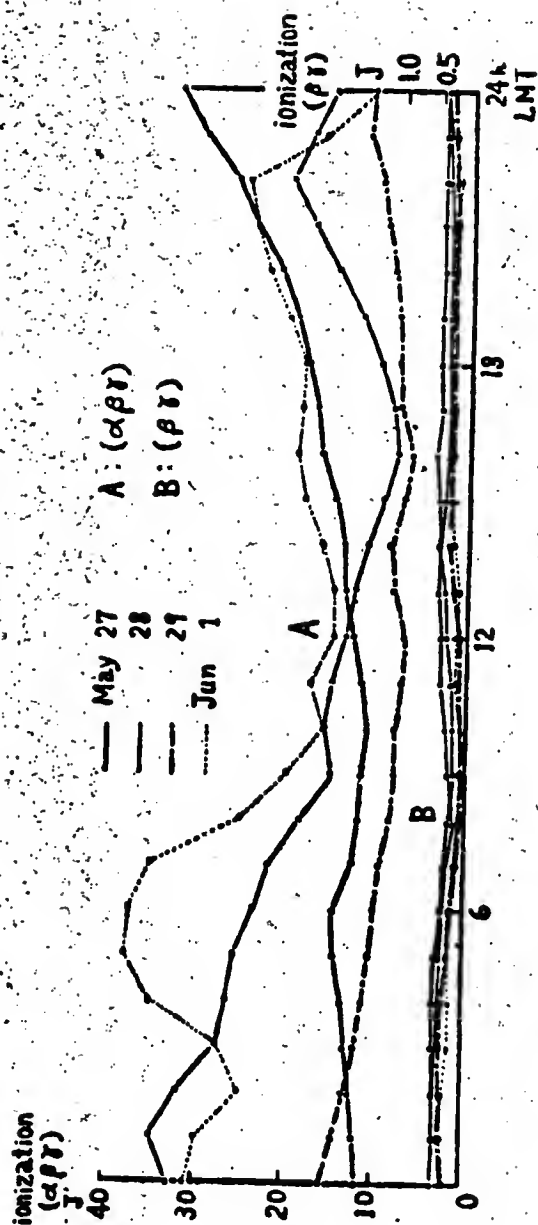


Fig. 10. The Diurnal Variation Curves of Ionization in the Atmosphere on Several fine Days.

19. 4. 1958. (Tanashi, Tokyo)

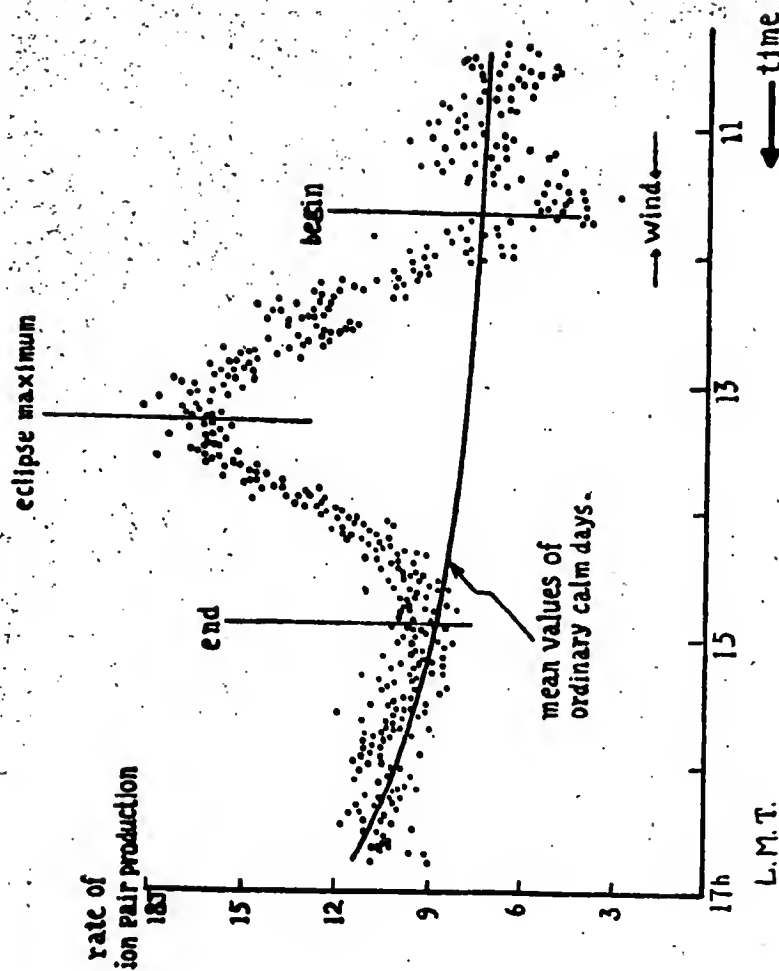


Fig. 11. The Record of the Ion Pair Production During the Solar Eclipse, April 19, 1958.

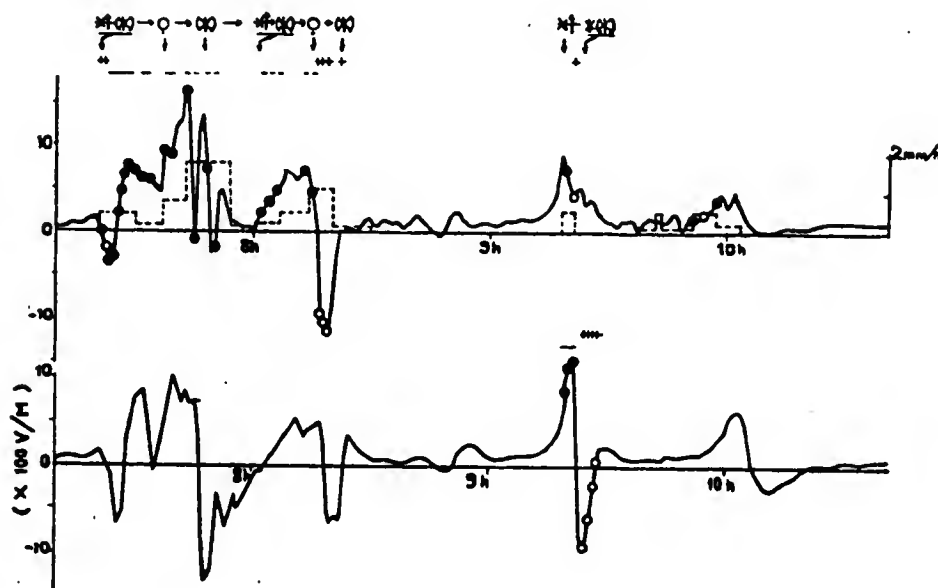


Fig. 12. An Example of the Simultaneous Observation of the Surface Electric Field, the Charge on Snow Particles The Form of Snow Particles and the Intensity of Snowfall During Snow Showers at Two Stations 1.2 km apart of each other.

Received December 17, 1962

SESSION 1.3

Report on Atmospheric Electricity in
Central Europe 1959-62

by R. Mühleisen

Preface: The following summary is based on publications, dispatched reports from "Atmospheric Electricity" in Central Europe. The author would regret it deeply, if any publication would have been disregarded, because it was not known to him. On the other side the dispatched reports and publications have been so numerous, that not every one has been mentioned. The gravity has been put on the new knowledges.

Disposition: The report is divided into various subjects:

- 1) General matters of atmospheric electricity, phenomena in fine weather.
- 2) Atmospheric electric aerology, atmospheric electric circuit and potential of the ionosphere.
- 3) Conductivity, ions, radioactivity.
- 4) Precipitation electricity.
- 5) Thunderstorms, lightnings, sferics, whistlers.
- 6) Electrical phenomena in space.
- 7) Biological action of atmospheric electricity.

1) General matters of atmospheric electricity, phenomena in fine weather.

In the International Geophysical Year registrations of the atmospheric electricity have been made at numerous stations such as: Arosa, Payerne (Switzerland), Swidrze (Poland), Murchison-Bay (Spitzbergen), Hohenpeielsenberg, Garmisch, Zugspitze, Black Forest, Eifel, Potsdam (Germany) and others. The results of these measurements

- 2 -

are manifold. The difficulties in separating the global and local influence have been explained. Therefore it must be concluded that atmospheric electrical registrations on the ground can give informations especially about the local events of atmospheric electricity in some cases, but only at excellent places and very seldom about the global events, such as the voltage between ionosphere and earth and therewith the world thunderstorm activity or about a spacious quality of the airmasses, such as the columnar resistance. The local and the global part are about equally large. There are always some informations not allowing an exact separation. This holds good for the single cases, but also very often for the temporal mean value.

Also the registration of atmospheric electricity by Saxer L. and Sigriet W.¹⁾ in Arosa (1800 - 2650 m above NN) proves that. Although Arosa is a place with great air-cleanness, the local influences can be found. Only the station in 2650 m NN shows squarized courses of the day in a few cases. Of some interest seems to be the discovered course in parallel of field at the ground and content of Ozon in the layer 0 - 20 km above the ground. The explanation of the relation between the O_3 and the columnar-resistance is the following: The percentage of O_3 increases as well as the electric field in sink processes because the columnar-resistance is getting less and the vertical-current-density is getting more.

Ierdel H.²⁾ brings the spacious atmospheric electric phenomena in connection with geophysical effects, as radioactivity of the atmosphere and the exchange. The atmospheric electric fluctuation means a quality to him which can be exploited on the synoptical way and can be used as an indication of the type of exchange.

Mühlstein R.³⁾ has continued the investigations about the atmospheric electric fluctuation at the coast of the German sea. The strong and short periodical variations of field, vertical-current and electric space-charge density have already to arise

- 3 -

on the open sea and will be caused by strong exchanges as it could be proved by registration of temperature, water-vapour and the speed of the wind and by observations of the low Sc-clouds at the same time. The exchange has to follow in big packages whereby the air near the water must to be exchanged by fresh air from a height of 100 - 300 m in a period of several minutes. The air near the water probably gets a positive space-charge by the electrode-effect, which the air from above does not possess, and as the steep changes of the atmospheric electric quality will arise at the fixed station.

The electrode-effect ⁴⁾ has also been discovered over the lake of Constance. The electric field E has been measured in various altitudes from 0 - 100 m at fixed stations and with captive-balloons. The value in an altitude of 10 m or more are just half of the value above the water surface. The measured and the calculated space-charge-density is in agreement. If these results will be transferred to the circumstances at the coast of the German sea, it can be found that the peaks of the field strength and the space-charge-density are in accordance with the very constant values of the lake of Constance.

N i n e t C. ⁵⁾ calculates a formula under consideration of the "eddy diffusion", which describes the correlation of the electric parameter of the atmosphere: space-charge, field-strength and conductivity. By the assumption of Whipple about the convection current this formula can be used in order to win the eddy diffusion coefficient by the values of the electrical quantities measured near the ground. The author has made these measurements and has got the eddy diffusion coefficient as function of the temperature-gradient, the speed of the wind and the Richardson number.

that
Ninet believes the values received by this method have come into accordance with the experiences, although he made some confined suppositions. This work is an valuable contribution to the problem "electrode-effect".

- 4 -

Reiter R. ⁶⁾ gives a summary about his registrations at the Zugspitz-massif in the last 6 years. Besides others he tries to explain some interesting observations. He found out a relation between the ratio of the small ions concentration n_+/n_- and the increasing speed of the wind. The herewith connected positive space-charge shall have the action of an exchange generator. In the evening decrease of the wind velocity the positive space-charge also disappears and herewith the atmospheric electric potential gradient sinks. That is Reiter's explanation for the sunset effect.

Kilinski E. ⁷⁾ disposed a difficulty with atmospheric electric measurements. The impairing of the isolation by spiders' webs can be prevented by rotation of the antenna such as a round vertical current plate.

2) Atmospheric electric aerology, atmospheric electric circuit, and potential of the ionosphere.

First there should be mentioned some of the general publications about the subject on atmospheric electric aerology. Israel H. ⁸⁾ describes measuring methods and measuring results in the free atmosphere in details. He puts them in connection with the conditions near the ground, and the meteorological conditions such as exchange, inversions etc.

A chapter by Georgii W. ⁹⁾ is devoted to the special atmospheric electric measuring opportunity in a glider. In his institute Reinhardt M. has instrumentated a doubleseat glider for meteorological and atmospheric electric measurements. He is able to measure the vertical component of the atmospheric electricity field with a field mill and two radioactive collectors on the wing and under the wing. Besides this the horizontal component of the potential gradient and the positive and negative conductivity of the air can be measured continuously during the flight. It can be reported about the already existing results after a concentrated exploitation.

- 5 -

M ü h l e i s e n R. and F i s c h e r H.J. ¹⁰⁾ report on the difficulties in exact measuring the atmospheric electrical field in the free atmosphere and its remedy, based on their numerous investigations with balloons and captive balloons. A special starting method has been developed in order to avoid a positive charging of the balloon team with triboelectrical effects at the suspending wire. A negative charging of the wire, what happened always during flights through the ice satisfied areas, has been cleared up by captive-balloon investigations as charge formations at rime.

The captive-balloon measurements by L u g e o n J. ¹¹⁾ give further explanations about the relation of the field and the conductivity in the lower atmosphere. The electrical quantities make possible an exact determination of the limits of atmospheric mist layers; they can be determined up to about 10 m by the conductivity. This is more exact than it is possible to derive from the course of temperature and humidity. It has been noticed that the meteorological quantities show these mist layers scarcely or even not at all.

An exploitation of the atmospheric electric work made by L u g e o n J., J u n o d A., W a s s e r f a l l e n P. and R i e k e r J. ¹²⁾ in the IGY gives some new and precise material about the course of the field and conductivity in the free atmosphere. These mean values given in the following table have been worked out from 28 atmospheric electric and 33 conductivity measurements above the Murchison-Bay and from 95 atmospheric electric and 81 conductivity sondages above Payerne (see table 1).

A comparison with former values also from other authors demonstrates that the field values in the stratosphere are eminently lower than it had been assumed in earlier times. These facts have also been worked out by M ü h l e i s e n R. and F i s c h e r H.J. ¹³⁾ Their mean values became less as well shown in table 1.

Table 1

$h_{NN}(\text{km})$	$dV/dz \text{ (V/m)}^{1)}$		$\lambda_{+}(10^{-14} \Omega^{-1} \text{m}^{-1})^{1)}$		$dV/dz(\text{V/m})^{2)}$
	Murch.B.	Payerne	Murch.B.	Payerne	Weissenau
0,007	89,0	-	1,70	-	-
0,49	-	107,3	-	2,55	-
1,0	53,1	98,3	3,27	3,07	104
3	24,5	50,7	5,13	5,32	26,2
5	13,8	18,4	8,44	8,32	12,4
10	5,3	5,2	27,1	25,3	4,4
15	3,0	3,3	68,9	66,6	1,95
20	3,5	2,3	118	143	1,40
25	0,4	1,1	180	-	0,70
32					0,35

Mean values of the potential gradient dV/dz and of the conductivity λ_{+} in the free atmosphere published by L u g e o n et al. (1) and M ü h l e i s e n u n d F i s c h e r (2)

To the global events there is a contribution by F i s c h e r H.J.¹⁴⁾
The atmospheric electrical potential gradient between earth surface and about 15 km above has been measured continuously by more than 50 balloon ascents. The ionosphere potential has been found out by integration of the altitude. The mean value was 282 kV in agreement with other authors. The precision of the measurements has been $\pm 8 \%$. The diurnal and annual courses of potential mean values agree very well with the mean values of the Carnegie measurements. But the single values fluctuate up to $\pm 30 \%$ of the mean-values. The same fluctuation can be found in the Carnegie mean values of single days. Therefore it seems not to be correct to compare single diurnal courses of stations on the continent with the mean diurnal courses on the oceans like it is sometimes done.

Fischer has found a seasonal maximum in the course of the ionosphere potential during the northern winter. He explains this in agreement with Whipple (1929) by a much larger electrical efficiency of the tropical thunderstorms. Considering all thunderstorms on the earth with the same importance, they would have their maximum of activity during the northern summer and no accordance with the mean results would be. If one gives however the tropical thunderstorms a greater weight than the other thunderstorms on the earth, a special explanation of the newest isobronch demonstration of the WMO material distributed to different degrees of latitude proves that the maximum of the thunderstorm activity is during the northern winter, indeed.

3) Conductivity, ions, radioactivity.

A great number of publications have been submitted on the subject of conductivity.

B r i c a r d J.¹⁵⁾ improves his former theories about the combination of small ions at aerosol particles. In calculation of the coefficient in the formula for the ionization equilibrium he takes in consideration, that the diffusion is not taking the normal

course, if the particle radii have the same dimension as the mean free path. For the radii more than 10^{-5} cm the deviation can be neglected. It gets new values for the combination coefficient in the radii range $0,6 \times 10^{-6}$ to 4×10^{-6} cm, which have a stronger deviation as the former ones, but they agree well with the results of Keefe, Nolan, and Rich.

Ninet's work (see 5 in chapter 1) concerns also the conditions in the ion concentration near the ground.

Besides others Reiter R. ¹⁶⁾ has registered the conductivity and the concentration of small ions at some places of his atmospheric electricity stations at the Zugspitze. Remarkable but not quite clear is the fact that the ratio n_+/n_- shall increase with the speed of the wind: For $v_w = 0$ he finds $n_+/n_- = 1,0$; for $v_w = 5 \text{ m/s}$ he finds $n_+/n_- = 2,0$.

Occasionally he finds a strong increase of the negative conductivity of the air at the sun radiated mist and fog layers. He supposes that it is caused by a photoemission by the solar UV. It does not seem to be correct, because there is no light of sufficient short wave length in the altitude of 3000 m.

There also appeared some new publications in the subject of measuring techniques. Hock A. and Schmeer H. ¹⁷⁾ describes a new small-ion counter, where they have disposed the counterfield effect by grounding the aspiration-condensator coat and by putting back the electrodes into the cylinder, where they have used double-electrometer valves in the entrance of the direct-current amplifier.

An interesting new method about the direct registration of the atmospheric small-ion spectrum has been published by Junod A., Sanger R., and Thams J. ¹⁸⁾ The authors used a measuring condenser with a linear, quickly increasing voltage, where

the currents become compensated by a bridge circuit. Not only the current voltage characteristic will be won, but also a mobility-spectrum by a thoughtful use of electronics. It is a great advantage, that all signals exist as alternating voltage and therefore the direct-current amplifier can be avoided.

H a e e n c l e v e r D. and S i e g m a n n H. ¹⁹⁾ published a new method of dust measurement using small ion dissipation. In a ionization chamber, working in the range of satisfaction, small ions will be produced with a radioactive probe. The measured ionization current changes when dusty air enters the chamber. The small ions become partly combined with the dust particles. These charged dust particles will not be measured for their lessened mobility; the decreased current is a measure for the concentration of dust. The authors show that not the dust concentration, but the product of dust concentration and medium particle radius has been measured. because of the dependence of the dissipation coefficient on the radius of the particles.

S i k s e n a R. ²⁰⁾ developed an aerosol measuring instrument at the same time, which works with the same system. Here the small ions will be produced in a separate tritium-ion generator and mixed with air in a special chamber. The content of small ions in the air will be measured with an aspiration condenser. The peculiarity is that the production of small ions, the mixing of the air, and the measuring of small ions is separated. The time of mixing is also independent of the speed of the wind and given by the speed of the air flow through the measuring condenser. Both arrangements can be calibrated only limited. The increase of small ions depends on the dissipation coefficient and this depends on the aerosol spectrum. The aerosol spectrum has a further influence on the result because the time up to the equilibrium is dependent also on the dissipation coefficient.

The mixing time at disposal has to be more than the time constant. Comparing measurements with the same aerosol spectrum can be made with this method, where it will also be the advantage of a continuous measuring. In spite of all it is not satisfying, because there will be kept only a single information.

S i k s n a R. and L i n d s a y R. ²¹⁾ developed a small-ion generator with a tritium source in a titan foil for the above mentioned instrument. Herewith they have been able to place in a small room a large activity and to produce a small ion concentration up to 5×10^6 per cm^3 of air. Of great advantage is the half-value time of the tritium of about 12 years and the assurance that no unwanted changes will happen with the aerosol.

There are also some works of interest on the subject of atmospheric radioactivity. They have only been mentioned if they are in connection with atmospheric electrical problems, such as the air conductivity near the ground, the electrode effect or the atmospheric exchange.

B u d d s E. and I s r a e l H. ²²⁾ discussed the diffusion coefficient of the radon in the air in soil. H. Israel compared the exhalation and the radon concentration in the lower atmosphere calculated with the various values of the diffusion coefficient with the measured values of these quantities. He receives the result that a value of $D = \text{about } 0,05 \text{ cm}^2/\text{sec}$ approaches best to the actual condition. This value depending on the sort of soil is about 50 to 500 times as high as the one of Budds.

L u g e n J., J u n o d A., W a s s e r f a l l a n P., R i e k s r J. ²³⁾ registered the radioactive content of the air near the ground besides the different qualities of atmospheric electricity in Paysne as well as at the Murchison-Bay (Spitzbergen).

R s i t s r R. ²⁴⁾ displayed his results of some of his investigations of the natural and the artificial radioactivity measured in his two

stations Wank and Farchant. Because these two stations have a difference in level of 1,1 km at a relative little difference of base, the author can make some declarations about the dependence of the components on the altitude. Out of it he derives the influences of the meteorological parameters on the natural and artificial radioactivity. He determines the exchange coefficient by the calculated half-value altitude and he compares it with the temperature gradient. These relations cannot be taken as the general, because they are based on the conditions in a tight valley of the mountains.

Ernst F., Prsining O., and Sedlacek M. ²⁵⁾ investigated the size distribution of the radioactive particles in the atmosphere of Vienna by using a Goetz-aerosol-spectrometer. The filter has been tested by the autoradiographic method, later the filter cut in single pieces has been investigated by a counter. They make the conclusion that the greatest activity of particles can be found in the area of less than $0,7/\mu$ Stokes' radius.

Bricard R., Pradel J., Renaux A. ²⁶⁾ employ their dissipation coefficient to work out the frequency of the dissipation of radioactive small ions on the aerosol particles of different radii. For that the size distribution by Junge has been used. It has been supposed that the RaA atoms caused by decay of radon, form small ions which combine later with the aerosol. Using the formula the distribution of the activity on the aerosol particles of different sizes can be worked out. The results have been compared with the values also measured by the authors.

4) Precipitation electricity and electrification.

Ritter R. ²⁷⁾ investigated the frequency of the signs of the potential gradient in his stations in the mountains of Wetterstein. By a statistic exploitation of the spacious measuring material he

found out the following proportions of signs during precipitation:

Table 2

Type of precipitation:	rain	rain shower	snow shower	snow fall
pos. signs of the PG:	10%	30-40 %	40-50 %	80 %
neg. " " " "	90%	60-70 %	50-60 %	20 %
change per hour:	0,8	2,5-3	2-2,5	0,9

He analysed the number of the changes of signs per hour in the various forms of precipitation in a similar way and he finds out the results in table 2.

It seems to be very interesting that the changes of signs are much more numerous in the valley than in higher altitudes. In the same work the dependence of the sign of the potential gradient on the altitude during steady precipitation in the two phases has been discussed. Above the melting zone the potential gradient is about 3 - 4 times greater than the value of fine weather, while it is negative and about $2/3$ of the value of fine weather beneath the melting zone.

- 5) Numerous and valuable work has been made about thunderstorm and thunderstorm theoriss, lightning phenomena and their electro-magnetic signals sferics and whistlers.

W o l f F. 28) discusses the present ideas of the cause of thunderstorms and the lightning-formation. Teepler's ideas about the formation of discharges have been put in the forefront again.

P ü h r i n g e r A. 29) put up for discussion a new thunderstorm theory, based on the electro-magnetic induction. In the author's opinion an electrical field will be induced by the

motion of a cloud in the magnetic field of the earth. This produces an electrical dipole moment which shall build up a strong electrical field in the outer room. The efficiency, necessary for a thunderstorm, shall be withdrawn from the kinetic energy of the wind.

M i c h n o w s k i St. ³⁰⁾ indicates the important part of the point discharge in the preservation of the charge exchange between the earth, thunder-clouds and ionosphere. Measurements of the sum of the point discharge for a longer period in Swidrze gave a result of the mean ratio of a charge run out of a point $\frac{Q_+}{Q_-} = 1,5$.

M ü l l e r - H i l l e b r a n d D. ³¹⁾ describes some interesting thunderstorm observations at Monte San Salvatore. The value of the electric field has formerly been estimated from about 20 kV/m to 330 kV/m. The author noticed only a field-strength of about 3-5 kV/m near lightning-strokes in the ground. He tries to explain whereby the strong fields have been screened by a larger space-charge area; registrations of the electric field, point discharge, precipitation current and precipitation strength of the same time support this assumption. An exact temporal analysis of the formation and discharge of a flash had been possible by the measuring of the lightning current at the place of stroke and the electrical and magnetic field-strength in a distance of 2,8 km at the same time. It had been shown that the steps of a leader stroke are extremely short. The single impulses can have a temporal interval down to 0,2 μ sec.

In another publication the author tries to extend the protective radius of lightning conductors by radioactive point discharges. At the approaching of a thundercloud, all points emit some corona currents, which will be led away by the wind as space charge. It had been asserted radioactive points could increase the point discharge current so much that the space charge cloud would

lead to catch discharge. In a laboratory experiment there was no difference noticed concerning the corona current of a radioactive point and a normal point after arising the corona discharge.

With another experiment it was however shown that a strong point discharge of 8 mA has a strong influence on the electrical field strength in the surrounding.

Outdoors the point discharge current of the radioactive points was always less than a current of non radioactive points. Obviously the ion cloud around the radioactive point delays the beginning of the corona discharge.

Müller - Hillbrand D.³²⁾ has won an interesting material about lightning frequency since 1958. With a rather narrow net of stations (115 stations) in Sweden he was able to register more than 100.000 earth flashes in 1958. These made 65 % of all registered discharges.

Malikowski G.³³⁾ determines the mean value of the diameter of a convective precipitation cell $d = 4$ km by a collective of 1000 radar observations during showers and thunderstorms. He gives a curve for the frequency distribution of these values. At the observation of echoes with the weather radar instrument it is of some interest whether a precipitation cell visible on the radar screen can be considered as a thunderstorm or a shower without lightnings. This had been undertaken by a spheric direction finding instrument by finding the position of thunderstorm centers at the same time.

Norinder H., Knudsen E.³⁴⁾ made spacious investigations about the discharge mechanism of lightnings in a free field station near Uppsala (Sweden). The collected data had been exploited. The length of the lightning path between cloud base and earth gave values of 0,6 - 2,4 km with a mean

value of 1,4 km. Observating 1135 flashes, there were 79 % between clouds and earth and 21 % within the clouds. Analysing the multiple discharges it had been displayed a decrease of the magnetic field-strength with the number of strokes. The intervals between the lightnings had been noticed from 16 thunderstorms. It was found, that the most intervals are 20 - 70 sec. At a single thunderstorm of extreme strength 80 % of the intervals had been shorter than 1 minute.

B e r g e r K. ³⁵⁾ made lightning observations with an oscillograph on the Monte San Salvatore in 1958-61. The registrations had been exploited concerning the front duration, the maximum current, the average and maximum current increase slope. On the base of this measurements there had been 4 different types of lightning discharges, which differ in front duration, maximum current, steepness of increase and current curve:

- a) flashes with leader strokes in upward direction; in general they only come from high and well grounded conductors. The form of current shows a slowly increasing with a current maximum of 20 to some 100 A;
- b) flashes with stepped leader from a negative cloud; the main discharge has a maximum current of 15 - 45 kA and a front duration of 4 - 12 μ sec;
- c) following strokes from a negative cloud. The maximum current strength is smaller. The front duration is shorter and less than 1 μ sec. in general;
- d) discharges from positive clouds to the earth with a slow current increase and a high discharge strength. A discharge exchange of more than 100 C is of no rarity.

N o r i n d e r H., K n u d s o n E., ³⁶⁾
made experimental investigations about the multiple-lightning strokes in the same lightning channel in 1956-57. Multiple lightning strokes have been regarded in the laboratory if a high ohm-resistance has been inserted in the discharge circuit. Because multiple lightning strokes can give some indications on the discharge mechanism in the thundercloud, oscillographic registrations of the strokes series and the discharge currents of natural multiple strokes. In order to registrate the front time and the discharge current three oscillographs with different time bases have been used. The electromagnetic field had been received from a frame aerial and led to the oscillograph by an aperiodical amplifier. Herewith the changes of the magnetic-field strength had been registrated and an estimate of the current changes in the lightning channel has been possible. The measuring results had statistically been exploited concerning the amplitude dispersion, front time and temporal intervals. Later on the method had been completed by day-light photography. The increase of voltage in the aerial triggered a connection circuit, which released the camera. This combined method made it possible to declare something about the discharge process in the cloud.

P a p e t L é p i n s J. ³⁷⁾ has been occupied with a theoretical work about the mechanism of the lightning discharge and the herewith existing change of the magnetic field. The author chose a method to calculate the temporal course of current in the lightning channel from the magnetic field changes measured near lightning discharges.

P r i t s c h V. ³⁸⁾ has been occupied with the problem of geological and geoelectrical influences on the place of lightning-strikes. He can confirm the opinion, that there are lightning nests. A special result was, that the danger by lightnings grows with increasing geological age of the terrain.

M i c h n e w s k i St. 39) describes an interesting observation in northern Viet-Nam, where electrical discharges had been in a cumulus cloud without any signs of existing ice crystals in the cloud. The altitude of the upper cloud limit was supposed to be 2500 m, while the 0° isotherm for this season should have been about 4000 m.

D e s s e n e H. and his coworkers⁴⁰⁾ made investigations with an installation of 100 burners which are arranged on a quadrat of a sidelength of 100 m. They tried to produce artificial cumulus clouds. During the first few experiments there have been developed sometimes tornado pipes with wind speeds of some hundreds of km/h. It had been noticed that lightning discharges ensue always along natural tornado pipes. Dessens hopes that an installed ventilator will stimulate the formation of a whirl of a tornado pipe. Dessens expects that the so called Metatron gives him the possibility for direct lightning investigations and for experiments in plasma-physics.

An earlier theoretical publication by W.O. Schumann refers to a resonance frequency of the condenser ionosphere earth. This frequency shall be about 9 c/sec. K ö n i g H.⁴¹⁾ investigated there upon atmospherics of this extremely low frequency. His receiver connected with a long-wire antenna enclosed the range from 0,5 - 13 c/sec. In fact he got signals with frequencies 8 - 9 c/sec. He believes that one part of these signals is caused by lightnings, which have excited the resonance circuit ionosphere earth to oscillations. Another part of signals arises at sun rise. König supposes, these signals would be caused by abrupt changes of the altitudes of the lower boundary of the ionosphere. Other types of signals with lower frequencies will be brought into correlation with local weather-phenomena. König has examined his interesting results by a simultaneous registration on a second station in a distance of 50 km resp. 450 km on one hand, on the other hand during the eclipse of the sun on 15.2.1961 (E.Haine).

M a l k o w s k i G. ⁴²⁾ determines the entrance-range of a sferics receiver by a decrease of the sferics frequency during a anticyclonic situation. At a field strength limit of 0,4 V/m he comes to a range of 850 km.

I s r a e l H. ⁴³⁾ compares the sunrise effect of sferics at 27 kc/sec registered at 3 different stations, Aachen 50,8° N, Tokyo 36° N, San Salvador 13,5° N. The beginning of the decrease of the sferics intensity varies from station to station during the annual course. The nearer the station is to the equator the earlier and more unregularly the effect begins.

M a t t e r n G. ⁴⁴⁾ dealt with the reception of sferics from great distances. He had built up his station on a solitary island without foreign electric installations. He is able to receive all lightning signals from the whole earth. This however leads to overlapping signals so that a lower limit of sensibility (about 50 μ V) must be fixed.

N o r i n d e r H. and K n u d s e n E. ⁴⁵⁾ investigated whistlers 1957 - 59 in order to explain the connection of thunderstorm activity and whistlers. It has been proved that only one part of flashes produces whistlers. They mostly appear in groups for a time of 1/2 to 2 1/2 hours. The longest time of observation had been 6 hours. These times favourable for whistlers have been interrupted by long periods of silence. Registrations of sferics at the same time showed that only sferics with the highest field-strength have been followed by whistlers. The exploitation of the field-course of the sferics with a harmonious analyser gave as a result that the energy maximum of the radiation is on about 5 kc/sec. A comparison between the temporal series of the multiple whistlers and the oscillographic registered multiple-lightning strokes showed accordance concerning the time intervals. Different whistler shapes had been regarded by the analysis with a "Sonagraph". One third of all registered whistlers during the

thunderstorm season 1959 could not have been put into relation of thunderstorm centers by a spheric-direction finder. All these whistlers appeared only during a short period and must have been produced in the neighbourhood of the conjugate geomagnetic point.

In another publication Norinder H. ⁴⁶⁾ supposes that the propagation of whistlers will be influenced by ionospheric irregularities. He follows the ideas of Budden, K.G. in a theoretical publication.

6. Space phenomena of atmospheric electricity

In this chapter only some investigations can be reported which are due to cosmic rays. The results come from balloon ascents made in one institute.

Waibel E. ⁴⁷⁾ determined the ionization spectrum of the cosmic rays. He was able to separate the protons from He- and Li-nuclei in the primary radiation. If one extrapolates to the limit of the atmosphere, the α -intensity is about one seventh of the proton intensity.

Erbe H. ⁴⁸⁾ finds a clear relation between the intensity in definite altitude measured by a Geiger-counter telescope and the intensity on the ground.

Ehmert A., Erbe H., Pfotzer G., Keppler E. ⁴⁹⁾ discussed the peculiarity of cosmic rays in a solar eruption in autumn 1960. During the summer season 23 balloon ascents had been made in Kiruna (Sweden). Some X-rays eruptions and injections of solar protons have been observed.

Ehmert A. ⁵⁰⁾ indicates that the experimental "rigidity spectra" of the primary cosmic protons and α - particles can be described by a variation of the electric potential of the earth

against far space. Its variation is correlated with the solar activity. The decelerating potential has a variation of 1 Gigavolt at sunspot minimum and 2,7 Gigavolt during a magnetic storm. The field is supposed to be beyond the radiation belt, as one can conclude from the intensity observations of moon rockets.

7. Biological action of atmospheric electricity.

K n o l l M., R h e i n s t e i n J., L e o n a r d G.F., and H i g h b e r g P.W. ⁵¹⁾ investigated the influence of artificial atmospheric small ions on the reaction time and the visual moment. An increase as well as a decrease of 7 % of the reaction time has been found for densities of about 10^3 to 10^6 ions/cm³, if the subject is breathing through the mouth. There is no influence when the subject is breathing through the nose. The polarity of ions does no matter at all. An influence for the optical moment - i.e. the shortest time between two flashes, which can be recorded separately - has not been found. The influence of ions resembles the effect of many drugs on the human system.

K ö n i g H. ⁵²⁾ has registered the atmospheric impulse radiation since four years. The receivers are able to record all spheres in three entrance ranges: 100, 300 and 1000 km. Until now there was not found any clear relation with aspects of illness on human beings.

R e f e r e n c e s

- 1) Saxer, L., Sigrist, W.: Tages- und Jahresgänge der luftelektrischen Elemente in Arosa.
Arch.Met.Geoph.Biokl. 12 (1961) 366-75 Ser.A
- 2) Israel, H.: Meteorologische Vorgänge im Spiegel der Luftelektrizität.
Annali di Geofisica 13 (1960) 327-367
- 3) Mühleisen, R.: Luftelektrische Verhältnisse im Küstenaerosol I.
Arch.Met.Geoph.Biokl. 11 (1959) 93-108 Ser. A
Mühleisen, R.: Luftelektrische Verhältnisse im Küstenaerosol II.
Arch.Met.Geoph.Biokl. 12 (1962)
- 4) Mühleisen, R.: Electrode effect measurements above the sea.
J.Atm.Terr.Phys. 20 (1961) 79-80
- 5) Ninet, C.: Relation entre les paramètres électriques de l'atmosphère et la diffusion turbulente.
Dissertation Université Paris 1961
- 6) Reiter, R.: Luftelektrisches Erscheinungsbild des Südföhne in den Nordalpen nach synoptisch-klimatologischen Untersuchungen im Wettersteinsgebirge von 1955-1959.
Arch.Met.Geoph.Biokl. 12 (1960) 72-124 Ser.A
- 7) Kilinski, E.: Verbesserung der Auffangvorrichtung des Potsdamer Vertikalstromgerätes.
Z.Met. 12 (1958) 352-54
- 8) Israel, H.: in W.Hesse Handbuch der Aerologie.
Leipzig (1961) 646-701
- 9) Georgii, W.: in W.Hesse Handbuch der Aerologie.
Leipzig (1961) 274-277
- 10) Mühleisen, R., Fischer, H.J.: Luftelektrische Aerologie.
Beitr.Phys.d.Atm. 34 (1961) 3-14
- 11) Lugeon, J.: Elctressendages à deux conductibilités pour la détection du niveau de la vase atmosphérique.
Act.Soc.Helv.Bienne (1961) 93-95

- 12) Lugeon, J., Juned, A., Wasserfallen, P., Ricker, J.:
Mesures des Parasites atmosphériques d'Electricité
atmosphérique et de Radioactivité de l'air à
Murchison-Bay (Spitsberg), Payerne et Zurich.
Zürich 1960
- 13) Mühleisen, B., Fischer, H.J.: Messung des luftelektrischen
Feldes in der freien Atmosphäre.
Naturwiss. 47 (1960) 36-37
- 14) Fischer, H.J.: Die elektrische Spannung zwischen Ionosphäre
und Erde.
Diss. Stuttgart 1962
- 15) Bricard, J.: La fixation des petits ions atmosphériques sur
les aérosols ultra-fins.
Geof.pura e Appl. 51 (1962/I) 237-242
- 16) Reiter, R.: Relationships between atmospheric electric
phenomena and simultaneous meteorological conditions.
Final Report, Contract AF July 1960.
- 17) Heck, A., Schmeer, H.: Über ein Gerät zur störfeldfreien
Luftionenmessung....
Z.f.angew.Phys. 14 (1962) 398-404
- 18) Juned, A., Sängler, R.; Thams, J.Ch.: Enregistrement direct du
spectre des petits ions atmosphériques.
J.de Math.Phys.Appl. 13 (1962) 272-278
- 19) Hasenclever, D., Siegmann, H.: Neue Methode der Staubmessung
mittels Kleinionenanlagerung.
Staub 20 (1960) 212-218
- 20) Sikana, R.: An ionometric counter for condensation nuclei.
Geof.pura e Appl. 50 (1961) 23-36
- 21) Sikana, R., Lindsay, R.: Air ions produced by a tritium-ion
generator.
Arkiv för Geofysik 3 (1959) 123-154
- 22) Israel, H.: Der Diffusions-Koeffizient des Radons in
Bodenluft.
Z.f.Geoph. 27 (1961) 13-17
- 23) Lugeon, J., Juned, A., Wasserfallen, P.:
Mesures d'électricité atmosphérique et de la
radioactivité de l'air à Murchison-Bay (Spitsbergen)
pendant l'AGI 1957-58
Actes de la Société Helvétique des Sciences
Naturelles Lausanne (1959) 122-126

- 24) Reiter, E.: Neue Ergebnisse alpiner Luftstrahlungsaktivitätsmessungen.
Zbl.f.biol.Aerosolforsch. 9 (1960) 3-27
- 25) Ernst, F., Preining, O., Sedlacek, M.:
Sizing of the Fall-out at Vienna.
Nature 195 (1962) 986-7
- 26) Bricard, J., Pradel, J., Renaux, A.:
Le Teneur de l'air en petits et gros ions radioactifs.
Geof.pura e Appl. 50 (1961) 235-242
- 27) Reiter, E.: see 16
- 28) Wolf, F.: Gewitter
Phys.Blätt. 17 (1961) 501-512
- 29) Pühringer, A.: Die elektromagnetische Induktion als Grundlage einer Gewittertheorie.
Arch.f.Met.Geoph.Biokl. 12 (1961) 262-70 Ser.A
- 30) Michniewski, St.: Point discharges in the interchange of electric charge between the earth and the atmosphere.
Acta Geoph.Polon. 5 (1957) 123-134
- 31) Müller-Hillebrand, D.: Beeinflussung der Blitzentladung.
ETZ A 82 (1961) 232-249
- 32) Müller-Hillebrand, D.: Lightning counter and results obtained in Sweden during the thunderstorm period 1958.
TVF, tekn.-vet.Forsk. 30 (1959) 1-16
- 33) Malkowski, G.: Über die Größe konvektiver Niederschlagszellen auf dem Radarschirm.
Geol.Beitr.z.Geoph. 70 (1961) 51-57
- 34) Norinder, H., Knudsen, E.: Some features of thunderstorm activity.
Arkiv för Geofys. 3 (1961) 367-374
- 35) Berger, K.: Frontzeit und Anstiegsteilheit des Blitzstromes bei Erdblitzes.
FKH 11 Zürich October 1962
- 36) Norinder, H., Knudsen, E.: Lightning discharge paths photographed in day-light and analysed by simultaneous variations of magnetic field components.
Ark.för Geof. 3 (1961) 375-390

- 37) Papet-Lépine, J.: Electromagnetic radiation and physical structure of lightning discharges.
Arkiv för Geoph. 3 (1961) 391-400

Papet-Lépine, J.: Rayonnement electromagnetique et structure interne des eclairs.
Dissertation Université de Paris Dex. 1959

- 38) Fritsch, V.: Geophysikalische Einflüsse auf die Blitzgefährdung.
Scientia 54 (1960) 1-7

- 39) Michnowski, St.: On the observation of lightning in warm clouds.
Private communication.

- 40) Dessens, H.: Un physicien francais cherche a canaliser la foudre.
Le Monde, 27.Juli 1962

- 41) König, H.: Atmosferics geringster Frequenz.
Z.f.angew.Phys. 11 (1959) 264-274

König, H., Haine, E.: Registrierung besonders niederfrequenter elektrischer Signale während der Sonnenfinsternis am 15.2.1961.
Z.f.angew.Phys. 13 (1961) 264-74 and 478-480

- 42) Malkewski, G.: Zum Einzugsbereich eines Sferic.-Empfänger.
Mat.Rundsch. 12 (1959) 64

- 43) Israel, H.: On the sun rise effect of sferic activity at 27 kc.
Z.f.Geoph. 26 (1960) 138-143

- 44) Mattern, G.: private communications.

- 45) Nerinder, H., Knudsen, E.: Lightning discharges as a source of whistlers.
Ark.för Geof. 3 (1960) 255-288

Nerinder, H., Knudsen, E.: Multiple lightning discharges followed by whistlers.
Ark.för Geof. 3 (1960) 289-298

Nerinder, H., Knudsen, E.: Occurrence of different kinds of whistler activity.
Ark.för Geof. 3 (1961) 347-366

- 46) Norinder, H.: Some comments on the penetration of whistlers through ionospheric layers.
Planet Space Sci 2 (1960) 261-262
- 47) Waibel, E.: Messungen von Primärteilchen der kosmischen Strahlung.
Mitt.a.d.MPI f.Aeronomie 1 (1959)
- 48) Erbe, H.: Auswirkungen der Variationen der primären kosmischen Strahlung auf die Mesonen- und Nukleonenkomponente am Erdboden.
Mitt.a.d.MPI f.Aeronomie 2 (1959)
- 49) Pfozser, G., Ehmert, A., Erbe, H., Keppler, E.:
X-Ray Bursts in the auroral zone on Sept. 27th October 1st and 2nd 1960. Space Research II.
Proc.of the 2nd Int.Space Science Symp.Florence
April 1961, 876-886
- Ehmert, A., Erbe, H., Pfozser, G.:
Peculiarities of the outburst of solar high energy particles on Nov.1960. Space Research II.
Proc.of the 2nd Int.Space Science Symp. Florence
April 1961, 778-786
- 50) Ehmert, A.: Electric field modulation.
Space Research I.
Proc.of the 1st Int.Space Science Symp. Nice,
Jan. 1960, 1000-1008
- 51) Knoll, M., Rheinstei, J., Leonard, G.P., Highberg, P.W.:
Influence of Light Atmospheric Ions on Human Visual Reaction Time.
Proc.of Int.Conf.on Ionization of the Air, Oct.1961
18, 1-25
- Rheinstei, J.: Der Einfluss von künstl.erzeugten atm. Ionen auf die einfache Reaktionszeit und auf den optischen Moment.
Dissertation TH München (1960)
- 52) König, H.: Atmosphärisch-elektrische Untersuchungen am Meteorologischen Observatorium Hamburg.
DWD Hamburg

SESSION 1.4

Atmospheric Electricity Research

in

Great Britain, Ireland, Africa and New Zealand.

W.C.A. Hutchinson,

Durham University, England.

1. Introduction
2. Ionization in the Atmosphere
3. Potential Gradient and Space Charges
4. Point Discharge and Precipitation Currents
5. Thunderstorm Electricity
6. References

1.

1. Introduction

The purpose of this paper is to present a survey of research in Atmospheric Electricity performed in the countries concerned and reported since the Second Conference on Atmospheric Electricity in 1958. The survey is not intended as an index to all the relevant literature, nor is the space allotted to any item to be regarded as a measure of its importance. I have arbitrarily left out work on atmospheric and electromagnetic wave propagation. To make the picture more complete it is well to refer to the present quite considerable and wide-spread interest in the subject of Atmospheric Electricity in these countries.

I will mention five centres in England. At Leatherhead the Electrical Research Association with over 1000 voluntary observers has since 1950 collected data on thunderstorms in Britain. At Imperial College, London, the experimental and theoretical studies of the electrical properties of ice and water are proceeding in Professor Mason's Sub-Department, and the work of Dr. Browning and Dr. Ludlam (1962) on the airflow in convective storms may well lead to a new approach to the problem of thundercloud electrification. Dr. Wormell's group at Cambridge University are extending their investigations on ions and Aitken nuclei, and are also studying low frequency fluctuations in the earth's electric field and the field spectrum of near lightning flashes. Dr. Latham, now at the Manchester College of Science and Technology, is continuing his studies on the frictional electrification of ice. At Durham University Dr. Chalmers' group are investigating precipitation and air-earth currents with mobile as well as static apparatus, point discharge, space charge, and electrical effects associated with water and ice. In New Zealand, at Auckland University, Professor Kreielsen is concerned with potential gradient and point discharge effects at balloon altitudes. There are reports from three centres in Ireland. Professor Pollak and his group at the Dublin Institute for Advanced Studies are working on the electrical equilibrium of aerosols and ice-nucleus concentration determinations, and have constructed a small portable photoelectric nucleus counter. At University College, Dublin, under Professor Nolan, research is on charged and uncharged nuclei and the application of the Boltzmann Law to earlier observations. Dr. O'Connor and his group at

2.

University College, Galway, are engaged in a study of natural sources of Aitken nuclei and space charge.

The African continent, with its fine opportunities for research in tropical and sub-tropical regions, now has several centres. In South Africa, at the Bernard Price Institute of Geophysical Research, Johannesburg, work under Dr. Malan includes the study of lightning flashes of various types, lightning photography, the study of upward discharges above clouds, and flash counting techniques. Also in South Africa, in the University of Natal, at Durban, Professor Clarence's Department is continuing research on whistlers and lightning. Observations are now being made at the University College of Sierra Leone, at Fourah Bay, of point discharge and precipitation currents. At University College, Ibadan, point discharge currents are being studied, and an interesting investigation of lightning by sound-ranging on the thunder has also begun. Other centres in Africa where there have been projects for Atmospheric Electricity research are at Salisbury, Southern Rhodesia, Makerere University College, Uganda, and University of Nigeria, Nsukka.

2. Ionization in the Atmosphere

The time required for a cloud of uncharged nuclei to reach equilibrium has been further investigated by Rich⁽¹⁾, Pollak⁽²⁾ and Metnieks⁽²⁾ (1962). Their calculations involve integrating the equations for the rate of change of concentration of small ions and charged nuclei respectively:

$$\frac{dn}{dt} = q - \alpha n^2 - \eta_0 n N_0 - \eta n N, \text{ and}$$

$$\frac{dN}{dt} = \eta_0 n N_0 - \eta n N.$$

Here n , N are the concentrations respectively of small ions and charged nuclei, assuming equal numbers for either sign, and N_0 the concentration of uncharged nuclei. The number of small ion pairs produced per cm^3 per sec is q , and η , η_0 are the appropriate combination coefficients. It is assumed that

(1) General Electric Company, Schenectady, U.S.A.

(2) Dublin Institute for Advanced Studies, Ireland.

3.

multiple charging or recombination of nuclei may be neglected. The authors started with initial values $N_0 = 10^4 \text{ cm}^{-3}$ and $n = 950 \text{ cm}^{-3}$ and $q = 1.6 \text{ cm}^{-3} \text{ sec}^{-1}$ and considered three different values for the fraction of nuclei charged at equilibrium, corresponding to three different values of nucleus radius. The results of the calculation show how much more slowly the charged nuclei approach their equilibrium concentration compared with the small ions, except for very small nuclei. With their arbitrary initial conditions the authors found that for nuclei of radius $3.6 \times 10^{-6} \text{ cm}$ n is at its equilibrium value after 7 minutes whereas N takes nearly an hour to reach 90% of its equilibrium value. These results together with the recent history of an air mass may be used to estimate whether the nuclei in it are in charge equilibrium. In one observation, however, upwind of a town, and where charge equilibrium might have been expected, the concentration of charged nuclei was only 0.6 to 0.8 of its equilibrium value, perhaps of undetected sources of nuclei.

Pollak and Metnicko⁽³⁾ (1962) measured the rate at which a stored aerosol approaches charge equilibrium. Nuclei of various sizes were produced by heating a nichrome resistance-wire inside a 4.2 m^3 balloon. At intervals during the decay of the resulting aerosol they took a sample and measured the fraction of the nuclei charged. Simultaneously another sample was brought to charge equilibrium, using a weak α -ray source, and the fraction of charged nuclei measured. A state of charge equilibrium was recognized when the fractions for the two samples were equal. For stored nuclei of equivalent radius $3 \times 10^{-6} \text{ cm}$ and concentration $22,000 \text{ cm}^{-3}$ equilibrium was reached within 15 min. As the size and concentration increased so did the time taken. Nuclei of radius 10^{-5} cm and in concentration falling with time from 234×10^3 to $59 \times 10^3 \text{ cm}^{-3}$ required several hours. The largest had not reached it even after several days. These results confirm the experimental predictions described above.

(3) Dublin Institute for Advanced Studies, Ireland.

4.

The use of an α -source in bringing an aerosol to charge equilibrium has been investigated theoretically and experimentally with a stored aerosol by Flanagan and O'Connor⁽⁴⁾ (1961). They conclude that it provides the best method at present available to test for charge equilibrium.

Following work briefly reported by Nolan⁽⁵⁾ (1955) at the First Conference on Atmospheric Electricity the problem of the equilibrium concentrations of charged and uncharged nuclei in air has been further examined by Keefe⁽⁶⁾, Nolan⁽⁶⁾ and Rich⁽⁷⁾ (1959) by applying the Boltzmann Distribution Law, assuming that because of their frequent collisions with small ions the particles should be in charge as well as in thermal equilibrium. A charged particle carrying x electronic charges e is treated as a spherical conductor of radius r so that it has electrical energy $\frac{1}{2} x^2 e^2 / r$ in addition to the energy E_0 of an uncharged particle. The particle energy is thus given by

$$E = E_0 + \frac{1}{2} x^2 e^2 / r$$

By Boltzmann's Law the number in unit volume $N(E)$ having energy E is given by

$$N(E) = Ag(E)e^{-E/kT}$$

where A is a constant and $g(E)$ is the statistical weight of the energy state E . Since a particle has the same energy whether its charge is positive or negative the statistical weight of the energy state $x > 0$ is $g_x = 2$. Hence the number per unit volume with x elementary charges regardless of sign is

$$N_x = 2 N_0 \exp(-\frac{1}{2} x^2 e^2 / r kT)$$

where N_0 is the concentration of uncharged particles and $|x| > 0$. If the numbers of positive and negative particles are equal, the number per unit volume carrying x elementary charges of one sign is $\frac{1}{2} N_x$. Writing $y = \frac{1}{2} e^2 / r kT$ the total number of charged particles of one sign in unit volume is given by

-
- (4) University College, Galway, Ireland
 (5) University College, Dublin, Ireland
 (6) University College, Dublin, Ireland
 (7) General Electric Company, Schenectady, U.S.A.

5.

$$\begin{aligned} N/N_0 &= e^{-y} + e^{-4y} + e^{-9y} + \dots \\ &= -\frac{1}{2} + \sqrt{\frac{\pi}{y}} \left(\frac{1}{2} + e^{-\pi^2/y} + e^{-4\pi^2/y} + e^{-9\pi^2/y} + \dots \right) \end{aligned}$$

The latter form is more convenient for the larger particles, say $r > 2 \times 10^{-6}$ cm, when all the exponential terms are negligible compared with $\frac{1}{2}$, so that

$$N/N_0 = -\frac{1}{2} + \frac{1}{2} \sqrt{\pi/y}$$

When $r > 2 \times 10^{-6}$ cm, and if the total concentration $Z = N_0 + 2N$, then

$$\begin{aligned} Z/N_0 &= \sqrt{\pi/y} \\ &= \sqrt{(2\pi r k T / e^2)} \\ &= K/r \text{ where } K \text{ is constant.} \end{aligned}$$

The values of Z/N_0 so deduced are in good agreement with the observations of Nolan and Kemman (1949) on the equilibrium charge distribution of nuclei, derived from hot platinum, in the size range $0.7 \times 10^{-6} < r < 14 \times 10^{-6}$ cm.

It is further shown that for the larger radii the Boltzmann Law treatment predicts an average charge per particle of $\sqrt{(2r k T / \pi)}$. For cloud droplets of radius 5×10^{-6} cm this would give a specific charge of 6.8 e.s.u. cm^{-1} . The average electrical energy per particle is shown to be $\frac{1}{2} k T$, the value to be expected from the classical law of equipartition of energy if the charge on a particle is regarded as a coordinate for one degree of freedom, the energy being proportional to the square of the charge.

Keefe, Nolan and Rich then apply the Boltzmann Law to an aerosol in charge equilibrium to deduce the ratios of the various combination coefficients for ions and nuclei when $r > 10^{-5}$ cm, but not for the smaller particles, the values of these ratios agree well with those deduced from earlier formulae based on diffusion of ions and ionic mobility - the "diffusion-mobility formulae".

An experimental investigation of ionization equilibrium in maritime air has been made by O'Connor and Sharkey⁽⁸⁾ (1950) on the west coast of Ireland. Upwind of the site there was no source of man-made nuclei within 15 km and no major source within 1500 km. Assuming that the Boltzmann Law applies,

(8) University College, Galway, Ireland

6.

particles of a given size should have a definite fraction of their number charged. O'Connor and Sharkey determined the radii r of nuclei in the sea air from the diffusion coefficient found using a diffusion box and photo-electric nucleus counters. They also measured the total nucleus concentration Z and that of uncharged nuclei N_0 . A graph of Z/N_0 plotted against r showed general but by no means complete agreement with the theoretical curve based on the Boltzmann law. The authors note particularly the frequent large and erratic fluctuations in Z when its average value was high, and claim that on these occasions equilibrium studies were impracticable except by enclosing a large sample in a gasometer. They discuss the possible lack of equilibrium due to the intrusion of small uncharged nuclei from natural sources on the sea shore.

Keefe and Nolan⁽⁹⁾ (1961, 1962) have suggested a model for the capture of small ions by uncharged nuclei. When $r < 10^{-7}$ cm the combination is assumed to be due mainly to simple kinetic theory collision effects with the effective target cross-sectional area increased by a factor due to electrical image forces. For large nuclei, when $r > 10^{-5}$ cm, diffusion effects are predominant. In the intermediate range with r about 10^{-6} cm, as in the air at sea level, capture is thought to be due jointly to both mechanisms. The authors calculated the combination coefficient for ions and uncharged nuclei and found moderately good agreement with values observed, but they emphasize the lack of good experimental data.

A study of nucleus and ion concentrations has also been made at Cambridge. The work, by Adkins and by Law⁽¹⁰⁾, is referred to later.

5. Potential Gradient and Space Charge

The fact that local concentrations of space charge often seriously modify the electric field near the ground in all weather conditions, but particularly in disturbed weather, has been emphasized by Adkins⁽¹¹⁾ (1970). He made continuous records of potential gradient with a field mill, of space charge concentration using a steel wool filter connected to a vibrating reed

(9) University College, Dublin, Ireland

(10) Cambridge University, England

(11) Cambridge University, England

7.

electrometer, and of small ion concentration with an Ebert ion counter. In fine weather he found large fluctuations in space charge concentration which made its mean value difficult to estimate, though it would probably be about $+2 \text{ pC m}^{-3}$. On several occasions in undisturbed weather he noted a close correspondence between the records of space charge and potential gradient. Sometimes this was associated with exhaust smoke from passing traffic; sometimes the records followed a similar course for an hour or more, usually in quiet, stable conditions, when the observed space charge concentration changes would need to reach up some tens of metres to account for the observed field variations. From his measurements in disturbed weather Adkins finds evidence for four processes. These are

- (a) the electrode effect (which he discusses in detail),
- (b) the modification of the potential gradient within some tens of metres of the ground by large-ion space charges resulting from point discharge, the small ion density remaining almost unaffected,
- (c) in heavy rain, modification of the potential gradient by space charges of small ions produced by splashing (Adkins reproduced this effect in a laboratory study and showed that the charge is proportional to the existing field), and
- (d) the control of the potential gradient near the ground by regions of high space charge associated with a column of rain.

Adkins discusses the effective current due to splashing both in steady rain and in heavy rain.

Lav⁽¹²⁾ (1961a,b) has developed an automatic condensation nucleus counter operating a pen recorder to study the vertical distribution of nuclei within 3 m of the ground in connexion with studies of space charge concentration. His unpublished work shows that convection plays an important part in the vertical transfer of electric charge.

The space charge concentration near the ground has been deduced by Smiddy and Chalmers⁽¹³⁾ (1959) from measurements at two heights using Smiddy double field mills to minimize field distortion. In fair weather a

(12) Cambridge University, England

(13) Durham University, England

8.

small negative space charge observed is explained in terms of radioactivity of the ground, and, in heavy rain, concentrations of negative charge up to 1000 pc m^{-3} are reported. The authors suggest that the lack of agreement with their simultaneous measurements using Obolensky filtration apparatus is due to the presence of small ions.

Following the construction by Stein⁽¹⁴⁾ (1958) of a field mill to be carried by a radiosonde balloon, an ingenious double field mill for radiosonde working has been designed and made by Currie and Kreibitz⁽¹⁵⁾ (1960). The stator and rotor members each comprise the opposite quadrants of a circular plate. With the two stators connected together the output is proportional to the mill self-charge if the two rotors move in phase but proportional to the external potential gradient if the rotors maintain a relative displacement of 90° . Errors in field measurement due to the charge on the instrument are thus automatically eliminated. The device has now been prepared for carriage in a glider of the Imperial College Gliding Club for thunderstorm investigations in England.

Adams⁽¹⁶⁾ (1960) has designed a field mill with overall negative feedback giving a very closely linear relation between output and field to be used in conjunction with an unshielded air-earth or rain current continuously recording system. The mill output is fed via a differentiating circuit into the current amplifier in such a way as to give compensation for the displacement current which is proportional to the rate of change of field. The apparatus has a time constant of 20 seconds excepting thunderstorms it is suitable for all weathers.

Wildman⁽¹⁷⁾ (1960) has devised a field mill suitable for use when the signal due to the conduction current is no longer small compared with the induction signal. His machine rotor has two concentric rings of holes covering and uncovering two sets of insulated studs, giving two separate signals with different dependence on field and conduction current, allowing the effects of these two to be distinguished.

(14) Auckland University, New Zealand

(15) Auckland University, New Zealand

(16) Durham University, England

(17) Durham University, England

4. Point Discharge and Precipitation Currents

A new method of measuring point discharge current down a tree has been introduced by Maund and Chalmers⁽¹⁸⁾ (1960). The ions leaving a discharging point cause a reduction in the potential gradient downwind. With one field mill upwind and another downwind the measured change in potential gradient can be used to find the point current. Although the method is indirect, no modification of the discharging object is necessary. The authors found evidence that a tree in full leaf gives much less point discharge current than had previously been assumed, a matter of importance in discussing the total charge brought to earth.

Milner and Chalmers⁽¹⁹⁾ (1961) report measurements of potential gradient and discharge current from a point fixed 2 m above a horse-chestnut tree 13 m high. For a given value of upwind speed their results show a linear relation between point current and potential gradient. These authors also describe a new method of measuring point discharge current down a tree. They drilled two holes through the bark of a lime tree, one 3 m above the other, and inserted tubes containing mercury to make electrical contact with the sapwood, connecting the leads to a galvanometer. This effectively short-circuited that section of the tree and the current measured was almost all the point discharge current. Here too they found a linear relationship with potential gradient, and some indication that a tree gives less point current when in leaf. Further observations with the same apparatus, by Chalmers (1962), underline the need to exercise caution when interpreting point discharge records. He reports that the tree current is not only always less than that through an artificial point, but that during the rapid field changes accompanying lightning the tree current has a quite different course from that of the artificial point, which follows the electrometer record in the usual way. An approximate relationship embracing the linear law for current to an earthed point has been deduced theoretically by Chalmers⁽²⁰⁾ (1961); the current $i = 2\pi\epsilon VW$ where ϵ is the electric permittivity of air, V the potential gradient and W the wind speed.

(18) Durham University, England

(19) Durham University, England

(20) Durham University, England

10.

Using Adamson's field-change compensated exposed collector system (1960) Ramsay and Chalmers⁽²¹⁾ (1960) have measured the current brought to earth during continuous non-stormy precipitation. The comparatively short time constant of 20 sec enabled them to examine in greater detail than before the connexion between current density and potential gradient. This was reasonably linear for observations in the winter 1957-8 and of the well-known form $I = a(F + C)$ where F is the potential gradient and a and C are constants. Correlation was poor in the summer of 1958. The connexion is most nearly linear during sleet and "wet snow", and supports the earlier conclusions of Chalmers (1956, 1959) that in nimbostratus clouds the precipitation, when in the form of snow, receives a negative charge, leaving positive behind in the cloud; but when it melts it acquires a positive charge, leaving negative behind.

5. Thunderstorm Electricity

A new theory of thunderstorm electrification has been advanced by Latham and Mason⁽²²⁾ (1961b). It is based on the results of their detailed laboratory experiments which are in excellent agreement with their theory of electric charge transfer associated with temperature gradients in ice by a kind of thermoelectric effect (1961a). To quote one of the authors, Mason (1961): "The positive hydrogen ions (protons) and the negative hydroxyl ions (OH-), formed by the thermal dissociation of a small fraction of the ice molecules, become separated under the influence of a temperature gradient. If we imagine a steady temperature difference maintained across a piece of ice, the warmer end will initially possess higher concentrations of both positive and negative ions. Ions of both types will diffuse down this concentration gradient towards the colder end, but because the mobility of the positive ions is at least ten times that of the negative ions, they will move ahead and produce an excess of positive charge in the colder part of the ice."

This charge transfer process is considered to operate, in a storm when supercooled water droplets captured by falling soft hail pellets, freeze on

(21) Durham University, England.

(22) Imperial College, London.

11.

contact, throw out small positively charged splinters, and so leave a negative charge on the hailstone. This charged splinter production was verified in the laboratory by the authors, working with a simulated hail pellet growing by accretion of supercooled water droplets. They confirmed the earlier experimental findings of Mason and Maybank⁽²³⁾ (1960) who observed the splintering and usually negative charging, on freezing, of a supercooled water droplet suspended on an insulated fibre. While a droplet is freezing it will have a liquid centre at 0°C and a solid outside part at a lower temperature, giving a radial temperature gradient in the ice shell. According to the charge transfer process there will be an excess of positive space charge in the outer layers of ice, and, when the droplet bursts, the outer layer will tend to carry off positive charge, leaving the residue negatively charged. Such negatively charged hailstones in falling away from the positive splinters would produce a positive dipole in agreement with that in a thundercloud.

Latham and Mason (1961b) proceed to calculate the rate of charge production in a thundercloud. For soft hail pellets of average radius \bar{R} and fall velocity v the volume swept out per sec is $\pi \bar{R}^2 v$ and so each pellet makes $E \pi \bar{R}^2 n_d v$ collisions with supercooled droplets in concentration n_d if E is the collision efficiency. If there are n_h hail pellets per unit volume there are thus $E \pi \bar{R}^2 n_d n_h v$ collisions per unit volume per second. The soft hail has an equivalent precipitation intensity p , i.e. the mass of water falling per unit area per second given by $\frac{4}{3} \pi \bar{R}^3 n_h v$ where $\bar{\rho}$ is the mean density of the hail. In terms of p the number of collisions becomes $\frac{3}{4} E \frac{p}{\bar{R} \bar{\rho}} n_d$. If the charge produced per droplet is q_d , the rate of charge production per unit volume is given by

$$\frac{dq}{dt} = \frac{3}{4} E \frac{p}{\bar{R} \bar{\rho}} n_d q_d$$

Using the values $E = 1$, $p = 5 \text{ cm h}^{-1}$ or $5/3600 \text{ cm s}^{-1}$, $\bar{R} = 0.2 \text{ cm}$, $\bar{\rho} = 0.5 \text{ g cm}^{-3}$, $n_d = 1 \text{ cm}^{-3}$ and the authors' laboratory value $q_d = 4 \times 10^{-8} \text{ e.s.u.}$, we have

(23) Imperial College, London

12.

$$\frac{dq}{dt} = 4 \times 10^{-8} \text{ c.s.u. cm}^2 \text{ s}^{-1} \\ = 1 \text{ C km}^{-2} \text{ min}^{-1}$$

The authors consider this rate adequate to provide enough charge to give the first lightning flash within about 20 minutes of the detection of precipitation particles by radar, and they suggest that their theory gives the principal mechanism of thunderstorm electrification.

Latham and Mason (1961a,b) have also investigated the charge produced by the momentary contact of two pieces of ice at different temperatures. From the temperature gradient charge transfer theory they predict a maximum charge transfer of $3 \times 10^{-8} \Delta T \text{ c.s.u. cm}^{-2}$, where ΔT is the temperature difference, for a contact time of 0.01 seconds. For longer times the samples rapidly come to the same temperature and the charge will tend to zero. These results were confirmed experimentally by the authors. Calculations of the rate of charge production in a storm by this process, with hailstones falling through a cloud of ice crystals, give only $10^{-4} \text{ C km}^{-2} \text{ min}^{-1}$, and the authors conclude that although the sign of the charge on the hailstone will be negative, as required, the contribution to storm electrification will be only slight.

The theory of the charging of hail pellets by these two processes has been extended by Latham and Mason (1962) to the case of collisions occurring in polarizing electric fields of up to about 1000 V cm^{-1} as found in thunderstorms. They also examined this question by laboratory experiment. They conclude that such fields have little effect on the rate of charging predicted by the main theory outlined above.

There is a serious discrepancy between the observed charge for ice-ice contacts reported by Latham and Mason and that by Reynolds, Brook and Gourley (1957), the latter being some five orders of magnitude larger. There seem to be no other measured values, but Hutchinson⁽²⁴⁾ (1960) reported that for momentary contact between two ice crystals grown from the vapour and having temperature differences up to 14 deg C any charges due to the contact

(24) Durham University, England

13.

were below the apparatus sensitivity of 6×10^{-8} e.s.u. The area in contact lay between 0.2 and 2 mm² and the contact time between 0.2 and 0.5 sec. A similar conclusion was reached by Evans ⁽²⁵⁾ (1962). Charges as large as those reported by Reynolds, Brook and Gourley should have been detected easily. The discrepancy has already led to some discussion by Reynolds and Brook (1962) and Mason and Latham (1962).

Evans (1962) also has measured the charge remaining when a supercooled drop on a fibre freezes, bursts, and ejects fragments. Although his results refer to only 50 drops there is an indication that the charge produced is often larger than the Latham-Mason theory can easily explain.

The production of ice splinters on exposing a frost deposit to an airstream at different temperatures has been examined by Latham ⁽²⁶⁾ (1962). The particles were found to carry a charge, its sign and magnitude depending on the difference in temperature between deposit and airstream, and explained by the Latham-Mason temperature-gradient charge transfer theory.

the
At the Electrical Research Association Laboratories at Leatherhead, England, an inexpensive and reliable lightning flash counter has been developed (Goide, 1962). It operates on positive potential gradient changes caused by negative strokes to earth up to a distance of 40 km. The recovery time is of the order of 1 second so that if multiple strokes occur only one will be recorded. Since the instrument is also triggered by the appropriate cloud to cloud discharges it is necessary to know the ratios of negative to positive earth and cloud strokes respectively.

(25) Durham University, England

(26) Manchester College of Science and Technology, England.

6. References

- Adams, J., 1960, Quart. J.R. Met. Soc. 86, 252.
- Adkins, C.J., 1959, Quart. J.R. Met. Soc. 85, 237.
- Browning, K.A. and Ludlam, P.H., 1962, Quart. J.R. Met. Soc. 88, 117.
- Chalmers, J.A., 1956, J. Atmos. Terr. Phys. 2, 311.
- Chalmers, J.A., 1959, Recent Advances in Atmospheric Electricity,
p. 309, Pergamon Press, New York.
- Chalmers, J.A., 1961, J. Atmos. Terr. Phys. 24, 339.
- Chalmers, J.A., 1962, To be published in J. Atmos. Terr. Phys.
- Currie, D.R. and Kreielaheimer, K.S., 1960, J. Atmos. Terr. Phys. 19, 126.
- Evans, D.G. 1962, M.Sc. Thesis, Univ. of Durham, England.
- Flanagan, V.P.V. and O'Connor, T.C., 1961, Geofis. Pur. Appl. 50, 148.
- Golds, R.E. 1962, Private communication.
- Hutchinson, W.C.A., 1960, Quart. J.R. Met. Soc. 86, 406.
- Keefe, D. and Nolan, P.J., 1961, Geofis. Pur. Appl. 50, 155.
- Keefe, D. and Nolan, P.J., 1962, Proc. Roy. Irish Acad. 62, 43.
- Keefe, D., Nolan, P.J. and Rich, T.A., 1959, Proc. Roy. Irish Acad., 60, 27.
- Latham, J. and Mason, B.J., 1961a Proc. Roy. Soc. A, 260, 523.
- Latham, J. and Mason, B.J., 1961b Proc. Roy. Soc. A, 260, 537.
- Latham, J. and Mason, B.J., 1962, Proc. Roy. Soc. A, 266, 387.
- Latham, J., 1962, not yet published.
- Law, J., 1961a, Geofis. Pur. Appl. 50, 53.
- Law, J., 1961b, Geofis. Pur. Appl. 50, 102.
- Mason, B.J., 1961, The Physics of Cloud, Rain and Lightning, p. 77,
Inaugural Lecture, Imperial College, London.
- Mason, B.J. and Latham, J., 1962, Quart. J. Roy. ^{Met.} Soc. 88, 551.
- Mason, B.J. and Maybank, J., 1960, Quart. J. Roy. Met. Soc. 86, 176.
- Maud, J.E. and Chalmers, J.A. 1960, Quart. J. Roy. Met. Soc. 86, 85.
- Milner, J.W. and Chalmers, J.A., 1961, Quart. J. Roy. Met. Soc., 87, 592.
- Nolan, P.J., 1955, Proc. Conf. Atmos. Elect. Geophysical Research Paper
No. 42, p. 113.
- Nolan, P.J. and Kennan, E.L., 1949, Proc. Roy. Irish Acad, 52, 171.
- O'Connor, T.C. and Sharkey, W.P., 1960, Proc. Roy. Irish Acad. 61, 15.

13.

- Pollak, L.W. and Metnieks, A.L., 1962, Geofis. Pur. Appl. 21, 225.
- Ramsay, M.W. and Chalmers, J.A., 1960, Quart. J. Roy. Met. Soc. 86, 530.
- Reynolds, S.E. and Brook, M., 1962, Quart. J. Roy. Met. Soc., 88, 550.
- Reynolds, S.E., Brook, M. and Gourley, M.F., 1957, J. Met. 14, 426.
- Rich, T.A., Pollak, L.W. and Metnieks, A.L. 1962, Geofis. Pur. Appl. 21, 217.
- Smiddy, M. and Chalmers, J.A., 1959, Quart. J. Roy. Met. Soc. 86, 79.
- Stein, J.M., 1958, M.Sc. Thesis, Univ. of Auckland, New Zealand.
- Wildman, P.J., 1962, Ph.D. Thesis, Univ. of Durham, England.

SESSION 7.3

ELECTROMAGNETIC ENERGY RADIATED FROM LIGHTNING

Atsushi KIMPARA

The Research Institute of Atmospherics
Nagoya University
Toyokawa
Japan

Abstract— This paper is to survey the study recently developed on the electromagnetic energy radiated from lightning, i.e. atmospherics, not including propagation. Characteristics of the electrostatic, induction and radiation fields of lightning are fully described, including the frequency spectrum in the neighbourhood of the source. Consequently this paper will supply a foundation to the study of propagation of atmospherics, slow tail, ELF and VLF propagations, whistlers, mechanism of lightning discharge, etc.

-1-

I. Introduction

feature

This paper is to survey the general of the developments of observation and theory which have been made recently in the field of electromagnetic radiation from lightning and at the same time to suggest the items of collaborated study for the future.

In order to study the characteristics of lightning discharge many kinds of measurement have been made and developed, i.e. optical, photoelectric, electrostatic and electromagnetic methods have prevailed all over the world. Here in this paper, specifically, the characteristics of electromagnetic energy, i.e. atmospherics in a broad sense, radiated from lightning, not including propagation, are described.

The atmospherics propagate through the space between the ionosphere and the earth in the wave guide transmission mode or in the ray mode reflecting between them. Some of the energy penetrate the ionosphere into exosphere along the geomagnetic line of force, and go to the other hemisphere where they are reflected back and return to the source again along the same geomagnetic line of force. As the exosphere is the medium ^{of} plasma with magnetic field, it is dispersive and during the journey atmospheric pulses become whistlers from which the density of electron in the exosphere is evaluated and the existence of proton in it is proved.

Frequency spectrum of atmospherics at the various distances from the source will show the propagation characteristics of LF and VLF waves. Since the long waves are not disturbed by geomagnetic storms and propagate with low attenuation,

-2-

they are very useful to the international comparison of the frequency standards as well as to the radio method of navigation. It is because the radio engineers and geophysicists make much of the study atmospheric and whistlers.

Consequently the investigation of characteristics of electric fields in the neighborhood of lightning discharge, are very useful to the study of the mechanism of lightning discharge, the propagation of longer radio waves and the interference of atmospherics to radio communications.

For this purpose workers have made so far the waveform measurement with wide band receivers, in which the band width is less than 1 kc/s to avoid interference in fairly clouded higher frequency region. ELF band, 1 c/s-3000 c/s, which attracts recently attentions of engineers and scientists, is measured with receivers of pass band 1 c/s-50 c/s for a lower frequency region and with waveform recorders for a higher frequency region, "slow tail". For HF, VHF and UHF regions observations are made with single frequency receivers of very narrow band width to avoid the interference of radio communications.

Lightning discharges are divided into 2 classes, i. e. the cloud-earth discharge and the intra-cloud discharge. The cloud-earth discharge consists of the pre-preliminary discharge, the preliminary discharge (I_p , ignition stage ^{or} Δ b, breakdown stage, I , intermediate stage and a , I , leader stage, Δ , b , R , the return streamer stage, c , J , the junction streamer stage, s , F , the final discharge stage, etc. Corresponding to each of these optically observed stages,

-3-

a characteristics change of electric field is observed with fairly good response. (1)(2)(3)(4)(5)(6)

The intra-cloud discharge displays also characteristic field changes somewhat different from those of cloud-earth discharges. Therefore the investigation of electrostatic, induction and radiation field of these stages and the comparison among them are very useful to investigate the details of characteristics of lightning phenomena. It is because the electronical methods, developed remarkably in the last decade, are recommended to reveal quantitatively the details of the phenomena better than the optical methods.

II. Electrostatic Field

In accordance with the observation at distances 25-250 km, Pierce⁽³⁾ found with capillary electrometers the relation between the positive and negative slow mean field changes with distance. The field obeys inverse cube relation and corresponds to a change of electric moment of 110 coul-km, i. e. to a field-change of 1 v/m at 100 km. It is well known that near a storm most field-discharges are positive, while as the distance of the activity increases negative field-changes become more frequent.

For any particular year and for magnitudes less than about 100 v/m, the ratio N_+/N_- , where N_+ and N_- are the number of all positive and negative field changes, is constant. This constant value may differ from year to year, but there is no significant change with magnitude between 100 and 0.1 v/m. Above 100 v/m positive field-changes become increasingly predominant as the magnitude of the field-change rises.

-1-

A field-change of 100 v/m corresponds to a distance of about 20 km; the constancy of $N+/N-$ below 100 v/m therefore implies that discharges, producing a reversal in the sign of the associated field-change beyond 20 km, do not occur. The changes from year to year in $N+/N-$, for field changes < 100 v/m, are therefore not to be regarded as characteristic of the year but rather as representing differences between particular storms.

Slow negative field-changes are due to air or cloud discharges which either lower positive charge or, more probably, raise negative charge. Slow positive field-changes are produced by flashes which do not reach the earth, and which probably involve the downward movement of negative charge. Slow positive field-changes with fast elements are produced by flashes conveying negative electricity to ground. Usually, a gradual L rise in field is succeeded by one or more rapid R elements separated either by quiet intervals or by slow J changes, and there is often a final S or F section.

Takari⁽⁶⁾ observed that in ground discharges the slow electrostatic change is negative for near flash (within 5 km), positive to negative at distances 5-15 km, positive at 15-20 km or more, and the large ground stroke pulse has almost always a positive and very steep front.

The difference between the slow field change of a ground discharge and that of cloud discharge is that the polarity of the dipole contributing to the slow change of a ground

-5-

discharge is negative and has a reversed relation to that of a cloud discharge, because the net field change is negative in a near distance and becomes positive in a long distance. (4a) Hillebrand obtained a rather unexpected result during his observation of lightning discharge. With lightning strokes at a distance of 3-8 km from his laboratory at Uppsala, it turned out quite often that the cathode ray was disappearing for a period of 5-10 μ s. The magnetic field was considerably greater than the field calculated for the return stroke with a velocity of about one-fifth to one-quarter of that of light. His interpretation would be postponed to future study and he wonders why was this fact not found in earlier observations.

1. Pre-preliminary discharges. Takeuti⁽⁷⁾ observed that about 50 % of the ground discharges are preceded by a pre-preliminary discharge, duration 50-800 ms with median of 177 ms, which occurs within 500 ms before the first ground stroke, and so this discharge precedes the "preliminary discharge". In some thunderclouds the greater part of the first ground stroke is preceded by the pre-preliminary discharge, while in others the strokes are preceded only by the preliminary discharge. On the average the ground discharges preceded by the pre-preliminary discharge have fewer ground strokes than those preceded only by the preliminary discharge; the pre-preliminary discharge probably neutralizes the negative charge in the ground stroke. The relation between the pre-preliminary discharge and the preliminary discharge is not yet known at present, but its characteristics

-6-

are almost similar to cloud discharges and it seems very likely to excite preliminary discharges.

2. B or Ig field change. (2)(6)

The B field change, duration 2-10 ms, is negative at distances upto 2 km, positive at distances in excess of 5 km and positive or negative between 2 and 5 km. (Malan); negative upto 6 km, positive in excess of 10 km and positive and negative or indeterminate between 6 and 10 km (Ishikawa). Taking into account that the maximum change of electric field occurs at a distance $D = \sqrt{2}H$, where H is the height of charge centre, E field change is attributed either to positive charge moving upwards from a minimum height of 1.4 km, or to negative charge moving downwards from a maximum height of 3.6 km. (2) The fact that the calculated heights of 1.4 and 3.6 km are in close agreement with the respective heights of the base of the cloud (1.5 to 2 km) and the lower region of the negative-charge centre N (3 to 4 km), strongly suggests that the B field change is due to a discharge between N and the positive charge centre p situated near the base of the cloud to make the discharge channel between p and N conductive.

3. I field change. (2)(6)

The I field change, duration 0-400 ms, is the part to connect the B and L field changes and the rate of change of field is either fairly uniform or variable.

4. L field change. (1)(2)(6)

The L field change, duration 4-30 ms, corresponds roughly to the photographed stepped leader process, but whenever a direct correlation is obtained

-7-

the L field change lasts from 1.14 to 4.5 times as long, the difference increasing with the order of the stroke in the series. This indicates that successive strokes come from progressively higher regions. The L field changes are negative and hook-shaped when near, and positive and approximately parabolic when far. The change in sign with distance shows that the leader lowers negative charge from the cloud and distributes this charge along its channel.

Two types of L variation preceding the first rapid R element are distinguished upon the field records.⁽³⁾ In the first, the increase in field is uninterrupted up to the R portion, while in the second the initial slow field-change is succeeded by a quiet part usually lasting until the rapid section, although there is sometimes a fairly short slow rise in field immediately preceding the R element. Somewhat similar effects have been noted by Schenland and given the titles α and β ; this nomenclature is retained here, the two kinds of initial field-change being denoted by L (α) and L (β). The average duration for the L (α) change is 50 ms, while the corresponding figure for the L (β) variety is 175 ms. The proportion of the total change of field, due to the whole discharge, occurring during the L section, is found to be significantly higher for L (β) than for L (α) variations; the appropriate percentages are 55 % and 40 % in Europe⁽³⁾ and 75 % and 9 % in Japan.⁽⁶⁾

5. R or Main discharge field change.⁽¹⁾ The R field change is made up of 2 parts. The rapid portion Rb has a duration of 50 to 250 μ s (most frequent value 165 μ s),

-6-

and evidently corresponds to the rapid upwards movement of the return streamer, its duration is between 1.5 and 2.0 times as great as the time taken for the return streamer to reach the cloud base. Rb is followed by slower field-change Rc which lasts from 70 to 900 μ s, corresponding roughly to the duration of continuing luminosity in the return streamer channel. Both Rb and Rc are of positive sign at all distances as would be expected if they were due to the removal to earth of negative charge from the leader channel and the cloud. But at the distance of more than 15 km Rb indicates a superposed pulse which deflects at first on the positive side and then negative.⁽¹⁾⁽⁵⁾⁽⁶⁾ Rc from a near flash to ground frequently shows small hook-shaped field changes which occur for a period up to 6 ms after Rb. Its duration is between 200 and 600 μ s and its amplitude is 0.2 to 0.01 times of Rb. It seems that these hook-shaped change can be directly related to the M components of luminosity in the return streamer channel. At a distance they show minor radiation pulses only.

6. J field change.⁽⁸⁾ This field change in the interval between separate strokes of the multiple discharge to ground is found to be negative for near flash (within 5 km), negative to positive at a distance 5-12 km, positive at 12-20 km. At distances between 20 and 150 km, Malan⁽⁵⁾ found 25 % positive, 37 % zero and 40 % negative, while Korwell and Pierce⁽⁹⁾ found 25 % positive and 75 % zero. It is believed that during this process there occurs a discharge between the positive charge brought to the top of discharge channel by

-9-

the return streamer and the negative charge in the cloud. This discharge makes conductive the part of a column in the cloud, which has abundant negative charges, to excite the next dart leader. Taking into account the change of sign of J field change with distance, Malan⁽⁶⁾ considered that the discharge proceeds upward in the cloud and at the same time the effect of positive charge, which is high above the cloud and discharges upwards, does not come out at a short distance due to the masking effect of the J field change and appears progressively with increasing distances. According to the observation at Socorro Mountain (alt. 7,200 ft or 2,200 m) by Crook⁽¹⁰⁾ the J process, in which a streamer moves slowly upward in the intervals between the return strokes was clearly visible as it penetrated the remote regions of the cloud. The upper most region from which the return stroke originated was observed to move (in steps reminiscent of darts) upward and outward, illuminating new regions of cloud, before a new section was added to the channel of the previous return stroke and a new stroke occurred. Some discharges to ground appeared to originate from a vertical column, but far the greater number were seen to progress horizontally or inclined at about 30° to the horizontal. The horizontally progressing junction streamer occurred about 3 times as often as the vertical streamer. These observations are consistent with the field measurement of Vorwell and Pierce.⁽¹¹⁾

Hewitt⁽¹¹⁾ employed a radar equipment at a frequency of 600 Mc/s for the study of streamer movement within

-10-

thundersclouds in the intervals between strokes to ground. The observations show that ascending echoes occur at increasing ranges and angles of elevation in the interstroke intervals, the heights increasing with the order of the intervals in the series. This is in accord with what would be expected if the echoes came from J streamers and the observed vertical velocity agrees with that found for the J streamer. A further observation shows that echoes at lower heights less than 4 km persist throughout the series of ascending streamers and often show considerable horizontal movement.

7. P field change. Malan⁽¹²⁾ found that the P field change is a large final slow positive field change most frequently occurs after flashes having fewer than 4 strokes in the multiple stroke process. It is shown that this field change is due to a continuous discharge to ground of part of the negatively charged column higher than that reached by the last stroke. The mechanism of progress of upward discharge in the column is similar to the J process. The discharge to ground changes from intermittent to continuous when the charge density becomes too low. It is believed that during this process there occurs a more active discharge between the positive charge at the top of the cloud and the negative charge above it, and the effect of this discharge is not clear at short distances due to masking effect of P process in the negatively charged column, but it appears remarkably with increasing distances.

-11-

3. Intra-cloud discharge field change. Cloud discharges show large slow continuous electrostatic field changes which are positive when the discharge is near and become negative when the distance increases.⁽⁵⁾⁽¹³⁾ Small rapid step-like or pulse form changes which are responsible for sudden bursts of bright luminosity are usually superimposed in sporadic fashion on the slow field change.

(5)

Takari found that in cloud discharges the slow electrostatic change is positive for near flash (within 5-10 km), negative at 10-20 km or more. It suggests that the cloud discharge generally dissipate a positive dipole in a cloud. The observed and estimated field intensities of the electrostatic field changes due to cloud discharges are shown in Table 1, where the estimated value is obtained by assuming that the charges +25 and -25 coul, are located at the height of 8 and 4 km respectively on a vertical line. The similar values are estimated on the ground discharge.

Table 1. The observed and the estimated field intensities of the electrostatic field changes due to cloud discharges.

Distance (km)	Observed		Estimated absolute values* (kv/m)
	Rapid process (v/m)	Slow process (kv/m)	
0-5	50-300	1 -30	2.6 -21
5-10	10-100	.1 - 5	0 - 2.6
10-15	2- 20	.1 - 1	.25- .31
15-25	.5- 10	.05- .5	.09- .25

* It is assumed that 25 and -25 coul of electricity are located at the altitudes 8 and 4 km respectively on a vertical line.

-12-

III. Induction field.

1. B or I_E pulsations. According to Ishikawa,⁽¹⁾ Clarence and Malan,⁽²⁾ at a distance more than 15 km the I or I_E field change starts with a train of large and predominantly positive pulses of varying and gradually decreasing amplitude. The interval between the pulses is irregular and varies from 80 to 230 μ s. The most frequent ^{duration} of the pulse train is between 2 and 4 ms, the longest train observed lasting for 12 ms, the durations corresponding with those of the electrostatic B field changes. Small amplitude pulsations of which time separations are between 5 and 10 μ s are often superimposed on the large low-frequency B pulses. They usually continue with varying amplitude up to the incidence of the return stroke.

2. I pulsations. ⁽²⁾⁽⁶⁾ The pulsations in the interval between the B and L stages are high frequency pulsations of very small amplitude. Periodic spurts of isolated pulses, of amplitudes comparable with those of the B pulses, often occur during the I phase. These pulses are positive when the rate of change of electrostatic field increases and negative when the rate of change of field decreases. When the return stroke follows the large B pulse train in less than 30 or 40 ms, the whole intermediate interval is occupied by the characteristic high frequency L pulsations described in the next paragraph, which suggests that in these cases the I stage is short or absent.

3. L pulsations. ⁽²⁾ The field changes immediately preceding the return stroke consist of a train of steep and

-13-

predominantly positive pulses following each other at 5 to 10 μ s intervals. Some of the pulses are of larger amplitude than those intervening. The larger pulses follow each other at intervals between 30 and 60 μ s, which is the same as the pause time between the bright steps of stepped leaders. The observation, however, that strokes subsequent to the first are often preceded by similar pulse trains indicates that they cannot wholly be due to the stepped process in the downward leader. Since the effects in the intervals between the strokes of a flash must be due to J streamers, it is reasonable to conclude that the similar field changes immediately preceding the first stroke are also mainly caused by streamer discharges inside the cloud, which supply charge to the advancing leader. The pulses during the L part of the discharge are smaller in amplitude than the E pulses. The amplitude ratio of E to L pulses varies from 3:1 to 20:1, the higher the rate of change of the electrostatic field during the B stage, the larger this ratio.

IV. The Radiation Field. (2)(12)(1h)

1. Preliminary discharge process. The radiation field of a preliminary discharge process in the ground discharge is remarkable in every frequency. It is observed even when the static field change is not clearly approved. The E, I and L stages show always some indication of high frequency radiation. Usually the amplitude of L is largest, and then that of E and I the smallest; the radiation field of B and I stages are negligibly small in the frequency

-14-

range between 200 c/s and 20 kc/s. The radiation field of subsequent dart leaders is not essentially distinguished from that of J process filling up in interstroke period especially at higher frequencies.

The records obtained during the daytime illustrate three common types of radiation L fields. (i) The α type (duration 2-25 ms) having a small almost uniform train of pulsations whose amplitudes are often less than 1/100 of that of the return stroke. (ii) The slow β type (duration 3-19 ms) whose initial pulsations are slightly larger than the later pulsations, which resemble those of the α type. (iii) The large amplitude fast β type (duration 1-7 ms) whose initial pulsations may have amplitudes up to half as large as the first return stroke pulsation. Intermediate types are also obtained. The time intervals between the L pulsations vary from 30 to 100 μ s which indicates that they originate from stepped leaders. Night time atmospherics show the same three types of leader, but the apparent time interval between the steps is smaller owing to successive ionospheric reflections.

2. The return streamer process. The salient points regarding the radiation field of ground discharge is as follows. At 3 kc/s the radiation is confined to the return strokes. This remains true up to about 20 kc/s except that preliminary and interstroke pulses occasionally appear with amplitudes 1 % to 2 % of those of the return strokes. With increasing frequency up to about 1-2 Mc/s return strokes

-15-

still have the largest amplitude, but radiation from other parts of the discharge become progressively large. At 4-12 Mc/s, especially at higher than 10 Mc, the latter surpass the return strokes in amplitude. An interesting phenomenon is observed at these higher frequencies. The radiation is intense and continuous during the course of the first few strokes of a flash, except for pauses varying from 2 to 20 ms immediately following a return stroke.⁽⁵⁾⁽¹³⁾ After the initial burst of activity the pulses become more and more spaced in time. With increasing frequencies, the intermittent impulsive radiations change gradually into continuous radiations, but at frequencies higher than 100 Mc/s they occur very often associated with electrostatic pulses.

3. The cloud discharge process. In the intra-cloud discharges small rapid step like field changes responsible for sudden burst of bright luminosity are usually superimposed in sporadic fashion on the slow field change. At frequencies from 3 to 10 Mc/s there are usually only one to three very small radiation pulses which are associated with rapid but not necessarily the largest E field changes. As the frequency increases to 2 Mc/s more and more radiation pulses appear, those associated with E field changes remaining the largest. At 4-12 Mc/s the radiation becomes practically continuous and the E pulses can no longer be distinguished from the rest of the radiation. The cloud discharge has somewhat similar high frequency characteristics to the J process in the ground discharge and it is generally composed of slow J-like streamers and many rapid local streamers. At higher

-16-

frequencies than 100 Mc continuous and intermittent radiations independent of any process like stepped leaders are observed. Lightning flashes within 5 km show very often a continuous radiation, which has a duration larger than 100 ms, accompanied by an electric field of complicated variation.

The following figures give the ratios of the amplitudes of the return stroke radiation of ground discharges to the amplitudes of the most intense radiation components of cloud discharges at different frequencies:

Frequency	Amplitude ratios
3 kc/s	20/1-10/1
6 "	10/1-20/1
10 "	10/1
20 "	5/1
30 "	2/1-3/1
50-100 "	1/1-1.5/1
1.5-12 Mc/s	1/1

The above figures agree with the suggestion of Alva that cloud discharges contribute little to the radio noise level below 1 Mc/s.

V. Frequency Spectrum.

The frequency spectrum of atmospherics is very important to the study of wave propagation, propagation of atmospherics, mechanism of lightning discharge, but it is also very difficult to obtain a frequency spectrum at various distances from the source, at various stages of lightning discharges, at various geographical ^a features, at various meteorological and seasonal conditions. Although the data available at present are very few, the followings are the main results of observation from ELF to UHF all over the world.

-17-

Taylor and Jeans⁽¹⁵⁾ recorded the intensity of atmospherics at 1-40 kc/s emitted from the ground discharge at distances between 150 and 600 km. Watt and Maxwell⁽¹⁶⁾ made similar observations at 1-100 kc/s at distances between 30 and 50 km. Horner⁽¹⁷⁾ measured at 11 Mc/s and 6 kc/s at distances between 1.5 and 6.5 km. Takagi⁽¹⁸⁾ measured at 100 kc/s-500 Mc/s at 15-20 km. Schafer⁽¹⁷⁾ measured at 150 Mc/s at 1-32 km. Summarizing these data and normalizing at a distance of 10 km for the receiver bandwidth of 1 kc/s, we obtain a frequency spectrum as shown in Fig.1. As the method of measurements and characteristics of the apparatus are different from each other, the curve in the figure is not fully reliable; it is only to show the general tendency. The waveform of atmospherics in the neighbourhood of lightning discharge depends on the geographical feature (sea, mountain, plain, city, town, tower, etc.), geographical position and the kind of discharge (ground discharge, cloud discharge, etc.) and changes from time to time during the discharge process.

Two widely quoted expressions have been given for the current i_t during the return-stroke of the lightning flash to earth. Both⁽¹⁹⁾ have the same double exponential form $i_t = i_0(e^{-\alpha t} - e^{-\beta t})$, where t is the time in sec. and i_t the current at time t , the origin of time being taken at the start of the return-stroke. Bruce and Golde⁽¹⁹⁾ gave the following figures for the parameters, namely, $i_0 = 28,000$ A, $\alpha = 4.4 \times 10^4$, $\beta = 4.6 \times 10^5$, while Norinder⁽²⁰⁾ suggested the values $i_0 = 20,000$ A, $\alpha = 7 \times 10^3$, $\beta = 4 \times 10^4$.

-18-

It is well known,⁽¹⁸⁾ for instance, that individual lightning flashes differ considerably in their spectral characteristics, the excitation of which may be anticipated to be related to conditions, and therefore currents, in the return-stroke channel. Perhaps the most striking evidence, however, for the existence of at least two main types of current surge is that derived from the study of atmospherics. The frequency spectra of the electromagnetic fields radiated respectively by return-strokes carrying the Norinder and Bruce-Golde forms of current surge, with the current assumed to be uniform along the channel, can easily be calculated.

Hill⁽²¹⁾ calculated the radiation energy of lightning in the VLF range, considering only the return stroke, and found that the spectral energy distribution is centred at about 11 kc, with a total width at half-maximum of 12 kc.

In 1952 it was suggested by Schumann⁽²²⁾ that the earth and ionosphere may together act as a cavity resonator for electromagnetic wave and that the first resonance should occur at 10.6 c/s. Refinement of the theory indicated that losses due to absorption by the ionosphere or radiation through the ionosphere should reduce the resonant frequency by at least 1.5 c/s. Experimental evidence^{for} the existence of the first resonant mode was reported first by Schumann and König⁽²³⁾ and, in considerably more detail by König.

The theory of ELF resonances was more recently discussed by Wait, and experimental evidence for the existence of the first and higher resonant modes, based upon measurements

-19-

of electric fields, was presented by Falser and Wagner.⁽²⁴⁾ Their results were also applied by Kaemer to the calculation of an ionospheric loss parameter which is a function of the height and the conductivity of the sharply bounded ionosphere assumed in the first order theory. Additional experimental results were published recently by König, by Maple, by Lokken, Shand and Wright, by Polk and Eichen, and by Sao, Jindo and Kumagai; König⁽²⁵⁾ reported that almost the same type of ELF were observed at Bonn and Munich which was classified into 5 types correlating with weather phenomena and on the occasion of solar eclipse the similar change were observed with the sunrise and sunset phenomena; Polk⁽²⁶⁾ confirmed the existence of comparatively strong natural oscillations in the 7 to 10 c/s frequency range, but the resonant frequency exhibits short-time variations and at night they are considerably weaker than during daylight hours and stronger than usual during periods of geomagnetic activity; Sao⁽²⁷⁾ suggested that only 25 % of lightning discharge emit ELF and 71 % of ELF come from sources, which radiate VLF, around the observatory and not from sources all over the world.

VI. The Study Programme for the Future.

1. According to the observation for a long time it seems that the characteristics of atmospherics, which define its frequency spectrum, depend on the configuration and development of thundercloud. They show variations in accordance with the seasonal and meteorological conditions as well as geographical features such as plateau, plain, mountain, sea, lake, town, city, tall tower, etc. Therefore it is recommended that the

-20-

frequency spectrum from ELF to UHF is to be measured at various distances from the source, at every meteorological and seasonal conditions as well as at every geographical feature. It will contribute to the study of wave propagation, mechanism of lightning discharge, properties of whistlers, etc. Really some authors showed that the occurrence of whistlers depend on the frequency spectrum of other atmospherics and on the propagation conditions, and those atmospherics which have a peak near 5 kc, in place of ordinary 10 kc, excite whistlers very often.

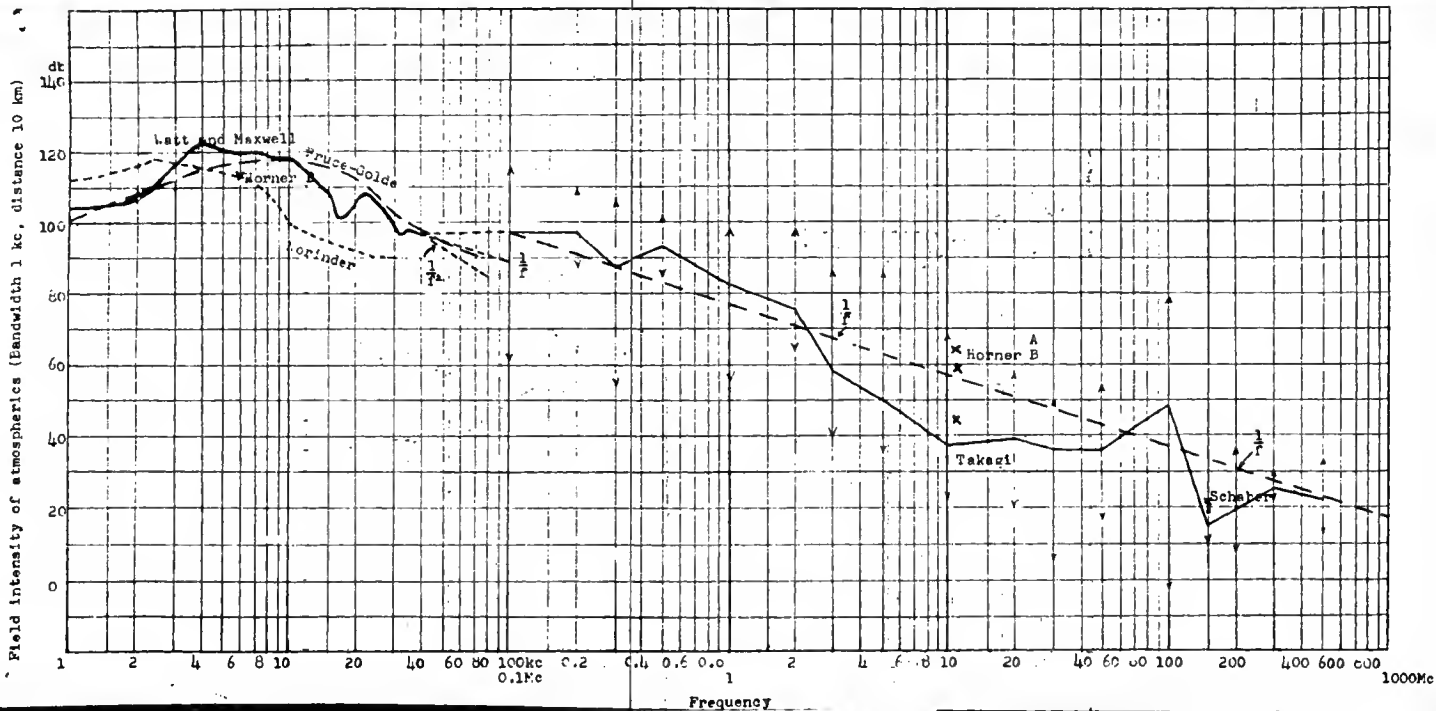
2. At present many scientists observe the production, development and destruction of thunderclouds at many points on the ground with electrical instruments, and evaluate the electrical configuration of thundercloud. But this is after all the indirect method and it is complicated, requires a large area, many manpower, etc. Therefore it is recommended to determine the specification of a radio-sonde and a Radar with PPI and RHI scopes suitable to observe horizontal and vertical configurations of thundercloud.

3. Although we could not succeed disturbed by a typhoon, we made a measurement of characteristics of a ground discharge with a large paper balloon, connected with a grounded conductor, at 200 m high upon the plateau of Mt. Maruno (1410 m), around which many equipments for measurements were arranged. It is therefore recommended that the ^{most} useful method of this kind would be discussed and determined so that a similar but more elaborate method may come out.

-21-

References.

- (1) F.F.J. Schenck: The **Lightning Discharge**. Handbuch der Phys. Bd XXII. (1956)
- (2) N. D. Clarence and D. J. Malan: **Q. J. Roy. Met. Soc.** 83, No. 356. (April 1957) p. 161.
- (3) E. T. Pierce : **Q.J. Roy Met. Soc.** 81, No. 340. (1955) p. 211
- (4a) G.D. Müller-Hillebrand: **International Conf. Gas Discharges Ele. Sup. Ind.** (1962), Pre-print, Session 1a, Paper 16.
- (4) E. T. Pierce : **Q.J. Roy Met. Soc.** 81, No. 340. (1955) p. 229
- (5) M. Takeuti : **Proc. Res. Inst. Atmospherics, Nagoya Univ.** 8, F. (1961)
- (6) H. Ishikawa : ditto, 8, A. (1961)
- (7) T. Takeuti : ditto, (1960) 7, p. 1.
- (8) D. J. Malan : **Ann. d. Géophys.** 11, Fas. 4. p. 420, (1955)
- (9) T. W. Wormell and E. T. Pierce : **Q. J. Roy. Met. Soc.** 79, p. 474, (1953)
- (10) H. Brook et al. : **J. Geophys. Res.** 65, No. 4, p. 1302 (April 1960)
- (11) F. J. Hewitt : **Proc Phys. Soc. Lond. E.** 66, p. 695, (1953)
- (12) D. J. Malan : **Ann. d. Géophys.** 10, Fas. 4, p. 271. (1954)
- (13) D. J. Malan : **Recent Advances in Atmospheric Electricity**, (1959) p. 557
- (14) M. Takeuti : **Proc. Res. Inst. Atmospherics, Nagoya Univ.** 10, (1963),
- (15) W. L. Taylor and A. G. Jean : **J. Res. NBS D** 63, p. 199 (1959)
- (16) A. D. Watt and E. L. Maxwell : **P. I. R. E.** 45, p. 787, (1957)
- (17) J. P. Schaefer et al. : **P. I. R. E.** 27, p. 262, March, (1939)
- (18) E. T. Pierce : **Recent Advances in Atmospheric Electricity**, (1959) p. 5
- (19) C. E. R. Bruce and R. H. Golde : **P. I. E. E. (Pt. II)** Vol. 88, p. 487, (1941)
- (20) H. Norinder : **Joint Com. Radio. Met. Int. Coun. Sci. Un.**, (1951)
- (21) E. L. Hill : **P. I. R. E.** 45, No. 6, (1957) p. 775.
- (22) W. O. Schumann : **Z. Naturforsch.** 7a, (1952) p. 149, p. 250, **Z. angew. Phys.** 4 (1952) p. 474, 6 (1954) p. 35, 2 (1957) p. 373
- (23) W. O. Schumann and H. König : **Naturwiss.** 41 (1954) p. 183, H. König : **Z. angew. Phys.** 11 No. 7 (July 1959) p. 264
- (24) M. Falser and C. A. Wagner : **J. Research NBS** 64D No. 4 (1960) p. 115, **Nature**, 188, (1960) p. 638
- (25) H. König et al : **Z. angew. Phys.** 13, No. 8, (1961) p. 364
- (26) C. Polk and F. Pitchen : **J. Research NBS** 66D No. 3, (1962) p. 313



SESSION 9.5

To be presented at the Third
International Conference on Atmospheric
and Space Electricity, May 6-10, 1963.

The Concepts of Atmospheric Electricity
as Applied to the Ionosphere

by
K. Maeda
(Kyoto University, Japan)

Abstract

1.1) Electric charges in the ionosphere are carried by free electrons and ions which are maintained by a balance of solar ionizing radiation and decay processes. The electron density can be measured by vertical radio sounding from the ground surface and the $N(h)$ profile is calculated from the data of this sounding. However, such $N(h)$ profile is not complete, but the whole profile can be obtained with the aid of sounding rocket bearing suitable sensors. As for the outer ionosphere extending to the magnetosphere, the $N(h)$ profile is estimated by topside sounding, satellite signal reception (Faraday rotation and Doppler shift experiments) and whistler observation. The $N(h)$ profile is a knowledge^{of} basic importance not only for radio propagation study but also for understanding the interrelationship between the geomagnetic variation and the ionospheric behaviour. For the latter problem the ion density profile is also essential, which could be revealed by sounding rocket so far, though incomplete.

1.2) The dynamic behaviour of electrons and ions will be described in terms of velocity distribution, drift velocity, collision, electrical conductivity and current, some of which are mutually connected.

Among others the velocity distribution and drift velocity of electrons are the most basic quantities. The classical magneto-ionic theory should be revised by taking into account the velocity distribution and some fruitful outcome from such revised concept can be expected in understanding the wave absorption, Doppler broadening and so forth. It is well known from laboratory experiments that a certain non-linearity exists in the electron drift velocity. However, when the problem should be treated under the influence of magnetic field, as in the case of ionosphere, a great difficulty arises in mathematics. Such is also the case of velocity distribution. Monte Carlo method will be one of the effective tools to attack these problems and some laboratory experiments will be designed to solve them. Also some possible methods of measuring directly those quantities by sounding rocket will be devised.

1.3) The Pedersen, Hall and Cowling conductivities ($\sigma_1, \sigma_2, \sigma_3$) based on the above dynamic behaviour of charge carriers play an important role in the dynamo-theoretical study on electric field and current, which is responsible for the geomagnetic variation. The result of such study tells us that the effective total conductivity has a peculiar characteristics, which can account for the abnormal intensification of dynamo current under the disturbed state of the ionosphere and that a large shear in the current flow can take place near the boundary of two zones having different conductivities. It is also noted that the wind system in the ionosphere is not yet established in spite of its great importance.

2.1) The measurement of radio noise over the ground has been made widely over the world and the world maps of radio noise intensity are available. This sort of noise is thought to originate in light-

ning discharge and other climatic phenomena. When we once go up into the ionosphere and still higher level, the situation will change. Radio noise originated near the ground can invade there by extraordinary wave mode (whistler mode) and such penetrated energy is expected to be fairly large especially during night. A spacial distribution of radio noise from such origin will be studied.

- 2.2) On considering the radio noise in the ionosphere and exosphere, one can imagine the possible existence of noise from extra-terrestrial source. If this is really the case, the noise distribution is subject ~~of~~ ^{to} wave propagation law which involves the frequency of the wave and geomagnetic field as important factors.
- 2.3) Moreover one might imagine the generation of radio noise by some certain electric phenomena occurring in the ionosphere and exosphere. Liberation of free charges by impinging meteors might be an example, and synchrotron radiation of high energy electrons in the radiation belts may be another source of noise.
- 2.4) Besides the above, we have to notice that there is an evidence to believe the existence of a certain amplifying action for radio waves in the exosphere. The phenomenon known as VLF emissions, such as dawn chorus, hooks etc. is the evidence. The problems of possible sources and amplifying mechanism should be studied, and one may suppose that such amplifying action, if it really exists, can contribute to raising the energy of radio noise.
- 2.5) All the above points will be finally consolidated to the problem on the nature and structure of radio noise in the ionosphere and its outer space. In connection to this problem one more important point must be added. That is the study of how the radio waves

penetrate the ionosphere. The problem is to know the rates of penetration and reflection of radio wave energy when the waves go up and come down through the ionosphere. The problem will be attacked analytically. The rocket experiments and satellite observations (such as LOFTI) will be very useful for the study of the problem as a whole.

STAATLICH AUTORISIERTE
VERSUCHSANSTALT FÜR
GEOELEKTRIK UND BLITZSCHUTZ
LEITER: DIPL.-ING., SC. TECHN. DR. VOLKER FRITSCH

Jänner 1963

Wien, am
III, Arsenal, Objekt 3
Postadresse: Wien, Postamt 62, Fach 389
Telefon: 65 63 73, 44 05 36
Postscheck-Konto: Wien 182.393

Volker FRITSCH, Wien 1.)

Geoelektrische Probleme der Blitzforschung =====

Die Frage, ob und wie der untere Teil der Blitzbahn durch die elektrische Beschaffenheit des Untergrundes beeinflusst wird, wird in der Fachliteratur schon lange diskutiert. Aber erst die moderne geoelektrische Meßtechnik konnte jene genauen Aufschlüsse über die elektrische Struktur des Untergrundes geben, die notwendig sind, um dieses Problem auf eine exakte Grundlage zu stellen.

Der Elektrotechniker ist im allgemeinen gewohnt mit recht homogenen Leitern zu rechnen. Der Untergrund ist aber, elektrisch betrachtet, ein Leitergebilde von meist sehr komplizierter Natur. Widerstandsschwankungen um mehrere Zehnerpotenzen über wenige Meter Entfernung sind keine Seltenheit. Ja, es sind auch scharf ausgeprägte elektrische Diskontinuitätsflächen vorhanden. Man versucht diese Frage durch statistische Erhebungen in Verbindung mit geoelektrischen Bodenuntersuchungen und durch Modellversuche zu klären.

Um das Problem statistisch eindeutig zu klären, wäre es zunächst nötig, für jeden Punkt der untersuchten Fläche einen Bruch anzuschreiben, der die durch Blitzentladung abgeleitete Elektrizitätsmenge pro Flächeneinheit angibt. Diese Angabe wäre dann zeitlich auf eine Gewitterperiode, also auf ein Jahr, zu beziehen.

Nehmen wir an, wir hätten diese Ziffern für eine große Fläche und für einen genügend langen Zeitraum, dann wäre unsere Frage, ob ein Zusammenhang zwischen der Entladungsdichte und geoelek-

Dr. Volker FRITSCH, Leiter der staatlich autor. Versuchsanstalt
für Geoelektrik und Blitzschutz und Professor der H.f.E.

trischen Faktoren besteht, aber noch nicht ohneweiteres zu beantworten. Wir wissen, daß die geoelektrische Struktur des Untergrundes möglicherweise eine Komponente ist. Ganz sicher aber existieren neben ihr noch mindestens zwei weitere: eine meteorologische und eine topographische. Wir müssen daher die geoelektrische Komponente isolieren. Darüber wollen wir noch später einiges sagen. Zunächst wollen wir aber untersuchen, mit welcher Genauigkeit wir die Entladungsdichte überhaupt schätzen können.

Leider stehen heute, wenn man von einigen Ländern absieht, nur sehr wenige und lückenhafte Statistiken zur Verfügung.

Auf den letzten internationalen Blitzschutzkonferenzen wurde die Frage der Blitzzähler diskutiert. Meßtechnisch bestehen da sicher keine Hindernisse, aber gewisse Probleme, wie zum Beisp. die Trennung der Erd- und Wolkenblitze, sind noch nicht geklärt. Auch hat jeder Blitz gewissermaßen eine "Meßreichweite", die von der eigenen Stromstärke, dem Verlauf der Blitzbahn und weiteren Faktoren ebenso abhängig ist, wie von der Meßempfindlichkeit des Anzeigegerätes. Während auf der einen Seite Doppelzählungen kaum zu vermeiden sein werden, dürften andere schwächere Einschläge wieder überhaupt nicht registriert werden. Unter diesen Voraussetzungen wird man erst nach vielleicht zehnjährigen Meßperioden einigermaßen repräsentative Vergleichswerte erhalten. Während so langer Zeiträume ändern sich aber oft die meteorologischen Voraussetzungen regional nicht unbedeutend. Ich habe zahlreiche Leitungsstatistiken untersucht. Man erkennt da sehr deutlich, daß die sogenannten Gewitterstraßen sich innerhalb oft recht weiter Grenzen verschieben. Jedes Jahr sind andere Abschnitte der von den Straßen senkrecht gequerten Leitungen besonders oft betroffen und daher kann man oft erst nach 30 Jahren wieder brauchbare Mittel erhalten, aus denen man Schlüsse ziehen kann.

Die topographische Komponente ist konstanter, obwohl, besonders im Gebirge, der Einfluß dieser Komponente durch die meteorologische mitbestimmt wird.

Es ist also sowohl die Ermittlung der Zahl der Blitzschläge und deren Einschlagstelle, als auch die Trennung der drei wichtigsten Komponenten in einfacher Weise nicht möglich. Wir müssen zu Untersuchungsmethoden greifen, die viel komplizierter und obendrein weniger zuverlässig sind.

Betrachten wir einmal die rein physikalischen Voraussetzungen. Wenn sich die Vorentladung des Blitzes der Erdoberfläche nähert, so wächst ihr bekanntlich aus dieser eine "Gegenentladung" entgegen, die auch "Ragentladung" genannt wird. Vereinigen sich diese beiden, dann ist der ionisierte Kanal geschlossen, in dem die Hauptentladung zustandekommt. Für jenen Punkt der Erdoberfläche, von dem die Hauptentladung daher ausgeht, ist somit sicher, im hohen Maße die Entwicklung der Gegenentladung bestimmend. Es ist nun aber klar, daß diese Gegenentladung in erster Linie von einer Zone ausgehen wird, in der unter dem Einfluß der vorwärtigen Vorentladung ein hoher Potentialgradient entstehen wird. Dadurch wird das Problem physikalisch etwas durchsichtiger, denn man erhält Hinweise auf den Einfluß der geoelektrischen Struktur und auf die Höhe, in der diese noch wirksam sein kann.

Die Äquipotentialflächen des normalen luftelektrischen Feldes werden durch die geoelektrische Beschaffenheit selbst eines inhomogenen Untergrundes, sicher nicht beeinflusst. Erst, wenn stärkere Entladungsströme fließen, gewinnen sie Bedeutung. Nun sind die Widerstandsunterschiede im Untergrunde aber oft recht bedeutend. Im Hochgebirge zum Beispiel, sind solche von mehreren Zehnerpotenzen über Entfernungen von nur wenigen Metern keine Seltenheit. Es ist dann physikalisch verständlich und auch durch Modellversuche erwiesen, daß die Gegenentladungen besonders aus schmalen gutleitenden Einschlüssen hervorquellen. Die geoelektrischen Diskontinuitätszonen unterscheiden sich daher wesentlich von ho-

mogenen Gebieten. Natürlich wird durch die Gegenentladung nur der unterste Teil der Blitzentladung beeinflusst, meist wohl nur die zwei bis drei letzten Stufen der Vorentladung, die zusammen eine Länge von ungefähr 80 bis 150 m im Mittel haben dürften. Über diesen Höhen ist dann der geoelektrische Einfluß des Untergrundes ohne Bedeutung für die Ausbildung der Blitzbahn. Diese Überlegung scheint übrigens auch vertretbar, wenn man verschiedene Blitzphotos näher analysiert.

Betrachten wir zuerst die Möglichkeit, das Problem auf statistischer Basis zu behandeln: Voraussenden möchte ich, daß nur Statistiken einen Wert haben, die sich über lange Zeiträume erstrecken.

Die Statistik, die in einigen Ländern gepflegt wird, ist natürlich mehr nach wirtschaftlichen als nach wissenschaftlichen Gesichtspunkten ausgerichtet. In erster Linie steht die meteorologische und die Schadenstatistik zur Verfügung. Kritische Vergleiche in Österreich haben gezeigt, daß als einzig sichere Bezugsbasis die Zahl der jährlichen Gewittertage angesehen werden kann. Die Angaben über Zahl der Gewitter, oder gar über deren Intensität, sind zu ungenau.

Die Schadenstatistik ist in den einzelnen Ländern verschieden organisiert. In manchen Ländern werden die Daten nicht veröffentlicht, oder sie sind unvollständig. In Österreich gibt es heute eine 15-jährige, für das Bundesgebiet einheitlich organisierte Statistik, bei der auch darauf geachtet wurde, daß sie Aussagen macht, die auch den Wissenschaftler interessieren. Da in Österreich das Versicherungswesen durchwegs in öffentlicher Hand ist, so besteht für die einzelnen Institute, die meist den Ländern gehören, kein Grund, Angaben geheim zu halten. In jedem der neun Bundesländer gibt es eine "Landesstelle für Brandverhütung", die auch die Blitzstatistik führt. Da praktisch alle wichtigen Objekte beobachtet werden und überdies auch alle Blitzschläge berücksichtigt werden, die irgendwie zur Kenntnis der Landesstellen gelangen, so ist diese Statistik ziemlich umfassend.

Gestatten Sie mir, daß ich nur einige Zahlen anführe: Österreich hat eine Fläche von nur 84.000 km². Trotzdem also Österreich ein sehr kleines Land ist, kann uns eine österreichische Statistik etwas sagen, denn dieses Land ist topographisch und siedlungsmäßig sehr verschiedenartig. Österreich umfaßt zunächst alle Landschaften, vom Hochgebirge, das fast bis 4000 m ansteigt, bis zur Tiefebene. Es hat ein stark differenziertes Klima. Siedlungsmäßig umfaßt es alle Einheiten, von der Millionenstadt bis zu den kleinsten Alpengehöften und schließlich sind Industrie und Landwirtschaft über bestimmte Zonen verteilt. So wird manches, das man in Österreich beobachtet hat, vielleicht auch für größere Länder interessant sein.

In Österreich werden jährlich ungefähr 1000 Blitzschläge statistisch erfaßt, also ein Blitzschlag auf ungefähr 80-100 km². Diese Ziffer liegt natürlich tief unter der tatsächlichen. Einen Anhaltspunkt erhält man, wenn man die Verhältnisse am Rande von Wien betrachtet. In der Stadt Wien wurden pro Flächeneinheit ungefähr achtmal, wenn man das dicht verbaute Gebiet betrachtet, ungefähr zehnmal so viel Blitzschläge beobachtet als in den unmittelbar angrenzenden Gebieten. In der Umgebung von Rom hat G. Bruckmann, allerdings auf Grund viel weniger zuverlässiger Unterlagen, ein Verhältnis 5:1 berechnet. Beide Städte sind ungefähr gleich groß. Diese Differenz ist nur darauf zurückzuführen, daß in der Stadt die Beobachtungsdichte viel größer ist als in den landwirtschaftlich besiedelten Gebieten der Umgebung. Man wird daher annehmen dürfen, daß ungefähr 95% aller Blitzschläge gar nicht beobachtet worden sind. Unter diesen Umständen darf man fragen, ob eine solche Statistik überhaupt eine Aussagekraft hat. Ich glaube, daß man diese Frage dennoch positiv beantworten darf, wenn man bedenkt, daß die Beobachtungsstellen zwar auf die jeweils dicht verbauten Gebiete zusammengedrängt sind, die vielleicht nur 5-10% der Gesamtfläche Österreichs ausmachen, daß diese aber wieder recht gleichmäßig über das ganze Staatsgebiet verteilt sind. Wenn man von Wien und vier weiteren Städten mit unge-

fähr 100.000 bis 250.000 Einwohnern absieht, verteilen sich die Beobachtungsstellen auf ungefähr 17.000 Siedlungseinheiten, die in 79 Bezirken zusammengefaßt sind. Wir haben nun diese Bezirke zur Grundlage der Blitzstatistik gewählt. Sie sind im Durchschnitt etwas über 1000 km² groß, also relativ klein, andererseits aber doch so groß, daß durchschnittlich auf einen im Jahr 12 beobachtete Blitzschläge fallen, und da die Statistik heute über 15 Jahre läuft, so erhält man für den Bezirk im Durchschnitt über 150 beobachtete Blitzschläge. Die örtliche Verteilung einer solchen Zahl kann doch schon einiges sagen.

Wir wollen daher unsere Statistik nicht auf die Flächeneinheit, sondern auf die Zahl der beobachteten Objekte beziehen, da nur diese exakt erfaßbar ist. Es ist, um die Zuverlässigkeit dieser Reduktion beurteilen zu können, wieder notwendig, die Verteilung dieser Objekte über die einzelnen Staatsgebiete zu untersuchen. Nur dann, wenn diese einigermaßen homogen ist, wird eine auf die Zahl der Objekte bezogene Statistik in den einzelnen Staatsgebieten vergleichbare Angaben liefern können.

Im ganzen Staatsgebiet entfallen, wenn man die Wald-, Wasser- und Odlandflächen abzieht, in denen kein Beobachtungsdienst besteht, durchschnittlich 22 Objekte auf den Quadratkilometer. Diese Verteilung ist in ungefähr 65% des Staatsgebietes fast die gleiche, in 10% der Gebietsfläche ist sie um 27% und in 25% der Gebietsfläche um 45% geringer. Es handelt sich bei den letzten beiden um die Hochgebirgsgebiete in Salzburg und Tirol. Man kann also von einer ziemlich homogenen Verteilung der Objekte über das ganze Staatsgebiet sprechen. Daher wird eine auf die Zahl der Objekte bezogene Statistik ausreichend repräsentativ sein. Selbst die erwähnten schwächer besiedelten Gebirgszonen werden ausreichend statistisch erfaßt, denn die Siedlungen sind in diesen Gebieten zwar auf die schmalen Täler beschränkt, diese aber sind wieder ziemlich gleichmäßig über die ganze Alpengrenze verteilt und sie reichen bis in bedeutende Höhen, bis in die Nähe des Zentralkammes.

Mir bilden nun für die einzelnen Bezirke Quotienten, in deren Zähler die jährlich beobachteten Blitzschläge und in deren Nenner die Zahl der beobachteten Objekte steht. Da dieser Bruch sehr klein ist, so wird er mit 10.000 multipliziert. Er gibt also die Zahl der Blitzschläge pro 10.000 Objekte an. Nun soll aber noch die topographische und meteorologische Komponente ausgeschieden werden. Der Einfluß der Höhenlage wurde genau untersucht; er ist kaum nachweisbar und überdies nicht systematischer Natur. Die meteorologische Komponente wurde in der Weise berücksichtigt, daß auf die Zahl der jährlichen Gewittertage, die in dem betreffenden Bezirk beobachtet wurden, bezogen wurde. Es bleibt also nur die durch die geophysikalische Bodenbeschaffenheit bedingte Komponente übrig.

Gestatten Sie mir nun, daß ich das Ergebnis dieser langjährigen Statistik vom Standpunkt der Geoelektrik aus kurz bespreche:

Sie sehen im Bilde eine Tabelle, in der für das ganze Staatsgebiet die besprochene, auf 10.000 Objekte bezogene Ziffer,

Bild 1. Angabe von Z_H für die geologischen Zonen

wir wollen sie Gefährdungsziffer nennen, angegeben ist. Das Staatsgebiet wurde zu diesem Zweck in Teilgebiete zergliedert, die geologisch einheitlich beschrieben werden können. Man sieht, daß die Gefährdungsziffer für die alten geologischen Formationen, besonders für die archaische "Böhmische Masse" weit höher ist als für die jungen Formationen. Man kann eine ziemlich gleichmäßige Zunahme der Gefährdungsziffer mit dem geologischen Alter feststellen. Diese Verteilung wurde von mir vor ungefähr 20 Jahren auch beobachtet, als ich für das Land Sachsen die Blitzstatistik von Lehmann und Schneider ausgewertet habe. Auch damals waren die alten Formationen durch eine besonders hohe Blitzgefährdung ausgezeichnet.

Diese Tatsache ist nun keineswegs leicht zu erklären. Eine Arbeitshypothese, die jetzt untersucht wird, werden wir noch besprechen.

Die Statistik zeigt aber auch, daß es eng begrenzte Zonen, deren Blitzgefährdung weit über jener der Umgebung liegt, gibt. Ich habe bereits 1934 auf eine kleine Gemeinde Absroth in Nordböhmen hingewiesen, in der die auf Grund der Angaben von J. Schwirtlich berechnete Blitzgefährdung ungefähr 140 mal so groß ist wie jene der nächsten Bezirke in Sachsen. Die statistische Auswertung der österreichischen Statistik durch Bruckmann hat nun zwei weitere Gemeinden in Kärnten eindeutig als Blitznester erkannt. In einer Ortschaft von 150 Häusern hat der Blitz in 6 Jahren zehnmal eingeschlagen, in der anderen, die 258 Häuser hat, zwölfmal. Die Blitzgefährdungsziffer ist ungefähr zwölfmal so hoch wie jene der Umgebung. Unter Annahme einer Poissonverteilung hat Bruckmann die Wahrscheinlichkeit für diese beiden Ereignisse mit 0,00009 und 0,0005, sowie die Wahrscheinlichkeit dafür, daß zwei Orte mit so hoher Blitzgefährdung im gleichen Bezirk existieren, mit 0,0019 berechnet. Man kann also von Blitznestern sprechen.

Ein weiteres Blitznest habe ich auf Grund der Angaben des Forstpersonales in der Steiermark konstatiert. Sie sehen es im nächsten Bilde. Auf diesem Plan sind die Einschlagstellen eingetragen, die

2. Bild. Blitznest bei Bad Aussee

in den letzten Jahren beobachtet wurden. Vergleicht man diese Beobachtungen mit der Statistik, so erkennt man folgendes: Im Bereiche des Blitznestes entfallen ungefähr 21 Blitzschläge im Jahr auf den Quadratkilometer, für das Bezirksgebiet kann man mit 0,3 bis 0,5 Einschlägen pro Quadratkilometer rechnen. Die Gefährdung des Blitznestes ist also 40 bis 50 mal so hoch wie jene der Umgebung.

Ich habe dieses Gebiet auch geoelektrisch untersuchen lassen und zeige Ihnen das Ergebnis im nächsten Bild.

3. Bild. Geoelektrische Untersuchung Bad Aussee

Das geoelektrische Profil, das mit einer Auslegung von 2x20 m gemessen wurde, zeigt einen Verlauf, wie wir ihn über tektonischen Störungen oft erhalten. Im Bereiche des Blitznestes und

an seinen Grenzen sind Widerstandsminima ausgeprägt. Außerhalb dieser Zone steigt der spezifische Widerstand zu beiden Seiten auf Werte von ungefähr 230 Ohm m, die in dieser Gegend als normal zu bezeichnen sind.

Es handelt sich also um eine ausgeprägte geoelektrische Diskontinuität.

Neben statistischen Untersuchungen steht die Auswertung von Modellversuchen. Wenn ich deren Ergebnis bespreche, so darf ich eine Bemerkung vorausschicken: Es ist vollkommen klar, daß der Modellversuch niemals die natürlichen Verhältnisse rekonstruieren kann, er wird stets nur Hinweise geben können. Diese aber sind wertvoll, wenn man bedenkt, daß z.B. in Österreich nach den Gesetzen der Wahrscheinlichkeitsrechnung innerhalb eines Zeitraumes von 20 Jahren erst jedes 79.000 Haus dreimal vom Blitz getroffen wird. Wollte man also diese Fragen nur aus Naturbeobachtungen heraus klären, so müßten Jahrzehnte vergehen, ehe man die ersten Hinweise für die Behandlung des Problems erhielte. Dagegen gestattet der Modellversuch eine beliebig große Zahl von Beobachtungen unter Bedingungen, die man ebenfalls beliebig wählen kann. Man wird daher auf den Modellversuch nicht verzichten, sondern seine Ergebnisse sinnvoll mit den Naturbeobachtungen verbinden.

Mit Schlagweiten von weniger als einem Meter haben u.a. H. Norinder und O. Salka in Uppsala gearbeitet. Ein Meßergebnis zeigt das nächste Bild. Das vordringende Entladungshaupt wird dadurch eine Spitzenelektrode ersetzt, die in der Mitte über einer mit

4. Bild. Modellversuch von NORINDER u. SALKA

Sand bedeckten Metallscheibe hängt. In dieser erkennen wir links eine gutleitende Einlagerung. Wir sehen, daß die Entladung zum größten Teil nach diesen Einlagerungen hin abgelenkt wird. Nur wenige feilientladungen gleiten nach den Punkten B und C hin ab. Gegen diese Versuche wurde eingewendet, daß in der Natur Einlagerungen von der Art, wie sie Norinder und Salka verwendet haben, nicht vorkommen. Ich habe daher diese Versuche im Hochspannungs-

feld der Technischen Universität Dresden wiederholt und dabei natürliche geologische Leiter - Sand, Humus und stark angefeuchteten Lehm . verwendet. Außerdem habe ich mit Entladungen bis zu 2 m Länge gearbeitet. Ein Meßergebnis sehen Sie im nächsten Bild. Die Entladungselektrode wurde bei A...B...C...D...E ange-

5. Bild. Versuche in Dresden

ordnet. Im oberen Bild sieht man die Verteilung der Einschlüge über einen gewachsenen Boden, in dem gutleitender Lehm eingelagert ist. Die meisten Einschlüge sind über der gutleitenden Zone konzentriert. Im unteren Teilbild ist der umgekehrte Fall dargestellt. Die schlechtleitende Zone ist aus ziemlich trockenem Sand gebildet. In ihr ist nur ein Einschlag zu verzeichnen. Dagegen sind diese an der Diskontinuitätsfläche konzentriert. Im nächsten Bild sind alle Ergebnisse miteinander verglichen.

6. Bild. Versuche in Dresden

Die Maxima und Minima sind besonders über der gutleitenden Einlagerung, bei positiver Spitze viel stärker ausgeprägt als bei negativer.

Das Ergebnis meiner Untersuchungen deckt sich also gut mit jenem der Versuche von Norinder und Salka. Auf der Hochschule für Elektrotechnik in Ilmenau hat K. Gopalan Modellmessungen gemacht, bei denen der Untergrund durch ein System Ohmscher Widerstände ersetzt wurde. Die Entladungslänge war leider nur gering, nämlich 44 cm.

Als Beispiel möchte ich die Analyse des Meßergebnisses zeigen, das Gopalan in Tafel 14 seiner Dissertation bringt. Man sieht,

7. Bild. Versuche von GOPALAN

daß über der Diskontinuitätsstelle ein bedeutender Anstieg der Einschlüge zu beobachten ist. Die Verteilungskurve zeigt über der rechten Diskontinuitätsstelle einen viermal so hohen Wert wie über der linken. Das Widerstandsverhältnis ist rechts: 1:20, links aber nur 1:4.

Im Zusammenhang damit sind auch Experimente interessant die K. Jummer auf der Hochschule für Elektrotechnik in Ilmenau ge-

macht hat. Von diesen will ich zwei Bilder zeigen. Dummer hat den Verlauf der Entladung in feuchtem Sand untersucht, also die sog. Blitzröhren. Im nächsten Bild ist der Verlauf einer Blitzröhre in einem homogenen Sandboden dargestellt. Sie verläuft von

8. Bild. Blitzröhre nach Dummer

der Einschlagstelle ziemlich geradlinig und ungefähr senkrecht zur Oberfläche in der Richtung zum Grundwasser. Im nächsten Bilde sehen wir den Verlauf in einem inhomogenen Untergrund. Der Sand hat wieder einen spezifischen Widerstand von ungefähr

9. Bild. Blitzröhre nach Dummer

150 Ohm m. Zu beiden Seiten sind aber gutleitende Einlagerungen mit spezifischen Widerständen von 4 und 12 Ohm m angeordnet. In diesem Falle teilt sich die Entladung nach beiden Richtungen hin und steuert die gutleitenden Zonen an. Diese Untersuchungen zeigen somit einen ähnlichen Verlauf der Entladungsbahn wie er in der Luft, nahe der Erdoberfläche, beobachtet worden ist.

Wir wollen nun damit die in der Natur beobachteten Ergebnisse vergleichen. Die Beobachtung von Blitzschlägen in Energieleitungen hat verschiedene Autoren zu verschiedenen Erkenntnissen geführt. G. Lehmann, der wohl über die älteste Statistik dieser Art verfügt - sie ist 30 Jahre alt - kommt zu dem Resultat, daß über geoelektrischen Diskontinuitätszonen mehr Einschläge zu verzeichnen sind als über geoelektrischen homogenen Zonen. Andere Autoren kommen zu entgegengesetzten Resultaten. Diese Verschiedenheit der Ergebnisse könnte aber physikalisch durchaus verstanden werden, wenn man bedenkt, daß die einzelnen Autoren ganz verschiedene Leitungen untersucht haben, nämlich solche über homogenen und inhomogenen Untergrund. Außerdem sollte man bei einem kritischen Vergleich nur solche Statistiken berücksichtigen, die sich über mindest 5 - 10 Jahre erstrecken. Bei kürzeren Meßreihen ist die Streuung zu groß und es können kaum brauchbare Durchschnitts ermittelungen werden.

Ich habe nun auch die bereits besprochene österreichische Statistik in dieser Richtung analysiert. Das österreichische Bun-

desgebiet ist mit einem Netz von ungefähr 10000 geoelektrischen Sondierungen überzogen, so daß man die geoelektrischen Eigenschaften der einzelnen Gebiete einigermaßen beschreiben kann. Zunächst kann man zeigen, daß die geoelektrische Homogenität der jüngeren geologischen Formationen im allgemeinen größer ist als jene der alten. Die bereits gezeigte Tabelle würde dann lehren, daß die Blitzgefährdung mit zunehmender Homogenität nimmt, was auch mit dem Ergebnis der besprochenen Modellversuche übereinstimmt. Ich habe nun weiter in Österreich zwei Gebiete von ungefähr 50.000 Objekten ausgewählt, von denen das eine geoelektrisch ziemlich homogen, das andere sehr inhomogen ist. Die Statistik zeigt nun, daß in der geoelektrisch inhomogenen Zone 83% der Bezirke mit extrem hoher Gefährdungsziffer (mehr als 12,6) liegen. Die stärkere Gefährdung des inhomogenen Gebietes ist also offensichtlich. Zur Erklärung wird jetzt eine Arbeitshypothese untersucht. Im homogenen Gebiet ist meist auch die Grundwasserverteilung eine homogene. Landwirtschaftliche Objekte sind daher nicht an bestimmte Zonen gebunden, an denen Wasser vorhanden ist. Im alten, geoelektrisch inhomogenen Gebirge aber ist Wasser nur aus einzelnen mächtigen wasserführenden Spalten zu gewinnen. Die landwirtschaftlichen Objekte werden daher meist in deren unmittelbaren Nähe angeordnet, da ja früher für den Standort einer Landwirtschaft die Möglichkeit, Wasser zu gewinnen, von größter Bedeutung war. Damit rücken aber alle diese Objekte auch in die Nähe von Zonen hoher Blitzgefährdung.

Wenn ich damit meine Ausführungen, die keineswegs vollständig sind, abschließe, so würde ich mich wirklich freuen, wenn mein Vortrag dazu beigetragen hätte, Sie zu Vergleichen anzuregen, die Sie vielleicht Ihren eigenen statistischen Untersuchungen entnehmen können. Gerade auf diesem Gebiete ist eine internationale Zusammenarbeit notwendig, denn die Probleme liegen nicht einfach. Es wäre vielleicht eine dankbare Aufgabe dieser Konferenz, eine einheitliche statistische Erfassung der Blitzschlage anzustreben.

Charge Generation in Thunderstorms

by

J. Alan Chalmers

Durham University, England

1. Introduction

I think I must first apologize for intruding into this discussion when I have no theory of my own to put forward; if what I have to say is more critical of the theories that have been discussed, rather than constructive suggestions of alternative theories, my excuse may be that it is difficult to formulate a new theory before we know what is wrong with the old ones.

2. Requirements of Theory

Mason has given a number of facts which must be explained by a satisfactory theory of thunderstorm electrification. However there seems to be one case where his remarks can be improved upon, and other requirements which can be added to his list.

Mason gives the requirement of generating current at the rate of about 1 amp. But this is the requirement just to provide the lightning flashes of an average storm, and to this must be added the charges which are used in the point-discharge current below a cloud, and the charges used in dissipating currents within the cloud. It is probable that a total generating current of 3-5 amp is a better estimate, with about 1 amp external current outside the cloud, including lightning flashes to ground, and 2-4 amp average internal dissipating current, including lightning flashes within the cloud. Wormell's (1953) results show that, after a

flash, the potential gradient due to the cloud returns towards its previous value approximately exponentially, and this indicates the building-up of a dissipating current.

Mason's figures refer to an average storm, but there are storms which are much more violent than the average, and if Mason's theory, or any other, is to be considered satisfactory, it must be able to account for the electrical phenomena in these. Vonnegut and Moore (1958) quote cases where there are 10-20 lightning flashes per second, as compared with Mason's figure of 1 in 20 seconds. Thus the lightning current must be 100 amp or more and the charge being separated of the order of 10^5 C. The question then is whether this remains within the bounds of possibility, or whether some theory is required in which the relative motion of charges of different signs is not limited to that provided by gravitation.

In nimbo-stratus clouds, the total separation of charge is approximately measured by the precipitation current at the ground. This seldom reaches a value of more than 10^{-10} amp/m², so that for an area of 10 km², corresponding to that of a thundercloud, the current is only about 10^{-3} amp, i.e. less than that of the thunder cloud by a factor of over 10^3 . An acceptable theory of thunderstorm electricity must be able to explain how it is that the process concerned gives so much smaller electrical effects in the nimbo-stratus than in the cumulo-nimbus clouds, although, for example, the amounts of precipitation show much less difference.

It has been pointed out several times by Vonnegut and others that the current carried down by precipitation in the thunder cloud is never more than a small fraction of the charge separation, though most theories consider precipitation to be the mechanism by which charge is separated. Even measure-

ments within the cloud at the Zugspitze (Kuettner, 1950) show that precipitation does not carry much charge. It is therefore necessary for a theory involving precipitation to be able to explain how the charge leaves the precipitation and becomes attached to cloud droplets.

Information available at present suggests that the external current, above and below the cloud, is probably less than the current of charge separation within the cloud and this leads to the conclusion (see Chalmers, 1961) that the source of the charging current must be within the cloud and not, as in Vonnegut's theory, outside.

3. Discussion of Mason's Theory

While Mason's theory appears to give an adequate explanation of the charges in a normal thunderstorm, it has yet to be shown whether it is able to account for very violent storms and whether it can explain why the nimbostratus cloud gives so much less charge generation. And the question of the transfer of the charge to the cloud droplets from the precipitation has not been discussed in detail though there may be an answer in the splashing that occurs at temperatures close to 0°C.

The measurements of Latham and Mason (1961b) on the production of charge and of splinters showed good agreement with their theory considering the average charge per drop. But the measurements of Mason and Maybank (1960) and the more recent measurements of Evans and Hutchinson (1963) have shown that some individual drops on freezing give much greater charges than the average and, in fact, give charges which are quite considerably greater than could be provided by the mechanism suggested by Latham and Mason (1961b). This forms a serious difficulty for their theory.

It seems surprising that Latham and Mason concerned themselves with electrical effects of temperature differences in ice, corresponding to the Thomson effect in metals and did not consider electrical effects at the surface of melting, corresponding to the peltier effect in metals. This is the more surprising when it is remembered that Workman and Reynolds (1950) have found very large electrical effects on freezing, even though, as Brook points out, they themselves no longer consider this as the main agency of charge separation in clouds.

Latham and Mason found that their theory of electrical effects in ice at different temperatures was adequate to account for the ice-impact results, when there was no water present; they then applied the same theory to riming phenomena, neglecting the ice-water boundary, and found it would give enough charge for a thunderstorm. But surely the ice-water boundary cannot be neglected and there is very likely to be preferential movement of ions across this boundary. It may be added that the total "freezing potential" measured by Workman and Reynolds (1950) involves not only the ice-water interface but also the metal-water and metal-ice interfaces.

4. Discussion of Workman-Reynolds Theories

There is at present a very serious discrepancy between the experimental results for the amounts of charge separated on ice impact, the results in New Mexico (Reynolds, Brook and Gourley, 1957) giving values greater by a factor of 10^5 than those in England (Latham and Mason 1961a, Hutchinson, 1960; Evans and Hutchinson, 1963). It is to be hoped that each side will attempt to repeat the experiments carried out on the other side.

The remarks made in regard to Mason's theory in respect of violent storms, of nimbo-stratus clouds and of the transfer of the charge to the cloud droplets apply also to these theories.

5. Discussion of Vonnegut's Theory

Some of the main arguments put forward for Vonnegut's theory seem to be more arguments against the theories that involve precipitation and ice. While Vonnegut's theory could more easily satisfy some of the conditions stated, such as those of the very violent storms, of the nimbo-stratus clouds and of the absence of much charge on precipitation, there still seem to be very serious difficulties in the theory.

It is difficult to visualise how it is that when negative charge has reached the base of the cloud in the down-draught, and there attracts positive charge produced by point discharge, it is the positive, rather than the negative charge which gets into the up-draught. Similarly, how is it that, when positive charge gets to the top of the cloud, it is not this charge but negative from above which gets into the down-draught? No answer can be contemplated in terms of the attachment of the charges to cloud droplets or precipitation particles, since this would again lead to differential motion under gravitation and a return of the problems that the theory is trying to avoid.

Also Vonnegut's theory is in opposition to the results discussed above regarding internal and external currents.

6. Warm Thunderstorms

It seems that the question of warm thunderstorms is a very vital one. If it can be confirmed that these do exist and do give the same separation of charge as normal thunderstorms, then this does seem to give a serious blow to those theories that involve ice as a necessary agent in the generation of thunderstorm charge. If, however, it should turn out that the polarity of a warm thunderstorm is opposite to that of the normal thunderstorm, this might be explained as due to the same process as is normally concerned in

the production of the lower positive charge, but acting with sufficient effect to produce lightning.

7. Conclusions

While there may be substance in some of the arguments against precipitation being the mechanism by which charge is separated in clouds, it does not seem that Vonnegut's theory is wholly satisfactory and up to the present there has been no other reasonable alternative, and we are left with a choice of theories, none of which appears quite satisfactory.

What appears to be required is a theory which might involve ice, but in which the separation in space is achieved not by gravitation but by some other agency. As a tentative suggestion, could there be some sort of centrifugal action in the main up-draught, where the electrification process occurs, flinging the heavier, negatively charged particles out of the up-draught while retaining the smaller positively charged particles to move upwards, giving a speed of separation much greater than the differential speed under gravity, and hence requiring a smaller content of charge in the cloud. The postulation of the up-draught would explain the absence of effects of such magnitude in the nimbo-stratus cloud, and allow of larger currents with very intense up-draughts. The effect need not be thought of as centrifugal action on a large scale, but rather as the throwing off sideways of the heavier particles by the turbulence that occurs in the up-draught. It does not seem that enough is yet known about the motion in the up-draught to be able to make any calculations to put this suggestion to the test.

References

Chalmers, J.A., 1961, "A criterion for thunderstorm theories", J. Atmosph. Terr. Phys., 21, pp. 174-176.

- Evans, D. G. and Hutchinson, W. C. A., 1963, "The electrification of freezing water droplets and colliding ice particles", not yet published.
- Hutchinson, W. C. A., 1960, "Ice-crystal contact electrification", Quart. J. R. Met. Soc., 86, pp. 406-407.
- Kuettner, J., 1950, "The electrical and meteorological conditions inside thunderclouds", J. Met. 7, pp. 322-332.
- Latham, J. and Mason, B. J., 1961a, "Electric charge transfer associated with temperature gradients in ice", Proc. Roy. Soc., A, 260, pp. 523-536.
- Latham, J. and Mason, B. J., 1961b, "Generation of electric charge associated with the formation of soft hail in thunderclouds", Proc. Roy. Soc. A. 260, pp. 537-549.
- Mason, B. J. and Maybank, J., 1960, "The fragmentation and electrification of freezing water drops", Quart. J. R. Met. Soc. 86, pp. 176-185.
- Reynolds, S. E., Brook, M. and Gourley, M. F., 1957, "Thunderstorm charge separation", J. Met. 14, pp. 426-430.
- Vonnegut, B. and Moore, C. B., 1958, "Giant electrical storms" in "Recent Advances in Atmospheric Electricity" (L. G. Smith, ed.) (New York: Pergamon Press), pp. 399-411.
- Workman, E. J. and Reynolds, S. E., 1950, "Electrical phenomena occurring during the freezing of dilute aqueous solutions and their possible relationship to thunderstorm electricity", Phys. Rev., 78 pp. 254-259.
- Wormell, T. W., 1953, "Atmospheric electricity: some recent trends and problems", Quart. J. R. Met. Soc., 79, pp. 3-50.

Received 11/23/62

RELATIONS BETWEEN LIGHTNING DISCHARGES AND DIFFERENT
TYPES OF MUSICAL ATMOSPHERICS

by

Harald Norinder
University of Uppsala

1. Introduction

When observing atmospherics at very low and audible frequencies by the use of a special amplifier, different types of musical (tonal) quality are heard. One type is classified as a usual whistler characterized by a steadily decreasing whistling tone from the upper limit of hearing and downwards with a frequency which falls first rapidly and then more slowly. Unusual musical atmospherics are characterized by irregular and shifting frequency variations.

The first to detect usual whistlers with an amplification set was Barkhausen (1) in 1918, and he alleged that the whistlers had connections with meteorological phenomena on warm summer days. In 1930 Barkhausen (2) indicated lightning discharges as a source of whistlers.

The first theoretical analysis of whistlers was made in 1925 by Eckersley (3). No information was presented of relations between lightning flashes and whistlers, and in 1928 he and Chapman (4) co-ordinated whistlers with powerful heard atmospherics. Later, Eckersley (5) cites relations observed between visible nocturnal individual lightning flashes and whistlers. Early investigations of whistlers were also carried out by Burton and Boardman (6). In Storey's (7) well as experimentally as theoretically comprehensive work a connection is assumed between atmospherics from lightning discharges and whistlers caused by them.

The theoretical investigations of whistlers stimulated extended experimental observations and have obviously influenced the comprehensive observation program of whistlers carried out in North America during the International Geophysical Year (1957-58). The main objective of this program was to record whistlers on a number of synoptically situated stations in North America. Magnetic tape recorders were used and the recording periods were not less than two minutes each hour round the clock.

2. Motivation for whistler investigations in Sweden

The IGY program did not include any particular investigations of lightning discharges which caused whistlers. Therefore it seemed to be of special value to start whistler investigations in Sweden. To some extent they could be considered as a complement to the mentioned IGY program. The aim of the new project was to analyse the relations between and the variation features of those individual lightning discharges which caused whistlers.

With its northern latitudes Sweden seemed to be well situated for whistler investigations. A special circumstance facilitated such a project. For the past few years a number of field stations outside Uppsala had been used and operated for simultaneous analysis of electromagnetic field variations of lightning discharges. Some of the results are given in the following publications (8-11).

A number of recording cathode-ray oscillographs and direction finders were at hand. Therefore the new investigation project only necessitated the construction of special whistler recorders.

Results obtained in the project will in brief be presented here; details are given in a number of publications (12-18).

3. Observation station, equipment, method of observation and supervision

In order to avoid man-made noise the whistler station was placed 17 km east of Uppsala. The geomagnetic coordinates are $\phi 58^{\circ}4$, $\lambda 107^{\circ}0$.

The following instruments were used:

- (a) Whistler recording equipment,
- (b) CRO recorder for lightning discharges and sferics wave-forms,
- (c) CRO recorder of multiple lightning strokes,
- (d) Direction finders of CRO type,
- (e) Sonagraph frequency analyser,
- (f) Harmonic frequency analyser.

The observation of whistler activities was done continuously at the station during the summer months June-August. There was a special reason for the concentration of the work during these months. It is well-known that the general occurrence of whistler activity is lower in summer, but on the other hand, it is only during this season that it is really possible in Sweden to observe thunderstorm activities at such distances as are necessary for a correlation with whistler phenomena.

During two seasons, 1958 and 1960, the observation and supervision program was carried out during the day, in 1959 both night and day, and

2. Motivation for whistler investigations in Sweden

The IGY program did not include any particular investigations of lightning discharges which caused whistlers. Therefore it seemed to be of special value to start whistler investigations in Sweden. To some extent they could be considered as a complement to the mentioned IGY program. The aim of the new project was to analyse the relations between and the variation features of those individual lightning discharges which caused whistlers.

With its northern latitudes Sweden seemed to be well situated for whistler investigations. A special circumstance facilitated such a project. For the past few years a number of field stations outside Uppsala had been used and operated for simultaneous analysis of electromagnetic field variations of lightning discharges. Some of the results are given in the following publications (8-11).

A number of recording cathode-ray oscillographs and direction finders were at hand. Therefore the new investigation project only necessitated the construction of special whistler recorders.

Results obtained in the project will in brief be presented here; details are given in a number of publications (12-18).

3. Observation station, equipment, method of observation and supervision

In order to avoid man-made noise the whistler station was placed 17 km east of Uppsala. The geomagnetic coordinates are $\lambda 58^{\circ}4$, $\Lambda 107^{\circ}0$.

The following instruments were used:

- (a) Whistler recording equipment,
- (b) CRO recorder for lightning discharges and sferics wave-forms,
- (c) CRO recorder of multiple lightning strokes,
- (d) Direction finders of CRO type,
- (e) Sonagraph frequency analyser,
- (f) Harmonic frequency analyser.

The observation of whistler activities was done continuously at the station during the summer months June-August. There was a special reason for the concentration of the work during these months. It is well-known that the general occurrence of whistler activity is lower in summer, but on the other hand, it is only during this season that it is really possible in Sweden to observe thunderstorm activities at such distances as are necessary for a correlation with whistler phenomena.

During two seasons, 1958 and 1960, the observation and supervision program was carried out during the day, in 1959 both night and day, and

in 1961 only at night.

The supervision was carried out in such a way that the thunderstorm activities were observed for 10 minutes every half hour. Simultaneously the occurrence of whistler activity was checked and detailed notes of the situations were made. Such notes formed the basis for the comprehension of the development of whistler situations.

When a whistler activity was ascertained, the observer either extended the continual observation or, if the whistler intensity seemed high enough, started a full recording procedure. This meant that all the mentioned apparatus were set into continual operation until the activity disappeared. In this way the following data were obtained: (1) the geographical position of the occasional lightning discharges, (2) the wave-forms of the produced atmospherics, (3) multiple lightning strokes, their intervals and time sequences, and (4) tape recordings of whistlers. These data will obviously make possible a rather detailed analysis.

4. Observations of local lightning paths producing whistlers

At the very beginning of the whistler investigations in 1956, an attempt was made to determine what direction of lightning paths was followed by whistlers, e.g. if they were only linked to vertical lightning paths or to those in other directions. This was singly possible by simultaneous local observations of lightning paths and whistlers. Earlier direct observations from other localities which might have answered this problem were not at hand.

Comprehensive measurements of lightning discharges combined with daylight photographs of lightning paths during the thunderstorm season of 1956, when three field stations were simultaneously operating in the vicinity of the whistler station, did not result in any simultaneous observations. On the other hand, in 1957, operations of the three stations resulted in the most comprehensive number of local thunderstorm and lightning flashes ever obtained. More than 100 daylight photographs and 600 cathode-ray oscillographic records were obtained. In spite of the great number of lightning discharges within the area in the numerous thunderstorms during the season, we succeeded only during a single day in confirming that certain lightning discharges were accompanied by whistlers. This constitutes a glaring and permanent proof of how rare and hazardous the conditions must be for whistlers to develop within a thunderstorm area. There must, consequently, be special pre-requisite conditions in the thunder atmosphere and in the layers existing outside in space for a

lightning discharge to give rise to whistlers.

The mentioned occasion during the 1957 thunderstorm season when two local thunderstorms were accompanied by whistlers occurred on August 6, with the first thunderstorm between 15.07 and 15.57. In one case it was possible to obtain a daylight picture (see Fig. 1) of a vertical lightning flash which according to simultaneous observations at the whistler

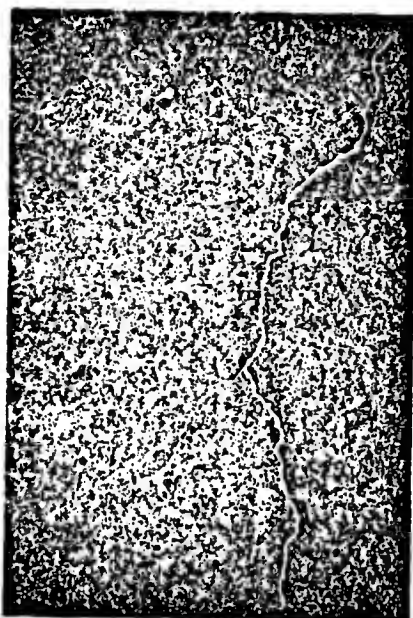


Fig. 1
Daylight photograph of vertical
whistler-producing lightning
flash.

station gave rise to a whistler. The distance from the station to the flash was 18 kilometres. The small distance of the stroke from one of the oscillographic recording stations allowed a calculation of the current in the path which reached a peak value of 7 kiloamperes. A second thunderstorm arrived at 19.15 on the same day. For half an hour the author was able to observe a number of typically vertical lightning paths which were all followed by whistlers. Observations based on the author's forty years' experience of studying lightning discharges characterized the thunderstorm observed as having an extraordinary and copious occurrence of vertical lightning strokes. Through the investigations of these two thunderstorms, it has accordingly been established that local vertical lightning paths generate whistlers. Oscillograms from the lightning stroke of Fig. 1 show to full evidence that negative charge was transported in the channel to the ground. The results obtained of the dominant role of vertical lightning strokes is quite in agreement with the current-jet hypothesis of whistler generation by Hoffman (19).

5. Occurrence of whistlers

It has been found that whistlers occur in groups during periods of time lasting up to several hours. Between these periods, whistlers are entirely absent. On going through the routine observations carried out every half hour no occasion occurred when the observer only heard isolated whistlers. During these periods are observed either cases in which no whistlers at all occur, or else cases in which groups of whistlers occur. Such situations as are characterized by activity as regards whistlers have therefore been designated throughout as "whistler situations". A typical survey of a whistler situation during an observation period of 46 days is exemplified in Fig. 2.

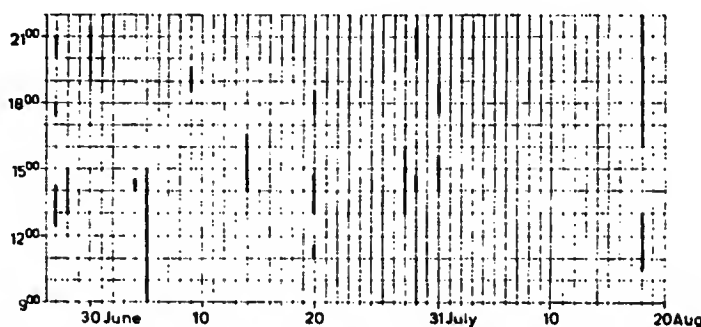


Fig. 2. General survey of whistler situations.

The following general conclusions can be drawn:

- (1) Whistlers occur in great numbers during shorter periods of time between which there is a total cessation - this may extend over hours, days, and, in isolated cases, even weeks.
- (2) Several whistler situations often occur on the same day or on consecutive days.
- (3) A cessation of whistler activity cannot be connected with a general cessation of thunder activity.

Through the investigation of whistlers and their occurrence carried out as described above, it is confirmed that, in addition to lightning discharges, there are certain other required, locally manifested, geophysical conditions which are necessary if whistlers are to be generated at all.

6. Synoptic direction-finder observations related to whistlers

By the use of a direction finder in combination with records of whistlers, it is obviously possible to obtain and follow synoptical si-

tuations of whistler activities. It has been found that a thunderstorm region located in one direction can be accompanied by whistlers while another simultaneous thunderstorm located at the same or at other distances and in other directions may or may not produce whistlers simultaneously. It is possible to illustrate such varying situations by the use of a graphic reproduction in which suitable circles provided with time and distance indications are used. Thunderstorms are marked in the sectors in such a way that no blackening represents no whistlers, half blackening an average number of whistlers, and full blackening a high number. The graphical method is e.g. illustrated according to direction finder observations of an interesting thunderstorm situation on 28/7/58 reproduced in Fig. 3. Two marked thunderstorm centres exist partly over

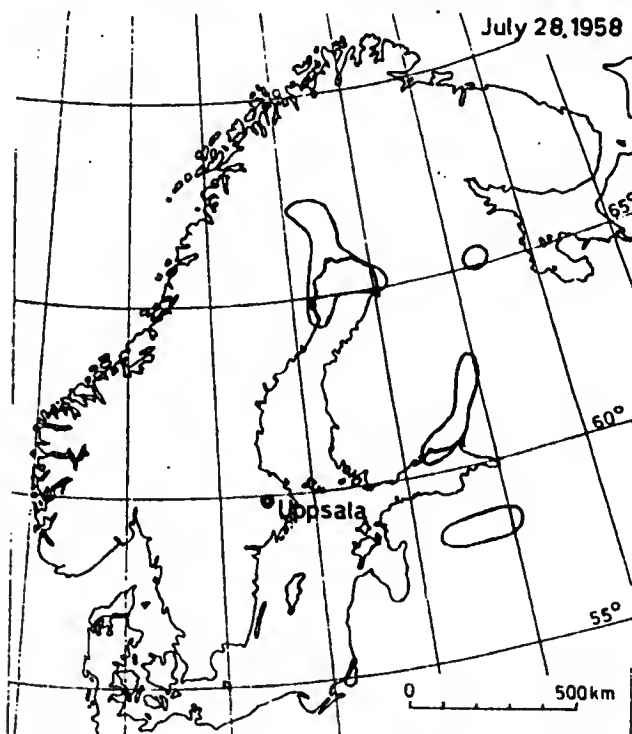


Fig. 3. Map with thunderstorm regions related to whistlers.

north-east Sweden and partly over the Gulf of Finland. The development of whistlers in these two thunderstorms during the course of the day is apparent from the graphic survey of Fig. 4. In this, very weak whistlers may be noted from both the thunderstorms during the observation period of 13.00. At 13.30 weak whistlers started at the centre in Sweden, and stronger whistlers which were very marked for both centres during 14.00-14.40 started at the centre in Finland. The whistlers' intensities decreased for both centres at 15.00 and ceased after 15.30.

According to direction-finder observations three thunderstorm areas appeared on 7/9/59 (see Fig. 5), one situated in southern Sweden, one in

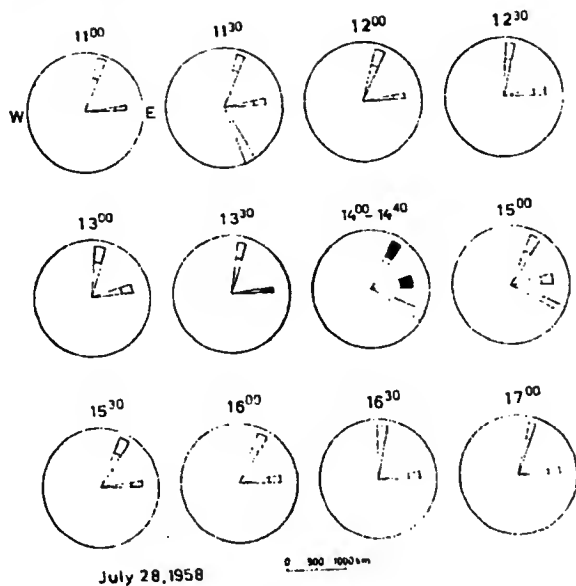


Fig. 4. Thunderstorm regions productive or non-productive of whistlers.

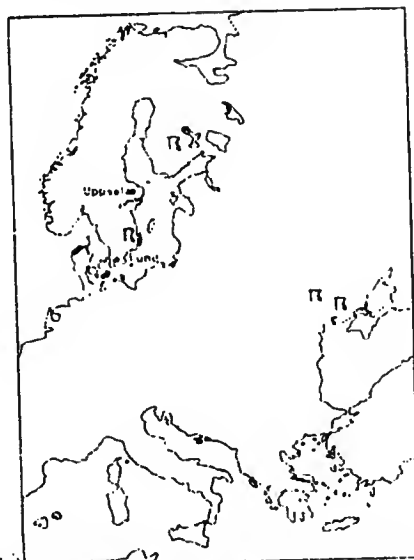


Fig. 5.

Fig. 5. Three simultaneous thunderstorms of which only one, located in Finland, was followed by whistlers.

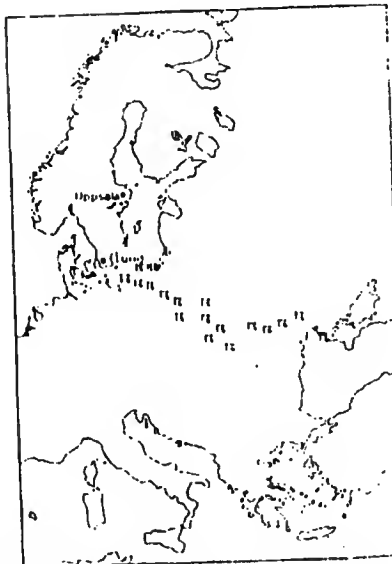


Fig. 6.

Fig. 6. An extensive thunderstorm front in which whistlers were produced and located only in the regions of the Ukraine.

central Finland and one in the Ukraine. The thunderstorm area in southern Sweden was very intense but in spite of that it yielded no whistlers. Only the area in Finland gave whistlers, whilst they failed to appear at all from the area in the Ukraine.

A particularly interesting case occurred in the night of 19-20/7/59. As shown on the map in Fig. 6, there appeared a very extensive thunderstorm front which stretched from northern Germany through Poland and the Ukraine down to the Crimea. The deflection of the direction finder alter-

nated between 15° and up to 190° . The closest flashes which were accompanied by the greatest amplitudes, were located in northern Germany at a distance of 600 km. These lightning discharges were not followed by any whistlers. On the other hand, lightning discharges located in areas in the Ukraine at ca. 1300-1700 km and with small field deflections at the Uppsala station, yielded clear whistlers.

Investigations carried out hitherto with the aid of direction finders cannot result in an accurate determination of the local positions within a thunderstorm area where lightning discharges accompanied by whistlers occur. This task is by no means easy but a solution is possible through the improvement of instrumental equipment. As follows from the foregoing, it is almost hopeless to draw conclusions by means of oscillographic analysis of local lightning discharges. This depends in the first place on the hazardous occurrence of whistlers. Through the development of a special direction finder system for locating whistlers this problem will obviously be nearer a solution.

7. Atmospherics producing whistlers

As has already been pointed out, the activity of whistlers will be associated with a limited region in the thunderstorm. It is evident in this respect that not all lightning discharges indicated by atmospherics give rise to whistlers. In this respect a manifest difference is found within different whistler situations. One day, for example, the number of observed atmospherics with subsequent whistlers amounted to 85 % of the total recorded atmospherics during an interval of 5 minutes. On other days the corresponding number may only amount to 10 % in spite of the fact that the lightning discharges emanated from the same area.

It is of special interest to illustrate how the relation between atmospherics, with or without subsequent whistlers, changes if an intensive whistler situation appears. Such a typical situation developed on 28/6/58 and lasted for two hours. On account of the high intensity level of whistlers that day continuous recording was started and allowed a percentage distribution of atmospherics with or without subsequent whistlers during every 5-minute interval. The result is given in Fig. 7, where filled piles represent atmospherics with subsequent whistlers and empty piles atmospherics without subsequent whistlers. The variability of occurrence of whistlers is rather striking.

It is evident that employing the direction finding procedure in the study of lightning discharges simultaneously combined with accompanied whistlers is of greatest value if correlation is to be shown between the

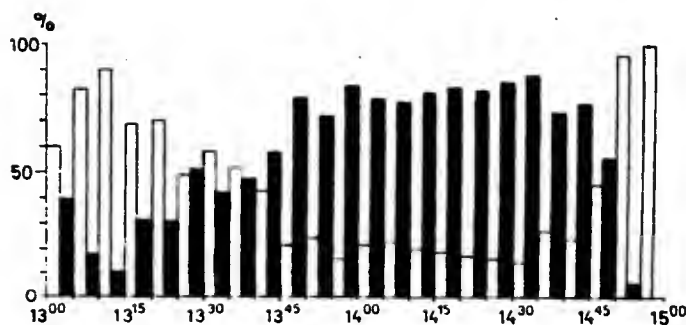


Fig. 7. Atmospherics productive of whistlers versus non-productive.

two phenomena. In the first place the method of analysis can be carried out after the following principles:

1. Comparison between the crest values of the electric field force of the atmospherics.
2. Comparison between the wave-forms of atmospherics.
3. Investigation by harmonic analysis.

8. Electric field variations of atmospherics in relation to whistlers

When it is a question of a comparison between the crest values of the electric field force of atmospherics, whether followed by whistlers or not, the whistler situation reproduced in Fig. 7 is especially valuable. It affords valuable material for comparison of the phases of development following on each other in whistler situations. The field force strength values have been directly determined by measurements from the original oscillograms in such a way that the values represent the highest amplitude difference between the two polarities.

The measured field strength values are, for a whistler situation on 28/6/58, graphically reproduced in Fig. 8, where a indicates the first period (79 observations) and b the second (119 observations). The field strength in volts/metre accompanied by whistlers is represented by filled circles and that without whistlers by empty circles. During the first half-hour of the whistler situation about 30 % of all oscillographic recordings gave subsequent whistlers within the actual sector fixed by the direction finder. During a later period 85 % gave subsequent whistlers. There is in Fig. 8 a very clear tendency to be seen for the relation of the field strength values to whistlers. In the area of the lowest field strength values atmospherics are not accompanied by whistlers. In a central area of the scale, atmospherics occur with or without whistlers. At the higher values on the scale all atmospherics are accompanied by whistlers.

10

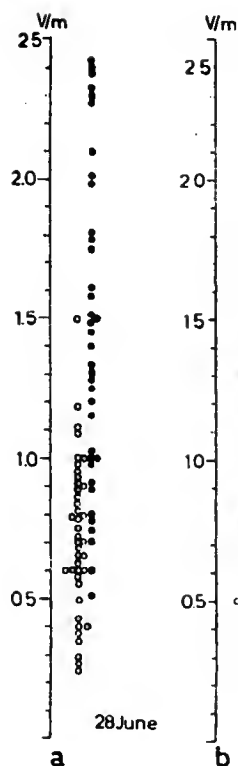


Fig. 8. Electric field of atmospherics related to whistlers.

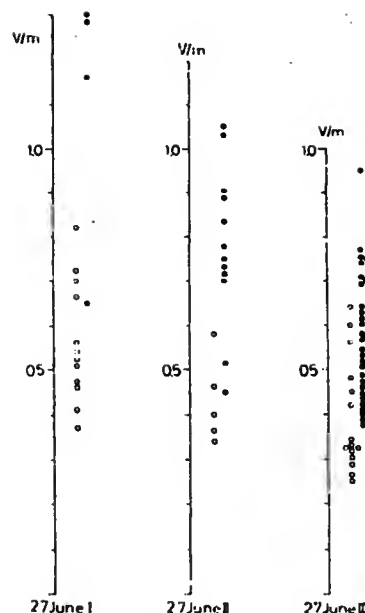


Fig. 9. Electric field of atmospherics related to whistlers.

Investigations on other whistler situations resulted in similar relations as obtained in Fig. 8. Another example of a characteristic situation from 27/6/58 is given in Fig. 9. The predominant occurrence of atmospherics producing whistlers at the groups of higher field-force values might to some extent be related to intensified current variations in the whistler-generating lightning discharges as compared with those lacking whistlers.

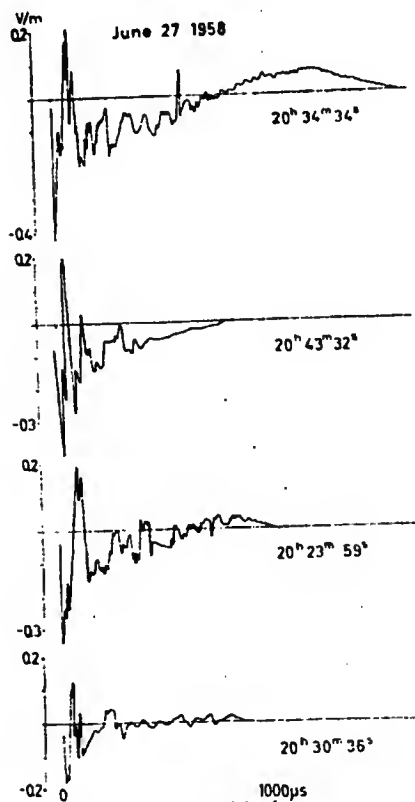
This indicates that the ionization in the channels when whistlers are produced has higher intensity values than in cases where no whistlers are produced. This fact is related to the typical preponderance of generating whistlers which, as will be demonstrated later, is characteristic of multiple lightning strokes. Another circumstance is related to the dependence of the transmission coefficient of the ionosphere in the very low frequency band from 1 to 5 kc, Wait (20, 21). As will be demonstrated further on, the frequencies around 5 kc are characteristic of lightning discharges followed by whistlers, and this must facilitate the entrance of the sferic signal through the ionosphere.

9. Wave-forms of atmospherics with or without whistlers

Evidently an attempt must be made to try to trace the characteristic variational quality factor in the lightning discharge which forms the prerequisite conditions for development of whistlers in a thunderstorm region. This problem will be treated by analysis of the oscillographic recordings of the atmospherics. During the 1958 observation period nearly 700 oscillograms of atmospherics have been recorded from whistler situations. Due to the large number of oscillograms at hand, it appeared especially suitable to divide up the plottable material by the use of the amplitude values of the field strength in conjunction with Figs. 8-9. In doing so three characteristic groups of amplitude variations of oscillograms from atmospherics were obtained:

- (1) Oscillograms of atmospherics not producing whistlers.
- (2) Oscillograms producing and not producing whistlers.
- (3) Oscillograms of only atmospherics which produced whistlers.

As it is a question of comparison, the suitable group is the one which contains atmospherics both producing and not producing whistlers. According to Fig 9 there is such a group from a thunderstorm centre with bearing between 40° and 65° and a mean distance of 450-600 km.



Within this observation area a number of atmospherics not producing whistlers were received and are illustrated in Fig. 10. The oscillograms show typically irregular variational forms, where particularly regular frequencies are absent. Another very important feature is that the atmospherics have in common the fact that they have been generated by single lightning strokes, which means one must reckon with high resistance in the lightning path.

From our investigations in other connections it has been found by special oscillographic analysis (22) that lightning discharges without multiple channels, as compared with multiple ones, occur only in 10 to 15 % of all

Fig. 10. Oscillograms of atmospherics not followed by whistlers.

lightning discharges.

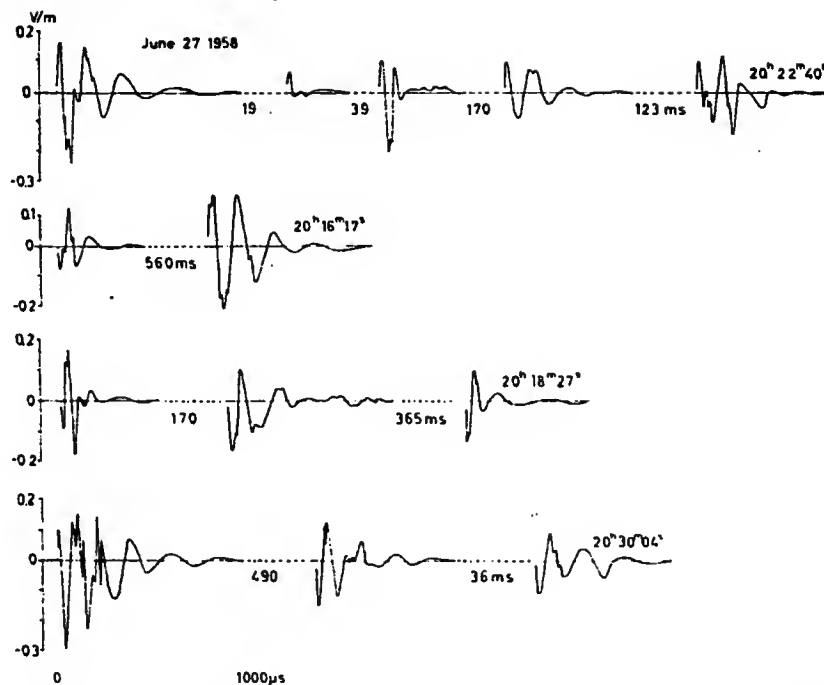


Fig. 11. Oscillograms of atmospherics followed by whistlers.

In Fig. 11 a number of whistler-producing atmospherics from the observation area are illustrated. Except in the initial stages these atmospherics are characterized by such very regular variational forms that they can, without further consideration, be designated as wave-forms, where the frequencies most nearly correspond to 5 kilocycles or to bands nearest this frequency.

The oscillograms reproduced in Fig. 11 are characterized by multiple discharges obtained by the method given in reference (11). The time intervals between the multiple discharges are given in milliseconds. In an oscillogram not reproduced in Fig. 11, only one single discharge was obtained with the same characteristic variational forms as given in that figure. Moreover, it is not out of the question that sometimes multiple strokes occur which do not appear in the recording because of their low amplitudes.

Multiple discharges which occur very often in the lightning path presuppose increased ionisation over that produced by single discharges both in the path and in the spaces within the thunderstorm atmosphere from which the large quantities of electric charges transformed into the lightning discharges are fed. The consequence on the whole must be a smaller resistance in the lightning path than in the oases where the burst

is characterized only by a single path.

This marked difference explains why only high-energy sferics appear capable of generating sferics, a fact thoroughly discussed by Hoffman (19).

10. Harmonic analysis of atmospherics with and without whistlers

In different connections, the necessary preponderance of frequencies around 5 kc has been mentioned as linked to the generation of whistlers. From this point of view it is obviously of special importance to compare the harmonic spectrum of lightning discharges followed by whistlers with that of discharges without whistlers. An indispensable condition for a comparison is that the lightning discharges occur during the same recording period and not very apart in time. This condition is very well fulfilled by an analysis of the oscillograms in Figs. 12-14.

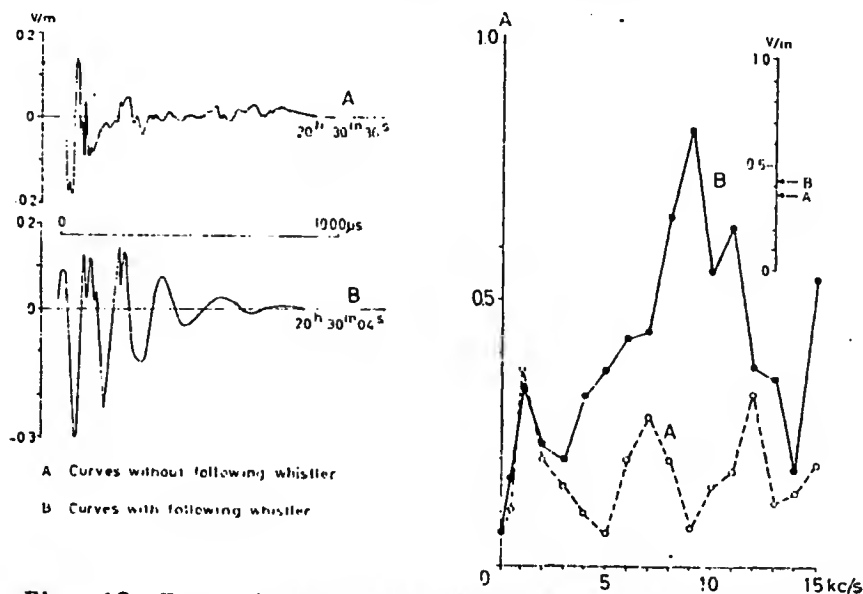


Fig. 12. Harmonic analysis of atmospherics not followed by whistlers, A, followed by whistlers, B.

Results of the harmonic analysis in these figures, where A represents oscillograms of atmospherics not followed by whistlers, and B oscillograms of atmospherics followed by whistlers. The harmonic analysis shows a striking predominance of frequencies in the region 5 to 8 kc for atmospherics followed by whistlers. Similar results have been obtained for other oscillograms in the same scale region of the field force. From the comparative analysis it follows that lightning discharges are followed by whistlers when the discharge contains a frequency distribution within the low frequency band as exemplified above. Evidently, a more exten-

14

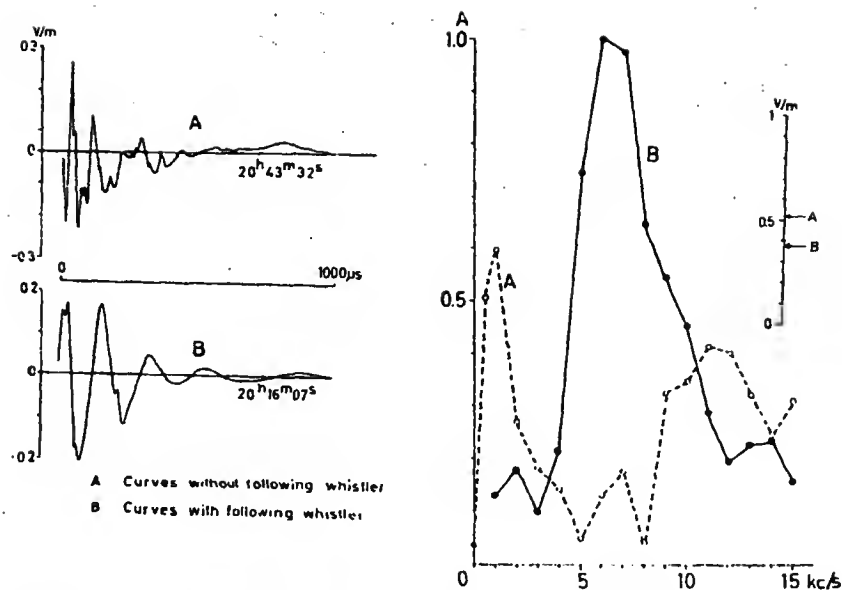


Fig. 13. Harmonic analysis of atmospherics not followed by whistlers, A, followed by whistlers, B.

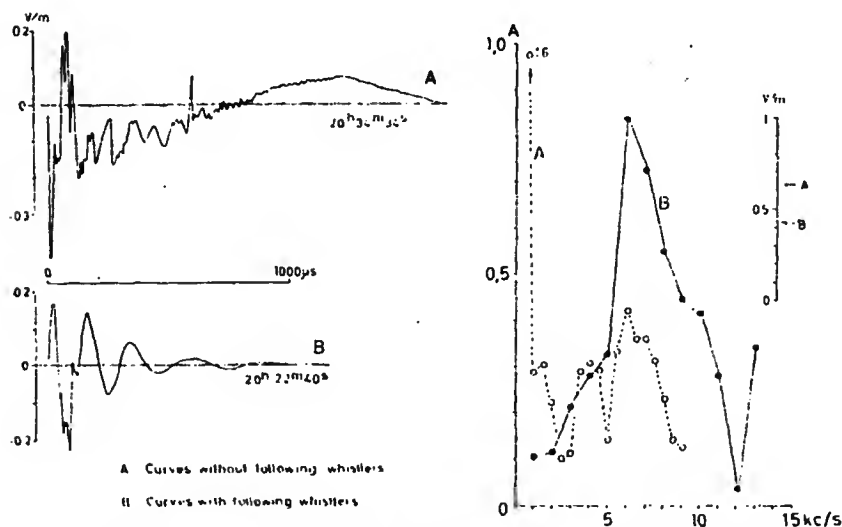


Fig. 14. Harmonic analysis of atmospherics not followed by whistlers, A, followed by whistlers, B.

sive comparative analysis is necessary, and such an analysis is already in preparation. A look at obtained frequency spectra of the extended comparison confirms agreement with what has already been shown in the above mentioned limited investigation.

11. Relations between multiple lightning discharges and multiple whistlers

In the previous discussion it was remarked that a lightning only followed by a single discharge does not in general produce whistlers. From our observations only about 10-15 % of all lightning strokes consist of a single discharge in the path. The reverse is very often true of multiple discharges in the path, and this difference is partially ascribed to the supposed higher ionisation in the paths of multiple discharges. Certainly it would be of special interest to examine more closely the occurrence of time differences of multiple whistlers passing in the same lightning channel. This is possible by frequency-time analysis using a suitable sound-spectrograph. For this purpose a Sonagraph of the Kay Electric Co design is especially well fitted. By the use of a narrow band filter and a heterodyne oscillator a record is obtained on a sensitized paper, a so-called sonagram. The frequency is given along the y-axis and the time along the x-axis. For multiple whistlers the time intervals are obtained on the sonagram. The only inconvenience is certain time uncertainties in the records of the sonagrams. This explains the time differences in intervals obtained by another more exact method.

An examination of the time intervals related to multiple whistlers can also in an exact way be obtained by simultaneous records on two cathode ray oscillographs (11, 22). The procedure allows a determination of the variational forms of successive discharges in the same channel here previously shown. It was also possible to obtain exactly, by cathode ray analysis, the time intervals between successive discharges in the channel. A comparative analysis of the time intervals of multiple whistlers is therefore possible.

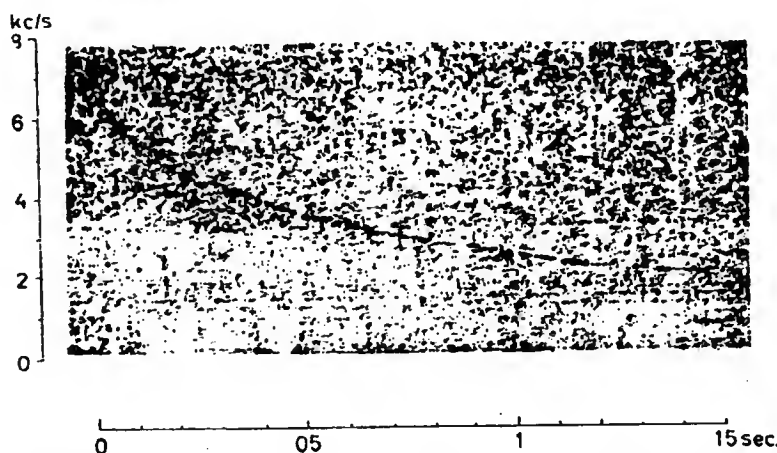


Fig. 15. Sonagram of a single whistler produced by a single lightning discharge in the channel.

In Fig. 15 is reproduced a typical sonagram of a whistler emitted from a lightning discharge which gives no indication by the oscillogram of more than one discharge having passed in the channel.

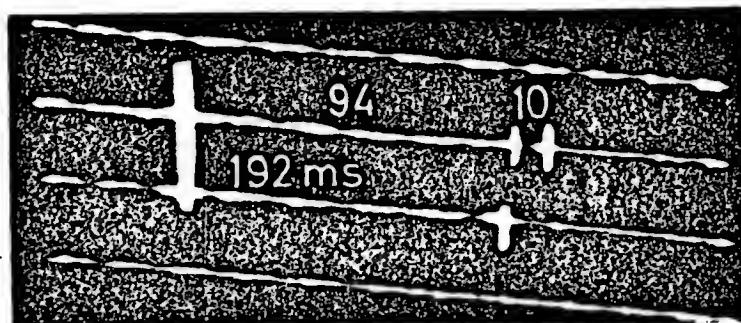


Fig. 16. Oscillogram of 3 multiple lightning discharges in the channel.

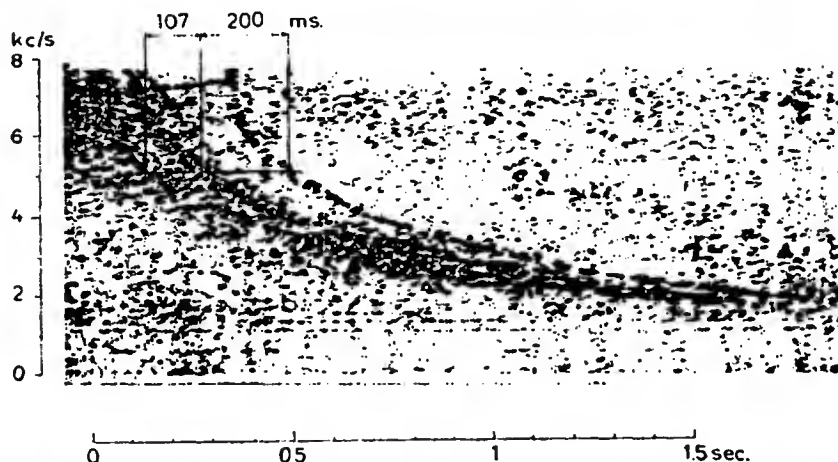


Fig. 17. Sonagram of 3 whistlers produced by multiple discharges in Fig. 16. Only 2 of the whistlers definitely visible.

An interesting case of a multiple-whistler situation is reproduced with oscillogram in Fig. 16 and with sonagram in Fig. 17. The differences in milliseconds between the oscillographed intervals of the discharges and the intervals in the sonagrams are ascribed to the mentioned uncertainty in time of the Sonagraph. Noteworthy is the long time intervals between the two discharges as compared with the third.

A contrary situation with more concentrated intervals are given in Figs. 18-19. The oscillogram shows 5 multiple discharges. Between two of them a very long time difference occurs as compared with the rest. A very dense accumulation of whistlers is shown in Fig. 20. This variation can be considered as a transition to the special variational type of condensed whistlers which is a typical transition to the form which has been

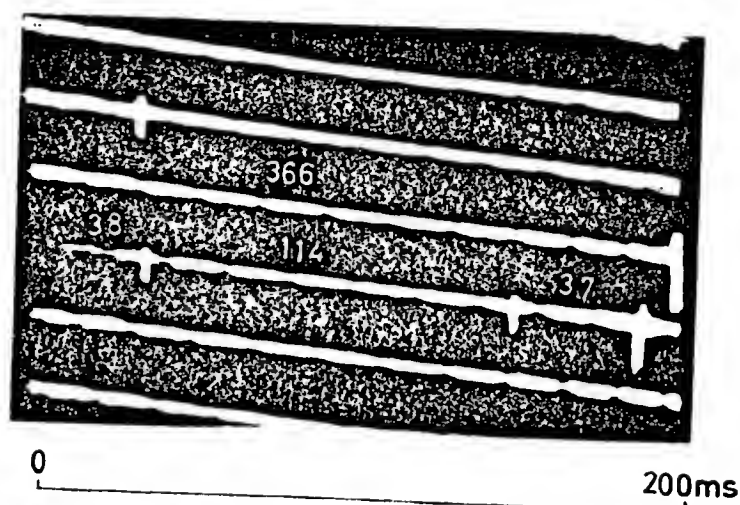


Fig. 18. Oscillogram of multiple lightning discharges with the first interval very long as compared with the following ones.

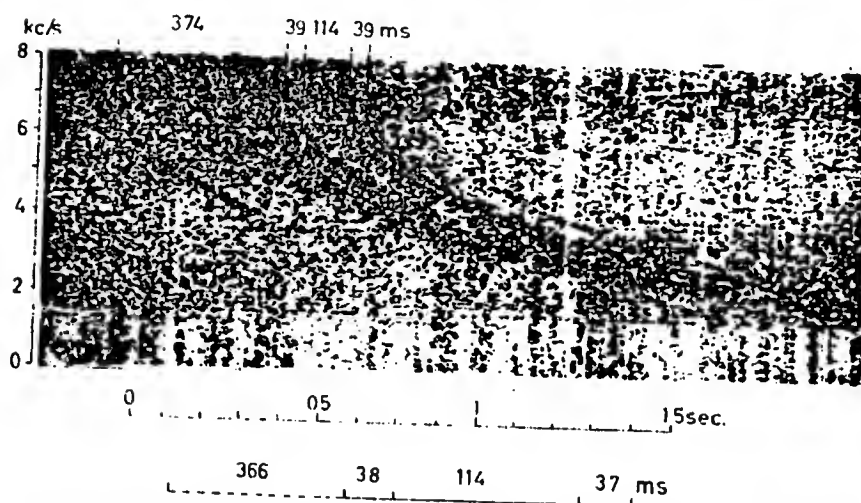


Fig. 19. Sonagram of 5 whistlers produced by the multiple discharges in Fig. 18.

called a swish shown in Fig. 21.

The haphazard occurrence of whistlers in local thunderstorms has up to now prevented the observance either vizually or by daylight photographs of lightning strokes followed by whistlers in separate channels. Nevertheless we have during two thunderstorm seasons (10, 23) samples of observations which in several cases show locally separated lightning strokes where the first has initiated the following ones. All strokes were bound together within time periods not exceeding 2 seconds. The occurrence of such locally separated lightning strokes can be accepted as indirect evidence that whistlers from adjacent separate lightning strokes will follow

separate propagation ducts. This opinion is supported by daylight photographs obtained in an earlier investigation (23).

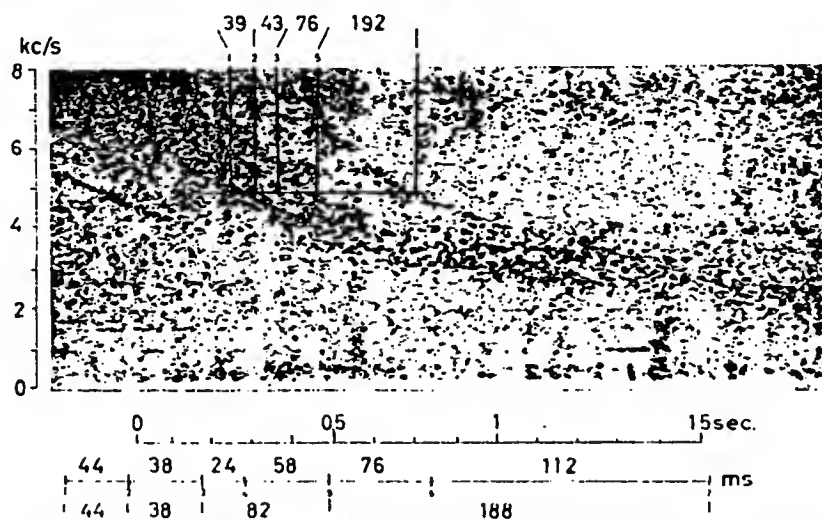


Fig. 20. Sonagram of 5 whistlers. Oscillogram shows 7 multiple discharges, 2 whistlers are missing.

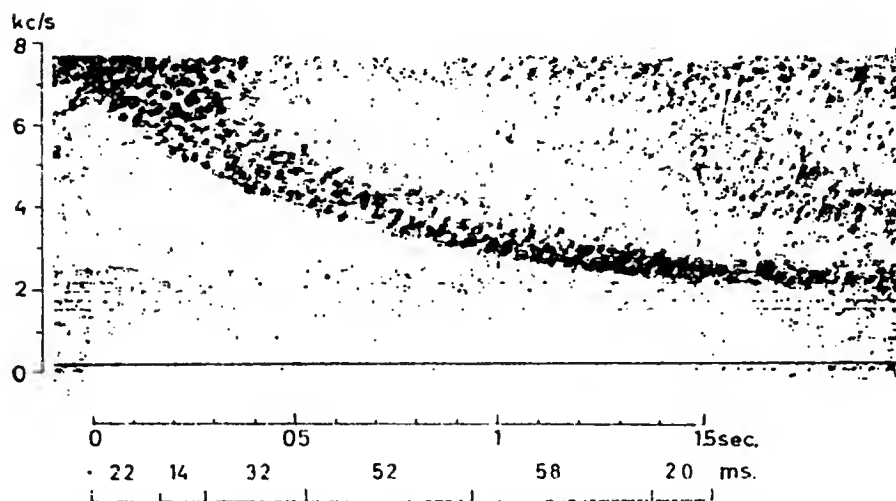


Fig. 21. Sonagram of a swish caused by 7 lightning discharges in the same channel.

12. Unusual musical atmospherics and their relations to lightning discharges

In the foregoing, musical atmospherics of the usual whistler type have been discussed. Different aural observations have shown that aside from usual whistlers other variational forms of musical atmospherics occur in great variety, a fact which becomes much more evident when whistler time-variations are resolved by a sound spectrograph. When in the following "variational type of whistlers" is used, it is meant the frequency-

time variational type of musical whistlers obtained on sonagrams. Such unusual musioal whistlers have received several suggestive names more or less well defined. Some of the most frequent are tweeks, single or multiple risers, hooks, constant frequency type, step type and combined types of some of the above mentioned.

As far as is known it has up to now only been possible to find a correlation between lightning discharges and usual whistlers and between lightning discharges and tweeks. It has been found to be of special interest to try to extend investigations of possible relations between lightning discharges and the quoted irregular variational types of unusual musical atmospherics.

In a publication (17) it was shown that several of the variational forms of musical atmospherics occur mainly in the day time. During the two thunderstorm seasons of 1958 and 1960 day-time observations of unusual musical atmospherics were carried out at the whistler station and about 700 individual observations that could be used as a basis for a special analysis (18) were obtained.

To this end during applied recording periods, continuous observations were carried out of the simultaneous occurrence of lightning discharges by means of the CRO direction finder and of musical atmospherics by the whistler-receiving set. Just as a whistler was taped, it was observed and noted if a correlation did or did not exist with a practically simultaneously recorded lightning discharge on the direction finder. A similar method applied in more southern latitudes with a comparatively high thunderstorm activity would no doubt lead to unreliable results. Because of the simultaneous occurrence of a considerable number of lightning discharges it would lead to some difficulties to correlate a musioal atmospheric with an observed individual lightning discharge. Owing to the comparatively low thunderstorm activity on the latitude of the station it was easy to determine the correlation. Occasionally it happened that a limited thunderstorm area could be used for observation of the correlation for a period of up to 1-2 hours. During such a situation all musical atmospherics without exception were found with correlation. In another limited thunderstorm situation not one of the musical atmospherics was observed as correlated. To some extent this difference can be explained in such a way that only a limited part of the thunderstorm area had necessary conditions favourable for production of musical atmospherics.

The explanation for the occurrence of similar variational types of correlated musical atmospherics versus not correlated ones will be discussed later on. In the following examples of the variational types ob-

tained by sonagrams have, with some exceptions, been reproduced types observed as correlated or not correlated with lightning discharges.

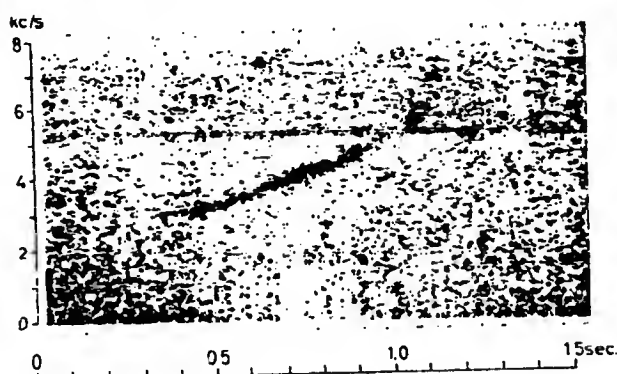


Fig. 22. Basic riser variation-
al type, correlated.

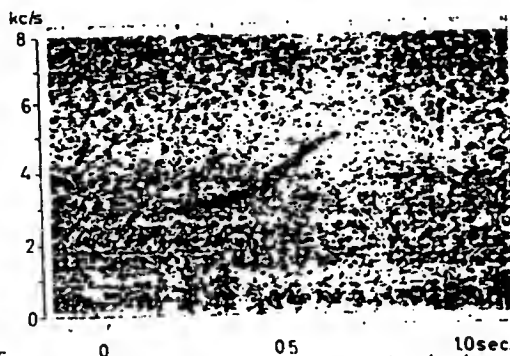


Fig. 23. Basic riser va-
riational type, not correlated.

In Figs. 22-23 a type of single risers is reproduced with or without correlation, and the same is given for typical multiple risers in Figs. 24-25. A single hook with or without correlation is reproduced in Figs. 26-27, and in Fig. 28 there are exemplified multiple hooks with correlation.

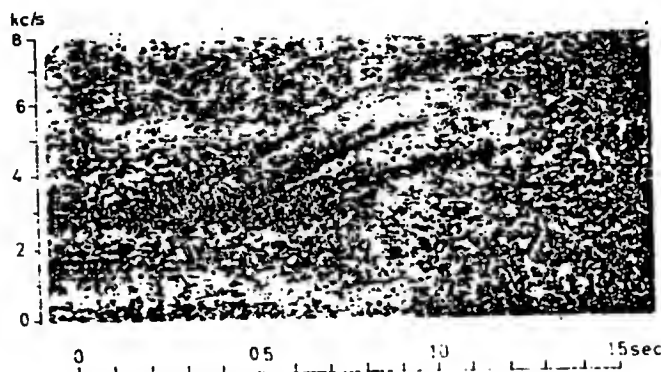


Fig. 24. Multiple risers
of basic variational types,
correlated.

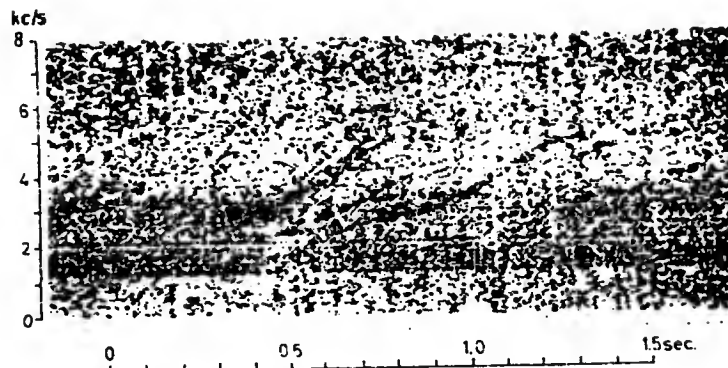


Fig. 25. Multiple ri-
sers of basic varia-
tional types, not cor-
related.

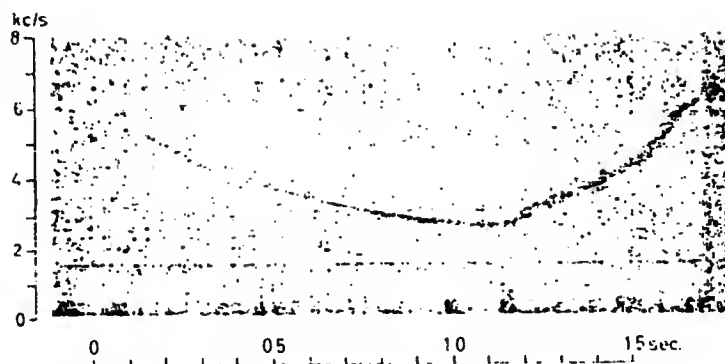


Fig. 26. Hook variational type, correlated.

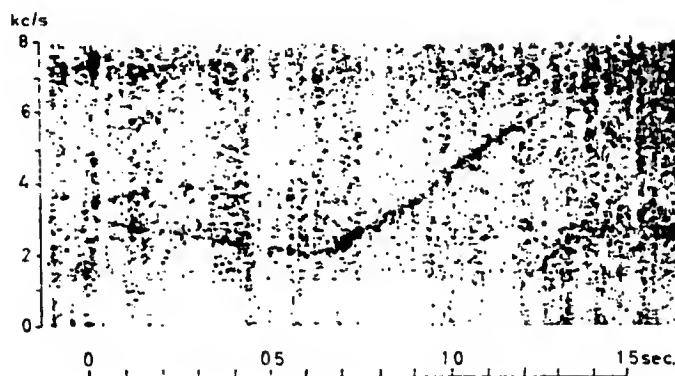


Fig. 27. Hook variational type, not correlated.

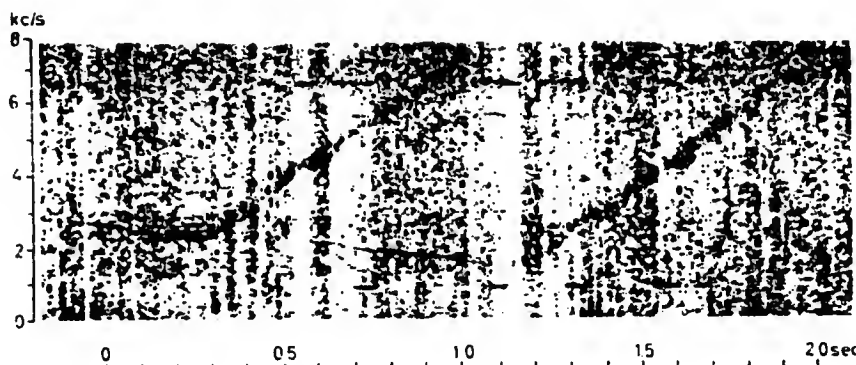


Fig. 28. Multiple hook variational types, correlated.

A nearly constant frequency variational type with or without correlation is reproduced in Figs. 29-30. A comparatively irregular variational type of frequency is reproduced in Figs. 31-32 with or without correlations. Multiple step variational types not correlated are given in Fig. 33, and in Figs. 34-35 single step variational types with or without correlation. Sometimes combinations of types were obtained, e.g. one or two risers preceding usual whistlers both correlated as exemplified in Figs. 36-37.

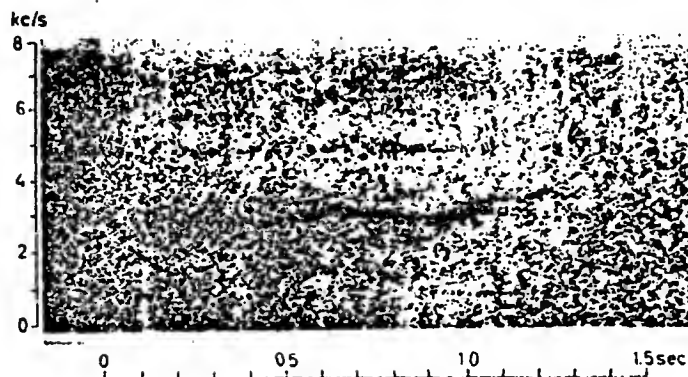


Fig. 29. Nearly constant frequency variational type, correlated.

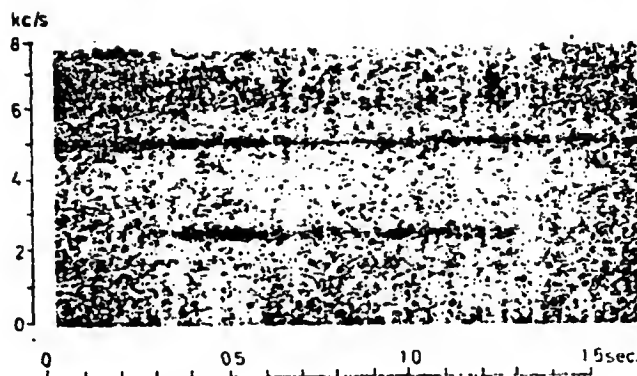


Fig. 30. Nearly constant frequency variational type, not correlated.

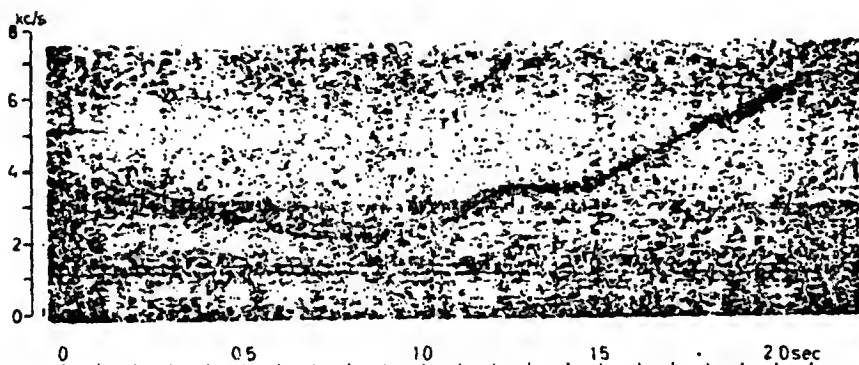


Fig. 31. Comparatively irregular variation of frequency, correlated.

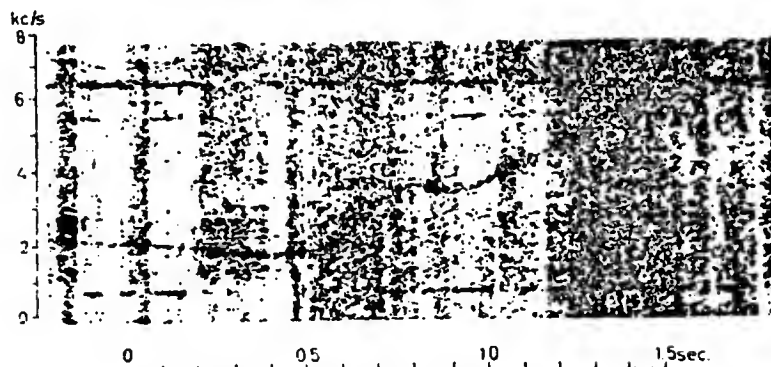


Fig. 32. Comparatively irregular variation of frequency, not correlated.

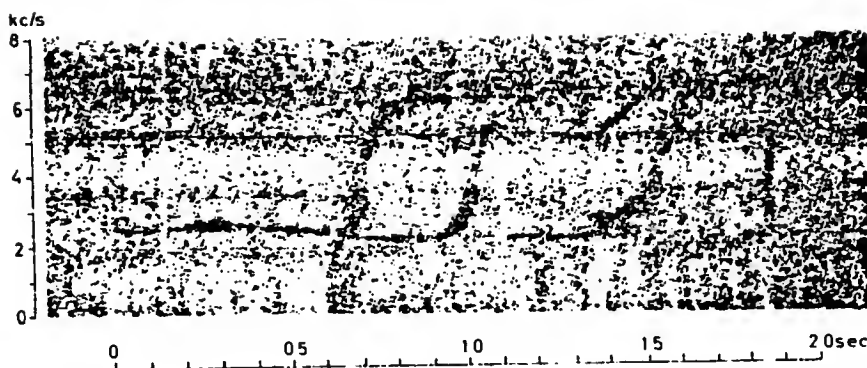


Fig. 33. Multiple step variational types, not correlated.

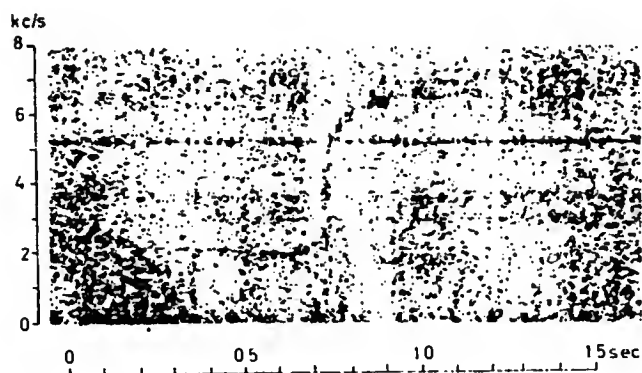


Fig. 34. Step variational type, correlated.

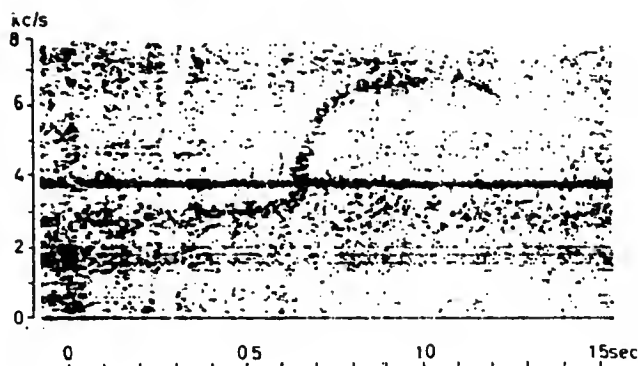


Fig. 35. Step variational type, not correlated.

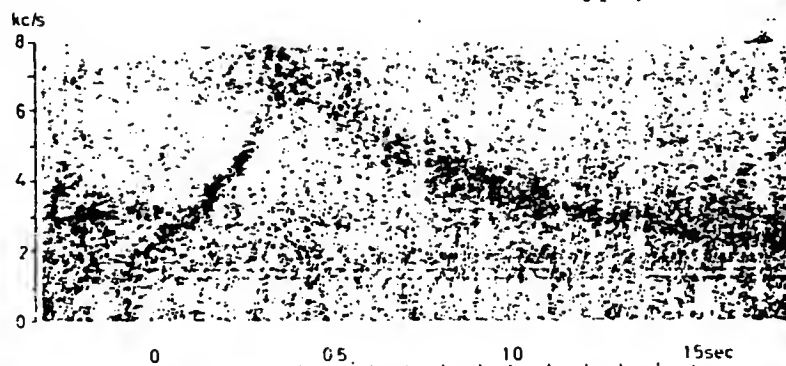


Fig. 36. Whistler of usual type preceded by one riser, correlated.

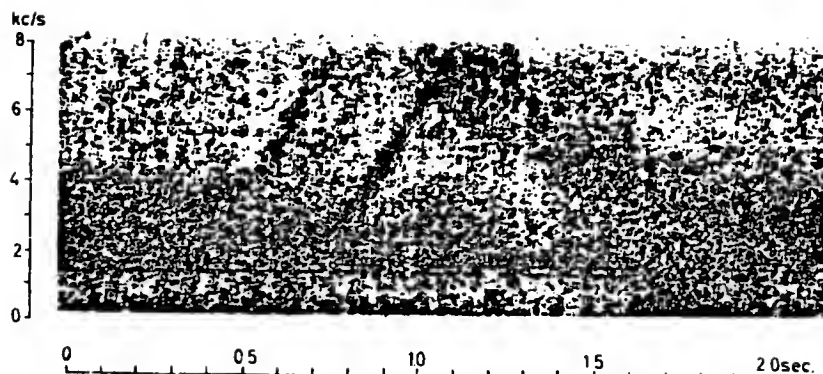


Fig. 37. Whistler of usual type preceded by two risers, correlated.

13. Special remarks of variational forms of unusual musical atmospherics.

The musical atmospherics of unusual types illustrated by Figs. 22-37 show plainly the most shifting variational aspects and forms. The conclusion must be that within the thunderstorm atmosphere there exist some very complicated, special modes of generation of unusual musical atmospherics. A theoretical explanation of the phenomena will for this reason require a more extended experimental analysis than has been obtained by the results presented here. It can only be confirmed that a theoretical treatment of the phenomena will be considerably more intricate compared with what was valid for musical atmospherics of the usual type.

It is especially striking that the analysed unusual musical atmospherics with or without correlation result in a conspicuous conformity in their characteristic variational forms. This shows that the unusual musical atmospherics originate from the same type of sources within the thunderstorm atmosphere. The conclusion is near at hand that the non-correlated musical atmospherics are also caused by lightning discharges.

The problem that non-correlated musical atmospherics have also been caused by lightning discharges without having been recorded as correlated has its explanation in the limitations of the equipment used with regard to distance sensitivity. For determination and recording of waveforms have been used CRO recorders and for the determination of the distances CRO direction finders. The acceptable distances for an accurate determination were estimated to be 2000 km at best. It seems quite acceptable that musical atmospherics beyond that distance have sufficient propagation to reach the observation station and to be observed and recorded there as not correlated.

Another explanation of the existence of non-correlated musical at-

muspherics within the sensitivity limit of the station is possible. In a thunderstorm region lightning discharges might occur producing musical atmospherics characterized by effective propagation qualities. On the other hand, in spite of their location within the sensitivity limit of the station, lightning discharges have sometimes insufficient propagation effectivity to reach the station. This can very well explain why in special situations musical atmospherics have not been correlated.

Summary

A station for analysis of relations between lightning discharges and musical atmospherics of usual (whistler) and unusual variational forms has been operated for some years near Uppsala.

Recording cathode-ray oscillographs were used for the analysis of the lightning discharges whose relations to musical atmospherics were investigated. Cathode-ray oscillographic direction finders placed at two stations with suitable distances between them made it possible to determine the sources of the lightning discharges investigated.

Through comparative harmonic analyses it was shown that lightning discharges producing musical atmospherics of the usual type - whistlers - were characterized by a preponderance of frequencies around 5-8 kc. Multiple lightning discharges were found to be followed by multiple whistlers.

The recording method of the station allowed also of an investigation of correlations between lightning discharges and musical atmospherics of unusual and irregular variational forms. It was found that out of 700 unusual musical atmospherics about 70 % were correlated to lightning discharges and about 30 % were not. The striking variational resemblance between correlated and non-correlated short-time variational types of unusual musical atmospherics indicated that the non-correlated variational types must also emanate from lightning discharges.

Acknowledgements

Special cathode-ray recording oscillographs and direction finders were used in this investigation. The instruments were constructed with the help of grants from Statens naturvetenskapliga forskningsråd (the Swedish Natural Science Research Council) and Statens tekniska forskningsråd (the State Council of Technical Research). Other instruments and other experimental equipment used for this whistler investigation were constructed with the support of a special grant from Statens naturveten-

26

skapliga forskningsråd.

The Swedish Board of Telecommunications has given valuable assistance with telephones between two direction-finder stations and with the construction of a special relay system for distance operation by telephone of the whistler station.

At the University of Lund the Institute of Physics and the Institute of Genetics made it possible to operate a direction-finder station used in the investigations.

For analysis of whistlers the author was permitted to make use of a sound-spectrograph which belonged to the Institute of Phonetics at Uppsala University.

The author is very much indebted for the valuable help given.

The geophysics research reported in this article has been sponsored and supported by Contract AF 61(052)-07, Geophysics Research Directorate and also by Contract AF 61(052)-171, Electronics Division, Cambridge Research Center, Office of Aerospace Research, United States Air Force through its European Office, Brussels.

References

1. BARKHAUSEN, H., Pfeiftöne aus der Erde. Physik. Zeitschr. XX. 1919.
2. BARKHAUSEN, H., Whistling Tones from the Earth. Proc. Inst. Radio Eng. 18, 7 (1930).
3. ECKERSLEY, T.L., A Note on Musical Atmospheric Disturbances. Phil. Mag. 6, 49 (1925).
4. ECKERSLEY, T.L. and CHAPMAN, S., Radio Echoes and Magnetic Storms. Nature 122, 768 (1928).
5. ECKERSLEY, T.L., Musical Atmospherics. Nature 135, 104 (1935).
6. BURTON, E.T. and BOARDMAN, E.M., Audio-Frequency Atmospherics. Proc. Inst. Radio Eng. 21. 1476-94, 10 (1933).
7. STOREY, L.R.O., An Investigation of Whistling Atmospherics. Phil. Trans. Roy. Soc. B. 246, 113 (1953).
8. NORINDER, E., Wave-forms of Electric Field in Atmospherics Recorded Simultaneously by Two Distant Stations. Arkiv för Geofysik 2, 10 (1954).
9. NORINDER, H., Magnetic field variations from lightning strokes in vicinity of thunder storms. Arkiv för Geofysik 2, 20 (1956).
10. NORINDER, H. and KNUDSEN, E., Combined Analysis of Daylight Photographs of Lightning Paths and Simultaneous Oscillographic Records. Recent Advances in Atmospheric Electricity. Book. Pergamon Press, London 1959.
11. NORINDER, H. and VOLLMER, B., Variation Forms and Time Sequence of Multiple Lightning Strokes. Arkiv för Geofysik 2, 25 (1957).
12. NORINDER, H. and KNUDSEN, E., The Relation Between Lightning Discharges and Whistlers. Planetary and Space Science, Pergamon Press 1959. Vol. 1, pp 173-183. Printed in Great Britain.
13. NORINDER, H. and KNUDSEN, E., Lightning discharges as a source of whistlers. Arkiv för Geofysik 3, 11 (1960).
14. NORINDER, H. and KNUDSEN, E., Recent Results in the Investigation of the relation between Lightning Discharges and Whistlers. Planetary and Space Science, Pergamon Press 1961. Vol. 5, pp 46-49. Printed in Great Britain.
15. NORINDER, H. and KNUDSEN, E., The dispersion of whistlers compared with the geomagnetic latitudes of their sources. (Research note). Planetary and Space Science, Pergamon Press 1961. Vol. 5, pp 326-328. Printed in Great Britain.
16. NORINDER, H. and KNUDSEN, E., Multiple lightning discharges followed by whistlers. Arkiv för Geofysik 3, 12 (1960).
17. NORINDER, H. and KNUDSEN, E., Occurrence of different kinds of whistler activity. Arkiv för Geofysik 3, 17 (1961).
18. KNUDSEN, E. and NORINDER, H., Different types of musical atmospherics and their relations to lightning discharges. Arkiv för Geofysik 4, 5 (1962).
19. HOFFMAN, W.C., The Current-Jet Hypothesis of Whistler Generation. Journal of Geophysical Research 65, 7 (1960).

28

20. WAIT, J., Symp. on Prop. of V.L.F. Radic Waves, Boulder, Colo. 4, 23 (1957).
21. WAIT, J., The Attenuation vs Frequency Characteristics of V.L.F. Radio Waves. Proc. Inst. Radio Eng. 45, 768 (1957).
22. NORINDER, H., KNUDSEN, E., and VOLLMER, B., Multiple Strokes in Lightning Channels. Recent Advances in Atmospheric Electricity. Book. Pergamon Press, London 1958.
23. NORINDER, H. and KNUDSEN, E., Lightning discharge paths photographed in daylight and analysed by simultaneous variations of magnetic field components. Arkiv för Geofysik 3, 19 (1961).

SESSION 2.1Problems of Fair Weather Electricity; Introducing Remarks.by H. Israël, Aachen1. Introduction

It is a task of our conference to review our knowledge and to recommend further investigations on the different branches of atmospheric electricity.

When I try to do this for the field of the "Fair Weather Electricity" ("FWE") I have the feeling that some of you may think:

Why still FWE? This is overdone! Moreover the results in this field are so complex and so contradictory that it seems senseless to continue!

But as scientists, I believe we should hesitate to use such an argument or to resign in view of difficulties. Besides there are quite different opinions concerning this question. Therefore let us examine critically the today's situation of the FWE.

The conception of "FWE" was the result of the old custom to consider only the fair weather values. These data seemed to be easier to explain than phenomena connected with disturbed weather. Today rather the opposite is true as we may see, e.g., when we look on the program of the present conference.

The division of the atmospheric electricity in the two parts; namely, the FWE and the "Disturbed-Weather Electricity," was justified afterwards by the dynamic conception of the atmospheric electricity: We have to distinguish generation - that is the disturbed weather electricity, or more precisely, the thunderstorm electricity, where the charges are separated - and consumption - even the FWE, where the separated charges will be

- 2 -

neutralized. So the two parts are connected together very closely, having the same importance in the explanation of the whole picture.

If we look now on the fair weather electricity we first remember the fundamental discoveries of the last thirty years: We understand why we find everywhere and always an electrical field in the atmosphere characterized by typical periodical and nonperiodical variations. But these results emerge only if they are based on a large quantity of data, while for shorter series of observations the average picture is disturbed more and more by local conditions and meteorological influences. In other words: we got a climatological picture only, based on statistical evaluation.

However, this method is quite insufficient to relate, for instance, the atmospheric electric with the meteorological phenomena. Thus, in my opinion investigation in this branch is rather underdone than overdone.

II. Modern Problems in FWE

A. The Stratosphere

Let us look now on the modern problems in FWE. As you know, it is one of the most difficult problems in this branch that frequently the results are ambiguous because, in general, there are worldwide influences superimposed on local effects - especially if we evaluate measurements near the ground. Therefore, we have to look first for suitable methods to separate the two districts of influences.

This may be achieved when we try to separate the researches with respect to space: We have to distinguish at least two spheres of a quite different behavior, the troposphere and the stratosphere/mesosphere. Furthermore, we usually divide the troposphere in two regions, a lower one which is characterized by the vertical turbulent connection, and an upper one which is governed generally by a horizontal movement of the air.

- 3 -

It is evident that the processes and the problems we have to clear up are quite different in these three regions, from the meteorological point of view as well as from the electrical one:

The electric behavior of the stratosphere/mesosphere is governed essentially by worldwide steering effects of the main generator and by variations of the ionization according to the latitude effect of the cosmic radiation only. On the other hand, tropospheric variations of the atmospheric electrical behavior are controlled by the influence of the "austausch" on the aerosol conditions.

Thus, I believe we can separate the "targets" of further researches in FWE in the two general groups of

- (1) stratospheric researches of the electric field and the conductivity and of
- (2) tropospheric results of the aerosol conditions.

Let me give some examples:

If we look on the first group, i.e. the stratospheric problems, we need first systematic measurements of the total potential difference V between the surface of the earth and the ionosphere and of their variations in time. Results of this kind can be obtained only by measurements in higher altitudes and at places not or less effected by the "austausch"! So we have there a special task for the aerological method of measurement as developed in the last time.

Two ways seem to be successful:

- (a) Integration of field measurements by airplanes or radiosondes (O.H. Gish, 1944; J.F. Clark, 1956; J.H. Kraakevik, 1958; H.J. Fischer, 1962 et al.)
- (b) Direct measurements of V and dV/dt in about 11 km altitude - by airplanes or constant level balloons with radiosondes -

- 4 -

as proposed by H.W. Kasemir, 1950.

Measurements of this kind promise a better insight into the mechanism of the worldwide atmospheric electrical circuit. I think there is no doubt that our basic hypothesis is correct, but up to now it is based only on mean results of a few polar expeditions and on those of the cruises of the Carnegie Institution. We are not able to control this in detail, e.g. to find out changes of the thunderstorm activity in different parts of the world - a target of special interest for the meteorology as well as for aviation. There are only first hints in this direction (H. Israël and E. Theunissen, 1957; H. Israël, 1957).

The aerological researches may be aided by continuous records of the atmospheric elements over the free oceans and at mountain tops. The first one could be done on the "weather ships" fixed now at different places of the oceans. Furthermore, I believe we should ask the permanent stations in the arctic and antarctic regions for atmospheric electrical records.

Another urgent question concerns the conductivity in the stratosphere/mesosphere. Here we have only scarce results up to now. The conductivity was measured directly, e.g. by radiosondes, up to about 30 km (C.G. Stergie, S.C. Coroniti, A. Nazarek, D.E. Kotas, D.W. Seymour, and J.V. Werme, 1955; R.H. Woessner, W.E. Cobb and R. Gunn, 1958). Furthermore the behavior of electro-magnetic waves in the higher atmosphere allows to measure the density of electrons or the conductivity respectively in the ionosphere, i.e. for altitudes above 80 km. In the interval between 30 and 80 km the conductivity values were computed (H. Israël and H.W. Kasemir, 1949; R.E. Bourdeau, E.C. Whipple, Jr. and J.F. Ciark, 1959) and measured directly only once by a rocket sonde (R.E. Bourdeau et al., 1959).

This first experiment shows already a considerable discrepancy in both the computation and the measurement, especially for the region above 50 km

- 5 -

of height. Therefore measurements of this kind should be continued.

Let us look into some of the most important problems in this field:

- (a) In the region of 30 km to 70 km the electron concentration is influenced by the intensity of ionizing radiation, by the recombination processes, and by electron detachment and attachment rates. To understand which of these quantities prevail in physical processes throughout this region, it is necessary to determine the chemical, molecular, and atomic components and their density, including their change with altitude.
- (b) In lower altitudes the conductivity of the atmospheres is determined by the density of the small ions, while in the ionosphere the conductivity is caused practically by free electrons. The transition is to be expected in the region between 30 and 80 km of height.
- (c) More knowledge of this kind will give a better understanding of the lower boundary of the ionosphere.
- (d) It also will yield more information on the global current circuit of atmospheric electricity, concerning questions such as the height distribution of the equalizing current, latitude effects, field gradients in horizontal directions, perhaps daily variations, etc.
- (e) Finally we may find in this region connections to geomagnetic events, solar influences, aurora and similar phenomena.

It is true, measurements of this kind may be much more difficult to carry out than the usual atmospheric electrical measurements; however, I believe the adaptation of measuring equipment to rockets and satellites is a technical and not a principal problem.

- 6 -

B. The Troposphere

A quite different picture of the electrical behavior we meet in the troposphere; we find a group of problems of another kind.

To characterize the situation we may remember the opinion of Lord Kelvin 100 years ago - that in the future the forecast of the weather would be done with the electrometer. This prediction, of course, was a too optimistical one; however, the essential point which provoked that statement is the same up to the time being: All meteorological events are accompanied by characteristic changes of the electric parameters.

What we have to do is to explain these connections and to classify the electric variations. Maybe this is easier to say than to do because at the first sight the results up to now seem to give a chaotic picture. We remember, e.g., wide ranges of variation spectra of the different elements including fluctuations from the annual variations down to the so-called "noise," the different combinations of the "electrode effect" with the aerosol conditions, the radioactive influences, the movements of air masses, etc. Although we know many details in this field, it is hard to find an integral view up to now.

This, I believe, is the reason why some people voiced the opinion it would be senseless to continue researches of this kind. But in my opinion we have here no more difficulties than in the field of meteorology in general. Therefore, rather we should examine our measuring methods if they are adequate for the problems arising here.

As mentioned above in the troposphere we have to distinguish two regions of a quite different behavior, i.e. the "Exchange Layer" and the upper troposphere. In addition to this we have to separate a third region near the surface of the earth which is governed by the so-called "electrode effect."

- 7 -

The boundaries between these spheres are fluctuating according to the specific weather conditions, to the time of day, and to that of the season.

1. The Electrode Effect

The electrode effect is caused by the electric field in ionized air near the electrodes, i.e. here near the surface of the ground. Considering the atmospheric conditions one can compute that this effect will be essential up to an altitude of one or at most a few meters. This altitude is smaller if the content of condensation nuclei in the air is greater (J. Scholz, 1931), and the effect is depending on the ionization conditions near the ground. They may limit it sometimes to the first decimeters above the ground (A.R. Hogg, 1935; J.A. Chalmers, 1946 et al.)

Summarizing the results we find only a rough conception of this effect. Especially we miss researches of the meteorological influences. Therefore, I believe we have to see here a first important problem for our future researches.

How will the electrode effect be influenced by the meteorological conditions, the radioactive conditions in the ground and in the air near the ground, the aerosol conditions etc?

Moreover the region of the electrode effect is accessible easily for all measurements and recordings we need. This enables us to examine the meteorologic-electrical connections in a small range, so to speak.

Of course, the usual measuring methods will be insufficient for researches of this kind. We have to measure at least the electrical field strength and the conductivity in small regions. Therefore, all kinds of disturbances should be avoided as much as possible as they occur due to the orographic situation, the installation or the working method, the equipment,

- 8 -

etc. It is true, this will raise the claims for our measurements. However, I believe the problems we have to investigate in the region of the troposphere require urgently a new effort in our work.

2. The Exchange Layer

In this region of the troposphere we meet in general quite similar problems as mentioned before. However, the researches are more difficult because this sphere is much more extended in both the horizontal and the vertical direction. Therefore, we have to combine measurements both near the ground and in the free atmosphere.

Looking into these problems we have to find out above all the numerous influences of the "austausch" on the aerosol conditions. They will give us the key to understand most of the meteorological electrical relations.

The next step will be a systematical examination of the effect of air mass movements, considering their aerosol conditions, their content or radon, thoron, and decay products, maybe the content of fission products, etc.

Although the measuring methods are insufficient here, too, a lot of results came out already. I recall your attention, e.g., (1) to the explanation of the different types of diurnal variations of the electrical elements (J.G. Brown, 1930, 1935; H. Israëli, 1948, 1950, 1952); (2) to the explanation of the so-called "sunrise effect" (H.W. Kasemir, 1956); (3) to the researches of the so-called "brightness effect" (G. Fries and H. Dolezalek, 1956); (4) to the "noise" of atmospheric electrical elements (H. Israëli, 1958, 1959); (5) to the steplike variations of the atmospheric electrical elements at the upper boundary of the exchange layer (F. Rossmann, 1950; Callahan, Coroniti, et al., 1951) and to other ones.

However, these results yield with few exceptions, average values, describing the climatological behavior. This may be the reason why we miss a systematic picture of the connections between the weather and the atmospheric electricity up to now. Therefore, we have to look for a suitable extension of investigation. We shall see that here, too, the usual measuring customs must be changed.

"Off-hand-solutions" and "ad-hoc-theories," as they are tried sometimes, do not help us. They fail today as they failed in the days of F. Exner*.

3. The Upper Troposphere

The problems arising here may represent the last step in the new program for atmospheric electrical researches.

Since the aerosol content in the air above the exchange layer in general is unimportant, (see, e.g. R.C. Sagalyn and G.A. Faucher, 1954, 1955) we can expect to be confronted in this region, first of all, with the influences of air masses and their movements, with effects of variations of radio-activity, and with stratospheric influences.

Researches in this region will be done with airplanes, gliders, radiosondes, and constant level balloons. Furthermore, it will be very helpful to record the atmospheric electric parameters at mountain tops of sufficient altitude.

First, results and important hints for future researches will be found, e.g., in the papers of F. Rossmann (1950); R.C. Callahan et al, (1951); R.C. Sagalyn et al, (1954, 1955); C.G. Stergis et al. (1955); L. Koenigsfeld (1955, 1957, 1958); J.F. Clark (1956, 1958); J.H. Kraakevik (1958); K. Uchikawa

*) so, e.g., the hypothesis of F.M. Exner (1886/1890) concerning a transport of charges by evaporation of water, which was refuted by H. Benndorf (**) and P. Lenard (1944); a revival of this hypothesis by R. Mühleisen (1958) was refuted by H. Israel and R. Knopp (1962; see also R. Knopp 1961).

**) H. Benndorf conducted in 1897/1898 field investigations in Siberia, which demonstrated that the mechanism as suggested by Exner is not verified.

- 10 -

(1961); G. Röncke (1963); and other ones. For observations on mountain tops see, e.g., the researches of R. Holzer et al. (1955) in California and Hawaii and of H. Israël et al. (1957) in the alps.

III. The Measuring Methods

The researches proposed above require changes and improvements of the measuring methods.

First of all we have to look on the comparability of the results.

For this the following demands must be fulfilled:

- (1) It is known that the so-called "Reduction on the Free Plane" involves a considerable uncertainty, because it is impossible to include the influence of the space charges. Therefore the necessity to reduce the observed values must be avoided. In other words, all measurements near the ground - especially those of the electric field - should be done on an open plane of sufficient size. The rules of H. Benndorf (1900, 1906) may be used for the critical examination what means "sufficient." This should be applied also to measurements in mountain regions where we have to look for planes of sufficient size (plateaus, glaciers, etc.).

Of course by measurements with aircraft, radiosondes, etc., a computation factor concerning the geometrical forms is inevitable.
- (2) Measuring techniques which disturb the natural conditions should be avoided as completely as possible. This concerns first of all the use of radioactive collectors for measurements near the ground. For airborne equipments the collector may be used provided that the aspiration is sufficient. When using radiosondes it is important to consider the researches of G. Röncke (1962)

- 11 -

concerning the mutual influences of the two radioactive collectors.

- (3) Different measuring equipments both for measurements near the ground and in the free atmosphere should be compared by simultaneous application at the same place and over a longer period of time.
- (4) All researches should include simultaneous measurements of the three parameters of Ohm's law, i.e. the potential gradient (field strength), the conductivity (conductivities), and the air-earth current density.
- (5) To avoid misunderstandings concerning the "sign," the remarks of H. Israëli (1961, 1963) may be mentioned.

For synoptical researches as proposed by H. Israëli (1954, 1955, 1961) and included in part II, B,2 of this paper the following difficulty should be considered.

- (6) Synoptical researches near the ground will be disturbed by the electrode effect which may be different at different stations. In order to avoid this difficulty it was proposed by H. Israëli (1962) to measure no more at the ground itself but in an altitude of at least two meters. If this proposition will be accepted the comparability may be improved. In this connection I like to refer to the researches of W.D. Crozier (1963). He tested a new method of field measurements which works with a minimum of disturbances.

IV. Some Indications for Practical Applications

Someone may ask for practical applications, if he thinks of the proposals given above for further investigation on Fair Weather Electricity, and the

- 12 -

expense connected with it. It is true, scientific work will not be criticized from this point of view; but, I believe we can answer questions of this kind also. Let me give some examples.

- (1) At first I like to mention here the method of M. Kawano (1958) to evaluate the "austausch" and its daily variation on the basis of atmospheric electrical measurements. Similar researches were done by W.B. Milin (1951, 1953, 1954). Researches of this kind will be very helpful for both climatological and meteorological purposes.
- (2) Some results concerning the ionizing effect of artificial radioactivity in the air (see e.g., D.L. Harris, 1955; E.T. Pierce, 1959; G. Kondo, 1959; K.H. Stewart, 1960; A. Oster, 1963 et al.) suggest the application of atmospheric electrical observations for watching the fission product content in the air.
- (3) Some years ago was discovered that the atmospheric electrical elements undergo specific variations about 1 to 2 hours before the onset of fog and about 1/2 to 1-1/2 hours before the dissipation of fog (see e.g., H. Dolezalek, 1957; G.P. Serbu and E.M. Trent, 1958; L.H. Ruhnke, 1961 et al.) The application of this results to the forecast of fog and fog dissipation will be of special importance for the practical meteorological work (H. Dolezalek, 1962).
- (4) Other possibilities for the application of atmospheric electrical results to practical problems came out from the researches of A. Gockel (1915) and others, concerning the prediction of thunderstorms; the results of J. Scholz (1935), concerning the prediction of blizzards; and the observations of G. Rott (1963)

- 13 -

concerning connections between the behavior of the electrode effect and the weather development during the day. - In all cases the prediction arised from observations during Fair Weather many hours before the event in question.

REFERENCES :

- BENNDORF, H. 1900 : Über Störungen des normalen atmosphärischen Potentialgefälles durch Bodenerhebungen. Sitz.Ber.Akad.Wiss. Wien 109, 923...940
- 1906 : Über gewisse Störungen des Erdfeldes mit Rücksicht auf die Praxis luftelektrischer Messungen. Sitz.Ber.Akad.Wiss. Wien 115, 425...456
- BOURDEAU, R.E., E.C. WHIPPLE, Jr., and J.F. Clark 1959 : Analytic and Experimental Electric Conductivity between the Stratosphere and the Ionosphere. Journ.Geophys.Res. 64, 1363...1370
- BROWN, J.G. 1930 : The relation of space-charge and potential gradient to the diurnal system of convection in the lower atmosphere. Terr.Magn.Atmos.Elect. 35, 1...15
- 1935 : The local variation of the earth electric field. Terr.Magn. 40, 413...424
- CHALMERS, J.A. 1946 : The Ionization of the Lowest Regions of the Atmosphere. Quart.Journ.Roy.Met.Soc. 72, 199...205
- CLARK, J.F. 1956 : The fair-weather atmospheric electric potential and its gradient. Diss.U.Maryland 1956
- CALLAHAN, R.C.; S.C. CORONITI; A.J. PARZIALE; and R. PATTEN 1951 : Electrical Conductivity of Air in the Troposphere. Journ.Geophys. Res. 56, 545...551
- CROZIER, W.D. 1963 : in print: Journ.Geophys.Res. 68
- DOLEZALEK, H. 1957 : Remarks on the electrical conditions during disturbed weather. Contract AF61(514)-640, Techn.Note No. 12
- : Examples for a synoptic evaluation of the measuring results of four atmospheric-electric stations in Switzerland. Contract AF61(514)-640, Techn.Note No. 16
- 1962 : Atmospheric Electric Parameter Study: Survey on an Effect Relating Atmospheric Electric Variations with Formation and Dissipation of Fcg. Contract Nonr 3388(00) Fin.Rep.
- EXNER, F. 1886/1890 : Über die Ursache und die Gesetze der atmosphärischen Elektrizität. Sitz.Ber.Akad.Wiss.Wien (IIa) 93 (1886) 222...285; and: 95 (1887) 1084 ff; 96 (1887) 419 ff; 97 (1888) 277 ff; 98 (1889) 1004 ff; 99 (1890) 601 ff.
- FISCHER, H.J. 1962 : Die elektrische Spannung zwischen Ionosphäre und Erde. Diss.Stuttgart 1962
- FRIES, G., and H. DOLEZALEK 1956: On parallelism occurring in the registration of potential gradient and general local brightness. Contract AF61(514)-640, Techn.Note No. 7

- 15 -

- GISH, O.H. 1944 : Evaluation and interpretation of the columnar resistance of the atmosphere. Terr.Magn. 49, 159...168
- GOCKEL, A. 1915 : Zur Gewittervorhersage. Das Wetter 32, 121...124
- HARRIS, D.L. 1955 : Effects of radioactive debris from nuclear explosions on the electrical conductivity of the lower atmosphere. Journ.Geophys.Res. 60, 45...52
- HOGG, A.R. 1935 : Mem. of Comm., Solar Observ. Canberra 7
- HOLZER, R.E. 1955 : Studies on the universal aspect of atmospheric electricity. Contract AF19(122)-254, Final Report
- ISRAEL, H. 1948 : Zum Tagesgang des luftelektrischen Potentialgefälles. Meteor.Rundschau 1, 200...204
- und H.W. Kasemir 1949 : In welcher Höhe geht der liftelektrische Ausgleich vor sich? Annales de Geophysique 5, 313...324.
- 1950 : Luftelektrische Tagesgänge und Luftkörper (Studien über das atmosphärische Potentialgefälle III). Journ. Atmosph.Terr.Phys. 1, 26...31
- 1952 : The diurnal variation of atmospheric electricity as a meteorologico-aerological phenomenon. Journ.Meteor. 9, 328...332
- 1954 : Luftelektrische Synopsis. Mitt.Dtsch.Wetterdienst, No. 7
- 1955 : Synoptic Researches on Atmospheric Electricity. Proc. Conf.Atmos.Electr., AFCHC Geophys.Res.Papers No. 42 11...20
- 1957 : Atmospheric Electric and Meteorological Investigations in High Mountain Ranges. Contract AF61(514)-640, Final Report
- und E. THEUNISSEN 1957 : Luftelektrisches Potentialgefälle und Weltgewittertätigkeit - ein Beitrag zur grossräumigen luftelektrischen Synopsis. Naturwissenschaften 44, 8
- et al., 1957 : Atmospheric Electrical and Meteorological Investigations in High Mountain Ranges; Microfilm of the Results. Contract AF61(514)640, Appendix to the Final Report.
- 1958 : The atmospheric electric agitation. In: Recent Advances in Atmospheric Electricity, ed. by L.G. SMITH, Pergamon press 1958, p. 149...160
- 1959 : The atmospheric electrical agitation. Quart.Journ.Roy. Meteor.Soc. 85, 91...104

- 16 -

- 1961 : Atmosphärische Elektrizität, Teil II: Felder, Ladungen
Ströme. Leipzig, Akadem. Verlagsges. Geest & Portig KG
- 1962 : The comparison of atmospheric electric results. Journ.
Atm. Terr. Phys. 24, 65...66
- 1963 : The sign of the atmospheric electrical field. Archiv
Meteor. Geophys. Bioklimat. (A), in print
- und R. KNOPP 1962 : Das Problem der Ladungsbildung beim Verdampfen.
Staub 22, p. 19 (see also R. KNOPP: Versuche zur
Ladungstrennung bei Phasenänderungen, Verdampfung
und Kondensation. Thesis Techn. Hochschule Aachen, Germany
1961).
- KASEMIR, H.W. 1950 : Studien über das atmosphärische Potentialgefälle IV:
Zur Strömungstheorie des luftelektrischen Feldes I.
Archiv Meteor. Geophys. Bioklimat (A) 3, 84...97
- 1956 : Zur Strömungstheorie des luftelektrischen Feldes III:
Der Austauschgenerator. Archiv Meteor. Geophys. Bioklim.
(A) 9, 357...370
- KAWANO, M. 1958 : The local anomaly of the diurnal variation of the
atmospheric electrical field. Res. Electrotechn. Lab.
(Japan) No. 569, July 1958
- The local anomaly of the diurnal variation of the
atmospheric electrical field. In: Recent Advances in
Atmospheric Electricity. ed. by L.G. SMITH, Pergamon
Press 1958, 161...174
- KOENIGSFELD, L. 1955 : Study of the variation of potential gradient with
altitude and correlated meteorological conditions.
Proc. Conf. Atm. Electr., AFCRC, Geophys. Res. Pap. No. 42,
21...25
- 1957 : La mesure du gradient du potentiel et de la conducti-
bilité par radiosonde. In: Atmospheric Electricity
During the IGY, ed. by H. ISRAEL, Aachen 1956, p. 84...90
- 1958 : Observations on the relations between atmospheric
electrical potential gradient on the ground and in
altitude and artificial radioactivity. In: Recent
Advances in Atmospheric Electricity, ed. By L.G. SMITH,
Pergamon Press 1958, p. 101...109
- KONDO, G. 1959 : The recent status of secular variations of the atmo-
spheric electric elements and their relation to the
nuclear explosions. Mem. Kakioka Magn. Observ. 9, 2...6
- KRAAKEVIK, J.H. 1958 : Electrical conduction and convection currents in the
troposphere. In: Recent Advances in Atmospheric Elec-
tricity, ed. by L.G. SMITH, Pergamon Press 1958, 75...88

- 17 -

- LENARD, P. 1944 : Probleme komplexer Moleküle. Sitz.Ber. Heidelberger Akademie der Wissenschaften Va, Abhandlung. No. 27, 28, 29.
- MILIN, W.B. 1951 : (New methods for the destination of the vorticity coefficient in the atmospheric layer close to the ground by using atmospheric electric factors - RUSSIAN) USSR Glavnoye Upravleniye Godrometeor. Slushby, Inform. Sbornik 1, 28...36
- 1954 : (Anomalous electric fields in the atmosphere - RUSSIAN) Dokl.Akad.Nauk SSSR 95, 983...986
- i S.G. MALAKHOV 1953 : (Air conductivity and turbulent mixing in the atmosphere - RUSSIAN) Izv.Akad.Nauk SSSR, Ser. Geofiz., No. 3, 264...270
- OSTER, A. 1963 : in print: Atomkernenergie 8
- PIERCE, E.T. 1959 : Some calculations on radioactive fallout with especial references to the secular variations in potential gradient at Eskdalemuir, Scotland. Geofisica pura e applicata 42, 145...151
- RÖNICKE, G. 1962 : Erfahrungen mit luftelektrischen Sondierungen in der freien Atmosphäre. Zs.f.Geophysik 28, 105...126
- 1963 : in preparation: results of atmospheric electric radiosonde ascents in San Salvador 1957/58
- ROSSMANN, F. 1950 : Luftelektrisches Feld und Wetter. Geofisica pura e applicata, in print
- RUHNKE, L.H. 1961 : The Change of Small Ion Density Due to Condensation Nuclei and the Relation to the Extinction Coefficient of Light. Proc.Intern.Conf. on Ionization of the Air, Philadelphia, V-1...V-13
- SAGALYN, R.C., and G.A. FAUCHER 1954 : Aircraft investigation of the large ion content and conductivity of the atmosphere and their relation to meteorological factors. Journ.Atm. Terr.Phys. 2, 253...272
- 1955 : Aircraft Investigation of the Large-Ion Content and Conductivity of the Atmosphere. Proc.Conf.Atm. Electr., AFCRC, Geophys.Res.Papers 42, 27...41
- : Investigation of charged nuclei in the free atmosphere Geofisica pura e applicata 31, 182
- SCHOLZ, J. 1931 : Theoretische Untersuchungen über die Feld- und Ionenverteilung in einem stromdurchflossenen Gas, das auch schwer bewegliche Elektrizitätsträger enthält. Sitz.Ber.Akad.Wiss.Wien (IIa) 140, 49...66

- 18 -

- SCHOLZ, J. 1935 : Luftelektrische Messungen auf Franz Josefs-Land
(cont.) während des Zweiten Internationalen Polarjahres
1932/33. Transact. of the Arctic Instit. USSR
16, 5...169
- SERBU, G.P., and E.M. TRENT 1958 : A study of the use of atmospheric-
electric measurements in fog forecasting. Trans.
Am.Geophys. Union 39, 1034...1042
- STERGIS, C.G.; S.C. CORONITI; A. NAZAREK; D.E. KOTAS; D.W. SEYMOUR; and J.V. WERME
1955 : Conductivity Measurements in the Stratosphere.
Proc.Conf.Atm.Electr., AFCRC, Geophys.Res.
Papers 42, 43...52
- : Conductivity Measurements in the Stratosphere.
Journ.Atm.Terr.Phys. 6, 233...242
- STEWART, K.H. 1960 : Some recent changes in atmospheric electricity and
their cause. Quart.Journ.Roy.Meteor.Soc. 86,
399...405
- WOESSNER, R.H.; W.E. COBB; and R. GUNN 1958 : Simultaneous Measurement
of the positive and negative light-ion conductivities
to 26 kilometers. Journ.Geophys.Research 63, 171...180
- UCHIKAWA, K. 1961 : Atmospheric Electric Phenomena in the Upper Air over
Japan; part I and II; Geophys.Mag. (Japan) 30, 619...672

Session 2.2

J. Bricard

Action of Radioactivity and of Pollution upon Parameters of Atmospheric
Electricity

Table of Contents:

	Page:
A b s t r a c t.....	1
<u>I. RADIOACTIVITY AND THE INTENSITY OF IONIZATION.....</u>	<u>1</u>
1. Intensity of Ionization.....	1
2. Intensity of Ionization Several Meters Above the Ground.....	3
3. Intensity of Ionization in the Altitude.....	4
a) Radiation from the ground.....	4
b) Derivates of Rn & Tn in suspension.....	4
c) Lower Stratosphere.....	6
4. Artificial Radioactivity.....	7
5. Qualities of Small Ions.....	8
General Remarks.....	8
Mobility.....	8
Diffusion Coefficient.....	10
Mean Free Path.....	10
Recombination Coefficient.....	11
6. Small Radioactive Ions.....	12
<u>II. AIR POLLUTION AND LARGE IONS.....</u>	<u>14</u>
1. General Remarks.....	14
2. Optical Properties.....	16
3. Condensation.....	17
4. Electric Charges.....	18
5. Mobility and Diffusion Coefficient.....	18
6. Coagulation.....	20
7. Radioactive Condensation Nuclei.....	21
8. Attachment of Small Ions to Charged and Neutral Nuclei.....	23
9. Attachment Coefficient Expression.....	24
a) Without Consideration of Small Ion's Mean Free Path.....	25
b) Introduction of the Mean Free Path of Small Ions.....	28

<u>III. IONIC EQUILIBRIUM OF THE ATMOSPHERE</u>	31
<u>A. Eddy Diffusion is Disregarded</u>	31
1. Equilibrium Conditions.....	31
2. Required Equilibrium Time.....	32
3. Ionic Densities.....	33
4. Account is Taken of the Inequalities of Positive and Negative Mobilities.....	36
5. The Case of Radio-Active Ions.....	39
a) Computation of Concentrations.....	39
b) Neutral Radio-Active Nuclei.....	41
c) Equilibrium Between Radioactive Small and Large Ions.....	43
d) Granulometric Distribution of the Activity of Natural Aerosols.....	44
<u>B. Introduction of Eddy Diffusion Coefficient, KAWANO's Theory</u>	45
1. Ionic Density.....	45
2. Other Electrical Parameters.....	48
<u>IV. CONCLUSIONS</u>	50
<u>References</u>	51
<u>Figures nos. 1 to 9</u>	after 53.

ACTION OF RADIOACTIVITY AND OF POLLUTION UPON PARAMETERS
OF ATMOSPHERIC ELECTRICITY

by J. BRICARD

ABSTRACT

Placing ourselves at an altitude of several meters above the ground, in order to avoid the perturbations, we recall the characteristic elements of radioactivity and of atmospheric pollution. It is shown that their actions are in the first case the formation of small ions, in the second case their disappearance and the formation of large ions. From that we deduce the ionic density of the air under given meteorological conditions, studying separately the ions, corresponding to the recoil atoms, which come from radioactive disintegrations in the troposphere and in the lower stratosphere.

Finally we introduce the relations between the radioactivity and the other parameters of the atmospheric electricity, close to the ground and in the free atmosphere.

I. RADIOACTIVITY AND THE INTENSITY OF IONIZATION

1. Intensity of Ionization.

We call Intensity of Ionization (or q) the number of small ions of each sign (air molecules, having lost or attached an electron), created in one cubic centimeter of air per second. It is hence a fundamental parameter of the atmospheric electricity. Disregarding the action of cosmic rays, which produce continuously about two pairs of ions per cm^3 of air per second at the sea-level, we can practically say that at this altitude the natural radioactivity of the air is responsible for 80% of the intensity of ionization.

We call one Curie the quantity of a radio-element, producing 3.7×10^{10} of disintegrations per second. If we know the concentration of a given element in the air, expressed in Curies, for instance, it is easy to deduce from it the corresponding intensity of ionization in the case of a disintegration producing Alpha-Rays. The calculation is much more complicated and not always possible in the case of disintegration producing Beta- and Gamma-Rays (Section I 3b). One Roentgen is the quantity of radiation, which per cm^3 of air at 0° under the pressure of 1 atmosphere generates a quantity of electricity of each sign equal to 1 esu or 2.08×10^9 pairs of ions.

In spite of its importance it does not seem that the measuring of q by the method of ionization chambers were satisfactory as a whole. (Difficulties in measuring the ionization of particles α because of the recombination in columns and the absorption of radiations by the wall-effect. Necessity to introduce in the ionization chamber not only air, but also the aerosols it contains, responsible for one part of the radioactivity α , and contributing by their charge to the saturation current. Absorption of β and γ on the walls of the chamber, etc.)

In spite of the improvements proposed (very thin walls of a known absorption [1] *, double-cage chambers [2]), we know but a few direct measurements of the intensity of total ionization. The instrument we applied for our calculations (double-cage) has not given so far sufficiently reliable results to allow us to use them at the present moment.

Thus, we are generally limited to indirect estimates of q , at least as far as α are concerned, made on the basis of the

*) Numbers in brackets refer to the list of references.

3.

content of radioactive products in the air and in the ground.

2. Intensity of Ionization Several Meters Above the Ground.

We shall suppose that the total intensity of ionization is on the order of 10 pairs of ions per cm^3 and second, 20% of which are of cosmic origin. It is then the production of 8 pairs of ions per cm^3 per second that we attribute to the radioactivity of the air and of the ground.

The radioactivity of the ground is about $3.5 \text{ pI}/(\text{cm}^3\text{sec})$; consequently the fraction of intensity of ionization, due to the radioactivity of the air, amounts to $4.6 \text{ pI}/(\text{cm}^3\text{sec})$. These values are divided in the following groups, according to their origin (Hess [3]):

Table I

-Radioactive substances of the air:

α	4.4	$\text{pI}/(\text{cm}^3\text{sec})$	
β	0.03		
γ	$\frac{0.15}{4.58}$	$\text{pI}/(\text{cm}^3\text{sec})$	(min 1.4 (max. 13.5)

-Radioactive substances of the surface soil:

β	0.3		
γ	$\frac{3.2}{3.5}$	$\text{pI}/(\text{cm}^3\text{sec})$	(min 2 (max. 6)

We see that in the case of radioactive substances of the air the radiation α plays the biggest role, while γ is the most important in the case of radiation from the ground.

4.

Above the oceans the total natural radioactivity is reduced to a few hundredths of its value above the ground.

3. Intensity of Ionization in the Altitude.

a. Radiation from the ground.

We see (table I) that the natural radioactive radiation of the surface soil, almost exclusively of γ origin, plays an important role in the lower layers. The following table (Israel) indicates its variation as a function of growing altitude.

Table II

Altitude above the ground	1m	10m	100m	500m	1,000m
% of radiation at the ground	97%	83%	33%	2%	0.1%

We may suppose an exponential law of absorption of this radiation in function of the thickness of the air-layer traversed. Let μ be the coefficient of absorption, supposed identical for all radiations. The intensity of ionization is proportional to the intensity of radiation in one given point. If we call q_{10} its value in the immediate vicinity of the ground, we shall have in the altitude z :

$$q_{1z} = q_{10} \exp(-\mu z). \quad (1)$$

The coefficient μ is in the order of $8 \times 10^{-3} \text{ m}^{-1}$.

b. Derivates (Daughter-Products) of Radon and Thoron in suspension in the air.

In the case of natural radioactivity the distribution of concentration of Tn and Rn (we neglect the presence of Actinon),

as well as that of their derivatives, is connected with the state of turbulency of the air. Taking a soil with average internal characteristics and a coefficient of turbulent diffusion K , independent of the altitude, of $8 \times 10^4 \text{ cm}^2 \text{ sec}^{-1}$, we find through calculations $[\text{ }^4\text{ }]$ for Rn and Tn ~~equal~~ concentrations at the ground level of 158×10^{-18} and $174 \times 10^{-18} \text{ c/cm}^3$, respectively.

Difficulties arise, if we want to calculate the concentrations in various altitudes, due to the disintegration of the various daughter-products of Tn and Rn (it is necessary to know the state of equilibrium mother-daughter products), and due to the attachment of the daughter-products on the aerosols in the air, due to their coagulation and to their disappearance with time.

On the other hand we have to make a distinction between Rn and Tn. The first-one, whose half life-period is long (4 days), disintegrates slowly as it raises higher, while Tn (half life-period 10 sec.) and the ThA (period 0.2 Sec) disappear in the vicinity of the ground. Thus, in higher levels only ThB remains (half life-period 10 h). In the altitude Z above the ground the concentrations of Rn and ThB in the atmosphere are given respectively by the relations:

$$C = C_0 \exp \left(-Z \lambda^{\frac{1}{2}} K^{-\frac{1}{2}} \right) \quad (2)$$

where C_0 represents the concentration of each on the ground level, K the coefficient of turbulent diffusion, and λ the radioactive decay constant, either of Radon or of ThB.

To simplify the reasoning, let us suppose that there exists a radioactive balance at any altitude between Radon on one hand and ThB on the other, and their daughter-products. This, of course, is very approximative, for if there actually exists a radioactive balance between Rn and RnA (3+ minutes period), it is not so for the other

6.

daughter-products, at least next to the ground. This is shown in the studies on the decrease in function of time of disintegration products of Radon, captured in the form of ions or aerosols. This is generally the case for ThB and ThC.- With the simplification we see that every disintegration α of Rn carries along simultaneously 2 α (RaA, RaC), and 2 β and 2 γ (RaB, RaC), and that every disintegration β and γ of ThB brings along simultaneously 1 β and 1 γ (ThC) and 1 α (ThC).

In order to obtain the corresponding value of intensity of ionization, it is necessary to know the number of pairs of ions, produced by each kind of disintegration, and to calculate the total at every altitude. This number is well-known for the α , which is monocinetic. It is poorly determined, however, for β and γ , whose spectra of distribution of energy we know little about at the present time. Table III represents the results, indicated by Israël, for a coefficient of turbulent diffusion $K = 8 \times 10^4 \text{ cm}^2/\text{sec}$ and supposing a middle-value of 2×10^5 pairs of ions through disintegration α and 2×10^4 pairs of ions through disintegration β and γ . These values are supposed the same, independent of the source of radiation.

Table III

Altitude km	0	0.1	0.5	1	2	3	4	5	6	8	10
q from radio-activity	7.6	5.1	3.8	2.7	1.5	0.9	0.5	0.3	-	-	-

It will be noticed that the values, indicated for the vicinity of the ground do not concord perfectly with those of Table I. This is explained by the very approximative mode of calculation used.

c. Lower Stratosphere

Fig. 1 represents variations of intensity of total ionization

in function of the altitude. We see that it begins by decreasing, passes through a minimum at about 3 km, increases again, and above several kilometers the effect of the radioactivity becomes negligible as compared to that of cosmic rays. The effect of cosmic rays, very weak in the vicinity of the ground, increases progressively with increasing altitude up to about 12 kilometers, passes a maximum and decreases then for the higher altitudes.

In the lower stratosphere, between 10 and 20 km of altitude, we find RaD (period 22 years, source of β and γ) in very low quantities on the order of 10^{-19} c/cm³. We find, in addition, radioactive elements originating in the action of cosmic rays upon the molecules of the air (principally Ar). Among them are Be₇ and P₃₂, which will be used later. The first one can also originate from atomic explosions. We find about 5×10^{-19} local c/cm³ of Be₇, and 5×10^{-21} local c/cm³ of P₃₂. As in the case of RaD, the resulting intensities of ionization are negligible as compared to the effects of cosmic rays.

4. Artificial Radioactivity.

With the exception of quite extraordinary conditions (vicinity of an nuclear station, or in the period after nuclear explosions [55]) the average content of artificial products in the air is now 2×10^{-18} c/cm³ of sources exclusively of β and γ . This corresponds to intensities of ionization in the order of 3×10^{-3} pI/(cm³ sec). In other words it is negligible as compared to natural radiation, except perhaps above the ocean, where the latter one is reduced to a few hundredths of its value above the ground. The situation is the same in the stratosphere layers, in spite of the accumulation of disintegration products manifesting itself there. At about 20 km of altitude

we find maximum concentrations $[5]$ of 10^{-17} and 10^{-13} c/cm³, the average concentrations being 10^4 and 10^3 times weaker. Thus the effect is negligible as compared to that of the cosmic rays.

The situation is not the same, if there is an accumulation of these products on the surface of the ground after precipitations, sedimentation of dust etc. According to Israël $[4]$, a rainfall of 10 mm containing 10^{-13} c/cm³, if all the water remains on the ground-surface, would give in its vicinity an intensity of ionization on the order of 75 pI/(cm³ sec). However, this is considerably minimized by the disappearance of water in the ground, and the effect is partially masked by the decrease of Radon exhalation during rainfall. Thus, it generally cannot be observed, yet it could become observable on a waterproof ground.

5. Qualities of Small Ions.

General Remarks. The small ions are generally present in the air in the order of a few hundreds per cm³, the concentration (n') of the positive ions being by some 20% higher than that (n'') of the negative ions. Their difference ($n' - n''$) amounts to several elementary charges per cm³. The concentration of the small ions, which is normally that of 300 to 500 per cm³ next to ground, can be reduced to less than 10% of its value in highly polluted atmospheres and in the clouds. It increases with increasing altitude..

Physical characteristics of the small ions, whose dimension (some 10^{-8} cm) makes direct observation impossible, are the following:

Mobility. This is the speed the ion has in the atmosphere under given conditions of temperature and pressure, if it is exposed to an electric field of 1 V/cm. Under normal conditions the mobility

9.

of the positive ions is in the average in the order of $K' = 1.4 \text{ cm}^2/(\text{V sec})$, that of the negative ions a little higher, $K'' = 1.9 \text{ cm}^2/(\text{V sec})$. (These are in fact the most probable values, the real values being dispersed around these average values). It varies with pressure and temperature according to the relation:

$$K(p,T) = K_0 (P_0/T_0) \frac{P_0}{P} \frac{T}{T_0} \quad (2a)$$

Electric conductivity of the air, more easily accessible for direct measurement than the ionic concentration, is proportional to it and to the mobility of ions. It is given by the following relation, where e stands for the elementary charge:

$$\Lambda = (K'n' + K''n'') e \quad (3)$$

On the ground level it is in the order of 0.5×10^{-16} to $2 \times 10^{-16} \Omega^{-1} \text{ cm}^{-1}$. It augments generally with increasing altitude under conditions depending essentially on meteorological circumstances. The figure 2, borrowed from M. H. Leisen, represent several examples of variation (Explorer II; Sagalyn and Faucher^[1]). According to curve I we can consider Λ as notably constant between the ground and 2.500 m (strong turbulence under a marked inversion). This is not so in the other cases.

The density of the vertical conduction current is given by:

$$i = \Lambda E = EK'n'e + EK''n''e = i' + i'' \quad (4)$$

where E is the electric field strength.

In good weather the vertical current is directed downwards, and we can suppose that its value is notably constant in the troposphere and in the lower stratosphere, whatever the spot the measuring has taken place may be. Its size is on the order of $2 \times 10^{-16} \text{ A cm}^{-2}$. The constance of this current permits to bring into connection the electric field and the conductivity of the air, which are two quantities

of different origin.

Diffusion Coefficient. Let there be $\frac{dn'}{dz}$ the gradient of concentration of the small ions, positive, for example, following a direction oz. The number of small ions traversing per sec. 1 cm² normal cross section at oz is equal to $D' \frac{dn'}{dz}$. D' stands for the coefficient of diffusion of the small positive ions. In principle, the same is valid for the negative ions. The coefficient of diffusion and the mobility are connected by the Einstein relation:

$$\frac{K}{D} = \frac{e}{kT} \quad (5a)$$

k being the constant of Boltzman and T the absolute temperature.

On the average, D' and D'' are under normal conditions in the order of 3.7×10^{-2} cm sec⁻¹ and 5.1×10^{-2} cm sec⁻¹, respectively [8].

Mean Free Path. In molecular dimensions, even if the charges are elementary, the electrical field produced by a small ion, animated by the Brownian movement, is sufficiently strong to polarize the neighboring molecules. Its trajectory, which is deviated by these charges between two successive collisions, is not straight, so that the results of the kinetic theory cannot be applied to it any more.

If we neglect this effect, we can calculate the mobility and the diffusion coefficient in function of the masses m of the ion and M of the gas molecules, from the average speed of thermic agitation of the ion and of the gas molecules and from a fictitious mean free path λ . Thus we obtain, for instance, the relation (1st formula of Langevin):

$$K = \frac{3}{8} e \lambda \sqrt{\pi} \left(\frac{m+M}{mM} \times \frac{1}{kT} \right)^{1/2} \quad (5)$$

11.

where k stands for the constant of Boltzmann.

If we take $M = m$ and $K = 1.5 \text{ cm}^2/(\text{V sec})$ (normal conditions of temperature and pressure), we find $\lambda = 1.3 \times 10^{-6} \text{ cm}$, a value notably different from the value, which corresponds to air molecules ($6.4 \times 10^{-6} \text{ cm}$), under the same conditions [9].

Recombination Coefficient. The small positive and negative ions recombine after their formation. A number of small ions of both signs disappear thus per sec. and per cm^3 ,

$$\frac{dn'}{dt} = \frac{dn''}{dt} = \alpha n' n''; \quad (6)$$

α , standing for the coefficient of recombination, is given by the relation:

$$\alpha = \pi \bar{g} \sqrt{2} \left(\frac{2}{3} \frac{e^2}{kT} \right) \epsilon. \quad (7)$$

$$\epsilon = \frac{\exp \frac{1}{4kT} \frac{\delta}{e^2}}{4 \left[1 - \frac{2}{9} \frac{\sqrt{2}}{\pi} \left(\frac{e^2}{3kT\lambda} \right) \left(1 - \exp \frac{3}{1 + 3kT\delta/e^2} \right) \right]} \quad (8)$$

$$\delta = \frac{kT}{\lambda e^2} \left[\left(\frac{e^2}{6kT} + \lambda \right)^2 - \left(\left[\frac{e^2}{6kT} \right]^2 + \lambda^2 \right)^{3/2} \right] - \frac{e^2}{6kT} \quad (9)$$

where k is the constant of Boltzmann and λ the mean free path, defined in (5), and \bar{g} is the average speed of thermic agitation. The expression (9), valid in a range of pressures between 10^2 and 10^5 mb is different from that of Thomson [8] and allows us to calculate the coefficient α under the various conditions of temperature and pressure. Under normal conditions we find [15] $\alpha = 1.6 \times 10^{-6} \text{ cm}^3 \text{ sec}^{-1}$.

6. Small Radioactive Ions.

Every disintegration of Rn, of Tn, and of their daughter-products in the atmosphere is accompanied by the appearance of a recoil atom. Let C be the concentration of the element considered, expressed in Curies per cm³. For Radon, for example, there will appear per cm³ and per sec. next to the ground a number of RaA atoms in the order of:

$$q_{\text{RaA}} = C_{\text{Rn}} \times 3.7 \times 10^{-10} = 8 \times 10^{-6} \text{ pI}/(\text{cm}^3 \text{ sec}); \quad (10)$$

the same as for the other constituents. A certain number of these atoms is neutral (20% in the case of RaA), the others with a positive unitary charge, constitute the small radioactive ions.

Studying the decrease of these small radioactive ions, as a function of the time, properly sampled, we find that they consist almost exclusively of RaA, with a very weak fraction of RaB. A more profound study allows us to evaluate the life-span of these atoms in the atmosphere before they disappear in a process we shall deal with further on. This life-span is found to be on the order of 20 to 60 sec. [10] [11] [12].

It is easy to determine their concentration in the air by direct capturing, and by measuring the activity of the captured sample. We find in the vicinity of the ground that this concentration is on the average of 10^{-4} to 2×10^{-4} atoms of RaA per cm³. Not having more precise results, so far (measurements are being carried out at the present time), we shall suppose that their mobility and their diffusion coefficient is the same as that of the ordinary small ions.

A study of the products of artificial disintegration, found in the lower stratosphere (accumulation zone) would lead us beyond the framework of this article. Without getting involved in the details, we can say that one part of the products of the explosions exists initially in the atomic form, neutral or electrically charged, as well as all the products of fissions of cosmic origin.

Let us take a simple example, that of Be_7 and P_{32} , generated by the fission of oxygen and nitrogen in the first case, of Argon in the second case. The period of the first (Be_7), which changes into Li_7 stable, is 53 days, that of P_{32} , which changes into S_{32} stable, is 14 days. All these are products, which are set free in the state of atoms, and they have probably an elementary positive charge.

Let us suppose at the altitude of 20 km [14] the concentration of 5×10^{-19} c/cm³ of Be_7 , and 5×10^{-21} c/cm³ of P_{32} . They remain in the stratosphere for a sufficiently long time so that we can suppose that the radioactive equilibrium is reached. According to the relation (10), in one cm³ of air and per sec. there will appear 2×10^{-8} atoms of Be_7 and as many of Li_7 , as well as 2×10^{-10} atoms of P_{32} , with as many atoms of S_{32} . These atoms exist for a certain time in a free state in the atmosphere before they are attached to aerosols, present at this altitude (section II, 1), and it should be possible to detect them (section III 5 a).

II. AIR POLLUTION AND LARGE IONS

1. General Remarks

Natural aerosols, the aggregate of which constitutes the normal atmospheric pollution, are liquid or solid particles, likely soluble in water, neutral or electrified, whose constitution is, as yet, not well known and to which we will assign a spherical shape. Their dimensions are included between 7×10^{-7} and about 10^{-4} cm radius (see Table IV). They are also called condensation nuclei (see section II, 3).

Condensation nuclei, appearing at the ground, are carried ^(easily) upwards by turbulent diffusion. They coagulate but slightly and fall back onto the ground by sedimentation, preferably at night, when turbulent convection is less intensive, or they are collected during the fall of precipitations.

They may come from the ocean (sprays), or from human activities (combustions), and, owing to their slow falling speed with regard to air, they are apt to be carried far from their place of origin. Their chemical composition may vary greatly [16], [17] (chlorides, sulphates, nitrates, ammonium salts, sodium, magnesium). They are usually mixtures of various matters, since they coagulate, coming from simple nuclei initially formed.

Their concentration ranges about 10^3 to 10^5 per cm^3 at a few meters above the ground. It decreases with the increase of the altitude, said decrease being more or less steady (see Large ions, electric charge, section II, 4). Figure 3, borrowed from Israël [4], shows, according to Wigand, [18] the relative variations of atmospheric concentrations in aerosols as the altitude increases

(measures made by a balloon). It may be seen that said distribution follows an experimental law, with a discontinuity corresponding to a temperature inversion. Towards 8,000 m it is reduced to $\frac{1}{10^4}$ of its value at the ground level, and it goes on decreasing as one goes up. According to Junge [19], there would be an increase of the concentrations, between 10 and 20 km; the concentration of particles averaging about 0.15μ radius, going from 0.01 to 0.1 cm^{-3} , before decreasing again. But this concerns rather large particles and it does not seem that, at these altitudes, smaller particles have been numbered.

Let us finally mention the case of natural clouds, made up of droplets of water of some μ in diameter, a few hundreds of which may exist in a single cm^3 . Some authors have mentioned, in addition to these droplets, the presence of particles inferior in size and much more numerous [20]. Above the altitude of 6,000 m, clouds are exclusively made of ice particles flat or elongated, over 0.5 mm in diameter. These crystals play an important part in charge generation in stormy clouds, but this will not be discussed here.

A direct observation of natural aerosols offers difficulties in particular with respect to their sampling. This is made either by collision (Konimeters), a method which does not seem to be applicable to small size particles under 10^{-5} cm or about; either by means of very fine threads (spider threads), which is possible only for liquid particles; either by electric precipitation of particles charged by corona effects, (particles with dimensions between approximately 0.2μ and 0.8μ escape more or less to that kind of precipitation); either by thermal precipitation (which is only good for solid particles); or by means of filters (one may moreover wonder how it comes that particles settle on the front surface of the filter

16.

and that, as a rule, only a few of them get inside the pores). On the other hand, particularly in the field of dimensions unattainable to an optical microscope, it will not be possible to use an electronic microscope for liquid particles, as long as there are no means available to realize supports liable to fix impressions of the droplets of these dimensions. In order to study condensation nuclei granulometry, we are compelled to use indirect methods based on their physical properties.

Their quantitative analysis in bulk in the air may be achieved directly by sampling on filters and by chemical analysis, or by radioactive computation. This proceeding, justly criticized [43] on account of the inefficiency of filter sampling in some dimensional fields, particularly between 1.5×10^{-6} and 10^{-5} cm, seems now perfected. It has been controlled thanks to the use of extra-thin calibrated aerosols and of large natural ions, the size of which were known. Filters with an efficiency of more than 98% may thus be obtained, whatever may be the dimensional field of aerosols to be filtered.

2. Optical properties

Light is diffused by these particles and, at least in the case where their constitution is known, (index, reflection, and absorption factors), it is possible to compute a diffusion indicator for particles the dimensions of which are given. Reciprocally, the measurements of the flux diffused by a group of particles, allows to figure, at least approximately, the atmospheric concentration in aerosols; and the measure of the flux diffused by an isolated particle, correctly lighted, allows to know its dimensions

without changing its constitution.

This method has been originally used for qualitative measures or for pollution detection, has been recently developed so as to become quantitative [20], [21]. It permits the access to dimensions bordering on the limit of the separative power of the optical microscope and we are now extending it to a field of lower dimensions.

3. Condensation

These particles, in a supersaturated atmosphere, act as condensation germs and give liquid droplets directly observable optically. The use of said property permits to determine their concentration in the air.

A droplet thus formed has a radius depending on its chemical nature, on the salt concentration or on the mixtures of salts of which it is formed and on atmospheric supersaturation. By measuring these droplets, under well defined conditions, it is possible to determine the primary dimensions of the corresponding germs in the air and to form an idea on the air pollution on the spot where they have been taken.

The following granulometric distribution may [22] be inferred from this:

$$\frac{dN}{d \log R} = \frac{C}{R^3} \quad (11a)$$

in which dN represents the number of nuclei in a logarithmic scale of radius R , and C a constant. This expression seems valid for particles whose dimensions are at least equal to 10^{-5} cm (see section II, 6).

4. Electric Charges

These particles can carry charges usually very low, (ranging about one or several elementary charges), either by attachment of small ions, or by means of other chemical or thermal processes, in order to give large ions. The statistical study shows that, on an average, the atmospheric concentrations of large ions of both signs are very close, so that the average space charge corresponding to them must be low. However, in the course of the various operations resulting from human activity (combustion, condensation), very important differences between these concentrations, as well as a very pronounced space charge, either positive or negative according to circumstances, may appear.

Under undisturbed circumstances, the proportion $\frac{Z}{N' + N''}$ of the total number of nuclei, to that of charged nuclei, is very variable, depending on authors [23]. it is included between 1.61 and 5.4. It increases with the number of nuclei; the lowest value nearest to that stated by Mme. Thellier [24], seems to correspond to undisturbed average statistical conditions.

The large ions concentration, proportional to that of condensation nuclei, decreases also as the altitude increases, under conditions depending on the meteorological situation; and they disappear above 3000 or 4000 m. Fig. 4, borrowed from Sagalyn and Faucher [25], represents examples of their distribution in altitude.

5. Mobility and Diffusion Coefficient.

Due to their rather great dimensions, the above mentioned particles have mobilities and diffusion coefficients defined in the same manner as in the case of small ions, but much smaller. The

19.

maximum values, under normal conditions are, ranging in about 10^{-2} $\text{cm}^2/(\text{V sec})$ and $3 \times 10^{-4} \text{ cm}^2/\text{sec}$, respectively. These quantities, as in the case of small ions, are interrelated by relation (5a).

It is known that, in a viscous fluid, the strength needed to give a constant speed B to a particle with a radius smaller than 10^{-5} cm is expressed as follows (Stokes-Cunningham law):

$$F = \frac{6 \pi R \eta}{1 + b/pR} \quad (12)$$

η is the air viscosity (at normal temperature and pressure $\eta = 1.7 \times 10^{-4} \text{ cgs}$), p is the atmospheric pressure expressed in cm of mercury, and b a constant, ($b = 0.000617$); R is the particle radius.

According to the mobility definition, we may write:

$$K = \frac{1}{6 \pi R \eta} n e \left(1 + \frac{b}{pR} \right); \quad (13)$$

e meaning the elementary charge and n the number of charges carried by the ion, said number being low and usually equal to the unit (see further down).

The following table IV gives an idea of the large ions mobilities and dimensions, derived from formula (8), a unit-charge carried by the ion being supposed.

Table IV

Small ions	$1,0 > k > 0,01 \text{ cm}^2 \text{ v}^{-1} \text{ sec}^{-1}$	$6,6 < R < 78 \times 10^{-8} \text{ cm}$
Average large ions	$0,01 > k > 0,001$	$78 < R < 250 \times 10^{-8} \text{ cm}$
Langevin ions	$0,001 > k > 0,00025$	$250 < R < 570 \times 10^{-8} \text{ cm}$
Ultra large ions	$k < 0,00025$	$R > 5.7 \times 10^{-6} \text{ cm}$

The diffusion coefficient of large ions may be derived from relations (5a) and (13). We then find for $n=1$:

$$D = \frac{kT}{6\pi R \eta} \left(1 + \frac{b}{pR} \right) \quad (14)$$

k representing Boltzmann's constant:

For average large ions, for instance, D , under normal conditions, is included between 10^{-6} and $10^{-7} \text{ cm}^2 \text{ sec}^{-1}$.

6. Coagulation

Suppose Z is the total number of nuclei, charged or neutral, per cm^3 . It is proved that everything happens, with respect to coagulation, as if every nucleus was neutral [56]. Smolukowsky's [26] coagulation theory may be applied to them and we may write:

$$\frac{dz}{dt} = -\gamma z^2. \quad (15)$$

With R the average radius,

$$\gamma = 8 \pi D R; \quad (16)$$

D being given by (14).

For the large tropospheric atmospheric ions, we find [25] $\gamma = 1.6 \times 10^{-9} \text{ cm}^3 \text{ sec}^{-1}$, which corresponds to an average radius of nuclei $R = 2.3 \times 10^{-6} \text{ cm}$.

The result is that the initial total volume of the nuclei, i.e. product ZR^3 , keeps a constant value. In the field of small dimensions, under 10^{-5} cm (Holl [27] and Mühleisen [28]), we obtain:

$$\frac{dN}{dR} = \frac{C}{R^3}. \quad (17)$$

Figure 5 represents, after Holl, the granulometry of natural

aerosols, as a whole. The fixation of condensation nuclei by cloud droplets may be discussed as a coagulation process; it may yield an explanation for the smaller concentration of large ions inside the natural clouds than in the surrounding atmosphere.

7. Radioactive Condensation Nuclei.

These are particles identical to those which have been described above, but they differ on account of the fact that they attached not small ordinary ions, but small radioactive ions, studied in section I-6. Here we shall only study those originated from natural radioactivity decay (Ra and Th); especially the first one. On these we now have a few informations, taken in the vicinity of the ground.

We have seen that small radioactive ions are, as a rule, largely made of RaA atoms. Due to the long stay of the large ions near the ground (about 15 minutes according to Renoux' measurements [12]), those atoms, once attached to the large ions, decay, giving birth to daughter-products RaB and RaC. As this stay is not sufficient for the radioactive equilibrium to be attained (nearly three hours would, as a rule, be necessary), they are therefore constituted by accumulation products coming from the Radon, corresponding to 15 to 20 minutes [12].

Their destination by sampling and activity measurements is unreliable, since it involves information on the duration of that stay.

Let us suppose that the radioactive equilibrium is reached between the Radon and the RaA, (section I, 3,b), whatever its condition may be (free or attached to aerosols). We shall write:

$$\lambda n_{Rn} = \lambda_A (n_A + Z_A)$$

in which n_A and Z_A mean the atmospheric concentrations of small ions and nuclei having attached RaA. The concentrations of Radon being known (1 to 2×10^{-16} c/cm³), we find that $n_A + Z_A$ averages 1 to 2×10^{-3} atoms of RaA/cm³, wherefrom the Z_A value is deducted by difference, i.e., 8×10^{-4} to 1.3×10^{-3} particles per cm³ under normal conditions [10] [11].

Their granulometric distribution is as follows:

Table V

(1)	(2)	(3)
$R > 1.7 \times 10^{-6}$ cm	$1.7 \times 10^{-6} < R < 10^{-5}$ cm	$R < 10^{-5}$ cm
55%	21%	24%

The 10^{-5} cm limit, actually under study, is not determined exactly. It seems well established that the greater part (60 to 70%) of the products responsible for natural radioactivity, is attached to the average large ions and on Langevin ions [11] [13] [39] [40].

Radioactive nuclei generated by the attachment of small RaA ions to neutral nuclei, carry a positive charge, but those generated by the attachment of RaA neutral atoms to neutral nuclei or of RaA positive atoms to negative nuclei are electrically neutral. Of the 55% of class (1) nuclei, 24% are charged, the remaining 31% are not [29]. These proportions are fairly the same as for neutral nuclei and for ordinary large ions.

Statospherical particles (section II, 1) attach small radioactive ions (section I, 6) and it is due to them that the atmospheric radioactivity at high altitudes is determined. Furthermore,

there are solid particles, entirely radioactive, generated directly by nuclear explosions.

8. Attachment of Small Ions to Charged and Neutral Nuclei.

Small ions, radioactive or not, sediment on condensation nuclei, charged and neutral, by diffusion and by electric action at the same time. Let us first suppose that nuclei are constituted by a monodispersed medium whose radius is equal to the average radius. The settling speed $\frac{dn'}{dt}$, $\frac{dn''}{dt}$ of the small positive and negative ions on the totality of nuclei, will be expressed as follows:

$$\begin{aligned} \frac{dn'}{dt} &= -n' \left[\beta'_0 N_0 + \sum_{p=1}^{\infty} \left(\beta'_{1p} N'_p + \beta'_{2p} N''_p \right) \right] \\ \frac{dn''}{dt} &= -n'' \left[\beta''_0 N_0 + \sum_{p=1}^{\infty} \left(\beta''_{1p} N''_p + \beta''_{2p} N'_p \right) \right] \end{aligned} \quad (18)$$

in which N_0 , N'_p , and N''_p represent per cm^3 the number of neutral nuclei, large positive and negative ions, respectively, carrying p elementary charges. β'_{1p} is the attachment coefficient of small positive ions on nuclei having p positive charges, and β'_{2p} the corresponding coefficient between the same small ions and nuclei having p contrary sign charges, and the same goes for small negative ions.

The only experimental values available as far as for attachment coefficients, are those corresponding to neutral nuclei and to ions having a single charge (we shall see later how to calculate those corresponding to several charges). Let us mention the following scale of sizes:

Table VI

	$\beta'_{c0} \times 10^{-6}$	$\beta''_{c0} \times 10^{-6}$	$\beta'_{21} \times 10^{-6}$	$\beta''_{21} \times 10^{-6}$
Scrase [30]	0.58	1.07	2.35	2.96
Parkinson [31]	0.6	1.1	2.4	4.5
Mme Thellier [24]	2.6	3.2	5.8	7.2
Nolan and de Sachy [32]	6.8	7.6	8.7	9.7

A great dispersion is noted in the above results; in some cases it may be due to difficulties in measuring.

9. Attachment Coefficient Expression.

In order to simplify, let us first suppose that charges are symmetrical. We consider a condensation nucleus, having radius R , charged or not. Let us compute the positive ions flux for instance, entering a sphere having radius r , centered on it. It is supposed that the medium is sufficiently diluted, so that the presence of the other possibly charged nuclei has no effect on the value of n' and n'' , concentrations in small positive and negative ions, in the vicinity of the nucleus considered; and that the nuclei, due to their mass, are motionless. The number of small ions, positive for instance, crossing, by diffusion and by unit of time, the surface unit of the sphere and proceeding towards the nucleus, will be $D \frac{dn'}{dr}$, D being the diffusion coefficient of the small ions.

The number of small ions of the same sign, crossing the same surface, under the same conditions, on account of the electric field, will be $Kn'X \frac{dU}{dr}$, U representing the electric potential at the distance r from the nucleus center and K the mobility of the small ions; (it is supposed that the diffusion coefficient and the

small ions mobility of both signs, have the same common value K and D). Under permanent normal conditions, there is no accumulation of ions and the ion flow ϕ crossing the sphere is constant and equal to the flow settling on the nucleus. Therefore we shall have:

$$\phi = 4 \pi r^2 \left(D \frac{dn'}{dr} + \frac{dU}{dr} Kn' \right) = \text{Cte}; \quad (19)$$

p be the number of elementary charges e , positive for instance, carried by the nucleus, whose surface is supposed to be conductor. Keeping into account the image force of the small ion with regard to this, we shall write:

$$\frac{dU}{dr} = -e \left[\frac{p}{r^2} + \frac{R}{r^3} - \frac{Rr}{(R^2 - r^2)^2} \right] \quad (20)$$

Let us write $r = Rx$ and $\eta = \frac{ke}{DR}$. The integral of relation (19) is expressed by:

$$n' = \exp \left[-\eta \left(\frac{p}{x} - \frac{1}{2x^2(x^2-1)} \right) \right] \left[\frac{A}{DR} \int \frac{1}{x^2} \exp \left(\frac{1}{x} - \frac{1}{2x^2(x^2-1)} \right) dx + B \right]. \quad (21)$$

a. Without Consideration of Small Ion's Mean Free Path.

Integration constants are determined by writing that n' is zero on the nucleus surface, supposed to be a perfect conductor, and that, far from the nucleus, limit densities have the same value n_0 , since the medium is supposed wholly neutral, and n'' is obtained by changing p to $-p$ in relation (21).

Combination coefficients β_{1p} and β_{2p} of a nucleus carrying elementary charges of same sign as that of the small ions and of opposed sign, are expressed as follows:

$$\left\{ \begin{array}{l} \beta_{1p} = \frac{1}{n_0} \quad 4\pi DR \left(\frac{dn'}{dr} \right)_{x=1} \\ \beta_{2p} = \frac{1}{n_0} \quad 4\pi DR \left(\frac{dn''}{dr} \right)_{x=1} \end{array} \right\} \quad (22)$$

from which

$$\beta_{1p} = \frac{4\pi DR}{I(R,p)} \quad \text{and} \quad \beta_{2p} = \frac{4\pi DR}{I(R,-p)} \quad (23)$$

with

$$I(R,p) = \int_1^{\infty} \frac{1}{x^2} \exp \left[\eta \left(\frac{p}{x} - \frac{1}{2x^2(x^2-1)} \right) \right] dx. \quad (23a)$$

Particularly, for neutral nuclei ($p = 0$) β_{10} and β_{20}

assume the form:

$$\beta_{10} = \beta_{10} = \beta_{20} = 4\pi DR. \quad (24)$$

Such are the expressions obtained independently by Fuchs [33] and Bricard [34]. In fact, for particle sizes in the range of large ions ($R > 5 \times 10^{-7}$ cm), and neglecting a few hundredths, we may disregard the action of the electric image (Fuchs [33], [35]; Nolan and Keefe [36]), and write (Pluvinaige [37], Gunn [38])

$$I(\eta, p) = \frac{e^{p\eta} - 1}{p\eta}, \quad I(\eta, -p) = \frac{1 - e^{-p\eta}}{p\eta}. \quad (25)$$

Whipple's approximation [41] consists in supposing that the quantity of small ions deposited by diffusion, is the same for a particle with a given radius, whether the latter is charged or not. This means to neglect the action of the charge carried by a particle on the ionic density in its vicinity, and to write that it follows the same distribution law, whether the particle is charged or not.

A small ion, situated at a distance r from the center of

a large ion, carrying an opposed unit charge, will support an attraction force $\frac{e}{r^2}$ and will proceed towards the large ion at a $\frac{Ke}{r^2}$ speed. So, for one unit of time, the number of small ions entering a sphere whose radius is r , centered on a large ion of contrary sign, by electric attraction, is $\frac{Ke}{r^2} 4 \pi r^2 n = 4 \pi Kne$. The difference $\beta_{21} - \beta_0$ is therefore equal to $4 \pi Ke$. By replacing $\beta_0 = \beta_{10} = \beta_{20}$ by value (24), Junge's relations are obtained [42].

Relations (22) and approximations stated above, which lead to fairly concordant results, when R is higher than 10^{-5} cm, show, if we take for the β the values mentioned on Table (VI), the radii R of about 10^{-6} cm, in full accordance with mobility measurements. However, they have been denied by Keefe, Nolan, and Rich [44], as when applied to smaller size nuclei. Keefe, Nolan, and Rich deny the validity of the theory, which has just been stated, and offer the following explanation: on account of their frequent collisions with small ions, condensation nuclei must go back to a state of equilibrium with them, as regards (at the same time) temperature and electric charge. Taking in consideration their electric energy, Boltzmann's distribution law can be applied to them. The concentration of particles carrying p elementary charges of both signs, may be written under the following form:

$$N_p = 2N_0 \exp(-p^2 e^2 / 2kTR) \quad (26)$$

in which N_0 represents the number of neutral particles per unit of volume, k the Boltzmann constant and T the absolute temperature. In fact, it does not seem that an equilibrium, in the Boltzmann meaning, can be established under these conditions and, as shown by Fuchs [33], [35], the expression (26) may be considered as an approximation

to relations (25), when radius R is sufficiently great (section III A3). Figure 6 shows a comparison between the various theoretical results stated above, according to Keefe, Nolan, and Rich; the points marked are their experimental results. It may be seen that the concordance is satisfactory when $R > 10^{-5}$ cm and that no computation is also satisfactory for the lower values of radius.

b. Introduction of the Mean Free Path of Small Ions.

Suppose that λ is the mean free path of small ions, stated by relation (5). Suppose that Δ is the average distance from the particle surface, with which the small ion had its last collision. It is supposed that everything happens as if said distance would be constant, i.e. as if the collision had taken place at the distance $R + \Delta$ from the large ion center, and that the thickness shell, Δ , may be considered as a void space. A first approximation, (Arendt and Kallmann [45]) used by Lassen [46], consists in taking $\Delta = \lambda$. In a more accurate way, (Smolukowsky [35]), we shall take [47]:

$$\Delta = \frac{1}{3 R \lambda} \left[(R + \lambda)^3 - (R^2 + \lambda^2)^{3/2} \right] - R; \quad (27)$$

which gives $\Delta = \lambda$ for very small values of R , and $\Delta = \frac{\lambda}{2}$ for great values.

It may be considered that, in the thickness zone Δ , between both surfaces, particles (in this instance small ions), move as in a vacuum and are impelled by thermic agitation speed v . Suppose that $n_{R+\Delta}$ is the small ion concentration on the outside surface of the shell. The ion flux reaching the particle (large ion or nucleus) is:

$$\phi_R = \pi R^2 v n_{R+\Delta} \quad (28)$$

At equilibrium we shall write:

$$\phi_R = \phi_{R+\Delta} \quad (29)$$

or, according to (19):

$$4 \pi (R + \Delta)^2 \left[\left(D \frac{dn'}{dr} \right)_{R+\Delta} + \left(\frac{dU}{dr} K n' \right)_{R+\Delta} \right] = \pi R^2 v n_{R+\Delta} \Delta \quad (30)$$

In saying that the above relation is satisfied and that, very far from the nucleus, ionic densities have the same n_0 value, we get A and B, integration constants of relation (21). Furthermore, we find that attachment coefficients β_{1p} and β_{2p} retain form (23) providing we write:

$$I = \int_{1+\frac{\Delta}{R}}^{\infty} \frac{1}{x^2} \exp \left(\eta \left(\frac{p}{x} - \frac{1}{2x^2(x^2-1)} \right) \right) dx + \frac{4D}{MvR} ; \quad (31)$$

with:

$$M = \exp \left[-\eta \left(\frac{p}{x} - \frac{1}{2x^2(x^2-1)} \right) \right]_{x=1+\frac{\Delta}{R}} \quad (32)$$

If we disregard the electric image, we get a good approximation by writing:

$$\left\{ \begin{aligned} \beta_{1p} &= \frac{\pi R^2 v p \frac{e^2}{kT} \exp \frac{-pe^2}{kT(R+\Delta)}}{p \frac{e^2}{kT} + \frac{v}{4D} R^2 \left[1 - \exp \frac{-pe^2}{kT(R+\Delta)} \right]} \\ \beta_{2p} &= \frac{\pi R^2 v p \frac{e^2}{kT} \exp \frac{pe^2}{kT(R+\Delta)}}{p \frac{e^2}{kT} - \frac{v}{4D} R^2 \left[1 - \exp \frac{pe^2}{kT(R+\Delta)} \right]} \end{aligned} \right\} \quad (33)$$

in which k represents always the Boltzmann's constant.

We find especially for β_o :

$$\beta_o = \frac{\pi R^2 v}{1 + \frac{4D}{R + \Delta}} \quad (34)$$

We see on figure 6, that the curve marked II, new theory calculated from (33) and (34), confirms the experimental points of Keefe, Nolan, and Rich, in a satisfactory way. Another argument in their behalf, is that relation (8), concerning the recombination coefficient of small ions, and equally proved right by experience, has been obtained through an argument identical to the above argument.

If r is greater than some 10^{-6} cm, relations (33) are simplified and become identical to those of Lassen [46]. For example we obtain for β_o :

$$\beta_o = \frac{4 \pi D R}{1 + \frac{4D}{vR}} \quad (35)$$

and if R is greater than 10^{-5} cm, we obtain relation (24), save for a few hundredths.

III. IONIC EQUILIBRIUM OF THE ATMOSPHERE.

We have studied, in chapter I, the radio-active origin of small ions and, in chapter II, the pollution characteristics, keeping strictly within the purpose of the Atmospheric Electricity viewpoint. We intend to study here the combined action of radio-activity and pollution, that is small ions versus condensation nuclei.

The consequences of the relations obtained, which are valid through the thickness of the entire atmosphere, will be studied circumstantially in the lower atmosphere, where experimental results are comparatively numerous. We shall state, furthermore, what may be their possible application to the problems of the higher atmosphere.

A. Eddy Diffusion is Disregarded.

1. Equilibrium Conditions. We suppose that the small ions, created in the air, disappear solely by fixation on neutral nuclei or on large ions having an opposite sign or the same sign; placing ourselves in a quiet atmosphere, free from turbulence, we disregard the nuclei coagulation (section II.6). At a given moment, at first we suppose that charges are symmetrical and that all the nuclei have the same radius (monodispersed medium), calling " N_p " the number of nuclei with the charge " $+pe$ " (large positive ions); and " N_0 " the number of electrically neutral nuclei. On account of the symmetry of the problem, the number per cm^3 of nuclei bearing the charge " $-pe$ " is also N_p . Under these conditions we may write:

$$\frac{dn}{dt} = q - \alpha n^2 - n \left[\beta_0 N_0 + \sum_{p=1}^{\infty} (\beta_{1p} + \beta_{2p}) N_p \right] - K \frac{d(nE)}{dz} \quad (36)$$

$\beta_0, \beta_{1p}, \beta_{2p}$ are defined by relations (33...), In the vicinity of the ground, the term depending on the re-combination coefficient α will be disregarded. This would not be allowable in altitudes where quantities $\beta_0 N_0 + \beta_{1p} N_{1p} + \beta_{2p} N_{2p} + \dots$ are much lower. We shall also disregard the term $Kn \frac{dE}{dz}$.

We write for large ions:

$$\frac{dN_p}{dt} = n \left[\beta_{1,p-1} N_{p-1} - \beta_{np} N_p \right]. \quad (37)$$

We shall state that an equilibrium exists between the large ion production and their attachment on the nuclei, consequently:

$$\frac{dn}{dt} = 0 \quad \frac{dN}{dt} = 0 \quad (38)$$

2. Required Equilibrium Time.

Let us suppose, in order to simplify, that there are no large ions having a charge greater than 1 elementary charge. If we consider the concentration of nuclei and large ions as constant, the concentration of the small ions at the time t will be written:

$$n(t) = N_0 \exp(-\beta t) + (q/\beta) [1 - \exp(-\beta t)] \quad (39)$$

If the total nuclei concentration (i.e. Z) is constant, the concentration N of the large ions of both signs will be:

$$\begin{aligned} N(t) &= \frac{Z}{(\beta_{21}/\beta_0) + 2} [1 - \exp(-pt)] + N_0 \exp(-pt) = \\ &= N_\infty [1 - \exp(-pt)] + N_0 \exp(-pt); \end{aligned} \quad (40)$$

N_0 is the value of N at the time $t = 0$ and N the equilibrium

concentration.

$$\theta = \frac{1}{k} = \frac{1}{\beta_0 N_0 + \beta_{21} N_1} \quad (41)$$

represents the average life time of a small ion, in a free state, that is the average time elapsing between the moment when it appears and the moment when it settles on a condensation nucleus.

In normal atmospheres, that quantity is included between 20 and 50 sec.

The quantity:

$$T = \frac{1}{p} = \frac{1}{(\beta_{21} + 2\beta_0)n} \quad (42)$$

represents the equilibrium time constant. Under normal conditions, it averages a few hundred seconds [4]. A direct measure of the average age of large radio-active ions, in the vicinity of the grounds, gives a value averaging 15 minutes. This represents the time of contact between large ions and small ions. The result is that in this time, as a rule, the ionic equilibrium corresponding to relations (38) is nearly reached, a few hundredths still missing.

3. Ionic Densities.

According to (36) we shall write to the equilibrium [49]

$$q = n\beta_0 N_0 + \sum_{p=1}^{\infty} (\beta_{1p} + \beta_{2p}) N_p. \quad (43)$$

It is easily established, according to (37) and (38), that;

$$N_p = N_0 \frac{\beta_0 \beta_{1,1} \beta_{1,p-1}}{\beta_{21} \beta_{22} \beta_{2p}} = N_0 a_p \quad (44)$$

wherefrom:

$$Z = N_0 (1 + 2 \sum_{p=1}^{\infty} a_p). \quad (45)$$

These are relations whose numeric computation is in progress and which permit the determination of the distribution of charges in terms of the nucleus.

We may state that if R does not exceed 2×10^{-6} cm, particles carrying a double charge do not exceed 1% of those carrying only one charge; that particles carrying three charges do not exceed by 2% in number those carrying a double charge.

We find the repartition of charges attached to particles with greater than 10^{-5} cm in (37) and (38). In particular, it is shown, that the maximum charge attached to cloud droplets is in the order of a few tens of elementary charges.

Relation (44) may be written:

$$N_p = \frac{N_0 \beta_0}{\beta_{1p}} \frac{f_{11} f_{1p}}{f_{21} f_{2p}}$$

or, according to (25)

$$N_p = N_0 \frac{\exp p\eta - 1}{p\eta} \exp \left(- \sum_{i=1}^{i=p} \eta^i \right)$$

$$= N_0 \frac{\exp (p\eta/2) - \exp (-p\eta/2)}{p\eta} \exp (-p^2\eta/2)$$

$$\text{If } R \text{ exceeds } 10^{-5} \text{ cm, the quantity } \frac{\exp \frac{p\eta}{2} - \exp (-\frac{p\eta}{2})}{p\eta}$$

is very near the unit, so that we may write (Fuchs [33]) for every sign:

$$N_p = N_0 \exp \left(- \frac{p^2 e^2}{2 R k T} \right).$$

The distribution of charges therefore follows, when the particles radius is not smaller than 10^{-5} cm, or so, a Boltzmann's

law, as regards electrostatic energy, according to the hypothesis expressed by Nolan, Keefe, and Rich [44], (section II, 8a), which may be considered as an approximation to the results stated above.

If we disregard particles carrying several charges (i.e. β_{11}, β_{1p}) and if we suppose that $(\beta_{21} / \beta_o) = 2$, (in fact the average of this ratio amounts to 1.7 according to table (VI)), we find, according to (24) and (43):

$$q = nZ\beta_o = nZ \frac{4\pi DR}{I(R_o)} ; \quad (46)$$

R is the average radius of nuclei. This is Schweidler's formula which connects density of small ions and condensation nuclei with ionization intensity.

In a more accurate way, we shall write, according to (43):

$$q = nZ\beta \quad (47)$$

$$\beta = \frac{\beta_o + \sum_{p=1}^{\infty} (\beta_{1p} + \beta_{2p})_{ap}}{1 + 2 \left(\sum_{p=1}^{\infty} ap \right)} = \frac{4\pi DR}{I(R)} \quad (48)$$

Figure 7 represents [49] the variations of function I (R) in terms of R, in the case as expressed by relation (23a) and in the case as relations (33) are used. We see then that, except for very small values of R, function I (R) is very close to the unit.

Introducing the atmospheric electric conductivity, relation (47) is written:

$$\Lambda = \frac{2q I(R) Ke}{4\pi DRZ} \approx \frac{2q Ke}{4\pi DRZ} \quad (49)$$

Figure 8, borrowed from Sagalyn and Faucher [25], represents ionic density variations, computed according to the above relations. The points marked show the results of measures made in the exchange zone, which had a thickness of a few km above the ground.

Let us now consider the case of a medium whose granulometry follows relation (17). Relation (47) is written as follows:

$$q = n \int_{R_0}^{\infty} \beta f(R) dR = Cn Z^{\frac{1}{2.3}}; \quad (50)$$

C being a characteristic constant of the granulometry for a certain ionic intensity, that is for a certain stated atmospheric radioactivity; we shall then write:

$$n \times Z^{\frac{1}{2.3}} = C^{te}, \quad (51)$$

an expression which is experimentally proven [27], [28].

4. Account is Taken of the Inequalities of Positive and Negative Mobilities [34].

Relations (47) will be expressed thus:

$$q = \frac{4\pi D' R Z n'}{I(R, p')} = \frac{4\pi D'' R Z n''}{I(R, p'')} ; \quad (52)$$

with

$$n' \approx \frac{q}{4\pi D' R Z} \quad n'' \approx \frac{q}{4\pi D'' R Z} \quad (53)$$

it results that:
$$\frac{n'}{n''} = \frac{D''}{D'} = \frac{K'}{K''} . \quad (54)$$

According to the above relations, the space charge constituted

by small ions, will be written as follows:

$$\rho_1 = e(n' - n'') = \frac{qe}{4\pi RZ} \frac{D' - D''}{D' D''} \quad (55)$$

in which R is always the average radius of the large ions.

This quantity ρ_1 represents a positive space charge; for an average ionic density near the ground it averages to 50 to 100 elementary charges per cm^3 , in accordance with the results which may be computed from direct measures of ionic concentrations of both signs.

As a rule, this represents only one part of the space charge, which, while preserving usually a near-by order of size, may be inversed in sign. Norinder's [50] results, valid at 8 or 9 m above the ground, show a negative charge (400 elementary charges per cm^3). Scrase [51] finds in case of marked turbulence, a charge always positive (under these conditions the electrode effect is masked); and negative in the first 5 meters above the ground, if the air is quiet; the average value measured ranging about 200 elementary charges per cm^3 . From here it may be inferred that there is a surplus of charge born by other particles and especially by large ions in excess over that corresponding to small ions; and this may reverse the sign of the whole.

On the other hand, positive and negative conductivities are such that:

$$\begin{cases} \lambda' = K' n' e \alpha \frac{q K'}{4\pi D' R Z} ; \\ \lambda'' = K'' n'' e \alpha \frac{q K''}{4\pi D'' R Z} . \end{cases} \quad (56)$$

It results from relation (54) that:

$$\lambda' = \lambda'' \quad (57)$$

According to relations (4) and (56) we find that the corresponding electric field of the earth is really proportional to the ionization and inversely proportional to the ionization intensity, which corresponds to the observations and permits particularly to explain the field variations related to radio-activity, on the ground as well as in altitude [55].

Finally, according to (23), (37), and (38):

$$\frac{N'_p}{N'_{p+1}} = \frac{N''_p}{N''_{p+1}} = \frac{I(\eta, p)}{I[\eta, -(p+1)]} \quad (58)$$

Particularly:

$$\frac{N'_1}{N''_1} = 1 \quad (59)$$

Relations (54), (57), (59) confirm usually stated experimental results. The following table gives a comparison with Mme. Thellier's experiments:

Theoretical Values

$$\frac{n'}{n''} = \frac{k''}{k'} = 1.25$$

$$\lambda' = \lambda''$$

$$\frac{N'_1}{N''_1} = 1$$

Experimental Values

$$\frac{n'}{n''} = 1.24$$

$$\lambda' = 1.42 \times 10^{-4}; \lambda'' = 1.40 \times 10^{-4}$$

$$\frac{N'_1}{N''_1} = 1.03$$

According especially to relation (59), the space charge born by large ions should be zero, which results seems inconsistent with the results recalled above. However, we must not forget (section III A, 2) that the ionic ^{equilibrium} is usually reached only to a few hundredths. Let us take 5%. It corresponds to a possible excess of large ions of the same order. For a slight pollution (2000 large ions/cm³), 100 elementary charges born by large ions may result, this being all the more marked when pollution is higher. We must furthermore add that artificial pollution causes important charges of a preponderant sign $[-6]$, which have no time to be neutralized by natural ionization, and whose action, superposing on that of natural pollution, alter ionic ^{equilibrium} equations.

5. The Case of Radio-Active Ions.

a. Computation of Concentrations. The following reasoning is prevailing, and valid whatever the nature of the radioactive body present in the atmosphere may be, providing that elements of the range of molecular dimensions be present and not aerosols of larger dimensions. It will be applied to the particular case of the Radon near the ground, which seems to have been the more accurately studied until now.

Supposing that:

$$q_A = \lambda_{Rn} N_{Rn} \quad (60)$$

is the number of RaA atoms appearing per cm³ of air and per second, N_{Rn} meaning the atmospheric concentration of Radon and λ_{Rn} its radio-active constant. We will write relation (36):

$$\frac{dn_A}{dt} = q_A - \alpha n_A - n_A \left\{ \beta_0 N_0 + \sum_{p=1}^{\infty} [(\beta_{1p} + \beta_{2p}) N_p + \beta_{pA} N_{pA}] \right\}. \quad (11)$$

n_A is the atmospheric concentration of small RaA ions, and N_{pA} that of the nuclei having attached RaA atoms.

Not knowing the exact value of the diffusion coefficient of neutral RaA atoms (mentioned in section (I,6)), which appear when the Radon disintegrates, we suppose as a first approximation, that every radio-active ion carries a positive elementary charge. The problem is then the same as that of the attachment of ordinary ions on condensation nuclei, with the difference that this concerns only positive ions.

Due to the fact that small radio-active ions have the same mobility as the small normal ions of the atmosphere, it results from relation (7) that they have also the same recombination coefficient as the small negative ions and we may, under normal conditions, disregard the quantity αn_A .

The β have the same meaning as in the previous section and the expression $\beta_{1p} N_A$ takes into account the formation of radio-active particles having a multiple concentration charge N_{pA} . The limit concentration reached at the equilibrium will be given by $\frac{dn_A}{dt} = 0$; that is, according to notations of section IIIA, 2 and disregarding multiple charges:

$$n_A = \frac{q_A}{\beta + \lambda_A}. \quad (62)$$

The quantity $\theta = \frac{1}{\beta}$ represents, as in the case of

relation (41), the average interval of time between the appearance of a radio-active atom coming from the Radon, disintegrated or not, and its attachment on a particle; it ranges therefore to about 20 to 50 sec, the same as for small normal ions.

This is, in fact, the order of magnitude corresponding to Renoux' direct measures $[12]$, taken close to the ground (study of the decrease of disintegration products of small ions, directly collected in the atmosphere during a very short period). RaA atom concentrations, corresponding to the conditions of relations (62), are of the same kind as those mentioned in section(I.6) for β -values consistent with experience.

Relation (62) may also be applied to the computation of the concentration of stratospheric recoil atoms. At an altitude of 20 km, we may suppose for them: $D \approx 1 \text{ cm}^2 \text{ sec}^{-1}$; $R = 10^{-5} \text{ cm}$; and $Z = 0.1 \text{ per cm}^3$. We find that β ranges at about 10^{-5} sec^{-1} , the attachment time for every present aerosol particle of these liberated atoms ranging at about 10^5 sec. , about 3 hours. If we take the case of Be_7 and P_{32} considered in section I-6, whose period is long compared with this attachment time, according to (62), corresponding concentrations would amount to 2×10^{-3} and 2×10^{-5} of free Be_7 and P_{32} atoms per cm^3 of the atmosphere, respectively.

b. Neutral Radio-Active Nuclei $[29]$ The whole of the Radon decay products is thus either free, in the form of small ions, mainly constituted by RaA, and by RaB and RaC in very small quantities, or in the form of radio-active condensation nuclei, electrically neutral, (coming from large ions originally negative), or of large radio-active ions (coming from neutral condensation nuclei), or

fixed on dust particles.

Radio-active neutral ions can also appear by neutralization of large radioactive ions, by small negative ions, and disappear by attachment of small ions of every sign. We will disregard, in a first approximation, these minor reactions.

If the disappearance of large radio-active ion and neutral nuclei, exclusively of N_A and N_{oA} concentration, is exclusively attributed to their decay, we will write, for instance for the second concentration:

$$\frac{dN_{oA}}{dt} = n_A \beta_{21} N'' - \lambda_A N_{oA}; \quad (63)$$

N'' is the concentration of large negative ions. The same relation will be obtained for N_A .

If we suppose that there is an equilibrium:

$$\frac{dN_A}{dt} = \frac{dN_{oA}}{dt} = 0; \quad (64)$$

and supposing a probable atmospheric ion concentration, we find for $n_A = 1.5 \times 10^{-4} \text{ cm}^{-2}$ (section I.6) that $N_{oA} = 5 \times 10^{-4} / \text{cm}^3$; $N_A = 4 \times 10^{-4} / \text{cm}^3$.

This corresponds to the experiments (section II.7).

However, (secondary reactions mentioned above), large negative radio-active ions should appear, originated by attachment of small ordinary ions, on neutral radio-active nuclei. In spite of all our efforts, we did not succeed in detecting the presence of these large negative ions in the atmosphere, which leads us to suppose that such a mechanism does not exist. It is, however, possible to realize it by the corona effect. An explanation could be the insufficient contact time between natural aerosol particles and Radon

products.

c. Equilibrium Between Radioactive Small and Large Ions.

[10], [11], [43]. Suppose that Z_A is the concentration of RaA atoms, corresponding to these two kinds of particle. Due to the small RaA period (3 min.), it may be supposed that the radio-active equilibrium is obviously reached between the Radon and the RaA resulting from its decay (10 minutes are indeed necessary to realize said equilibrium to 10%). We shall therefore write:

$$q_A = \lambda_{Rn} n_{Rn} = \lambda_A (n_A + Z_A); \quad (65)$$

and, starting from (62) and (65), we find that:

$$Z_A = q_A \frac{\beta}{\lambda_A} \quad (66)$$

from which:

$$\frac{n_A}{Z_A} = \frac{\lambda_A}{\beta}. \quad (67)$$

We see that the ratio $\frac{n_A}{Z_A}$ is independent of the quantity of Radon existing in the A_{air} .

Relation (67) shows for the RaA (period 3 min), near the ground, under normal conditions, ($\beta = 4 \times 10^{-2} \text{sec}^{-1}$), that $\frac{n_A}{Z_A}$ ranges at about 10%, which corresponds to the measures. These relations are also valid for stratospherical decay products. For Be_7 and P_{32} with $\beta = 10^{-5} \text{sec}^{-1}$, orders of magnitudes of 0.02 and 0.06 are respectively found for n/Z .

44.

d. Granulometric Distribution of the Activity of Natural Aerosols [46], [49]. First, let us go back to the case of the attachment of small ions on natural aerosols, but in a polydispersed medium. According to (47) and (48), we may write:

$$q(R) = 4\pi Dn \int_{R_0}^R \frac{Rf(R)}{I(R)} dR. \quad (68)$$

$f(R) = \frac{dZ}{dR}$ represents the granulometric distribution of the medium as given by the relation (17). Function $q(R)$ is represented, in relative values, in fig.9 for two values: $R_0 = 5 \times 10^7$ and $R_0 = 10^{-6}$ cm of minimum radius R , corresponding to inferior limits, reasonable for large average ions: the maximum radius was chosen equal to 1. The distribution, thus computed from relation (68), is practically identical with that computed by Lassen [46] from relation (35) for $R_0 = 10^{-6}$ cm.

On the same figure, a dotted line shows the distribution obtained by making $I(R) = C^{te}$ in relation (68). We may see, especially for $R_0 = 10^{-6}$ cm, that the corresponding distribution is very similar to the former, and that, due to the accuracy of measuring methods now available, this approximation is largely satisfactory, which justifies Mühleisen and Holl's [27], [28] arguments $[I(R) = 1]$.

We derive from the curves that the average nuclei ($R \leq 2.5 \times 10^{-6}$ cm) attach 78 to 80% in the first case and 83% to 86% in the second; the remaining, i.e. about 15 to 20%, being attached by particles of larger size. These results define the role of these particles, the nature of which has been discussed before [34].

Relation (68) is general and applies to small radio-

active ions derived from the Radon; for instance, attached to aerosol particles; n is to be replaced by n_A and q by $q_A(R)$, which represents the accrued granulometric distribution of the activity attached to natural aerosol particles. Points marked in fig. 9 represent the experimental results directly obtained, corresponding to table V. We see that categories (1) and (3), table C, are well placed, (points marked c and d), with respect to the computed curves in fig. 9.

The experimental device used in these investigations does not permit to know accurately the value of the radius corresponding to class 2, which may be either a or b on fig. 9. However, even if we take the farthest, we are again in the neighborhood of the computed curve. We may then conclude, in consideration of the slight quantities measured and of the difficulties encountered in such experiments, that the experimental points thus obtained, constitute a first checking of the theoretical consideration stated above. They are also in agreement with the theoretical distribution foreseen by Lassen [46], concerning the attachment of Thoron by-products on artificial aerosol particles.

B. Introduction of Eddy Diffusion Coefficient. Kawano's Theory
[52] [53].

1. Ionic Density.

In order to know the vertical distribution of ionic densities, we must introduce the eddy diffusion coefficient into the equilibrium equations. This allows to determine the distribution of the various electric parameters, depending on the altitude. Let n be the concentration of small positive ions, for instance, supposing that, as in (36), charges are symmetrical and that K is the eddy diffusion coefficient. The rate of variation of n with altitude Z will be

46.

expressed, on account of eddy diffusion, as follows:

$$\frac{dn}{dt} = \frac{d}{dz} \left(K \frac{dn}{dz} \right). \quad (69)$$

The contribution of ions, coming from lower parts, adds itself to the production of ions by the various ionizing agents, considered in chapter I. Let $q(z)$ be the corresponding total ionization intensity. Equations (36) and (38) become, at altitude z^* :

$$\frac{d}{dz} \left(K \frac{dn}{dz} \right) + q_z = B Zn - K \frac{d(nE)}{dz} + \alpha n^2. \quad (70)$$

Account may be taken of possible variations of K with the altitude (Milinc [54]), which complicates the computations. We will merely consider K as constant (Kawano) and disregard possible variations of the conduction current, as well as the small ions recombinations, which leads to relation:

$$K \frac{d^2 n}{dz^2} + q_z = B Zn. \quad (71)$$

The ionization intensity is the sum of 3 terms:

$$q_z = q_{z1} + q_{z2} + q_{z3}. \quad (73)$$

The first term, q_{z1} , represents the action of the γ -radiation from the ground. At z altitude, it is given by relation (1). The second term represents the action of radio-active gases and of their active decay products suspended in the atmosphere. By limiting ourselves, in a first approximation, to the Radon daughter-products and

*) K is not well known close to the ground. However, we shall suppose, that the value of K as well as that of dn/dz is much smaller at ground level than in some height. This justifies the equations (37) and (38).

47.

by reverting to the reference level h , we will write, according to (2):

$$q_2(z) = q_{2h} \exp - \left[\sqrt{\frac{\lambda}{K}} (z - h) \right]. \quad (73)$$

where λ is the Radon radio-active constant. (It would be easy to take into account the other radio-active bodies, possibly present. They would reveal themselves through a sum of terms of the above type).

Relation (70) will then be written under the form mentioned by Kawano:

$$K \frac{d^2 n}{dz^2} + q_{10} \exp(-\mu z) + q_{2h} \exp - \left[\sqrt{\frac{\lambda}{K}} (z-h) \right] + q_3 = B Z n; \quad (74)$$

$Zn;$ (74)

q_3 is the cosmic radiation contribution, supposed constant, in terms of the altitude.

The integration of the above relation has been made by KAWANO, in the case when product BZ is constant with the altitude. It is evident that this condition is in contradiction with the other conditions brought in relation (74), (other characteristics variable with the altitude), as well as with experience, (section II,1). Therefore, the expression of n thus obtained can only be very approximative and would most probably be improved if Z would be given an exponential form. However, with the following limit conditions:

$$\begin{aligned} n &= n_h & \text{at } z &= h \\ n &= n & \text{at } z &= \infty \end{aligned}$$

we obtain:

$$n = \left[n_h - \frac{q_{1h}}{BZ - \lambda} - \frac{q_{20}}{BZ - K\mu^2} - \frac{q_3}{BZ} \right] \exp \left[-\sqrt{\frac{\lambda}{K}} (z-h) \right] + \frac{q_{1h}}{BZ - \lambda} \exp \left[-\sqrt{\frac{\lambda}{K}} (z-h) \right] + \frac{q_{20}}{BZ - K\mu^2} \exp(-\mu z) + \frac{q_3}{BZ}. \quad (75)$$

This expression allows numerical calculation of the ionic density with these simplifying hypotheses and according to (3), the conductivity, resistivity, etc., at various altitudes.

2. Other Electrical Parameters.

By calling E the earth's electric field supposed vertical and ρ the charge density at altitude:

$$\frac{dE}{dz} = -4\pi\rho \quad (76)$$

or, according to (4):

$$S = \frac{1}{4\pi\Lambda^2} \frac{d\Lambda}{dz}. \quad (77)$$

i is the density of the vertical conduction current.

Starting from (3), (75), (76), and (77), we may therefore bring in the pollution and radio-activity on all other atmospheric electricity parameters, and especially on the space charge and the electric field. Let us write $q_{20} + q_3 = q_2$ and $\mu = 0$, which means to disregard ground radiation absorption (table III). Noting that $\lambda = 2.09 \times 10^{-6} \text{sec}^{-1}$ is negligible compared with BZ (whose order of magnitude under low pollution is nearing 10^{-2}sec^{-1}), we obtain, according to (75), (76), and (77), a relation between the electric field E and space charge density at the height h , which is written

$$E_h = 4\pi \epsilon_h \frac{n_h K^{\frac{1}{2}}}{(BZ)^{\frac{1}{2}} (n_h - \frac{q_h + q_z}{E Z})} \quad (78)$$

At zero altitude, if we take $K = 4 \times 10^4 \text{ cm}^2 \text{ sec}$, $BZ = 10^{-2} \text{ sec}^{-1}$, $q_h = 10 \text{ pI cm}^{-3} \text{ sec}^{-1}$, and $n = 1000 \text{ cm}^{-3}$ according to (46), we find that E ranges about 0.3 esu/m , i.e., about 100 V m^{-1} , normal size range. Relation (78) allows to explain, in a satisfactory way, the electric field local anomalies.

IV CONCLUSIONS

Although the relations established in the course of this report are general, their application to problems of atmospheric electricity is restricted, as regards the equilibrium between small ions and natural aerosols, at altitudes higher than a few km. Above, ionization intensity of radio-active origin and atmospheric pollution play a negligible part, compared with ionization intensity of cosmic origin and re-combination between small ions. In other words, relations (70) and (72) remain valid, providing all other terms besides q_3 and αn^2 are disregarded even in the stratospheric accumulation zone.

We have shown that ionic equilibrium conditions may also be applied to the attachment of ions or radio-active atoms on natural aerosol particles. Although their concentrations are extremely low, compared with those of large and small natural ions, their experimental study is already well in progress, in the neighborhood of the ground. It presents an interest in the exchange layer where pollution and radio-activity are still noticeable, but seems useless between the latter and the tropopause. On the contrary, in the accumulation zone, towards 20 km in height, where exist at the same time, radio-active atoms (fission and artificial radio-activity) and an appreciable quantity of pollution, it presents certainly an interest and could constitute a new stage in the study of the atmospheric radio-activity.

REFERENCES

1. G.R.Wait and A.G. McNish - Month. Weath. Rev. 62
p. 1 - 1934
2. F. Pluvinage et R. Utzmann - Ann. Géophys. - 4, p. 161
1948
3. V.F. Hess - Ergebnisse der Kosmisch. Phys. 2, p.95 -
1933
4. H. Israël - Atmosphärische Elektrizität - Leipzig,
1957 und 1961
5. See 3rd report H A S P - Vol. 2B
6. R. Mühleisen - Handb. d. Phys. - Vol. 48, p. 544, 1957
7. R.C. Sagalyn and G.A. Faucher - Journ. Atm. a. Terr.
Phys. 5. p. 253, 1954
8. L.B. Loeb - Basic Processes of Gaseous Electronics
University Press of California Berkley, 1960
9. E.H. Kennard - Kinetic theory of gases. New York and
London, 1938
10. J. Bricard, J. Pradel, et A. Renoux - C.R. Acad. Sc.
Paris, 252, p. 2119, 1961
11. J. Bricard, J. Pradel, et A. Renoux - Geofisica pura
e applicata 51, p. 237, 1962
12. A. Renoux - to be published in C.R. Acad. Sc. Paris
13. J. Bricard -to be published in C.R. Acad. Sc. Paris
14. Rama and Honda - Journ. of geophys. Res. 66, p. 3227, 1961
15. O.H. Gish and K.L. Sherman - Terr. Mag. 49, p. 159, 1944
16. H. Cauer - Archiv Met. Geophys. Biokl. 1, p. 221, 1949
17. C. Junge - Journ. of Met. 11, p. 323, 1954
18. E. Everling und A. Wigand - Ann. Phys. 66, p. 261, 1921
19. C. Junge - Journ. of Met. 18, p. 746, 1961
20. M. Deloncle - Journ. de Phys. 23, p. 269, 1962
- R.G. Eldridge - J. Meteorology, 18, p. 171, 1961

21. J. Bricard, M. Deloncle et G. Israël - Ann. Géophys.
15, p. 415, 1959
22. C. Junge - Ber. Deutsch. Wetterdienst U.S. Zone No 35,
p. 201, 1952
23. J.A. Chalmers - Atmospheric Electricity; Pergamon Press
1957
24. O. Thellier - Ann. Inst. Phys. Globe, Paris, 19, p. 107,
1941
25. R.C. Sagulyn and G.A. Faucher - Quart. Journ. Roy. Met.
Soc. 82, p. 428, 1956
26. M. Smolukowsky - Z. Phys. Chem. 92, p. 129, 1918
27. W. Holl - Beitr. z. Phy. d. Atm. 29, p. 83, 1956
28. W. Holl and R. Mühleisen - Geofisica pura e applicata
31, p. 115, 1955
29. J. Bricard, J. Pradel, et A. Renoux - C.R. Acad. Sc.
Paris, 253 - p. 1476, 1961
30. F.I. Scrase - Geophys. Mem. Met. of London, No. 64, 1935
31. W. D. Parkinson - Trans. of Oslo Meeting, 1948
32. J.J. Nolan and G.P. de Sachy - Proc. Roy. Ir. Acad.
A. 37, 71, 1927
33. M.A. Fuchs - Iz - Akad - Nauk USSR - Geogr. Geophys
I - p. 341, 1947
34. J. Bricard - C.R. Acad. Sc. Paris, 226, p. 1536, 1948
Journ. Geophys. Res. 54, p. 39, 1949
35. M.A. Fuchs - The Mechanism of Aerosols, U.S. Army,
Chemical Laboratories. Special Publications
CWL. 4, 12, 1955
36. D. Keefe and P.J. Nolan - Geofisica Pura et Applicata
50, p. 155, 1961
37. P. Pluvinaige - Ann. de Géophys. 2, p. 31, 1946;
3, p. 2, 1947
38. R. Gunn - Journ. Met. 11, p. 339, 1954
39. M.H. Wilkening - Rev. Sc. Inst. 23, p. 13, 1952

40. M. Kawano - Geofisica pura e applicata 51, p. 243, 1961
41. F.J.W. Whipple - Proc. Phys. Soc. London, 45, p. 367, 1933
42. C. Junge - Journ. of Met. 12, p. 13, 1955
(En: Israël & Krebs?)
43. C. Junge - Nuclear radiation in geophysics, p. 169
Springer, 1962
44. D. Keefe, P.J. Nolan and T.A. Rich - Proc. of the Roy. Irish Acad. A - 60, p. 27, 1959
45. F. Arendt und H. Kallmann - Z. Phys. 35, p. 421, 1926
46. L. Lassen - Zeits. für Phys., 163, p. 363, 1961
47. J. Bricard - Geofisica pura e applicata, 51, p. 237, 1962
48. V.P.V. Flanagan et T.C. O'Connor. Geofisica pura e applicata, 51, p. 148, 1961
49. J. Bricard, J. Pradel, et A. Renoux - to be published in Annales de Géophysique, 1962
50. H. Norinder - Geogr. Ann. Stockholm, I, p.1, 1921
51. F.J. Scrace - Geophys. Mem. London, 67, 1935
52. M. Kawano - Journ. of Geom. and Geoelectricity, 9, p. 123, 1957
53. M. Kawano - Journ. of the Met. Soc. of Japan, 35, p. 29, 1957
54. V.B. Milin i S.B. Malakev - Isv. Acad. Sc. U.R.S.S. Section Geophys. - 3, 1953
55. E.T. Pierce, L. Koenigsfeld, H. Israël, D.L. Harris - in: J.C. Smith: Recent advances in atmospheric Electricity, Pergamon Press, 1958
56. P.J. Nolan - Journ. Atm. and Terr. Phys. 6, p. 205, 1956

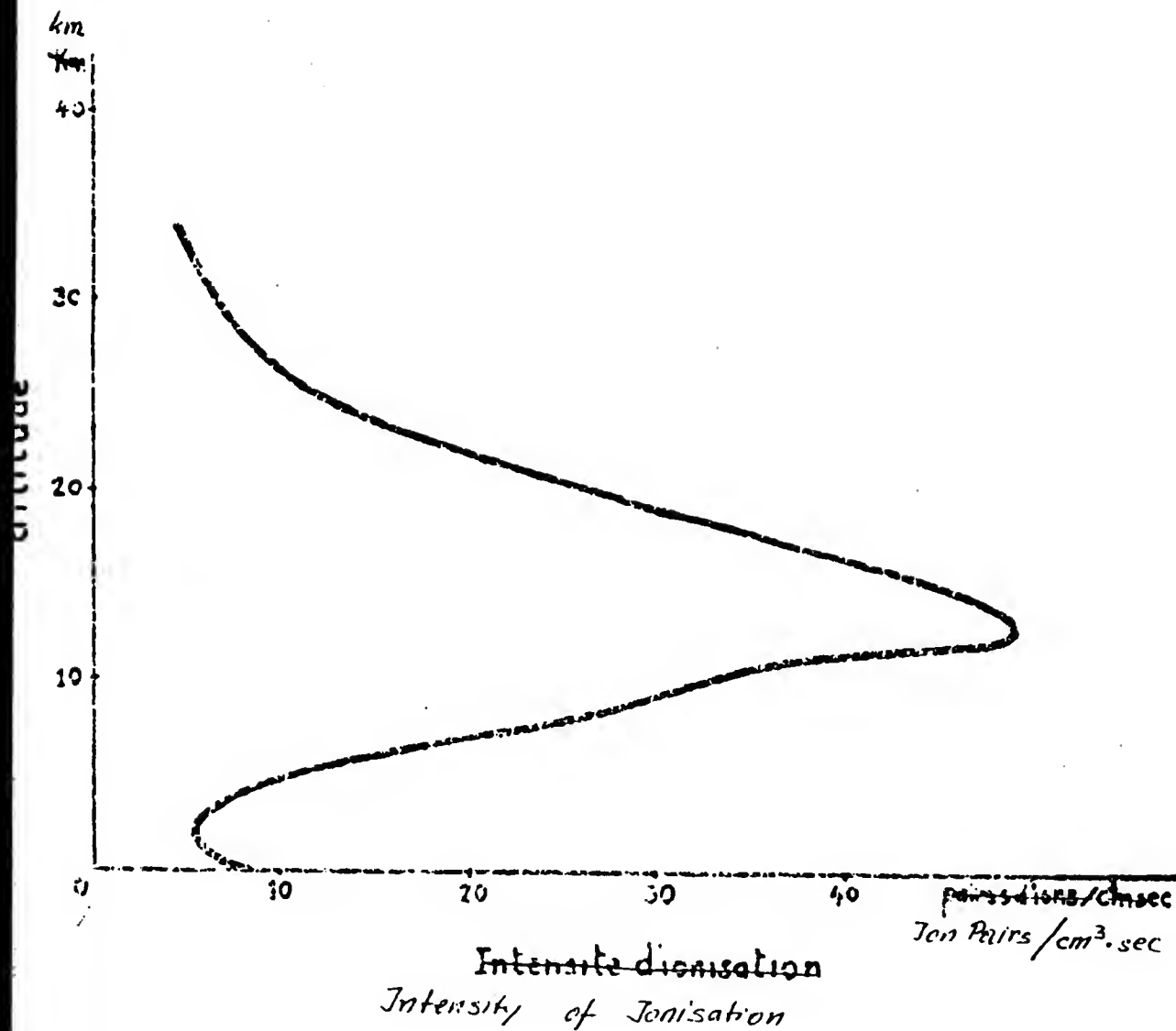


fig. 1

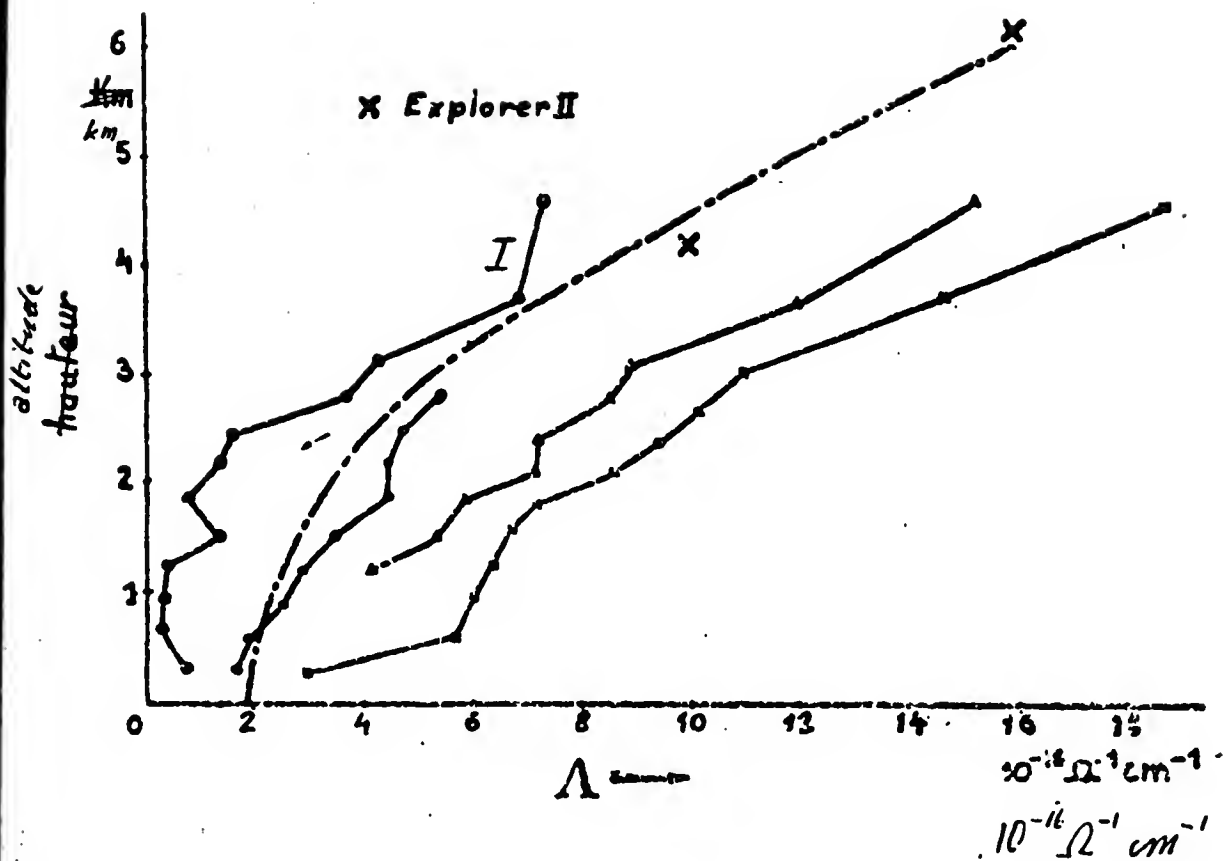


fig.2

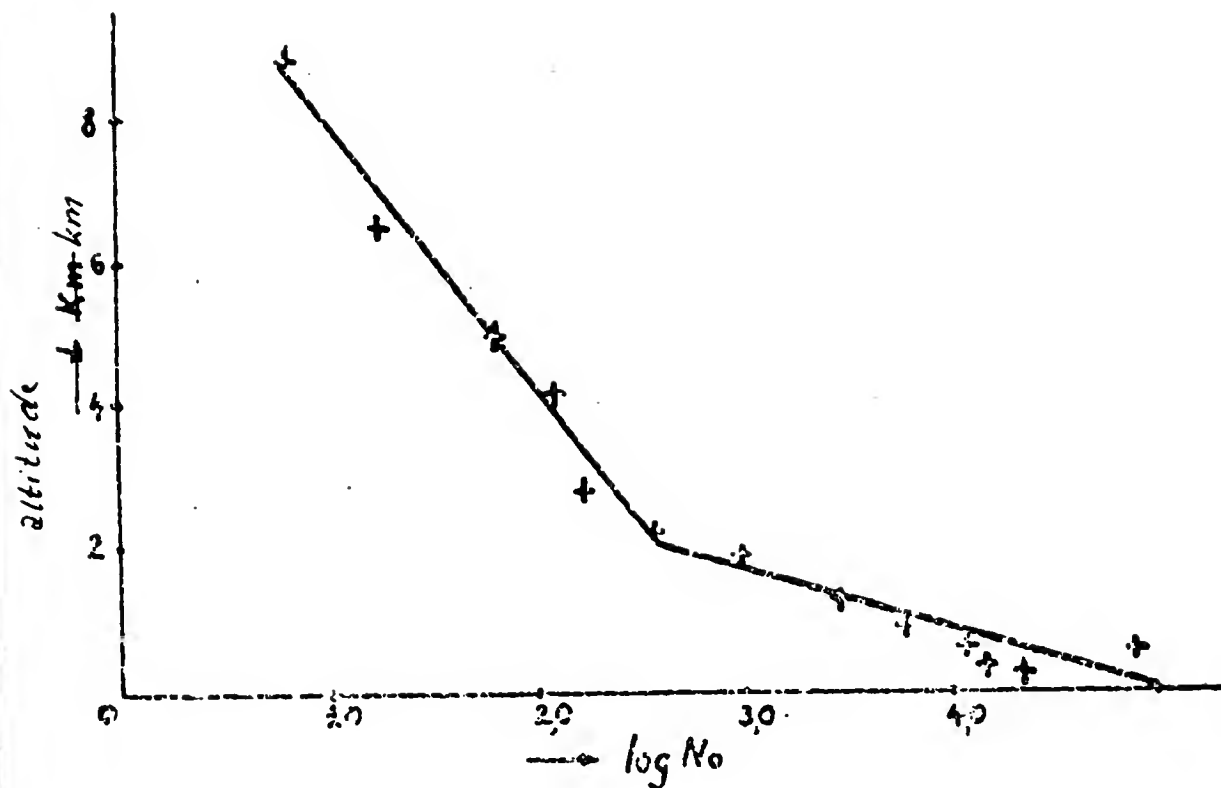
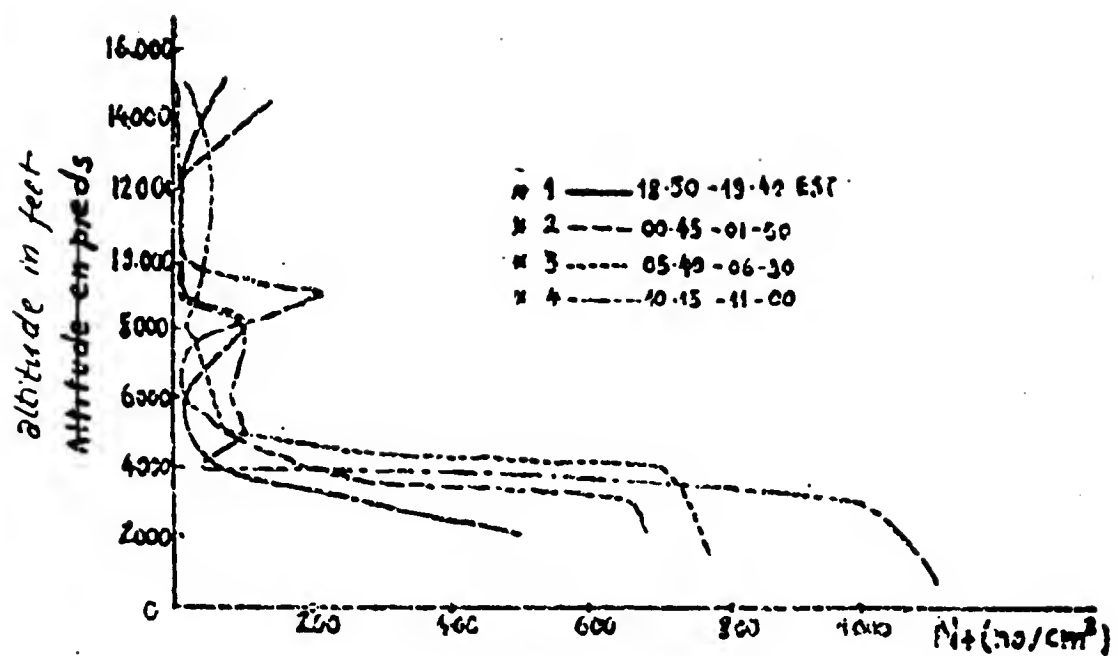


fig.3



~~21-22 Janvier 1954~~
21/22 January 1954

fig. 4

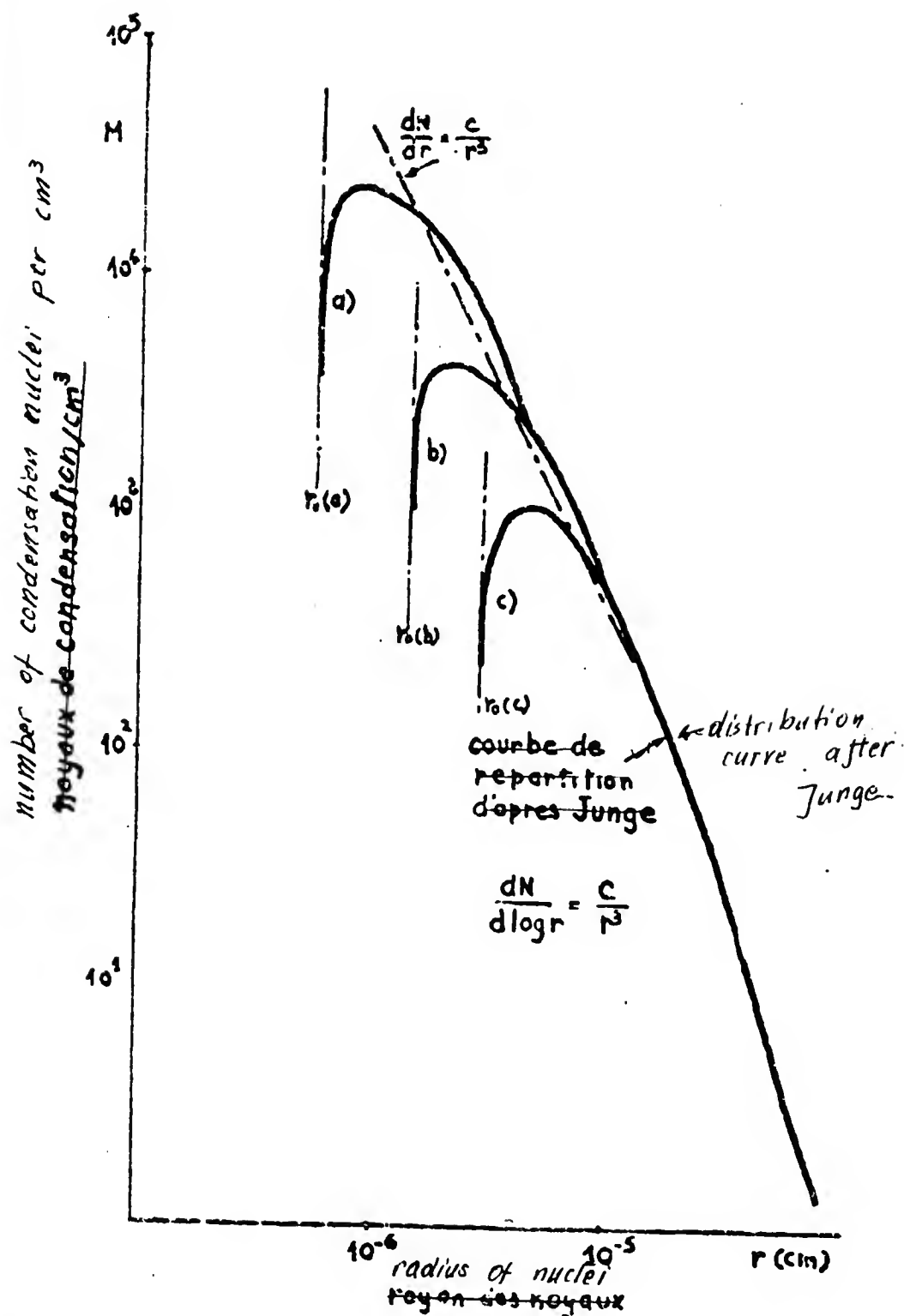


fig. 5

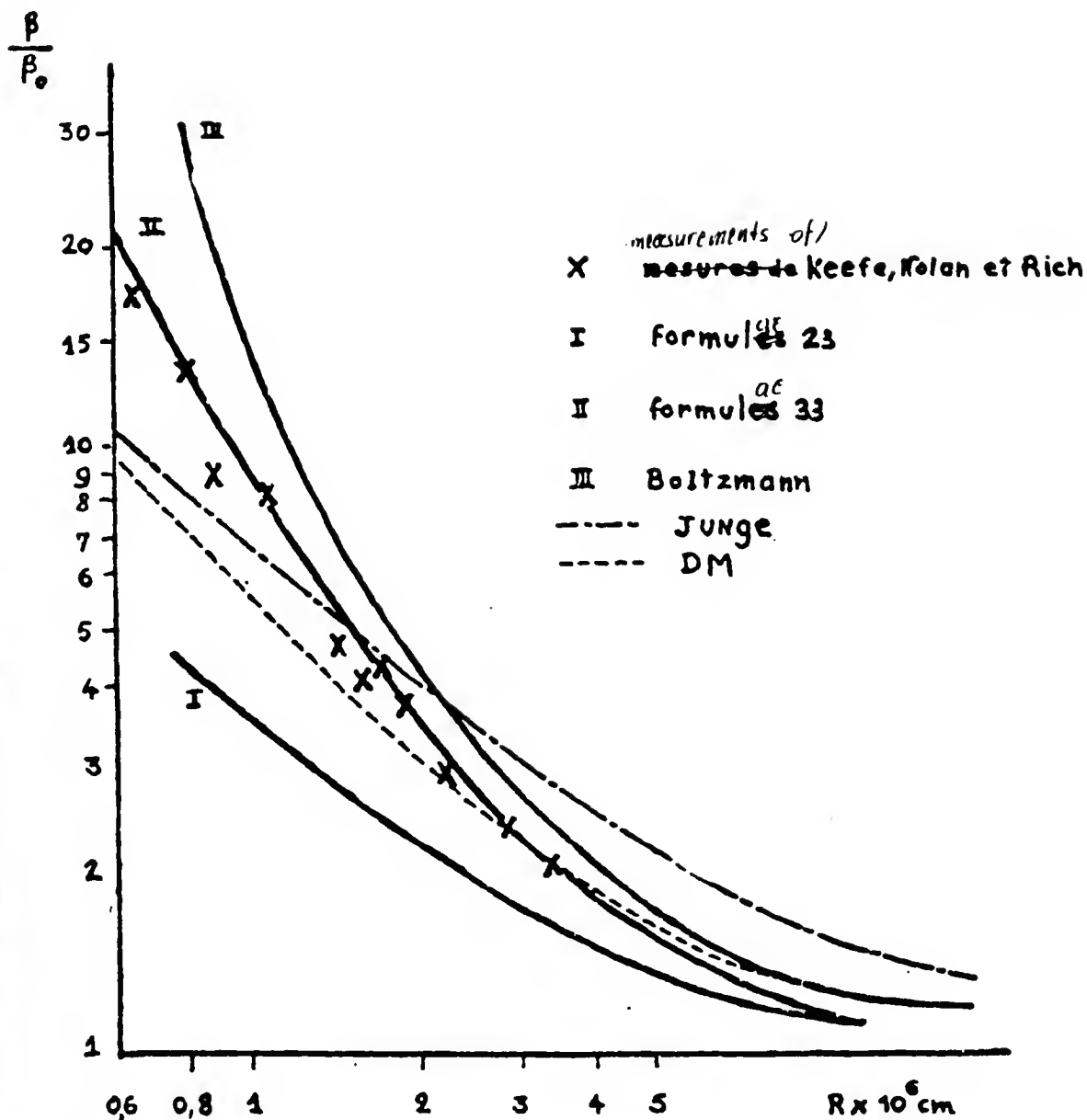


fig.6

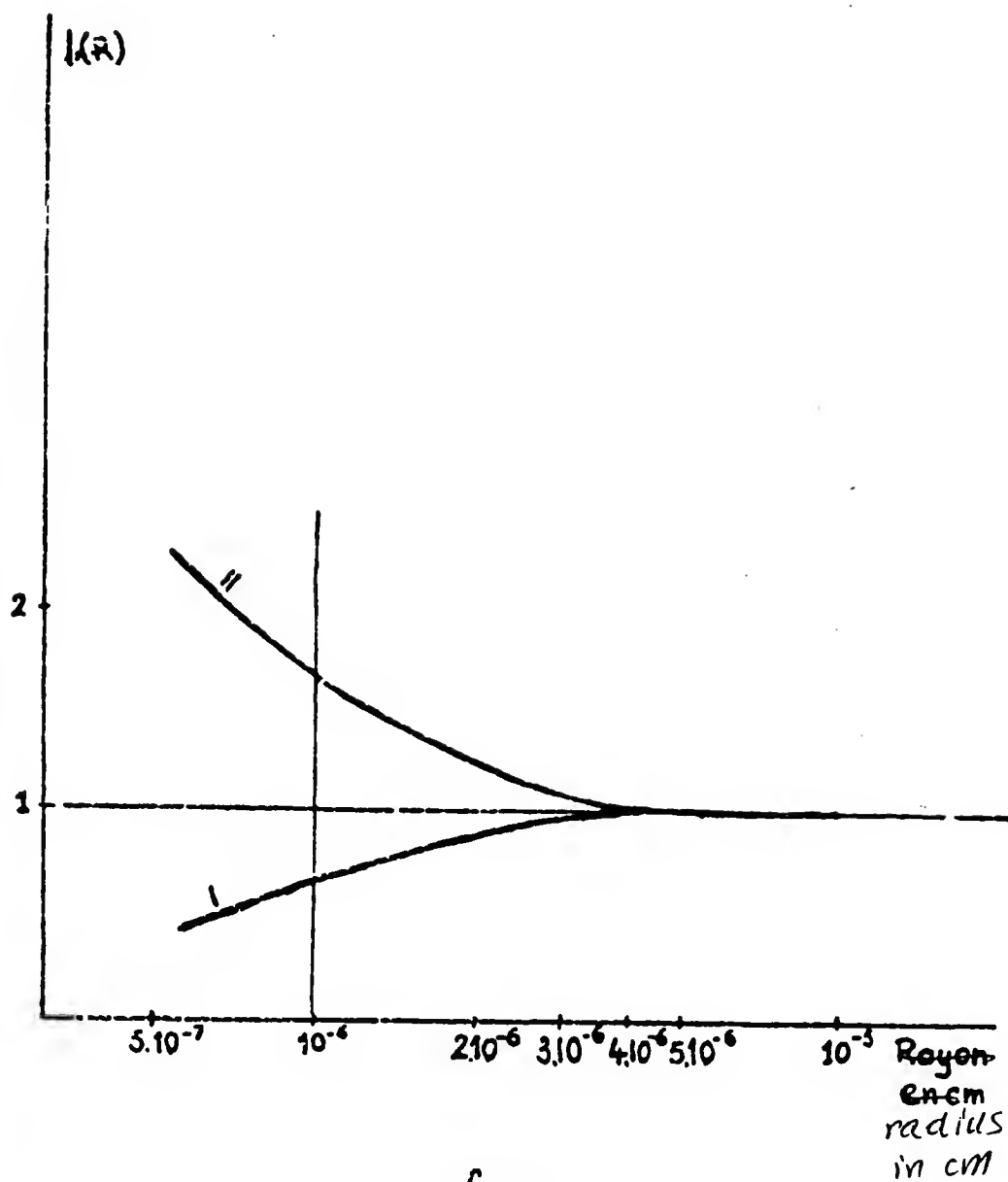


fig. 7

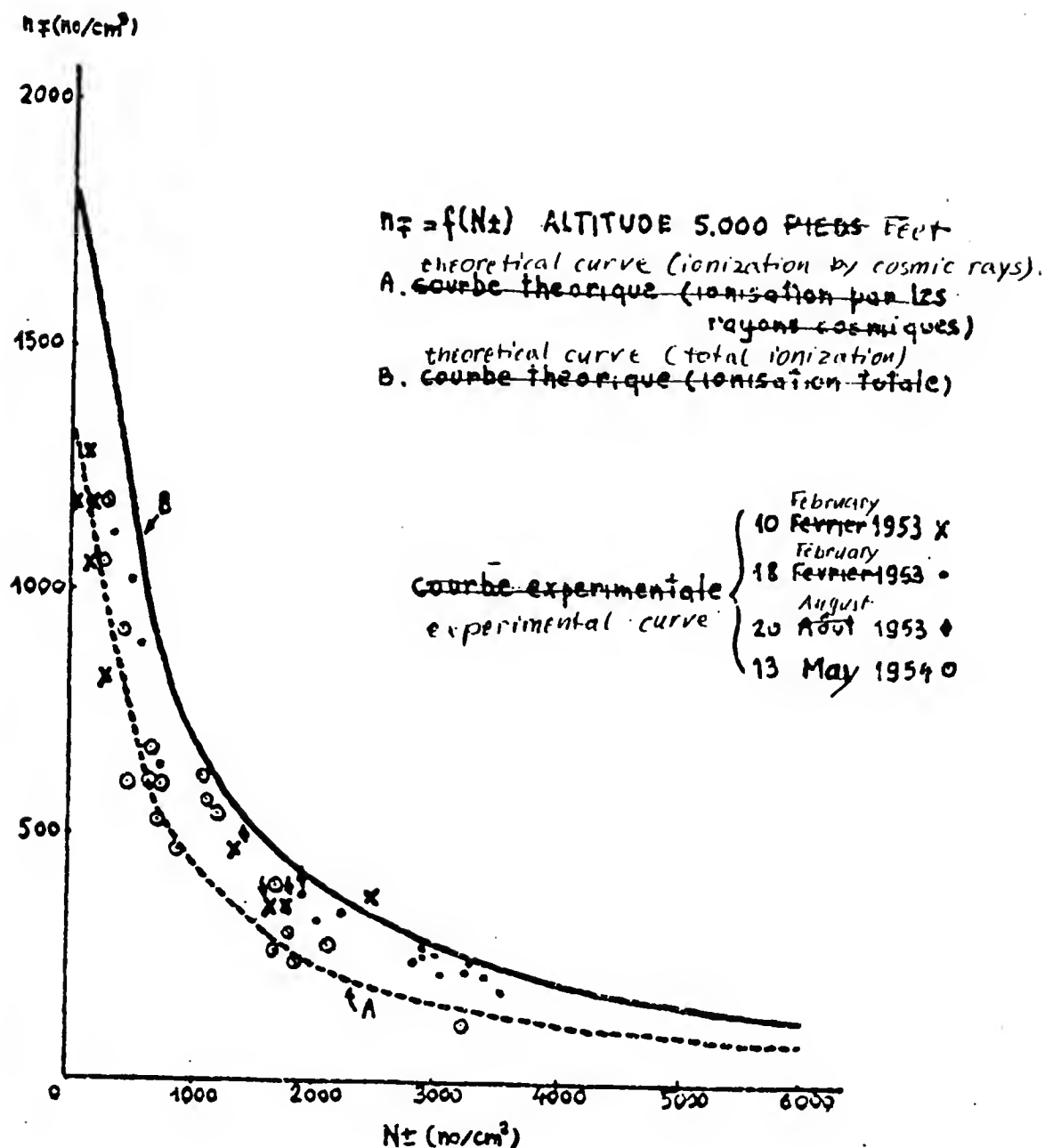


fig. 8

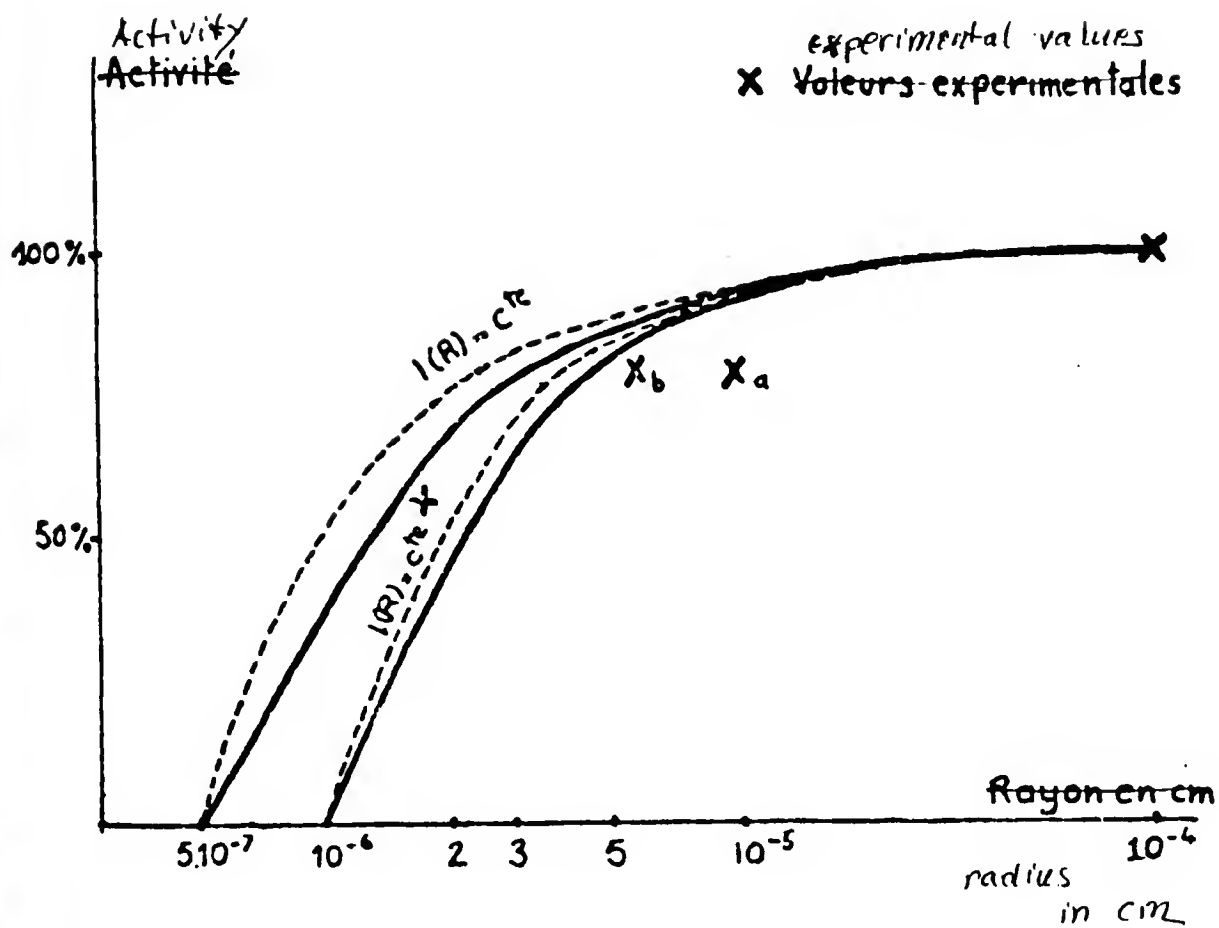


fig.9

SESSION 3.1

Generation of Electric Charges Outside Thunderclouds

by

J. Alan Chalmers, M.A., Ph.D., F.Inst.P.,

Reader in Physics,

Durham College in the University of Durham, England.

1. Introduction

It can scarcely be denied that the most important processes of electrification in the lower atmosphere are those within thunderclouds, but nevertheless there are many other electrical processes at work in various regions of the atmosphere that ~~are~~ have been discovered and that will have small or large effects on the electrical state of the atmosphere.

It is hoped that, at the risk of becoming a mere catalogue, something can be said about most of these processes, though naturally there will be more that can be discussed about some than about others.

As in the thunderstorm, it is possible to distinguish between two stages in the generation of charge, first the actual separation of the two charges of opposite sign from previously neutral matter and, second, the segregation of these two charges in such a way that they reach different places. In some of the processes discussed, the separation is that which produces the natural conductivity of the atmosphere, namely the ionization of the atmosphere by cosmic rays and by radioactivity. And in some processes the segregation is by the ordinary process of electric conduction in the electric field that is present, moving charges of opposite sign in opposite directions.

2. Point Discharge

Point discharge can be considered as a generator of charge, since the breakdown separates charges from neutral matter and the electric field segregates them.

When an earth-connected point exists above the surface of the earth, the lines of electric force in the atmosphere concentrate on the point and the local field strength is ^{at} greater than that of the earth's surface. In the simple case of an isolated point, this local field strength would depend on the potential difference between the point and its surroundings, i.e. the free atmosphere

2.

at the same level, and so on the height of the point and the potential gradient in the atmosphere; for a point which is one of a number at comparable heights, the other points modify this simple approach.

When the potential gradient in the atmosphere reaches a certain value, the field strength near the point becomes sufficiently large for local breakdown, involving ionization by collision, to occur, and, as the potential gradient increases, breakdown can occur over wider volumes and for more points. The local breakdown near points has been studied under laboratory conditions as "corona discharge", but the details need not concern us here.

The result of the local breakdown is to produce ions of both signs; those of the same sign as the potential gradient move quickly into the point and form a current to earth, while those of the opposite sign remain in the atmosphere and form a space charge, ultimately moving upwards to the cloud which is the origin of the potential gradient. The presence of the space charge near the point diminishes the actual field strength at the point, and under suitable circumstances the discharge may occur in pulses; averaging effects over periods of time long compared with the pulses, it is easy to see that, in steady conditions, there will be an adjustment to give a steady current and space charge, the local conditions near the point providing just sufficient current for the purpose; it is then unnecessary to discuss details of the actual processes at work near the point, just as, in an analogous case of the Langmuir-Child law for thermionic emission, the details of the emission process need not be discussed.

With a particular point and one value of the potential gradient, it follows that the current would be altered only if the space charge is altered, and this is achieved only by wind removing it from the neighbourhood of the point. An approximate theoretical calculation of the current in its dependence on potential gradient and wind speed for an isolated point has recently been made (Chalmers, 1962) and work is progressing on an attempt to carry out a more accurate computation with a computer. The theoretical problem of a point which is not isolated, but one of a number similarly or differently situated remains to be tackled.

On the experimental side, the earlier measurements of the relation between point-discharge current and potential gradient did not recognize

3.

the part played by wind, but the more recent work has shown that this must be included and the results are in fair agreement with the approximate theoretical calculations.

The work so far discussed has been carried out by simply erecting a metal point in the atmosphere and connecting it to earth through a measuring instrument; this, therefore, does not give a great deal of information about the effect of natural point discharge, which must take place largely through trees. The problem therefore arises as to how closely a metal point and a tree correspond in regard to point-discharge currents.

Schönland (1938) cut down a bush, typical of the neighbourhood, mounted it on insulators and measured the current through it; while this was an approach to natural conditions, it did not reproduce the conditions of a living tree. More recently, Masud and Chalmers (1960) attempted to measure the current through a tree, not directly but by measuring the effect of the space charge on the potential gradient downwind; the results suggested that a tree in leaf gives less current than a point at the same height. Milner and Chalmers (1961) inserted electrodes into a tree, so as to short-circuit the current down the tree through a galvanometer and found smaller currents than for a point. Quite recently, with the same apparatus, Chalmers (1963) found that, at the time of a close lightning flash, the tree and a neighbouring metal point gave appreciably different currents, showing that the tree does not behave like a simple conductor. It would be very desirable if such measurements could be attempted in the parts of the world where thunderstorms are frequent.

The question of the effect of the presence or absence of neighbouring points on the current through one particular point is another which requires further investigation. Chiplunker (1940) and Chalmers and Mopleson (1955), using natural point discharge, found that the total current through a number of points close together was less than if they were replaced by a single point, but Bellin (1948), in a laboratory experiment, found that each point of a group gave the same current whether the others were present or not.

4.

3. Non-Stormy Rain and Snow Clouds

Although the electrical effects in non-stormy clouds are less than those of thunderclouds, they are still appreciable, and some processes of charge separation must be present.

One of the important problems in this field is the discussion as to whether the charge-separation processes in non-stormy clouds are the same as in thunderclouds or not. If they are the same processes, then the problem is why the magnitude of the charge separation is so different; what are the conditions in the thundercloud that make the processes so much more efficient there than in the non-stormy cloud? It should perhaps be pointed out that the difference is much greater than the mere difference in intensity of precipitation. If, on the other hand, charge separation in the non-stormy cloud takes place by totally different processes, then these processes must be such that they are not much magnified by the change from non-stormy to stormy conditions, and, further, the processes in the thundercloud must be such that they cannot operate significantly in the non-stormy cloud. These considerations are a strong justification for increased study of nonstormy cloud electrification, particularly when it is realized that such clouds are much more frequent in many parts of the world than thunderclouds and conditions are much steadier and more amenable to measurement.

In this connection, an important principle has been used, namely that of the quasi-steady state, so that one can assume that the total vertical electric current is the same at all levels. This assumes that there is no differential horizontal electric current at any level, and it might be profitable to consider this question in more detail, particularly in the case of warm-front clouds where the movement of the air is much more horizontal than vertical.

An important result in the measurements of the effects of non-stormy clouds is the difference of both potential gradients and precipitation currents between rain and snow. Unless there are effects at the earth's surface, or near to it, this seems to indicate that there must be electrical effects in the process of melting, since most of the precipitation concerned has started as ice particles and, if finally falling as rain, has melted later. The simple discussion of the quasi-steady state lends to the conclusion that the potential gradient above a cloud would alter in sign when the precipitation

5. changes from rain to snow or vice versa; it would be most desirable if this conclusion could be confirmed or refuted by actual observations above the clouds.

4. Non-Raining Clouds

The charges in warm clouds which are not precipitating have been measured by a number of workers and, although there is some disagreement, the general results appear to be that the larger droplets more often carry positive charges and the smaller negative, the actual charges being only a few electronic units.

Some laboratory experiments by Barklie, Whitlock and Habertfield (1958) have shown that these charges are directly related to the presence of ions and this is in accord with theoretical work by Gunn (1955).

Though these effects provide the only separation of charge in clouds of this type, it seems unlikely that similar processes could be appreciable, compared with others, in clouds which give precipitation.

Another effect in non-raining clouds is that which is termed the "traffic-jam effect". Since the conductivity within a cloud is less than that outside, in order to maintain continuity of current across a cloud boundary, there must be a greater potential gradient within the cloud than outside, and this, in turn, means a region of space charge at the boundary.

5. Precipitation

Precipitation, as it reaches the ground, is usually charged; if the charge it carries is that which it has received in the cloud, then this is not to be considered separately from the problems of charge generation within the cloud; but if the charge on the precipitation has been altered as it falls, then the processes by which this occurs must be considered as separate. If precipitation is an important factor in charge generation in thunder clouds, then there must be a large change of charge during fall, since it is certain that the precipitation current reaching the ground is much smaller than it would be in the charge-generating region of the cloud.

When precipitation leaves the cloud, the only ways by which it would seem possible that it could acquire charge would be 1) melting 2) capture of ions and 3) shattering.

6.

The fact that the charges and the potential gradients during snowfall differ from those during rainfall (see, for example, Chalmers 1956), show that it is likely that something occurs during melting and it is very desirable that more should be found out about this, both by observations during precipitation and, if possible, by laboratory measurements.

The "inverse-relation" between precipitation current and point-discharge current (Simpson 1949) can be explained if the precipitation acquires charge from the point-discharge ion and a more detailed consideration of this (Chalmers 1951) has shown fairly satisfactory results. For the correlation of rain current with potential gradient when there is no point discharge, the matter does not appear so simple and further work is required. At the time this is being written, work is in progress on the measurement of rain current simultaneously at the top and foot of a 60-foot tower; results and conclusions may be available by the time of the Conference.

Kelvin (1860) and Chauveau (1900) have found a change of sign of the potential gradient at the top and foot of a tower on certain occasions during rain, and this requires a negative space charge in the air below the top of the tower; measurements of charges due to splashing cannot entirely explain these results and it might be that shattering of rain drops occurs in this region.

6. The Electrode Effect

It is perhaps questionable whether the electrode effect should be included as a charge-generating process, since the actual charges concerned are only the ions produced by cosmic rays and radioactivity. But recent work has suggested that the electrode effect, and the convection of the charges separated by it, are of appreciable importance in the atmosphere.

The electrode effect comprises a space charge near an electrode, in the case of the atmosphere the earth's surface, and arises because there can normally be no ions leaving the electrode, so that the conductivity at the surface of the electrode is due to ions of one sign only. In normal fine-weather conditions, the electrode effect would give a positive space charge near the earth's surface; this is, in fact, found only in special conditions, e.g. over the Greenland ice-cap (Ruhnke, 1962) or over water (Mühlstein, 1961); in other cases it is reduced or absent because of higher ionization close to the earth.

7.

7. Other Natural Sources of Charge

There are several other natural phenomena which give rise to charges in the atmosphere.

In blizzards, there are charges generated by, presumably, the impact of snow particles on one another and on the snow on the ground (Simpson 1919) and the same occurs in drifting snow. Obstacles such as wires become charged in a blizzard (Barre, 1953).

Dust-storms give rise to quite large electric potential gradients, sometimes even giving lightning (Hodge, 1914), and volcanoes also give considerable effects to be ascribed to frictional effects of the ash (Hatekmyama and Uchikawa, 1951).

It has long been known that positive charge is generated by the splashing of water, e.g. at waterfalls (Lenard, 1892); Mühleisen (1958) has found charge separation with change of humidity; there is evidence (Mühleisen 1959) for positive charges originating at the sea-shore in the breaking of the waves. Blanchard (1961) has found that positively charged particles move upwards from the sea surface, produced by the breaking of air bubbles in the sea.

It is probable that only the last two of these are likely to be of appreciable importance in the whole balance of charges in the atmosphere, but there is scope for more investigations of all these phenomena.

8. Artificial Sources of Charge

Mühleisen (1955) has investigated in detail the generation of charge by burning and other industrial processes and has found that different processes produce different signs of charge; the amounts of charge taken into the atmosphere may be quite appreciable. An earlier example of the same was the positive charge arising from locomotives (Kelvin, 1860).

Chalmers, (1952) found that negative charges can be liberated into the atmosphere from high-tension cables in conditions of high humidity when the insulation partially breaks down; sufficient charge is liberated to produce negative potential gradients several km. downwind.

8.

Another example of an artificial source of charge is the observation of Moore, Vonnegut, Semonin, Bullock and Bradley (1962) who found positive space charge downwind of a television tower in fine weather; this they explained as due to the removal by wind of a space charge formed at the top of the tower by the electrode effect.

Deliberate attempts to produce space charges in the atmosphere by electric discharge have been made by Vonnegut and Moore (1958), Vonnegut, Maynard, Sykes, and Moore (1961) and Vonnegut, Moore, Stout, Staggs, Bullock and Bradley (1962).

References

- Barklie, R.H.D., Whitlock, W. and Huberfeld, G. 1958, "Observations on the reactions between small ions and (a) cloud droplets, (b) Aitken nuclei", in "Recent Advances in Atmospheric Electricity - Proceedings of the 2nd Wentworth Conference, May 1958" (ed. L.G. Smith, New York: Pergamon Press).
- Barre, M. 1953, "Propriétés électriques du blizzard" Ann. Géophys. 2, pp 164-183.
- Belin, R.E. 1948, "A radio-sonde method for atmospheric potential gradient measurements", Proc. Phys. Soc. Lond. 60, pp 381-387.
- Blanchard, D.C. 1961, "The electrification of the atmosphere by particles from bubbles in the sea", Unpublished paper from Woods Hole Oceanographic Institution (reference 61-9).
- Chalmers, J.A., 1951, "The origin of the electric charge on rain", Quart. J.R. Met. Soc. 77, pp 249-259.
- Chalmers, J.A., 1952, "Negative electric fields in mist and fog", J. Atmosph. Terr. Phys. 2, pp 155-159.
- Chalmers, J.A., 1956, "The vertical electric current during continuous rain and snow", J. Atmosph. Terr. Phys. 2, pp 311-321.
- Chalmers, J.A., 1963, "Point-discharge currents through a living tree during a thunderstorm", J. Atmosph. Terr. Phys.
- Chalmers, J.A. and Mapleson, W.W. 1955, "Point discharge currents from a captive balloon", J. Atmosph. Terr. Phys. 6, pp 149-159.
- Chauveau, B. 1900, "Études de la variation de l'électricité atmosphérique", Annales de BCM 2, p.1.

9.

- Chiplonkar, M.W., 1940, "Measurement of point discharge current during disturbed weather at Colaba", Proc. Indian Acad. Sci. A 12, p.50.
- Gunn, R., 1955, "The statistical electrification of aerosols by ionic diffusion", J. Coll. Sci. 10, pp 107 - 119.
- Hatekayama, H. and Uchikawa, K. 1951, "On the disturbance of the atmospheric potential gradient caused by the eruption smoke of the volcano Aso", Gen. Ass. Int. Un. Geod. (Brussels), Ass. Terr. Magn. Elect.
- Kelvin, Lord, 1860, "Atmospheric Electricity", Royal Institution Lecture; reprinted in "Papers on Electricity and Magnetism" (London : Macmillan & Co.) pp. 208-226.
- Lenard, P. 1892, "Über der Elektrizität der Wassertropfen", Ann. Phys. Lpz., 46, pp. 584-636.
- Maud, J.E. and Chalmers, J.A. 1960, "Point discharge from natural and artificial points", Quart. J. R. Met. Soc. 86, pp. 85-90.
- Milner, J.W. and Chalmers, J.A. 1961, "Point discharge from natural and artificial points (Pt II)", Quart. J. R. Met. Soc. 87, pp. 592-596.
- Moore, C.B., Vonnegut, R., Semonin, R.G., Bullock, J.W. and Bradley, W., 1960, "Fair-weather atmospheric electric potential gradient and space charge over Central Illinois, Summer 1960", J. Geophys. Res. 67, pp. 1061-1071.
- Mühleisen, R. 1953, "Die luftelektrischen Elemente in Grossstadtbereich", Z. Geophys. 29, pp. 142-160.
- Mühleisen, R., 1958, "Elektrische Ladungen auf Kondensationskernen bei der Wasseraufnahme und - abgabe", Naturwissenschaften 45, pp 1-2.
- Mühleisen, R. 1959, "Die luftelektrischen Verhältnisse im Küstenaerosol, I", Arch. Met. Wien A 11, pp. 95-108.
- Mühleisen, R. 1961, "Electrode effect measurements above the sea", J. Atmosph. Terr. Phys. 23, pp 79-81.
- Rudge, W.A.D.; 1913, "On the electrification associated with dust clouds," Phil. Mag. 25, pp 481-494.
- Ruhnke, L.H., 1962, "Electrical conductivity of air on the Greenland ice-cap", J. Geophys. Res. 67, pp 2767-2772.
- Schonland, B.F.J. 1928, "The interchange of electricity between thunderclouds and the earth", Proc. Roy. Soc. A. 118, pp 252-262.

10.

- Simpson, G.C. 1919, "British Antarctic Expedition 1910-13 Meteorology", (Calcutta), 1, pp 302-312.
- Simpson, G.C., 1949, "Atmospheric electricity during disturbed weather", Geophys. Mem., Lond. 84, pp 1-51.
- Vonnegut, B., Maynard, K., Sykes, W.G. and Moore, C.B., 1961, "Technique for introducing low density space charge into the atmosphere", J. Geophys. Res. 66, pp 823-830.
- Vonnegut, B. and Moore, C.B., 1958, "Preliminary attempts to influence convective electrification in cumulus clouds by the introduction of space charge into the lower atmosphere" in "Recent Advances in Atmospheric Electricity - Proceedings of the 2nd Wentworth Conference, May 1958" (ed. L.G. Smith, New York: Pergamon Press) pp. 317 - 331.
- Vonnegut, B, Moore, C.B., Stout, G.E., Staggs, D.W., Bullock, J.W. and Bradley, W.E., 1962, "Artificial modification of atmospheric space charge", J. Geophys. Res. 67, pp 1073-1083.

CHARGE GENERATION IN THUNDERSTORMS

By B.J. Mason

(Imperial College, London)

Introduction

It is proposed that the principal mechanism of thunderstorm electrification involves the accretion, freezing and splintering of supercooled droplets on pellets of soft hail. Gravitational separation of the small positively-charged ice splinters and the much heavier negatively-charged hail pellets then produces an electric field of the observed polarity.

Evidence in support of this theory comes from: (i), observation of the disposition of electric charges and fields in thunderclouds; (ii), observed correlations between the appearance of soft hail and strong electric fields; (iii), laboratory observations that rising elements acquire a negative charge as positively-charged splinters are ejected from freezing drops; (iv), the discovery that this separation of charge arises from a basic property of ice, viz a protonic thermo-electric effect which has been investigated experimentally and theoretically in some detail; (v), application of the laboratory results on the rate of charging of artificial hail pellets to a model thunderstorm which reveals that the proposed mechanism is capable of producing and separating charge at the rate required by observations on lightning flashes while other mechanisms appear to work much too slowly. These arguments will now be presented in more detail, but first it seems worthwhile to list the more important and relatively undisputed features of the thunderstorm with which any satisfactory theory of electrification must be consistent.

2. Requirements of a satisfactory theory of thunderstorm electrification

The theory must explain quantitatively how electric charge is generated and separated in a thundercloud at a rate equivalent to that at which it is dissipated in lightning flashes. It must account for

-2-

the observed polarity of the thunderstorm and be consistent with what is known about the electrical and dynamical structure of the storm, the nature of the electrical field changes accompanying lightning, the size and duration of the storm, and the nature, scale and intensity of the precipitation processes which are generally considered to be closely correlated with the electrical activity. More specifically, the theory must be consistent with the following facts:

- (i) The average duration of precipitation and lightning from a typical single thunderstorm cell is about 30 min.
- (ii) The average electric moment destroyed in a lightning flash is about 100 C.km, the corresponding charge being 20-30 C. A typical cell produces flashes at intervals of about 20 sec so the average lightning current is about 1 amp.
- (iii) The magnitude of the charge which is being separated immediately after a flash, by virtue of the falling speed of the precipitation elements, is of order 1,000C.
- (iv) In a typical cell this charge is generated and separated in a volume bounded by the 0 and -40°C levels and having a typical radius of 2 km and therefore a volume of about 50 km^3 .
- (v) The negative charge is centred near the -5°C level, while the main positive charge is situated some kilometres higher up; a subsidiary positive charge often exists near cloud base where the temperature is usually a little warmer than 0°C .
- (vi) Sufficient charge must be generated and separated to supply the first lightning flash within 10-20 min. of the first appearance of precipitation particles large enough to produce a radar echo.

In round figures, the requirement is to generate about 1000 C of charge in a volume of about 50 km^3 in a period of about 20 min. i.e. at an average rate of $1 \text{ C/km}^3/\text{min}$.

3. Observational evidence for an ice mechanism

- (i) Lightning is usually accompanied by heavy precipitation although,

-3-

in warm, dry climates, this may not reach the ground. Most theories on the origin of the electric charge have assumed that the precipitation plays an important role, and as the main charge centres appear at levels in the cloud where the temperature is below 0°C , it is natural to associate that generation with the presence of supercooled water and/or the ice phase.

(ii) Kuettnner (1950), from observations made inside thunderclouds capping the Zugspitze in Germany, reported that solid precipitation elements were predominant in the greater part of the thundercloud and were present on 93% of the occasions. Snow pellets and pellets of soft hail were the most frequent form of hydrometeor being present on 75% of occasions but large hail was relatively rare.

(iii) Fitzgerald and Byers (1962), using aircraft fitted with electric-field meters, have reported that the actively building regions of thunderstorms are regions of excess negative charge. The strongest fields, of up to 2300 V/cm, were associated with regions of heavy precipitation. In particular, a large hail shaft produced a strong, smoothly increasing field indicating a negative charge on the hail.

(iv) Malan and Schonland (1951, a, b) find that, in South African storms, the negative charge is often distributed in a nearly vertical column which may extend up to but not beyond the -40°C level. This is consistent with the charge being generated by growing hail pellets because supercooled droplets exist at temperatures down to, but not below -40°C .

4. The charging of rime deposits

In recent years, several workers have reported that when supercooled water droplets impinge and freeze on an ice surface, the resulting layer of rime acquires a substantial charge. The experimental results, which have been reviewed by Mason (1957), may be summarized as follows.

Findeisen (1940, 1943) formed a rimed layer by spraying water droplets on to a cold metal surface and found that it acquired a

-4-

positive charge. The charging ceased if the surface became smooth and glassy, as was the case if the drops froze slowly, or if it became wet. Rather stronger charging was obtained with a natural supercooled cloud than with an artificial spray, the difference being ascribed to more rapid freezing of the smaller cloud droplets. The rate of charging in the cloud was $3 \times 10^{-13} \text{ C cm}^{-2} \text{ s}^{-1}$.

In a later investigation, Kramer (1948) found the rime deposit acquired a negative charge which increased in proportion to the impact velocity of the droplets. With a velocity of 0.5 m s^{-1} the charging rate was $2 \times 10^{-14} \text{ C cm}^{-2} \text{ s}^{-1}$ and, for a velocity of 5 m s^{-1} , ten times larger.

Lueder (1951 a,b) made experiments in natural supercooled clouds on a mountain top in order that the contaminants in the water should be those occurring in nature. He states that the growing rime deposit acquired a negative charge, an equal positive charge being communicated to the air, probably on the parts of the drops which were flung off without freezing. Unfortunately, it is difficult to interpret his experiments and to deduce the actual rate of charging.

Meinhold (1951) measured the electric field strength at the surface of the fuselage of an aircraft flying at 80 m s^{-1} through a supercooled cumulus congestus cloud. The deposition of rime was accompanied by a rapid rise in the field strength in a sense which indicated that the aircraft was acquiring a negative charge, and the rate of charging was calculated to be $5 \times 10^{-12} \text{ C cm}^{-2} \text{ s}^{-1}$.

The charging of a rime deposit on a cold metal surface was also studied by Weickmann & aufm Kampe (1950). Water droplets in the diameter range 5 to 100μ were sprayed at velocities varying from 5 to 15 m s^{-1} on to a metal rod of 5 mm diameter in a cold room kept at either -5 or -12°C ; they were therefore slightly supercooled on reaching the rod. The rate of charging, which was not sensitive to the presence of dissolved salts, increased with increasing velocity of the air stream, and for a velocity of 15 m s^{-1} , attained a value of

-5-

$5 \times 10^{-12} \text{ C cm}^{-2} \text{ s}^{-1}$. When water at temperatures slightly above 0°C was sprayed on to the rod it acquired a slight positive charge. Later the authors indicated that the results of these experiments may have been seriously affected by electrification associated with the production of the spray.

The balance of the evidence from all these experiments points to the acquisition of a negative charge by a growing layer of rime, Findeisen's result being an outstanding contradiction. In light of the recent experiments of Latham and Mason (1961), described below, it now appears that some of the differences between the results of different workers may be ascribed to the use of differing drop sizes, temperatures, and impact velocities, while spurious effects may arise from initial charging of the spray droplets and electrification produced by the splashing of droplets on the ice surface.

5. The splintering and electrification of freezing water drops.

Some evidence for the production of charged splinters by a growing rime deposit was obtained by Kramer (1948), and their production during the freezing of individual water drops was investigated in detail by Mason and Maybank (1960).

Nucleation of a water drop, at temperature $-T^\circ\text{C}$, is followed by rapid solidification of a fraction $T/80$ of its mass in the form of an ice shell. Subsequent freezing of the liquid interior now proceeds at a rate determined by the dissipation of the latent heat to the surroundings. The expansion which accompanies this freezing sets up stresses in the ice shell which may disintegrate to produce a number of ice splinters. Mason and Maybank found that, for drops suspended in still air, the number of splinters produced was almost independent of the drop diameter in the range 0.1 to 2 mm but that for drops of diameter $< 60\mu$, splinter production was much reduced. They also measured the charges on the residues of fragmenting drops. If only a minor fraction of the drop was blown off the residue was invariably negatively charged. Typically, a drop of 1 mm diameter

-6-

freezing at -5°C produced about 20 splinters and acquired a negative charge of about 10^{-4} e.s.u.; a similar drop freezing at -15°C produced about 5 splinters and acquired a charge of about 3×10^{-5} e.s.u. The average positive charge per splinter was therefore 5×10^{-6} e.s.u. These experiments suggested an explanation for the electrification of growing rime deposits and that a similar mechanism operating during the growth of hail pellets might be an important factor in the electrification and ice-crystal economy of clouds.

6. Charging associated with the growth of soft hail pellets.

Latham and Mason (1961) measured the electrification of artificial pellets of soft hail as they grew by the accretion of supercooled water droplets, and determined how this varied with the temperature, size and impact velocity of the drops.

The experiments were conducted in a cold room, at air temperatures ranging from 0°C to -17°C , with the apparatus shown in Fig. 1.

The hailstone, simulated by a 5 mm diameter, electrically insulated, copper sphere coated with a $\frac{1}{2}$ mm layer of ice, was suspended in the centre of an earthed vertical brass tube through which the air stream carrying the droplets could be drawn at velocities ranging from 0 to 30 m s^{-1} . Water drops of uniform diameter in the range 20 to 90μ produced by the spinning-top apparatus of Walton & Frawett (1949), or rather larger drops produced by an atomizer, were allowed to fall several feet in the cold room where they became supercooled to very near the air temperature before reaching the hailstone target. For a given droplet size and air-stream velocity, the flux of droplets hitting the target was determined by allowing them to strike, for a given time, a Formvar-coated glass sphere of the same dimensions, and counting the droplet impressions under the microscope. The impaction and freezing of the droplets was accompanied by the ejection of ice particles from the target surface; their number and sizes were determined by inserting Formvar-coated slides just beneath the hailstone

-7-

and later examining the plastic replicas of the crystals.

The electric charge accumulating on the hail pellet during the freezing of droplets on its surface was measured by a Vibron vibrating-reed electrometer of resistance $10^{12} \Omega$ and time constant 200 s. The minimum detectable charge was about 5×10^{-4} e.s.u.

The surface temperature of the target, measured by a thermocouple, was higher than that of the surrounding air because of the latent heat released by the freezing drops and could be raised artificially by irradiating the surface with the beam of a 50 W tungsten lamp.

The experimental operations, which could be performed from outside the cold room, consisted of setting the cold room (air) temperature, the air-stream velocity and the drop size and reading the electrometer after the target had been exposed to the droplets for a known time, usually 10 s. Then the effect, on the rate of charging, of raising the surface temperature of the hailstone (this being previously calibrated in terms of the air speed and the current supplied to the lamp) was investigated. Meanwhile, slides for collecting the ice crystals shed by the target were inserted at regular intervals. The whole procedure was then repeated for a different set of conditions.

The freezing of droplets of distilled water on the surface of the hailstone caused it to become negatively charged and was accompanied by the ejection of small ice splinters. The manner in which the average charge and number of splinters produced per drop varied with the drop diameter, impact velocity and air temperature is shown in figures 2, 3 and 4.

In a typical experiment, with the air temperature at -15°C and the air stream moving at 10 m s^{-1} , 10^4 drops of diameter 80μ struck the hailstone within 10 s and produced a total charge of 4×10^{-2} e.s.u., i.e. an average charge of 4×10^{-6} e.s.u. per drop. On average, each droplet produced 12 ice splinters; their mean diameter on collection

-8-

was 20μ but they were probably smaller on ejection and had grown in the meantime.

Droplets of $d < 30\mu$ produced few splinters and little charging. Figure 2 shows that the production of both was enhanced as the droplet diameter was increased to about 50μ , remained fairly constant for diameters between 50 and 80μ , and fell again for still larger drops. These results are in fairly good agreement with those which Mason and Maybank (1960) obtained for individual droplets suspended on fibres except that they did not observe a reduction in splintering for large drops. This tendency, in the present experiments, may be explained by the fact that, in impinging at several metres per second, the larger drops shattered before freezing and that splashing communicated a positive charge to the ice target in the manner observed originally by Faraday and more recently by Gill & Alfrey (1952). Positive charging of the target at high impact velocities is shown in figure 3; this occurred although there was still a considerable production of splinters.

As shown in figure 4, the rates of charge and splinter production are almost independent of the air temperature in the range -6 to -17°C but both fall off rapidly at higher temperatures and, in our experiments, were no longer detectable at -2°C . The explanation is as follows. The impacting droplets can be frozen only at a rate determined by the rate of dissipation of their latent heat to the environment; at air temperatures close to 0°C the rate of freezing was slow and consequently the hailstone surface became wet and, as the replicas showed, considerable splashing occurred as the drops struck it.

A number of tests were carried out to make sure that charging of the hailstone was due entirely to the collision and freezing of the droplets. No detectable charging occurred when the air stream carried no droplets and when droplets, impacting at very low velocity, froze on the surface without producing splinters. The parallelism

-9-

between the curves of charge and splinter production in figures 2 to 4 is, perhaps, the strongest evidence for the one being a consequence of the other.

Irradiation of the hailstone by the lamp caused a reduction in the rate of charging. For example, with the air temperature at -12°C , raising the surface temperature of the hailstone by 2°C reduced the rate of charging by about 20%; when the surface was warmed by 5°C , the charge production was halved; but, in both cases, the rate of splinter production was not appreciably altered.

When the impinging water droplets were contaminated with sodium chloride in concentration corresponding to the average found in cloud water (3.6 mg/l.), the rate of charging was decreased by about 20%.

These experiments appear conclusive in showing that the negative charging of the hailstone is caused by the ejection of small splinters of ice during the freezing of droplets on its surface. The influence of droplet size and the presence of salt are in fair agreement with the observations of Mason and Maybank apart from the effects which were produced by splashing of large drops.

In a later paper, Latham and Mason (1962) reported that when the above experiments were repeated in the presence of an external electric field the charging rates of the hailstones were altered by only about 10 per cent by application of fields of $\sim 1000 \text{ V cm}^{-1}$. The inference is that the charging of hailstones will not be greatly accelerated by the cumulative build-up of polarizing fields in thunderstorms.

7. Application of laboratory results to computation of the production of charges and electric fields in a model thundercloud.

We consider a thunderstorm in which above a level Z_0 the updraught U contains an exponential size spectrum of hailstones such that the concentration of stones within the radius interval R to $R + dR$ is

$$N(R) dR = N_0 \exp(-\lambda R) dR, \quad (1)$$

where N_0 and λ are constants independent of position in the updraught.

-10-

Since splinters and charge are produced only by the freezing of droplets on the surfaces of hailstones which remain dry, we write the fractional volume $F_D(z)$ swept out per unit time by the dry hail at level z as

$$F_D(z) = \int_0^{R_c(z)} \pi R^2 V(R, z) N(R) dR, \quad (2)$$

where V is the hailstone fallspeed and $R_c(z)$ is the critical radius at which a hailstone becomes wet at level z . We now assume that this flux of dry hail encounters a concentration $n(z)$ of supercooled droplets of radii greater than 25μ ; smaller droplets produce few splinters and little charge. Since these droplets are continually being swept up by the entire spectrum of hailstones, their concentration will decrease with increasing height according to

$$n(z) = n_0 \exp\left(-\int_{z_0}^z \frac{F(z)}{U(z)} dz\right), \quad (3)$$

where n_0 is the concentration of drops at z_0 and $F(z)$ refers to the entire hail spectrum.

The total rate of charge production between levels z_0 and z owing to the impaction, freezing and splintering of large cloud droplets on dry hail is then given by

$$\frac{dQ}{dt} = A n_0 q_d \int_{z_0}^z F_D(z) \exp\left(-\int_{z_0}^z \frac{F(z)}{U(z)} dz\right) dz, \quad (4)$$

where A is the mean cross-sectional area of the updraught and q_d is the average charge produced by the freezing of a drop of $r > 25\mu$.

We have seen that a typical single-cell storm generates about 1000 coulombs of charge in about 20 min., i.e. at an average rate of about 1 amp. Putting $\frac{dQ}{dt} = 1 \text{ amp} = 3 \times 10^9 \text{ e.s.u.}$, $A = 9\pi \times 10^{10} \text{ cm}^2$ (a mean radius of 3 km for the cell), $q_d = 4 \times 10^{-6} \text{ e.s.u.}$ (Latham and Mason 1961), and values of F_D and F based on the observations of Atlas and Ludlam (1961) for a storm having an updraught increasing linearly with height according to $U(z) = 5(z-1) \text{ m sec}^{-1}$ with z measured in km and a liquid water content of 3 gm^{-3} , we find $n_0 = 5 \text{ cm}^{-3}$.

-11-

This does not seem an unreasonable value since droplets of $r > 25 \mu$ have been found in concentrations exceeding 1 cm^{-3} in rather small cumulus (Durbin 1956), while concentrations of 5 cm^{-3} in Cb have been observed by Weickmann and aufm Kampe (1953).

The corresponding concentration of splinters, assuming a freezing drop to produce on average, 10 splinters, is calculated to be about 1 cm^{-3} between the -20°C and -50°C levels (Browning and Mason, 1963). This, too, seems a reasonable figure.

The rate of building of the vertical electric field E by separation of the hail pellets and ice splinters is given by

$$\frac{d^2 E}{dt^2} + \beta \frac{dE}{dt} = -4\pi n q_a \sum \pi N(R) R^2 V(R) \quad (5)$$

$$= -3\pi (p/\rho_i) (\bar{V}/\bar{R}) \quad (5a)$$

where β represents the leakage of charge through point-discharge and conduction currents, p the precipitation intensity, ρ_i the average density of the ice particles, \bar{V} and \bar{R} are respectively weighted mean values for the fall speed and mean radius of the hailstones. For particles sizes ranging from $R = 0.1 \text{ mm}$ to 1.0 mm ,

$\bar{V}/\bar{R} = \text{const} = 8500$. If we assume that the precipitation intensity increases rather rapidly with time at first, and then levels off at a value p_m which is maintained for several minutes, we may write $p = p_m (1 - e^{-\alpha t})$ and Eq 5(a) becomes

$$\frac{d^2 E}{dt^2} + \beta \frac{dE}{dt} = \delta (1 - e^{-\alpha t}), \quad (5b)$$

where $\delta = -3\pi \times 8500 \times \left(\frac{n_a q_a}{\rho_i} \right) p_m$.

The solution of (6) with the conditions $E = 0$ and $dE/dt = 0$ when $t = 0$ is

$$E = \delta \left[\frac{t}{\beta} - \frac{\alpha + \beta}{\alpha \beta^2} + \frac{1}{(\beta - \alpha)} \left(\frac{e^{-\alpha t}}{\alpha} - \frac{e^{-\beta t}}{\beta} \right) \right]. \quad (6)$$

Taking $\beta = 2 \times 10^{-3} \text{ e.s.u.}$ and $p_m = 5 \text{ cm hr}^{-1}$, $\rho_i = 0.5 \text{ g cm}^{-3}$, $\frac{1}{\alpha} = 600 \text{ s}$, $n_a = 1 \text{ cm}^{-3}$ and $q_a = 4 \times 10^{-6} \text{ e.s.u.}$, Eq (6) predicts that the field will reach a value of 9400 V cm^{-1} within 10 min of the appearance of precipitation elements. But, before large-scale fields of this magnitude are reached, lightning discharges will almost

-12-

certainly occur and destroy the field. However, it appears that the accretion, freezing and splintering of supercooled droplets on hail pellets can readily account both for the production of charge in thunderstorms and for the generation of large-scale fields of several thousand volts per cm during periods of about 10 min.

If the field were destroyed by a lightning flash but the soft hail continued to fall at a steady rate β_m , the field would recover at a rate given by

$$\frac{d^2 E}{dt^2} + \beta \frac{dE}{dt} = \mathcal{J} \quad (7)$$

$$\text{or} \quad E = \mathcal{J} \left(\frac{t}{\beta} - \frac{1}{\beta^2} \right) + \frac{\mathcal{J}}{\beta^2} e^{-\beta t} \quad (8)$$

With β and \mathcal{J} taking the same values as above, the field would build up again to 4000 V cm^{-1} in 30 s, which is about the average interval between lightning flashes from a modest single-cell storm.

8. The basic mechanism of charge-separation during the freezing and splintering of droplets.

The fundamental problem is to explain how the electric charge can be separated during the bursting of a freezing drop and why the splinters are ejected with a positive charge leaving a negative charge on the hailstone. Mason and Latham (1961) have proposed that this is a manifestation of a protonic thermo-electric effect in ice by which the hydrogen and hydroxyl ions formed by the dissociation of a small fraction of the ice molecules become separated under the influence of a temperature gradient.

The process depends essentially on two facts. One is that the concentrations of positive and negative ions increase quite rapidly with increasing temperature; the other, that the hydrogen ion (proton) diffuses much more rapidly through the ice crystal than does the hydroxyl ion (Eigen and de Maeyer, 1958). Thus, if we imagine a steady temperature difference maintained across a piece of ice, the warmer end will initially possess higher concentrations of both

-13-

positive and negative ions. The more rapid diffusion of H^+ ions down this concentration gradient leads to a separation of charge, with a net excess of positive charge in the colder part of the ice. A detailed theoretical treatment by Mason and Latham (1961) leads to the following expression for the potential V produced by a temperature difference T across the ends of an ice specimen

$$V = \frac{k}{2e} \frac{(u_+/u_- - 1)}{(u_+/u_- + 1)} \left\{ \frac{\phi}{kT} + 1 \right\} \Delta T \quad (9)$$

$$= 1.86 \Delta T \quad \text{millivolts}$$

where u_+ , u_- are respectively the mobilities of the H^+ and OH^- ions, $u_+/u_- = 10$, e the electronic charge, k Boltzmann's constant, $\phi = 1.2\text{eV}$ the activation energy for dissociation in ice and T is the absolute temperature. Latham and Mason (1961) have measured the potential differences across specimens of pure ice and find excellent agreement with Eq. (9). Moreover, the potentials are not markedly affected by the presence of dissolved salts and gases in the ice.

When two pieces of ice at different temperatures are brought into temporary contact and separated, the warmer piece acquires a negative charge and the colder one an equal positive charge. Theory indicates that there should be a maximum charge separation of $5 \times 10^{-5} \Delta T$ e.s.u. between each cm^2 of contacting surface when the surfaces are separated after about 0.01 sec. If they are left in contact for longer times, the charge separation will be decreased as the two pieces of ice become more nearly equal in temperature. These conclusions have been confirmed by experimental measurements that show that very little charge separation occurs if the contact period exceeds 0.5 sec.

The electrification of freezing water droplets is explained by the preferential migration of protons down the temperature gradient established across the ice shell. During the early stages of freezing, a radial temperature gradient is established across the ice shell, the inner surface being held at 0°C by the water that is still liquid inside, the outer surface cooling towards the air temperature. According to the above theory, protons will migrate preferentially down this

-14-

temperature gradient and produce an excess positive space charge in the outer layers of the ice. When the droplet bursts by the expansion of the centre as it freezes, splinters ejected from the outer layer will tend to carry away a positive charge and leave the remainder of the drop negatively charged. This is in accord with the experimental observations.

It is difficult to calculate the temperature gradient across the ice shell, which varies with time, and therefore the space charge density in the outer layers at the time of rupture. During the formation of the initial shell, the temperature of the drop is everywhere 0°C ; as freezing of the interior proceeds, a temperature gradient is built up; when freezing is completed the droplet finally assumes the air temperature everywhere and again the temperature gradient disappears. However, near the end of the freezing process, when the centre of the drop is still 0°C and the temperature of the outer surface close to that of the air, we may take the average temperature gradient across the ice to be T_c/r . In fact, shattering usually occurs before this late stage but we may use this value of the gradient to calculate a minimal value for the separated charge. According to Eq. (9), this will be $4\pi r^2 \cdot 5 \cdot 10^{-5} T_c/r$ e.o.u. If $T_c = -15^{\circ}\text{C}$ and $r = 40\mu$, this becomes 4×10^{-5} e.o.u. If $r = 0.5$ mm, the charge becomes 5×10^{-4} e.s.u. Thus the measured charges of 5×10^{-6} e.s.u. and 3×10^{-5} e.s.u. could be accounted for by the fragmentation of one-tenth of the surface area of the drops.

The Reynolds-Brook Charging Mechanism

Reynolds (1954), Reynolds, Brook and Gourley (1957), have attributed the negative charging of hailstones not to the freezing and splintering of droplets but to collisions between the hailstones and much smaller ice crystals. Laboratory experiments in which an ice sphere was rotated in a mixed cloud of ice crystals and super-cooled droplets showed that the sphere acquired a negative charge;

-15-

but if the cloud was composed entirely of droplets or entirely of crystals, there was negligible charging.

Reynolds believed that charging was caused by rubbing contact between the simulated hail pellet and the ice crystals which bounced off with a positive charge, and that the sole function of the freezing droplet was to warm the rimed surface and to create a temperature difference between it and the colliding crystals. It was estimated that, with a temperature difference of a few degrees, the average charge carried away by a crystal of radius 50 μ was 5×10^{-4} e.s.u.

Following up these ideas, Reynolds, Brook and Gourley (1957) investigated the electrification which resulted from rubbing contact between two rods of ice of different temperatures. When both pieces of ice were formed from distilled water, their resistivity being about $10^8 \Omega$ cm, the warmer became negative after rubbing. If, however, one of the ice specimens was made from a 10^{-4} molar solution of NaCl it became negative even though it was 25°C colder than the 'pure' ice. This reversal of potential was attributed to the formation of a liquid layer during rubbing and, on refreezing, a selective incorporation of Cl^- ions into the colder ice. Later, Brook (1958) investigated the potentials developed when two pieces of ice of different temperatures are brought into temporary contact and separated with a minimum of frictional contact. The sign of the charging was related to that of the temperature gradient, for both 'pure' and 'salty' ice, in the same manner as before, but the potentials were an order of magnitude smaller than those developed during rubbing contact.

These phenomena have been re-investigated by Latham and Mason (1961, a, b). They found, in agreement with Reynolds et al, that when two pieces of highly purified ice were brought into temporary contact (with minimum friction) and separated, the warmer acquired a negative charge. A theoretical calculation based on the protonic thermo-electric effect, indicated that a maximum charge transfer of $3 \times 10^{-3} \Delta T$ e.s.u. cm^{-2} should occur with a contact time of about

-16-

1/100 sec. and that it should thereafter decline as the two pieces become more nearly equal in temperature. The theoretical value for the charge developed for a contact time of $\sim 1/100$ sec. was well confirmed by experiments which also showed that very little charge separation occurred if the contact period exceeded $\frac{1}{2}$ sec. Contamination of the ice with CO_2 , HF, and NaCl in concentrations of up to 50 times that normally present in rainwater, did not greatly influence the electrification.

Latham and Mason also investigated the charging of a simulated hailstone by collisions with ice crystals. In order to eliminate charging by the freezing of supercooled droplets, these were rigidly excluded from the cloud, and the surface temperature of the hailstone was controlled by an internal electric heater or by irradiating its surface. Charging of the hailstone by the colliding crystals was measured as a function of their temperature difference, and of the size and impact velocity of the crystals. The sign of the charging was directly proportional to the temperature difference but rather insensitive to the size (diameter ranging from 20μ to 50μ) and impact velocity (1 to 50 m sec^{-1}) of the crystals. With a temperature difference of 5°C , a rebounding crystal of diameter 50μ produced, on average, a charge of 5×10^{-9} e.s.u.

This is five orders of magnitude smaller than Reynolds' value of 5×10^{-4} e.s.u.:

Reynolds' value may be questioned on two grounds. First, the field produced by such a charge at the crystal surface would exceed $10,000 \text{ V cm}^{-1}$; surely a discharge would occur between the pointed crystal and the hail pellet before the charge on the crystal could build up to this value.

Secondly, the charge of 5×10^{-4} e.s.u. is about 1000 times greater than that of all the charged carriers that would be present in the ice crystal if this were pure ice! Additional carriers might be produced as the result of local frictional heating of the ice at the points of contact but even if the whole ice crystal

-19-

fall in a vertical electric field and collide with the much smaller cloud-droplets that they overtake. The raindrop will be electrically polarized by the field; in a downwardly directed field such as exists in the atmosphere in fine weather, the lower half of the drop will carry a positive charge and the upper half an equal negative charge. Elster and Geitel suggested that, after collision, some of the cloud particles would rebound from the underside of the raindrop, carry away some of its positive charge, and leave the raindrop with a net negative charge. The falling drops, in carrying their negative charge towards the base of the cloud, would enhance the original field, and so the whole electrification process would build up rapidly. A detailed mathematical treatment of the problem shows that if only one per cent of the cloud droplets striking the lower half of the raindrops were to bounce off, and if this percentage were independent of the electric field strength, the field would grow exponentially with time and, in a cloud producing rain at the rate of 1 cm/h, would reach 1000 times its initial fine-weather value in only 10 minutes.

Now laboratory experiments indicate that, in the absence of an electric field, the fraction of cloud droplets that actually rebound after striking raindrops is small; the great majority of collisions result in coalescence. However, no experiment sufficiently accurate to detect non-coalescence to the extent of only a few per cent has yet been performed. This problem, which becomes complicated further by the presence of electric fields and of free charges on the drops, is now being studied by the author. It has been found that although droplets of 10-100 μ diameter may rebound after striking an uncontaminated plane surface of water or a much larger drop, they can always be made to coalesce by applying vertical fields of only about 10 volts per cm. The droplets become distorted as they approach the water surface, small protuberances develop at their ends in the direction of the field, and complete coalescence occurs, probably because small electric discharges occur at the protuberances and cause rupture of

-20-

the intervening air film. This suggests, perhaps, that once fields of about 10 V/cm are established in the cloud, coalescence between colliding cloud droplets and raindrops is assured. In this case the Elster-Geitel charging mechanism will cease long before fields strong enough to initiate lightning are produced.

At the present time we are unable to suggest a mechanism that would convincingly account for the origin of lightning in clouds consisting wholly of liquid water. But there is strong evidence in favour of the riming-hailstone mechanism being the dominant one in the typical large thunderstorm.

REFERENCES

- ATLAS, D., and LUDLAM, F.H. 1961. Quart. J. Roy. Met. Soc., 88, 117.
- BROOK, M. 1958. Recent Advances in Thunderstorm Electricity, p 383. New York; Pergamon Press.
- BROWNING, K.R., and MASON, B.J. 1963. Quart. J. Roy. Met. Soc., (in press).
- DURBIN, W.G. 1956. Air Ministry, Met. Res. Cttee., M.R.P., No991.
- HIGEN, M., and DE MAEYER, L. 1958. Proc. Roy. Soc., A247, 505.
- ELSTER, J., and GEITEL, H. 1913. Phys. Z., 14, 1287.
- EVANS, D.G. 1962. M.Sc. Thesis, Durham University.
- FINDEISEN, W. 1940. Met. Z. 57, 201.
1943. *ibid* 60, 145.
- FITZGERALD, D. and BYERS, H.R. 1962. University of Chicago Contract Report AFCL/TR/62/805.
- GILL, E.W.B. and ALFREY, G.F. 1952. Nature, Lond., 169, 203.
- HUTCHINSON, W.C.A. 1960. Quart. J. Roy. Met. Soc. 86, 406.
- KRUMER, C. 1948. Neth. Met. Inst. Vehr. A54, 1.
- KUETTNER, J. 1950. J. Met., 7, 322.
- LAHAM, J., and MASON, B.J. 1961a Proc. Roy. Soc., A260, 523.
1961b *ibid* A260, 537.
1962 *ibid* A266, 387.
- LUEDER, H. 1951a Z. angew. Phys. 3, 247.
1951b *ibid* 3, 288.
- MALAN, D.J. and SCHONLAND, B.F.J. 1951a Proc. Roy. Soc. A206, 145.
1951b *ibid* A209, 158.
- MASON, B.J. 1953 Tellus, 5, 446.
1957 The Physics of Clouds. (Clarendon Press, Oxford)
p 402-4.
- MASON, B.J., and MAYANK, J. 1960. Quart. J. Roy. Met. Soc., 86, 176.
- REINHOLD, H. 1951. Geofis. pur. appl. 19, 176.
- REYNOLDS, S.E. 1954. Comp. of Thunderstorm Elect. p 77. New Mex. Inst. Min. Tech.
- REYNOLDS, S.E., BROOK, M., and GOURLEY, M.F. 1957. J. Met. 14, 426.
- SARTOR, J.D. 1961. J. Geophys. Res., 66, 831.
- WALTON, W.H. and IREJETT, W.G. 1949. Proc. Phys. Soc. B62, 341.
- WEICKMANN, H.K. and AUFM KAMPE, H.J. 1950 J. Met. 7, 404
1953 *ibid* 10, 204.

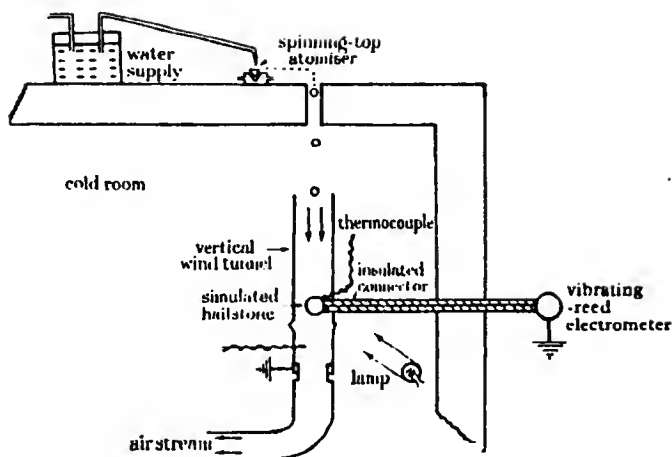


FIGURE 1 Apparatus for measuring the charge on hail pellets growing by riming.

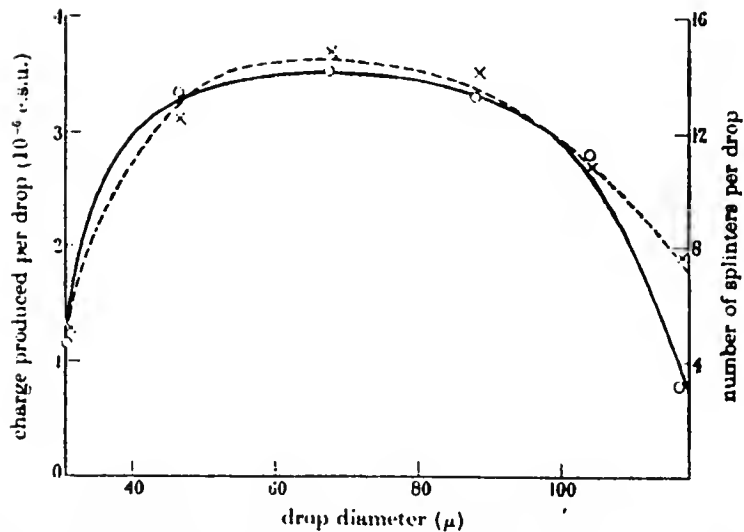


FIGURE 2 The production of ice splinters (x) and electric charge (O) as a function of the diameter of the freezing droplets. Air temperature, -15°C ; air velocity 10 m/s.

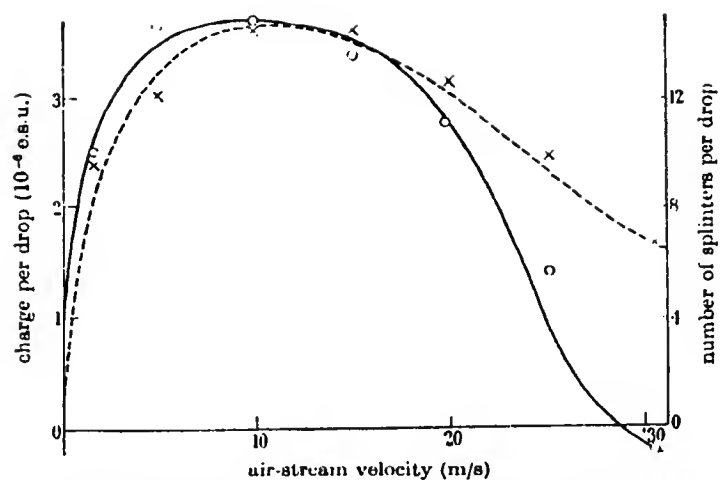


FIGURE 3 Splinter (x) and charge (O) production as a function of the impact velocity of the droplets. Air temperature, -15°C ; drop diameter, 70μ .

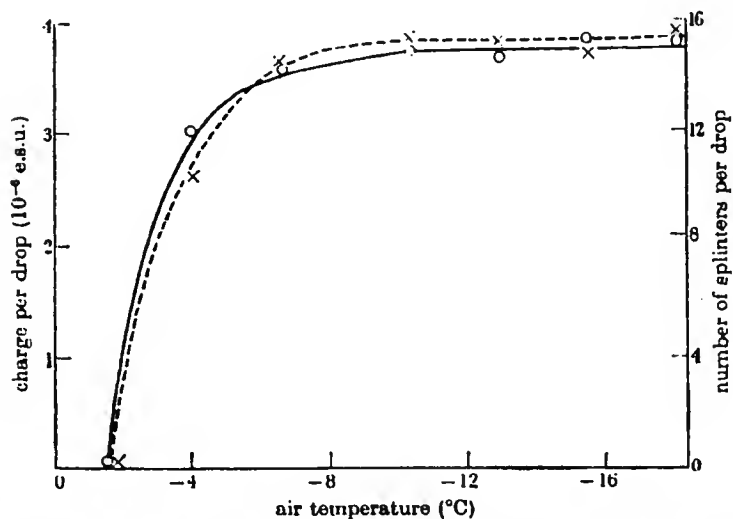


FIGURE 4 Splinter (x) and charge (O) production as a function of the air temperature. Air velocity 10 m/s; drop diameter, 70μ .

1.

SESSION 7.1

THE THEORY OF LIGHTNING

D.J. Malan

Bernard Price Institute of Geophysical Research
Johannesburg.

The title of this discussion covers a very wide field since a discussion on any aspect whatever of the lightning discharge or its manifestations involves a certain amount of theorizing.

I shall confine this talk firstly to the theory of the stepped leader, and shall then discuss discharge processes taking place inside and above the cloud.

Experimental data on the latter processes are extremely scanty so that the suggested mechanisms are mostly speculative and as such fall in the realm of theory.

THE THEORY OF THE STEPPED LEADER.

Very little new information based on photography of the stepped leader of a lightning flash has materialized since its discovery about thirty years ago. Photographic studies of laboratory sparks on the other hand have yielded a large amount of new information but difficulties arise when attempts are made to apply the knowledge gained to the leader of a lightning stroke. A case in point is the recent work of Stekolnikov and Shkilyov (1962) who used an image converter tube to photograph negative rod-to-plane sparks. They state that the bright steps they photographed are /.....

2.

are impulse corona discharges and are not preceded by a pilot streamer, from which they conclude that the leader process in laboratory sparks is different from that of natural stepped leaders.

Apart from the observation that the bright step is not accompanied by a pronounced steplike electrostatic field change, electrical studies of lightning have given little information which can be usefully applied to stepped leader theory.

In studying the radiation fields of flashes in the distance range of 50 km., both Clarence and Malen (1957) and Kitagawa (1957) found that when the stepped leader approaches the ground, radiation pulses follow one another at intervals of the order of $10\mu\text{sec}$. Kitagawa ascribes these pulses to short interval leader steps. Clarence and Malen, however, conclude that since the radiation field comes from the whole lightning channel, intracloud streamers which take part in supplying current to the advancing leader also contribute to the radiation pulses. The evidence for this conclusion is based on the observation that of the numerous stepped leaders photographed by us, none except perhaps the last step, show intervals as short as $10\mu\text{sec}$ between steps. Furthermore, we also argued that because exactly similar short interval pulses are often observed to precede strokes subsequent to the first, it is evident that all the pulses need not necessarily originate in a stepped leader process.

The question now arises: which explanation of the

profuse /.....

3.

profuse radiation pulses is the correct one? The answer to this question is important from the point of view of stepped leader theory. It is especially necessary to have conclusive evidence showing whether dart leaders are propagated by short steps or continuously.

The latest attempt to formulate a stepped leader theory known to the speaker is that of Wagner and Hileman. The theory of these authors is a sort of combination of the well-known earlier theories of Schonland, Bruce and Komelkov. Wagner and Hileman distinguish between the channel which consists of a 2 mm. diameter highly conducting arc plasma and a surrounding corona sheath of diameter about 30 m. When the channel is arrested a space charge develops in front of it, being fed by a multitude of filamentary streamers. At some instant the current in one of the filaments reaches a critical value of 1 ampere when an arc plasma begins to develop from the tip of the channel. This filament now robs the other space charge filaments of their charge and emerges as the new channel (or step).

According to Wagner and Hileman the intensity of the current at any point along the advancing step rises suddenly when the tip of the newly formed arc plasma reaches that point and thereafter remains constant until the tip has reached its maximum extension. The current which remains at about 1 ampere at the starting point of the step increases uniformly along the new channel to reach a maximum value of about 7000 amperes at the tip of the fully

developed /.....

4.

developed step. At any point the product of current and duration of current flow is constant during the advance of the step.

The assumption that the current which flows in the plasma channel during step formation is mainly derived from the surrounding space charge can explain why the bright step produces practically no sudden electrostatic field change although it carries a heavy average current.

THE POSSIBLE EFFECT OF HEAVY RAIN ON THE STEPPED
LEADER PROCESS.

It has been postulated that the preliminary electrical breakdown in the base of the cloud takes place by the mechanism of filament formation on large water drops. In a heavy thundershower the base of the cloud virtually extends down to ground level. The question now arises as to what extent, if any, heavy rain is likely to affect the stepped leader breakdown to earth.

Let us first consider the information available from the radiation fields occurring immediately before first strokes of flashes to ground. When using very high amplification, radiation pulses which may be ascribed to stepped leaders, can be detected in practically all cases. For a very large percentage of flashes the radiation pulses are surprisingly small, however. Does this indicate that the breakdown process for flashes in rain is a hybrid between the ordinary stepped process and the filamentary process, or can the effect be wholly attributed to the low

radiation /.....

5.

radiation propensities of stepped leaders in general, or as first suggested by Pierce, are stepped leaders totally absent?

Let us now consider the photographic evidence. Under favourable conditions for photography all flashes show stepped leaders. By favourable conditions it is meant that the flash is not obscured by rain or that the stray light scattered from rain has not caused overall blackening of the picture. It is obviously almost impossible to photograph a faint stepped leader in heavy rain, except perhaps when the flash is very near indeed.

Berger has taken many pictures of flashes in close proximity but has only obtained pictures of stepped leaders on very few occasions. It will be interesting to hear from professor Berger whether the absence of stepped leaders on so many of his photographs bears any relation to the intensity of rainfall while taking the photographs.

THE MECHANISM OF INTRA-CLOUD DISCHARGES.

It can be confidently concluded that intra-cloud discharges are not propagated by a stepped leader process because these discharges do not emit the radiation pulses which are characteristic of stepped leaders.

In regions near the base of the cloud where there are large water drops, the discharge can be propagated by the process of filament formation when the field reaches 10 kV/cm, provided that the diameters of the drops exceed 2 mm. At high altitudes in the cloud where its content

may /.....

6.

may consist of ice particles and droplets smaller than 2 mm., or of ice particles alone, this process can no longer take part in propagating the discharge. The following is a tentative explanation of the mechanism of the discharge process at high levels.

The droplets and also ice particles, as Chalmers (1947) has shown, will become polarized in the electric field. When the field between a neighbouring pair of droplets or ice particles reaches a value of about 30 kV/cm (the exact value depending on the pressure), electrical breakdown occurs. The discharge is subsequently carried forward from particle to particle, probably in a channel of large cross-section.

The presence of discrete pockets of high charge density in fairly close proximity to each other will cause the tip field to increase rapidly with the advance of the streamer so that it is not arrested as in the case of the stepped leader to ground. Furthermore, if this is the case it may not be necessary for the tip field to build up to 60 kV/cm which, according to Schonland, is the field required to produce the thermal ionization required for the progress of a stepped leader.

PROCESSES CONTRIBUTING TO INTERSTROKE FIELD CHANGES.

There are several factors which can contribute to the change of electric field as observed at ground level during the intervals between the strokes of a flash to ground.

Effect /.....

7.

Effect of space charge below the cloud.

A re-arrangement of space charge between the base of the cloud and the ground will influence the field in close proximity to the flash. However, since the conductivity of the air near ground level is small the relaxation time is long which makes it unlikely that this effect will contribute noticeably to the field changes observed during the short time intervals between the successive strokes of a flash.

Effect of transient changes in the charging process.

The separation of charge in the cloud under the influence of gravity is also relatively slow. It is bound to be profoundly affected during the development of the discharge, but to what extent is difficult to judge owing to the lack of experimental data. Moore, Vonnegut et al. (1962) found by Radar observations that the large drops responsible for gushes of rain following after lightning flashes were not present prior to the electrical discharge. They suggest that after a return stroke the droplets in the streamer channels and the surrounding droplets are oppositely charged so that coalescence takes place by electrostatic attraction. This observation will have to be taken into account when formulating a theory relating to the transient effect of a lightning flash on the normal separation of charge in a cloud.

The J process.

The interstroke J process is considered to be a positive streamer discharge progressing mainly upwards from

the /.....

8.

the upper regions of the previous return stroke channel. It was found that at distances nearer than 5 km interstroke field changes were nearly always negative in sign, whereas at distances between 12 and 20 km there were very few negative field changes, about 2/3 of them being positive and 1/3 zero.

In the intermediate range between 5 and 12 kms distance the tendency was for the initial interstroke field changes of a flash to be positive changing to negative between the later strokes.

The above distribution of sign of interstroke field changes at short range are in support of the suggested mechanism of the J process.

Effect of continuous discharge to ground.

A continuous discharge to ground during the intervals between the intermittent strokes of a flash brings negative charge to earth and will thus contribute a positive component to the interstroke field change at all distances.

Brook, Kitagawa and Workman (1962) have carried out a detailed study of continuing currents by simultaneous electrical and photographic observations in New Mexico. They find that a continuing current flows to ground in about 25% of interstroke intervals.

THE INTERSTROKE FIELD CHANGES DUE TO DISTANT FLASHES.

At distances beyond 20 km, J field changes although small should be positive so that it would have been expected that most of the interstroke field changes in this range

would /.....

9.

would be positive. Such is not the case, however.

In England, Pierce (1955) found that only 25% of such interstroke intervals showed positive field changes whilst in the remainder no field changes could be detected. The above percentage of positive field changes agrees with the frequency of occurrence of continuing currents in New Mexico, so that it may be assumed that large positive interstroke field changes observed at great distances are mainly caused by continuing currents in the channel to ground. The contribution by the J process may be so small as to be undetectable.

At Johannesburg the distribution of sign is somewhat different. At distances between 25 and 100 km, 19% of interstroke field changes are positive. Here too, these field changes may be ascribed to continuing currents. Of the remaining field changes, however, 37% are zero and 44% negative. Fig. 1 shows three examples of field changes of flashes in the 50 km range. In (A) a positive interstroke field change is followed by 4 negative interstroke field changes. All the field changes are relatively small compared with those due to the preceding return strokes. The sequence of sign in this type of flash is not random but follows in the order positive, zero, negative, except for the occasional random occurrence of an exceptionally large positive field change which is obviously due to continuing current.

Of far less common occurrence are the field changes shown in (B) and (C) where negative interstroke field changes are comparable in amplitude with, and may even surpass, the preceding return stroke field changes. The occurrence at

large /.....

10.

large distances of negative interstroke field changes at Johannesburg and not in England is possibly connected with the large vertical extent of thunderclouds at the former locality which is situated on an extensive plateau 1800 metres above MSL.

As outlined above, the basic data on which to base a theory for explaining the negative field changes are scanty but it appears that the effect can be explained in terms of a readjustment of space charge above the top of the cloud. A possible theory will now be briefly outlined.

THEORETICAL STUDY OF SPACE CHARGE EFFECTS.

Consider unit volume of air above a thundercloud at an altitude z above the ground.

Let the conduction current be j , the potential φ , field E , conductivity σ and density of charge ρ .

If the field is not too high

$$j = \sigma E \quad \dots\dots\dots (1)$$

since

$$\nabla^2 \varphi = -4\pi\rho$$

and

$$E = -\text{grad } \varphi$$

it follows that

$$\nabla^2 \varphi = -\text{div}(j/\sigma)$$

giving

$$4\pi\rho = (1/\sigma)\text{div } j + (\text{grad } 1/\sigma) \cdot (j)$$

for steady state conditions, $\text{div } j = 0$ so that

/.....

11.

$$4\pi \rho = (g \tan \theta / \sigma) \cdot (\sigma E)$$

since the conductivity is constant in the horizontal plane,
we get

$$\rho = \frac{\sigma}{4\pi} \left[\frac{\partial}{\partial z} \left(\frac{1}{\sigma} \right) \right] E_z \quad \dots\dots\dots (2)$$

Gish (1944) has shown experimentally that in fair weather
 $1/\sigma$ can be empirically expressed as the sum of three
exponential terms. Two of these can be neglected at high
altitudes, so that for the region above the cloud his
equation may be written

$$1/\sigma = 0.37 e^{-0.12z} \times 10^{15} \quad \text{ohm. cm, } z \text{ being in km.}$$

If it is assumed that the thundercloud does not alter the
conductivity of the air above it (Gish and Wait 1950),
equation (2) becomes

$$\rho = - \frac{0.12}{4\pi} E_z \quad \dots\dots\dots (3)$$

A similar expression was derived in a rather more lengthy
way by Holzer and Saxon (1952)

It follows then that the space charge density at
a point in the air above the cloud is proportional to the
electric field at that point.

Using equation (3) it is possible to obtain an
approximate estimate of the distribution of space charge in

a /

12.

a vertical column above the cloud and to calculate the field change produced at a point on the ground by the relaxation of space charge after the occurrence of a stroke to ground.

Tamura (1954) expanded the theory of Holzer and Saxon to prove that the difference in the recovery curves after an intra-cloud discharge for near and distant flashes could be explained by taking into account the readjustment of space charge above the cloud after the occurrence of a flash. Tamura's expressions for the field component of the space charge will also be used in what follows.

The interstroke field change due to the space charge effect will be called the U field change. A stroke to ground removes negative charge from the cloud so that E_z of equation (3) becomes more positive and the U field change will consequently be negative at all distances.

To circumvent the uncertainty in estimating the magnitudes of the charges involved in the discharge processes, the ratio U/J of the respective field changes was calculated assuming arbitrary values for the charges. Furthermore, it was assumed that the ratio U/J is unity at a distance of 20 km. Justification for this assumption depends on the experimental observation that at distances up to about 20 km the interstroke field changes correspond in sign with the expected J field changes whereas at larger distances this is no longer the case.

The variations of the ratio U/J with distance, starting from 20 km, are shown in figs. 2 and 3.

In fig. 2 the J process advances from 4 to 5 km. altitude and in fig. 3 from 7 to 8 km. The former thus represents conditions at the commencement and the latter those at the end of a flash with several strokes.

Curves /.....

13.

Curves A have been calculated on the simple assumption that the U charge disappears from the top of the cloud at 12 km altitude as first tentatively suggested by Malan and Schonlend (1951). Since these curves are approximately parallel to the abscissae they show that removal of charge from such a low altitude does not account for negative interstroke field changes.

Curves B were calculated by the simplified method outlined above and represent the effect of the adjustment of space charge in a column reaching from 20 to 30 km altitude and taking place after a stroke.

Curve C was calculated from Tamura's equations which assume that the space charge is distributed from the top of the cloud to infinite height.

The difference between curves B and C is not significant except in the range 20 to 30 km where curve B seems to fit the experimental observations somewhat better.

Both curves show that at large distances the negative U field change can be much larger than the positive J field change.

E_z of equation (3) increases in a steplike fashion after each partial discharge with the result that the U field change also increases. This can account for the observation that the interstroke field change is often positive or zero after the initial strokes and becomes negative after the later strokes of a flash.

As Brook, Kitagawa and Workman have pointed out the J field changes become very small at a distance of 50 km from /....

14.

from which it follows that the curves of figs. 2 and 3 do not account quantitatively for the relatively large negative field changes shown in fig. 1 (B) and (C).

It is possible that the field above the cloud occasionally becomes so large that equation (1) is not valid and the outlined theory breaks down. This may conceivably happen in a cloud of large vertical extent where the main positive and negative centres are widely separated so that flashes to ground are more frequent than intra-cloud flashes. When the records shown in fig. 1 B and C were obtained, flashes to ground were 2 to 3 times more frequent than cloud flashes.

In the extreme case, the field above the cloud may become high enough to initiate a glow discharge between the space charge and the ionosphere (Malan 1937). In this case the conductivity of the air above the cloud will increase and cause a decrease in the relaxation time thus giving large and rapid U field changes.

It will be interesting to determine whether the rare large negative field changes have any connection with solar flares which cause increased ionization in the D layer of the ionosphere.

REFERENCES.

- Brook M., Kitagawa H. and Workman E.J. 1962
Quantitative study of strokes and continuing
currents in lightning discharges to ground.
Journ. Geophys. Res. 67, 649
- Chalmers J.A. 1947
The capture of ions by ice particles.
Q. Journ. Roy. Met. Soc. 73, 324.
- Clarence N.D. and Malan D.J. 1957
Preliminary discharge processes in lightning
flashes to ground.
Q. Journ. Roy. Met. Soc., 83, 161.
- Gish O.H. 1944
Evaluation and interpretation of the columnar
resistance of the atmosphere.
Torr. Magn. and Atm. Electr., 49, 159.
- Gish O.H. and Wait G.R. 1950
Thunderstorms and the earth's general electrification.
Journ. Geophys. Res. 55, 473.
- Holzer R.E. and Saxon D.G. 1952.
Distribution of electrical conduction currents in
the vicinity of thunderclouds.
Journ. Geophys. Res. 57, 207.

Kitagawa /.....

Kitagawa N. 1957

On the electric field change due to the leader processes and some of their discharge mechanisms.

Papers in Meteorology and Geophysics vol.VII, no.4 published by the Met. Res. Inst., Tokyo.

Kitagawa N., Brook M. and Workman E.J. 1962.

Continuing currents in cloud to ground lightning discharges.

Journ. Geophys. Res. 67, 637.

Malan D.J. 1937

Sur les décharges orageuses dans la haute atmosphère

Comptes Rendus 205, 812.

Malan D.J. and Schonland B.F.J. 1951.

The electrical processes in the intervals between the strokes of a lightning discharge.

Proc. Roy. Soc,A, 206, 145.

Moore C.B., Vonnegut B., Machado J.A. and Survilas H.J. 1962.

Radar observations of rain gushes following overhead lightning strokes.

Journ. Geophys. Res. 67, 207.

Pierce E.T. 1955.

Electrostatic field changes due to lightning discharges and The development of lightning discharges.

Q. Journ. Roy. Meteorol. Soc. 81, pp. 211 and 229.

Stekolnikov /.....

Stekolnikov I.S. and Shkilyov A.V. 1962.

New data on negative spark development and
its comparison with lightning.

Conference on Gas Discharges and the
Electrical Supply Industry.

In course of publication by Butterworth.

Tamura Y. 1954.

An analysis of electric field after lightning
discharges.

Journ. of Geomag. and Geoelectr. 6, 34.

Wagner C.F. and Hileman A.R.

The lightning stroke II

(Typed memorandum. Has it already been
published?)

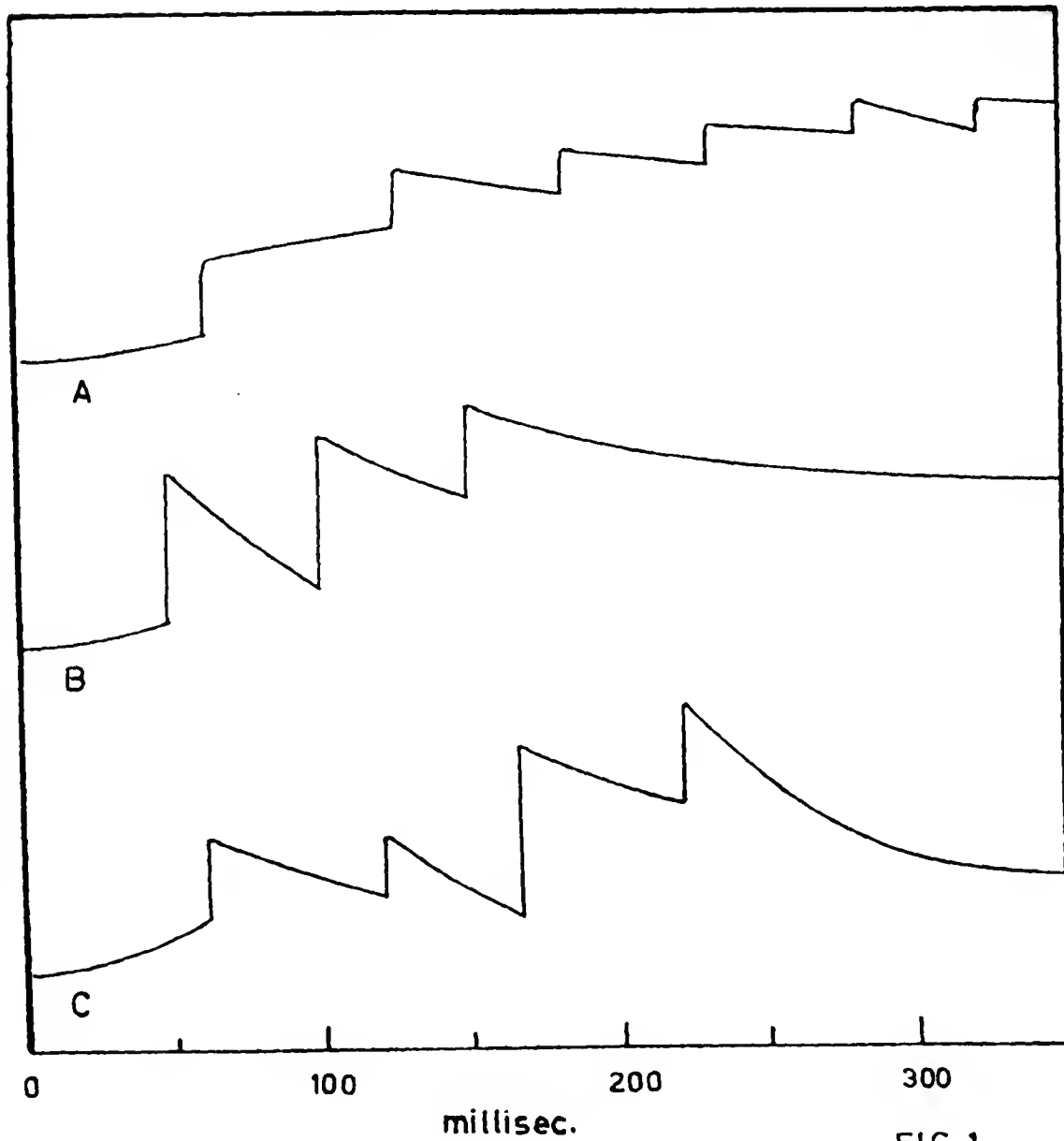


FIG.1.

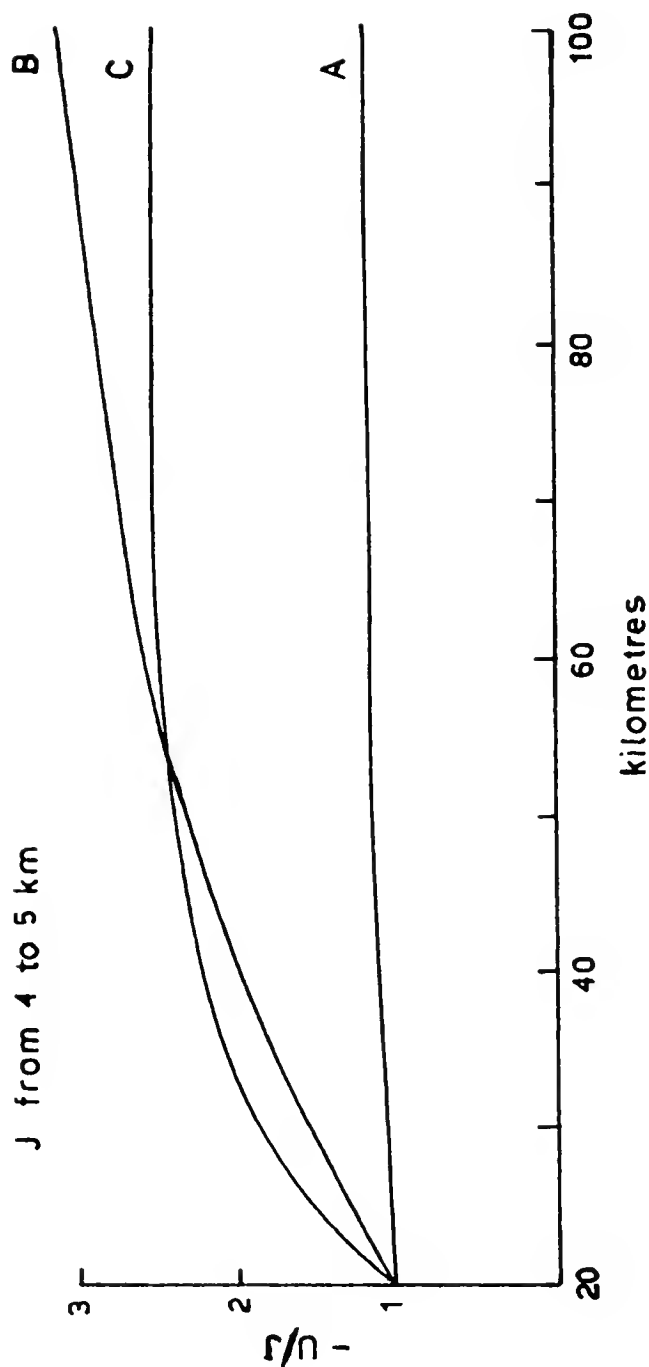


FIG. 2.

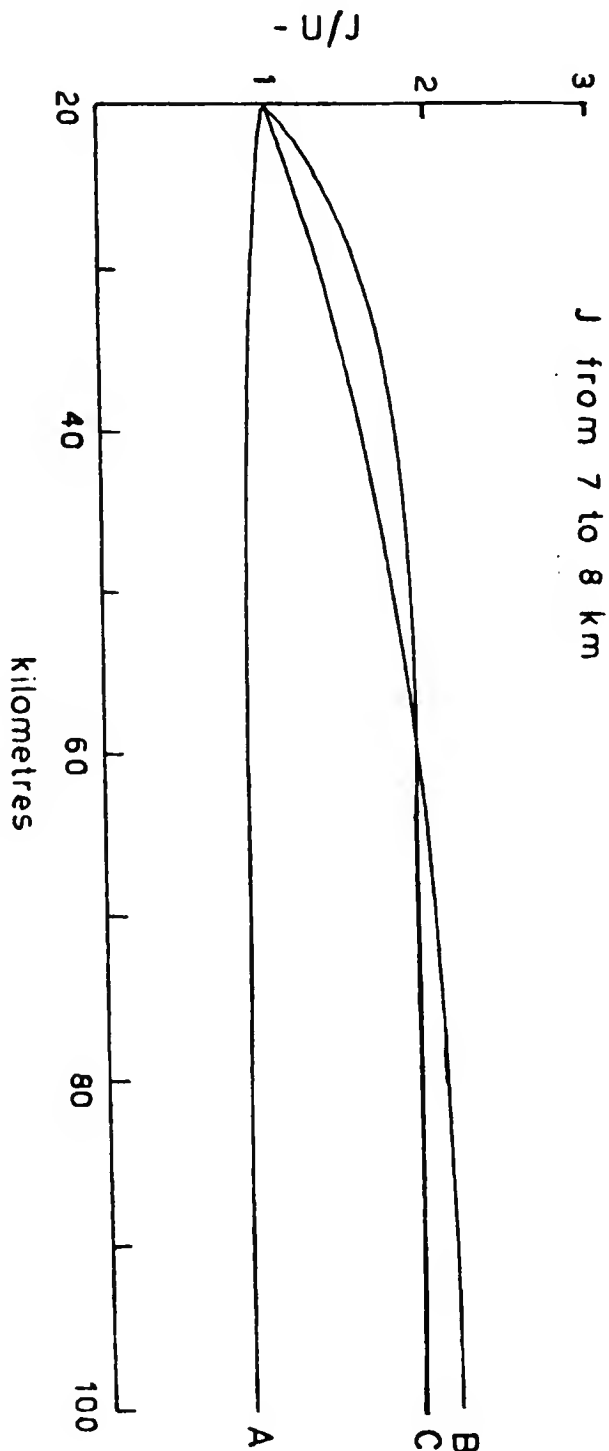


FIG. 3

SESSION 7.2

Types of Lightning

N. Kitagawa

Introduction

The mechanism of lightning discharge can best be studied by the simultaneous measurement using photographic and electric-field recording technique. Lately in New Mexico lightning measurements on this line with improved technique have been done extensively. The result thus obtained have revealed new aspects of lightning discharges as well as the detailed structure of the discharge mechanism. (Kitagawa, Brook and Workman, 1962; Brook, Kitagawa and Workman, 1962)

Based mainly upon these results, the author will try to depict the picture of the lightning, pointing the accompanying unsolved problems at the same time.

Terminology

The author adopts the terminology of Shonland (1956) in describing the various processes in the lightning discharge. A flash is a lightning discharge in its totality. A stroke is a partial discharge consisting of downward-moving return streamer. A flash may consist of a single stroke or a series of strokes in the same or an adjacent channel. A M component is a sudden enhancement of the continuing luminosity which occasionally follows a stroke in the channel (Malan and Shonland, 1947). The M components are not preceded by leaders.

Long-continuing luminosity is arbitrarily defined as luminosity which persists in the channel for a time longer than 40 msec i.e., luminosity which lasts as long as or longer than the usual stroke

interval. A stroke followed by such luminosity will be called a long-continuing stroke. Occasionally a stroke is followed by continuing luminosity which lasts less than 40 msec; such a stroke will be called a short continuing stroke. A stroke whose luminosity decays abruptly will be called a discrete stroke. A K change is a small, rapid electric field change which occurs in the intervals between and after the strokes of a multiple stroke flash (Kitagawa, 1957; Kitagawa and Brook, 1960). The K changes are generally associated with streamer activity within the cloud. There is a slow electric field change which occurs during the interval of continuing luminosity, this will be referred to as a continuing or C change to distinguish it from the junction or J change which occurs without the accompanying channel luminosity between or after the strokes.

In analogy with the definitions given by Malan (1954), a lighting flash which involves one or more continuing strokes is called a hybrid flash. A flash which involves discrete strokes or short continuing strokes is called a discrete flash. Cloud-to-Ground, in-cloud and cloud-to-cloud discharges will be referred to by the symbols, C-G, I-C and C-C discharges respectively. A cloud-to-clearair flash is called a air discharge.

General nature of C-G discharges

As a result of New Mexico lightning measurements it has been found that hybrid flashes i.e. flashes involving one or more long continuing strokes are found to be observed very commonly in C-G discharges.

In multiple flashes which constitute 86 per cent of all C-G discharges, the occurrence rate of discrete and hybrid flashes is about fifty to fifty. The percentage of single flashes with long continuing luminosity is exceptionally low (only 2 of 193). The long continuing strokes does not either occur as the initial stroke of a multiple flash.

Figure 1 is a comparison of the luminous events of a discrete and a hybrid flash as recorded by the moving-film camera and by the electric field and electric field-change records. In the schematic representation of the luminous events, a straight, vertically oriented channel is assumed. The electric field record represents the actual variation of electric field, whereas the electric field-change record emphasizes the rapid components through the use of an antenna with a short time constant and a high amplification. Both of the flashes are about 20 km distant from the recording station. It can be noted in Figure 1 that the magnitude of slow electric field changes (J changes) is very small or practically zero during the intervals of non-luminosity between strokes of both discrete and hybrid flashes. On the contrary, it has been found that a large positive, slow electric field change (C change) is always associated with a continuing luminosity on the photographic record. The average number of strokes per flash in both discrete and hybrid flashes is 7. If we include the single flashes, the average number of stroke per flash is 6. Thus the number of strokes per flash has found^{to} be appreciably larger than the statistics by Schonland (1956) based upon electric field-change records. It is not uncommon to find several strokes which produce field-changes

of 1/10 to 1/20 of the field change caused by the largest stroke. Without the positive identification of the leader-return combinations on the high speed photographs, it is highly probable that R changes of such small magnitude might have been interpreted as K changes or overlooked.

Malan (1954) found that the large slow field change of the same nature as defined C change here, often occurs as a final stage of a multiple flash which involves fewer stroke elements. In New Mexico measurements such a hybrid flash found to be observed more frequently that its earlier stage is very similar to that described by Malan but involves one or more stroke elements of very small R changes in its very late stage.

In England Pierce (1955 a) sometimes recorded $S(\beta)$ field change. The field change of this type can reasonably interpreted as a continuing current field change in which the stroke field change initiating the C change is barely discernible on the electric field record. It is because of the occurrence of such small stroke field changes that the number of strokes per flash appears to be less when counted on the electric field records than when measured on the high speed photographs.

While the duration of long continuing luminosity varies widely as shown in Figure 3, the duration of the no-luminous interval i.e., the interval from the end of the luminosity ^{of the preceding stroke} to the following stroke tends to fall in certain limited range around 80 msec (from 50 to 200 msec). Though the duration of a no-luminous interval appears to be longer than a usual stroke interval, the value still lies within the

range of discrete or short stroke intervals (5 to 180 msec).

The methods and assumptions used in calculating value for the charge which is brought to earth by individual discharge elements of a flash are described and discussed in detail by Brook, Kitagawa and Workman (1962). Here the method will be outlined. The electric field change due to a lightning stroke measured at the surface of the earth is given by

$$\Delta E = 90 \frac{2 Q_R H_R}{(D^2 + H_R^2)^{3/2}}$$

where ΔE is in volts/cm, Q_R is in coulombs and H_R and D are in km. D is the horizontal distance from the field meter to the flash and H_R is the vertical height to the assumed center of charge Q_R .

The height H_R is determined by

$$H_R = h t_e / t_p$$

Where h is cloud base height, t_e is the total duration of the dart leader measured on electric field change records and t_p is the time for the dart leader to travel from the cloud base to ground determined by photographic records. From the first equation, with the measured value of H_R , D and ΔE , the charge Q_R can be written

$$Q_R = \frac{\Delta E [D^2 + (h t_e / t_p)^2]^{3/2}}{180 h t_e / t_p}$$

The above method is also applicable to the continuing current intervals. Let H_1 and H_2 be the heights determined for two successive strokes between which a continuing current to ground was evidenced on both the electric field records and the photographs. The charge Q_C is assumed

to be centered at H_c , a distance midway between the tops of the two return stroke channels; i.e.,

$$H_c = \frac{1}{2} (H_1 + H_2)$$

The corresponding slow electric field change ΔE is then measured, and the charge Q_c is calculated.

The negative charge (no strokes carrying positive charge to earth were observed) lowered by individual stroke is shown in Figure 2(a) and 2(b) in two histograms showing the number of occurrences of strokes in which charge was (a) lowered by strokes which were preceded by stepped leaders and (b) lowered by strokes preceded by dart leaders. A striking contrast is seen to exist between the two types of strokes. The minimum charge lowered by the strokes associated with stepped leaders is 3.0 coul; for the others a minimum value is 0.21 coul. Both of the histograms exhibit a sharp cut-off at their minimum end. The most frequent value of charge brought down by first strokes lies between 3 and 4 coul; for subsequent strokes the most frequent value lies between 0.5 and 1 coul. For single flashes the average value of the charge lowered was calculated to be 4.6 coul. The charge lowered by the continuing current is shown in Figure 3 as a plot vs. its duration. The maximum duration of a continuing current interval was found to be 300 msec. The greatest amount of charge lowered during one of these long intervals was 31.2 coul. Though both the amount of charge and the duration vary widely, the plot shows that the average current i.e., the charge divided by the duration tends to be far less variable from current to current. It ranges from 38.4

to 130 amp around the mean value of 79.2 amp. Thus the continuing current turns out to be very efficient agent for carrying the cloud charge to earth. Because of this agent the total charge lowered by a hybrid flash is remarkably larger than that lowered by a discrete flash. The calculation shows that the average values for a discrete and a hybrid flashes are 20 and 34 coul respectively.

The result of the calculation of the charge center height for each stroke element is shown in Figure 4 as a plot vs. the stroke order. The figure shows the definite tendency that the height of charge center, exactly speaking, the length of the stroke channel increases from stroke to stroke. The most frequent height difference for the discrete flash is 0.3 km. The value for the discrete intervals of the hybrid flash is also 0.3 km. The continuing-current intervals are most frequently associated with a value of 0.9 to 1.6 km. Figure 4 suggests that hybrid flashes usually involve greater cloud volumes than do discrete flashes.

Continuing currents and the junction Process

With the realization that the continuing currents to earth often occupy the intervals between strokes previously assigned to in-cloud processes alone (i.e. J changes), it is desirable that we reexamine the interpretation of the inter-stroke field changes, as discussed by Malan and Schonland (1951 b), Malan (1955) and Pierce (1955 a,b)

Table 1 shows the electric moment change $2HQ$ associated with a flash, a stroke, a long continuing current and a J process, obtained

in the present measurement. J change, identified by the absence of

Table 1 Electric Moment Change Associated with a Flash,
a Long Continuing Current and a J process

Discharge	Electric Moment Change 2HQ (coul km)	
Flash	248	(average)
Stroke	22	(average)
Long Continuing Current	135	(average)
Junction Process	1.62	(maximum observed value)

a continuing channel luminosity on the photographs turns out to be remarkably small. As shown in Table 1 the maximum change was found to be 1.62 coul km. Large slow field changes ~~does~~ occur, but invariably the photographs show these to be associated with continuing current to ground. When we consider the average change in moment associated with the flashes in this study is 248 coul km (Table 1), it is not surprising to find that the J-change moment, having values much less than 1.6 coul km, are not detectable. Taking the maximum value as 2 coul km, we see that the J process produces a change in moment which is about 10 per cent of the average change in moment for strokes (22 coul km), and about 1 per cent of the

average change in moment for continuing currents (135 coul km). It is now clear that the value $2RQ = 50$ coul km used by Pierce (1951 b) for the J change in moment is really to be associated with the C change.

We shall assume that the most favorable conditions of noise allow the measurement of slow field changes of magnitude 10^{-3} of the earth's fair weather field, i.e., of magnitude 10^{-3} volt/cm. Using the value 1.6 coul km for the upper limit of the J change in moment, we calculate that the maximum distance at which a J change will produce an electric field change of 10^{-3} volt/cm is 52 km. Since only a C field change is expected to be detected as a slow electric field change on the record beyond this distance, it is highly probable that most of the J changes reported by Pierce (1955 a) for distances between 50 and 90 km were produced by continuing currents to ground. He was able to measure slow field change in approximately 25 per cent of the intervals between strokes and for the remainder no variation in field could be detected. This figure of 25 per cent is reasonably consistent with our own statistics for the occurrence of continuing currents in lightning discharges. These statistics also reinforce the conclusions that C changes, and not J changes, are detectable for distances beyond 50 km. A new process involving a discharge from the cloud top to the high conducting layers was postulated by Malan and Schonland (1951 b) and Malan (1955) to explain the apparent absence of J changes in the measurements of Pierce (1955 a) and Malan (1955) for distant storms (20 to 150 km). Since we now see that the absence of J change is actually to be expected for distances beyond 50 km, the com-

compensating process (a discharge to the upper air) is unnecessary. Also, it appears that it is not necessary to postulate a difference between thunderclouds in England and in South Africa (Pierce and Wormell, 1953).

During the interval between successive strokes of a multiple flash, there found to be two different stages of channel conditions, a continuing luminosity stage and a non-luminosity stage. We have done some experimental approach to the luminous conditions, but the channel condition during non-luminous intervals remains entirely unknown. A number of problems concerning this channel condition should be the subjects of future studies. For instances, what is the amount of the dark current in the channel? How the J process is connected to the ground? How such a conductive condition is maintained in the channel that allows the dart leader of a subsequent stroke to follow the same channel?

M components and K changes

During the continuing luminosity M components are found to be associated with field changes similar to K changes on electric field-change records as can be seen in Figure 1. Separations of M components are very small and tend to increase very rapidly with elapsed time within the first 15 msec from the return stroke. Later on this tendency disappears and M-component intervals exhibit no dependence on the elapsed time. Figure 5 (a) shows the frequency histogram of M-component intervals in this later stage of continuing

luminosity. For the comparison the frequency histograms for K changes in discrete intervals of G-C discharges (b) and for K changes in I-C discharges (c) are shown in the figure.

So far the luminosity continues in the channel, streamers connected to the channel keep developing within the cloud into the flash charged region. The M components is the presentation of the current surge in the luminous channel produced by the momentary increase of the cloud charge supply. Thus, the occasional appearance of M components in a continuing current is considered to be the reflection of the non-uniform distribution of charge in the cloud. The similarity in three histograms (a), (b) and (c) in Figure 5 also suggests that M-component intervals and K-change intervals both in discrete stroke intervals of C-G discharge and in later stages of I-C discharges are all controlled by the same conditions, by the conditions attributable to the cloud structure, not by the conditions of the discharge process. Ogawa (1962) calculated the average developing velocity for the streamers associated with the long continuing current to be 1.6×10^6 cm/sec. This value, combined with the most frequent M-component interval of 6 msec, gives the linear dimension of 100 M for the spacing of the densely charged regions in the cloud. This dimension can be compared reasonably well with that of the unit cell of the convection suggested by Reynolds (1954) i.e., the microstructure in the so-called cloud cell, evidenced by the radar echoes of the storm or by the visual observation of cumulus towers and striation in the rain sheet.

The K change is a rapid luminous small scale discharge within

the cloud. Usually the duration is less than 1 msec and the moment change involved varies from a few hundredth to about 1 coul km. Ogawa's (1962) analysis based on New Mexico measurements shows that the main discharge process which constitutes the K change is the rapid flow of the cloud negative charge into an already existing channel. Comparing the discharge processes associated with M components with those produces K changes, there seem to be no essential difference in the way of the streamer development within the cloud. A junction or J process described by Malan and Schonland (1951 b) is now reasonably interpreted as a whole series of K-change discharges involved in a stroke interval. The J change turns out to be the smoothed trace of the electric field record which actually consists of a number of very small K-change steps during the non-luminosity interval of a multiple C-G flashes.

Nature of I-C discharge

Figure 6 shows a typical example of electric field and electric field-change records of a I-C discharges. The records is usually divided into two different portions; the earlier active portion and the later portion. The later portion of field and field-change records are very similar to those between strokes of a C-G discharge i.e., J or C field changes; K changes follow each other on the electric field-change record with the identical time intervals with those of K changes and M components in C-G discharges (Figure 5). During the earlier portion pulse activity is much higher; amplitudes

of some of pulses are much larger and pulses are spaced so densely that quiescent intervals are seldom recorded. Occasionally an earlier active portion may be preceded by a less active portion, called an initial portion, which is characterized by pulsations of high repetition rate and of relatively small amplitude. The rate of the moment change estimated on electric field record is generally higher during active portions than during later portions. The electric field and electric field-change records of a later portion obviously show that the discharge mechanism is essentially the same as that of discharge processes which take place in the cloud during the intervals of a multiple C-G discharge. Though there is no strict distinction between the discharge of the M-component type and of the K-change type in the case of a I-C discharge, the discharge mechanism is considered to be closer to that of the continuing current interval of a C-G discharge, because the moment change in this portion is generally larger than that in the discrete stroke intervals (i.e. J field change). And it is highly probable that continuing channels of considerable length are usually established in a later stage of a cloud discharge as occasionally evidenced on moving camera records of C-C or Air discharges. Occasionally a moment variation in a K change is appreciably larger compared with that in C-G discharges. A measurement by Ogawa (1962) shows that for the I-C discharge the average moment change associated with the K change is about 6 coul km and the charge involved is estimated to be 2 coul. The average current during the change is 2000 amp.

A very frequent occurrence of pulses in an active portion apparently suggests that a number of different streamer channels develop in the cloud at the same time or with slightly different time phases. Sometimes the development of relatively small scale streamers is repeated for the duration of some 50 to 100 msec before the burst of larger streamers takes place (an initial portion). At present quantitative information about streamer processes in an initial or in an active period of the I-C discharge are not available. However, we can point out one aspect of the initial stage of the I-C discharges. Regardless the discharge starts with an initial portion or immediately with an active portion, the pulse activity is much more irregular than that recorded in the very beginning stage of the leader field change of C-G discharge, both length of pulse intervals and pulse amplitude tend to be larger and more variable in the first several ^{milliseconds} ~~msec~~ compared with those in the later stage. Still the regularity in both period and amplitude well reflects the step-wise development of stepped leader streamers. In fact the pulse intervals during this stage lies in the range from 10 to 150 μ msec. On the contrary for corresponding initial stage of the field change of a I-C discharge, pulse intervals spread over the extremely wide range from 10 μ sec to several msec. Pulse intervals along with much irregular pulse shapes indicate that the mechanism of the associated discharge is entirely different. While the initial breakdown of a C-G discharge takes place in the water droplets region of a cloud, the initiation of a I-C discharge starts at much higher altitude where the cloud consists of ice particles and

A very frequent occurrence of pulses in an active portion apparently suggests that a number of different streamer channels develop in the cloud at the same time or with slightly different time phases. Sometimes the development of relatively small scale streamers is repeated for the duration of some 50 to 100 msec before the burst of larger streamers takes place (an initial portion). At present quantitative information about streamer processes in an initial or in an active period of the I-C discharge are not available. However, we can point out one aspect of the initial stage of the I-C discharges. Regardless the discharge starts with an initial portion or immediately with an active portion, the pulse activity is much more irregular than that recorded in the very beginning stage of the leader field change of C-G discharge, both length of pulse intervals and pulse amplitude tend to be larger and more variable in the first several ~~msec~~ ^{milleseconds} compared with those in the later stage. Still the regularity in both period and amplitude well reflects the step-wise development of stepped leader streamers. In fact the pulse intervals during this stage lies in the range from 10 to 150 μ sec. On the contrary for corresponding initial stage of the field change of a I-C discharge, pulse intervals spread over the extremely wide range from 10 μ sec to several msec. Pulse intervals along with much irregular pulse shapes indicate that the mechanism of the associated discharge is entirely different. While the initial breakdown of a C-G discharge takes place in the water droplets region of a cloud, the initiation of a I-C discharge starts at much higher altitude where the cloud consists of ice particles and

super-cooled droplets of very small size. The author suggested that the difference between the two initial breakdown processes is attributable to the difference in the breakdown impedance affected by the above two different environmental conditions i.e., the difference in the relative populations of water drops and ice particles in the cloud (Kitagawa and Brook, 1960). In addition to the difference in the breakdown impedance, it is probable that the kind of breakdown streamers, positive streamers mostly, not negative streamers and the configuration of channels, extensively branched or separated into a number of channels will account for the different character ^{of the initial} ~~in the very early~~ breakdown process ~~stage of the field change~~ of I-C discharges.

We have tried to depict the nature of the I-C discharge in the comparison with the C-G discharge. As to discharge processes, however, which take place entirely in the cloud, we have very little quantitative informations. For the further study of the lighting discharge, quantitative measurements of these processes are desired, e.g. an initial breakdown streamer process, a streamer process in an active portion, a K-change process and a streamer process of continuing luminosity. The approach for these will be simultaneous measurements by field meters of high time-resolution at several stations on the surface.

References

- Brook, M., N. Kitagawa, and E. J. Workman, Quantative Study of strokes and continuing currents in lightning discharges to ground, J. Geophys. Research, 67, 649-659, 1962.
- Kitagawa, N., On the mechanism of cloud flash and junction or final process in flash to ground, Papers Meteorol. and Geophys. Tokyo, 7, 415-424, 1957.
- Kitagawa, N., and M. Brook, A comparison of intracloud and cloud-to-ground lightning discharges, J. Geophys. Research, 64, 1189-1201, 1960.
- Kitagawa, N., M. Brook, and E. J. Workman, Continuing currents in cloud-to-ground lightning discharges, J. Geophys. Research, 67, 637-647, 1962.
- Malan, D. J., Les décharges orgeuses intermittentes et continues de la colonne de charge négative, Ann. géophys., 10, 271-281, 1954.
- Malan, D. J., Les décharges lumineuses dans les nuages orageux, Ann. géophys., 11, 427-434, 1955.
- Malan, D. J., and B. F. J. Shonland, Progressive lightning, 7, Directly-correlated photographic and electrical studies of lightning from near thunderstorms. Proc. Roy. Soc. London A, 191, 485-503, 1947.
- Malan, D. J., and B. F. J. Shonland, The distribution of electicity in thunderclouds, Proc. Roy. Soc. London A, 209, 158-177, 1951a.
- Malan, D. J., and B. F. J. Shonland, The electrical processes in the intervals between the strokes of a lightning discharge, Proc. Roy. Soc. London A, 209, 158-177, 1951b.
- Ogawa, T. Private communication, 1962.
- Pierce, E. T., and T. W. Wormell, Field changes due to lightning discharges, in Thunderstorm Electricity, edited by H. R. Byers, University of Chicago Press, 1953.
- Pierce, E. T., Electrostatic field changes due to lightning discharges, Quart. J. Roy. Meteorol. Soc., 81, 211-228, 1955a.
- Pierce, E. T., The development of lightning discharges, Quart. J. Roy. Meteorol. Soc., 81, 229-239, 1955b.

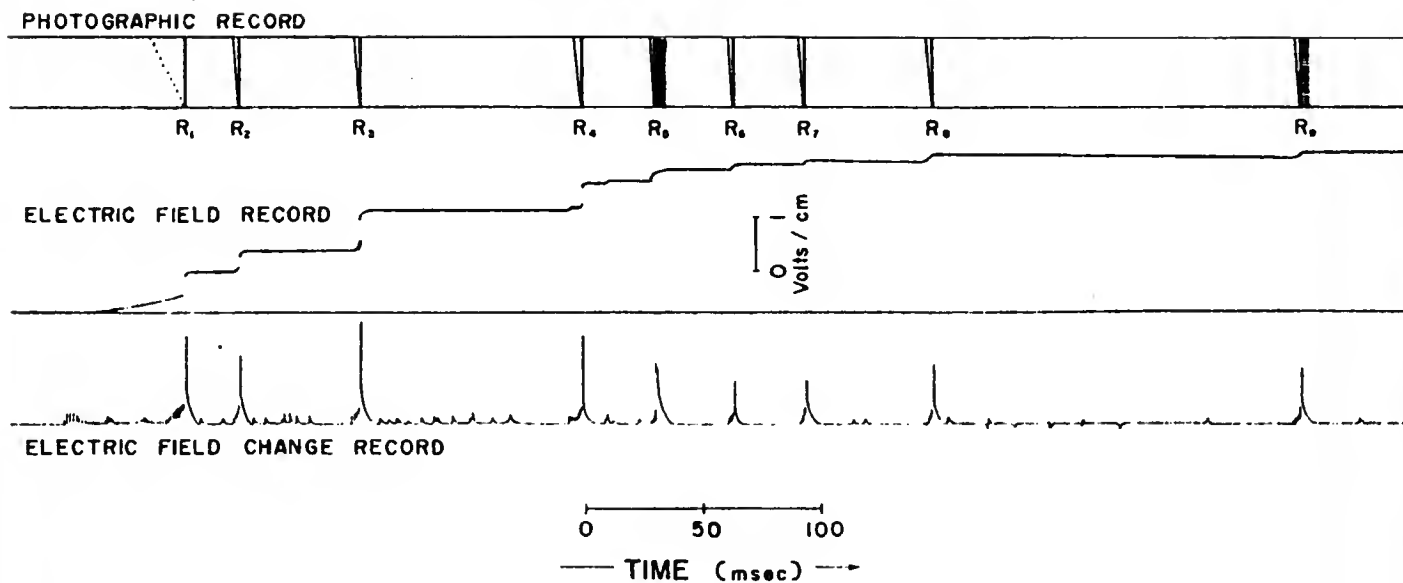
Reynolds, S. E., Compendium of Thunderstorm Electricity, (Signal Corp Project, 172-B), New Mexico Institute of Mining and Technology, Socorro, New Mexico, 1954.

Schonland, B. F. J., The lightning discharge, Handbuch der Physik, 22, 576-641, 1956.

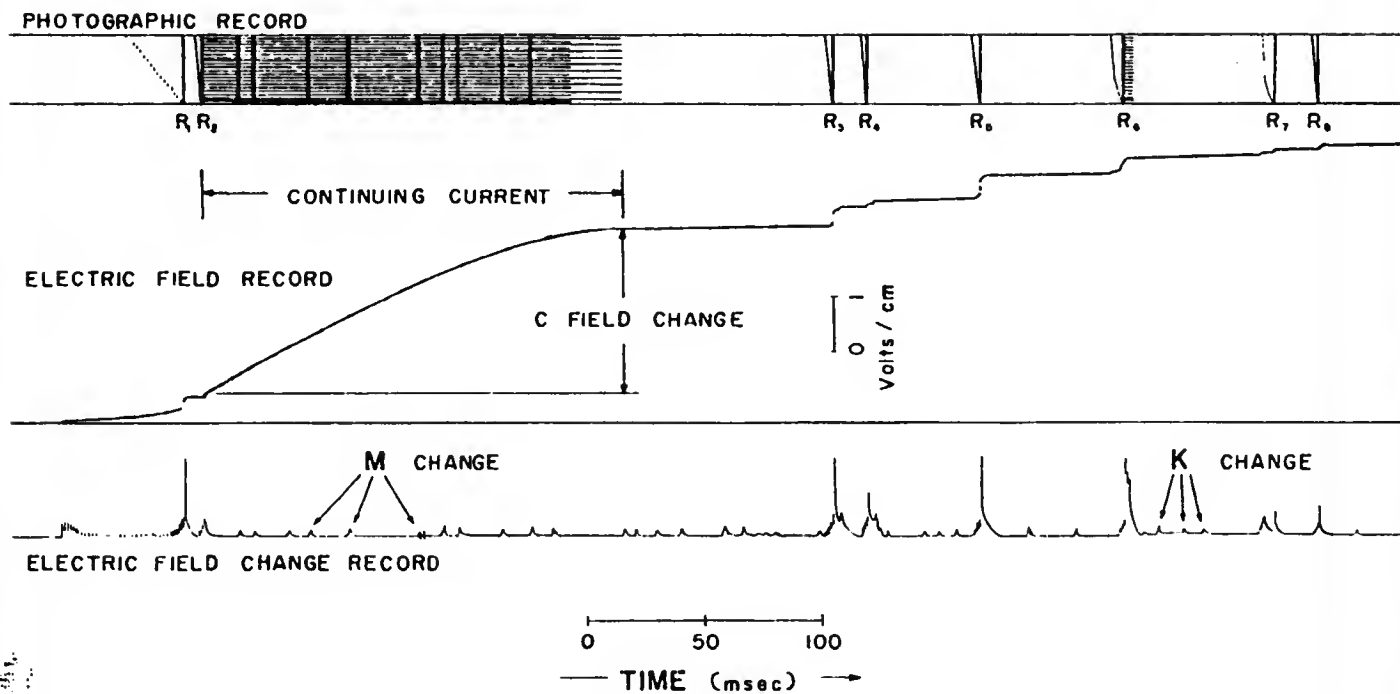
List of Figures

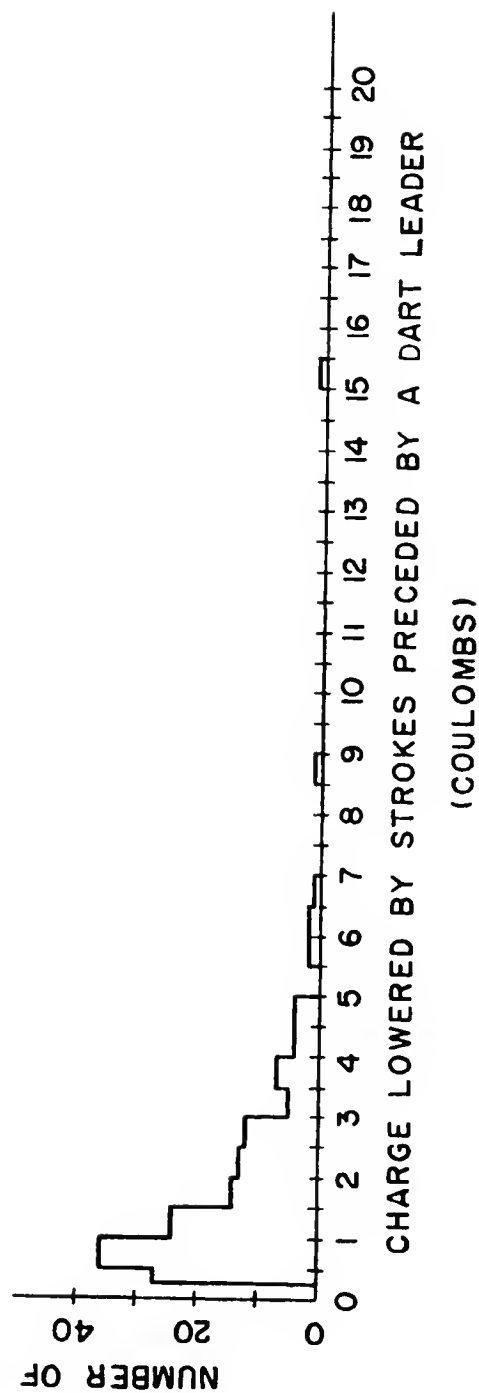
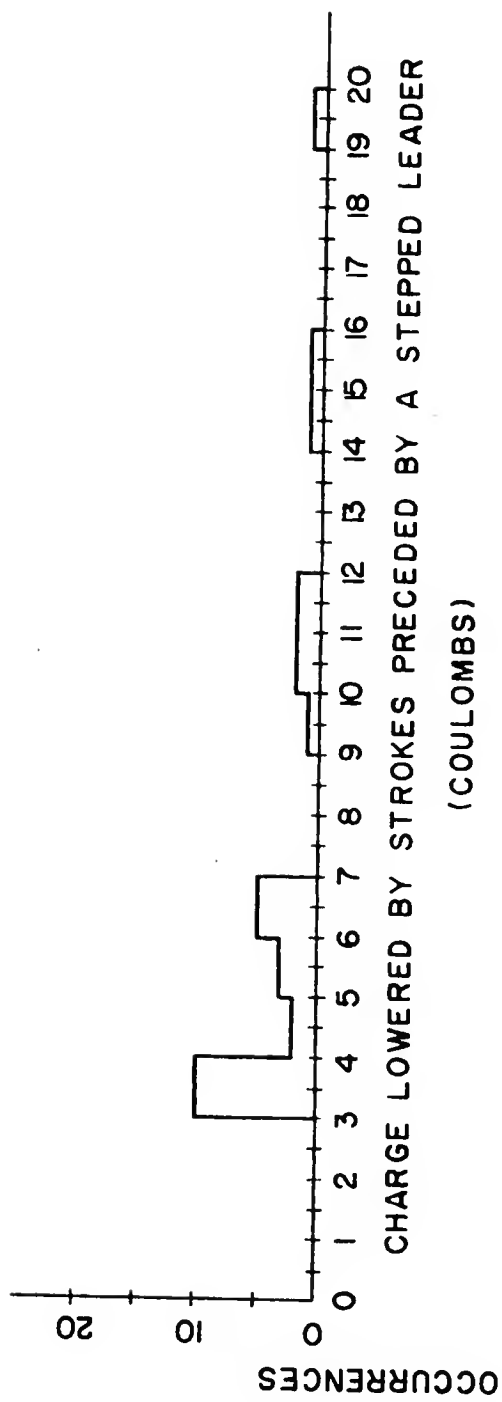
- Figure 1 : Examples of simultaneous photographic, electric field, and electric field-change records of discrete and hybrid flashes. Positive deflections are upward.
- Figure 2 : Frequency histograms of (a) charge lowered by strokes preceded by a stepped leader, and (b) charge lowered by strokes preceded by a dart leader.
- Figure 3 : Graph of charge vs. duration for the continuing current.
- Figure 4 : Apparent height vs. stroke order for strokes in discrete and hybrid flashes.
- Figure 5 : Frequency histograms of (a) M-component intervals in continuing luminosity; (b) K-change intervals in discrete intervals of C-G discharges; and (c) K-change intervals in later portions of I-C discharges.
- Figure 6 : Examples of simultaneous electric field-change (above) and electric field (below) records of a I-C discharge. Positive deflections are upward.

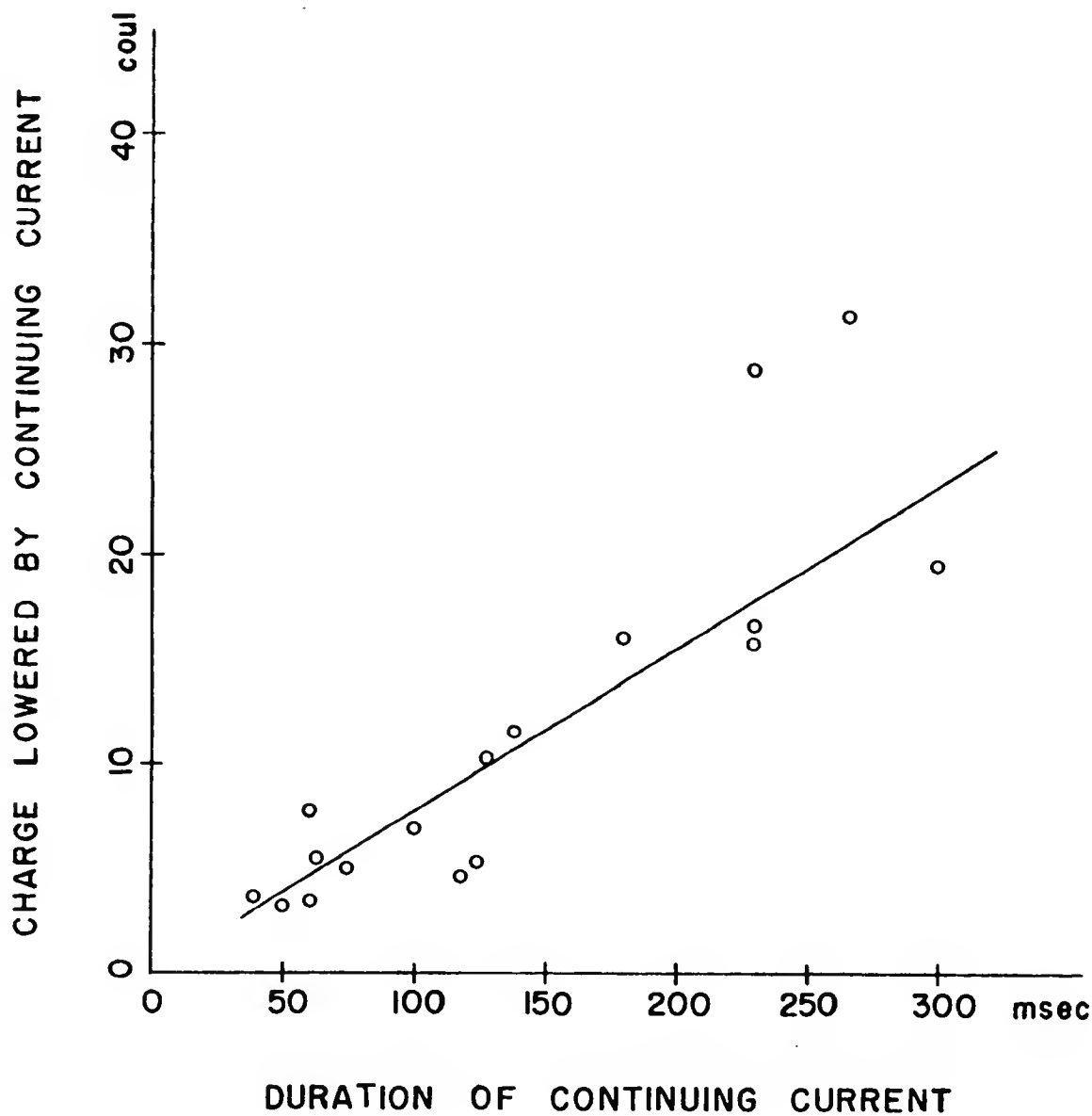
DISCRETE FLASH



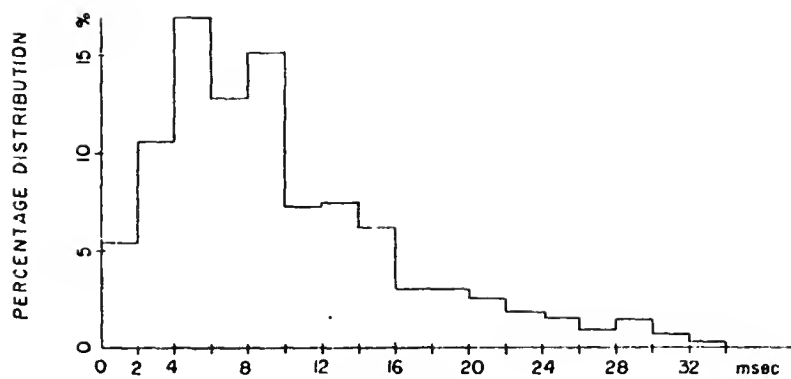
HYBRID FLASH



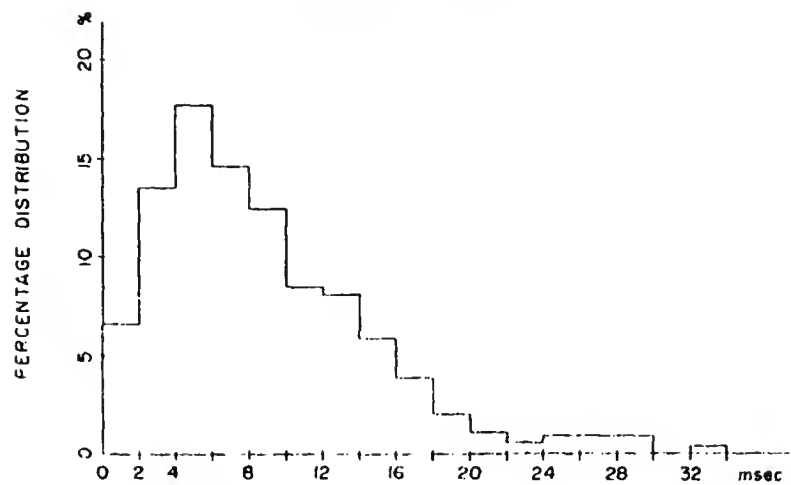




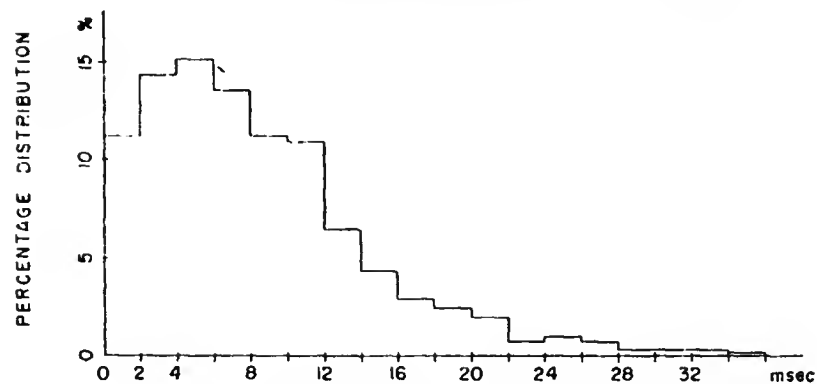




(a) M COMPONENT INTERVALS



(b) DISCRETE K-CHANGE INTERVALS—C-G DISCHARGES



(c) K-CHANGE INTERVALS—I-C DISCHARGES

SESSION 8.1

Lightning Protection

D. Müller-Hillebrand

Institute of High-tension Research, University of Uppsala,
Uppsala, Sweden

Physical research on lightning and the practical application of its results are intimately related to each other. The demand for security against damage by lightning has greatly stimulated research. Lightning discharges affect buildings, power lines, machines and equipment, and telecommunications systems. They can cause damage to aircraft and during tunnel blasting deep down in a mountain. They kill and injure living creatures and cause fires and accidents. All this has given rise to innumerable investigations and publications in the majority of civilized countries in which lightning is a problem. Summaries on lightning protection matters have often been published. An early work by Goodlet (1) deals with questions such as the shattering of poor conductors, damage to buildings, oil-tank fires, damage to aircraft and effects on living creatures. A more recent work by McEachron (2) gives, in the first place, an account of protective measures for communications and power-supply systems. The present report can only give a limited survey of such protection questions as have still not been completely elucidated; they relate, on the one hand, to physical phenomena and, on the other, to statistical and probability investigations, which are often connected with financial problems.

The publications from the Golden Age of lightning research - from about 1750 to 1780 - often show acute observation of nature in connection with protective measures. As an example, I quote two observations by Benjamin Franklin which touch on quite topical questions. The first shows his view of the limited protective range of an elevation rod - a question which is always being discussed. In "Poor Richard's Almanac" for 1753 Franklin writes:

- 2 -

Provide a small Iron Rod (it may be made of the Rod-iron used by the Nailers) but of such a Length, that one End being three or four Feet in the moist Ground, the other may be six or eight Feet above the highest Part of the Building. ... If the House or Barn be long, there may be a Rod and Point at each End, and a middling Wire along the Ridge from one to the other. ...

The instruction is later repeated in Franklin's 24th letter (3).

The second observation makes clear the protective effect of a thin wire, in a case which is topical today, as regards finance. The church at Newsbury in New England had been badly damaged by lightning in the summer of 1754. Franklin gives a detailed account of the destruction. I reproduce extracts from his letter to Dalibard (3):

The spire (of wood, reaching 70 feet higher than the 70 feet high steeple) was split all to pieces by the lightning, and the parts flung in all directions over the square in which the church stood, so that nothing remains above the bell. ... From the end of the pendulum, down quite to the ground, the building was exceedingly rent and damaged, and some stones in the foundation wall torn out and thrown to the distance of twenty or thirty feet. ...

The central portion was not damaged. The lightning current had destroyed a thin wire which connected the clapper of the bell to the clock mechanism 20 feet away. The flash was conducted to the pendulum wire, which had the thickness of a goose quill. Franklin draws the following conclusions:

1. That lightning, in its passage through a building, will leave wood to pass as far as it can in metal, and not enter the wood again till the conductor of metal ceases. And the same I have observed in other instances, as to walls of brick or stone.
2. The quantity of lightning that passed through this steeple must have been very great, by its effects on the lofty spire above the bell, and on the square tower all below the end of the clock pendulum.
3. Great as this quantity was, it was conducted by a small wire and a clock pendulum, without the least damage to the building so far as they extended.
4. The pendulum rod, being of a sufficient thickness, conducted the lightning without damage to itself: but the small wire was utterly destroyed.
5. Though the small wire was itself destroyed, yet it had conducted the lightning with safety to the building.
6. And from the whole it seems probable that, if even such a small wire had been extended from the spindle of the vane to the earth, before the storm, no damage would have been done to the steeple by that stroke of lightning though the wire itself had been destroyed.

- 3 -

Before concluding this short historical survey, I show (Fig. 1) one of the earliest lightning-conductor drawings ever published - a lightning conductor designed by Torbern Bergman for a building in Uppsala, Sweden, in 1765. Even at that period the special instruction is given that large metal parts in the building should be connected to the lightning conductor (4).

The Lightning Path near the Ground

Space charges between cloud and earth greatly affect the lightning path. A visible proof of this is the "Type β leader" according to Schonland (5, 6), which has a high velocity (more than 6×10^7 cm/sec = 600 m/ms) between the base of the cloud and the space-charge layer (first stage) and a low velocity (about 1×10^7 = 100 m/ms) and often a pronounced fork in its further career to the ground (second stage). About 30% of the leaders in South Africa showed this phenomenon (7). The charges in the water-vapour cloud are transported to and distributed over the space-charge cloud. These charges consequently become "over-neutralized". The leader's space-charge channel receives additional charge and thereby has a greater volume than it would have had if the space-charge layer had not existed. On the return stroke the lightning channel accordingly receives a substantial additional charge. The current strength is increased. The course of the lightning current, according to Berger (8), who recorded it on the summit of Monte San Salvatore, shows that a current maximum is reached after 5-10 μ s. The vertical length of the lightning channel after 5-10 μ s is approximately 400-1200 m (5). The order of magnitude of the distance between the space-charge cloud and the ground agrees with the length of the leader's "second stage" measured by Schonland *et al.* At Monte San Salvatore the space charges may be particularly heavy. The two 70-metre-high towers on the 600-metre-high mountain both generate glow discharges in the static electric field. The charges - approximately 1 Coul in 10 minutes - may affect the lightning path. The statistics of

- 4 -

lightning strokes to ground show this clearly (9). The annual number of lightning strokes to these towers is 29. If this is converted to 10 lightning days (corresponding to an isocerannic level of 47 lightning days) we obtain 6.2 strokes per year, the same order of magnitude as on the Empire State Building in New York and approximately 25-75 times greater than on a 70-metre-high tower on level ground (10).

How a leader develops near the ground is not known in detail. To calculate the field strength on the ground near the leader certain assumptions have to be made as to the charge distribution in the leader channel. Schonland assumed that the charges are evenly distributed over the length of the leader (5). Bruce and Golde (11), on the other hand, assumed that the charges decrease exponentially with height, corresponding to e^{-h/h_0} . The constant h_0 is between 54 m and 1430 m. Pierce (12) points out that the line density of charge along the channel cannot be uniform. It is probably greatest towards the middle portions. In the immediate vicinity of the cloud the charges are slight, as the potential difference is comparatively small. At the ground end the potential difference is great, but the time is not sufficient for the extensive production of charge. Griscorn (13) evolved a theory according to which the space charges at the end of the leader are concentrated in a ball with a relatively large diameter. The reason for his discussions was an unexpectedly large number of flashovers in a high-tension network. Fig. 2 shows the charge distribution according to these different assumptions. In calculating the attraction distance between the leader and an object on the ground, the charge distribution in Fig. 2 plays an essential part. Thus Golde (14) calculates the distance between the leader, according to Fig. 2b, and the ground with different intensity values of the space charge for one field strength on the ground. A leader charge of 1 Coul, according to Golde, corresponds to a lightning current of 20 kA. Distributed exponentially, with $h_0 = 1000$ m, this charge at a distance of 17 m from the ground generates a field strength of 10 kV/cm. With a lateral distance of 45 m, calculated in the same way, the field strength is 3 kV/cm and consequently sufficient to start

- 5 -

a capture discharge from an object about 20 m high to the leader. The attraction distance is thus $\sqrt{17^2 + 45^2} = 48.1$ m. This ^{method of} calculation of the attraction distance for smaller space charges and consequently smaller current strengths receives support from many observed lightning strokes on lower objects adjacent to high objects or horizontally to low objects. Fig. 3 shows an example (15), a stroke horizontally on a farmhouse roof to the lightning-conductor cable, which was located the width of two bricks from the edge of the roof. The damage was comparatively slight, a fact which is often observed in connection with such phenomena, for example, in the first "classical" lightning stroke at Purfleet, England, in 1777 (16) on the Meeting House of the Artillery College, which was furnished with a lightning arrester. The lightning did not strike the rod but struck an iron corner clamp above the cutlery. The tip of the rod formed a protective angle of 31° and was 14 m from the point struck. Here also the damage was insignificant, but the fact that a lightning conductor with a protective angle of 31° could not prevent it caused a great sensation at the time, without it being possible to give any explanation.

The protection of high-tension lines against direct lightning strokes with the aid of earth wires is an important technical problem which has given rise to many investigations, both theoretical and experimental. Davia (17) took up afresh the problem of calculating the protective value of these earth wires and consequently the frequency of lightning strokes to high-tension lines. He calculated the flashover voltage between the end of the leader and the ground with the aid of an impulse flashover gradient based on extrapolated experimental values. He determined by geometrical calculations the effectiveness of the ground wires' shielding angle in relation to the high-tension line. The shielding angles ranged from 45° to 15° . With a shielding angle of 45° in an earth wire at a height of 20 m, flashes with a current strength of over 37 kA would be intercepted by the earth wire. With a shielding angle of 20° the corresponding current strength is 20 kA. It can be deduced from the statis-

- 6 -

tical distribution of lightning currents that the number of lightning strokes to the transmission line would be reduced from about 40% to 17% (10 to 4.25). This does not tally with practical experience. The quantitative calculation is dependent on very approximate assumptions as to the distribution of the charges in the leader. The geometrical method cannot take into account metre-long corona discharges which are generated from the cables and alter the geometrical picture.

Grindley (18) calculated the magnitude of the charges bound on earth wire and on phase conductor by the leader in some distant part of the wires. Equality of charges is taken as a condition in which both wires are equally likely to be struck. The charges are calculated from the field due to the leader and it is shown that equality of charges corresponds to both wires being at the same equipotential of the leader. Calculation suggests that shielding is normally adequate for conductors in a wedge, of which the apex line is the earth and of semi-vertical angle 45° . At a shielding angle of 45° an earth wire would consequently offer perfect protection. Fig. 4 shows that this does not agree with experience. This figure is a collocation of lightning faults in high-tension lines operating at 275-400 kV and a few lines below 275 kV with a low earth resistance in the pylons. The majority of these faults arose from lightning strokes to the line. The values are derived from a tabulation by Kastenka (19) and have been converted to a line length of 100 km, 100 lightning days and a line height of 30 m. According to this tabulation, the faults are reduced from about 10 to 0.25 when the shielding angle is reduced from 45° to 20° . In addition to Kastenka's values for protective lines about 30 m high, the values published by Burgsdorf (20) for 220 kV, 150 kV and 110 kV lines in the USSR are also reproduced (Fig. 4). These lines have an average height of 15 m. The original values have been converted from 30 lightning hours (= 20 lightning days) to 100 lightning days. The number of lightning strokes to the phase conductor increases very substantially with increasing shielding angle. The risk of a stroke increases approximately quadra-

- 7 -

tically with the height of the object (10). If these values, which were established for lines 15 m high, are converted to a height of 30 m by a factor of 4, the agreement is then satisfactory.

T. Horváth (21) has attempted to avoid the disadvantages of a geometrical calculation by means of an experimental model investigation. He determined the probability distribution of the critical distance between the leader and the grounded object with the guidance of Golde's calculations and of the statistical distribution of lightning currents. By model experiments on a scale of 1:30 to 1:100 he determined the probability of a lightning stroke on the conductor, which was protected by an earth line with shielding angles of 20° and 30° . By reducing the shielding angle from 30° to 20° , the number of lightning strokes was reduced in the ratio of 10:1 in these model experiments on a scale of 1:50. This agrees with experience, as shown in Fig. 4. But the problem is not thereby solved, as the experiments are based on uncertain assumptions as to the critical distance. The relative amplitude of the pre-discharges in these model experiments is not in accord with reality. These model experiments do not reproduce correctly the influence of the height of the line on the frequency of lightning strokes. An alteration in the scale of the model and thereby the height of the line in the ratio of 2:1 results in a change in the stroke frequency in the ratio of 30:1 with a shielding angle of 20° and of 10:1 with a shielding angle of 30° and therefore not in agreement with observed values.

The question of the influence on the lightning path of corona discharges from lightning-conductor points is as old as lightning research. This complex of questions includes Dauzère's inquiries concerning an accumulation of lightning strokes on a boundary line between two different geological formations. According to Dauzère, the emanation of radium from geological discontinuities influences the lightning path through the ionization of the air. About ten investigations ensued. Some showed a tendency to strive after ~~clap-trap~~ ^{commercial}. The question would long ago have been laid ad acta if substantial ~~financial~~ interests had not been

- 8 -

involved in protecting buildings centrally by a single radio-active point. The γ -radiation generated by these radio-active lightning conductors can be demonstrated by sensitive instruments at a distance of several hundred metres. But the ionization of the air should be 10^6 to 10^8 times more powerful than the ionization that can be produced by a radio-active point, to have any possible effect on the lightning path (23). Uncertainty in judging electrical effects in the atmosphere is often a result of incorrect measurements. Unfortunately, many investigations made before 1942 are valueless on account of fundamental errors in measurement, particularly as regards the electrostatic field in thunderstorms. In low-lying land with plants, trees and grass the field is limited to values which seldom exceed 10 kV/m. Incorrect measurements at a height of 600 m above sea-level at the High Knob station in

, for example, resulted in field strengths with an average value of 200 kV/m. Ten per cent of the measured values showed a field strength of more than 260 kV/m (24). Even with a field of 6-10 kV/m all plants produce such intense space charges that the electrostatic field seldom exceeds 10 kV/m. With a field of 70 kV/m, discharges on a man's fingers are visible. Only in areas without these "points", for example, at sea, can such powerful electric fields arise that St. Elmo's fire can be formed on a ship. There is consequently a conceivable risk of lightning strokes on ships, but with the steel ships of today this is no longer of current interest.

The Lightning Path on the Ground

The statistical frequency of lightning currents and charges is fairly well known through many investigations (25). Their probability distribution is represented within certain limits by a normal logarithmic distribution. If the percentual number of the magnitude x (current or charge) within the limits Δx is denoted by Δz , the distribution is expressed by

-9-

$$\frac{\Delta x}{x} = \frac{1}{\sqrt{2\pi}} \cdot \frac{1}{M s x_0} \cdot \frac{(x_0)}{x} e^{-(\log(x/x_0))^2 / 2s^2}, \quad (1)$$

where x_0 is the ~~mean~~ ^{median} value, M the base of the natural logarithm (2.303) and s the standard deviation. The mode of distribution x_{mod} is

$$x_{\text{mod}} = x_0 e^{-(Ms)^2} \quad (2)$$

and the arithmetical average value x_{arith}

$$x_{\text{arith}} = x_0 e^{+(Ms)^2 / 2}. \quad (3)$$

The probability of the magnitude x is calculated by the Gaussian distribution

$$P = \frac{1}{\sqrt{2\pi}} \int_{-\infty}^t e^{-t^2/2} dt \quad (4)$$

$$t = \frac{1}{s} \log(x/x_0). \quad (4a)$$

where

Table 1

Some typical values are given in Table 1. Column 1 reproduces the values ~~values~~ recommended by the AIEE for lightning currents above 5 kA (26). According to this tabulation, with 18 kA as ~~mean~~ ^{median} value, the current strength which occurs most frequently is 10 kA. The arithmetical mean is calculated as 23.7 kA. Column 2 shows the average values in investigations by both Berger and Stekolnikov and measurements in Sweden (25) which take into account current strengths below 5 kA. The current strength which occurs most frequently is 4.25 kA. The arithmetical mean is 22.8 kA. The charges in column 3 are values for a single lightning stroke. Column 4 gives charges for a complete lightning discharge consisting of multiple discharges and prolonged discharges (25).

Extrapolation for a cumulative value less than 2% would give values too large for the current strength. If the percentage of lightning currents greater than 50 kA is drawn on log-lin paper, P_J for $J(A)$ lightning currents, according to columns 1 and 2 in Table 1, is represented by the following expressions:

$$P_{J_1} = e^{-0.384 \times 10^{-4} (2 \times 10^4 + J)}, \quad (5a)$$

$$P_{J_2} = e^{-0.288 \times 10^{-4} (3 \times 10^4 + J)}. \quad (5b)$$

with J the current in A.

- 10 -

Table
2

If the current strength is calculated for a probability $P = 0.1$ and less, according to (5a) and (5b), the values given in Table 2 are obtained. Powerful strokes with current strengths exceeding 200,000 A occur very seldom.

Table
3

The ~~current-heat~~ current-heat impulse $\int i^2 dt$ has not been systematically investigated. Practical experience is available from investigations with a power transmission line from Boulder to Los Angeles (27) carrying 287 kV in an area with about 30 lightning days a year. Three stations are shielded against lightning strokes by capture towers 50 m high, carrying earth wires. These towers and some pylons, 80 towers in all, are furnished with elevation points, magnetic links for current measurement and six copper wires connected in series (see Table 3). The current-heat impulse values given have been calculated from experimental investigations by Poitzik (28).

Experience over 20 years shows that, in lightning strokes on these towers, 1, 2 or 3 wires are destroyed, never 4. One example mentioned is a current strength of 43 kA, which destroyed wires nos. 1-3. On another occasion 36 kA were measured without wire no. 1 being destroyed. Bellaschi (29) determined experimentally the connection between the current impulse (decreasing exponentially) and the half-value period T_H required for fusing copper wire:

$$I = 3,2 \times 10^5 \times \frac{A}{\sqrt{T_H}} \quad (6)$$

where A is the cross-section in mm^2 and T_H the half-value period in μs .

With a 36 A peak current which does not fuse 0.81 mm wire, the half-value period, according to (6), is less than 40 μs . The probability of these towers being struck would seem to be at least 0.15 per year. With 80 towers and 20 years' experience the probability of the current-heat impulse being sufficient to destroy a 2.09 mm^2 copper wire is thus less than 0.4%.

After 16 years of measurements at San Salvatore, Berger (9) confirms that the current-heat impulse was greater than $1.5 \times 10^6 \text{ A}^2 \text{ sec}$ on five

- 11 -

occasions and greater than $6.4 \times 10^6 \text{ A}^2$ s on one occasion. The corresponding probabilities are about 0.75% and about 0.15% respectively. These results are collated in Table 4.

Table
4

The maximal velocity at which the lightning current increases in strokes to the ground (di/dt) has not been so comprehensively investigated as to enable the observational material to be treated statistically. Direct measurements on tall chimneys, carried out by Hyltén-Cavallius and Strandberg (30), showed on several occasions di/dt values greater than $30 \text{ kA}/\mu\text{s}$ and once a value of about $100 \text{ kA}/\mu\text{s}$. At $30 \text{ kA}/\mu\text{s}$ the inductive voltage drop in a ~~cable~~ ^{line} with an inductance of $1.67 \mu\text{H}/\text{m}$ is $50 \text{ kV}/\text{m}$. Oscillographic measurements of the lightning current make an analysis possible. Berger (8) was able to show a current rising to the maximum value after $5-10 \mu\text{s}$ as a consequence of a first downward-progress leader from a negative cloud and of an upward midgap streamer from the air (Fig. 5a). Ten per cent of the measured course shows a steepness greater than $25 \text{ kA}/\mu\text{s}$. Partial strokes from negative clouds, which follow either the first discharge, in accordance with Fig. 5a or the prolonged discharge typical of San Salvatore of a few tens or hundreds of ampères, have a front period of only one or a few microseconds (Fig. 5b). The specific steepness is thus substantially ^{greater} than with a current course in accordance with Fig. 5a. The method of measuring the current course with the aid of a delay cable has been used since 1960. The results are consequently not ^{yet} so numerous as to ^(enable) a statistical analysis to be carried out.

The multiplicity of courses which lightning current can take on and in the ground results in numerous and varying phenomena connected with questions of protection. Extreme and uncommon phenomena attract particular attention in this connection and are naturally more conspicuous than the more common cases. The following phenomena are mentioned briefly and are illustrated in individual cases by examples.

1. Power phenomena, for example, in a lightning-conductor ~~cable~~ ^{line}. The power increases as the square of the current strength. With a

- 12 -

lightning current of 100 kA there comes into existence a power of 500 kp in a ~~cable~~ ^{line} which follows a very pronounced cornice on a building. In addition breaking forces arise in straight lengths.

2. The following are some of the manifold voltage phenomena at the place of striking, and starting from the point of striking:

(a) Voltages of up to several million volts as a result of the resistance in transit to earth.

(b) Sliding discharges from the point of striking to the surroundings up to a distance of 50 m, arising in very poorly conducting bedrock, for example, granite.

(c) Voltage differences in a cable as a result of rapid change in the lightning current. The voltage difference may be 100 kV per metre of ~~cable~~ ^{line} at 60 kA/ μ s.

(d) "Displacement" of voltages to distances of many hundreds of metres through fissures in rock (tunnel building), wire fences, power lines or underground cables.

3. Heat phenomena.

(a) When the striking place consists of metal, power is supplied to the surface of the metal equivalent to the strength of the lightning current times the anode voltage drop. At 100 kA a power of about 1000 kW is supplied. The ^{w)}power density in copper is about 800 kW/cm² and in aluminium 350 kW/cm² in the first 10 μ s and then decreases owing to the reduction of the current density.

(b) In the interior of the metal current heat arises, which is inversely proportional to the fourth power of the linear dimensions of the conductor, for example, the wire diameter or the plate thickness.

(c) Transmission of heat from the lightning channel to the surroundings, thereby causing fire. With a lightning stroke in sand fulgurites may be formed. At 100 kA the power is approximately 150,000 kW/m in sand.

4. Pressure phenomena.

(a) In the rapid expansion of the lightning path as a result of

- 13 -

a rapid growth in the lightning current, a pressure wave arises which is released from the lightning channel at supersonic speed. The ~~pressure~~ pressure and the wave impulse may produce considerable damage.

(b) The same phenomenon may arise in the vaporization of metal wires.

(c) Turbulent forces ~~are~~ arise in the evaporation of water in a cleft. Trees split in most cases. At 100 kA blocks of stone weighing 5 tons may be torn off and rocks weighing 100 kg thrown 20 m.

This short tabulation will be illustrated by a few examples.

1. On June 15, 1956, lightning struck the church at Rudolzhofen (Bayern, Germany) and did extensive damage to the lightning-conductor installation and to the church (31). Fig. 6 shows a semi-diagrammatic picture. From the top of the tower two copper conductors ran to earth, one ($4 \times 3 = 12$ wires, 30.6 mm^2) directly and the other (7 wires, 24.2 mm^2) over the body of the church. The cables were torn to pieces in at least seven places, denoted in Fig. 6 by the figures 1 to 7. (The conductor with lightning faults 1 and 2 ran down the other side of the tower. The power input similarly took place on the other side. Fig. 6 was drawn with this down lead on the front side for the sake of a more perspicuous survey.) At 1 the slate roof was damaged. At the grounding point 8 a hole appeared in the concrete pipe which had been used as a mechanical protection. The rainpipe was damaged at I and II. A flashover had occurred from the down lead to the rainpipe at a distance of about 30 cm and from the rainpipe to the power cable, similarly at a distance of 30 cm. The cable in the church ($4 \times 1.5 = 6 \text{ mm}^2$) was vaporized for a length of 10 m, equal to 0.5 kg of copper. Considerable pressure damage was done to the organ and the electrical installation. Examination of the material showed that the temperature of the cable had been about 700°C . To heat copper cables of 54.8 mm^2 to red heat, a current-heat impulse of $1000 \times 10^6 \text{ A}^2 \text{ s}$ is required and to vaporize 6 mm^2 copper, $37 \times 10^6 \text{ A}^2 \text{ s}$. From these power and heat phenomena the strength of the

- 14 -

lightning current can be estimated as 300,000 kA, which, with an effective duration of at least 11 ms, meant a cloud charge of over 330 Coul. Such phenomena occur with a probability of less than 1:100,000 (see Table 2).

2. Fig. 7 shows the situation in a lightning stroke which caused considerable damage to a house without the lightning conductor being able to prevent it (32). The flash had struck a birch tree about 20 m high at a distance of 35 m from the house. The tree stood on granite covered with a thin layer of soil. The area was strewn with large and small stones. Several traces led from the tree, which was totally splintered. One trace, more than 35 m long, led to the house. Several cubic metres of earth and stones had been thrown up, six windows had been smashed and 40 or 50 litres of earth and stones had been flung into the upper floor of the house. Via the cellar the flash had struck a wall socket for the electric cable in the kitchen, about 1.5 m above ground level. The cable ($2 \times 1.5 \text{ mm}^2$) was vaporized. The trace then disappeared into a 4 mm^2 cable (and) thence to a water-pipe with a flashover approximately 10 cm in length. Four persons who on this occasion were sitting only 2 m away from the vaporized cable were uninjured. This phenomena - that a house may be struck and damaged from under ground - is not particularly uncommon in Scandinavia when granite is the bedrock (33). Experimental investigations of peak currents in clefts permit an extrapolation to a current strength of 100 kA with a half-value period of 200 μs . In damp sand the amount of energy developed in such cases is approximately 1000 kWs per metre of the lightning path. This is equivalent to the energy developed in the detonation of 215 g of dynamite or 350 g of gunpowder per metre.

"Displacement" of the voltage plays an important technical part. In tunnel construction in high mountains, primers prepared for blasting have been exploded too soon and accidents have been caused. As a safety measure the cables are provided with a metallic sheath (34) and special primers are used which require substantially greater power for firing than the ordinary primers, which ignite even with a power of 1 mWa (35). The cables in the ground may be exposed to a direct lightning stroke at a distance of several tens of metres from the place of striking. Telephone

- 15 -

cables connected with overhead lines are exposed to indirect and direct lightning action. Conious specialist literature shows the importance of safety measures (36-40, a limited selection).

3. In a lightning stroke on a lightning conductor, high voltages may arise in the ~~cable~~^{line}, with the result that a flashover may occur indoors to electric cables or telephone wires 40 or 50 cm away. Many fires have been caused in this way. These high voltages are then transferred via power or telephone lines to adjacent houses. It is, however, often possible to establish that the damage at a distance of about ~~about~~ 10 m from the point of striking is fairly slight. McCarthy et al. (41) analyse a lightning stroke on a church in north-western Pennsylvania with the aid of installed oscillographs and magnetic links. The lightning stroke shattered a 4" by 6" by 18' wooden rafter, left the steeple and terminated on the wiring above the ceiling. The church had no lightning conductor - the electrical installation was the lightning conductor. Some fuses were blown and some lamps vaporized, but neither the watt-hour meter nor the 7.2 kV transformer 60 metres away was damaged or affected by the flash. The lightning current was established as having been 31.7 kA. Of this, 4.6 kA went to earth in the transformer, 19.5 kA to the high-voltage-grounded conductor and 6.7 kA to the high-voltage phase conductor via the transformer. The duration of this partial current was determined oscillographically as longer than 2000 μ s. Similarly the damage to the electrical system in the case of the powerful flash at Rudolzhofen (Fig. 6) was very slight. Fig. 8 shows the damage in the general plan, denoted by figures 1-8; fuses blown, lamps vaporized and flashovers in junction boxes. No meter was damaged, in spite of the fact that the distance to some installations was less than 30 m from the place of striking.

4. Very high voltages may arise in lightning strokes on a thick bed of sand, the foundation of which consists of a better conductor, for example, clay. The lightning channel goes almost perpendicularly down. The voltage gradient is about 100-150 kV/m. After about 100 μ s of contact with the lightning channel pressed into the sand, fulgurites arise. The temperature of the lightning channel, according to spectroscopic

- 16 -

measurements by Mandelstam (42), is 16,000-25,000°C. Fulgurites arise at 1900°C. Their generation can only be established in a chance direct observation of a lightning stroke in sand (43). In the atmosphere the pressure is propagated as a detonation wave, which can shatter window panes at a distance of about 10 m. Fig. 9a shows a remarkable case of damage caused by pressure to a window pane. An almost circular disc (160/170 mm in diameter, glass thickness 2.5 mm) with sharp edges had been cut out of the pane. The window was an external one, separated from the undamaged inner one by a space of about 50 mm. The round disc had fallen down between the two windows. (The window is in the Institute's archives, initiated by Professor H. Norinder.) Böckmann (44) describes similar damage (Fig. 9b) in June 1754 to a hothouse in Karlsruhe. The window was torn out of the frames in which it was nailed and thrown out into the garden - a result of the negative pressure. The explanation of the damage may be that the stress on the glass through the pressure wave and ~~the pressure~~ ^{depression} wave of the lightning channel was reinforced to breaking point through the wave's being propagated in the glass and reflected at the edge of the glass.

Lightning Protection in the Light of Standard Codes

The knowledge and practice of that time was summarized by the Lightning Rod Conference in London in 1878 (45). About 25 years later individual countries - England, the USA and Germany - began to draw up instructions and guiding principles dealing with the protection of different kinds of buildings, towers, chimneys, ships and last but not least structures containing inflammable liquids, gases and explosives. A tabulation of the codes available to me is given as ref. (46). On the whole, the instructions are much the same but on closer scrutiny show divergent views which are not due to the individual character of particular countries.

The question of the zone of protection is not dealt with in a uniform manner. In the USA (16, m) a shielding angle of 45° in important cases and 63° in less important cases is considered sufficient (Fig. 10).

- 17 -

In England (46, 1) a shielding angle of 45° is given, but not, however, for particularly important buildings, such as explosives factories, oil and petrol tanks, etc. In the USSR (46, n) the shielding angle is subdivided. In a chimney 52 m high the shielding angle for the upper part is very limited (Fig. 11). For the lower part a protective radius of 40 m is stated on the basis of model experiments.

Contrary views on elevation rods are made clear by Figs. 12 and 13. In the USA several elevation rods are recommended, for example, 15 on "the typical installation on a barn group". In Germany special rods are not recommended on the roof of a farmhouse. The roof conductors act as an air terminal. Some awe-inspiring objects (Fig. 14) included in the Code for Protection against Lightning (1959) in the USA are probably of most use on the psychological plane. According to British Standard BS (46.1), an air termination need not have more than one point and should be at least 1 foot above the salient point on which it is fixed. We accordingly see that the dimensions of the elevator rod, which was formerly 10 feet high or more, are now only rudimentary (Fig. 15).

In all the instructions the question of reliable grounding plays an important part. In England a maximum value of 10 ohms is prescribed (45, 1, 308c). In Austria this is not possible at ^{economically} ~~financially~~ justifiable expense in certain provinces. The Austrian instructions (46, a, 10, 3) therefore allow higher ^{resistance} ~~transition~~ values than 10 ohms for a specific earth resistance of more than 250 ohms/m. For this, exact instructions with various examples are given. In the USA (46, m, 217h) it is laid down that low resistance is, of course, desirable but not essential. By a building resting on a base of solid rock it would be impossible to make a ground connection in the ordinary sense of the term. The most effective means would be an extensive wire network laid on the surface of the rock surrounding the building, after the manner of a counterpoise to a radio antenna. Here we approach the standpoint of James Clerk Maxwell (47) that "earth" does not exist in the protection of buildings against lightning. The essential thing is to prevent potential differences. Maxwell in 1876 suggested making a construction like a cage with 6 mm^2 copper wires. In

- 18 -

modern houses with heating systems, water-pipes and electric cables, not many wires would be needed to complete the whole arrangement according to Maxwell's suggestion (Fig. 16).

The cross-section of the conductor necessary for the discharge has for many decades been fixed more on the basis of the craftsman's experience of mechanical strength and of practical knowledge of very powerful lightning strokes than on the basis of physical investigations and calculations of probabilities. For the protection of aircraft, however, it was necessary to determine the cross-section of the conductor for bonding purposes. The current-carrying capacity of the bonding system has to be such that a lightning discharge current can be carried between any two extremities of the airplane without risk of damaging flight controls and external surfaces or of producing excessive voltages within the aircraft. The investigations were carried out with peak currents up to 100 kA, reaching the crest value at 10 μ s and dropping to 50 kA at 20 μ s. For this a copper cable with a cross-section of 3.3 mm² or an aluminium cable with a cross-section of 5.1 mm² was necessary (48). With a few exceptions the cross-section prescribed in the standards of different countries is a result of experience in building technique *and is much bigger.*

Lightning protective systems can be divided into three groups: (1) super-installations, in which relatively large sums of money have to be spent to obtain perfect protection; (2) standard installations, which are designed, in the first place, for valuable ^(public buildings) buildings and buildings in which financial considerations play a small part; (3) "do-it-yourself" installations, in which the financial aspect of protection plays the main part and which are designed for the numerous small dwellings in the provinces, for which a standard installation would be too expensive.

An example of a super-installation is shown in Fig. 17, an explosives factory built on poorly conducting ground. The surroundings of the building are protected by banks of earth. On these banks stand wooden posts carrying a network of 50 mm² copper wires with a mesh width of about 8 m. This network is grounded through a ring conductor with outgoing earth wires at a relatively ~~small~~ ^{great} distance from the building.

- 19 -

This is constructed like a Faraday cage and grounded separately. All the metal parts in the building are carefully grounded in order to avoid the generation of small sparks by a lightning stroke. There is no permanent metallic connection between the building and its surroundings. If the supply of electricity is necessary, this is done by means of a cable, the last 10 m of which are arranged overhead and are separated from the building at this distance when lightning is forecast.

Standard installations are so thoroughly described in the instructions of the respective countries (46) that it is not necessary to give an account of them. Only one point may be mentioned: the practical difficulty of connecting large metal parts to the lightning protective system. A relatively large amount of damage has been brought about by, amongst other things, television antennae. The difficulty is that in many cases the supports for the antennae, usually iron pipes affixed to the roof or a chimney, are not grounded at all. Obviously they are virtually ungrounded lightning rods with only the twin lead of small wires as a circuit to ground, either through a small arrester, probably poorly grounded, or through the TV set. The twin lead is easily vaporized and thereby produces an explosion (49).

In the majority of countries lightning protective systems are not economical for small houses: other considerations play the main part in their ~~production~~ ^{installation}. Insurance statistics show that lightning damage in the countryside seldom exceeds a value of 3% per insured small dwelling and year. As a rule, it is not possible to produce a standard lightning protector for an economical sum of $20 \times 3 = \$60$. In Poland Szpor has suggested protecting small houses with 10 mm^2 iron wire (50). Several hundred thousand installations have yielded a surprisingly good result as regards lightning (16). More detailed investigations of current-heat impulses and their probability showed that 10 mm^2 copper wires are completely adequate (51). The installation is made cheaper not so much by reducing the cross-section of the conductor but by the fact that it is possible to use lighter fittings and brackets, which are available mass-produced. It is possible to stretch the wires over the building oneself, without having

- 20 -

to depend on the experts who are required for erection work with the heavier standard wires. It is requisite, however, that owners of small dwellings who wish to build a lightning conductor themselves should receive the essential instructions. This system is permitted in Sweden (46, 1, 9).

References.

1. B.L. Goodlet Lightning,
Journal of the Inst.El.Eng. 81 (1937) July
82 (1938) Febr.
2. K.B.No. Eachron Lightning protsotion since Frankline day.
Journal of the Franklin Institute 253 (1952)
441 - 470
3. I.B. Cohen Benjamin Frankline Experiments.
A new edition of Franklins Experiments and
Obseervations on Electricity.
Cambridge Maes. Harvard Univ. Press 1941
4. T. Bergman Om möjligheten at förekomma Askans skadeliga
verknningar.
(On the poesibility of preventing damaging effects
of lightning)
Kongl. Vetenekape Aademie Stockholm 1764.
5. B.F.I. Schonland, D.B. Hodgee, H. Collane
 Progressive Lightning V.
Proc.Roy.Soc. A 166 (1938) 56-75
6. B.F.I. Schonland, D.I. Malan, H. Collens
 Progressive Lightning VI.
Proc.Roy.Soc. A 168 (1938) 455-469
7. B.F.I. Schonland
 Progressive Lightning IV.
Proc.Roy.Soc. A 164 (1938) 132 - 150
8. K. Berger
 Front time and current steepness of lightning
strokes to earth.
Proc.Internat.Conf.Gas Discharges and the
Electrioity Supply Industry 1962.
9. K. Berger
 Gewitterforechung auf dem Monte San Salvatore.
ETZ (A) 82 (1961) 249-260
(Compl. by pers. information)
10. D. Müller-Hillebrand On the frequency of lightning flaesches to high
objects.
Tellue 12 (1960) 444-449
11. C.E.R.Bruce, R.H. Golde The lightning discharge.
Journal of the Inst.El.Eng. 88 (1941) 487-505

12. E.T. Pierce Some Topics in atmospheric electricity.
Recent advances in atmospheric electricity
Pergamon Press 1958
13. S.E. Griscom The prestrike theory and other effects in the
lightning stroke.
Trans.Amer.Inst.Electr.Eng. 77 (1958) 919-931
14. R.H. Golde The frequency of occurrence and the distribu-
tion of lightning flashes to transmission lines.
Trans.Amer.Inst.Electr.Eng. 64 (1945) 902-910
15. F. Schwenkhausen Blitzechäden trotz Blitzschutz.
Elektrotechnik 1959 Nr 18
Moormanns Periodische Pers N.V. Den Haag (Holland)
16. D. Müller-Hillebrand The protection of houses - an historical review.
Journal of the Franklin Institute 274 (1962)
34-56
17. R. Davis Frequency of Lightning Flashovers on overhead-lines.
Proc.Internat.Conf.Gas Discharges and the
Electricity Supply Industry
18. I.H. Gridley The shielding of overhead lines against lightning.
Proc.Inst.Electr.Eng. 107 A (1960) p. 325-335
19. M.V. Kostenko Contribution to the Conference of Cigré study
committee 8 in Athen (1962). Not published.
20. V.V. Burgsdorf Lightning protection of overhead transmission
lines and operating experience in the USSR.
Cigré report 326/1958
21. T. Horváth The probability theory of lightning protection.
(In hungarian language)
Elektrotechnika 55 (1962) 48-61
22. C. Dautère, I. Bouget Influence de la constitution géologique du sol
sur les points de chute de la foudre.
C.R. Acad. Sc. 186 (1928) 1565
23. D. Müller-Hillebrand Beeinflussung der Blitzbahn durch radioaktive
Strahlen und durch Raumladungen.
E T Z A 83 (1962) 152-157

24. L.M. Robertson, W.W. Lewis,
C.M. Foust Lightning investigation at high altitudes in
Colorado.
Trans.Amer.Inst.Electr.Eng. 61 (1942) 201-208
25. D. Müller-Hillebrand Zur Physik der Blitzentladung.
E T Z (A) 82 (1961) 232-249
26. A method of estimating lightning performance
of transmission lines.
Trans.Amer.Inst.Electr.Eng. 69 (1950) 1187-1195
- 27.a) B. Cozzano Symposium on operation of the Boulder Dam
Transmission Line-Insulation and Lightning-
Protection.
Trans.Amer.Electr.Eng. 58 (1939) 140-146
- b) T.M. Baksaase, E.L. Kanouse
Thirteen years lightning performance of Boulder
287 kV transmission lines.
Trans.Amer.Electr.Eng. 69 (1950) 796
Results completed by personal information
28. R. Foitzik Versuche mit grossen Stossströmen.
E T Z 60 (1939) 89-92, 128-133
29. P.L. Bellaschi Heavy surge currents-generation and measurement.
Trans.Amer.Electr.Eng. 53 (1934) 86-94
30. N. Hyltén-Cavallius,
A. Strandberg Field measurements of lightning currents.
Elteknik (Stockholm) 2 (1960) 109-113
31. A. Hölzel Blitzschäden an Kirchen.
E T Z (a) 82 (1961) 288-293
32. D. Müller-Hillebrand Åskrisk och åskskydd. (Lightning danger and
lightning protection)
Teknisk Tidskrift Stockholm (1960) 625-630

33. D. Müller-Hillebrand Rückwärtiger Blitzeinechlag in Häuser und Energieumsets im eingeeengten Blitzkanal.
E T Z (A) 78 (1957) 548-553
34. K. Berger Notwendigkeit und Schutzwert metallischer Mäntel von Sekundärkabeln in Höchstspannungsanlagen und in Hochgebirgestollen als Beispiel der Schutzwirkung allgemeiner Faradaykäfige.
Bull. S.E.V. 51 (1960) 549-563
35. K. Berger, I.P. Fourestier, H.F. Schwenkhagen Blitzschutz für elektrische Sprengsünder im Stollenbau.
Nobelhefte 25 (1959) 149-160
36. B.L. Coleman The direct lightning stroke to a buried cable.
The Electrical Research Association
Leatherhead, Surrey
Technical Report S/T71 (1951)
37. H. Meister Blitzschutz an Telephonanlagen.
Technische Mitteilungen P T T
36 (1958) 13-32
38. D.W. Bodle, P.A. Gresh Lightning surges in paired telephon cable facilities
The Bell System
Technical Journal 40 (1961) 547-576
39. S.I. Little Protection of exchange equipment and subscribers installations from damage due to lightning and contacts with power lines.
The Post Office
Electr.Eng.Journal London 53 (1961) 219-225
40. E. Foretay, R. Buchet Schute von Kabeln in Wassereitollen gegen Blitzschäden.
Bull S.E.V. 52 (1961) 33-39
41. D.D. Mac Carthy, D.R. Edge, D.A. Stann, W.C. Mc Kinley Lightning Investigation on a rural distribution System.
Trans.Amer.Inet.El.Eng. 68 (1949) 428-437

42. S. Mandelelam Über die Temperatur des Blitzes und die
Stärke des Donners.
Proc. Ionization phenomena in gases.
Edited by H. Maecker 1962 North-Holland Publ. Co
Amsterdam
43. M.N. Reed Fulgurites in the making.
Rocks and Minerals 33 (1958) 406
Earlier references in:
J.I. Petty. The origin and occurrence of Fulgu-
rites in the Atlantic Coastal Plain.
American Journal of Science V, 31 (1936) 188-198
(86 references)

A.F. Rogers. Sand fulgurites with enclosed Lechate-
lierite from riverside country, California.
The Journal of Geology 54 (1946) 117-122
(15 references)
44. J.L. Böckmann Ueber Blitzableiter.
Karlsruhe 1. Aufl. 1783. 2. Aufl. 1830
45. G.I. Symone Lightning Rod Conference.
Report of the delegates. London 1882
see also: Engineering 1882 p. 225
- 46.a) Austria Leitsätze für die Errichtung und Überprüfung von
Blitzschutzanlagen.
Wien (1960)
Elektrotechnischer Verein Österreichs
- b) Czechoslovakia Instruction for the installation of lightning
protective systems.
Prague (1955)
- c) Denmark Vejledende Regler for Udførelse af Lynaflederanlæg
paa Bygninger m.m.
København Valby (1944)
Elektricitetsrådet

46.d) Finland

Äsekydd för byggnader.
Helsingfors (1943)
Elektriska Inspektoratet

e) Germany

Blitzschutz..
Berlin (1957)
Ausschuss für Blitzableiterbau e.V.

f) Netherlands

Richtlijnen voor Bliksemafleiderinstallaties.
NEN 1014
Den Haag (1958)
Nederlandsche Elektrotechnisch Comité

g) Norway

Lynavlederboka.
(1951)
Norsk Brannvern Forening

h) Polen

Protection of building against atmospheric discharges. General instructions.
Warsaw (1955)

i) Sweden

Byggnadsåskledare.
SEK Handbok 2
(1960)
Sveriges Standardiseringskommission

k) Switzerland

Leitsätze für Blitzschutzanlagen
(1959)
Schweizerischer Elektrotechnischer Verein, Zürich

l) U.K.

Protection of structures against lightning.
(1948)
British standard code of practice CP 326.101

m) U. S. A.

Code for Protection Against Lightning.
(1959)
National fire protection association

n) U.S.S.R.

Lightning protection for industrial and other buildings.
Moskva (1951)
I.S. Stekolnikov, V.S. Komsikov, A.F. Bogomolov,
F.A. Lihachev, V.N. Borisov, L.M. Lopehitz

47. J.C. Maxwell On the protection of buildings from lightning
Rep.Brit.Assoc. for the advancement of science
(1876) p. 45
48. A.O. Kemppainen, I.H. Merriman
Aircraft bonding for lightning protection.
Proc. 1948 Symposium Lightning protection for
aircraft.
Lightning and Transients Research Institute
Minneapolis, Minnesota
49. E. Beck Westinghouse El.Co. East Pittsburgh personal
information.
50. St. Szpor Paratonnières bureaux de type léger.
Rev.Gen. de l'Electricité 68 (1959) 263
51. D. Müller-Hillebrand Über die Beanspruchung und Bemessung von
Blitzschutzanlagen.
E.u.M. 77 (1960) 345-349

Tables

Table 1. Normal log distribution.

Column	1	2	3	4
Magnitude	Current, kA		Charge, Coul	
Average Median	18	13	3.1	15
Deviation	0.32	0.46	0.40	0.51
Mode	10.4	4.25	1.33	3.8
Arithmetical mean	23.7	22.8	4.7	30

Table 2. Extreme current strengths.

Probability	Current 1, A	Current 2, A
1:10	42,000	50,000
1:100	100,000	130,000
1:1000	160,000	210,000
1:10000	220,000	290,000

Table 3. Current heat impulse

No.	Wire diameter, mm	Wire cross section mm ²	Current heat impulse, 10 ⁶ A ² sec
1	0.81	0.52	0.019
2	1.02	0.82	0.048
3	1.29	1.31	0.12
4	1.63	2.09	0.303
5	1.83	2.63	0.49
6	2.05	3.30	0.77

Table 4. Probability of current heat impulses.

Region	Probability %	Current heat impulse 10 ⁶ A ² sec
Boulder	< 0.4	0.303
San Salvatore	0.75	1.5
	0.15	6.4

- 29 -

Figures

Fig. 1. Lightning conductor proposed by Torbern Bergman for a building.
in Uppsala, in 1764.

Fig. 2. Diagrammatic survey of the charge distribution in a leader channel, according to various proposals.

Fig. 3. Marks left by a lightning stroke on a farmhouse. (a) General view. (b) Detail of point of striking.

Fig. 4. Lightning faults on high-tension cables protected by earth wires with various shielding angles.

Fig. 5. Course of lightning current, according to Berger. (a) First stroke from negatively charged cloud. (b) Subsequent partial discharge.

Fig. 6. Damage caused by a powerful flash of lightning striking the church at Rudolzhafen (Bavaria, Germany).

Fig. 7. Traces of lightning over poorly conducting ground from a distance of 35 m to a house.

Fig. 8. Distribution of insignificant damage caused by lightning to the electrical installation near the powerful flash mentioned in Fig. 6.

Fig. 9. Holes in window panes as a result of lightning discharges.
(a) Window in Stockholm in August 1944. (b) Window in Karlsruhe in June 1754.

Fig. 10. Shielded zone of a mast, according to NEPA № 78

Fig. 11. Shielded zone of a chimney, according to Russian model experiments.

Fig. 12. Typical installation of a group of barns, according to the Code of Protection against Lightning (1959). (NEPA № 78)

Fig. 13. Lightning-conductor installation on a farmhouse, according to German recommendations.

Fig. 14. Air terminals, according to NEPA No. 78.

Fig. 15. Modern air terminal.

Fig. 16. A modern house with oil-fired heating etc. and lightning protection.

Fig. 17. Installation of a protective network on wooden poles over a building used for the manufacture of explosives.

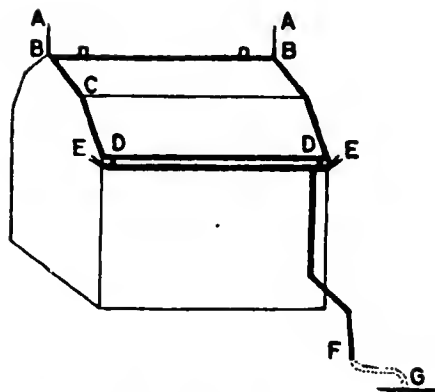


Fig. 1. Lightning conductor proposed by Torbern Bergman for a building. Uppsala, 1764

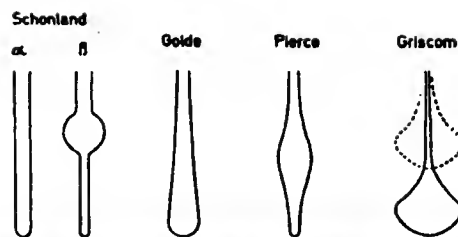


Fig. 2. Diagrammatic survey of the charge distribution in a leader channel, according to various proposals.

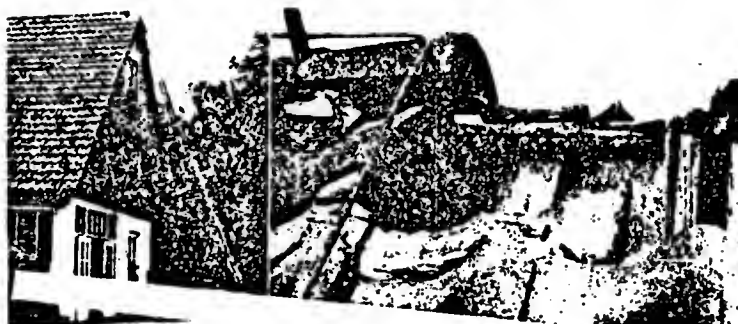


Fig. 3. Marks left by a lightning stroke on a farmhouse
a) General view. b) Detail of point striking

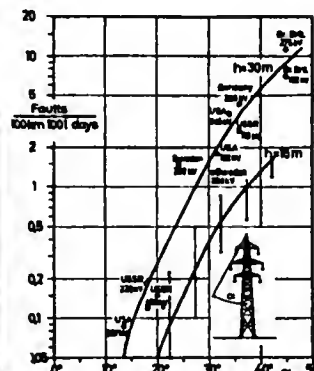


Fig. 4. Lightning faults on high-tension lines protected by earth wires with various shielding angles.

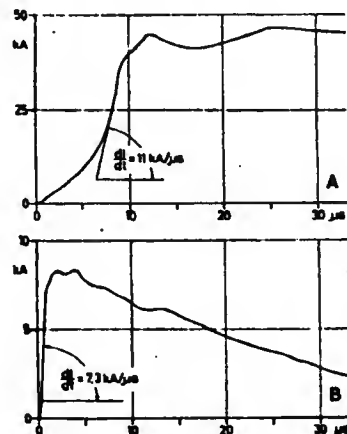


Fig. 5. Course of lightning current, according to Berger
a) First stroke from negatively charged cloud.
b) Subsequent partial discharge.

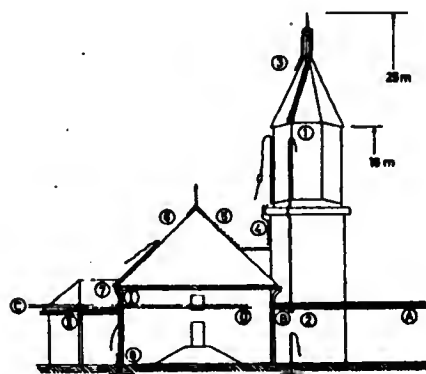


Fig. 6. Damage caused by a powerful flash of lightning striking the church at Rudolzhofen (Bavaria, Germany).

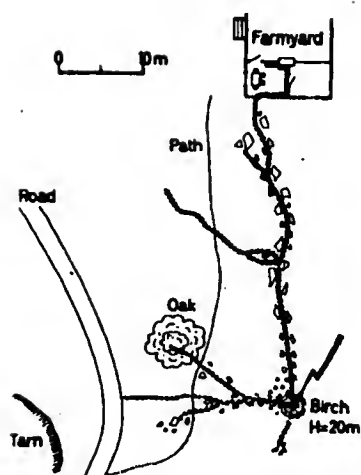


Fig.7. Traces of lightning over poorly conducting ground from a distance of 35 m to a house.

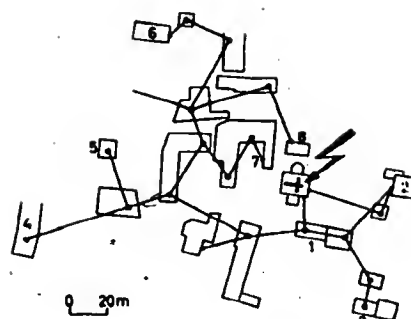


Fig.8. Distribution of insignificant damage caused by lightning to the electrical installation near the powerful flash mentioned in Fig.6.



Fig.9. Holes in window panes as a result of lightning discharges.

a) Window in Stockholm in August 1944.



b) Window in Karlsruhe in June 1754.

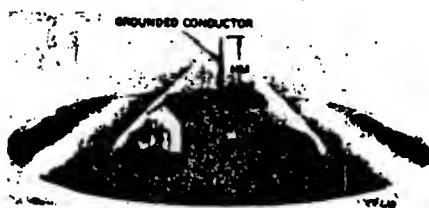


Fig.10 Shielded zone of a mast, according to NEPA No 78.

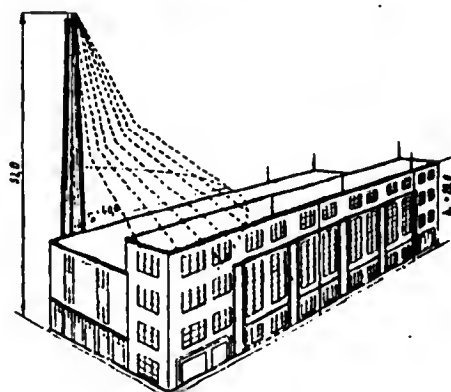


Fig.11. Shielded zone of a chimney, according to Russian model experiments.

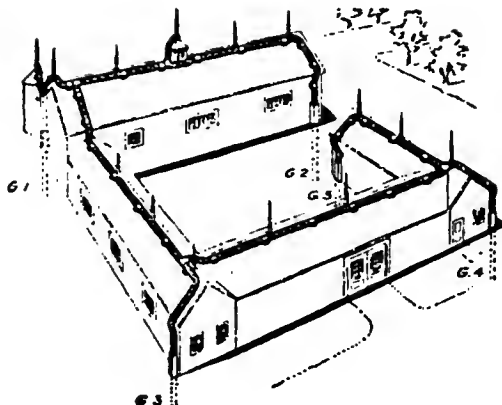


Fig. 12. Typical installation on a group of barns, according to the Code of Protection against Lightning (1959). (NEPA No 78).

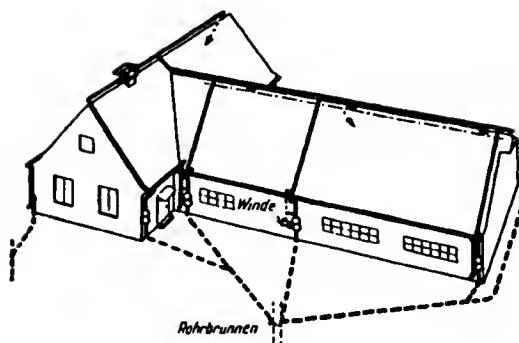


Fig. 13. Lightning-conductor installation on a farmhouse, according to German recommendations.

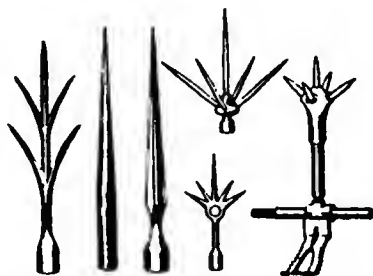


Fig. 14. Air terminals, according to NEPA No 78.

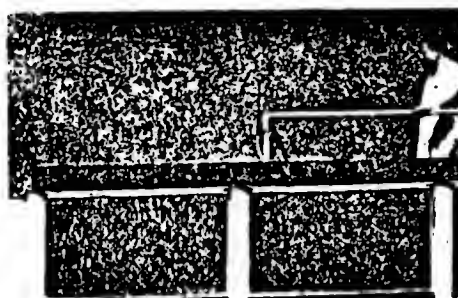


Fig. 15. Modern air terminal.

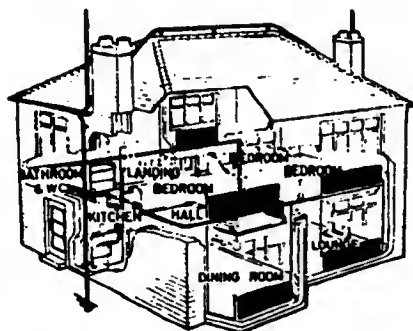


Fig. 16. A modern house with oil-fired heating etc. and lightning protection.

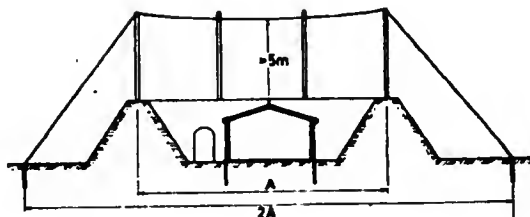


Fig. 17. Installation of a protective network on wooden poles over a building used for the manufacture of explosives.

SESSION 9.1

Whistlers as a Phenomenon to Study Space Electricity.by N.D. Clarence.

Part of the data used in this paper have been taken from the results of a joint project by the author and Dr. P.A. P'Brien now of the University of Khartoum. The results of this project are now in the course of preparation for publication elsewhere.

SUMMARY.

After a brief resumé of evidence supporting the contention that whistling atmospherics may be generated by lightning discharges to ground, and that the components of a multiple flash whistle arise from the separate strokes in the flash, an analysis of the measurement of dispersions of multiple flash whistlers is given. It is shown that there is an increase of about 3% in the dispersion of the second component as compared with that of the first. An explanation of this is tentatively given in terms of an upward electron jet originating from runaway electrons in the thundercloud. Further supporting evidence for such a jet is sought from a study of the records of electrostatic field changes during a lightning discharge to ground.

SESSION 9.1

Whistlers as a Phenomenon to Study Space Electricity.by N.D. Clarence.

Part of the data used in this paper have been taken from the results of a joint project by the author and Dr. P.A. P'Brien now of the University of Khartoum. The results of this project are now in the course of preparation for publication elsewhere.

SUMMARY.

After a brief resumé of evidence supporting the contention that whistling atmospherics may be generated by lightning discharges to ground, and that the components of a multiple flash whistle arise from the separate strokes in the flash, an analysis of the measurement of dispersions of multiple flash whistlers is given. It is shown that there is an increase of about 3% in the dispersion of the second component as compared with that of the first. An explanation of this is tentatively given in terms of an upward electron jet originating from runaway electrons in the thundercloud. Further supporting evidence for such a jet is sought from a study of the records of electrostatic field changes during a lightning discharge to ground.

Introduction.

During the International Geophysical Year whistling atmospherics were recorded in South Africa at Durban (geomagnetic co-ordinates $31^{\circ}34' S$, $93^{\circ}04' E$) by sampling incoming atmospheric for two minutes each hour during the day and night. All records were made on magnetic tape from which frequency-time curves of whistlers were made using a Kay Electric Sona-Graph. The records referred to below were all obtained during the period September 1957 to August 1959.

Multiple Whistlers.

Multiple whistlers, consisting of several components were frequently recorded and may be classified as either multiple path or multiple flash type (Helliwell and Morgan 1959). It is not possible to determine, merely by inspection of a spectrogram, the group to which any particular example belongs. It is known, however, from the Eckereley dispersion law that $t^2 = D^2/f$ where t is the time interval between the occurrence of the lightning stroke producing the whistler and the arrival at the observer of the component of radiated energy of frequency f . A plot of $f^{-1/2} \propto t$ give a straight line the slope of which is the reciprocal of the dispersion, D , of the whistler. Grouping may be carried out by drawing the Eckereley plot for each component and producing the straight line back to cut the time axis. In the case of the multiple path type the lines produce back to a single point indicating the same source for all components. For the multiple flash type the lines cut the time axis at points which are separated by from 10 ms. to several hundred milliseconds indicating a discrete source for each component. Typical examples are shown in fig. 1(a) and (b).

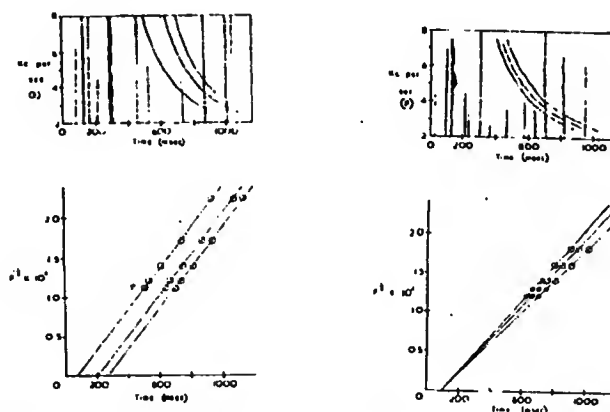


Fig.1. Eckereley plots for (a) multiple path whistlers and (b) multiple flash whistlers.

Of the Durban records of multiple whistlers selected for analysis, over 90% were of the multiple flash type. The ensuing remarks refer specifically to multiple flash whistlers.

The origin of whistlers.

Although sources other than lightning discharges cannot be excluded, there is a great deal of evidence supporting the contention that whistlers arise from lightning discharges.

The strong correlation found between thunderstorm activity in the region near the geomagnetic conjugate point of a recording station and short whistler activity at the station suggests that lightning discharges are the source of whistlers.

Helliwell, Taylor and Jeane (1958) found correlation between observed vertical discharges and long whistlers heard. The atmospheric waveforms recorded at the time were typical of those for flashes to ground.

By the simultaneous recording of long whistlers and the waveform of the related lightning discharges, and by direct comparison of the time intervals between whistler components and strokes in the lightning discharge, Norinder and Knudsen (1961) have shown clearly, for the records published, that the components of the whistlers arose from multiple discharges in the same lightning channel.

Although similar direct comparisons could not be made in Durban, as only short whistlers were recorded, the Durban results do provide further indirect evidence that lightning discharges are the source of whistlers. The distribution of the time intervals, Δt , between components of whistlers is shown in fig.2, together with the distribution of the time intervals between strokes of a lightning flash to ground.

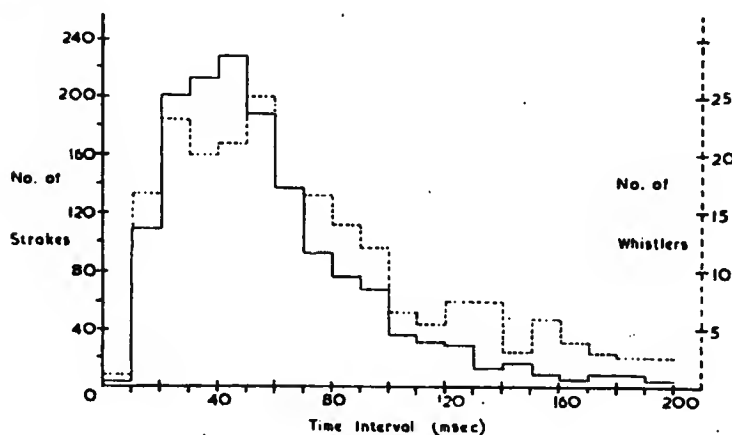


Fig.2. Distribution with time interval of
(a) lightning strokes to ground (full curve) and
(b) whistler components (dotted curve).

3.

The modal value for Δt of between 20 and 60 ms. is in agreement with the value for the most probable time interval between strokes of lightning discharges to ground given by Bruos and Golde (1941) for records in Europe. Also the distribution may be compared with that for the time intervals between strokes to ground given by Schonland (1956) where the similarity of the two curves is again obvious.

It seems clear that where a multiple flash whistler has several components it is generated by a lightning flash to ground which consists of several separate strokes. For this reason it is felt that this type of multiple whistler could be more appropriately termed a "multiple stroke" whistler but for the sake of consistency with published literature the term "multiple flash" whistler is retained.

In the case of cloud flashes the modal value of the time interval between rapid field changes is significantly less than the above value and of the order of 10 ms (Malan 1955; Kitagawa and Kabayashi, 1958). Furthermore, the radiation energy from cloud discharges in the 3-6 Kc/s range is at best only 1% of the corresponding energy for ground flashes (Malan 1958). It seems unlikely therefore that whistlers are generated by discharges within the cloud.

The Dispersion of Multiflash Whistlers.

The Ratio of the Dispersions of successive Components.

Whistlers with two components only.

For multiple whistlers with two components only, there was often a significant difference between the intensity of the components. The records could be divided approximately equally into three groups where the intensity of the second component was (a) greater than, (b) approximately equal to and (c) less than, the intensity of the first component. Also the dispersion of the second component was often slightly greater than that of the first.

In Table 1 the results of an analysis of the ratio of the dispersion of the second component to that of the first, D_2/D_1 , are given. In the column giving the mean value of D_2/D_1 , the standard error of the mean is also shown, and the final column gives the level of significance between the measured dispersion and a ratio of one.

This result proved particularly interesting in view of the fact that previous authors have stated that the dispersions of successive components are either identical or approximately equal. (Storey 1953; Iwai and Otsu 1956; Helliwell and Morgan 1959; Norinder and Knudsen 1961;). Because of the small difference between the measured values of D_2/D_1 and the value one, selected groups of records were analysed

4.

Intensity Group	No. of records.	No. with D_2/D_1	Mean value of D_2/D_1	Significance level, P.
(a)	31	29	1.052 ± 0.011	0.001
(b)	41	28	1.026 ± 0.007	0.001
(c)	31	24	1.016 ± 0.006	0.01
All groups	103	81	1.031 ± 0.005	0.001

Table 1. Ratio of dispersions of components in a two component whistler.

by several different workers. All agreed with the main finding that $D_2/D_1 > 1$. Significance tests have also been carried out between the mean values of the dispersion ratio for the various intensity groups. Significance was calculated to be at the 0.04 level for groups (a) and (b) and at the 0.29 level for groups (b) and (c).

It is concluded, therefore, that the dispersion of the second component of a two component whistler is about 3% greater than that of the first and that there are significant differences between the dispersion ratios when two component whistlers are grouped according to the relative intensity of the two components.

Whistlers with more than two components.

A similar analysis of the dispersion ratio for successive components in the case of whistlers with more than two components, leads to a similar conclusion. Results for records of whistlers with three, four and five components are shown in Table 2.

No. of records.	Mean value of Dispersion Ratio.	Significance level P.
52	$D_2/D_1 = 1.023 \pm 0.007$	0.005
52	$D_3/D_2 = 1.031 \pm 0.007$	0.001
20	$D_4/D_3 = 1.018 \pm 0.015$	0.30
7	$D_5/D_4 = 1.011 \pm 0.020$	0.70

Table 2. Ratio of dispersions of successive components for whistlers with more than two components.

5.

Although the dispersion ratios D_4/D_3 and D_5/D_4 are both greater than one the number of available records is too small for any great reliance to be placed on these figures.

The Relationship between Dispersion and the Time Interval between Components.

An investigation was carried out to see whether the difference in dispersion between successive components was in any way related to the time interval between components. The analysis was made by plotting ΔD , the difference in dispersion between successive components, against Δt , the time interval between components. Time intervals of 20 ms were used and the results were obtained from all records of $D_2 - D_1$ and $D_3 - D_2$. In both cases it was found that there was an initial increase in ΔD , as Δt increased, followed by a decrease. The maximum value for ΔD occurred for a value of $\Delta t = 30$ ms.

The results for $D_2 - D_1$ are shown in figure 3, the numbers in brackets indicating the number of records, in the particular time interval, available for calculation.

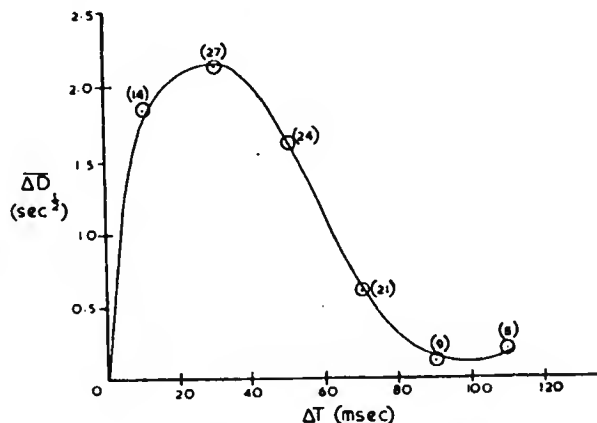


Fig. 3. Relationship between the difference in dispersion between the first two whistler components and the time interval between them.

Speculations on a Possible Explanation of these Results.

From the above it would appear reasonable to assume that (a) in the majority of cases the source of a whistling atmospheric is a lightning discharge between cloud and ground;

6.

- (b) in multiple flash whistlers the several components arise from the separate strokes of the lightning discharge,
- (c) there is a small increase in dispersion between the successive components of a multiple flash whistler;
- (d) the increase in dispersion between whistler components is related to the time interval between them.

Point (d) is of particular interest as it suggests that the dispersion measurements may be related to the physical processes occurring in the thundercloud during the interval between strokes. A possible explanation of the variation in D might be sought in terms of these processes.

Factors Influencing the Dispersion of a Whistler.

The dispersion D of a whistler is given by $D = \frac{1}{c} \int \frac{f_o}{f_H} ds$. (Storey, 1953), provided the frequency of the whistler is much less than either the gyrofrequency f_H or the plasma frequency f_o . ds is an element of path length and the integration is taken over the whole path. By substituting for f_o and f_H , $D = \left(\frac{e}{2}\right)^2 \int \frac{N}{H^2} ds$, where e is the electronic charge in e.m.u., N the electron density per cc and H the magnetic field strength in oersted.

It is known that the ducting of whistlers, giving rise to the multiple path type, occurs very much more frequently in higher latitudes than it does at lower latitudes. It would seem reasonable, therefore, that the energy in each component of a multiple flash type has traversed the same path. In the short time interval between components the values of the magnetic field strength along the path will not change. Consequently, any change in dispersion between one component and another can only be due to a change in electron density along the path.

The fact that D initially increases with t, as shown in Fig. 3, suggests that the change in dispersion is related in some way to the physical processes occurring in the thundercloud during the time interval between strokes. Could then the source of electrons, necessary to account for the increase in dispersion originate in the thundercloud?

Runaway electrons were postulated by J.T.R. Wilson (1925) who showed that in the presence of electric fields such as are found in thunderclouds, the energies of such electrons could be as high as 10^9 Mev. Evidence for such penetrating particles of high energy has been found by Schonland and Viljoen (1933), using geiger counters and by Halliday (1941) using an expansion chamber. In the former case there was a pronounced tendency for the counting rate to increase at the moment of the flash and in addition more impulses were registered during the few seconds

7.

before a flash than during a similar interval after the flash. The radar studies of Atlas (1958), Hewitt (1957) and Rumi (1957) have shown the existence of upward ionized jets during discharges of a thundercloud to ground. Such jets extend to heights well above the top of the thundercloud and are estimated by Rumi to have a velocity of approximately 2×10^7 cm/sec.

Using data given by Nelms (1956) for the range of electrons in various media it is estimated that for an electron to penetrate the remaining atmosphere from a height of 10 Km. it must have an energy of the order of several hundred Mev. It is possible therefore that runaway electrons, accelerated within the thundercloud, could provide an upward jet of electrons.

Assume, in the first place, that such a jet of electrons moves upwards during the time between one stroke and the next. The modal value of Δt between first and second strokes is 40 ms. and for this time interval $\Delta D = 2.0 \text{ sec}^{\frac{1}{2}}$. If the upward velocity of the jet is assumed to be 2×10^7 cm/sec., in 40 ms. an ionized column 8 Km long will be formed. The electromagnetic energy radiated from the second stroke would thus pass through this charged column in addition to traversing the whistler path traversed by the energy from the first stroke.

The question now arises as to whether this column of enhanced ionization can satisfactorily account for the increase in dispersion of the second component over that of the first. Assuming a magnetic field strength of 0.12 oersted the value of the electron density in such a column, which could account for an increase in dispersion of $2.0 \text{ sec}^{\frac{1}{2}}$ is 9.7×10^7 electrons/cc. For such a medium the quasi-longitudinal approximation of the magneto-ionic theory, upon which the expression for D is based, is applicable and, assuming a collision frequency of 10^{10} /sec., the medium would have a refractive index of 22 for a 5 Kc/sec wave.

The above value for the electron density necessary to account for the measured dispersion is the effective density required in the assumed column. It could be used to estimate the current density in the jet and the total charge moving upwards from the thundercloud. In this case, however, values obtained would be minimum values for two reasons. Firstly the picture of the upward moving column has been greatly oversimplified and no account has been taken of the effect of recombination. This would increase the value of the electron density by at least an order of magnitude. From the intensity of radar reflections the electron density in upward jets has been estimated at 3×10^{11} per cc. as it leaves the cloud and 2.8×10^7 per cc. at a height of 60 Km. These figures are consistent with the known values for recombination coefficients at these heights which are of the order

8.

of 10^{-7} . The calculated value for the electron density necessary to account for increased dispersion falls satisfactorily within this experimental range of densities.

Secondly it has been assumed that the jet current flows for the whole of the time interval between strokes. From the work of Schonland and Viljoen (1933) this assumption appears to be justified, but it is likely that the intensity of the upward jet increases to a maximum at the time of the discharge.

The current density, J , in the jet is given by $J = Nev$, and using the calculated value of $N = 9.7 \times 10^7$ per cc. and $v = 2 \times 10^7$ cm./sec. is equal to 0.31 ma/cm².

The total charge carried upward by the jet is given by $Q = A.L.N$ e. when A and L are the area of cross section and length of the ionised column respectively. Substituting known values $Q = A \cdot \frac{1.24}{10^5}$ coulombs with A in square centimetres. Estimates of the radius of upward jets vary over a wide range from a few centimetres to several kilometres depending on the assumed model of the thundercloud. With the uncertainty in the value of A it is difficult to make an estimate of Q . However, assuming a radius of 1 metre, approximately 0.7 coulombs of charge would be carried upward by the jet. Increasing the radius soon leads to enormous values for the charge carried upwards and unless the radius of an upward jet is of the order of 1 metre or less the assumptions made above become untenable bearing in mind that the charge brought to ground is approximately 4 coulombs.

The effect of upward jets on field change measurements.

If upward jets of electrons as postulated, do in fact exist some evidence for them might be expected from field change studies of lightning discharges. Malan and Schonland (1951 A) have considered the electrostatic field which would be produced by an upward moving charge and have shown that there is a reversal in the sign of the measured field change as the charge passes through a reversal height. Assuming that measurements are made at a distance D from a vertical discharge, the reversal height, H_r , is given by $H_r = D/\sqrt{2}$.

For
~~From~~ upward moving positive charge, electrostatic field changes would be positive whilst the charge was below the reversal height and negative when above this height. In the case of upward moving electrons the sign of the field changes would be reversed.

Malan and Schonland explain the observed results in terms of an upward moving positive junction streamer between strokes and having a velocity of approximately 3×10^6 cm/sec. Final slow positive field changes observed for flashes at a considerable distance may also be

9.

due to positive streamers from the top of the thundercloud.

Consider the simultaneous existence of upward moving junction streamers of positive charge and upward jets of electrons. If both processes are below H_r the electrostatic field changes produced by them would be of opposite sign. Since both streamers originate in the thundercloud the faster moving electron jet would be the first to pass through the reversal height. When this happens the field changes due to each process would be positive and a sudden increase in the rate of change of the electrostatic field might be expected. Such field changes are occasionally observed in the final field changes of fairly distant discharges. A typical example of such a field change is shown in Fig. 4.

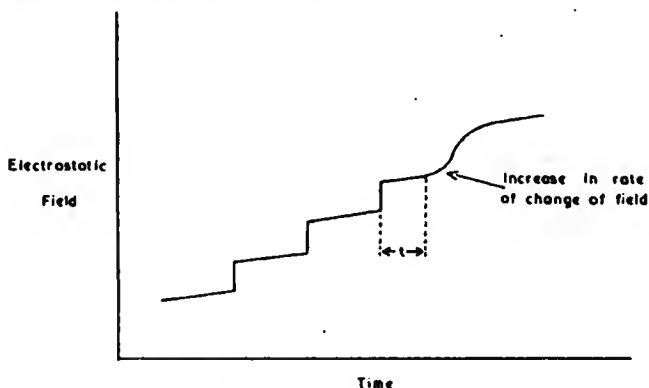


Fig. 4. The electrostatic field of a fairly distant discharge showing a sudden increase in the rate of change of field during the final field change.

Suppose now that the following information is available: Distance of the discharge from the observer and hence H_r ; the height of origin of the final stroke; the time interval, t , between the final stroke and the increased rate of change of the field. From these data it is simple to estimate the velocity of the upward electron jet, assuming that the increased rate of field change may be attributed to its passing through the reversal height.

The results of these calculations are shown in Table 2. for nine records generously provided by Dr. D.J. Malan, of the Bernard Price Institute, from data collected by him over many years. The stroke heights used in the calculations have been taken from Malan and Schonland (1951 B). In all cases the increased rate of field change occurred after the final stroke which originated below the reversal height.

10.

Record No.	Distance (Km)	H _r (Km).	Field change increase after stroke No.	Assumed height of discharge (Km)	t (ms)	Velocity of electron jet. (cm/sec x 10 ⁻⁷).
DA1,3	30	21.2	3	5.4	65	2.4
DAE3,1	20	14.1	2	5.1	14	6.4
DE2,3	16	11.3	3	5.4	20	2.9
DAE1,1	15	10.6	2	5.1	32	1.7
DAB5,9	15	10.6	3	5.4	60	0.9
DX4,6	10-20	10.6	9	8.9	28	0.6
DO3,5	13	9.2	2	5.1	16	2.6
DE4,6	12	8.5	2	5.1	46	0.7
DO2,3	10	7.1	1	3.7	50	0.7

The calculated values of the electron jet velocity lie within the range 0.6×10^7 - 6.4×10^7 cm/sec. Bearing in mind that there could be a considerable difference between the assumed and actual height of the final discharge, these estimated values of the velocity may be regarded as consistent with those obtained from radar studies.

The results of the above paragraphs appear to lend support to the assumptions made. In spite of this, the suggestion that the increased rate of field change is due to the processes outlined must be regarded as tentative for several reasons. The 9 records analysed were the only ones showing the effect out of a total of 285 records and a more frequent occurrence of the effect might be expected. Similar increases in the rate of field change between strokes earlier than the last might also be expected but there is little evidence for this. Finally, out of a total of 159 field change records of flashes which occurred at a distance of 8 km. or nearer there are three instances of an increase in the rate of field change occurring after the final stroke. These results cannot, however, be explained in a similar fashion as it is likely that all processes took place above the reversal height.

In spite of these difficulties it is felt that further radar studies, designed specifically to investigate the existence of ionised jets above thunderclouds during the intervals between strokes, would be justified.

ACKNOWLEDGEMENT.

The interest shown by the members of staff of the Department of Physics, at the University of Natal, and their assistance with calculations is appreciated.

BIBLIOGRAPHY.

- Atlas, D. 1958 Recent Advances in Atmospheric Electricity. Pergamon Press, 441.
- Bruce, C.E.R. and Gold, R.H. 1941 J.I.E.E. 88(11) 487.
- Halliday, E.C. 1941 Phys. Rev. 60, 101.
- Hellivell, R.A. and Morgan, M.G. 1959 Proc. I.R.E. 47, 200.
- Hellivell, R.A. Taylor, W.L., and Jeans, A.G. 1958 Proc. I.R.E. 46, 1760.
- Hewitt, P.J. 1957 Proc. Phys. Soc. B70, 961.
- Iwai, A. and Otsu J. 1956 Proc. Res. Inst. Atms., Nagoya University, 4, 29.
- Kitigawa, N. and Kobayashi, M. 1958 Recent Advances in Atmospheric Electricity. Pergamon Press. 485.
- Malan, D.J. 1955 Ann. Geophys. II, 427.
- Malan, D.J. 1958 Recent Advances in Atmospheric Electricity. Pergamon Press. 557.
- Malan, D.J. and Schonland, B.F.J. 1951A P.R.S.A. 206, 145.
- Malan, D.J. and Schonland, B.F.J. 1951B P.R.S.A. 209, 158.
- Nelms, A.T. 1956 N.B.S. Circ. 577, July, 28.
- Norinder, H and Knudsen, E. 1961 Planet Space Science. 2, 46.
- Rumi, G.C. 1957 J. Geophys. Res. 62, 547
- Schonland, B.F.J. 1956 Handbuch der Physik. 22, 578.
- Schonland, B.F.J. and Viljoen, J.P.I. 1933 P.R.S.A. 140, 314.
- Storey, L.R.O. 1953 Phil. Trans. Roy. Soc. A 246, 113.
- Wilson, C.T.R. 1925 Proc. Camb. Phil. Soc. 22, 534.